140 AK

Data Analysis : Wind / Wave Interaction of Compliant Offshore Structures

Table of Contents

1 INTRODUCTION

Offshore Systems and Analysis Corporation was asked by the University of Western Ontario to review model test data results from the Joint Industry Project (JIP) Wind/Wave Interaction on Compliant Offshore Structures. The following report documents this work.

Model tests for the JIP were performed by the Boundary Layer Wind Tunnel Laboratory at the University of Western Ontario. Three structures were tested in a wind tunnel/wave tank test facility : a semi-submersible, a TLP, and a compliant tower. All models were all built to a scale of 1:160, and were installed in a test section representing 1800 ft. water depth in full scale.

The purpose of the work described in this report was to assess the overall quality and general integrity of the data by performing response analyses from selected tests. In exploring the data, it was anticipated that any problems or unusual features in the data sets could be identified and, if necessary, be acted upon while the project was still active.

Offshore Systems and Analysis has experience in evaluating and interpreting field measurements and model test data from compliant offshore structures. In performing this work, we have attempted to evaluate the data sets with regard to responses which are generally expected, to understand any unusual features in the data, and to explain the system responses in physical terms. Where effects have apparently been introduced by the instrumentation, we have attempted to identify them as such.

The results of the analysis performed for this study are presented almost exclusively as plots. The report, which is a discussion and interpretation of the plots, is organized by response data-type with cross-reference to all relevant test sequence numbers. The plots have been organized by vessel-type, test sequence number and input data- or response data-type. Keeping the plots for each test together facilitates a review of the overall system performance for each set of met-ocean forcings.

The analysis methods used in this report include conventional spectral FFT based techniques, as well as a number of specialized procedures.

The standard analysis sequence includes the following:

- removal of spikes (bad points) from the time series;
- calculation of standard statistics : minimum, maximum, mean, standard deviation, skewness, and kurtosis for each channel;
- plotting time series for visual examination of data, with zooming to examine suspicious features;
- calculation of histograms with appropriate theoretical distributions plotted as overlays;
- removal of mean and trends;
- calculation of the extremal distributions of the maxima and minima using either a generalized Weibull distribution (Type III, three parameters) or a two-parameter Weibull distribution;
- calculation of the spectrum and transfer functions using a block averaging procedure or a frequency-band averaging procedure;

Note : the transfer function magnitude represents a total response, both coherent and incoherent. Phase is defined as positive for the response peaks lagging the input peaks.

Other processes includes :

- X-Y scatter plots with best-fit correlation lines;
- high- and low-pass filtering;
- time-domain integration;
- Hilbert transforms to obtain envelope functions and quadrature series;
- correlations;
- rotation of data to principal axes.

Spectral Resolution

Spectra and transfer functions are calculated using FFTs after removing the mean. The number of points in the data sets vary from 5000 to 6000 points, and are sampled at 10.35 Hz. The maximum frequency (Nyquist frequency) is 5.175 Hz. For most of the test data, 10 overlapping time segments of 1024 points (50 percent overlap) were FFT'd and ensemble averaged for spectral and transfer function estimation. The frequency resolution for most of the spectral plots was $1.011\ 10^{-2}$ Hz, which corresponds to a full-scale frequency resolution : $(160)^{-1/2}\ 1.011\ 10^{-2} = 0.791\ 10^{-3}$ Hz. This resolution was sufficient to separately resolve low-frequency surge and tank seiche modes. The model scale spectral peak frequency at approximately 1 Hz, corresponds to a full scale spectral peak at 0.07906 Hz (spectral peak period = 12.65 s).

Statistics

The summary statistics are provided in a table for each of the closely examined model tests. The primary statistics for all channels that were used include minimum value, mean, maximum value, standard deviation, skewness and kurtosis. The skewness and kurtosis are useful indicators of the Normality of a distribution. Zero skewness implies a symmetric distribution. Positive skewness indicates a tendency for the distribution to have a longer tail in the positive extremes, a negative skewness indicates a longer tail for the negative extremes. Kurtosis measures the peakedness of the distribution. A positive kurtosis indicates a tendency toward a double-exponential distribution (spiked near 0, with broad tails). A negative kurtosis indicates a tendency toward a uniform (top-hat) distribution (blockier than Gaussian with a lower peak and shorter tails).

Extremal Statistics

Extremal statistics are displayed in plots of non-exceedence probability *vs.* maxima (or (-) minima) normalized by the standard deviation of the process. The degree of non-Normality of the process is often visually more apparent in these plots than in the histograms. At the one-in-a-thousand occurrence level, the ratio of the maxima to the rms value should be approximately 3.72 for a Gaussian process. Since the Rayleigh distribution is the distribution for the envelope of a Normal process, it represents an upper bound for the distribution of the peaks (or negative troughs) of a spectrally spread process. Distributions of maxima (or (-) minima exceeding this bound, are strong indicators of the non-Gaussian nature a

response. Distributions of maxima that fall below the Rayleigh distribution do not necessarily indicate non-Normality, since the effect may be due to spectral spreading. With the information provided by the skewness and kurtosis, the histograms and extremal distribution plots, the nature of the process can usually be clarified.

3 DATA DESCRIPTION and NOTATION

Detailed descriptions of the model tests, including the facility, instrumentation and models, are available in the reports provided by BLWT and will not be belabored in this report.

Of the three structure/vessel configurations tested, OSAC was provided with the data for the semi-submersible and the TLP. This data was transmitted to OSAC as compressed ASCII files on 3 1/2" diskettes. The 15 data channels recorded for the semi-submersible are listed in Table 2.1; the 21 data channels recorded for the TLP are listed in Table 2.2.

Although all data channels were examined, only the following data channels were extensively explored and used for the response analyses :

Semi-submersible

SURGE
HEAVE
PITCH/ROLL
YAW
CENTRE WAVE
HOTWIRE (Windspeed)

TLP

SURGE
HEAVE
YAW
TENDON TENSION (1, 2, 3, 4)
ACCELERATION (X, Y)
CENTRE WAVE
HOTWIRE (Windspeed)

Model Test Notation The model tests are identified by a six character alpha-numeric code. The first two characters identify the vessel-type : TR (semi-submersible) and TL (TLP); the next two numerals indicate the vessel heading : 00 (0°), 45 (45°) and 90 (90°); the last two numerals indicate the test sequence number for that vessel and heading : 00, 01, ...

Figure Notation Figure identifiers for all plots displayed in this analysis use following notation :

- the six character test number (followed by a period);
- a letter code identifying the variable or combination of variables displayed in the plot (followed by a period). The letter codes used are :

W	Wave (Centre Wave)
NW	Wave (Near Wave)
FW	Wave (Far Wave)
HW	Hotwire (Windspeed)
S	Surge
A	Acceleration principal direction (maximum variance)
H	Heave
Pi	Pitch
Ro	Roll
Y	Yaw
VX	Water particle velocity X-direction
VY	Water particle velocity Y-direction

For the TLP, the additional letter codes are :

Tn	Tendon Tension (*e.g.*, **T1** = Tension Tendon 1)
HTavg	*Heave* ⇔ average of all four tendon tensions : (T1+T2+T3+T4) / 4
PiT13	*Pitch* ⇔ tendon tension difference : (T1 - T3) / 2
RoT24	*Roll* ⇔ tendon tension difference : (T2 - T4) / 2

If the data has been filtered, then the additional notation is attached to the variable to indicate this :

HF	High-Frequency

LF Low-Frequency

- a numeral is used to indicate the type of plot :

1 Histogram

The Histograms will normally have one to three overlays of theoretical distributions. These overlays are indicated on the plot as :

Norm (Normal or Gaussian);
C-Gsk (Gram-Charlier, using both skewness and kurtosis);
GNorm (Generalized Normal, the exponent is variable).

2 Distribution of the Maxima (peaks)

The peaks are normalized by the standard deviation of the process, and fit by a generalized Weibull distribution (3 parameters). In addition, a Rayleigh distribution is plotted (with dashed lines) as a reference to a narrow-band Gaussian process.

3 Distribution of the (-) Minima (troughs)

The absolute value of the troughs are normalized by the standard deviation of the process, and fit by a generalized Weibull distribution (3 parameters). In addition, a Rayleigh distribution is plotted (with dashed lines) as a reference to a narrow-band Gaussian process.

4, 4* Spectra (* refers to smoothed spectral estimates)

4t,4t* Transfer Function, Coherence and Phase

An overlay of the input spectrum is often plotted with the transfer function to indicate the frequencies with input energy (* refers to smoothed spectral estimates).

Examples of the figure notation are:

TR0001.W.1, indicates a histogram of the wave elevation (Centre Wave) for the semi-submersible at 0° heading, test number 1;
TL4504.W/S.4, indicates a spectral plot of both the wave and surge for the TLP at heading 45°, test number 4.

A total of twelve combinations of wave and wind conditions were utilized in the tests (three sea-states and four wind conditions).

	Model Scale		*Full Scale*	
	H_s	f_p	H_s	f_p
WAVE 1	**0.056**	**1.01**	**9.0**	**0.0800**
WAVE2	0.080	0.84	13.0	0.0667
WAVE3	0.108	0.74	17.0	0.0581
	Windspeed		Windspeed	
WIND1	**0.0**		**0.0**	
WIND2	2.0		25.3	
WIND3	3.0		37.9	
WIND4	**4.0**		**50.1**	

In this study, the detailed responses analyses were concentrated on a single sea-state :

- WAVE1, corresponding to a 9 m. significant wave height and 12.6 second spectral peak period in full-scale.

For this sea-state, responses for two wind conditions were contrasted :

- WIND1, no wind;
- WIND4, the maximum wind corresponding to 50.1 m/s, full-scale.

As discussed below (see Wave Statistics) the statistics for the highest sea-state (WAVE3), consistently displayed a behavior that we cannot account for. Prompted by the unusual WAVE3 crest-trough statistics, a large sample of tests for the shortest spectral peak period sea-state - WAVE1 - were examined. Since the data quality was good and the wave statistics normal (and because of time and budget constraints), the results of the WAVE1 tests were emphasized. To this extent the selection of WAVE1 rather than WAVE2 was arbitrary.

Wave Spectra

Generally, the data quality for the waves appears to be good from viewing the time series and the basic statistics. The spectral distribution of the model-test wave energy is highly concentrated near the spectral peak. In a test report (BLWT-SS31-88, Preliminary Report No. 1), comparisons of the model-test wave spectra to various JONSWAP forms consistently reveal relatively small spectral densities in the model-test waves above the spectral peak frequency. The narrow-bandedness of the sea-state would tend to enhance the second-order bound waves, although no extraordinary secondary peaks were noted in any of the wave spectra analyzed.

Seiche Modes

The predicted tank seiche modes (personal communication, S. Ramsey) are 0.364 Hz (transverse) and 0.0424 Hz (longitudinal). Although a small peak corresponding to the longitudinal mode is often seen in the wave, heave and tendon tension spectra, its effect appears to be small, even though it is near the TLP's surge resonance peak. The transverse mode is not apparent in the wave spectra (centre, near or far), but it is close to the semi-submersible pitch resonance peak.

Spatial Variability

There is evidence of some spatial variability of the wave-field in the tank data. Table 4.1 displays the standard deviation of the wave elevation for each of the six tests analyzed. The centre wave (C.Wave) and near wave (N.Wave) were quite close in their estimates, well within the limits that can be accounted for statistically. However, statistics for the far wave sensor were clearly different. The estimates for the rms wave elevation fall outside the range one could reasonably expect from statistical variability.

Wave Statistics

The prime reason for not concentrating on the most extreme sea-state (WAVE3) was the anomalous behavior of the wave elevation extrema statistics. The wave crests and troughs were not distributed asymmetrically as one would expect in a normal sea-state (Longuet-Higgins, M. S., 1963 , *J. Fluid Mech.* 17, 459-480). Rather, both crests and troughs exceeded the amplitudes predicted for a Rayleigh-distributed process (the Rayleigh distribution being the expected distribution of a instantaneous amplitude of a Gaussian process).

Of the six tests that were emphasized in this study, only TL4504 displayed wave statistics for the WAVE1 sea-state that were out-of-line with the other tests. The skewness and kurtosis for the waves of test TL4504 differ considerably from the other tests (contrast the histograms and extremal crest probability distributions of TL4504.W.1,2 with TR4511.W.1,2, for example). There are some large wave events in the test with perfectly reasonable time histories. Therefore, the results appear valid, but we are unable to account for the behavior.

Wind

The detailed discussions of the model-test winds are very competently covered in the BLWT reports BLWT-SS01-1989, BLWT-SS02-1989, BLWT-SS03-1989.

Current

The behavior of the velocity sensors (see Appendix 1) precluded any effort to estimate wind-generated currents and their effects on the models.

Two vessel orientations were selected for the response analyses, zero and forty-five degrees. For both headings, responses from tests without wind , TR0001 and TR4501 were contrasted with the responses obtained from tests with the maximum wind, TR0004 and TR4511.

Surge

The surge response is characterized by two frequency regimes : wave-frequency surge (SHF) and low-frequency surge (SLF), or slow-drift. By filtering at approximately 0.5 Hz, the drift-frequency surge (SLF) and wave-frequency surge (SHF) can be separated. As can be seen from the histograms (SHF.1 and SLF.1) and the spectral plots (W/S.4), the low-frequency drift tends to dominate the response, especially with the maximum wind. Virtually the entire increase in rms surge response that occurs due to wind can be accounted for by the increase in the low-frequency surge (SLF) variance.

Surge HF

From the histograms, one sees that the smaller amplitude wave-frequency surge (SHF) is only mildly non-Gaussian in the absence of wind (TR0001, TR4501), but very non-Gaussian, tending toward a peaked double-exponential distribution with the maximum wind (TR0004, TR4511). The effect of the wind on the wave-frequency surge is to statistically re-distribute the energy, rather than to significantly increase it. Comparing the spectral plots (W/S.4), one sees that the wind does increase the level of the high-frequency surge well above the spectral peak (1 Hz), with out changing the energy density near the peak of the wave spectrum. It does not appear likely, however, that the effect is due to the high-frequency waves introduced by the wind. As shown in Figure 5.2.5 in the report preliminary report (BLWT-SS31-88), the variance of these high-frequency waves is only 10^{-2} the variance of the dominant waves.

A high-frequency surge-pitch coupling due to the wind may account for the effect. The increase in high-frequency energy, although small, manifests itself in a greater number of small amplitude surge zero-crossings. Hence, a tendency toward a peaked exponential distribution of the high-frequency surge (SHF) is developed.

Surge LF

The low-frequency surge distributions are moderately skewed and peaked (kurtosis > 0) in the absence of wind (TR0001.SLF.1, TR4501.SLF.1). The down-wave surge maxima are well above the values predicted from Rayleigh statistics, at the one-in one thousand exceedence level ((TR0001.SLF.2, TR4501.SLF.2). With the maximum wind introduced, the distribution of low-frequency surge becomes more symmetric with a flattened peak (TR0004.SLF.1, TR4511.SLF.1), mimicking the form of the wind distribution (TR0004.HW.1, TR4511.HW.1). The down-wave surge maxima are still above the values predicted from Rayleigh statistics (at the one-in one thousand exceedence level), but not to the extent seen without wind.

The large amplitude low-frequency surge (SLF) is broadly increased by the wind at all frequencies below the spectral peak frequency of the waves. As can be seen from the wind-surge transfer function plots (HW/S.4t), there are no regions of particularly high coherence.

While the overall effect of the wind is to increase the down-wave surge maxima- due to the static offset and the increased surge variance - the divergence of the extremes from Rayleigh statistics is apparently reduced by the introduction of the wind. This same effect is seen in the TLP response, so it is unlikely that an explanation can be attributed to idiosyncrasies of the semi-submersible model.

Heave

The heave sign convention is reversed from the wave elevation, being positive downward. As one would expect, the strong correlation of heave with wave elevation, causes the heave distributions to closely mimic the wave distribution, regardless of the wind.

The heave resonance peak near 0.67 Hz is evident in the spectral plots (W/H.4, W/H.4t). When the wind is introduced, the pitch resonance near 0.34 Hz also appears. This heave/pitch coupling maybe due to wind lift effects on the structure.

Pitch/Roll

At the zero degree heading, the roll is very much smaller than the pitch, as expected. For the forty-five degree heading, pitch and roll

are comparable. The distribution of pitch is moderately non-Gaussian, skewed toward the downwave direction in the absence of wind (TR0001.Pi.1,2,3 and TR4501.Pi.1,2,3). With the maximum wind, the pitch distributions become symmetric and approach the Gaussian distribution (TR0004.Pi.1,2,3 and TR4511.Pi.1,2,3).

The resonant peak near 0.34 Hz contributes substantially to the overall pitch response as can be seen in the spectral plots (W/Pi.4, W/Pi.4t). Although not displayed, no significant coherence between wind and pitch was observed at any frequency, even though the increase in pitch amplitude with wind was substantial. The character of this behavior is substantially that observed for the surge, where the increased amplitudes in the response are limited to low frequencies, and the coherence remains small.

Yaw

The yaw response is small regardless of the vessel heading or the windspeed, although it does increase with the windspeed. Even at the highest winds, the rms yaw is only about 0.02 radians (1°), with the majority of the energy in the low-frequency.

The spectral plots, TR0001.W/Y.4 and TR4501.W/Y.4, clearly show separate yaw responses at the periods of low -frequency surge and pitch resonance in the absence of wind. At the maximum wind, the yaw response peaks at low -frequency increase, with the response peaking at the pitch resonance period (TR0004.W/Y.4 and TR4511.W/Y.4).

A single vessel orientation was selected for the TLP response analyses, the forty-five degree heading. The responses from the WAVE1 test without wind, TL4501, were contrasted with the responses obtained from tests with the maximum wind, TL4504.

Surge

As for the semi-submersible, the TLP surge response is characterized by two frequency regimes : wave-frequency surge (SHF) and low-frequency surge (SLF), the slow-drift. By filtering at approximately 0.5 Hz, the drift-frequency surge (SLF) and wave-frequency surge (SHF) can be separated. As can be seen from the histograms (SHF.1 and SLF.1) and the spectral plots (W/S.4), the low-frequency drift tends to dominate the response, especially with the maximum wind. Like the semi-submersible, virtually the entire increase in rms surge response due to wind can be accounted for by the increase in the low-frequency surge (SLF) variance.

The total surge response in the absence of wind displays the same skewed behavior (TL4501.S.1) we have noted in other tests. The down-wave surge maxima and the up-wave surge (-) minima differ substantially from the Rayleigh distribution at the one-in-one thousand level (TL4501.S.2,3).

Surge HF

The small amplitude wave-frequency surge (SHF) is nearly symmetric and only mildly non-Gaussian with or without the maximum wind (TL4501.SHF.1,2,3). Unlike the behavior of the semi-submersible the effect of wind on the wave-frequency surge is negligible, neither changing its rms value (as for the semi) nor its distribution. Comparing the spectral plots (W/S.4), one sees that the wind does slightly increase the level of the high-frequency surge well above the spectral peak (1 Hz), with out changing the energy density near the peak of the wave spectrum.

Surge LF

The low-frequency surge distribution is strongly skewed and peaked (kurtosis > 0) in the absence of wind (TL4501.SLF.1). The down-wave surge maxima are well beyond the values predicted from Rayleigh statistics, at the one-in one thousand exceedence level ((TL4501.SLF.2). With the maximum wind, the distribution becomes symmetric with a flattened peak , mimicking the form of

the wind distribution (TL4504.HW.1, TL4504.SLF.1). The down-wave surge maxima are still slightly above the values predicted from Rayleigh statistics (at the one-in one thousand exceedence level), but not to the extent seen without wind.

As was seen in the surge response of the semi-submersible, the large amplitude low-frequency surge (SLF) is broadly increased by the wind at all frequencies below the spectral peak. From the wind-surge transfer function plots (HW/S.4t), there are no regions of particularly high coherence observed at any frequencies.

The overall effect of the wind is to increase the down-wave surge maxima due to the static offset and the increased surge variance, but to reduce the divergence from Rayleigh statistics in the prediction of the extremal statistics.

Heave

The heave channel is included for completeness. Because of the smallness of the signal (30 times smaller than the semi-submersible heave) the average of the tendon tension are used as indicators of the heave dynamics (see the discussion in Heave-Tension)

Pitch/Roll

Again due to the smallness of the signal the pitch/roll sensors output are ignored (and not included in this analysis). The differences in tendon tensions are used as indicators of pitch and roll dynamics.

Yaw

TLP yaw responses amplitudes are similar to those observed for the semi-submersible, although no pitch resonance contributes. The yaw response is concentrated near the low-frequency surge resonance. The response remains small even at the highest winds, where the rms yaw is about 0.02 radians (1°) .

Tendon Tension

The distributions of up-and down-stream tendon tensions (T1 and T3) display a noticeably non-Gaussian form (T1.1-3, T3.1-3). Although skewed toward the maxima, both maxima and minima exceed the Rayleigh estimates at the one-in-a-thousand level. The ratio of down-stream to up-stream tension variance of is approximately 1.5, regardless of the wind.

Resonant Peak

In the spectral plots (W/T1.4, W/T3.4) there are two distinct high-frequency peaks above the wave spectral peak frequency. From the wave-to-tension transfer plots (W/T1.4t, W/T3.4t), one sees that the highest peak near 3 Hz (0.24 Hz full-scale) is probably a resonant response since the coherence approaches zero. This probably corresponds to the vessel natural pitch period.

Secondary Peak

The peak near 2 Hz (0.158 Hz full-scale) is most pronounced in the no-wind test for the up-stream tendon (TL4501.T1), although it is visible in the down-stream tendon, T3. When the maximum wind is introduced, the peak is reduced in T1 and essentially eliminated in T3 (contrast TL4501.W/T3.4 and TL4504.W/T3.4). Although there is some coherence between wave and tension at the secondary peak, there is strong coherence with wave-squared, indicating a non-linear origin of the peak (the wave-squared to pitch transfer functions are shown in TL4501.WSQ/PiT13.4t and TL4504.WSQ/PiT13.4t). There are a number of second order wave forces, including but not limited to the second order wave potential, which could be driving this response.

Heave-Tension

Because of the small TLP heave response, the average of the four tendon tensions (HTavg) are used as the measure of the heave dynamics, since the tension is a sensitive measure of vertical motion. Comparing the spectral plots of the direct measure of the heave (W/H.4) to the average-tension estimate of the heave (W/HTavg.4) clearly shows the superiority of the tension estimate to resolve both the narrow-band low-frequency peaks and the small amplitude high-frequency peaks. The high-frequency heave spectral estimates in the direct heave measurements have the character of a uniform (white) noise.

The distribution of the heave-tension is very non-Gaussian, with a highly peaked near-exponential distribution. The wind exaggerates the differences between the maxima and (-)minima, by increasing the skewness. In both cases, with or without the wind, the heave-tension extrema greatly exceed the Rayleigh estimates at the one-in-a-thousand level.

The resonance near 3 Hz, seen in the individual tendons, the heave-pitch (PiT13) and heave-roll (RoT24), is much less pronounced for

the heave-tension, when compared to pitch-tension, indicating the resonance is pitch dominant . This resonant peak in the heave-tension signal is reduced even further in the presence to the maximum wind (compare figures TL4501.W/HTavg.4 and TL4504.W/HTavg.4).

The effect of the tank seiche on the heave-tension is very clearly displayed in TL4501.HTavg.4 and the low-pass filtered response shown in TL4501.HTavgLF.4. When the maximum wind is introduced, another low-frequency peak appears (see TL4504.W/HTavg.4) due to the slow-drift / set-down effect. This oscillation is significant and is very clearly seen in the time segment displayed in TL4504.HTavgHF/LF.

Time series showing the "springing/ringing" and contrasting the heave-tension and pitch-tension response are deferred to the pitch-tension discussion.

Pitch-Tension

The pitch-tension mode (PiT13) is defined as one-half the difference of up- and down-stream tendon tension, 0.5 (T1 - T3). This mode displays a very non-Gaussian behavior, moderately skewed toward the (-) minima and tending toward a peaked, nearly exponential distribution. The wind only moderately affects the distributions.

"Springing-Ringing"

High-pass filtering the pitch-tension at 2.5 Hz to isolate the high-frequency oscillations near the resonant peak at 3 Hz leads to the histograms seen in TL4501.PiT13HF.1 and TL4504.PiT13HF.1. Distributions of this form (mixture processes) may be hypothesized to consist of the sum two zero-mean Gaussian processes with very different variances - small amplitude background process ("springing") sporadically interrupted by a much larger response ("ringing"). This interpretation is supported by the time series segments shown in TL4501.PiT13HF.TIM and TL4501.PiT13HF.TIM .

The correlation of the bursts of "ringing" to larger wave events is seen in the figures TL4501.W/PiT13HF.TIM and TL4504.W/PiT13HF.TIM. The wave and high-frequency pitch - tension (PiT13HF) have been normalized and offset vertically on the plots. Since the wave sensor is down-stream of the TLP, the peak

of the wave events appear after the "ringing" event has been initiated.

Figures TL4501.PiT13HF/LF.TIM and TL4504.PiT13HF/LF.TIM show the relative contribution of the high-frequency pitch-tension events, pitch (HF), to the pitch-tension without the high-frequency, pitch (LF) for the same time segment. Total pitch-tension and heave-tension are contrasted in TL4501.HTavg/PiT13.TIM and TL4504.HTavg/PiT13.TIM.

TL4501.HTavgHF/LF.TIM and TL4504.HTavgHF/LF.TIM emphasize the relative importance of the pitch-tension at high-frequency resonance by showing the small amplitude of the high-frequency heave-tension signal compared to the remainder of the heave-tension.

Non-linearities

The secondary peak in the tension near 2 Hz is emphasized in the pitch-tension. Squaring the wave elevation, removing the mean and Fourier transforming, the wave-squared to pitch-tension transfer function can be computed. In the absence of wind, figures TL4501.WSQ/PiT13.4, 4t provide convincing evidence of the non - linear origin of the secondary tension peak, showing high coherence near 2 Hz. The introduction of the maximum wind clearly erodes the coherence of this secondary peak, but it still remains moderately high (see figures TL4504.WSQ/PiT13.4, 4t).

Miscellaneous

Acceleration and roll-tension plots have been included, but provide little additional information beyond the obvious. The accelerations are highly correlated to the pitch-tensions, and the roll-tension are similar in structure to the pitch-tension but of much smaller amplitude.

Several interesting effects associated with the wind have been observed for the semi-submersible and the TLP. Both vessels displayed similar rms surge responses, with similar distributions of wave-frequency and low-frequency surge.

For the semi-submersible, it was noted that even though the rms wave-frequency surge was virtually unchanged when maximum wind was applied, the probability distribution of this component of the surge was substantially altered. For the TLP, neither the rms wave-frequency surge nor its probability were affected by the application of the maximum wind.

The rms low-frequency surge for both the semi-submersible and the TLP sharply increased when the maximum wind was applied. The coherence between wind and surge, however, was relatively low at all frequencies, although tending to be higher at the low frequencies. In the absence of wind, the low-frequency surge was strongly skewed in the down-wave direction, differing considerably from the Rayleigh statistics at the one-in-a-thousand exceedence level. When the maximum wind was applied, the low-frequency surge distribution was strongly modified, acquiring more of the symmetric character of the wind distribution. This modification could be caused by :

- a change in character of the wind, as opposed to wave drift, forcing ;
- by the change in the mooring system stiffness with increased offset.

The latter explanation seems most plausible, but cannot be resolved since the no-wind tests did not include offsets (due to equivalent wind forcing).

The overall effect of applying the maximum wind is to increase the down-wave surge maxima through the increase in the rms surge (as well as mean). However, when the maximum wind is introduced, the surge extremes tend to deviate much less dramatically from the Rayleigh inferred estimates at the one-in-a-thousand exceedence level.

Pitch-tensions display high-frequency "springing / ringing" to a much greater extent than the heave-tension mode. For pitch-tension, a low-level background ("springing") is sporadically interrupted by much larger bursts ("ringing") induced by large wave events.

The heave-tension shows very much lower levels of the high-frequency "springing / ringing" than the pitch-tension. However, in the presence of the maximum wind, a large amplitude low-frequency oscillation appears induced by the surge / set-down effect. This effect is barely evident in the absence of the wind.

TABLES

Channel	*Probe*
1	SWAY
2	SURGE
3	HEAVE
4	PITCH
5	ROLL
6	YAW
7	NEAR WAVE
8	CENTRE WAVE
9	FAR WAVE
10	HOTWIRE
11	NEAR PITOT
12	FAR PITOT
13	VELOCITY X
14	VELOCITY Y
15	REFERENCE PITOT

Table 2.1 Semi-submersible Channel Assignments

Channel	*Probe*
1	SWAY
2	SURGE
3	HEAVE
4	PITCH
5	ROLL
6	YAW
7	NEAR WAVE
8	CENTRE WAVE
9	FAR WAVE
10	HOTWIRE
11	NEAR PITOT
12	FAR PITOT
13	VELOCITY X
14	VELOCITY Y
15	ACCELEROMETER X
16	ACCELEROMETER Y
17	TENDON 1
18	TENDON 2
19	TENDON 3
20	TENDON 4
21	RISER

Table 2.2 TPL Channel Assignments

FIGURES

Test	TR0001	TR0004	TR4501	TR4511	TL4501	TL4504	Mean	Coff. Var.
Channel								
Near Wave	0.0145	0.0167	0.0147	0.0150	0.0147	0.0150	0.0151	0.0542
Centre Wave	0.0151	0.0150	0.0151	0.0147	0.0148	0.0143	0.0148	0.0223
Far Wave	0.0129	0.0130	0.0132	0.0134	0.0138	0.0133	0.0132	0.0245

Table 4.1 Wave Elevation Standard Deviations

DATA FILE : TR0001

Channel	Minimum	Mean	Maximum	Stand. Dev.	Skewness	Kurtosis
SWAY	-0.0041	0.0022	0.0083	0.0020	0.0179	-0.1559
SURGE	-0.0478	0.0057	0.0818	0.0166	0.4266	0.7459
HEAVE	-0.0251	0.0004	0.0249	0.0061	-0.1248	0.4565
PITCH	-0.1019	-0.0013	0.1332	0.0279	0.1892	0.6164
ROLL	-0.0161	0.0042	0.0239	0.0056	0.0056	0.0129
YAW	-0.0174	-0.0002	0.0117	0.0031	-0.3549	1.2776
NEAR WAVE	-0.0511	0.0001	0.0838	0.0145	0.1594	0.7161
CENTRE WAVE	-0.0479	0.0009	0.0743	0.0151	0.2496	0.5782
FAR WAVE	-0.0535	0.0001	0.0586	0.0129	0.1802	0.6627
HOTWIRE	0.0000	0.0000	0.0000	0.0000	0.0000	0.0000
VEL X	-0.6644	-0.0387	0.6375	0.1459	-0.2694	0.6047
VEL Y	-0.6677	-0.0016	0.5696	0.1408	-0.2684	2.4851

NUMBER OF DATA POINTS PER CHANNEL = 5960
DELTA TIME (DT) = .09662

Table 5.1

DATA FILE : TR0004

Channel	Minimum	Mean	Maximum	Stand. Dev.	Skewness	Kurtosis
SWAY	0.0000	0.0158	0.0313	0.0047	0.0491	-0.0337
SURGE	-0.0105	0.0672	0.1820	0.0282	0.1129	-0.0546
HEAVE	-0.0296	-0.0040	0.0255	0.0066	-0.0588	0.6463
PITCH	-0.0831	0.0923	0.2904	0.0551	0.0454	-0.1719
ROLL	-0.1004	0.0090	0.0669	0.0187	-0.1243	0.0920
YAW	-0.0423	-0.0086	0.0234	0.0094	0.0601	-0.1744
NEAR WAVE	-0.0531	0.0048	0.0781	0.0167	0.2330	0.7258
CENTRE WAVE	-0.0500	0.0054	0.0800	0.0150	0.2425	0.6737
FAR WAVE	-0.0452	0.0045	0.0661	0.0130	0.1842	0.9977
HOTWIRE	1.9715	3.7468	5.9939	0.5343	0.1999	-0.3454
VEL X	-0.7432	-0.0138	0.6397	0.1454	-0.1544	1.7050
VEL Y	-0.7121	0.0036	0.7374	0.1570	-0.5026	2.2893

NUMBER OF DATA POINTS PER CHANNEL = 5408
DELTA TIME (DT) = .09662

Table 5.2

DATA FILE : TR4501

Channel	Minimum	Mean	Maximum	Stand. Dev.	Skewness	Kurtosis
SWAY	-0.0195	0.0001	0.0215	0.0059	0.0279	-0.3269
SURGE	-0.0333	0.0042	0.0612	0.0130	0.6182	0.9661
HEAVE	-0.0248	0.0002	0.0181	0.0055	-0.1792	0.3017
PITCH	-0.0836	0.0025	0.1204	0.0218	0.4765	1.1829
ROLL	-0.0900	0.0036	0.1071	0.0254	0.2936	0.3568
YAW	-0.0227	-0.0023	0.0161	0.0056	-0.0683	0.0828
NEAR WAVE	-0.0572	0.0003	0.0577	0.0147	0.1388	0.4655
CENTRE WAVE	-0.0514	0.0004	0.0740	0.0151	0.1605	0.5539
FAR WAVE	-0.0495	0.0002	0.0716	0.0132	0.1839	0.6316
HOTWIRE	0.0000	0.0000	0.0000	0.0000	0.0000	0.0000
VEL X	-0.6507	0.0408	0.6693	0.2293	-0.1944	-1.2260
VEL Y	-0.7890	-0.0181	0.7459	0.1792	-0.0345	0.5253

NUMBER OF DATA POINTS PER CHANNEL = 5863
DELTA TIME (DT) = .09662

Table 5.3

DATA FILE : TR4511

Channel	Minimum	Mean	Maximum	Stand. Dev.	Skewness	Kurtosis
SWAY	-0.0328	-0.0005	0.0332	0.0110	-0.0125	-0.3053
SURGE	0.0264	0.0982	0.1962	0.0266	0.0774	-0.3258
HEAVE	-0.0324	-0.0040	0.0208	0.0059	-0.1432	0.5388
PITCH	-0.0755	0.0882	0.2705	0.0413	-0.0517	-0.0684
ROLL	-0.0628	0.0947	0.3319	0.0491	-0.0602	-0.1431
YAW	-0.0724	-0.0197	0.0322	0.0164	-0.0179	-0.2938
NEAR WAVE	-0.0573	-0.0001	0.0693	0.0150	0.1370	0.7552
CENTRE WAVE	-0.0496	0.0001	0.0778	0.0147	0.1791	0.6339
FAR WAVE	-0.0526	-0.0002	0.0605	0.0134	0.1928	0.7836
HOTWIRE	2.3119	3.9680	6.1472	0.5705	0.0937	-0.3430
VEL X	-0.8368	-0.1291	0.6842	0.2176	-0.0606	-0.5381
VEL Y	-0.7890	-0.0313	0.7956	0.1590	-0.1780	1.9055

NUMBER OF DATA POINTS PER CHANNEL = 5576
DELTA TIME (DT) = .09662

Table 5.4

DATA FILE : TL4501

Channel	Minimum	Mean	Maximum	Stand. Dev.	Skewness	Kurtosis
SWAY	-0.0069	0.0000	0.0076	0.0019	-0.0277	0.0101
SURGE	-0.0340	0.0127	0.0847	0.0177	0.5499	0.4610
HEAVE	-0.0014	0.0002	0.0025	0.0004	0.3370	0.8507
PITCH	-0.0159	-0.0003	0.0164	0.0046	-0.0147	-0.1285
ROLL	-0.0056	0.0007	0.0118	0.0018	0.5125	1.1457
YAW	-0.0247	-0.0005	0.0267	0.0077	-0.0376	0.1218
NEAR WAVE	-0.0617	0.0001	0.0598	0.0147	0.2101	0.6961
CENTRE WAVE	-0.0476	0.0002	0.0668	0.0148	0.1649	0.4899
FAR WAVE	-0.0535	0.0001	0.0538	0.0138	0.2449	0.6514
HOTWIRE	0.0000	0.0000	0.0000	0.0000	0.0000	0.0000
VEL X	-0.5264	0.0024	0.4775	0.1117	0.1170	1.0999
VEL Y	-0.4767	-0.0191	0.5363	0.1008	-0.3256	2.7325
ACCEL X	-0.0926	0.0000	0.1321	0.0266	0.2427	0.3502
ACCEL Y	-0.1194	0.0000	0.0911	0.0259	-0.0401	0.4406
TENDON 1	-1.6603	0.1713	2.5643	0.4267	0.5289	1.4420
TENDON 2	-1.1861	-0.0296	1.1626	0.2236	-0.1531	1.5357
TENDON 3	-3.0865	-0.0308	4.2317	0.7817	0.2301	1.3891
TENDON 4	-1.3119	-0.0353	1.7927	0.2487	0.2581	2.3251
RISER	-1.7132	0.0618	0.6356	0.1135	-3.4322	44.3570

NUMBER OF DATA POINTS PER CHANNEL = 6002
DELTA TIME (DT) = .09662

Table 6.1

DATA FILE : TL4504

Channel	Minimum	Mean	Maximum	Stand. Dev.	Skewness	Kurtosis
SWAY	-0.0192	0.0030	0.0265	0.0064	-0.0068	-0.0834
SURGE	0.0846	0.1544	0.2211	0.0238	0.0142	-0.5741
HEAVE	0.0007	0.0040	0.0086	0.0014	0.3335	-0.3323
PITCH	-0.0167	0.0010	0.0166	0.0048	-0.0497	-0.2419
ROLL	-0.0036	0.0023	0.0115	0.0019	0.3774	0.4990
YAW	-0.0096	0.0424	0.1104	0.0184	0.1116	0.3330
NEAR WAVE	-0.0594	-0.0007	0.0658	0.0150	0.2206	0.6013
CENTRE WAVE	-0.0468	-0.0001	0.0827	0.0143	0.4533	1.2183
FAR WAVE	-0.0527	-0.0003	0.0599	0.0133	0.1934	0.9496
HOTWIRE	2.1879	3.8508	5.5092	0.5284	0.0217	-0.4268
VEL X	-0.5764	0.0269	0.5625	0.1242	0.0385	0.6774
VEL Y	-0.5369	-0.0286	0.5042	0.1110	-0.5728	2.3255
ACCEL X	-0.1133	0.0000	0.1257	0.0303	0.1868	0.3574
ACCEL Y	-0.1168	0.0000	0.1131	0.0311	0.0686	0.0541
TENDON 1	-0.9698	0.6414	2.6893	0.4415	0.4215	0.8645
TENDON 2	-0.7893	0.2990	1.7118	0.2655	0.3122	1.4500
TENDON 3	-2.9288	-0.2020	4.3242	0.6972	0.4788	2.2810
TENDON 4	-0.7247	0.3812	2.4723	0.2877	0.6150	2.3045
RISER	-2.2026	0.0193	0.7878	0.1403	-6.4047	70.7120

NUMBER OF DATA POINTS PER CHANNEL = 5981
DELTA TIME (DT) = .09662

Table 6.2

APPENDIX

APPENDIX Velocity Sensor

Introduction

The velocity measurements in all tests that were examined for the semi-submersible and the TLP showed a tendency toward the following types of distributions :

- Bi-modal distribution seen in the histogram (Figure TR4501.VX.1) from test TR4501;
- Tri-modal distribution seen in the histograms (Figures TL4501.VX.1, TL4506.VX.1) from tests TL4501 and TL4506;
- Almost uni-modal distribution seen in the histogram (Figure TR45016.VX.1) from test TR4516.

The appearance of two large peaks displaced somewhat symmetrically to either side of the mean suggests at least two possible time series representations that could lead to the observed bi-modal distribution :

1. the sum of a nearly sinusoidal oscillation and Gaussian noise;
2. an episodic lightly damped oscillation plus the persistent Gaussian noise.

The Gaussian noise in these instances is the wave-induced signal, with the sinusoidal oscillation triggered either by resonance (1) or a non-linearity due to an impulsive force. The first scenario will be analyzed below since it is easily modelled and interpreted. The distribution for the second scenario can be described, but requires more analytic effort - and is beyond the scope of this investigation.

RMS Velocity

If the water particle velocities were being correctly measured (ignoring any mean velocities), their probability density distributions should mimic the surface wave distribution. Since the surface waves are nearly Gaussian (we will ignore the weak non-Gaussian effects in this discussion), the water particle velocities should also be nearly Gaussian. Just to be sure, the distribution for the surface waves in plotted in Figure TR4501.W/VX.4 and as expected it is

nearly Gaussian with a zero-mean and standard deviation, σ_ζ = 0.0151 m.

But as Figure TR4501.VX.1 shows, the measurements are far from Gaussian. To estimate the standard deviation of the "correct" water particle velocities, σ_v, spectral definitions will be used. By definition :

$$\sigma_\zeta^2 = \int_0^\infty S_{\zeta\zeta}(\omega)\, d\omega \quad , \quad \sigma_{\dot{\zeta}}^2 = \int_0^\infty \omega^2\, S_{\zeta\zeta}(\omega)\, d\omega$$

The ratio of these two variances, provides a measure of the average zero-crossing frequency, $\langle \omega_{02} \rangle^2$, so that :

$$\sigma_v = \langle \omega_{02} \rangle\, \sigma_\zeta$$

Very typically, if one estimates the zero-crossing frequency from the spectral peak and the spectral width of the process, one finds that $\langle \omega_{02} \rangle \approx 1.25\ \omega_p$, where ω_p is the spectral peak frequency.

With these approximations, and the measured σ_ζ and ω_p, one should expect the standard deviation of the velocity to be :

$$\sigma_v = 1.25\ (2\pi)\ (1.0\ \text{Hz})\ (0.0151\ \text{m.}) = 0.1186\ \text{m/s}$$

The standard deviation of the measured velocities, $\sigma_{v\text{-}m}$, rotated to the principal direction in test TR4501, is :

$$\sigma_{v\text{-}m} = 0.2905\ \text{m/s}$$

This amplification by a factor of nearly 2.5 times strongly suggests are resonance phenomenon.

Time Series / Statistical Model

As described in the introduction, the simplest model to compare to the velocity measurements, **V**, consists of a pure sinusoid at frequency, ω_o, amplitude, A, and randomly selected phase, φ, plus zero-mean Gaussian noise, $\mathbf{n}(t;\sigma_v)$, with standard deviation, σ_v :

$$\mathbf{V} = A \cos(\omega_o\, t + \varphi) + \mathbf{n}(t;\sigma_v)$$

The random phase, φ , is uniformly distributed on [0, 2π].
Assuming φ and $n(t;\sigma_v)$ are uncorrelated, the distribution of V can be obtained from the convolution of the individual distributions :

$$p(V;\frac{A}{\sigma_v}) = \frac{\sigma_v^2}{\pi\sqrt{2\pi}}\int_0^{\pi} d\varphi \exp -\frac{1}{2}[\,V - \frac{A}{\sigma_v}\cos(\varphi)\,]^2$$

where, $V = V / \sigma_v$.

To compare directly to the measurements, the variance of V can be calculated from :

$$\sigma_{v\text{-}m}^2 = \langle V^2 \rangle = \sigma_v^2 \int_0^{\pi} p(V;\frac{A}{\sigma_v})\, V^2 dV = \sigma_v^2\,(\,1 + \frac{A^2}{2\sigma_v^2}\,)$$

which provides the expected result for independent processes.
Using the measured value for $\sigma_{v\text{-}m}$ (= 0.2905 m/s) and the estimated value for σ_v (= 0.1186 m/s), the estimated amplitude of the resonant oscillation is A = 0.3750 m/s, with the signal-to-noise ratio, A / σ_v = 3.1622

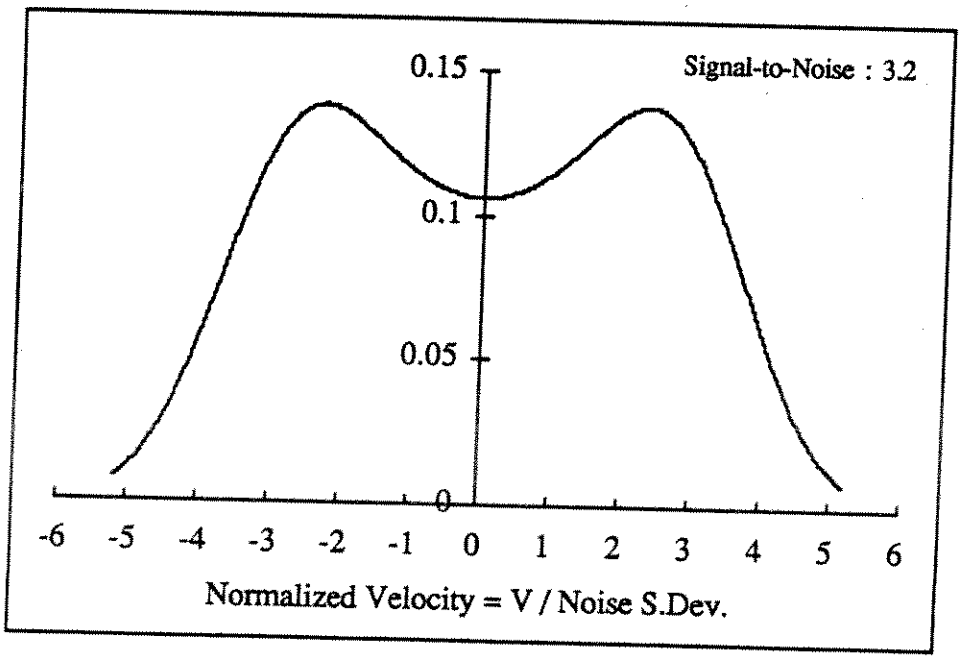

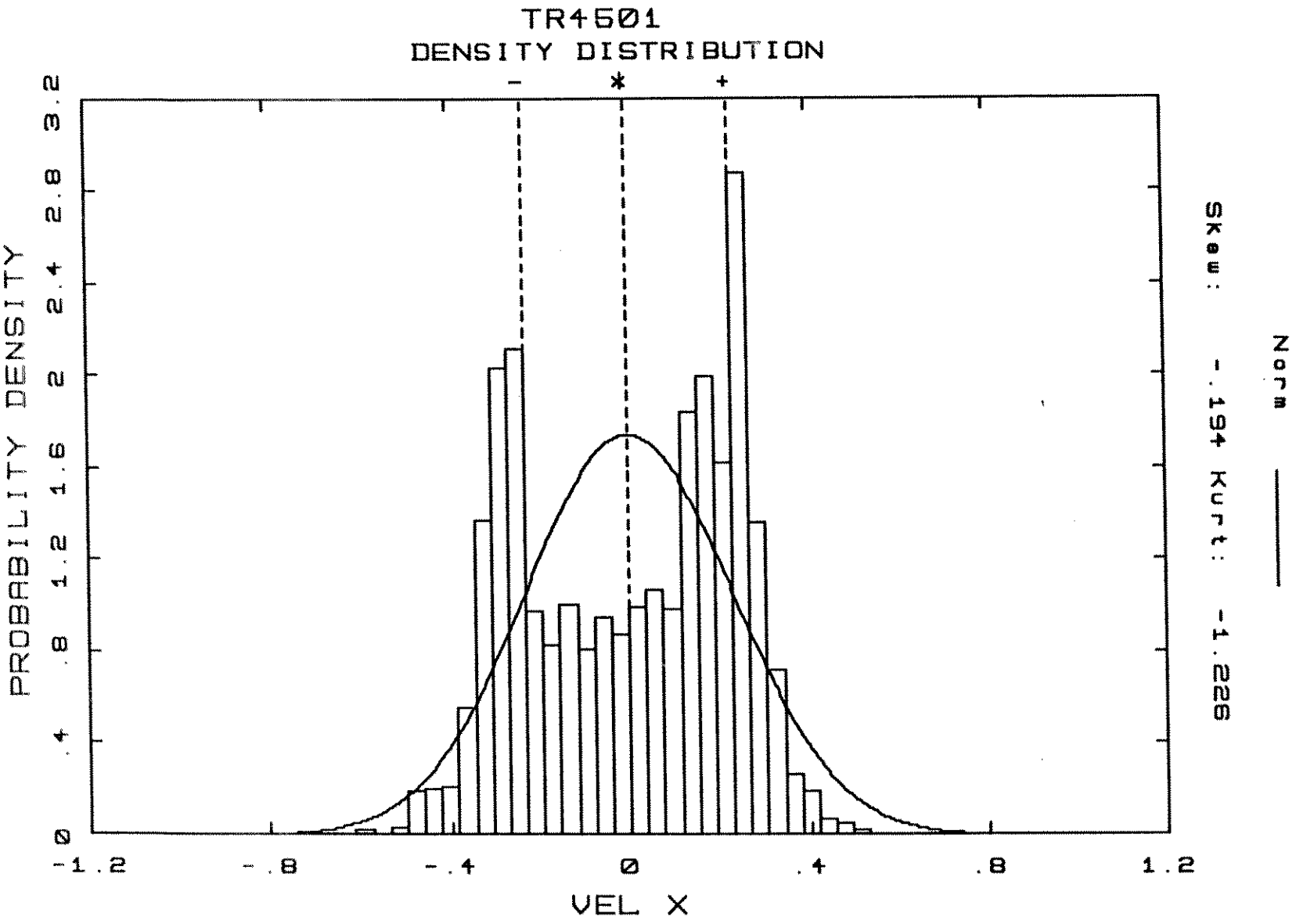
TR4501
DENSITY DISTRIBUTION
- * +
PROBABILITY DENSITY
0 .4 .8 1.2 1.6 2 2.4 2.8 3.2
-1.2 -.8 -.4 0 .4 .8 1.2
VEL X
Norm
Skew: -.194 Kurt: -1.226

TR4501.VX.1

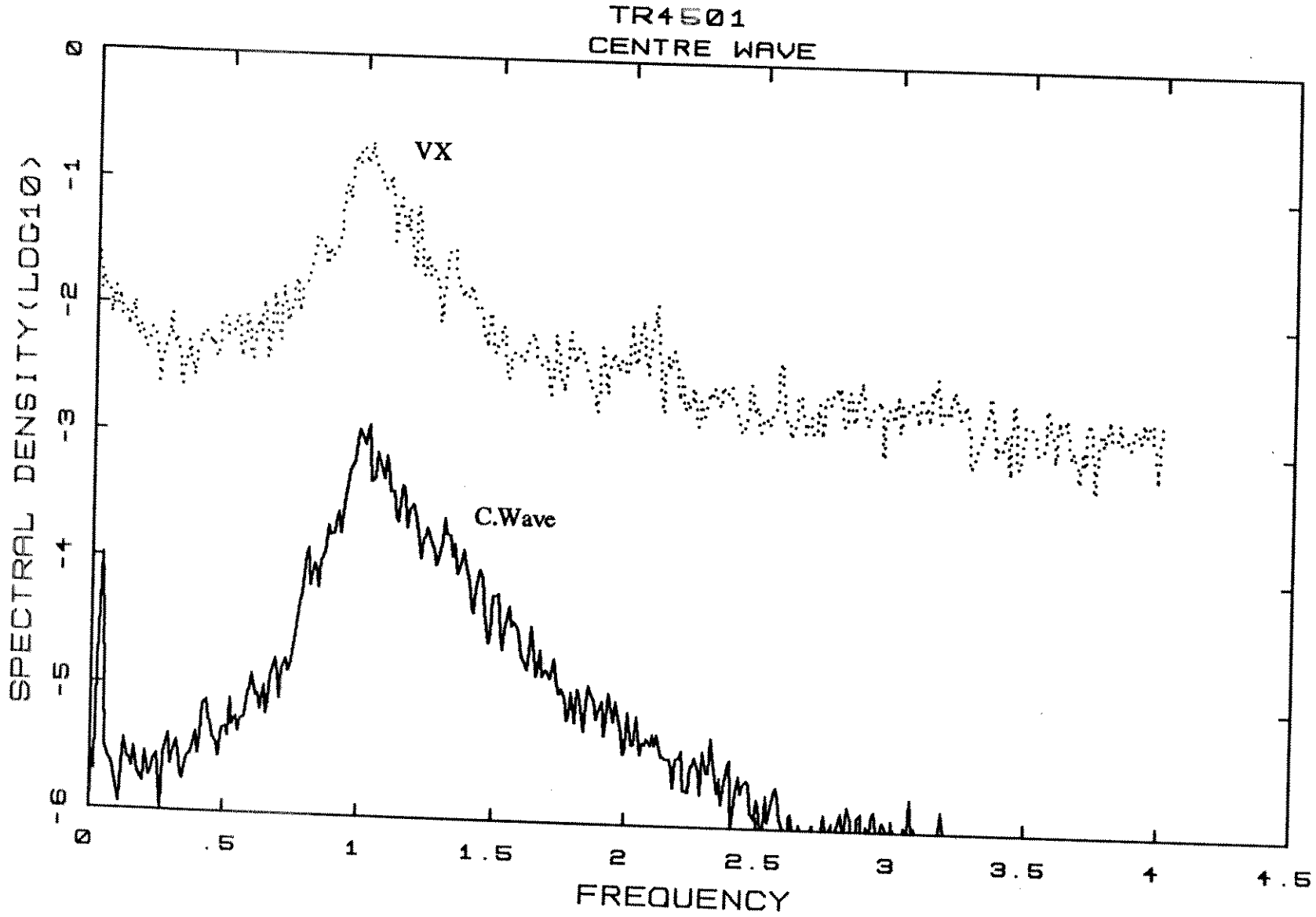
TR4501
CENTRE WAVE
VX
C.Wave
SPECTRAL DENSITY(LOG10)
0
-1
-2
-3
-4
-5
-6
0
.5
1
1.5
2
2.5
3
3.5
4
4.5
FREQUENCY

TR4501.W/VX.4

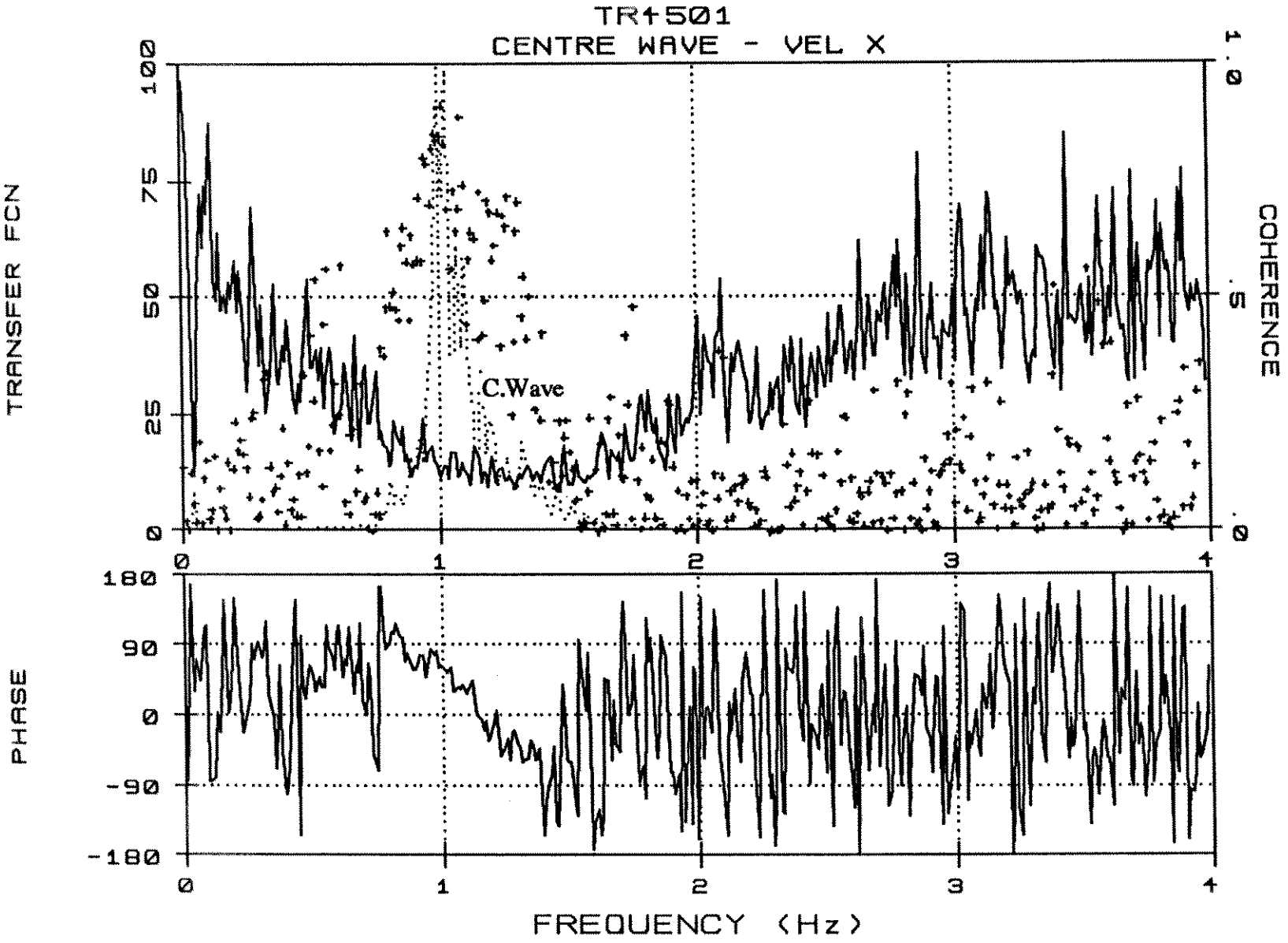

TR4501.W/VX.4t

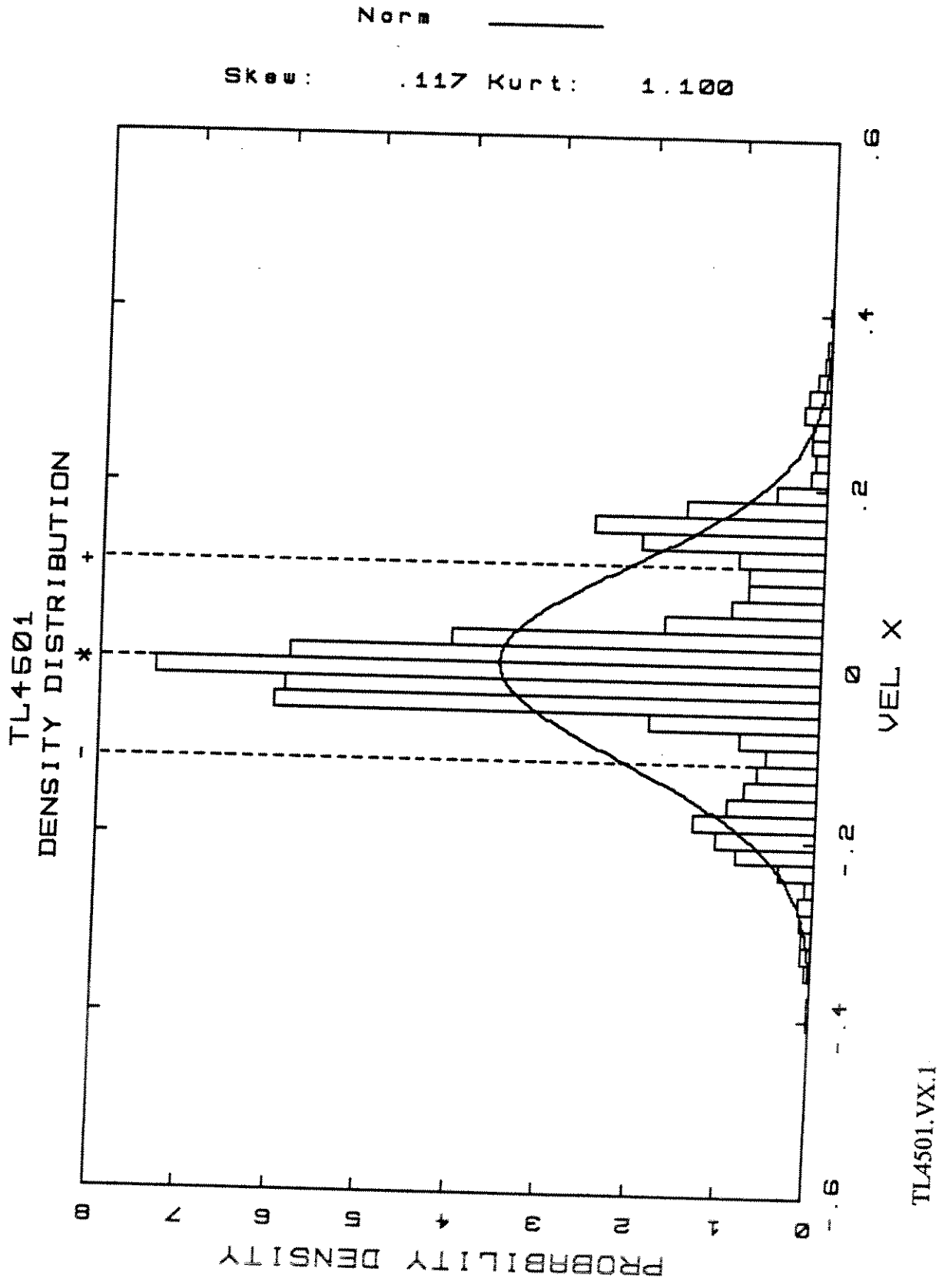
Norm
Skew: .117 Kurt: 1.100
TL4501
DENSITY DISTRIBUTION
PROBABILITY DENSITY
VEL X
TL4501.VX.1

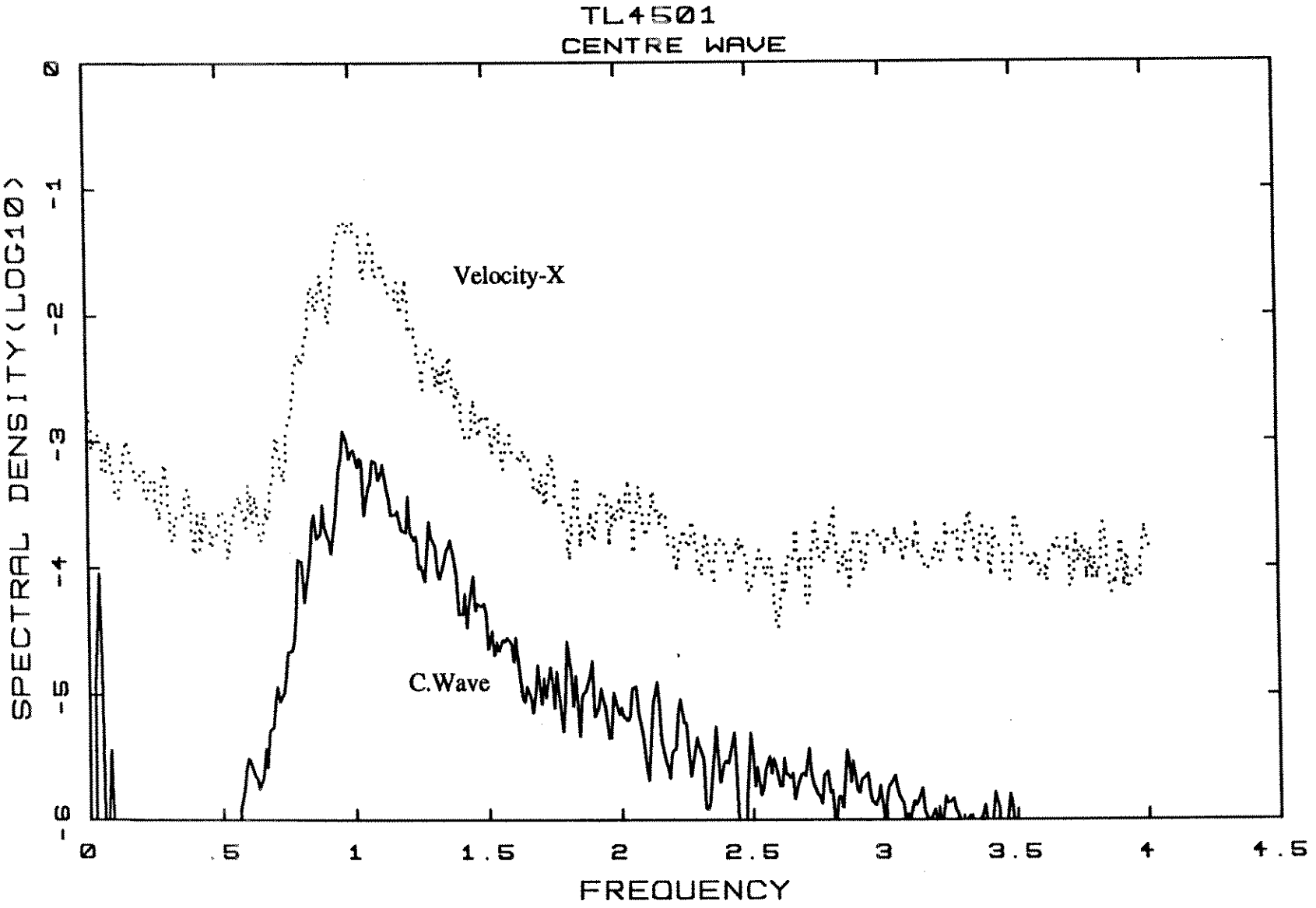
TL4501
CENTRE WAVE
SPECTRAL DENSITY(LOG10)
0
-1
-2
-3
-4
-5
-6
Velocity-X
C.Wave
0
.5
1
1.5
2
2.5
3
3.5
4
4.5
FREQUENCY

TL4501.W/VX.4

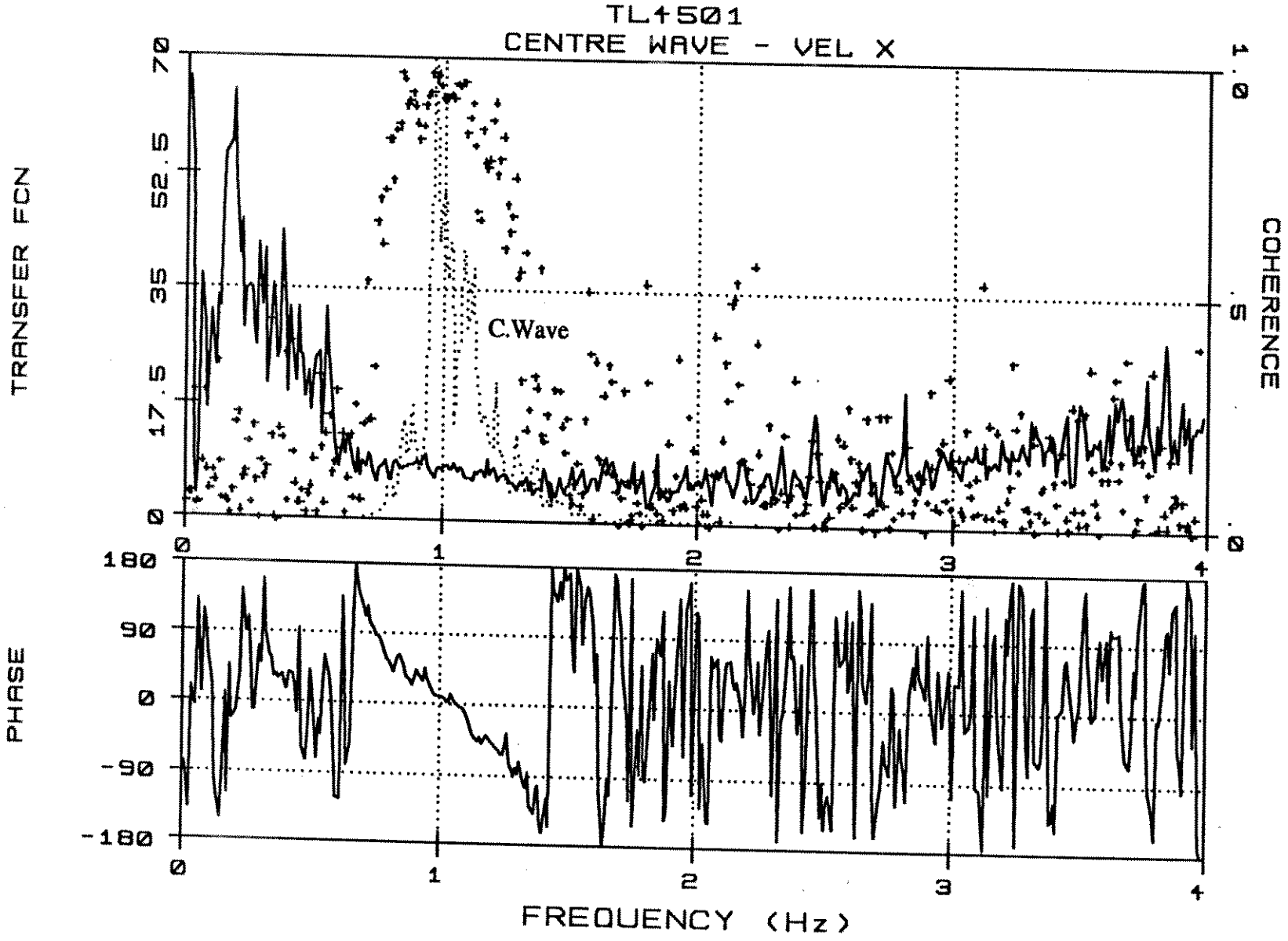

TL4501.W/VX.4t

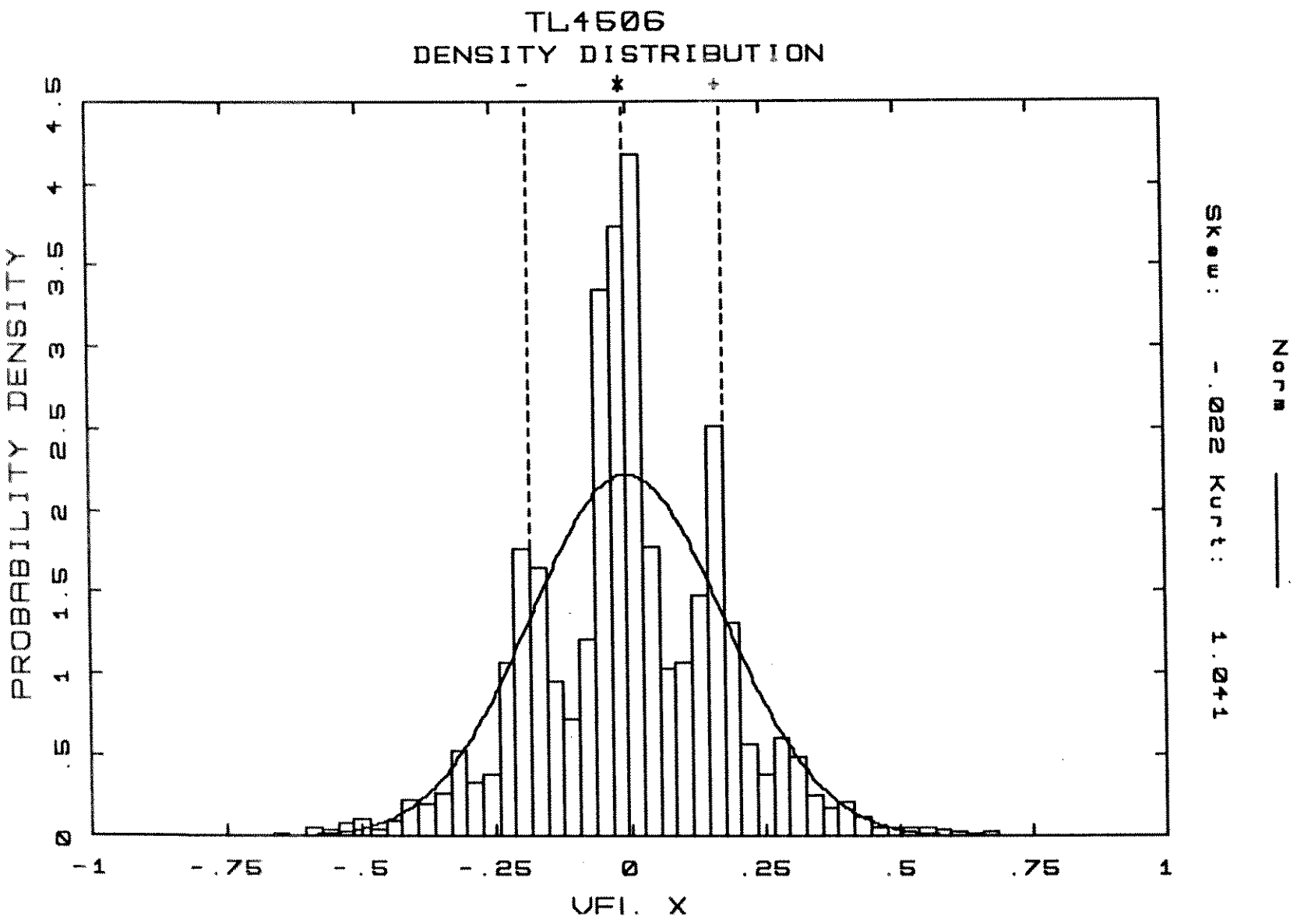
TL4506
DENSITY DISTRIBUTION
PROBABILITY DENSITY
0
.5
1
1.5
2
2.5
3
3.5
4
4.5
-1
-.75
-.5
-.25
0
.25
.5
.75
1
VFI. X
Skew: -.022 Kurt: 1.041
Norm

TL4506.VX.1

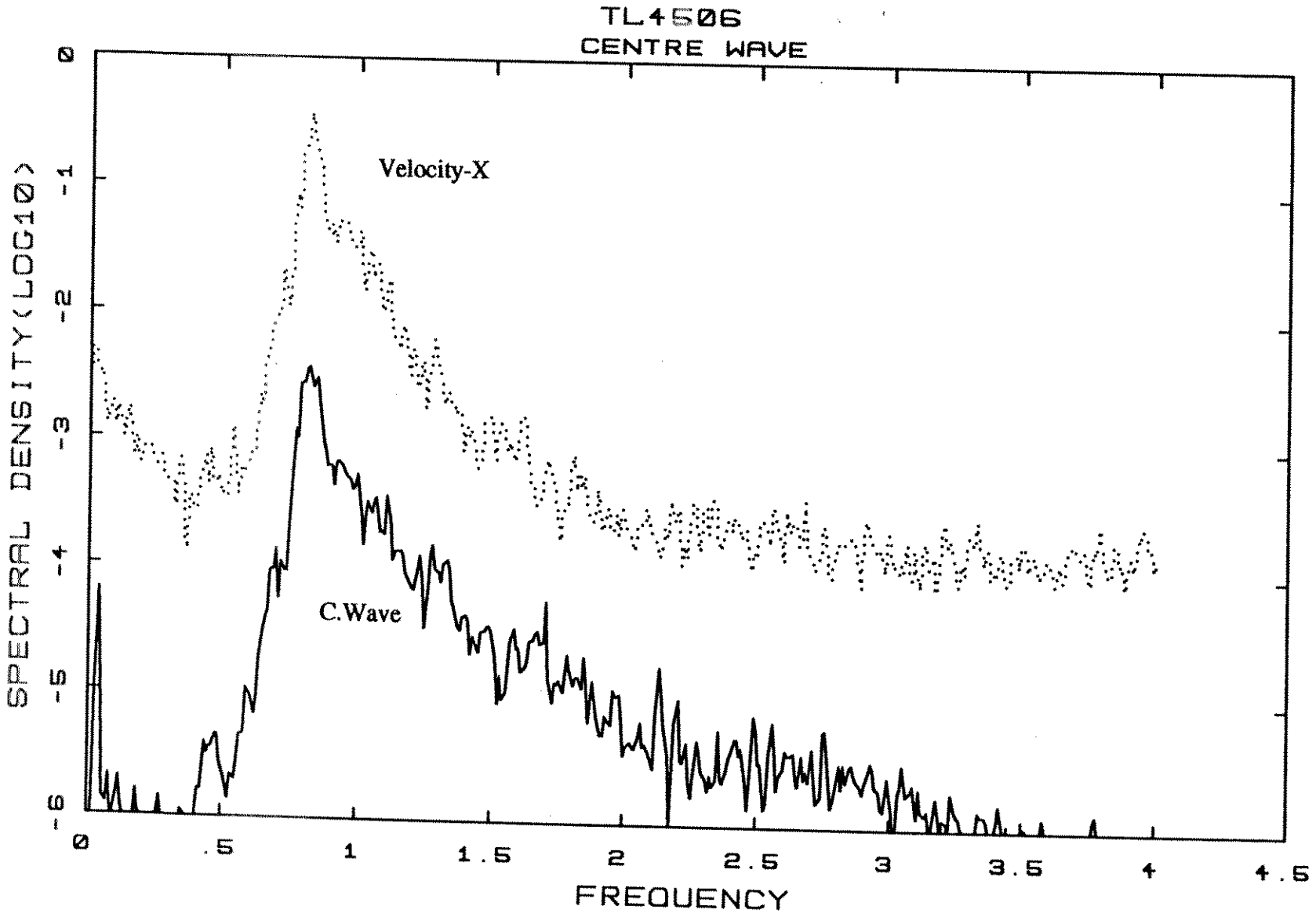
TL4506
CENTRE WAVE
SPECTRAL DENSITY(LOG10)
0
-1
-2
-3
-4
-5
-6
Velocity-X
C.Wave
0
.5
1
1.5
2
2.5
3
3.5
4
4.5
FREQUENCY

TL4506.W/VX.4

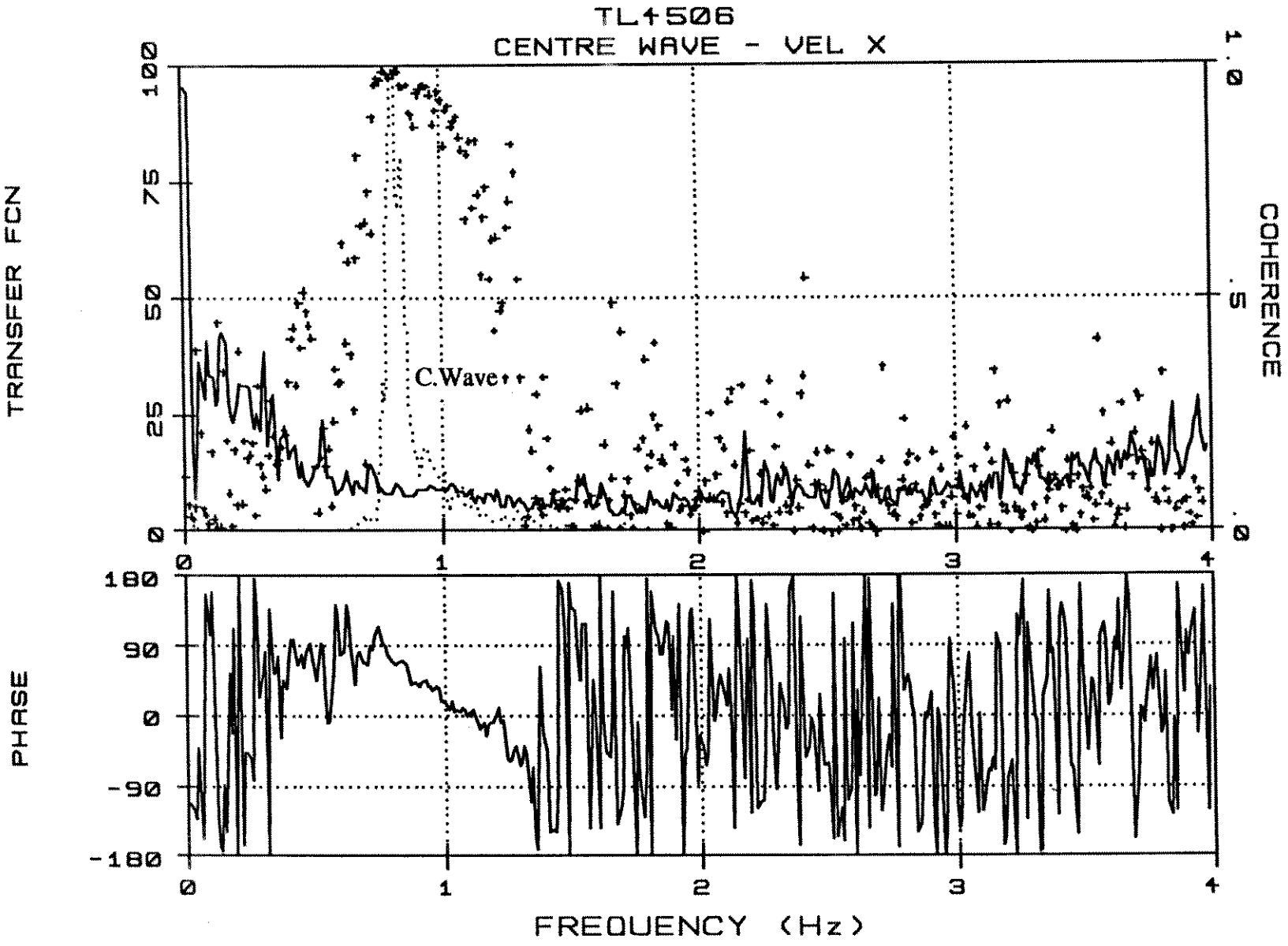

TL4506.W/VX.4t

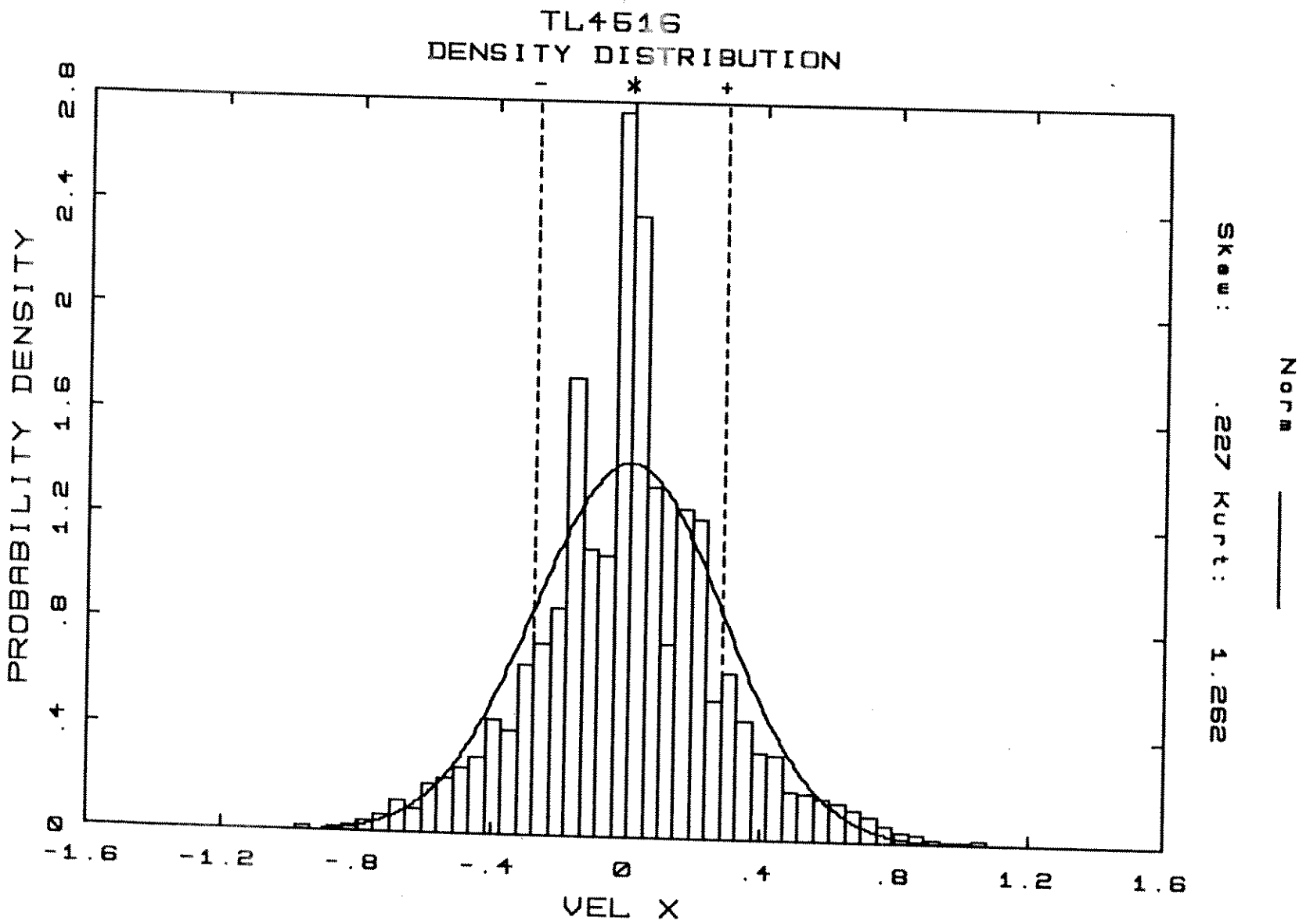
TL4516
DENSITY DISTRIBUTION
PROBABILITY DENSITY
0
.4
.8
1.2
1.6
2
2.4
2.8
-1.6
-1.2
-.8
-.4
0
.4
.8
1.2
1.6
VEL X
Skew: .227 Kurt: 1.262
Norm

TL4516.VX.1

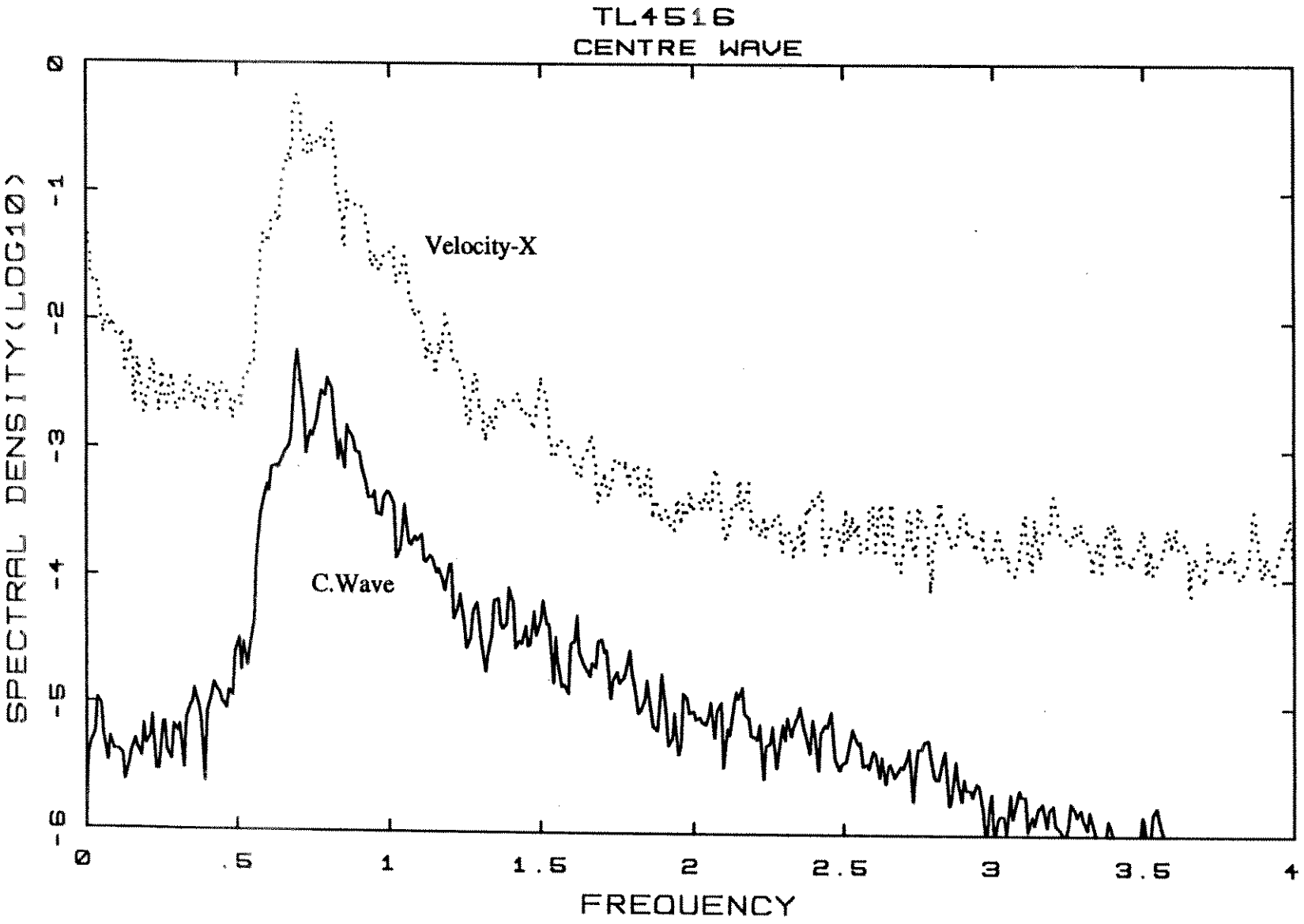
TL4516
CENTRE WAVE
SPECTRAL DENSITY(LOG10)
0
-1
-2
-3
-4
-5
-6
Velocity-X
C.Wave
0
.5
1
1.5
2
2.5
3
3.5
4
FREQUENCY

TL4516.W/VX.4

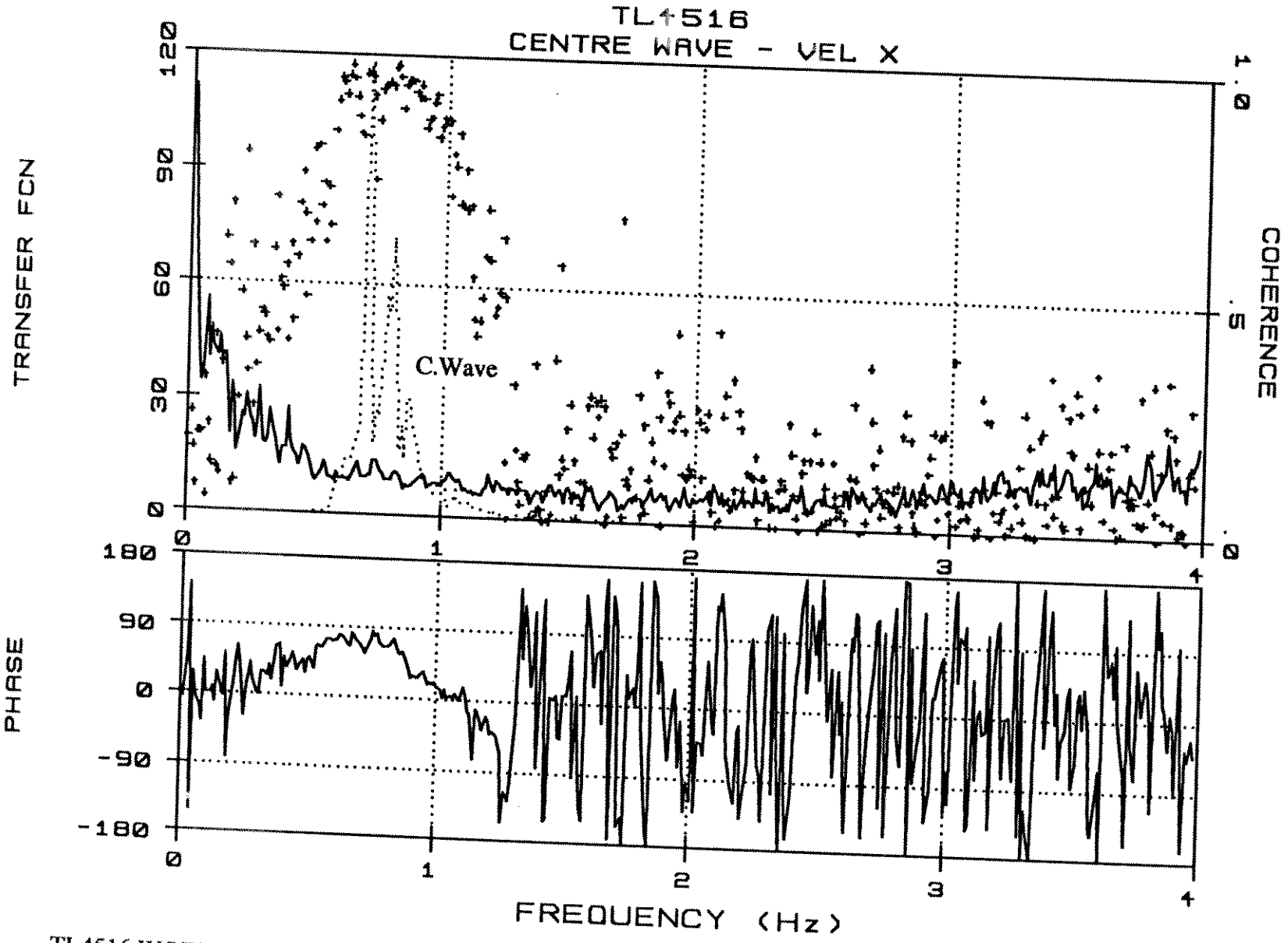

TL4516.W/VX.4t

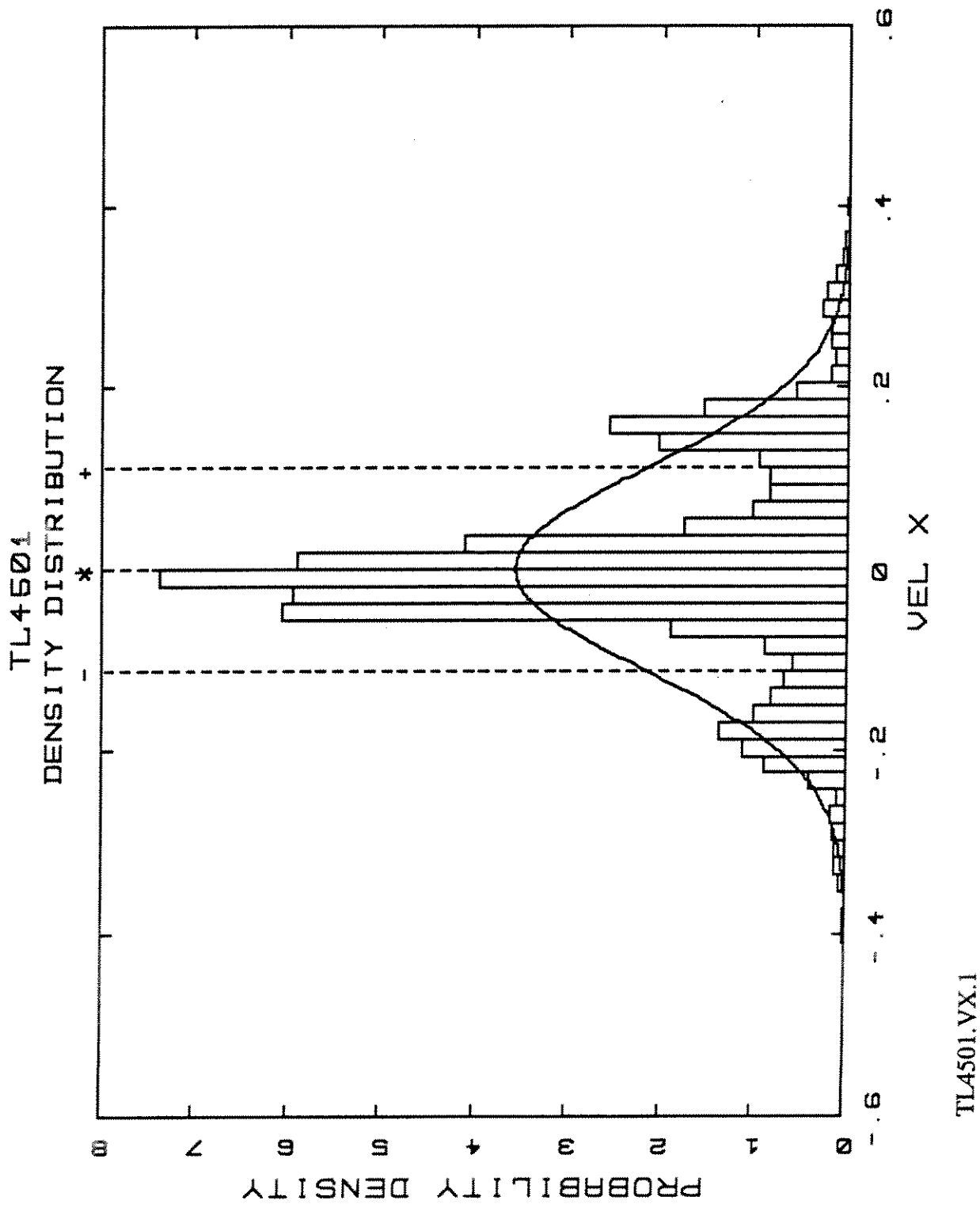
Norm
Skew: .117 Kurt: 1.100
TL4501
DENSITY DISTRIBUTION
PROBABILITY DENSITY
VEL X
TL4501.VX.1

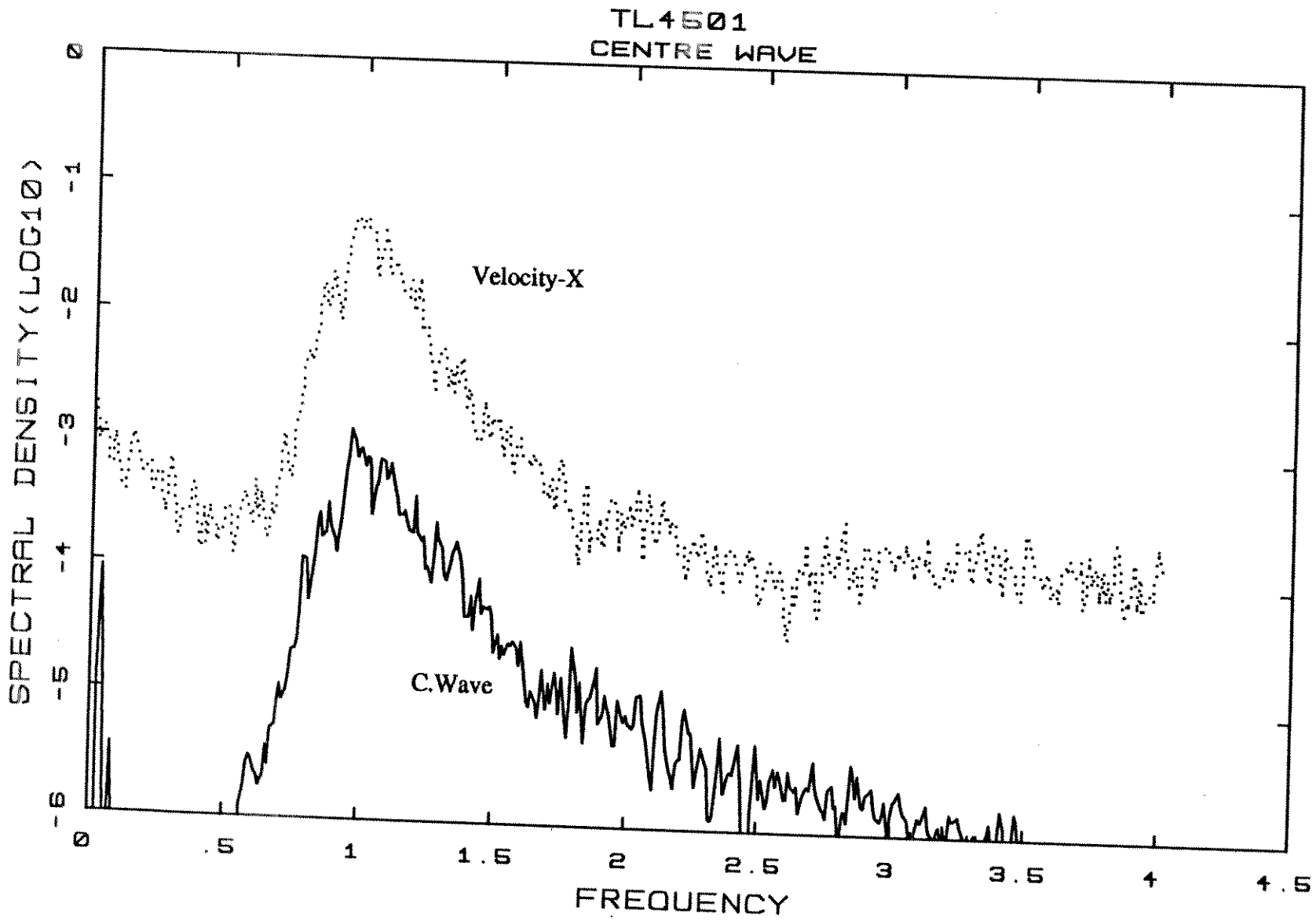
TL4501
CENTRE WAVE
SPECTRAL DENSITY(LOG10)
0
-1
-2
-3
-4
-5
-6
Velocity-X
C.Wave
0
.5
1
1.5
2
2.5
3
3.5
4
4.5
FREQUENCY

TL4501.W/VX.4

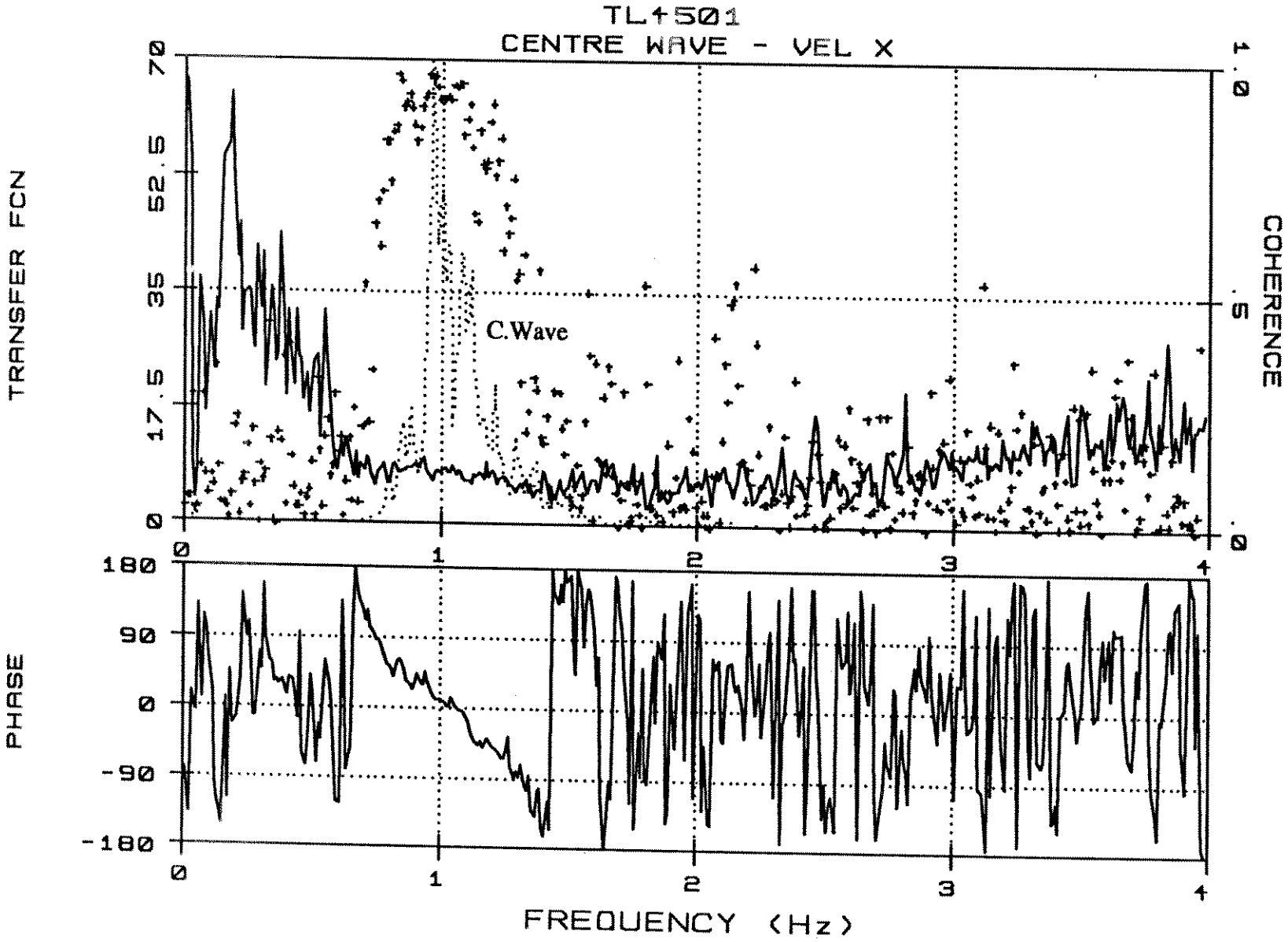

TL4501.W/VX.4t

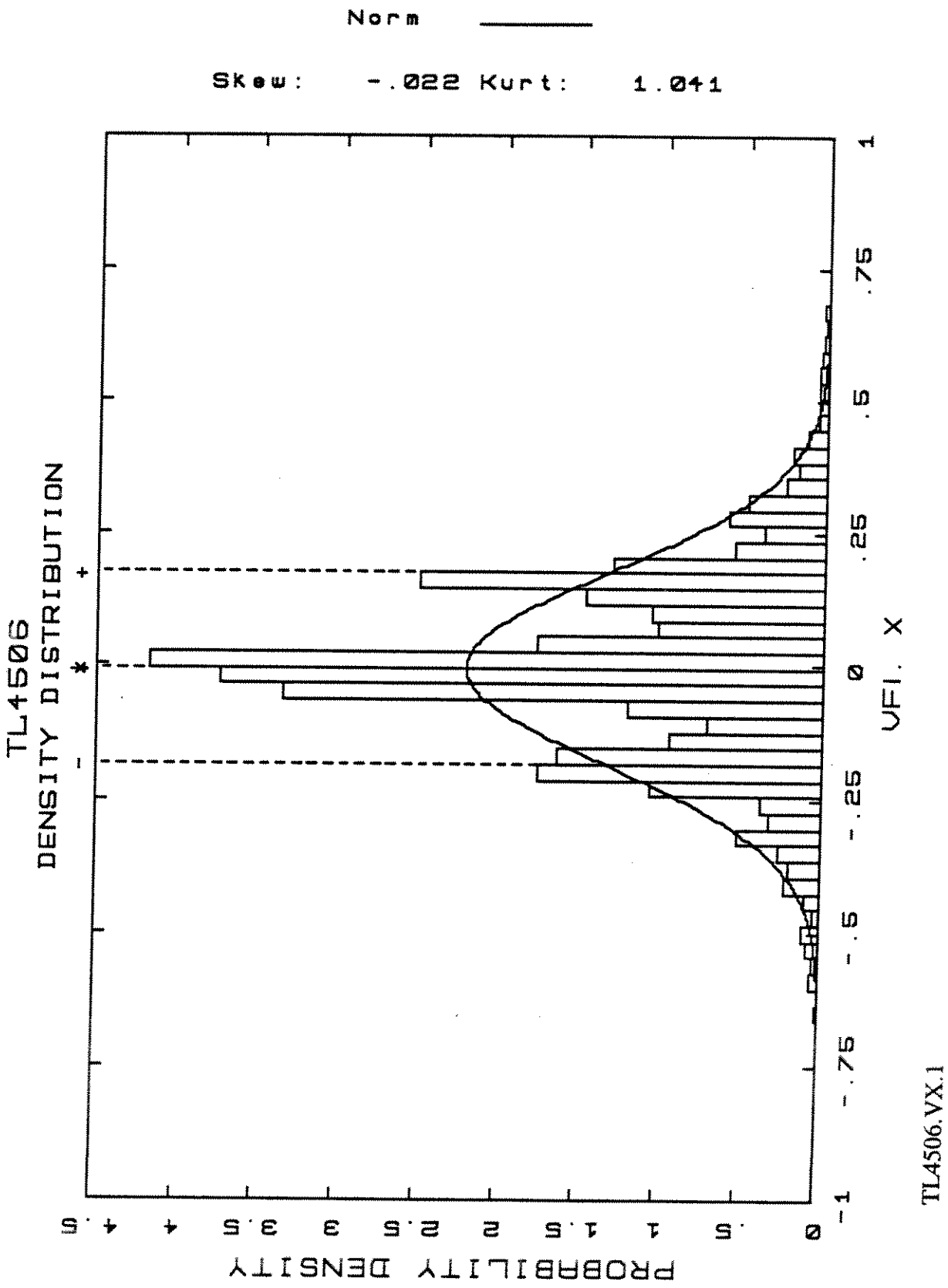
Norm
Skew: -.022 Kurt: 1.041
TL4506
DENSITY DISTRIBUTION
+
*
-
PROBABILITY DENSITY
0 .5 1 1.5 2 2.5 3 3.5 4 4.5
-1 -.75 -.5 -.25 0 .25 .5 .75 1
VFI. X
TL4506.VX.1

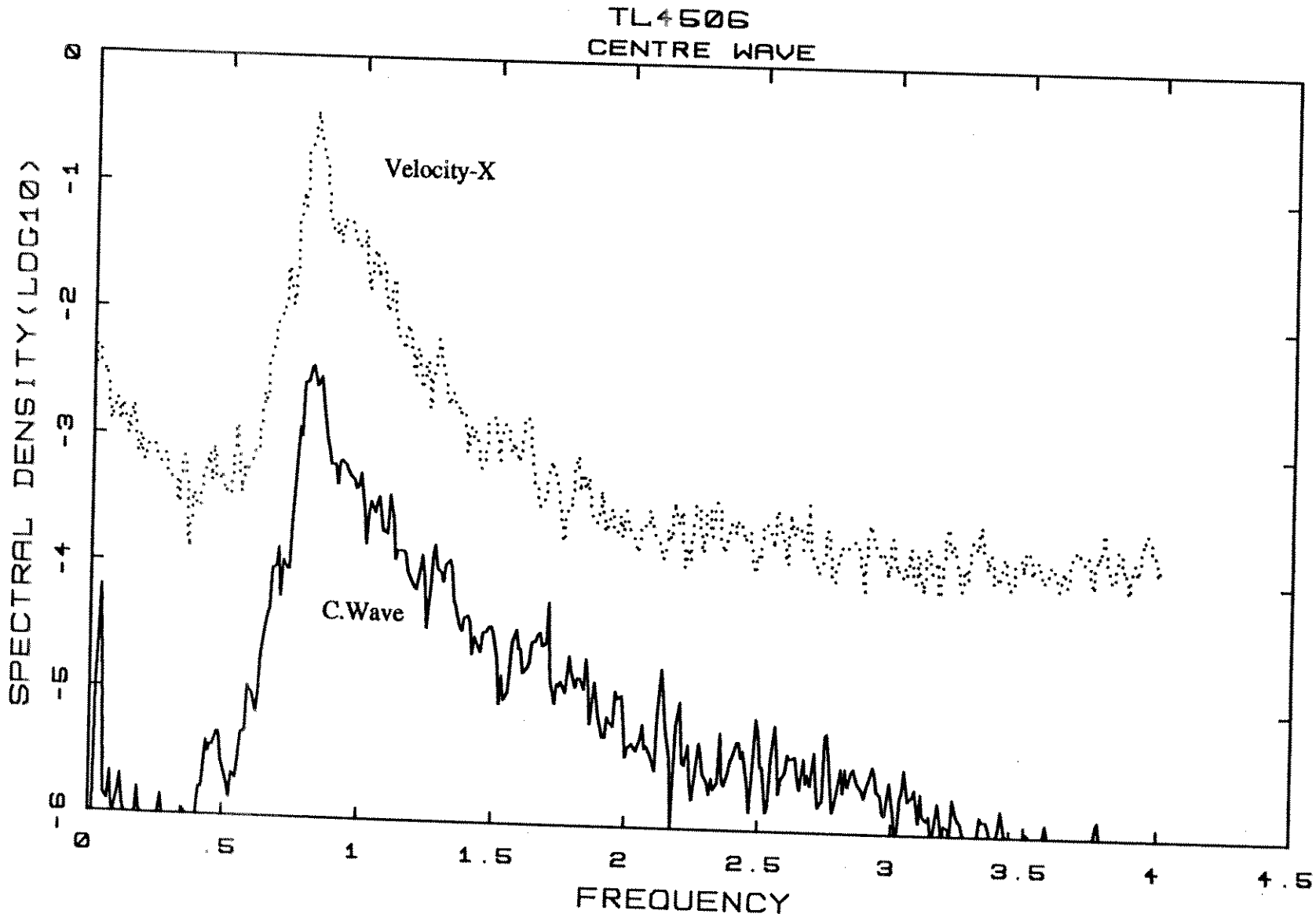
TL4506
CENTRE WAVE
Velocity-X
C.Wave
SPECTRAL DENSITY(LOG10)
0
-1
-2
-3
-4
-5
-6
0
.5
1
1.5
2
2.5
3
3.5
4
4.5
FREQUENCY

TL4506.W/VX.4

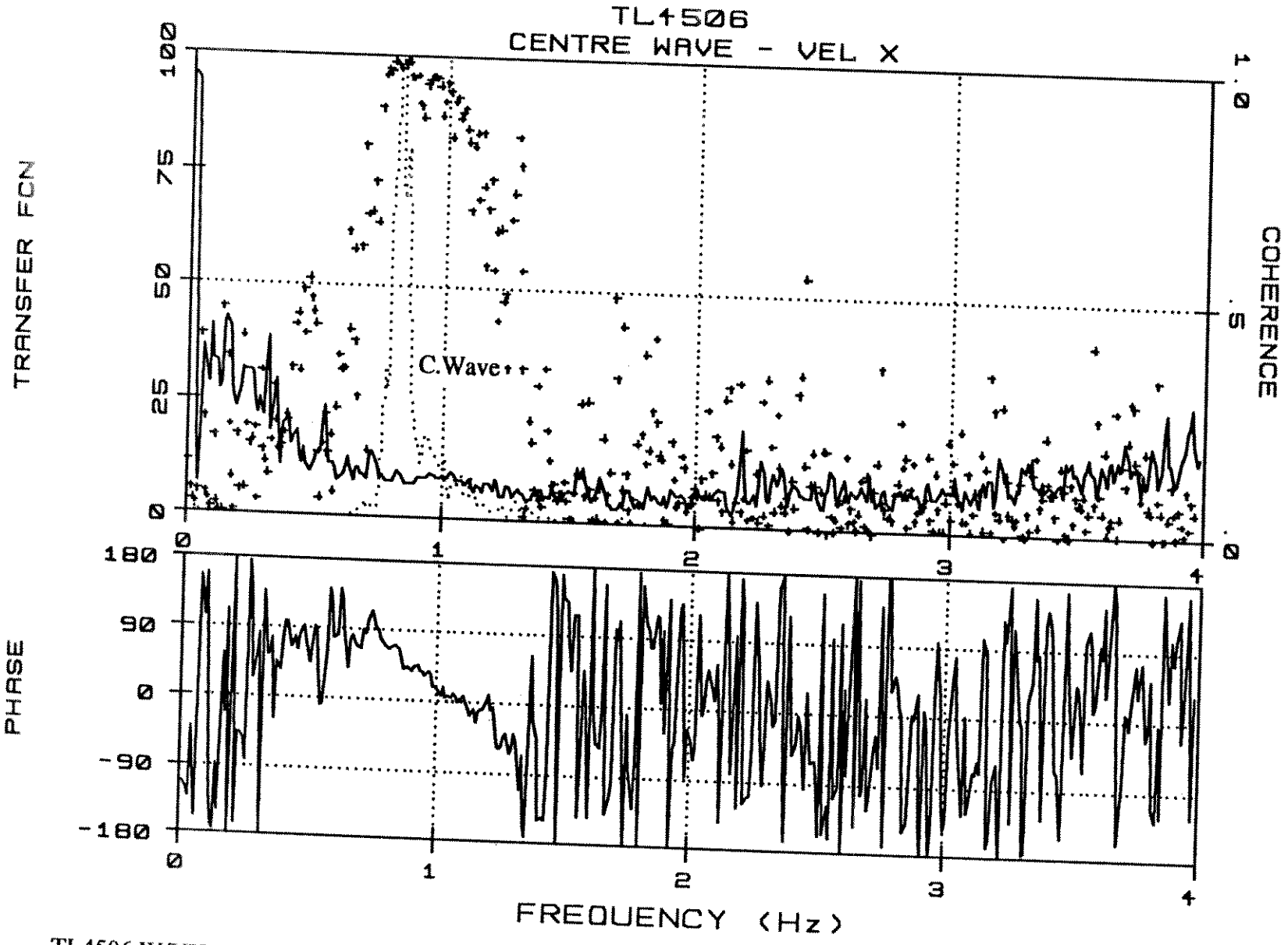

TL4506.W/VX.4t

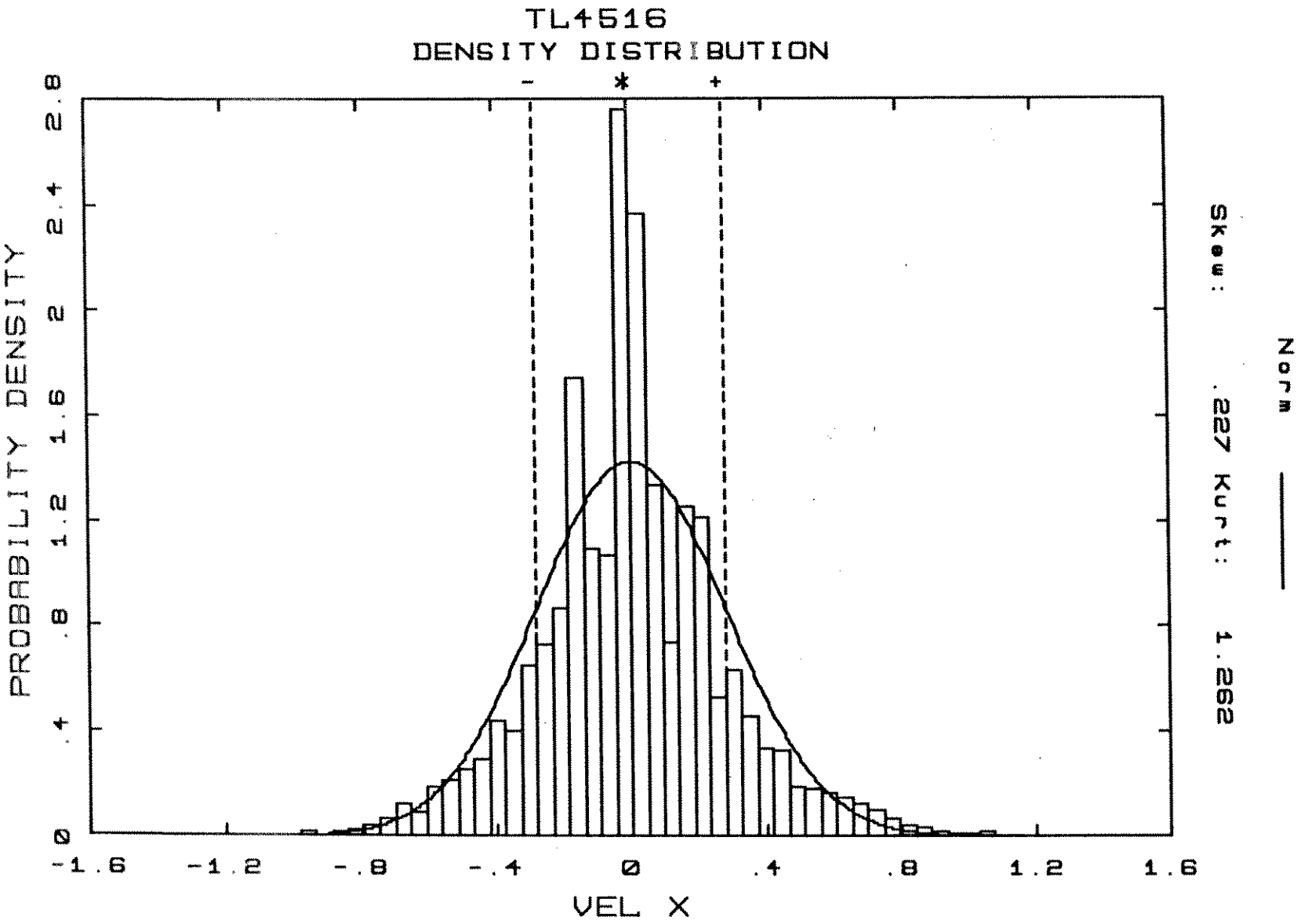
TL4516
DENSITY DISTRIBUTION
- * +
PROBABILITY DENSITY
0
.4
.8
1.2
1.6
2
2.4
2.8
-1.6
-1.2
-.8
-.4
0
.4
.8
1.2
1.6
VEL X
Skew: .227 Kurt: 1.262
Norm

TL4516.VX.1

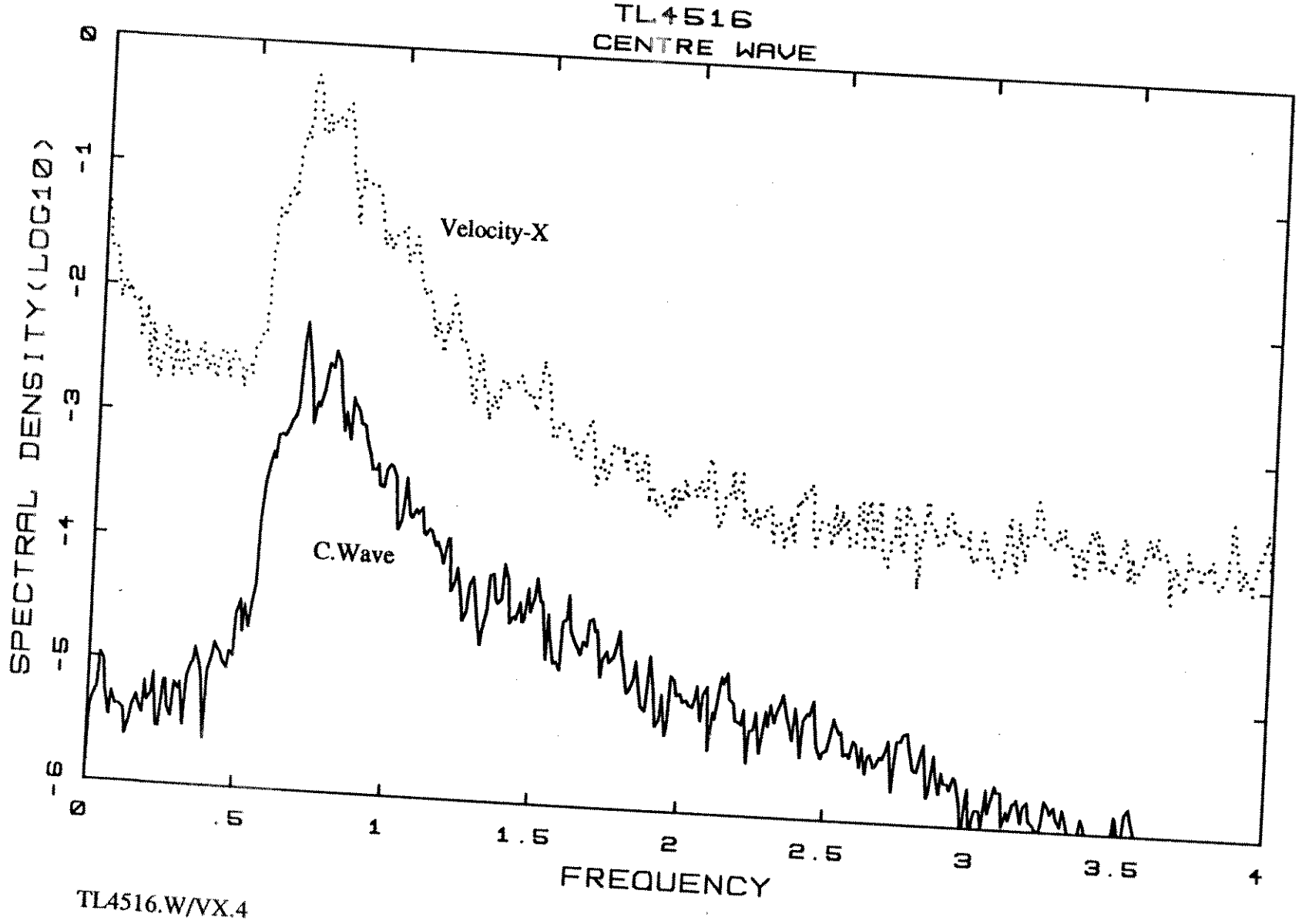
TL4516
CENTRE WAVE
SPECTRAL DENSITY(LOG10)
0
-1
-2
-3
-4
-5
-6
Velocity-X
C.Wave
0
.5
1
1.5
2
2.5
3
3.5
4
FREQUENCY

TL4516.W/VX.4

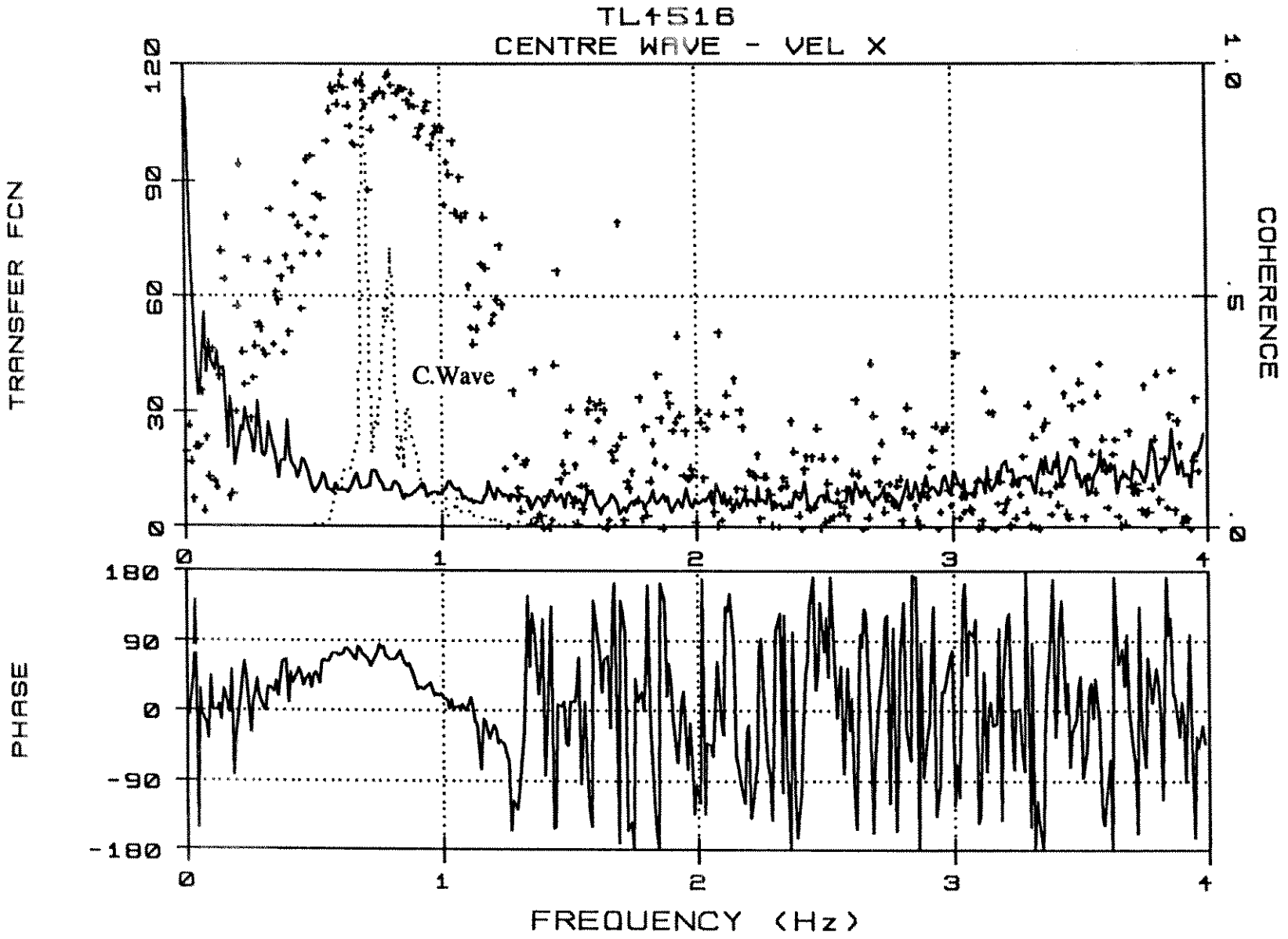

TL4516.W/VX.4t

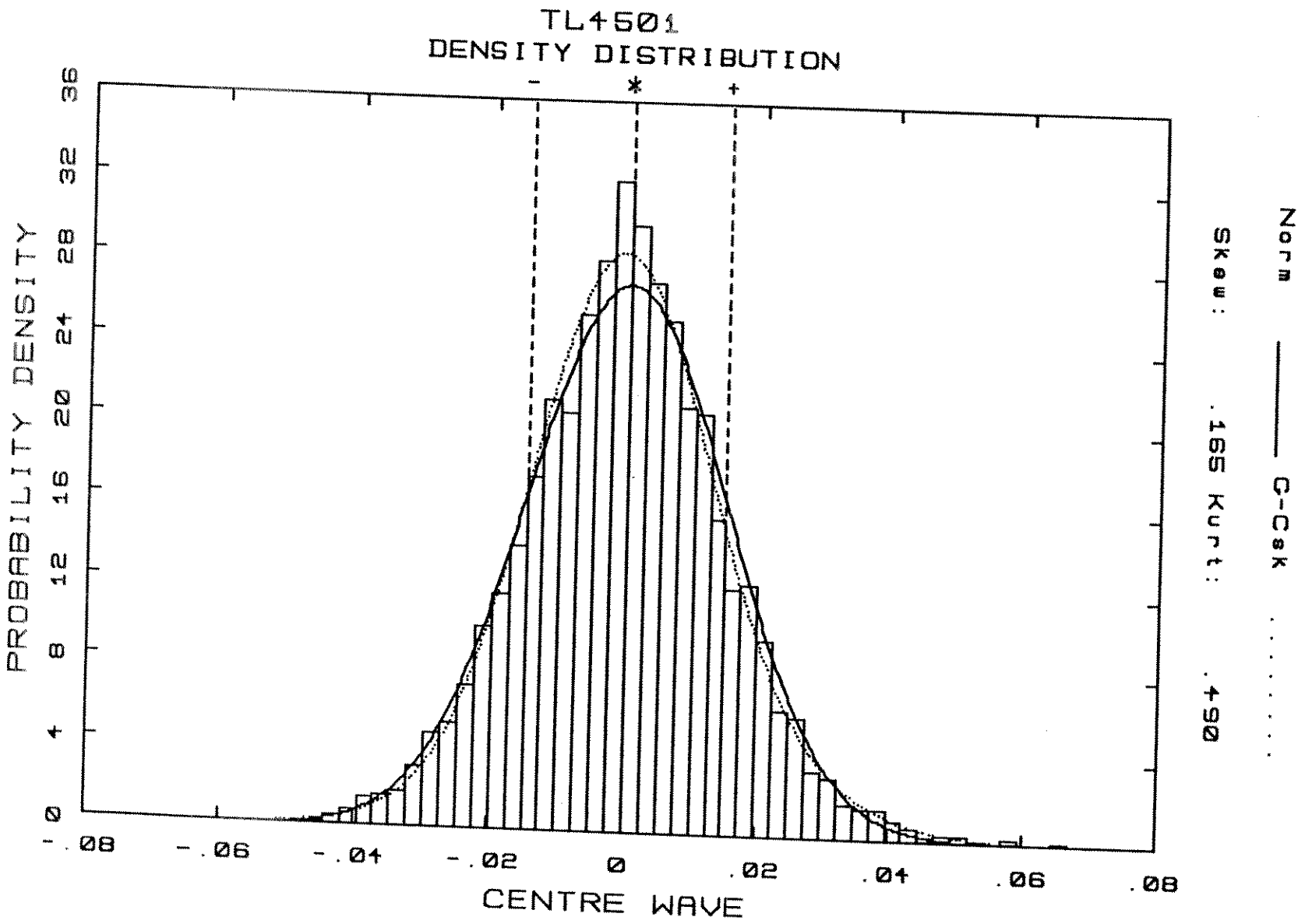
TL4501
DENSITY DISTRIBUTION
PROBABILITY DENSITY
0
4
8
12
16
20
24
28
32
36
-.08
-.06
-.04
-.02
0
.02
.04
.06
.08
CENTRE WAVE
Norm
C-Csk
Skew: .165 Kurt: .490

TL4501.W.1

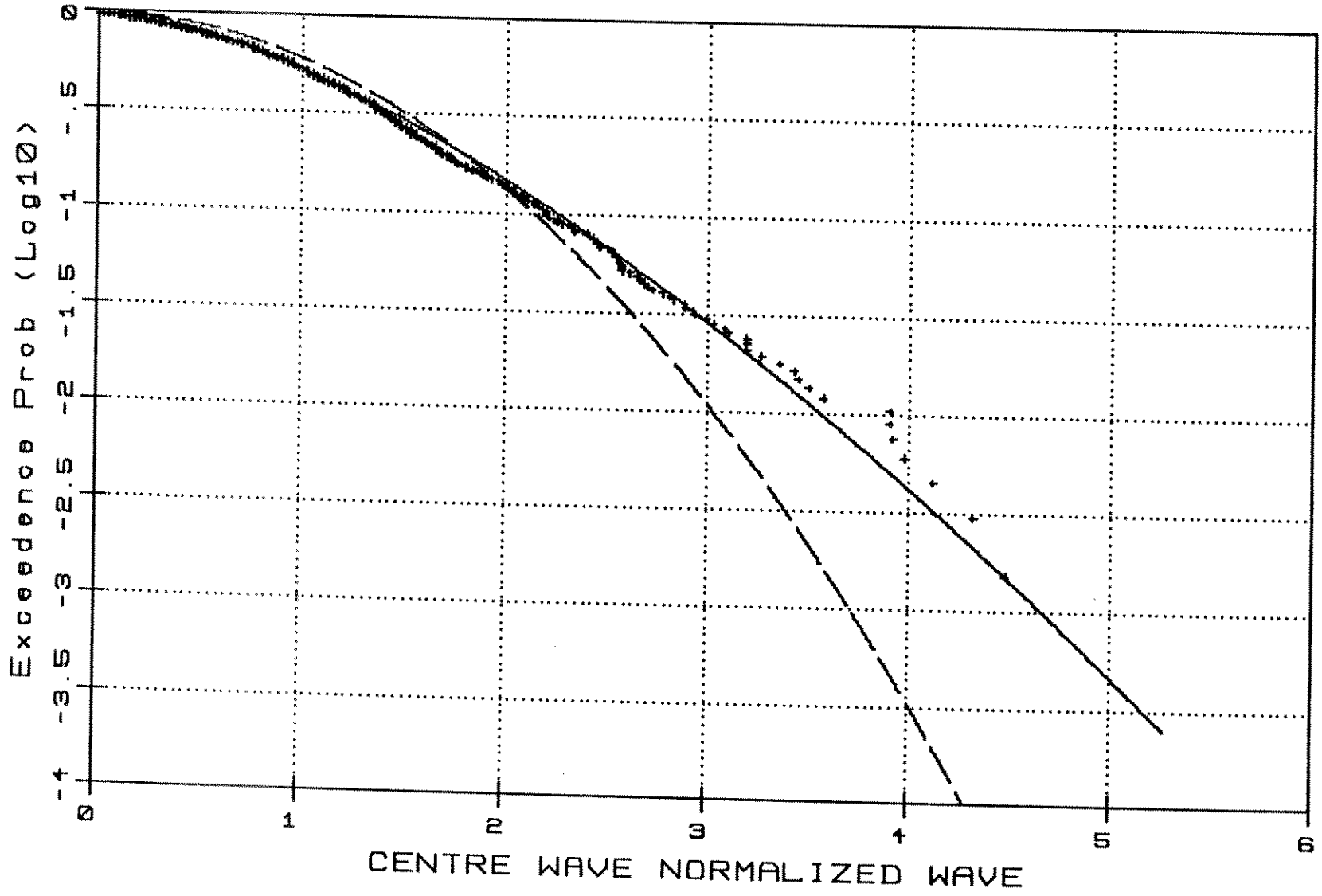
TL4501 -Weibull Type III/Rayleigh
Exceedence Prob (Log10)
0
-.5
-1
-1.5
-2
-2.5
-3
-3.5
-4
0
1
2
3
4
5
6
CENTRE WAVE NORMALIZED WAVE

TL4501.W.2

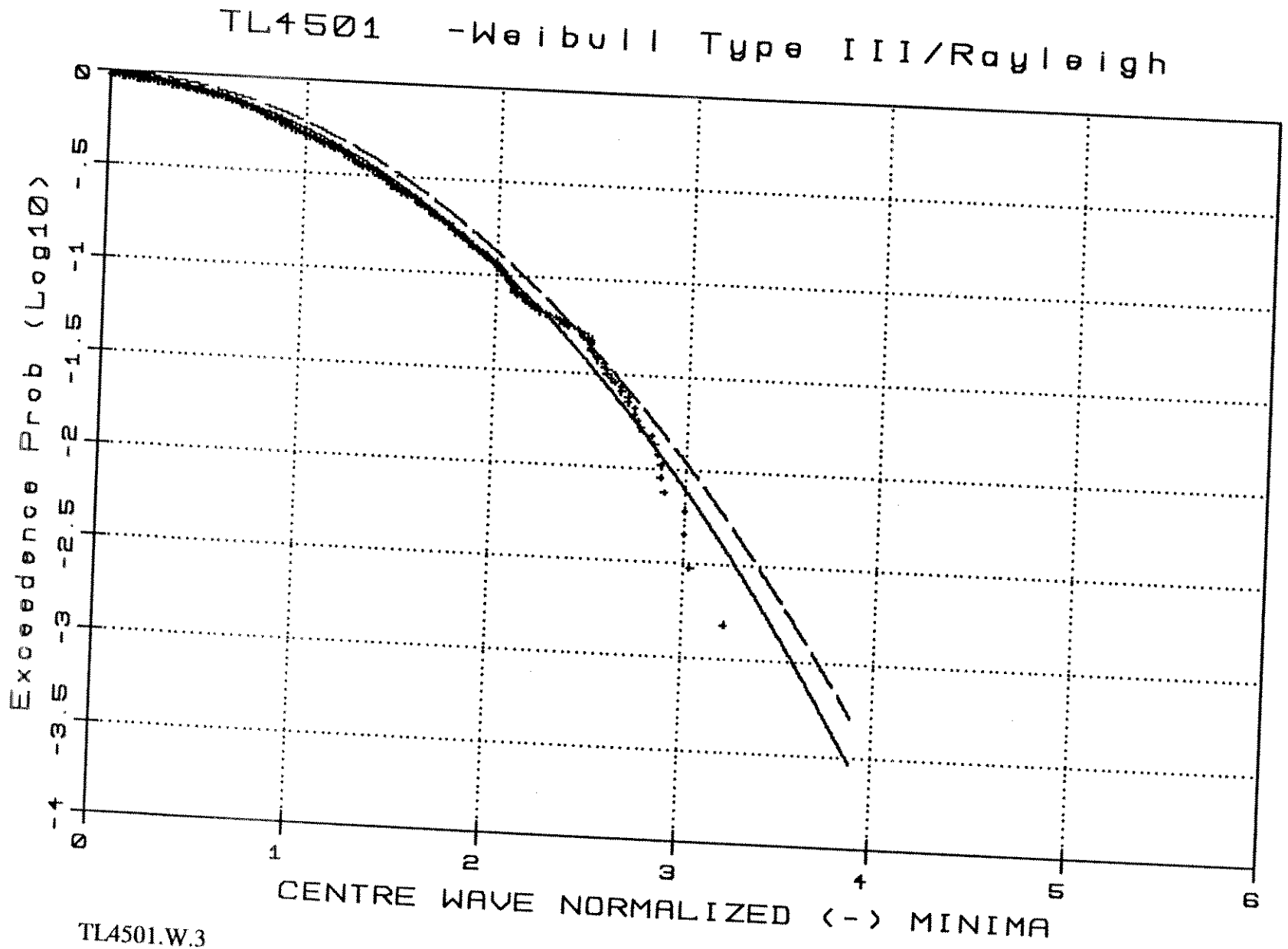
TL4501 -Weibull Type III/Rayleigh
Exceedence Prob (Log10)
0
-.5
-1
-1.5
-2
-2.5
-3
-3.5
-4
0
1
2
3
4
5
6
CENTRE WAVE NORMALIZED (-) MINIMA

TL4501.W.3

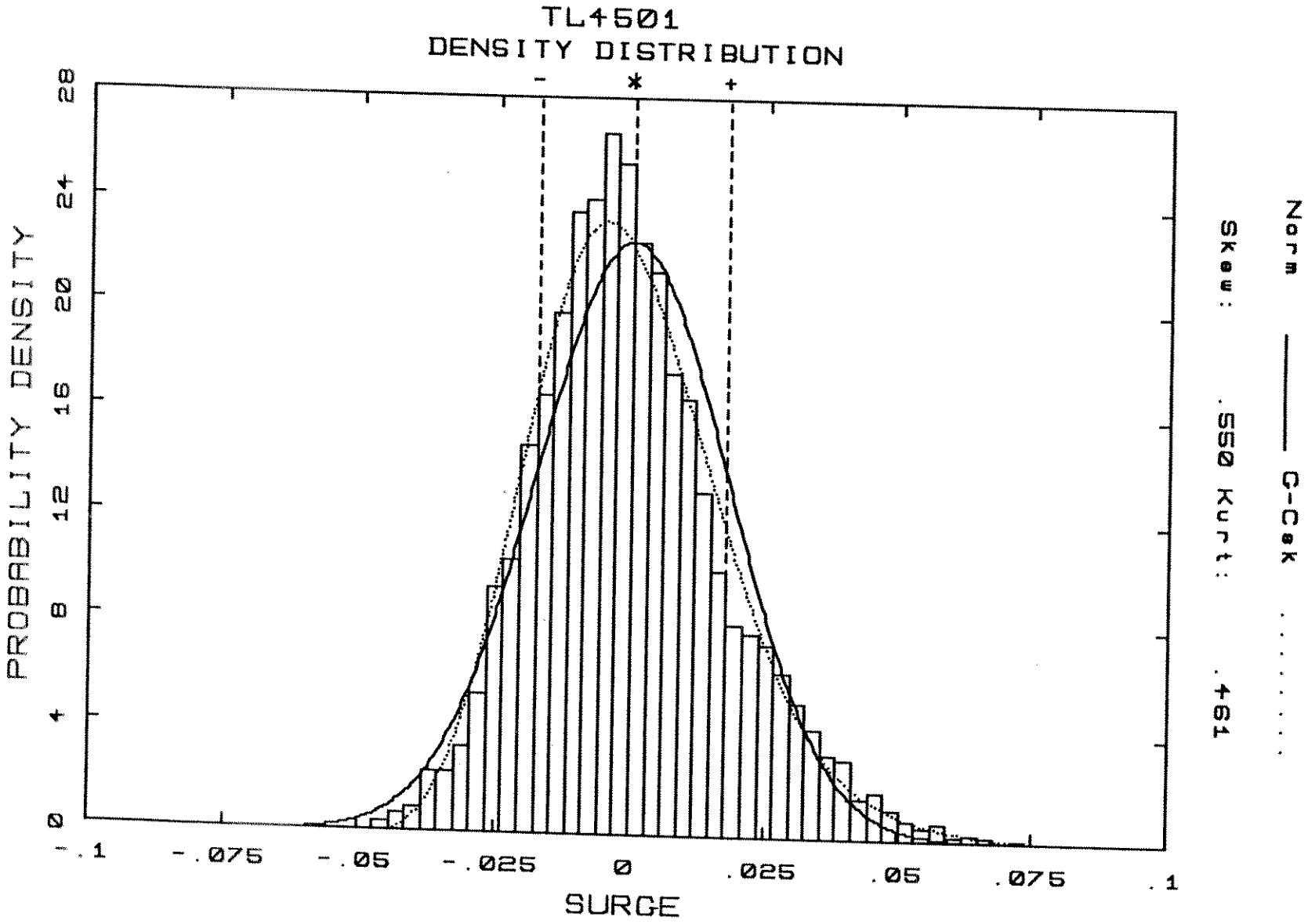
TL4501
DENSITY DISTRIBUTION
- * +
PROBABILITY DENSITY
0
4
8
12
16
20
24
28
-.1
-.075
-.05
-.025
0
.025
.05
.075
.1
SURGE
Norm
C-Cek
Skew: .550 Kurt: .461

TL4501.S.1

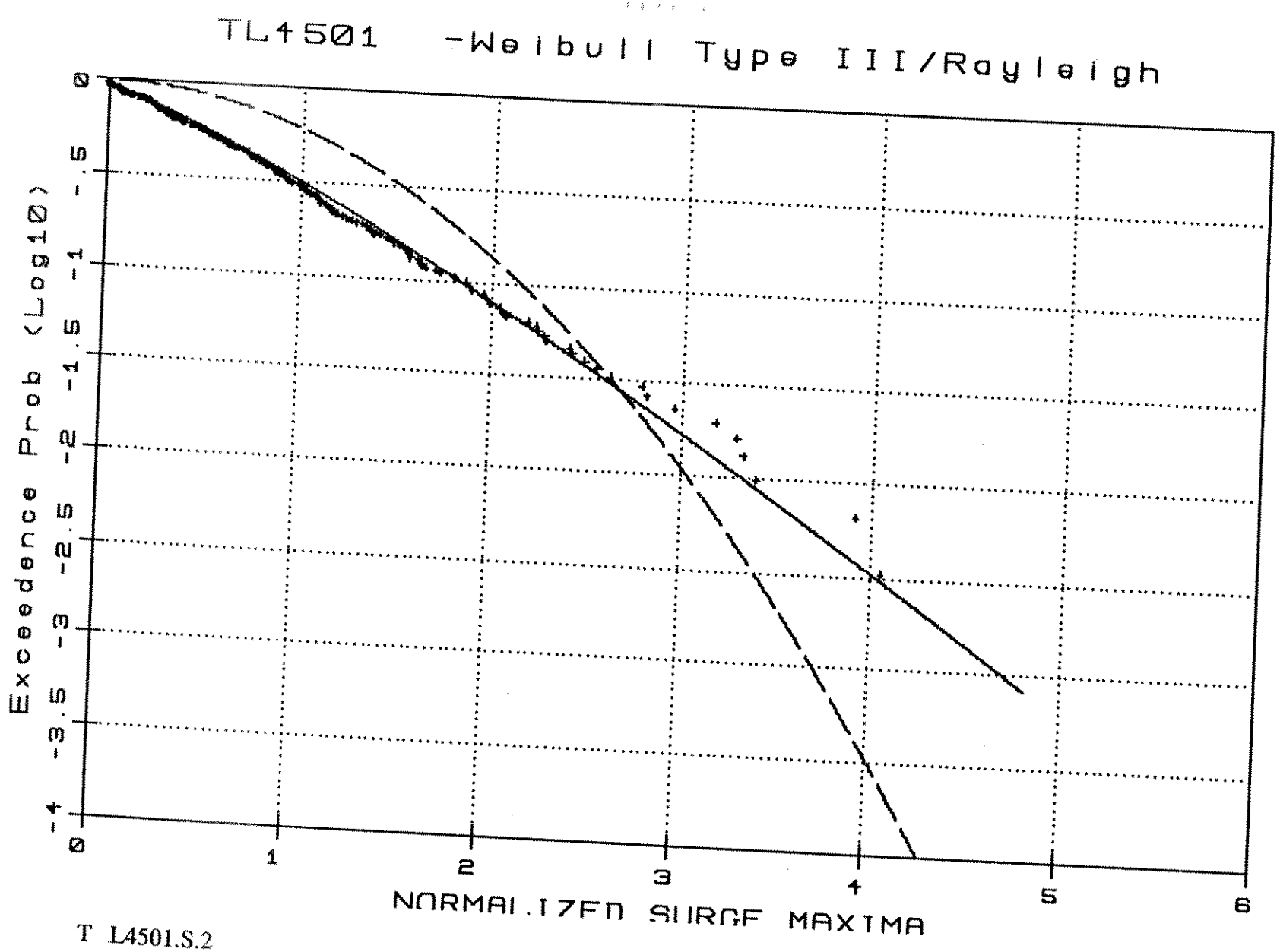
TL4501 -Weibull Type III/Rayleigh
Exceedence Prob (Log10)
0
-.5
-1
-1.5
-2
-2.5
-3
-3.5
-4
0
1
2
3
4
5
6
NORMALIZED SURGE MAXIMA

T L4501.S.2

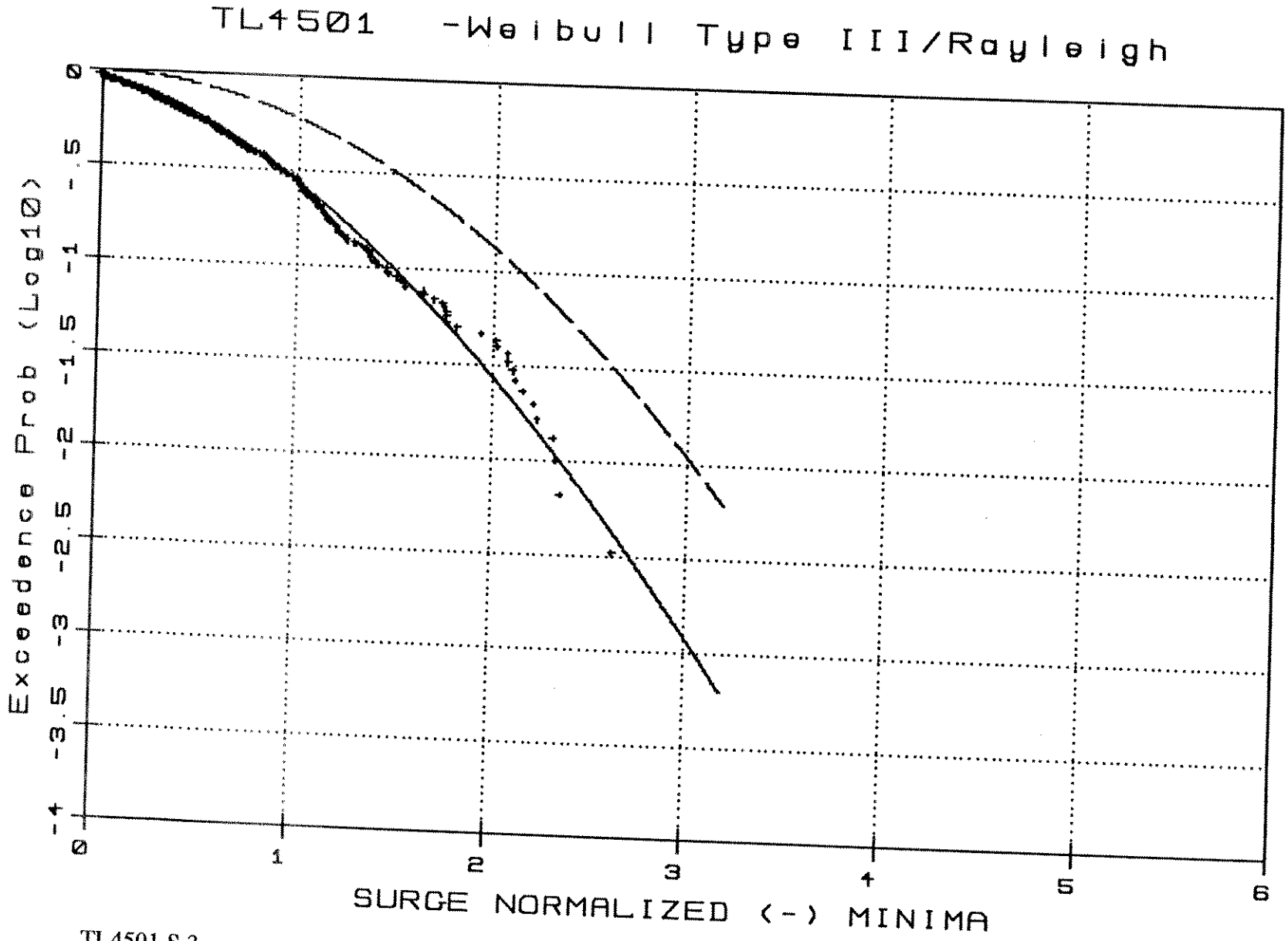
TL4501 -Weibull Type III/Rayleigh
Exceedence Prob (Log10)
0
-.5
-1
-1.5
-2
-2.5
-3
-3.5
-4
0
1
2
3
4
5
6
SURGE NORMALIZED (-) MINIMA

TL4501.S.3

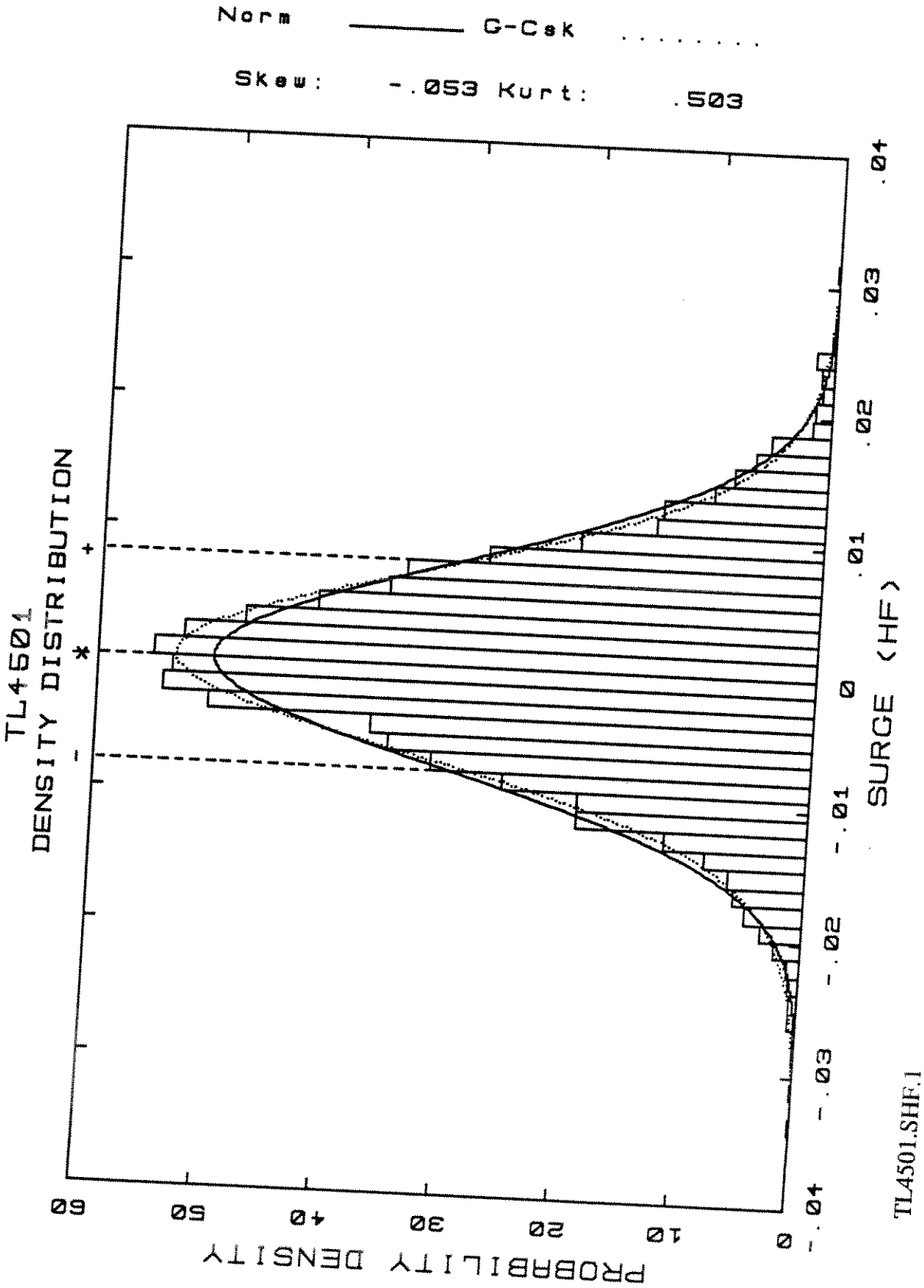
Norm ——— G-Csk .....
Skew: -.053 Kurt: .503
TL4501
DENSITY DISTRIBUTION
+
*
-
PROBABILITY DENSITY
0
10
20
30
40
50
60
-.04
-.03
-.02
-.01
0
.01
.02
.03
.04
SURGE (HF)
TL4501.SHF.1

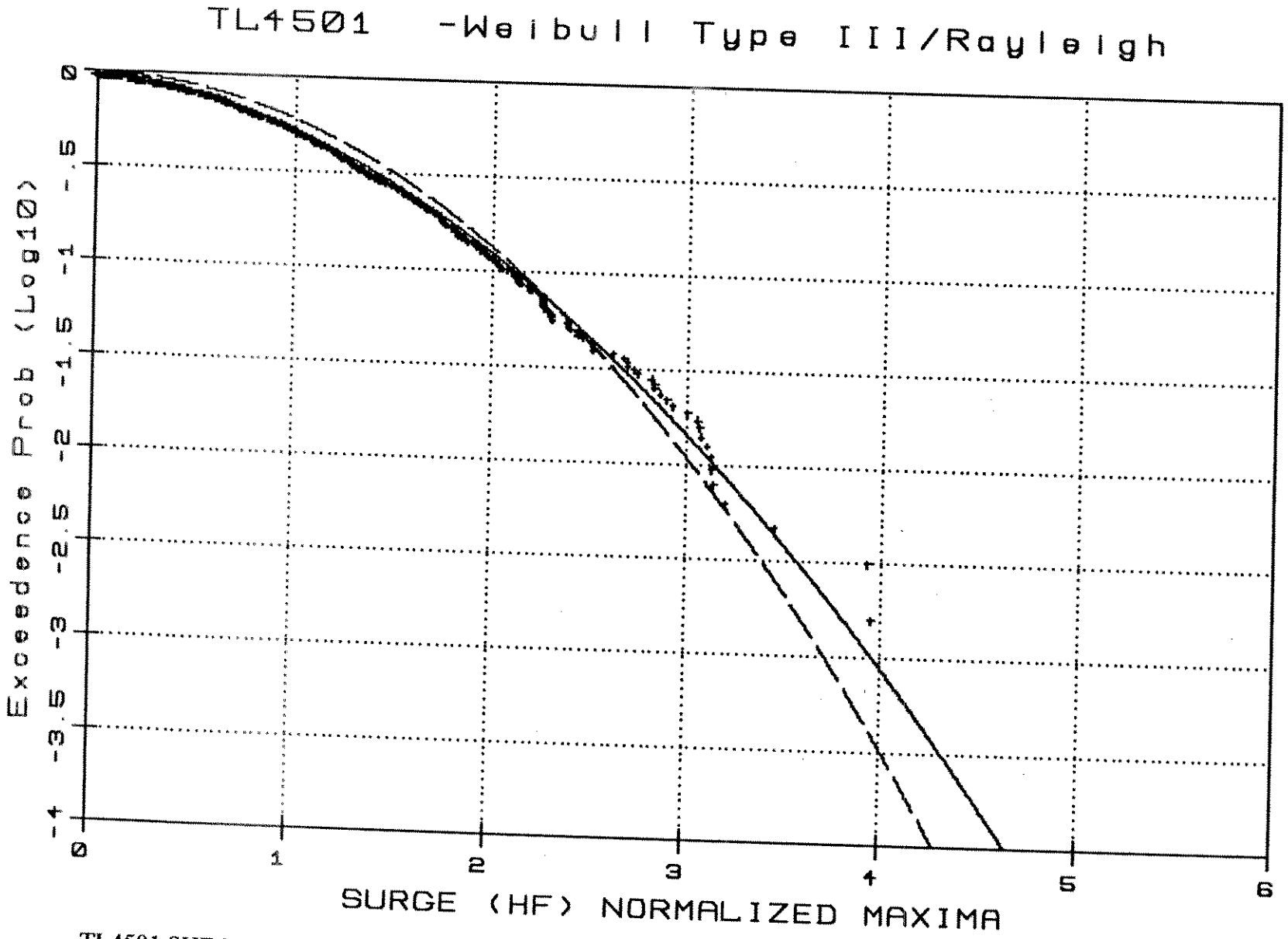
TL4501 -Weibull Type III/Rayleigh
Exceedence Prob (Log10)
0
-.5
-1
-1.5
-2
-2.5
-3
-3.5
-4
0
1
2
3
4
5
6
SURGE (HF) NORMALIZED MAXIMA

TL4501.SHF.2

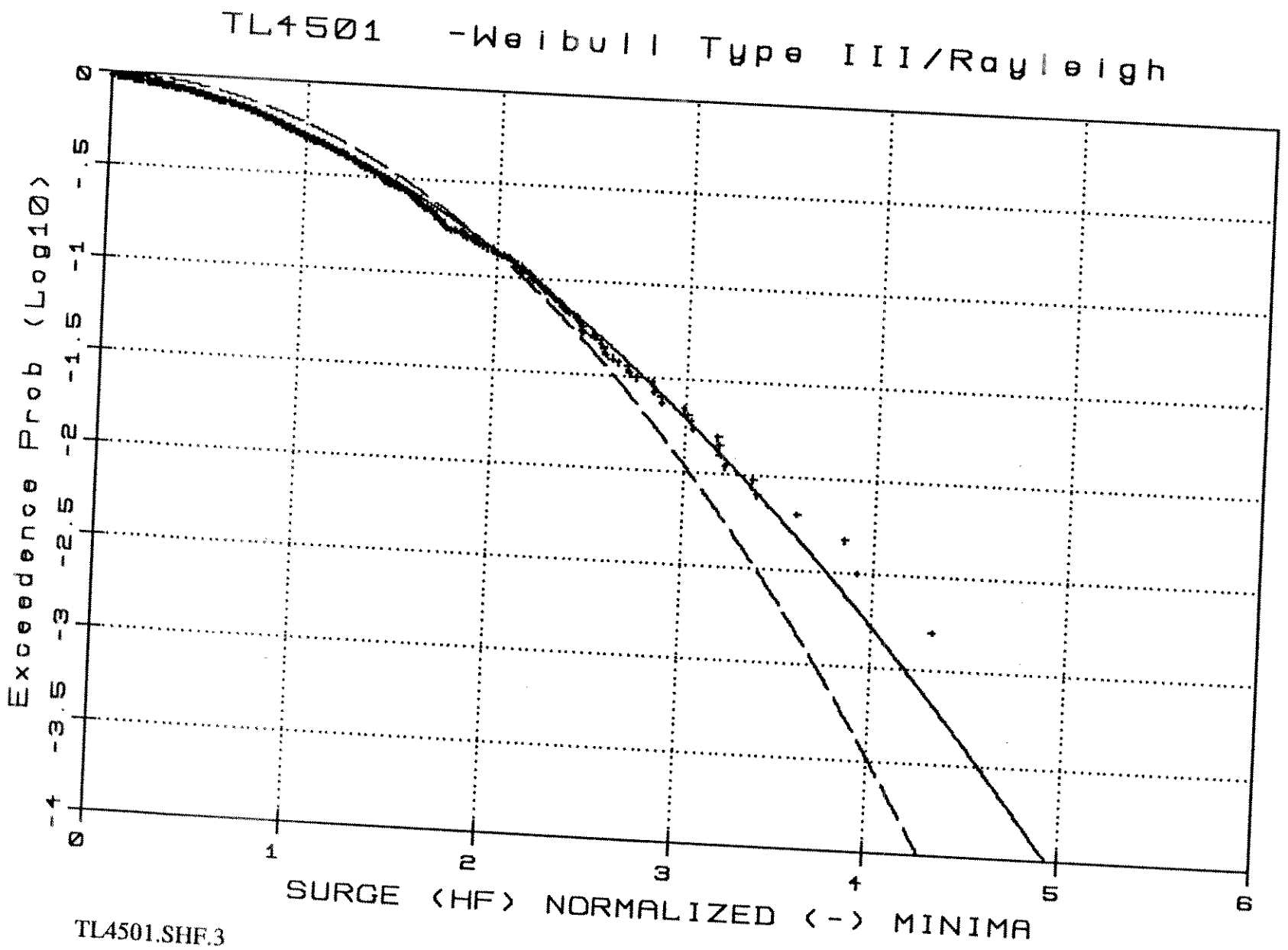
TL4501 -Weibull Type III/Rayleigh
Exceedence Prob (Log10)
0
-.5
-1
-1.5
-2
-2.5
-3
-3.5
-4
0
1
2
3
4
5
6
SURGE (HF) NORMALIZED (-) MINIMA

TL4501.SHF.3

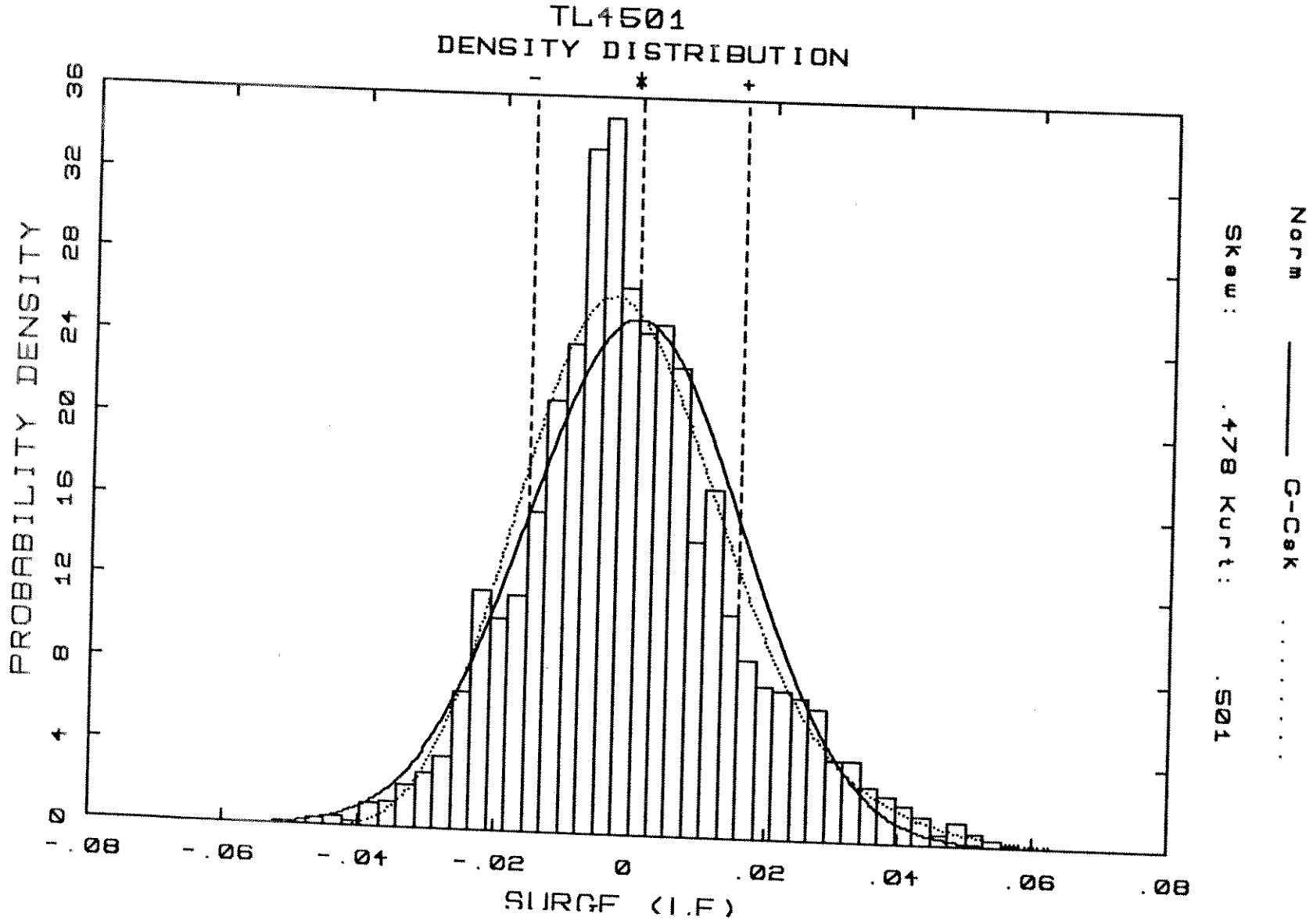
TL4501
DENSITY DISTRIBUTION
PROBABILITY DENSITY
0
4
8
12
16
20
24
28
32
36
-.08
-.06
-.04
-.02
0
.02
.04
.06
.08
SURGE (I.F)
Norm
C-Cek
Skew: .478 Kurt: .501

TL4501.SLF.1

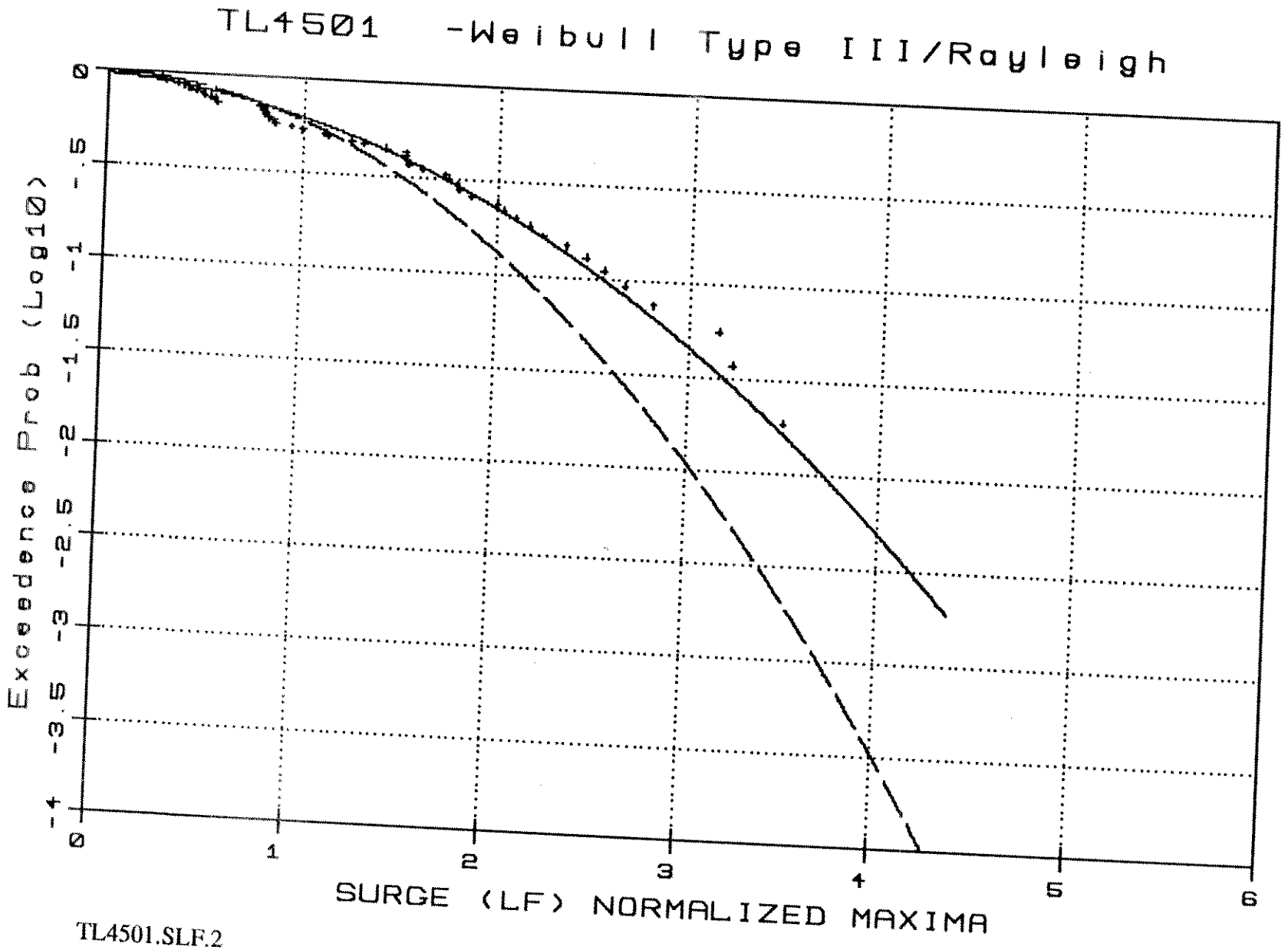
TL4501 -Weibull Type III/Rayleigh
Exceedence Prob (Log10)
0
-.5
-1
-1.5
-2
-2.5
-3
-3.5
-4
0
1
2
3
4
5
6
SURGE (LF) NORMALIZED MAXIMA

TL4501.SLF.2

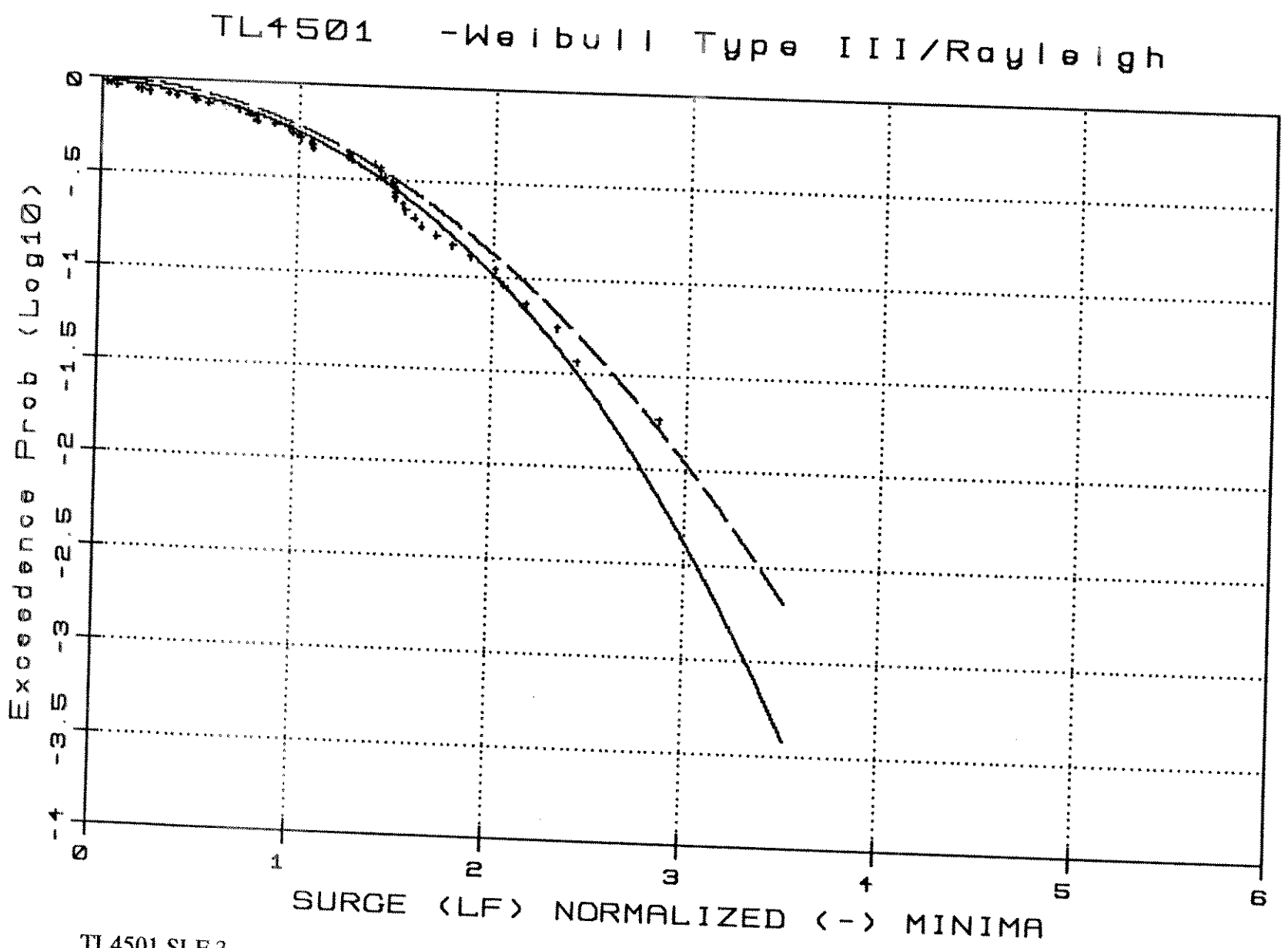
TL4501 -Weibull Type III/Rayleigh
Exceedence Prob (Log10)
0
-.5
-1
-1.5
-2
-2.5
-3
-3.5
-4
0
1
2
3
4
5
6
SURGE (LF) NORMALIZED (-) MINIMA

TL4501.SLF.3

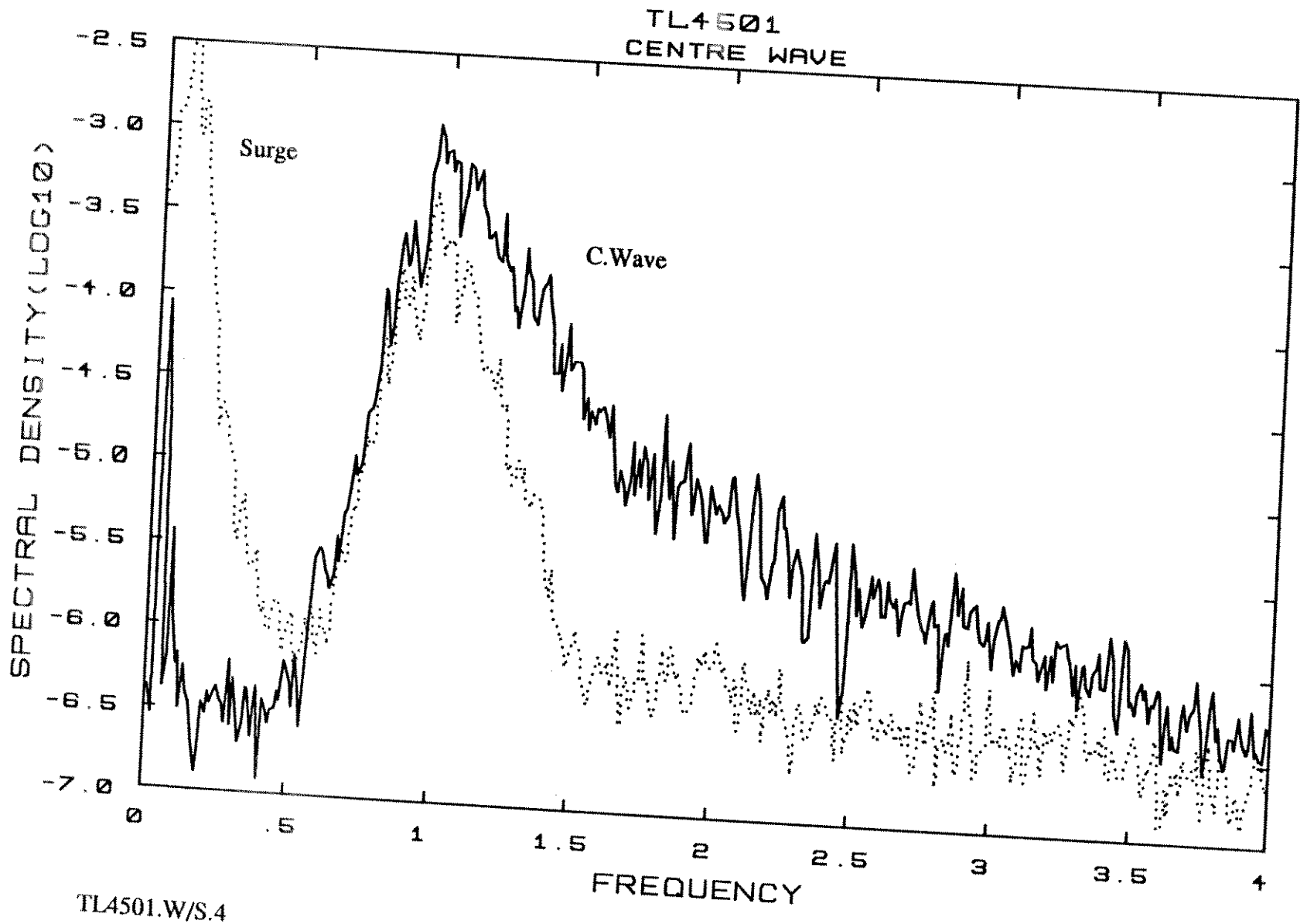
TL4501
CENTRE WAVE
Surge
C.Wave
SPECTRAL DENSITY(LOG10)
-2.5
-3.0
-3.5
-4.0
-4.5
-5.0
-5.5
-6.0
-6.5
-7.0
0
.5
1
1.5
2
2.5
3
3.5
4
FREQUENCY

TL4501.W/S.4

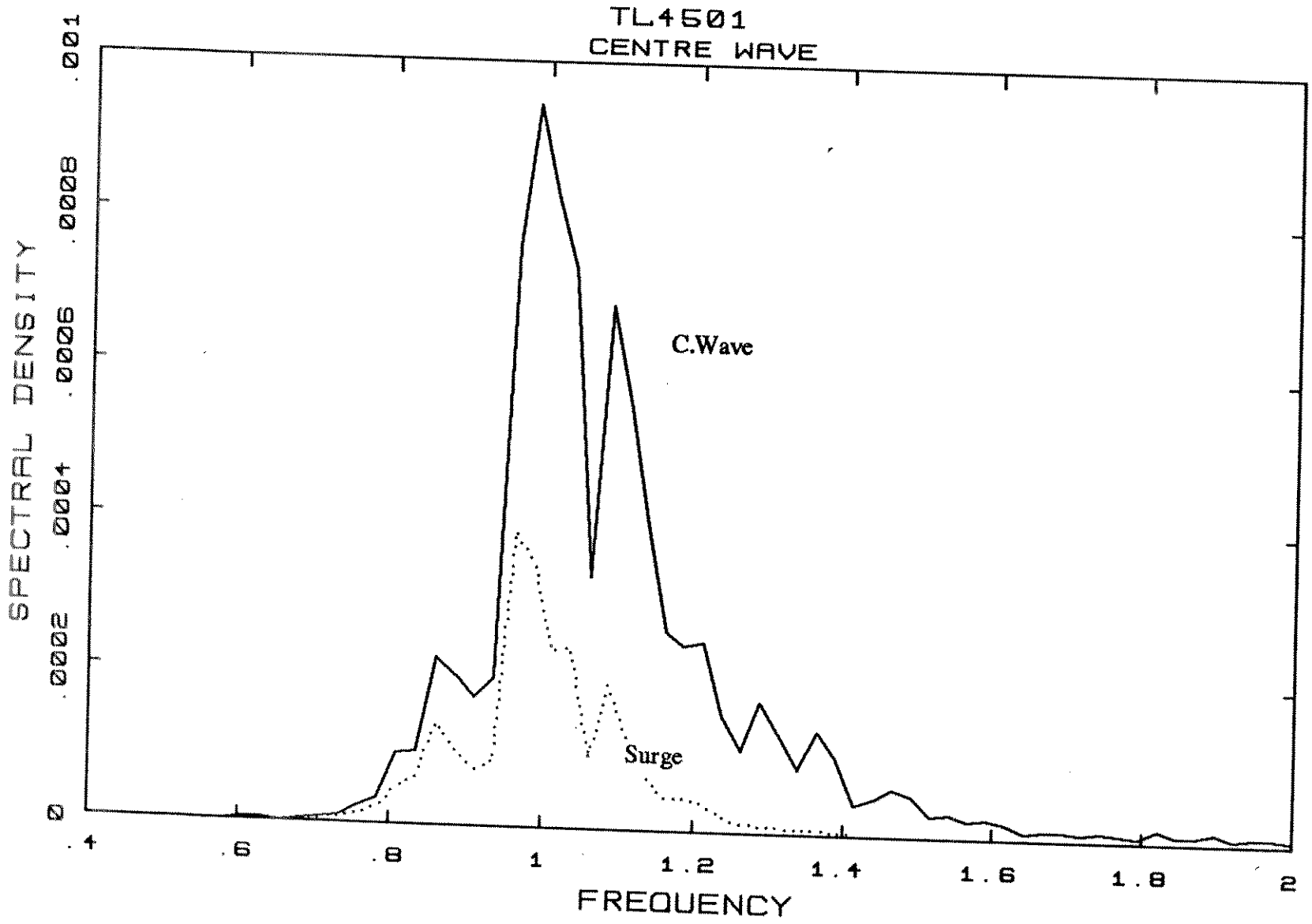
TL4501
CENTRE WAVE
SPECTRAL DENSITY
.001
.0008
.0006
.0004
.0002
0
C.Wave
Surge
.4
.6
.8
1
1.2
1.4
1.6
1.8
2
FREQUENCY

TL4501.W/S.4*

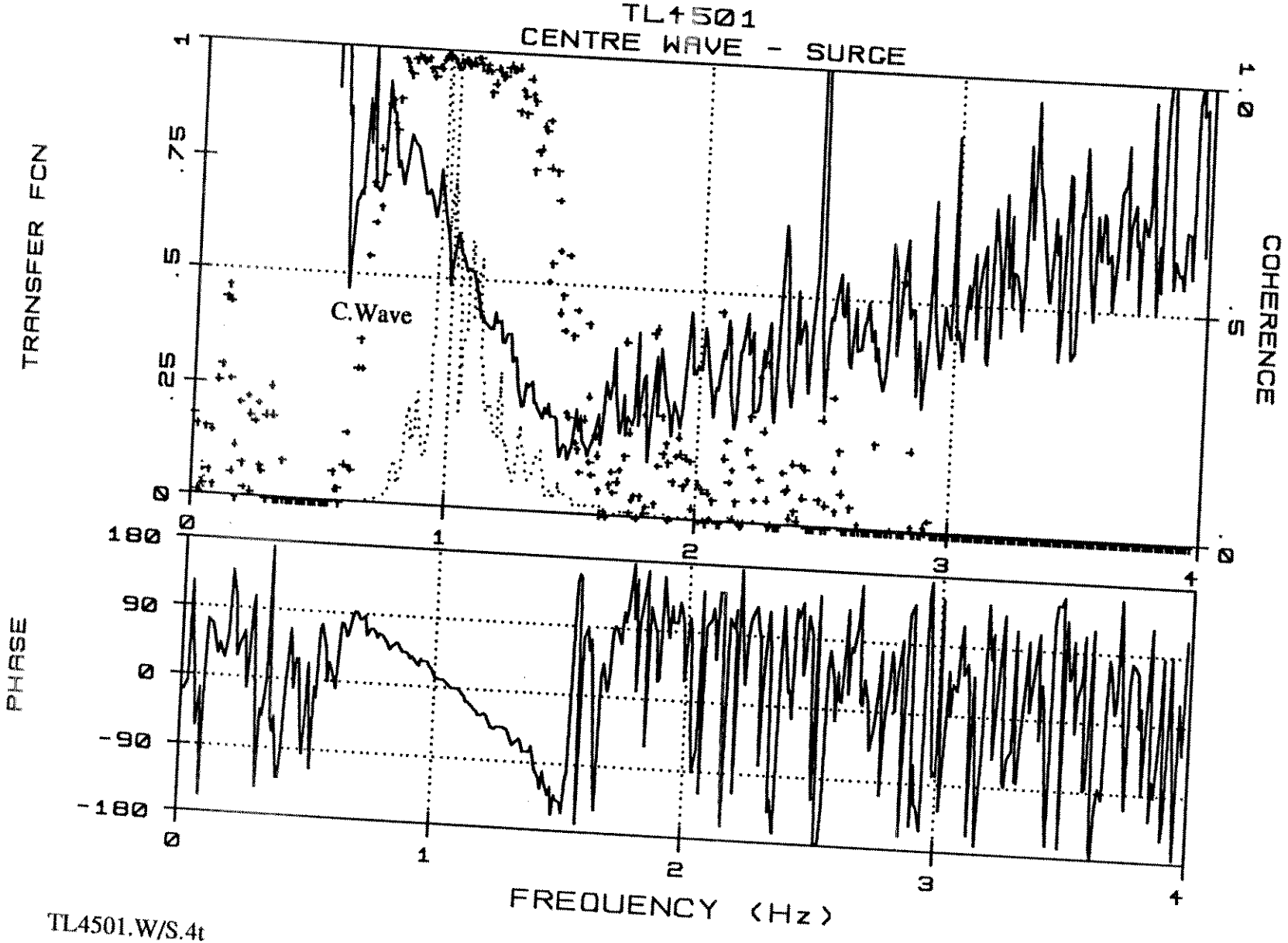
TL4501
CENTRE WAVE - SURGE
TRANSFER FCN
COHERENCE
C.Wave
PHASE
FREQUENCY (Hz)
1
.75
.5
.25
0
1.0
.5
0
180
90
0
-90
-180
0
1
2
3
4

TL4501.W/S.4t

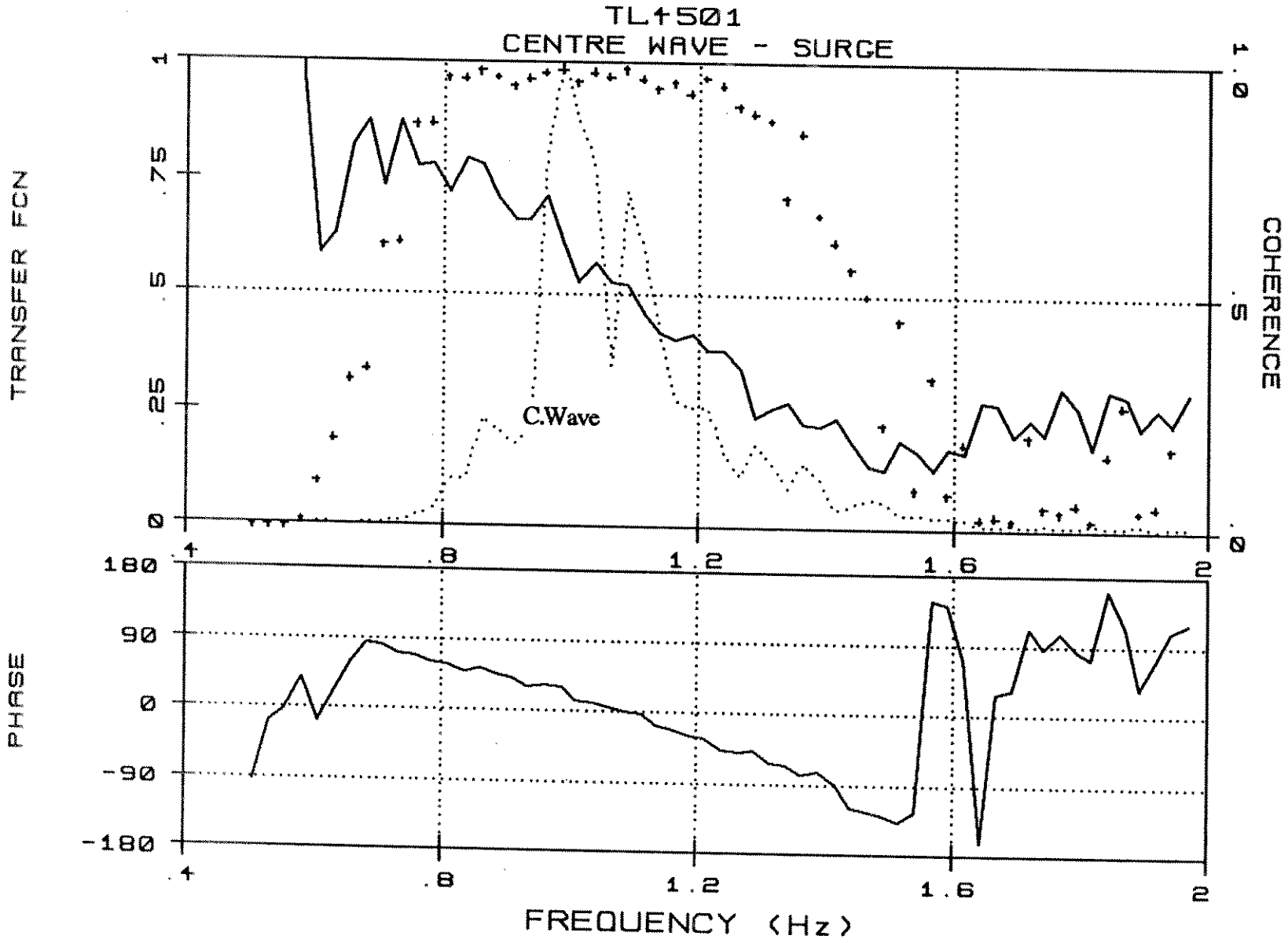
TL1501
CENTRE WAVE - SURGE
TRANSFER FCN
COHERENCE
C.Wave
PHASE
FREQUENCY (Hz)
1
.75
.5
.25
0
1.0
.5
0
180
90
0
-90
-180
.4
.8
1.2
1.6
2

TL4501.W/S.4t*

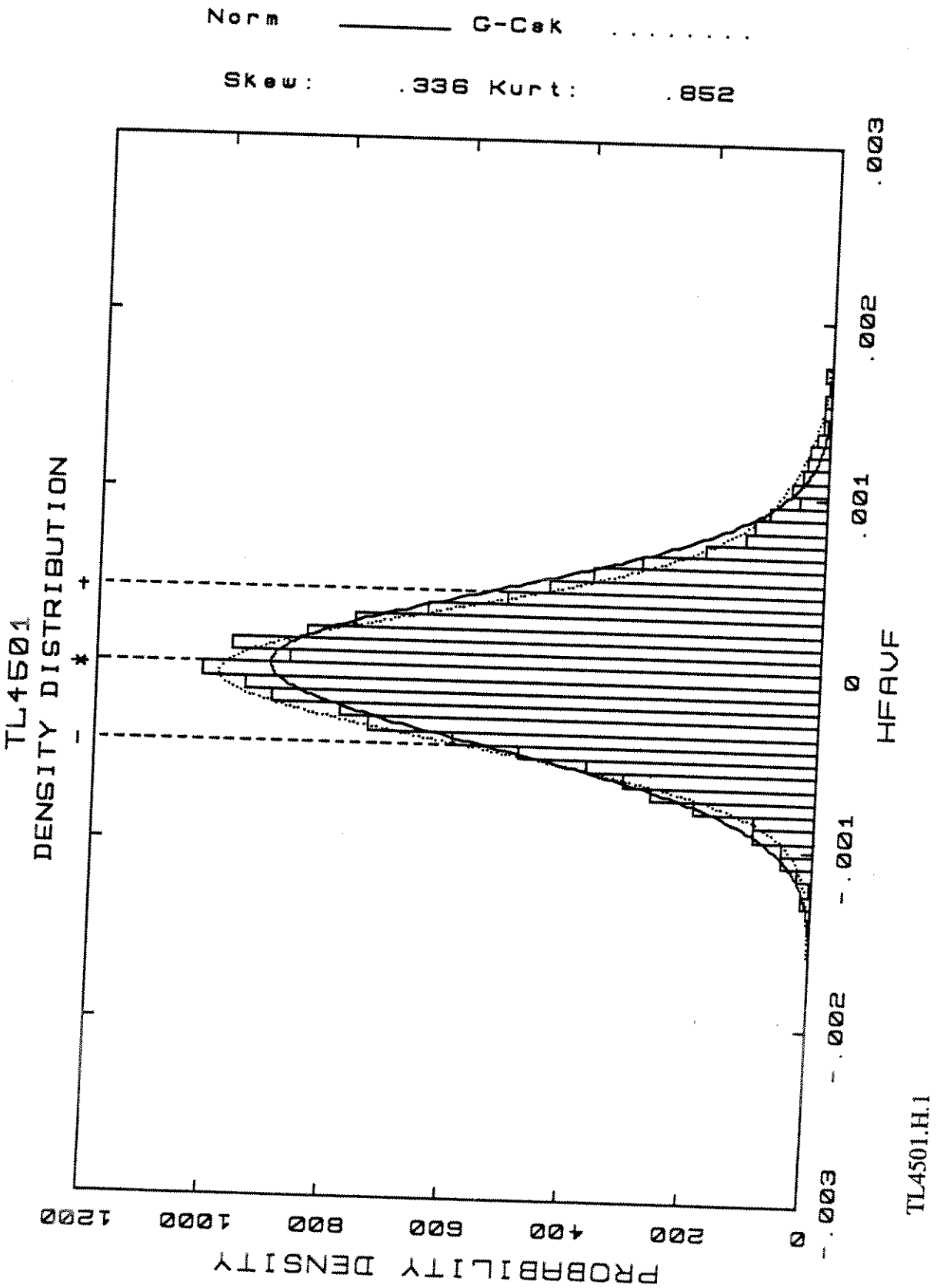
Norm
G-Cek
Skew: .336 Kurt: .852
TL4501
DENSITY DISTRIBUTION
+
*
-
PROBABILITY DENSITY
0
200
400
600
800
1000
1200
-.003
-.002
-.001
0
.001
.002
.003
HFAVF

TL4501.H.1

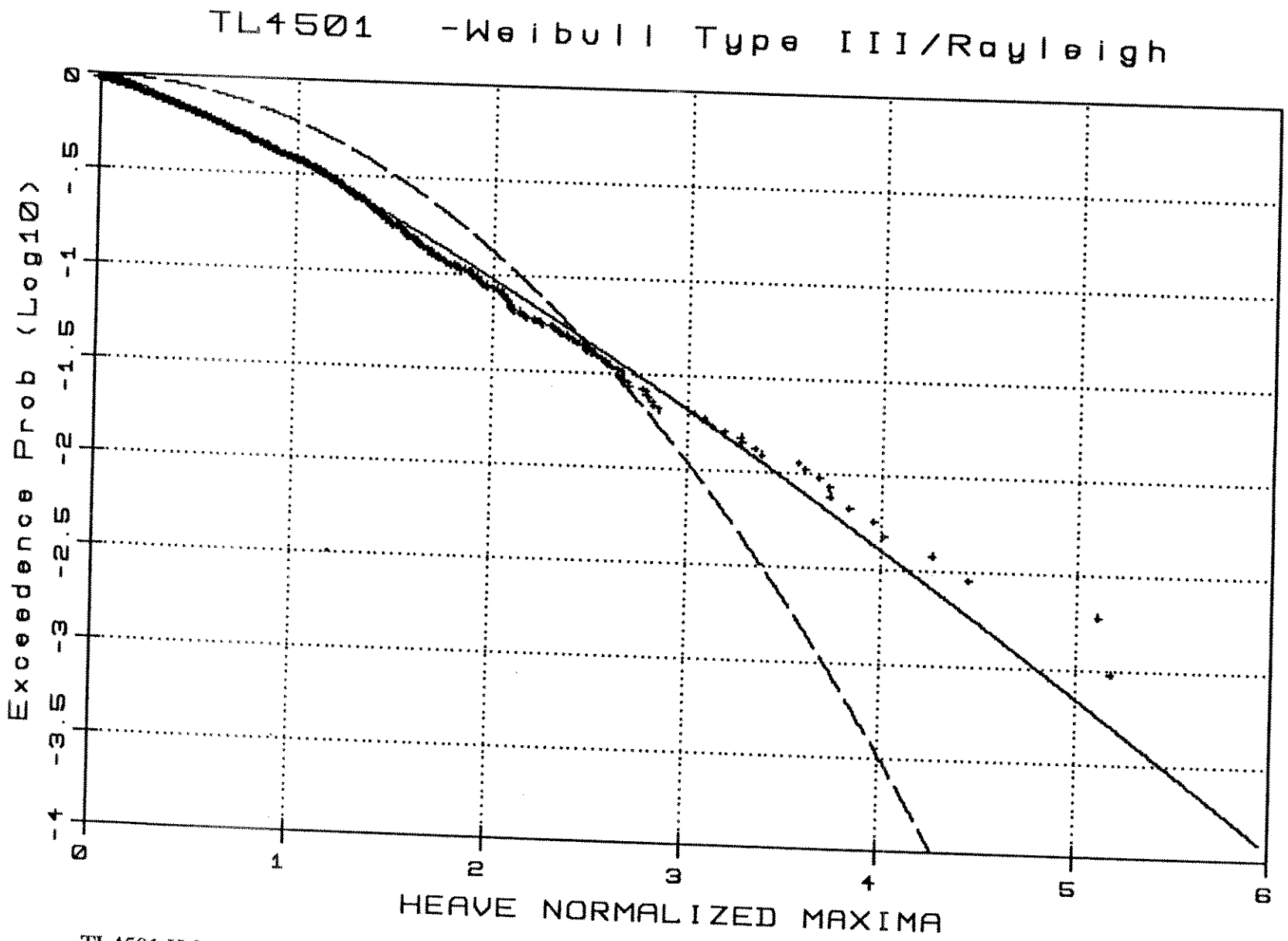
TL4501 -Weibull Type III/Rayleigh
Exceedence Prob (Log10)
0
-.5
-1
-1.5
-2
-2.5
-3
-3.5
-4
0
1
2
3
4
5
6
HEAVE NORMALIZED MAXIMA

TL4501.H.2

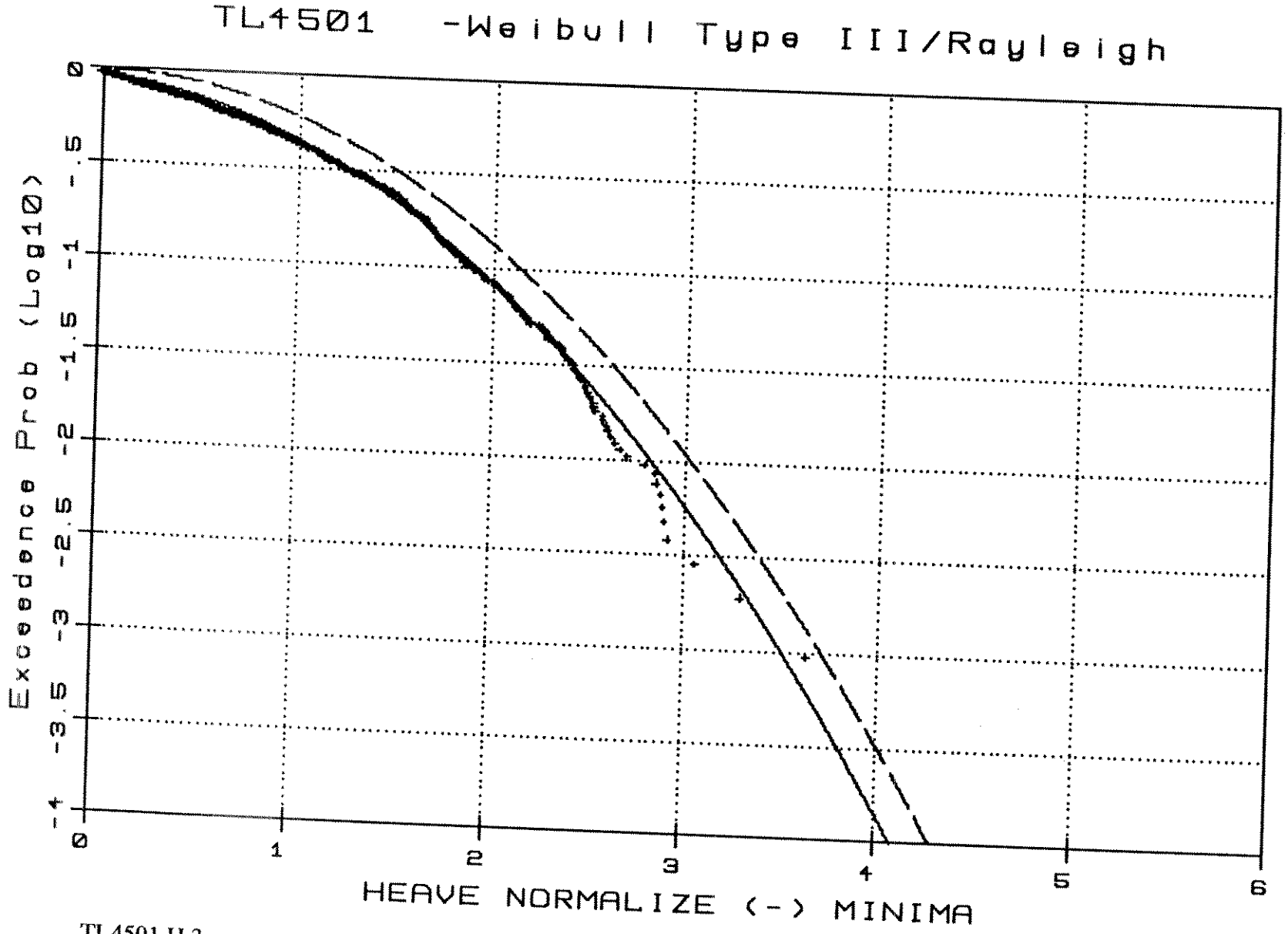
TL4501 -Weibull Type III/Rayleigh
Exceedence Prob (Log10)
0
-.5
-1
-1.5
-2
-2.5
-3
-3.5
-4
0
1
2
3
4
5
6
HEAVE NORMALIZE (-) MINIMA

TL4501.H.3

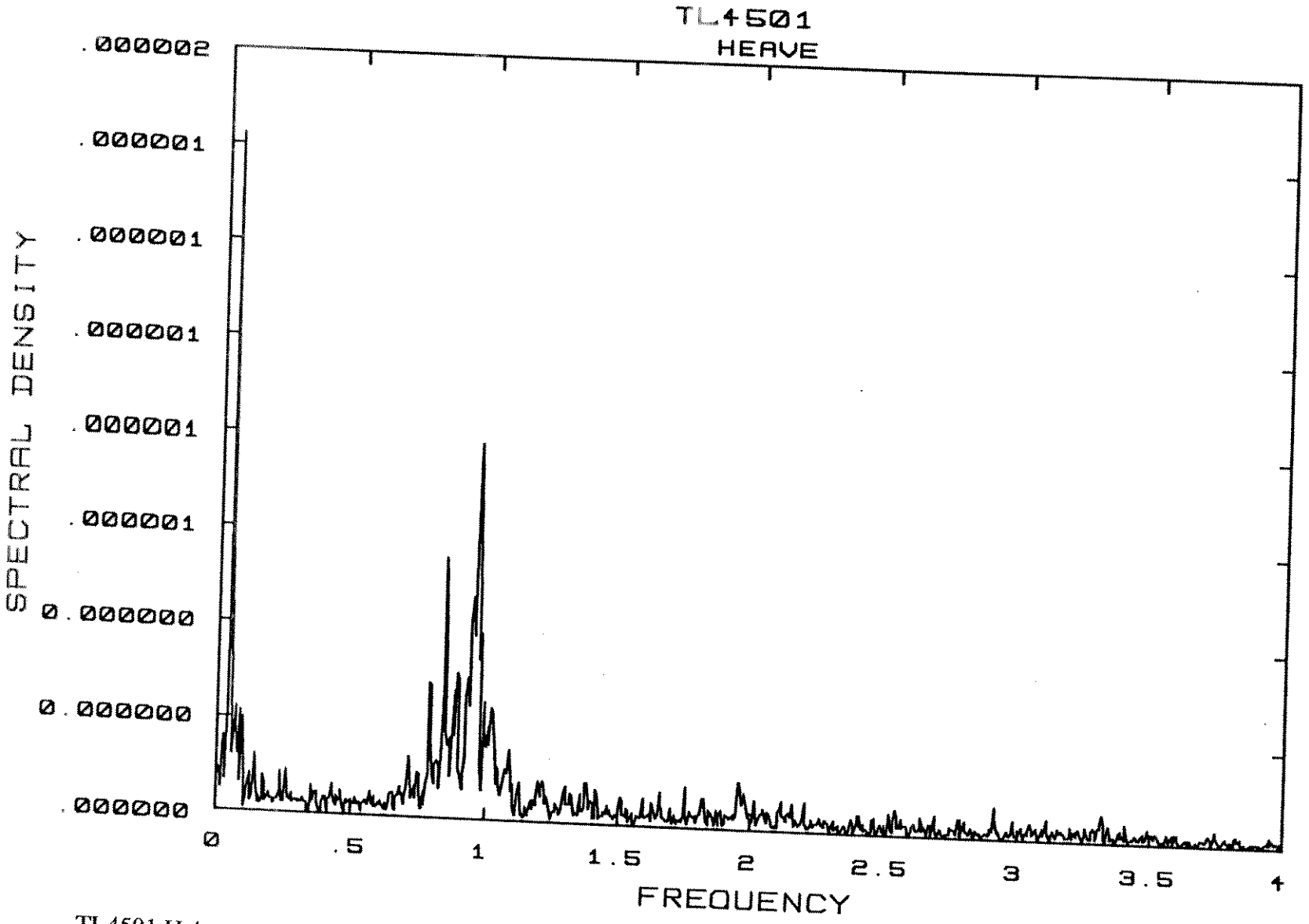
TL4501
HEAVE
.000002
.000001
.000001
.000001
.000001
.000001
0.000000
0.000000
.000000
SPECTRAL DENSITY
0
.5
1
1.5
2
2.5
3
3.5
4
FREQUENCY

TL4501.H.4

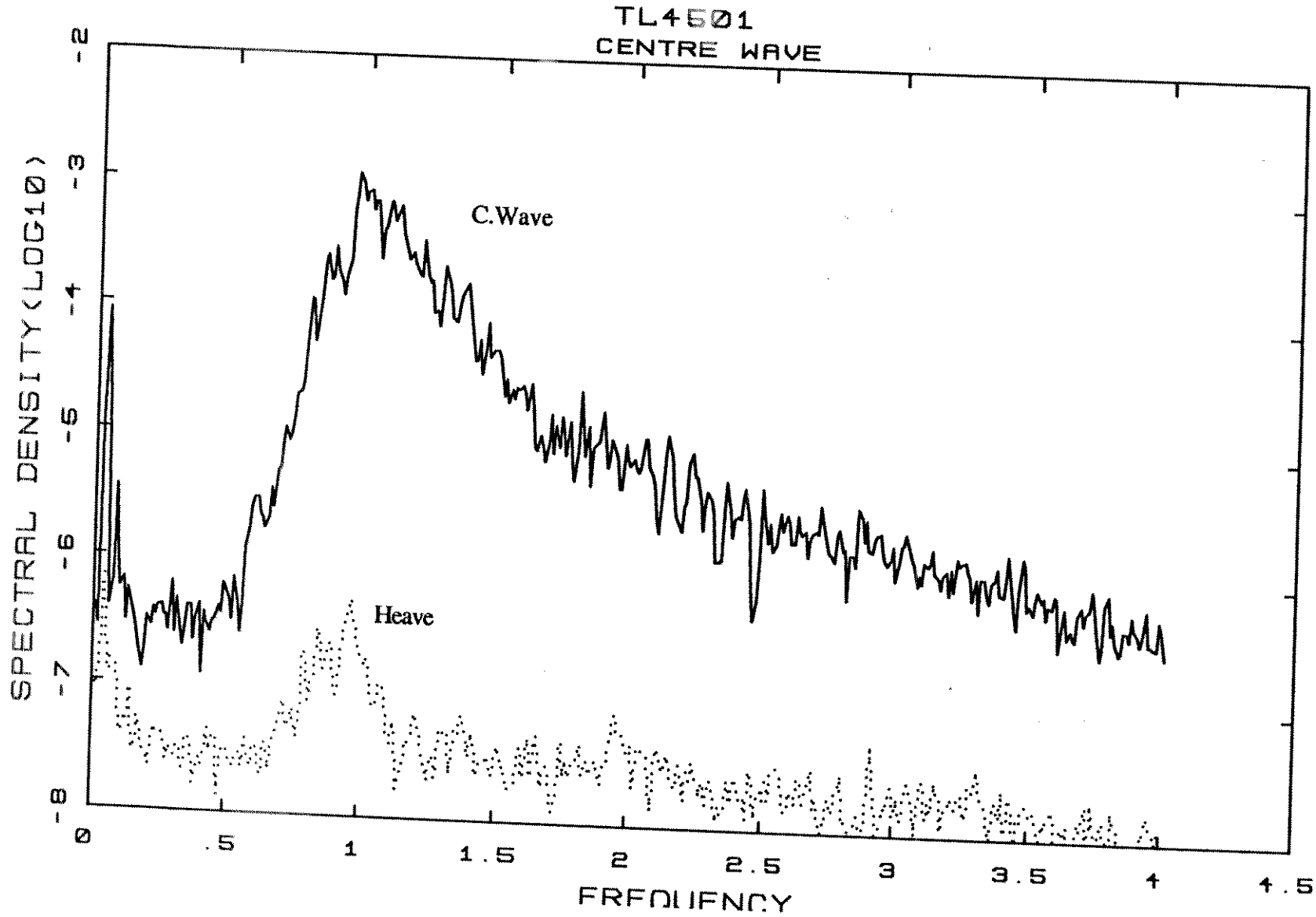
TL4501
CENTRE WAVE
SPECTRAL DENSITY(LOG10)
-2
-3
-4
-5
-6
-7
-8
C.Wave
Heave
0
.5
1
1.5
2
2.5
3
3.5
4
4.5
FREQUENCY

TL4501.W/H.4

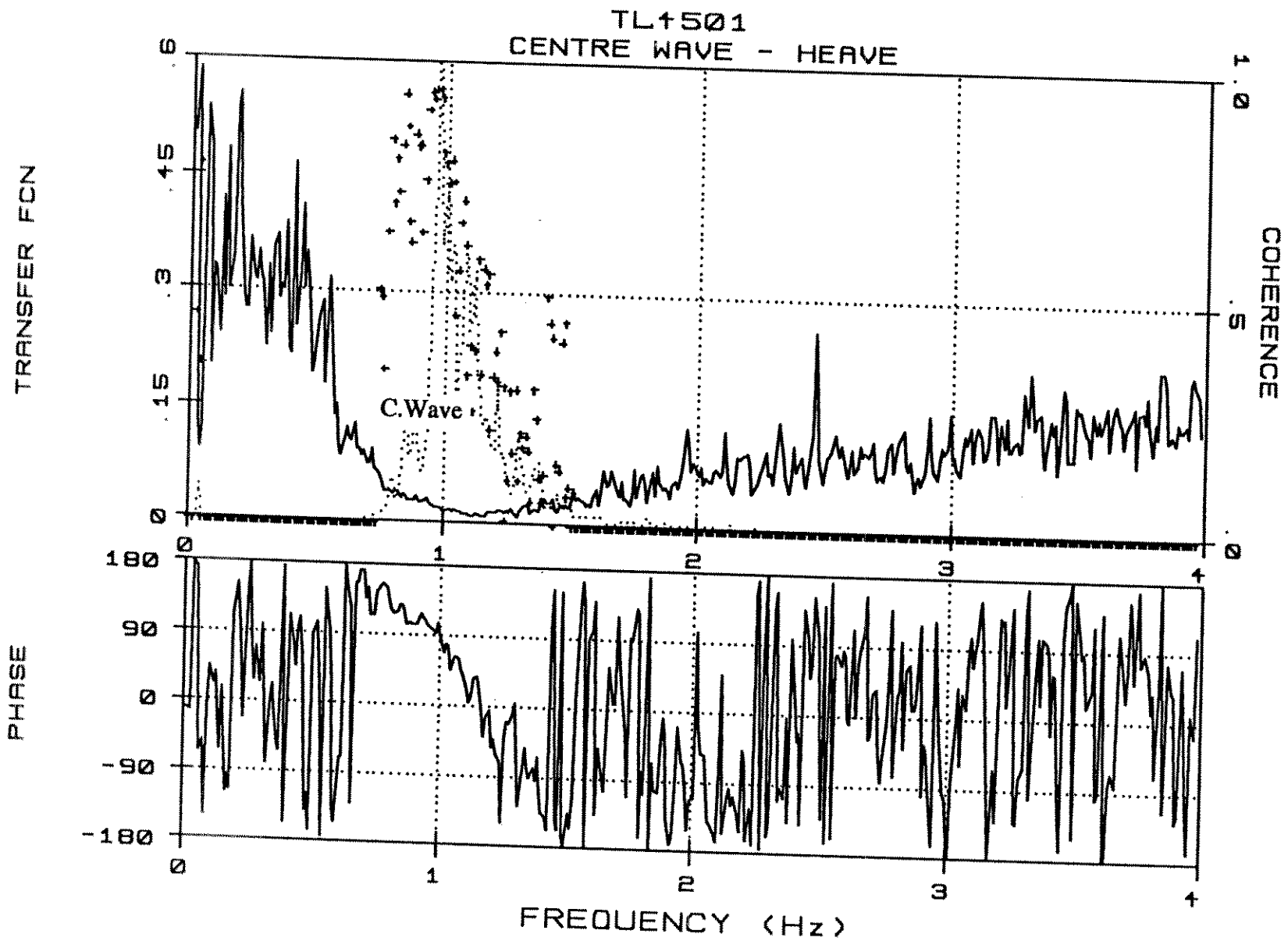
TL1501
CENTRE WAVE - HEAVE
TRANSFER FCN
.6
.45
.3
.15
0
COHERENCE
1.0
.5
0
C.Wave
0
1
2
3
4
PHASE
180
90
0
-90
-180
FREQUENCY (Hz)

TL4501.W/H.4t

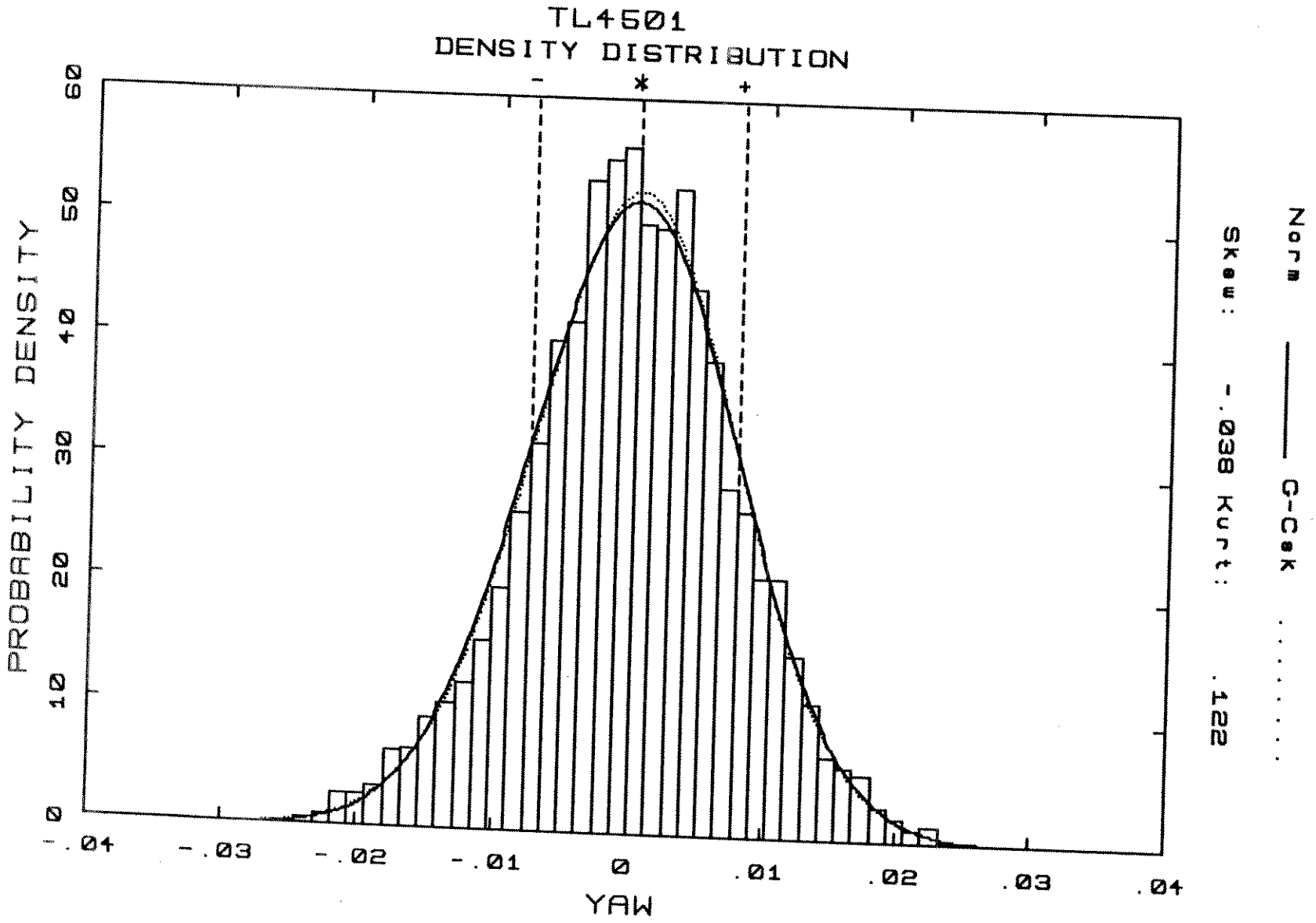
TL4501
DENSITY DISTRIBUTION
PROBABILITY DENSITY
0
10
20
30
40
50
60
-.04
-.03
-.02
-.01
0
.01
.02
.03
.04
YAW
Norm
G-Cak
Skew: -.038 Kurt: .122

TL4501.Y.1

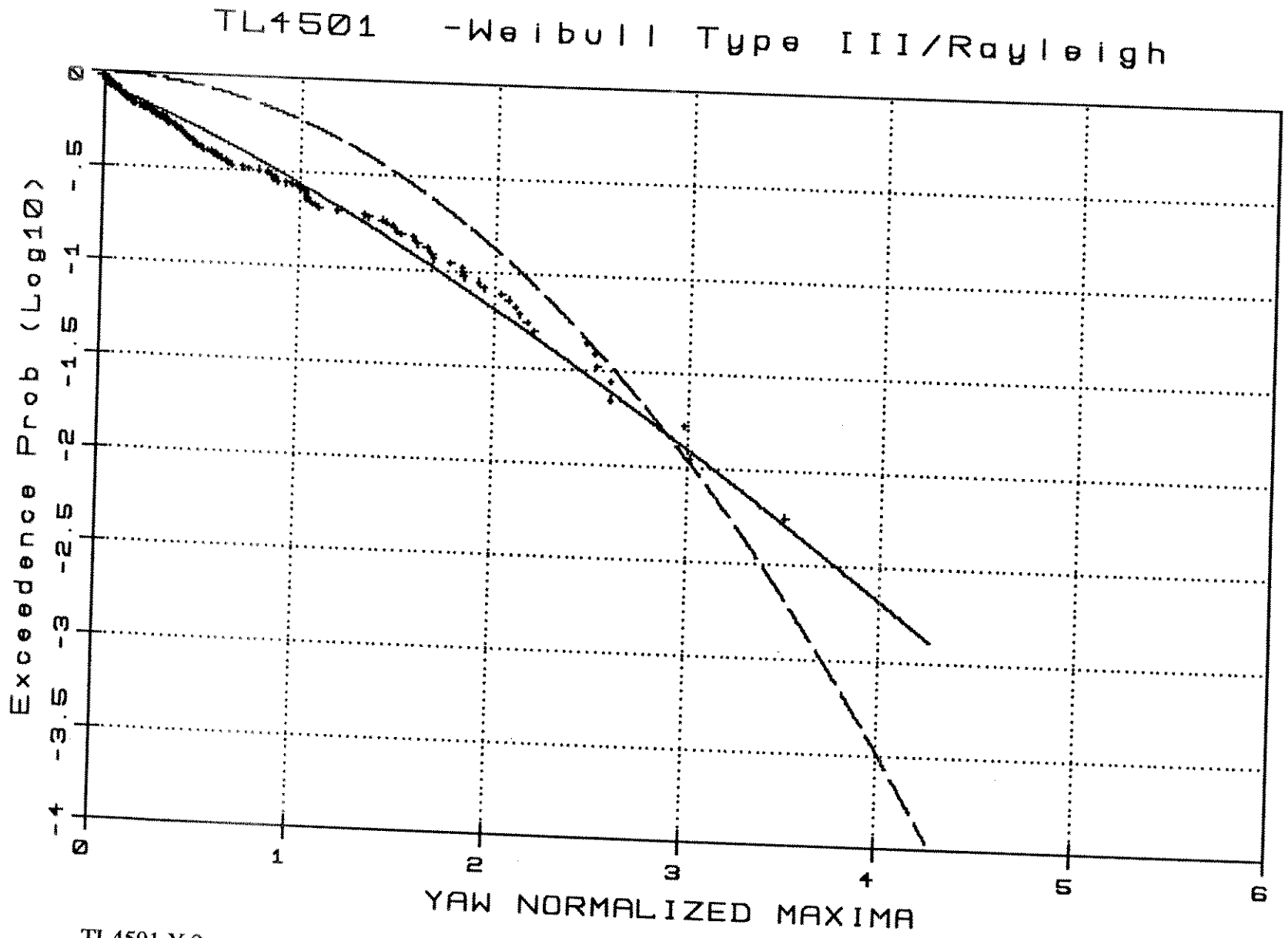
TL4501 -Weibull Type III/Rayleigh
Exceedence Prob (Log10)
0
-.5
-1
-1.5
-2
-2.5
-3
-3.5
-4
0
1
2
3
4
5
6
YAW NORMALIZED MAXIMA

TL4501.Y.2

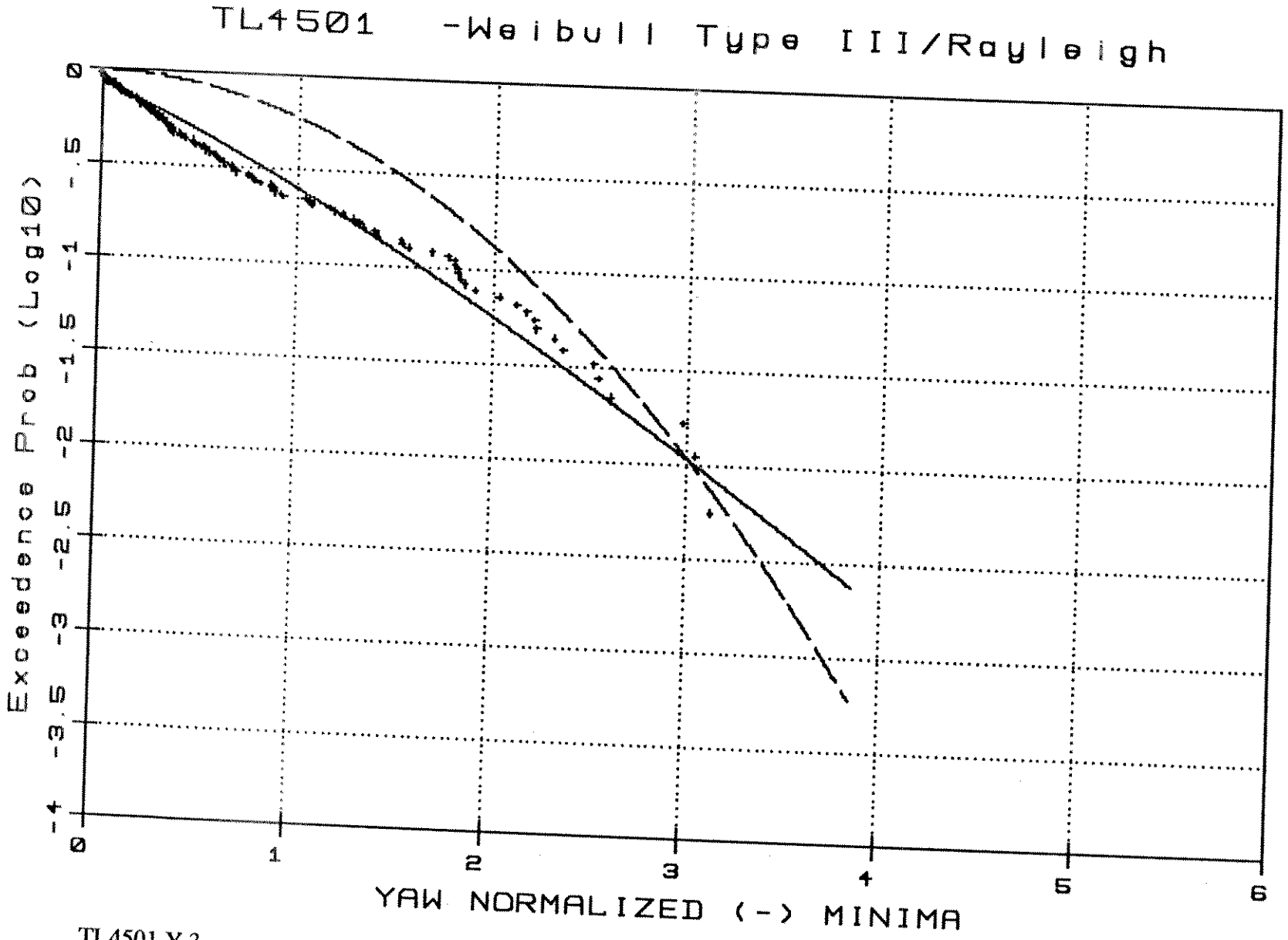
TL4501 -Weibull Type III/Rayleigh
Exceedence Prob (Log10)
0
-.5
-1
-1.5
-2
-2.5
-3
-3.5
-4
0
1
2
3
4
5
6
YAW NORMALIZED (-) MINIMA

TL4501.Y.3

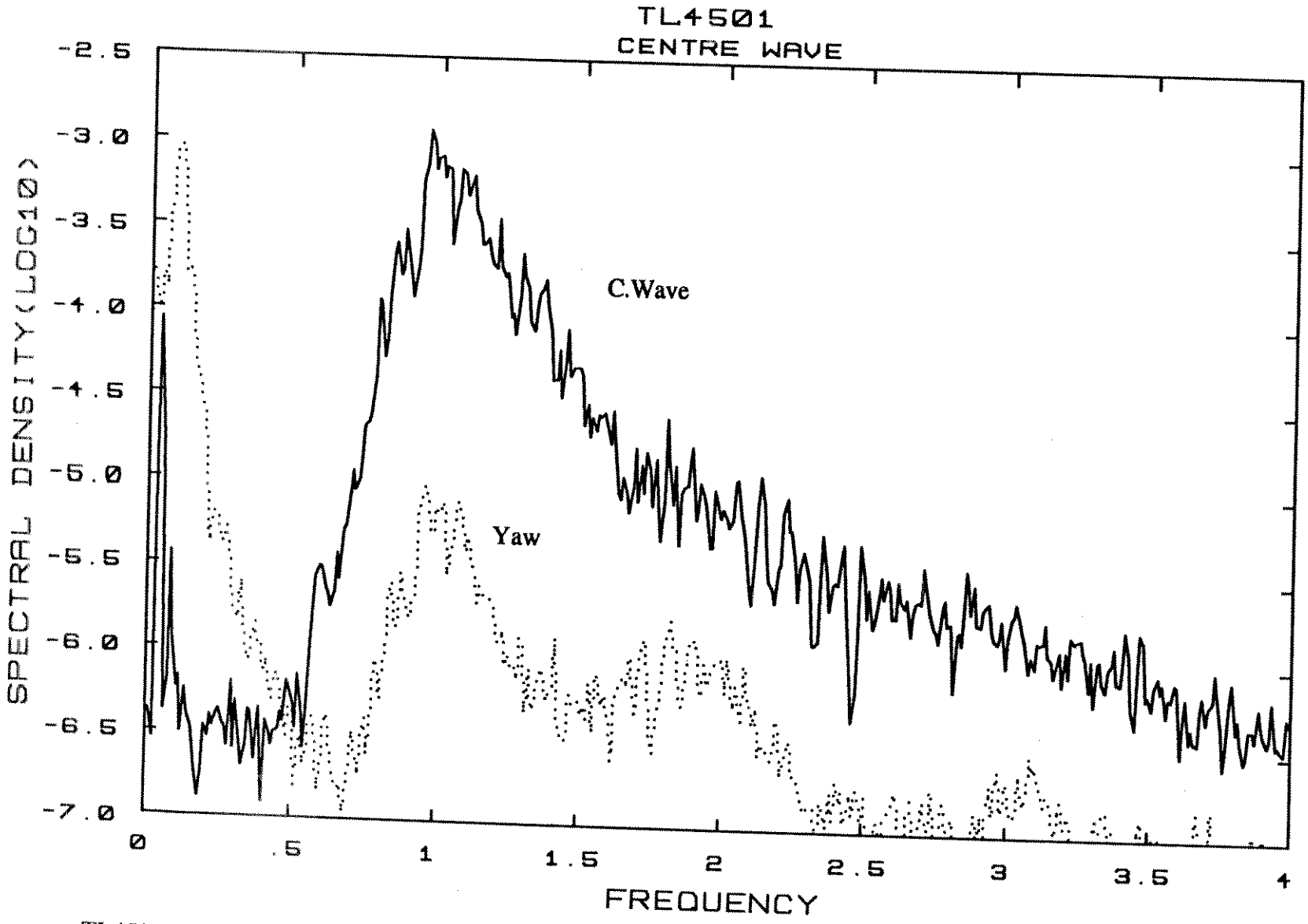
TL4501
CENTRE WAVE
SPECTRAL DENSITY(LOG10)
-2.5
-3.0
-3.5
-4.0
-4.5
-5.0
-5.5
-6.0
-6.5
-7.0
C.Wave
Yaw
0
.5
1
1.5
2
2.5
3
3.5
4
FREQUENCY

TL4501.W/Y.4

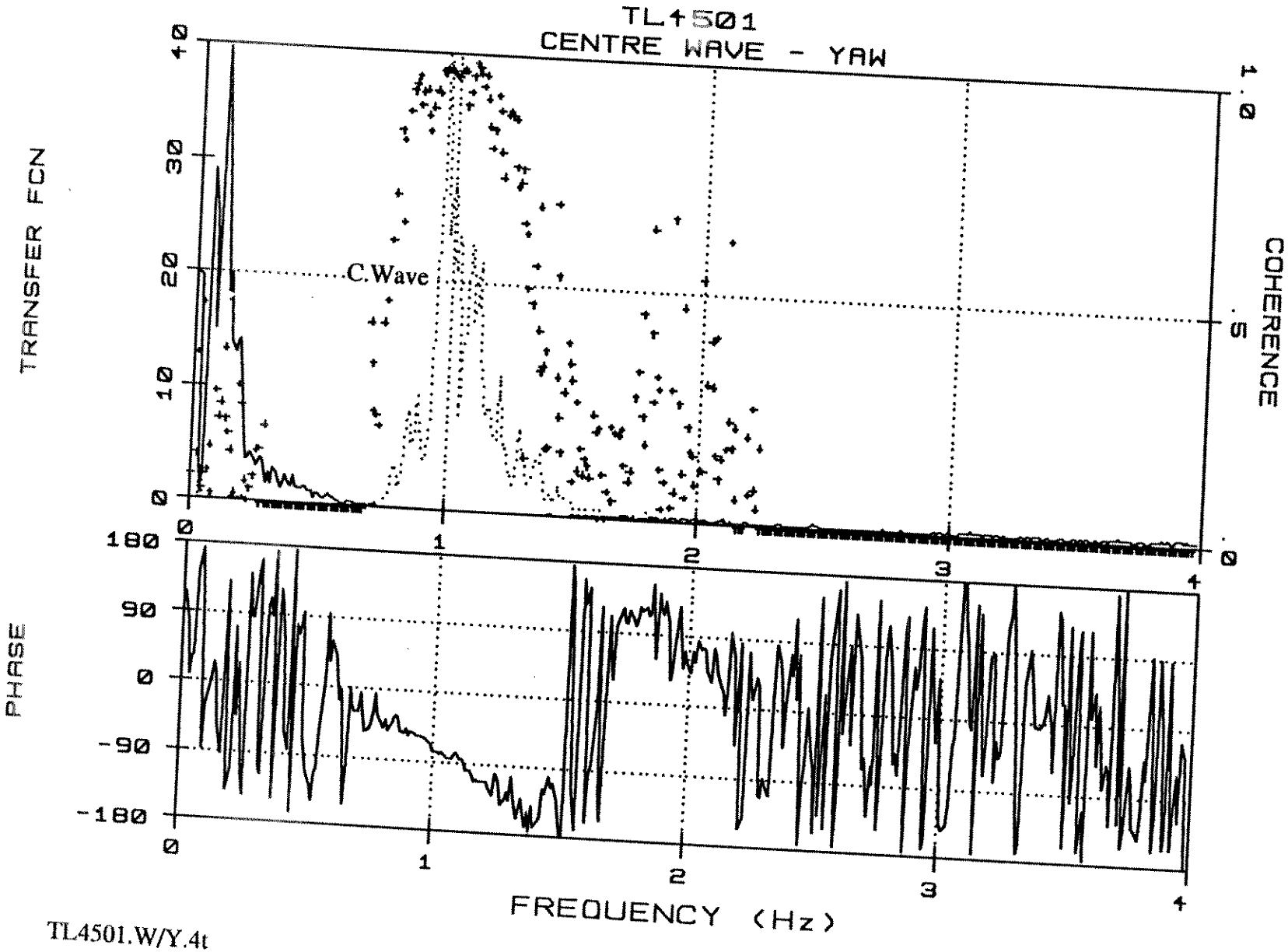
TL4501
CENTRE WAVE - YAW
TRANSFER FCN
40
30
20
10
0
C.Wave
COHERENCE
1.0
.5
0
0
1
2
3
4
PHASE
180
90
0
-90
-180
FREQUENCY (Hz)

TL4501.W/Y.4t

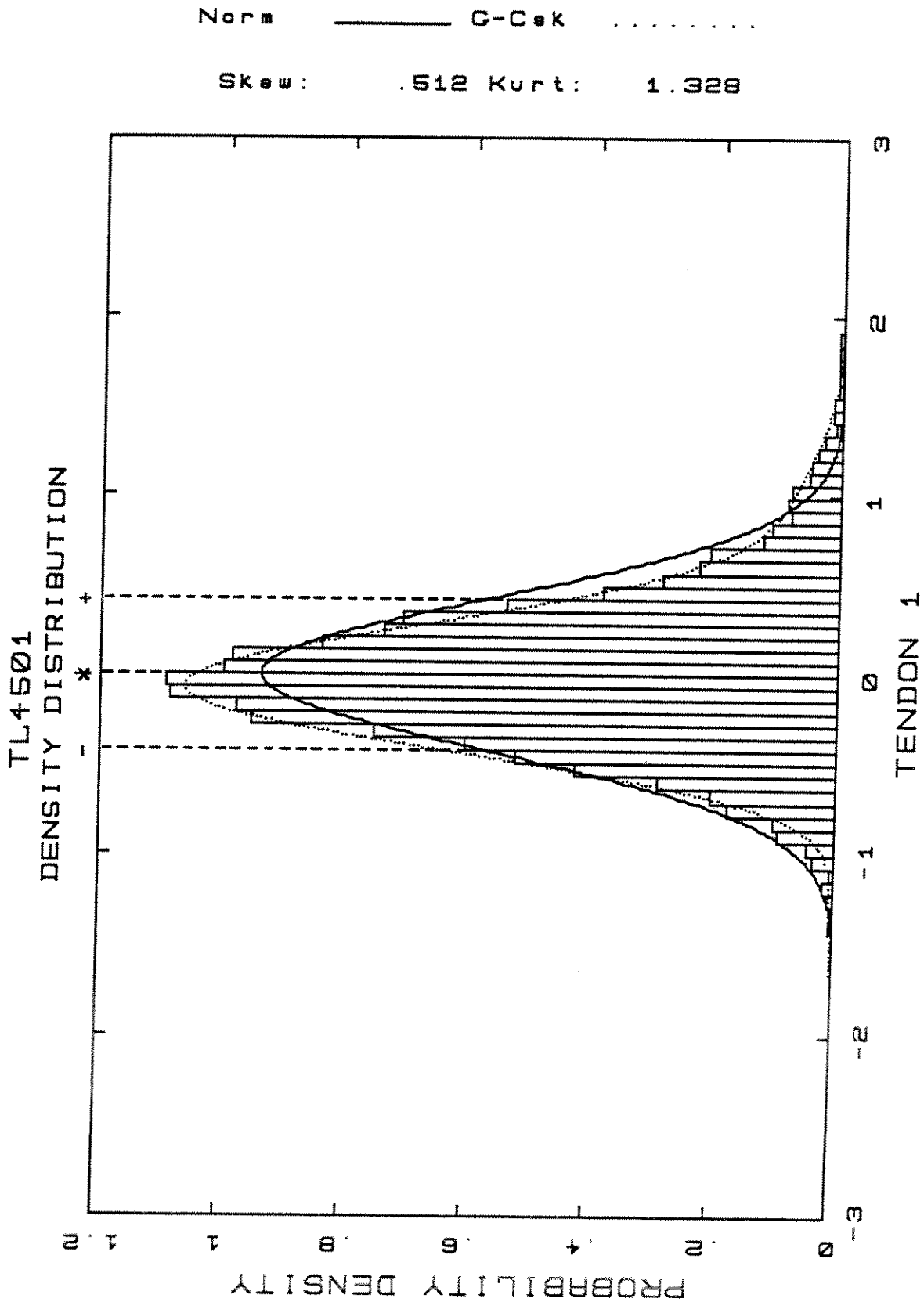
Norm ——— G-Cek .....
Skew: .512 Kurt: 1.328
TL4501
DENSITY DISTRIBUTION
+
*
-
PROBABILITY DENSITY
0
.2
.4
.6
.8
1
1.2
-3
-2
-1
0
1
2
3
TENDON 1

TL4501.T1.1

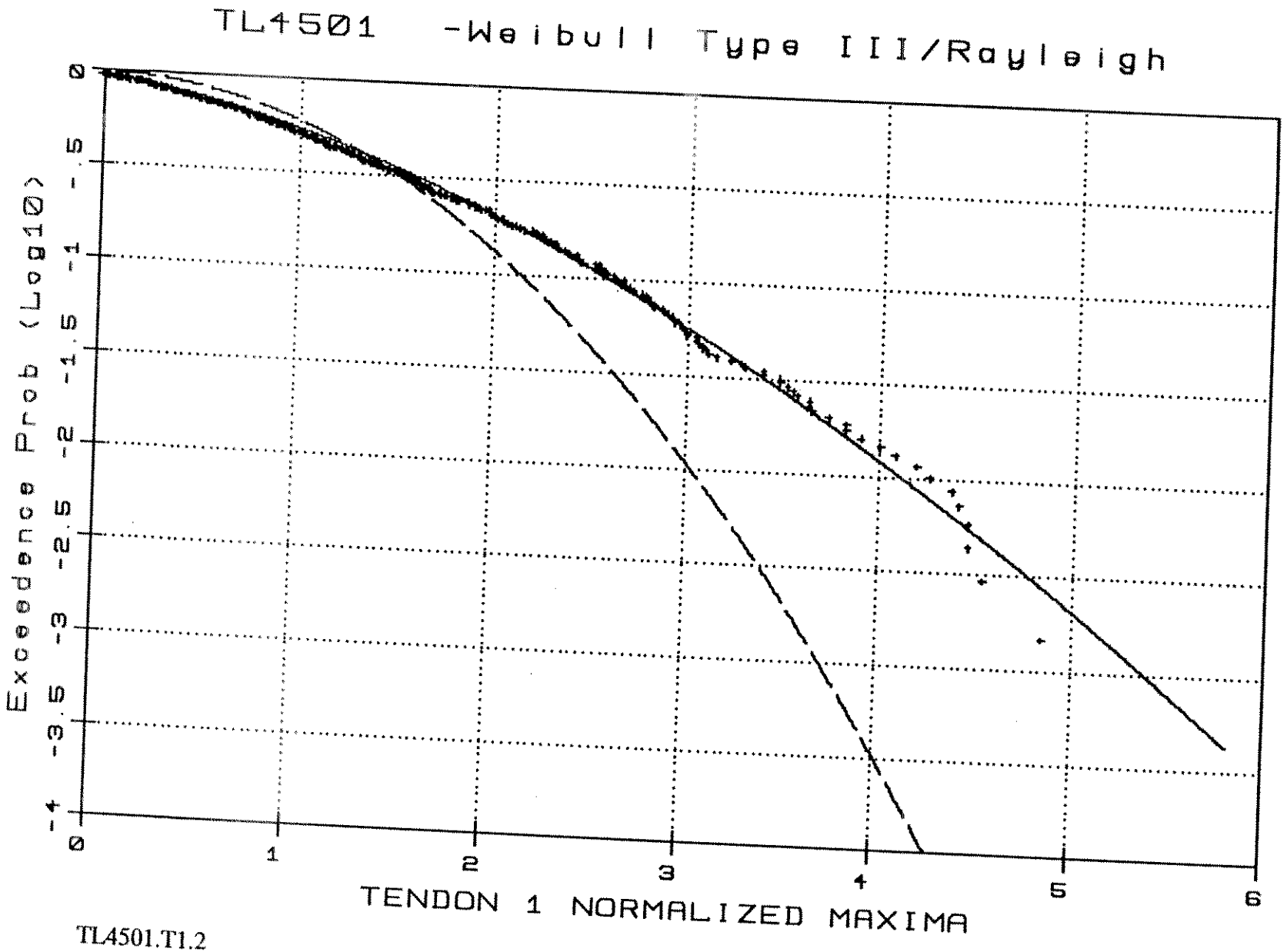
TL4501 -Weibull Type III/Rayleigh
Exceedence Prob (Log10)
0
-.5
-1
-1.5
-2
-2.5
-3
-3.5
-4
0
1
2
3
4
5
6
TENDON 1 NORMALIZED MAXIMA

TL4501.T1.2

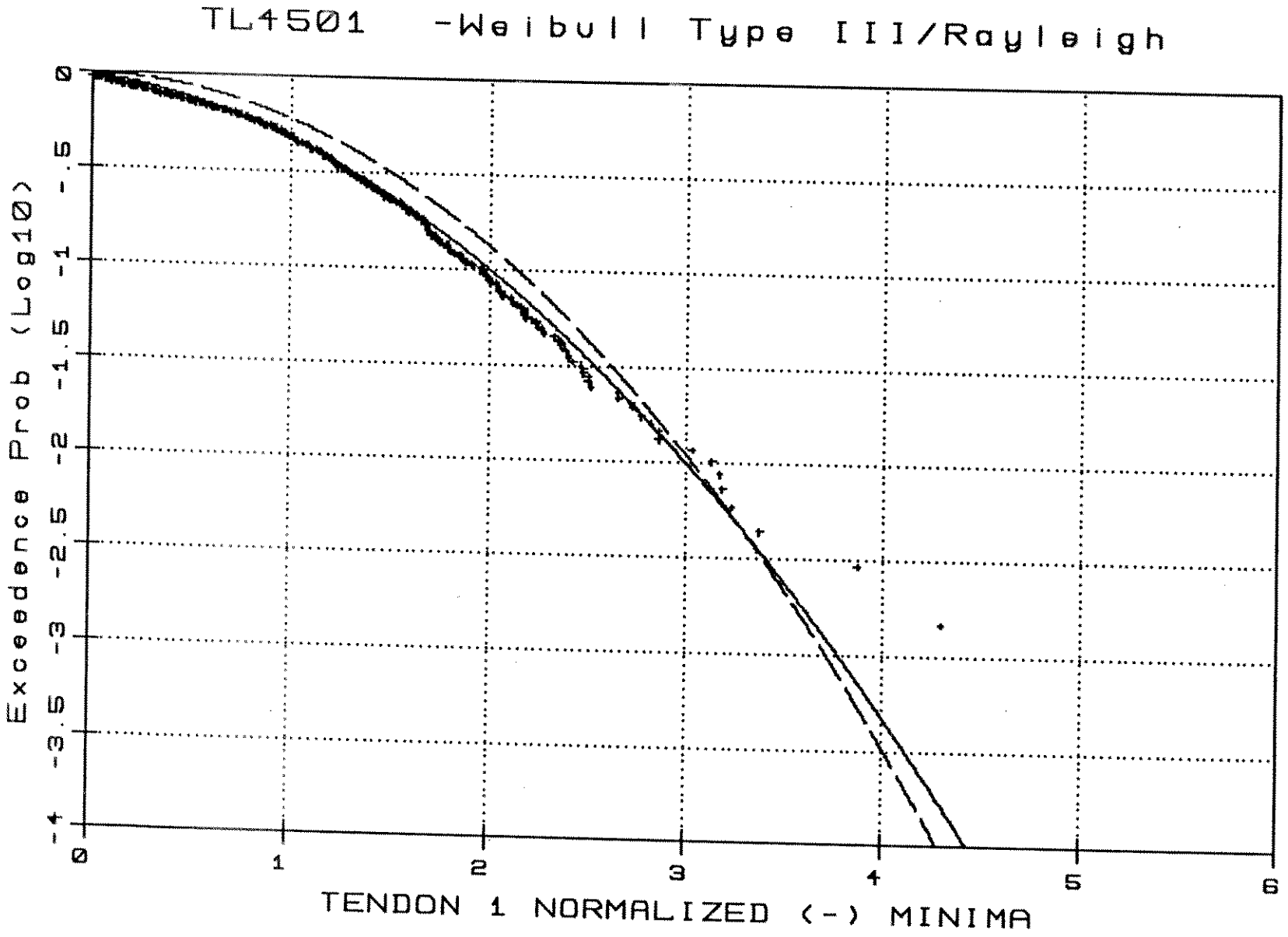
TL4501 -Weibull Type III/Rayleigh
Exceedence Prob (Log10)
0
-.5
-1
-1.5
-2
-2.5
-3
-3.5
-4
0
1
2
3
4
5
6
TENDON 1 NORMALIZED (-) MINIMA

TL4501.T1.3

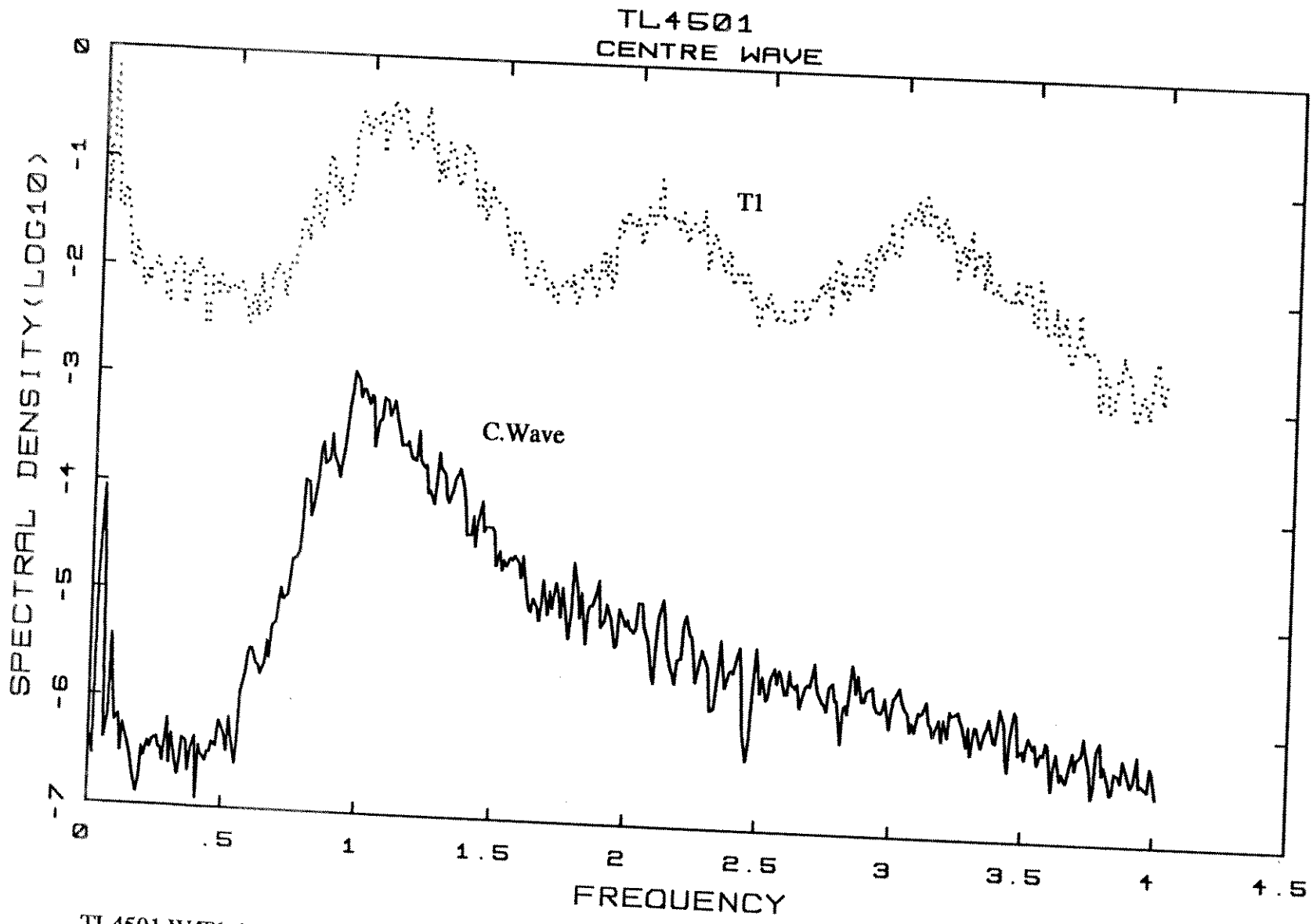
TL4501
CENTRE WAVE
T1
C.Wave
SPECTRAL DENSITY(LOG10)
0
-1
-2
-3
-4
-5
-6
-7
0
.5
1
1.5
2
2.5
3
3.5
4
4.5
FREQUENCY

TL4501.W/T1.4

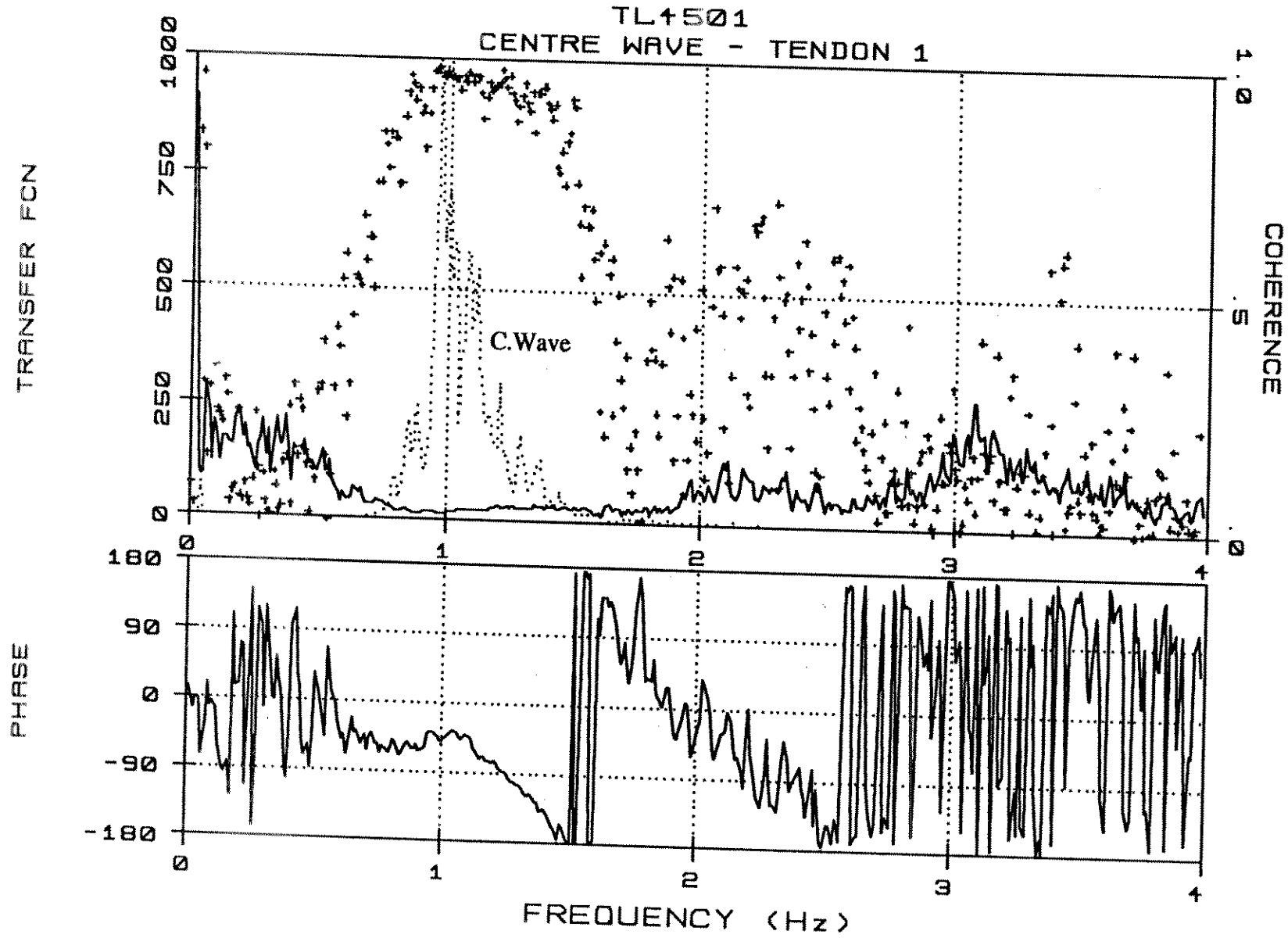

TL4501.W/T1.4t

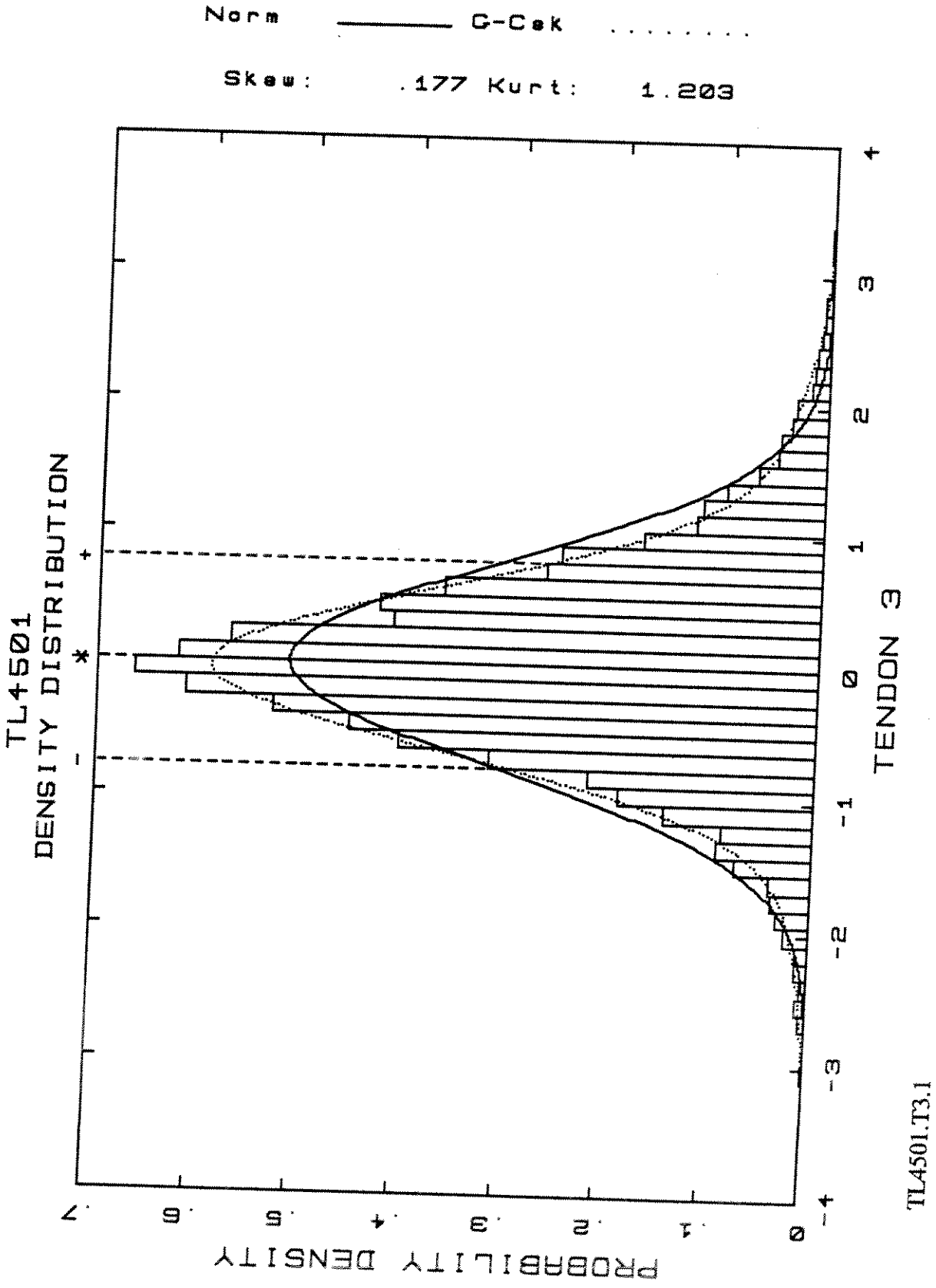
Norm
G-Cek
Skew: .177 Kurt: 1.203
TL4501
DENSITY DISTRIBUTION
TENDON 3
PROBABILITY DENSITY
TL4501.T3.1

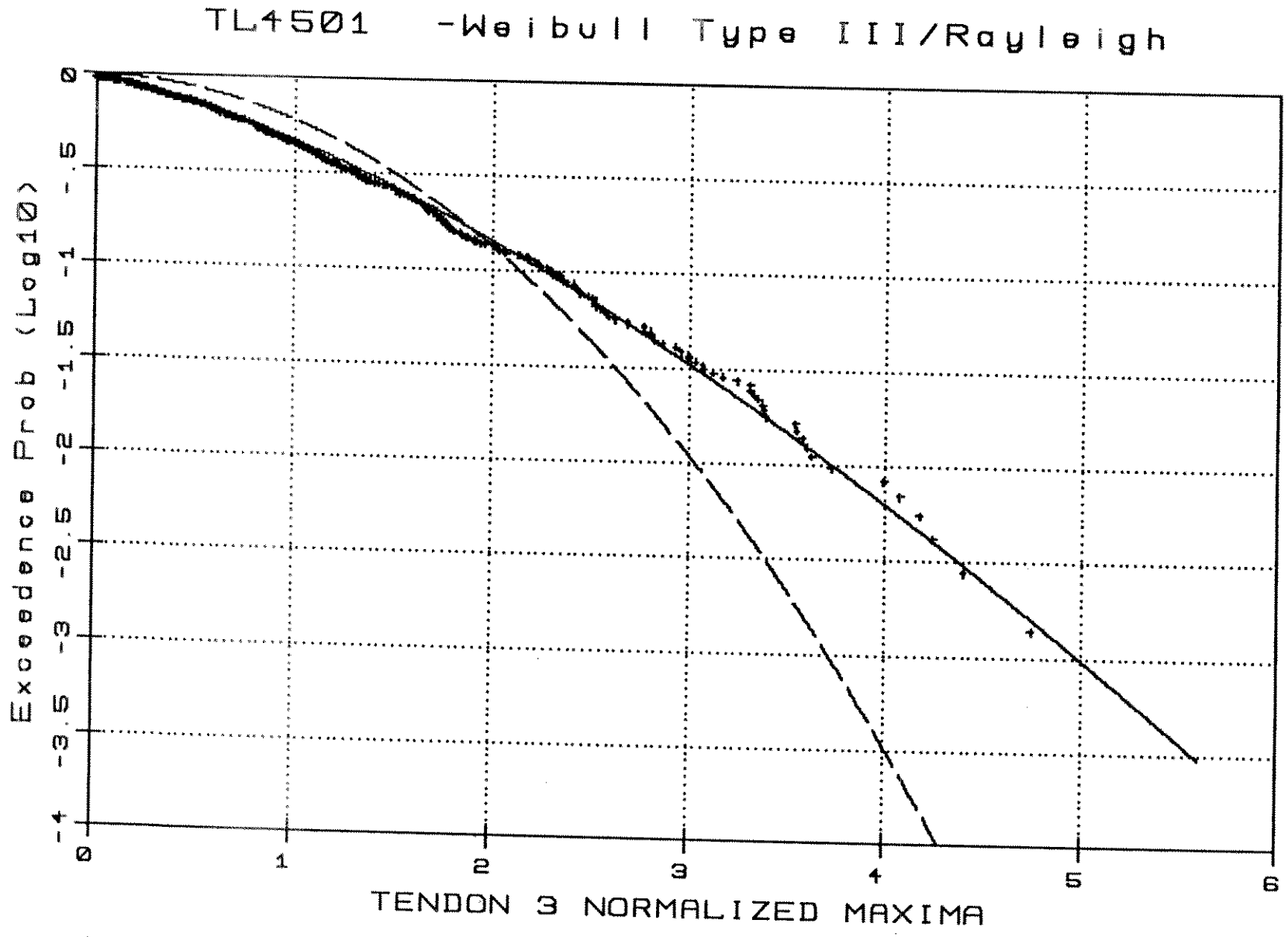
TL4501 -Weibull Type III/Rayleigh
Exceedence Prob (Log10)
0
-.5
-1
-1.5
-2
-2.5
-3
-3.5
-4
0
1
2
3
4
5
6
TENDON 3 NORMALIZED MAXIMA

TL4501.T3.2

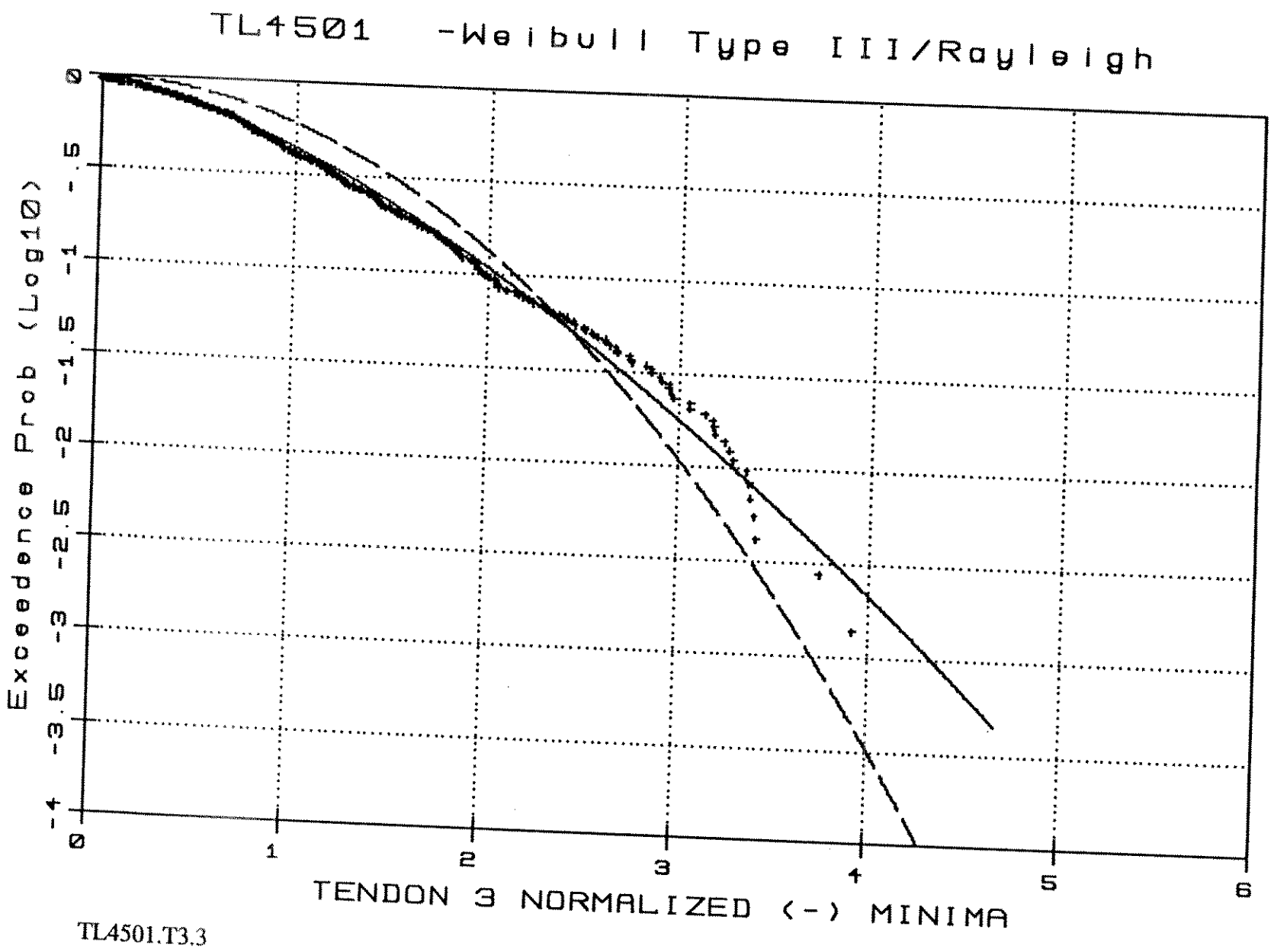
TL4501 -Weibull Type III/Rayleigh
Exceedence Prob (Log10)
0
-.5
-1
-1.5
-2
-2.5
-3
-3.5
-4
0
1
2
3
4
5
6
TENDON 3 NORMALIZED (-) MINIMA

TL4501.T3.3

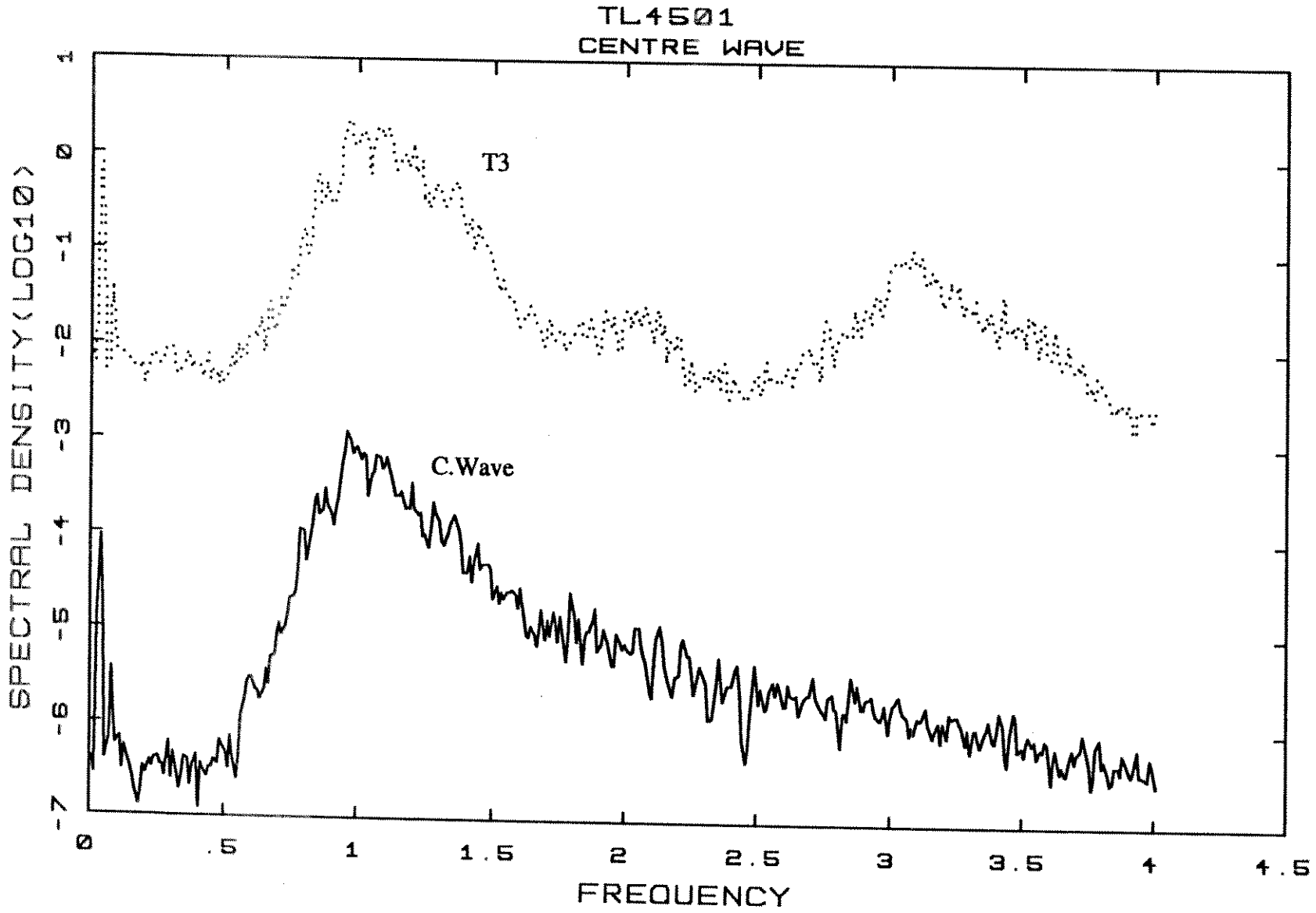
TL4501
CENTRE WAVE
T3
C.Wave
SPECTRAL DENSITY(LOG10)
1
0
-1
-2
-3
-4
-5
-6
-7
0
.5
1
1.5
2
2.5
3
3.5
4
4.5
FREQUENCY

TL4501.W/T3.4

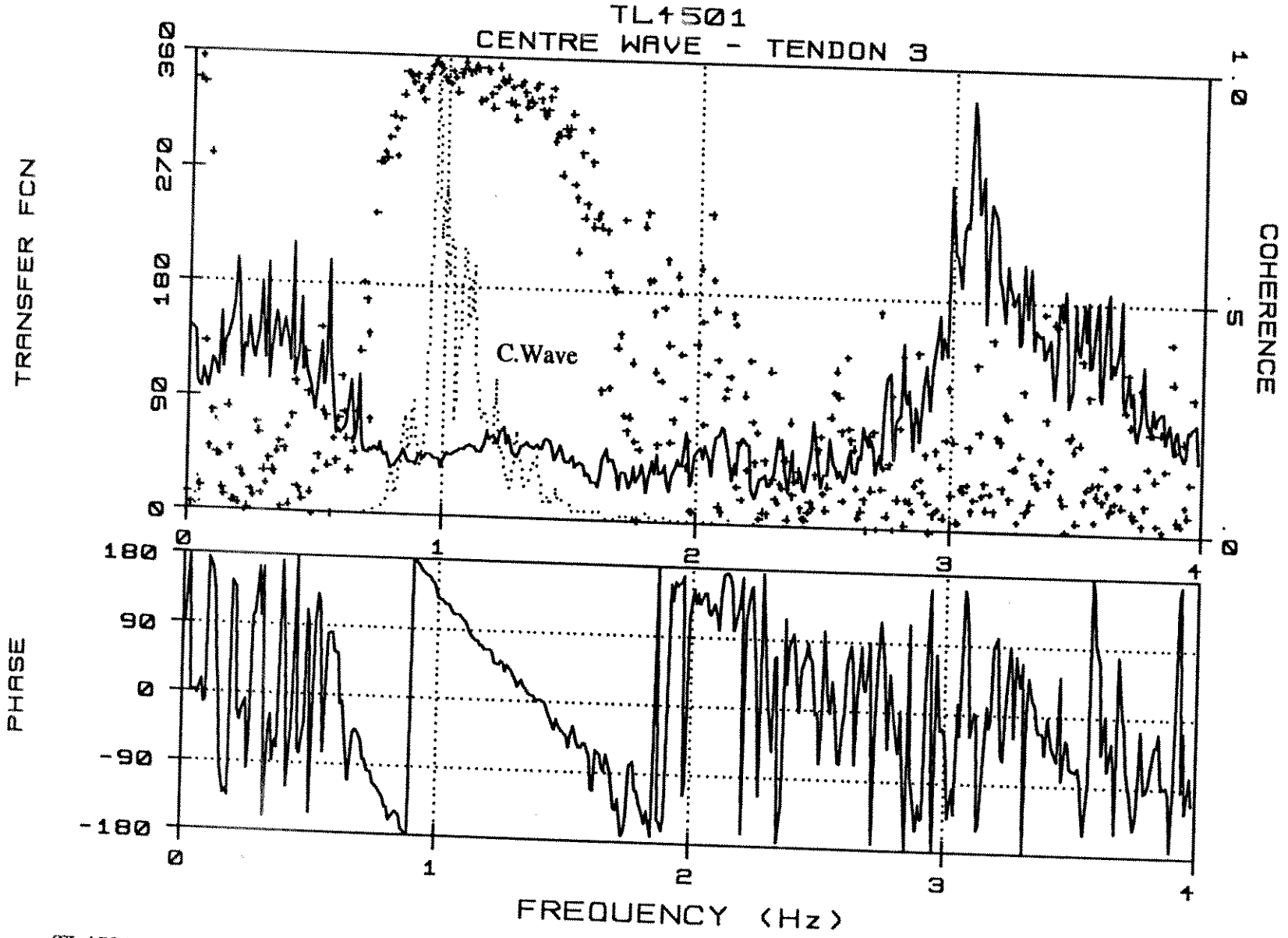

TL4501.W/T3.4t

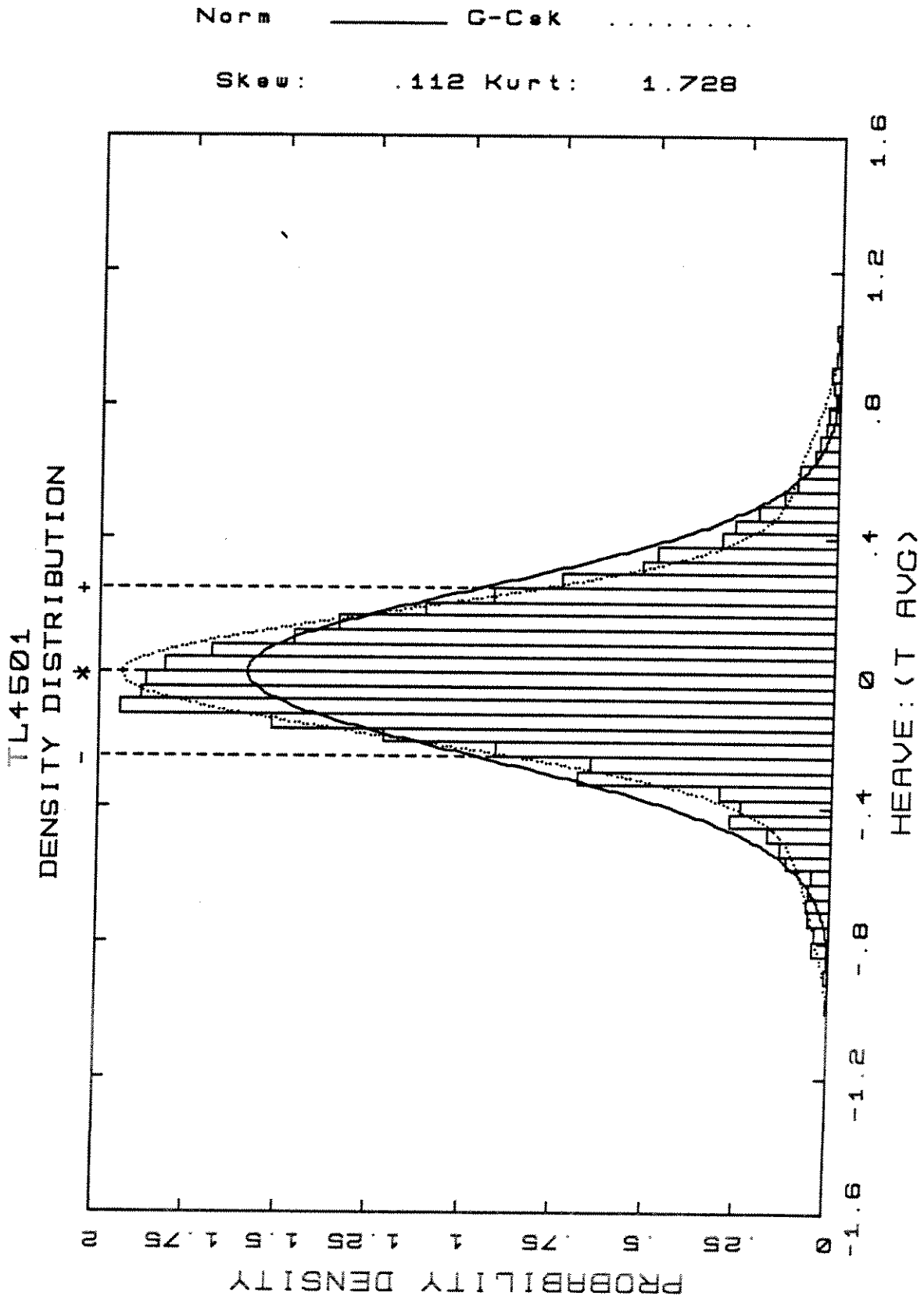

TL4501.HTavg.1

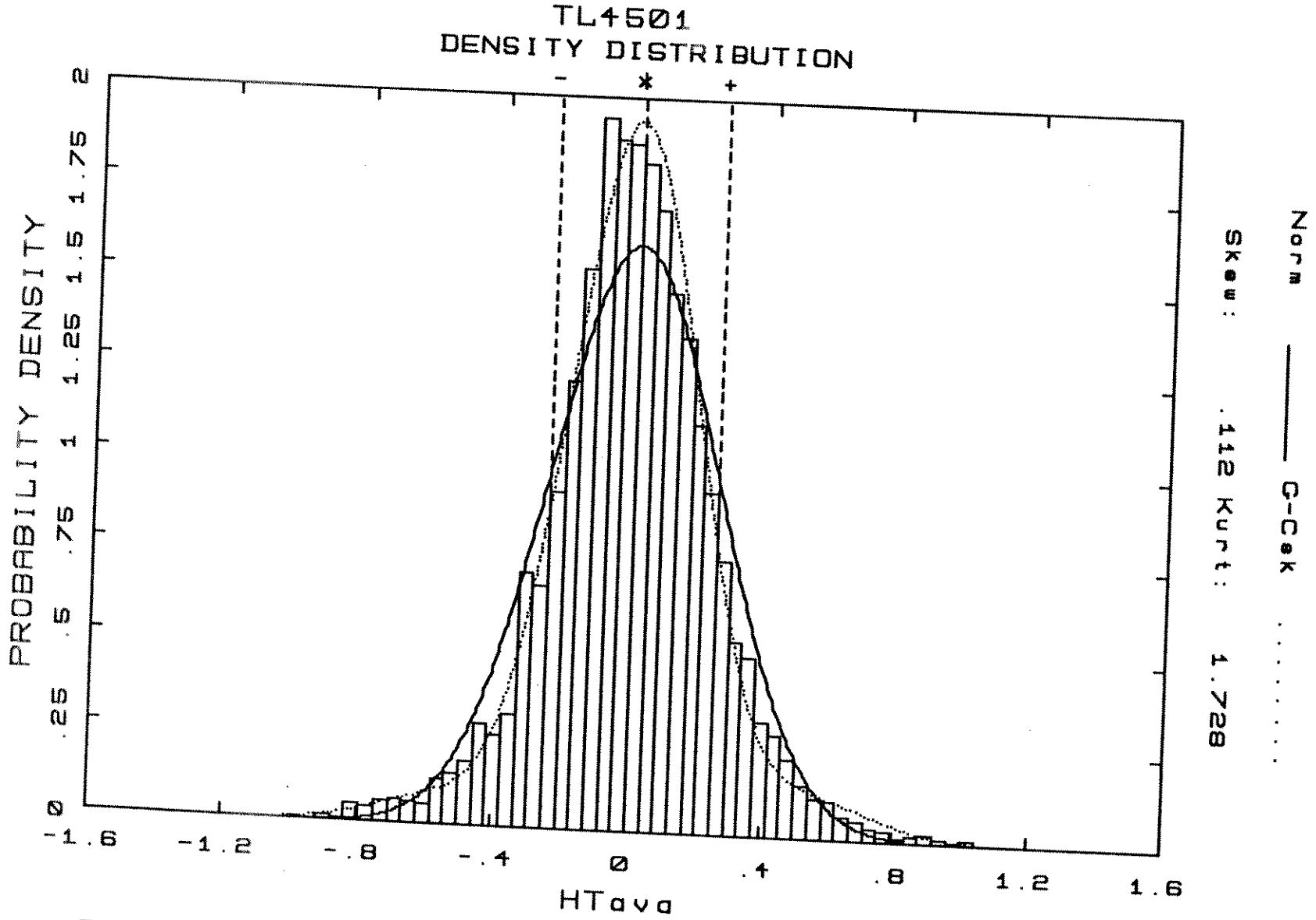

TL4501.Tavg.1

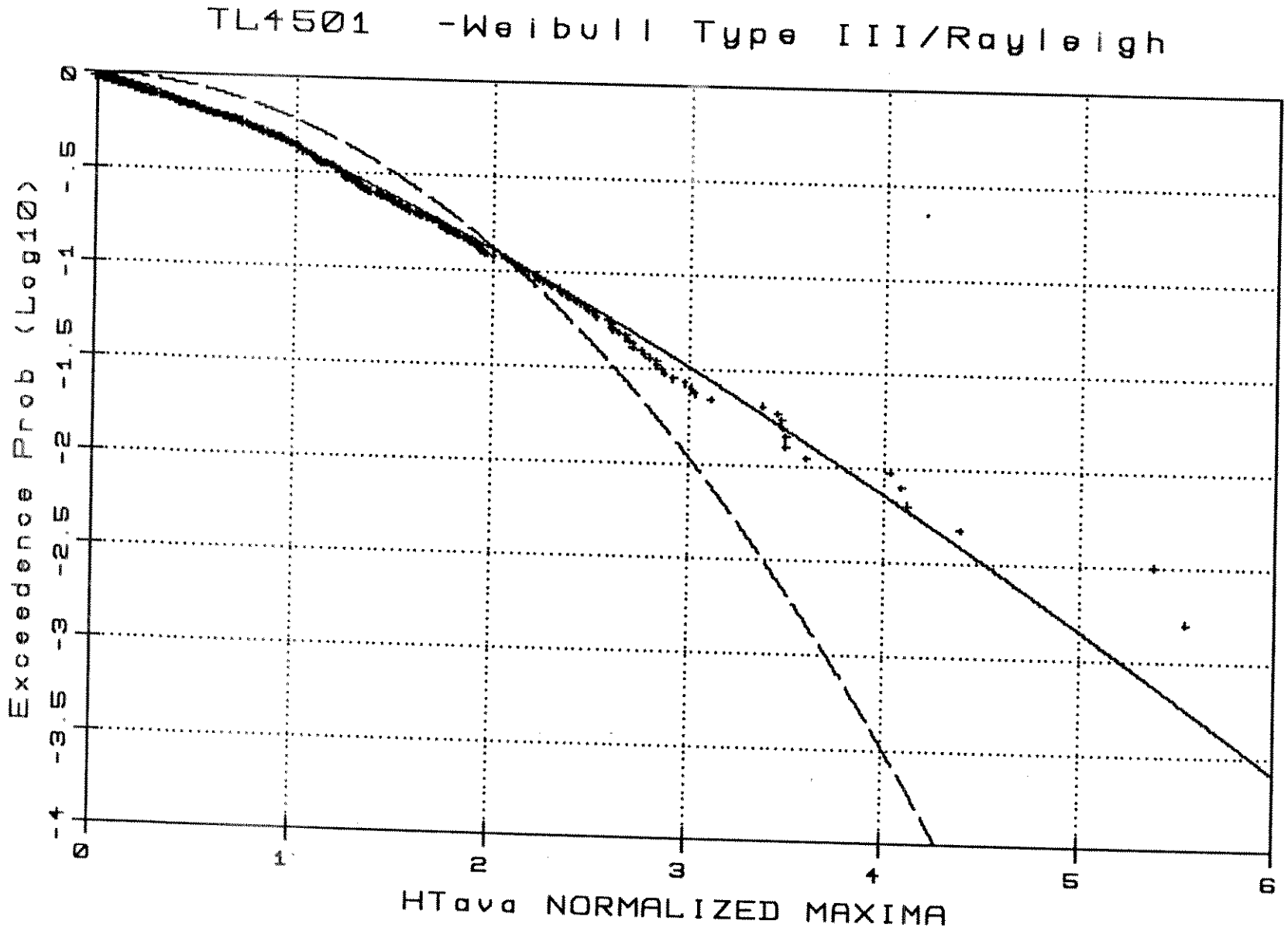

TL4501.Tavg.2

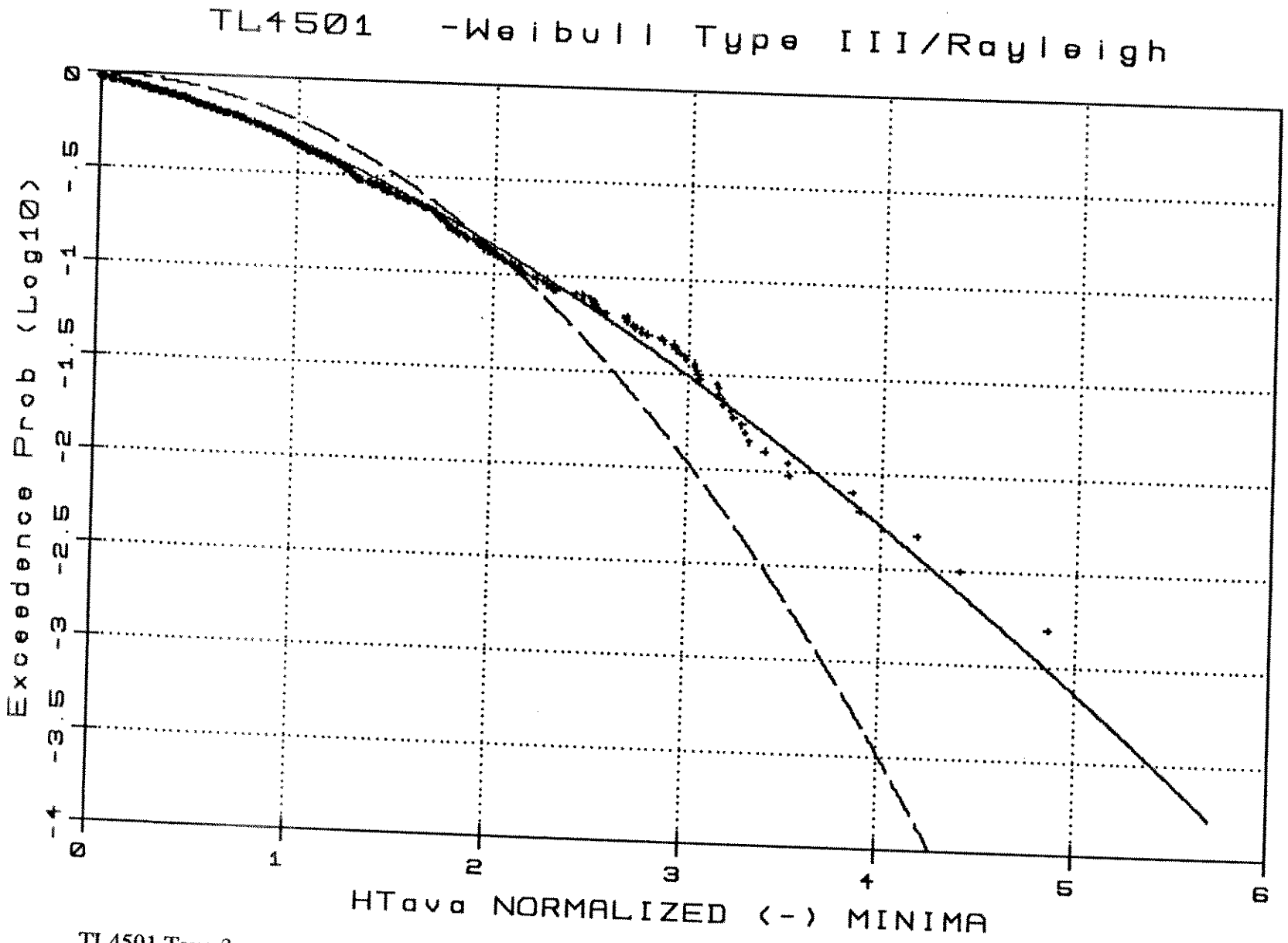

TL4501.Tavg.3

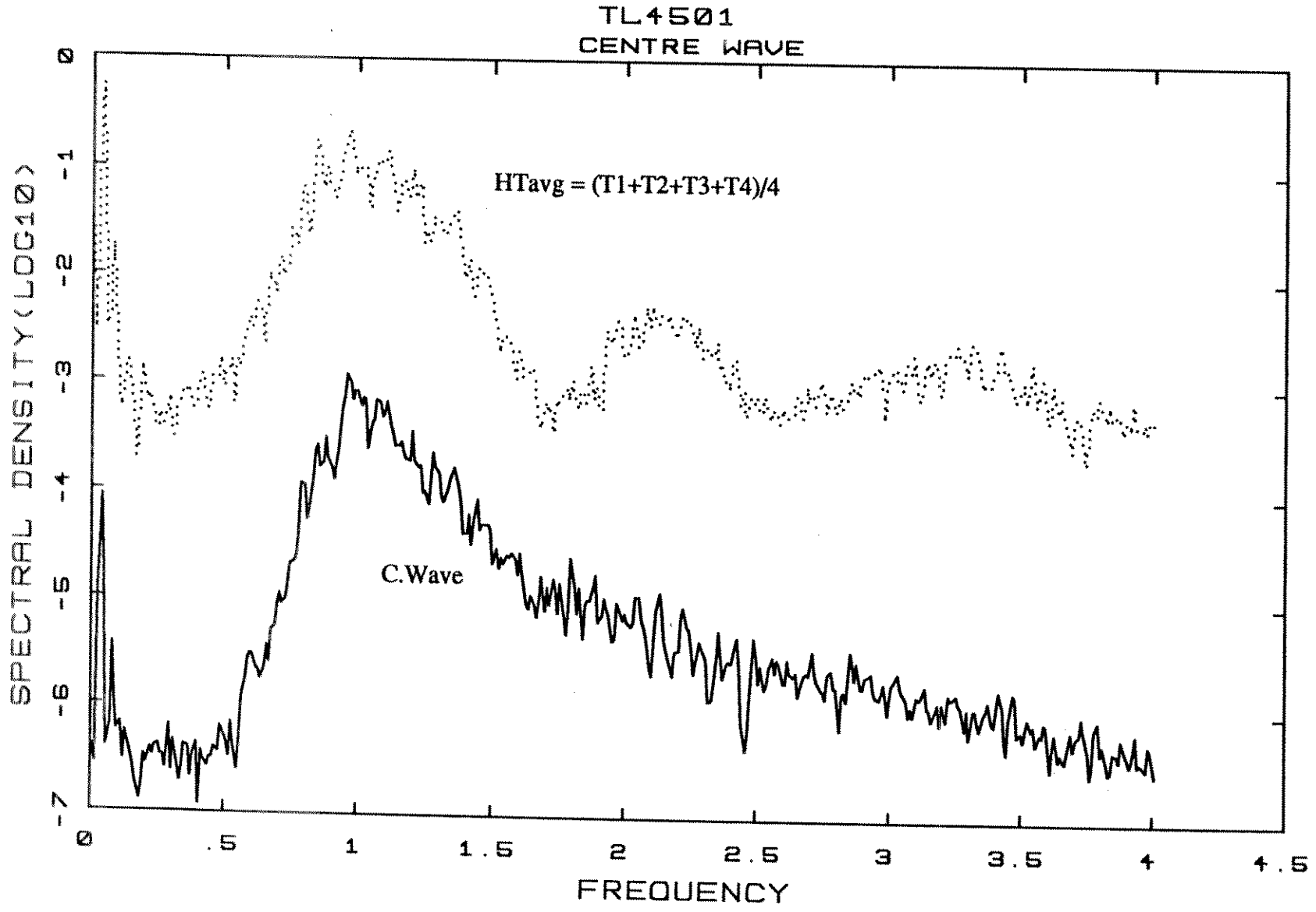

TL4501.W/HTavg.4

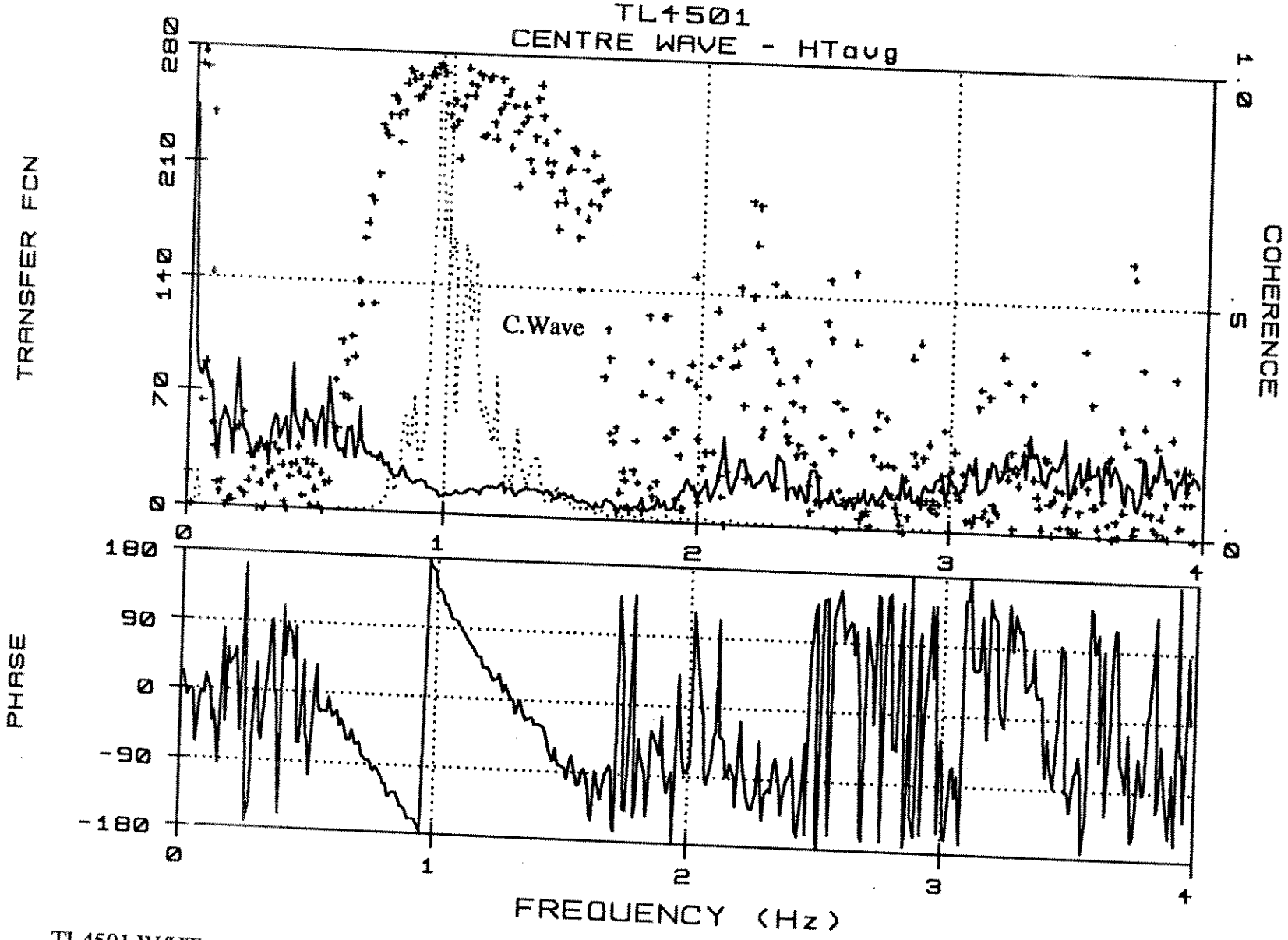

TL4501.W/HTavg.4t

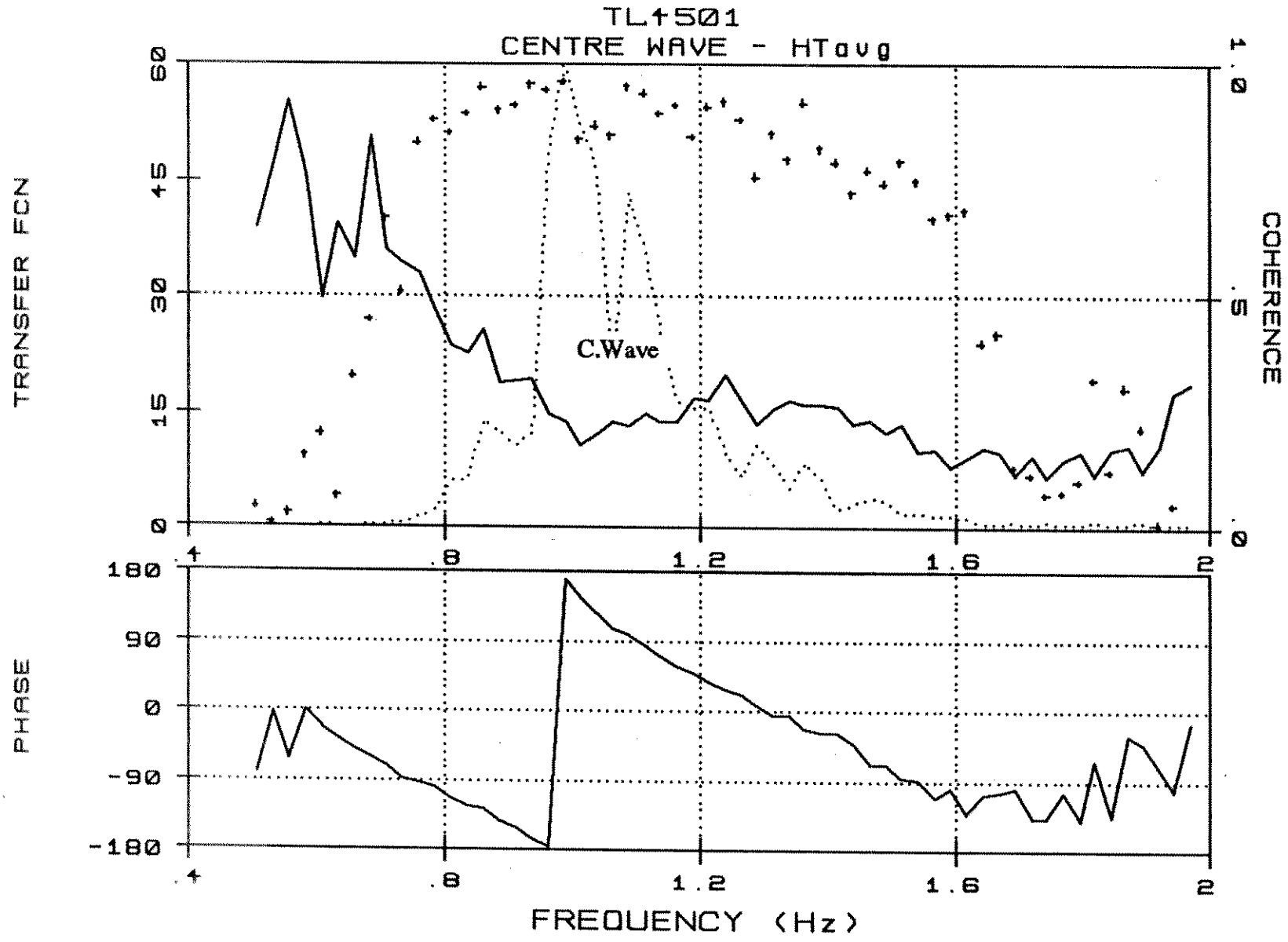

TL4501.W/HTavg.4t*

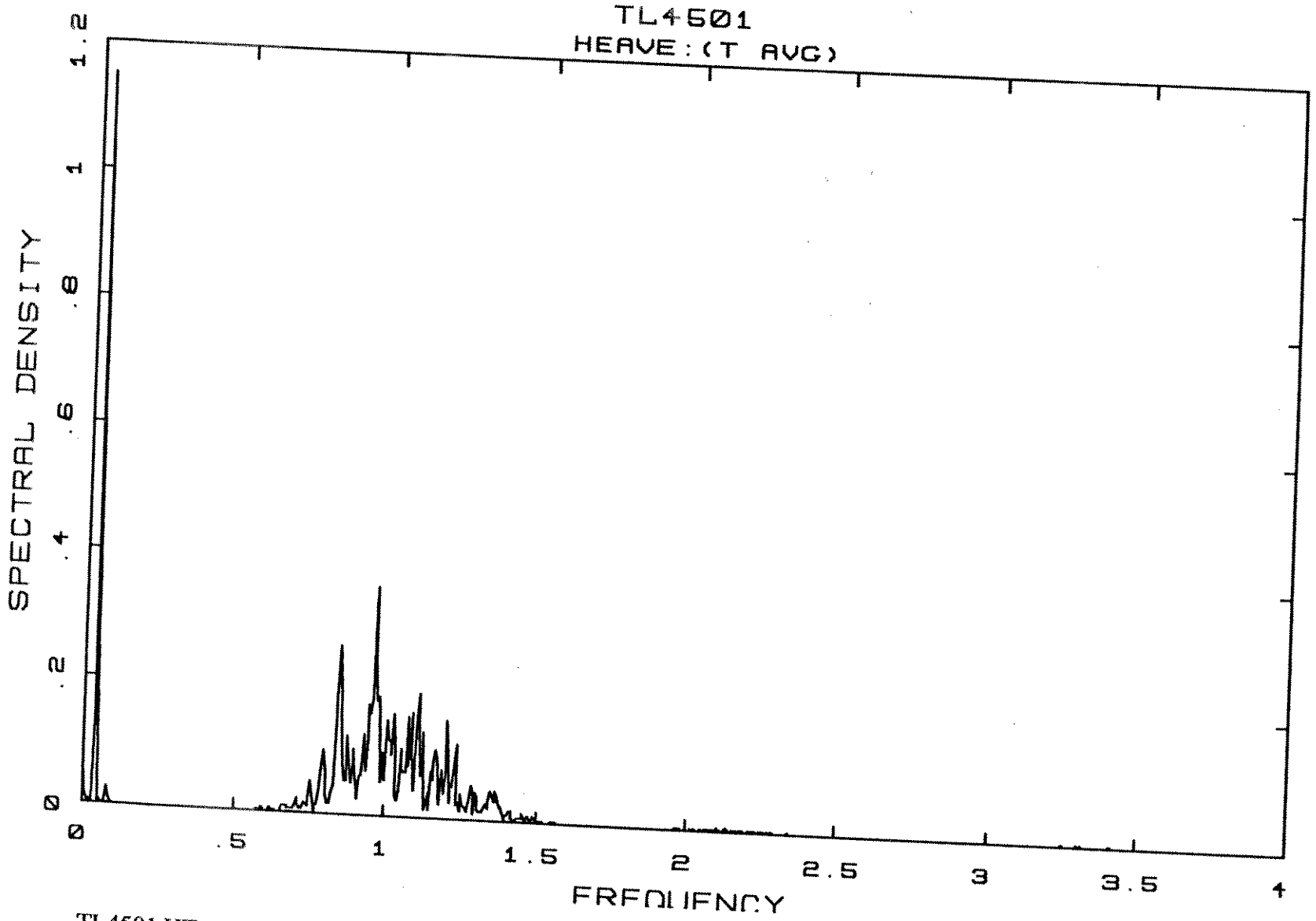

TL4501.HTavg.4

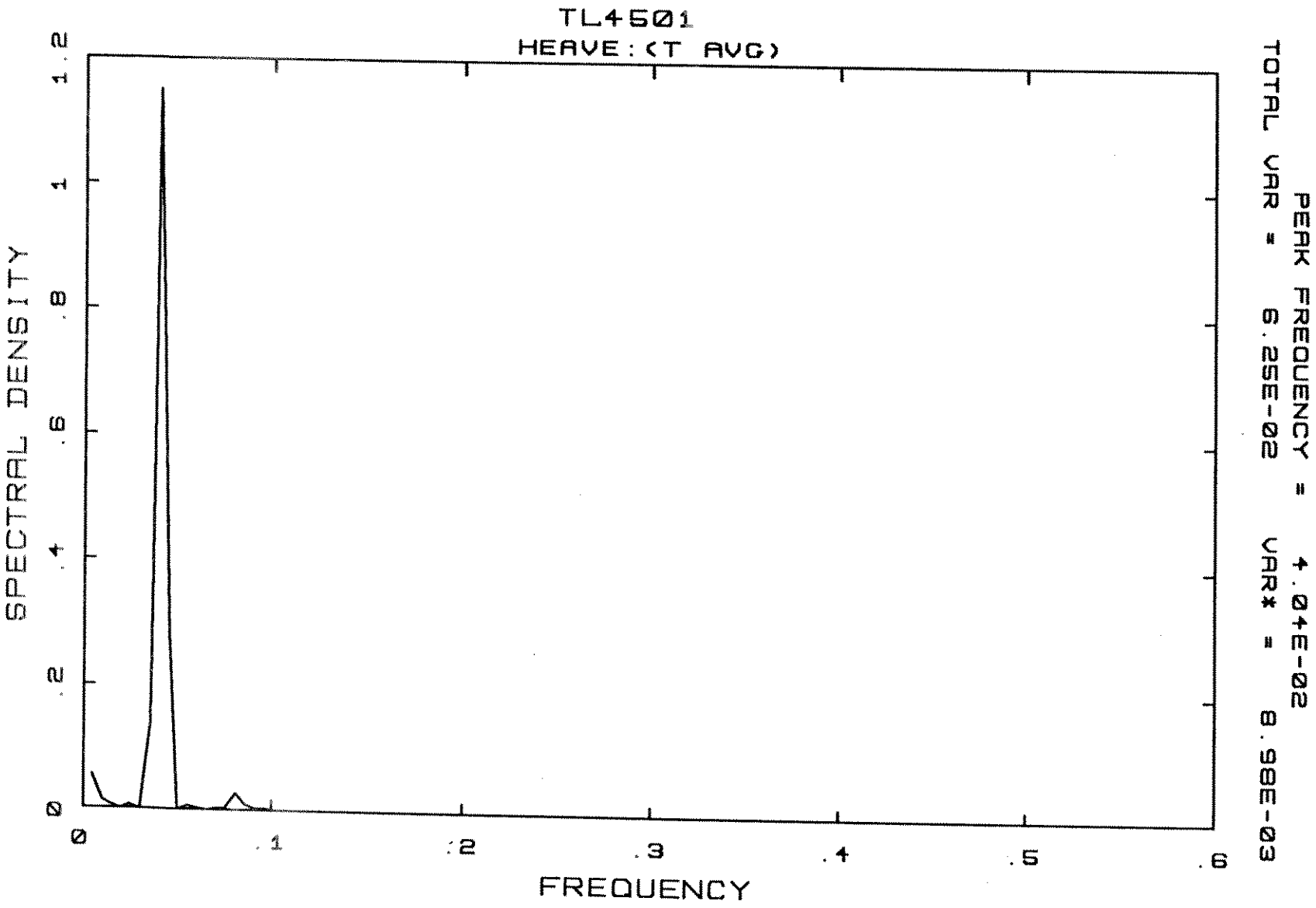

TL4501.HTavgLF.4

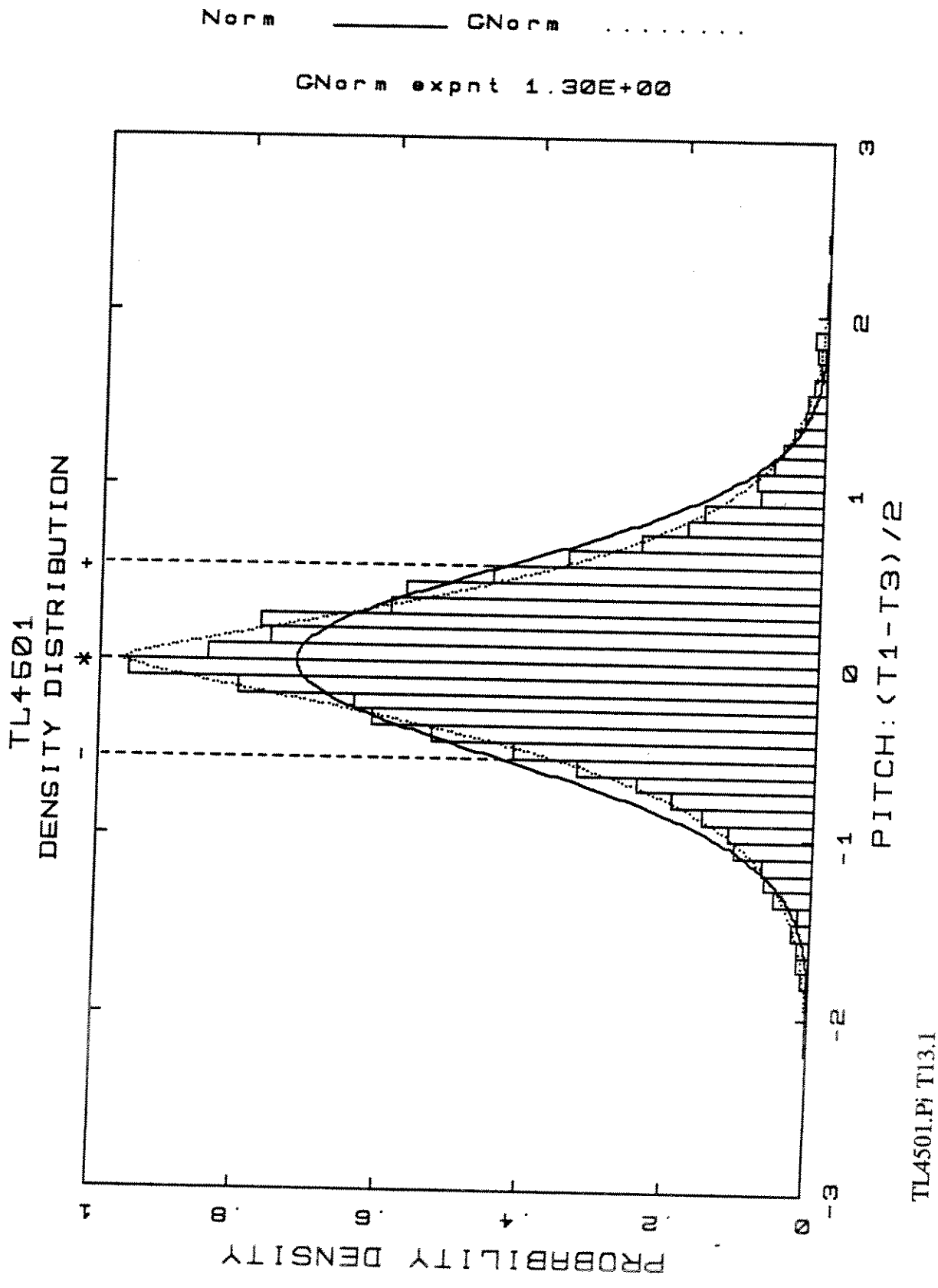
Norm
GNorm
GNorm expnt 1.30E+00
TL4501
DENSITY DISTRIBUTION
PROBABILITY DENSITY
PITCH: (T1-T3)/2
TL4501.P; T13.1

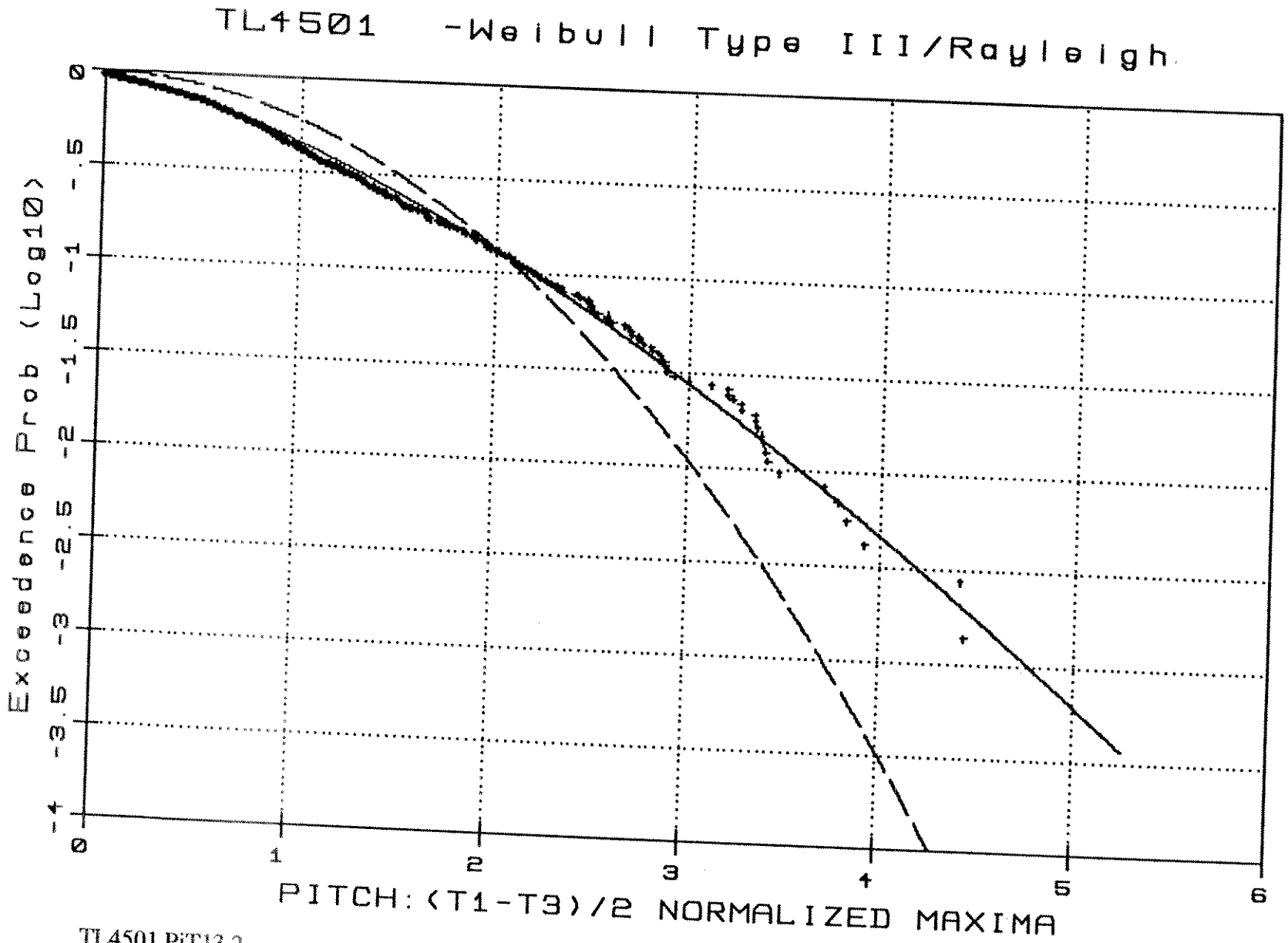

TL4501.PiT13.2

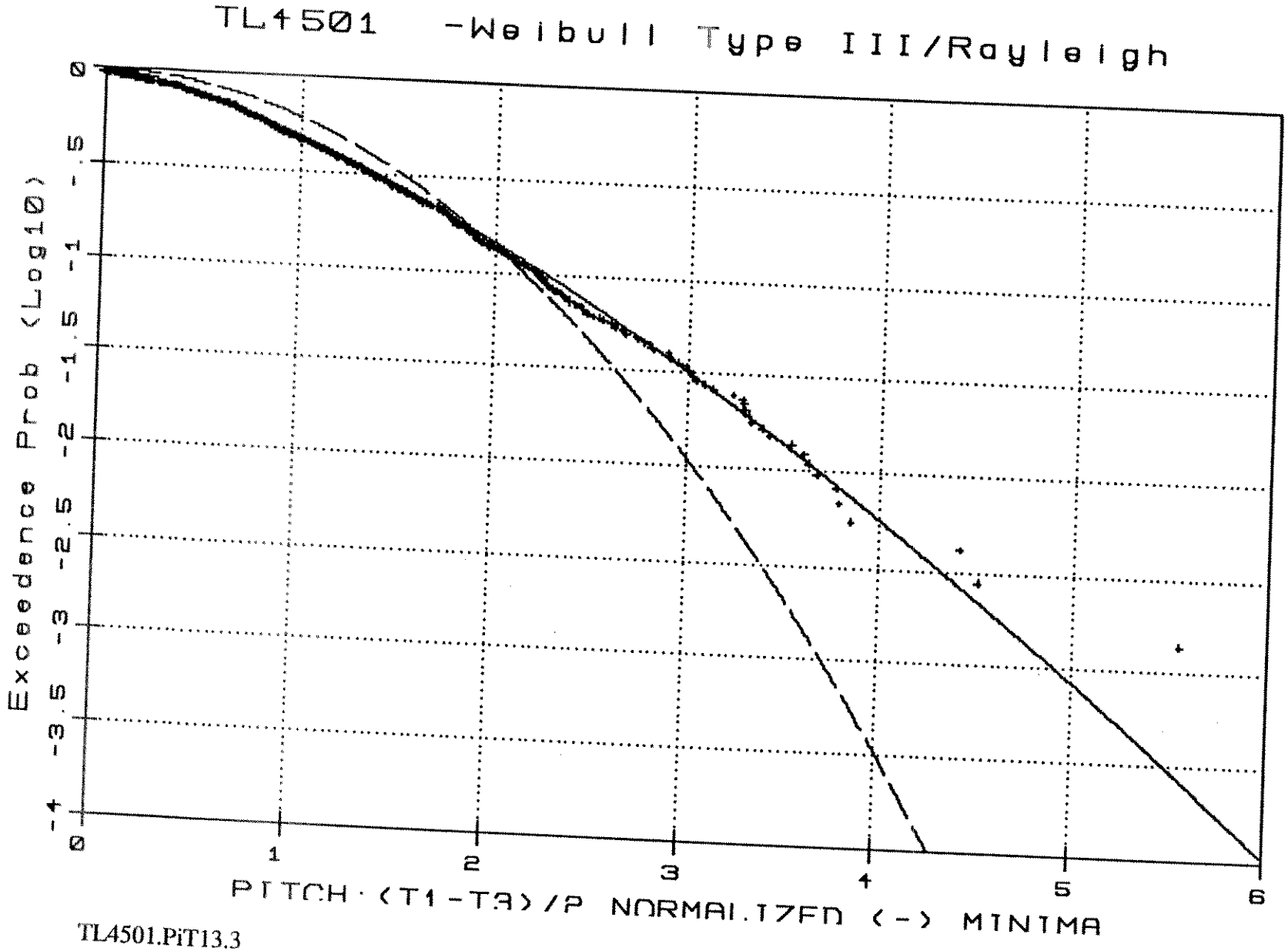

TL4501.PiT13.3

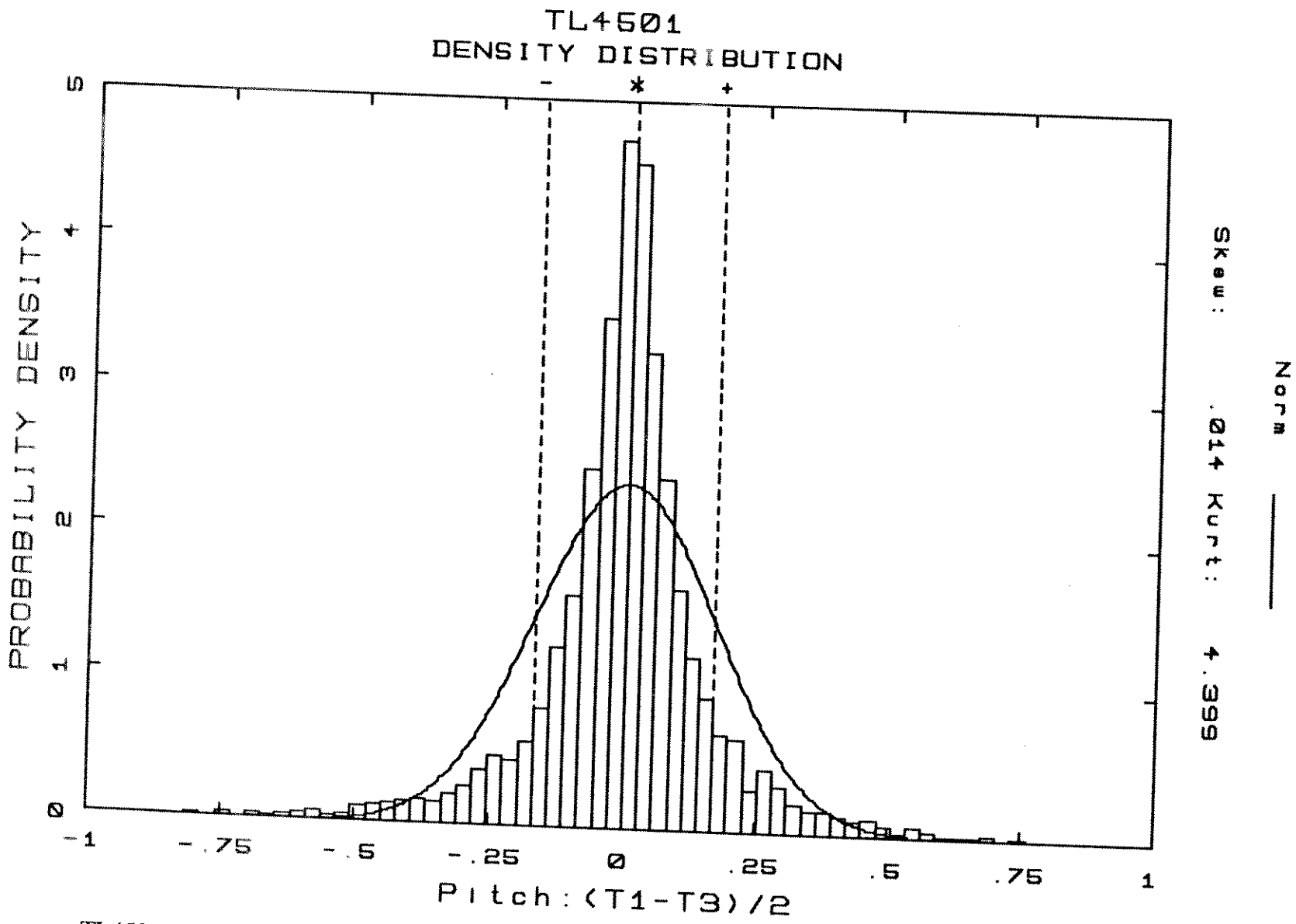

TL4501.PiT13HF.1

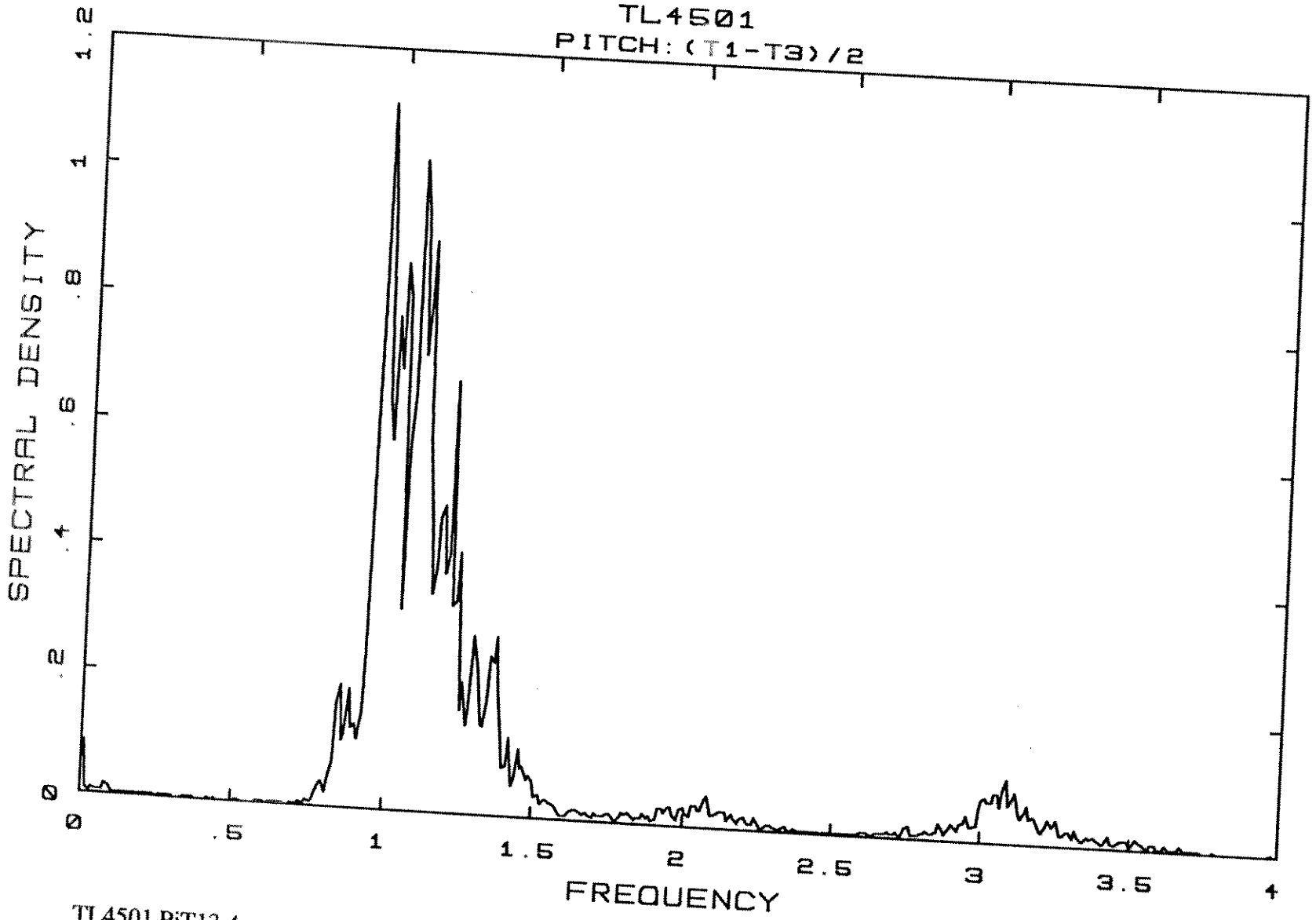

TL4501.PiT13.4

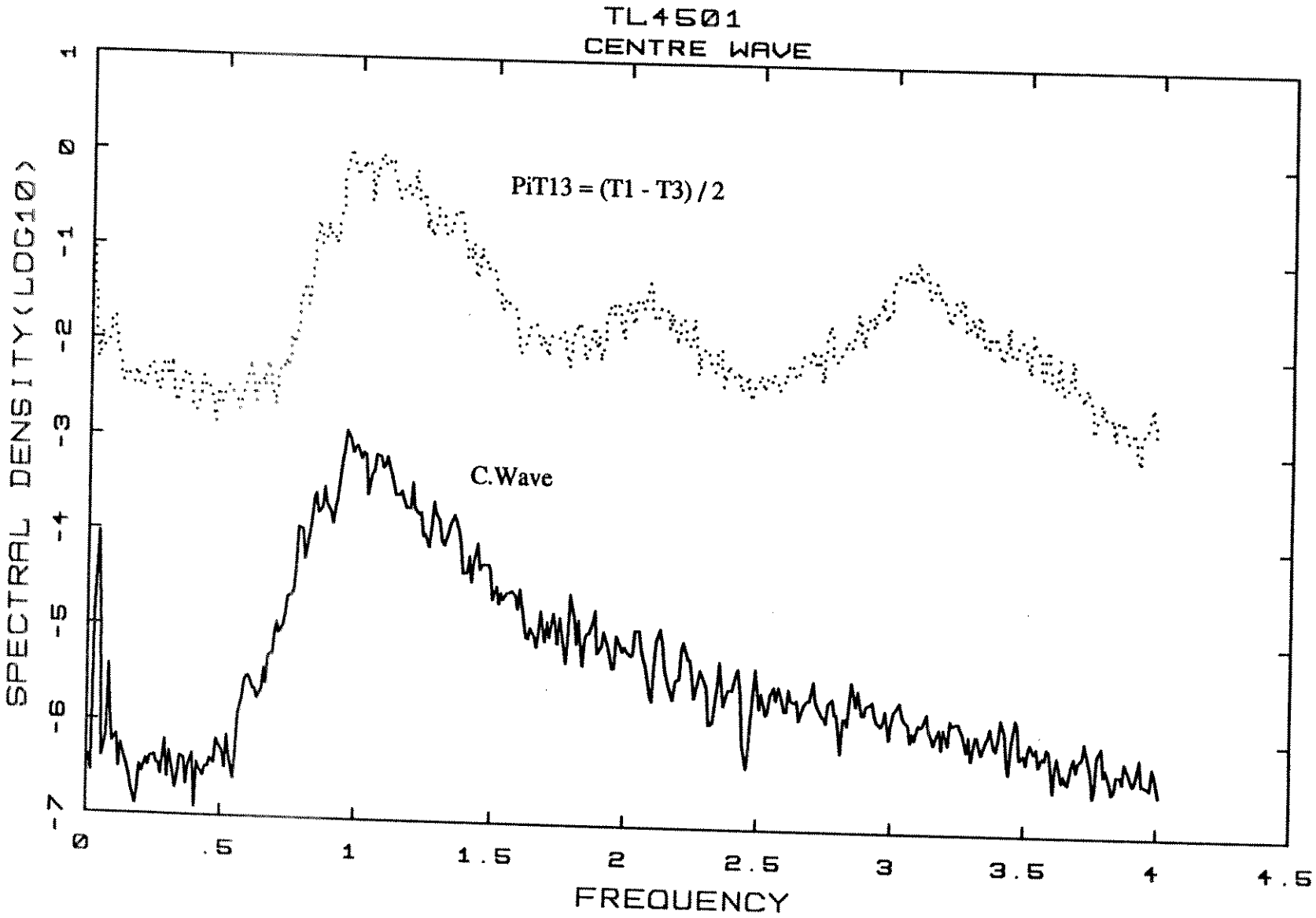

TL4501.W/PiT13.4

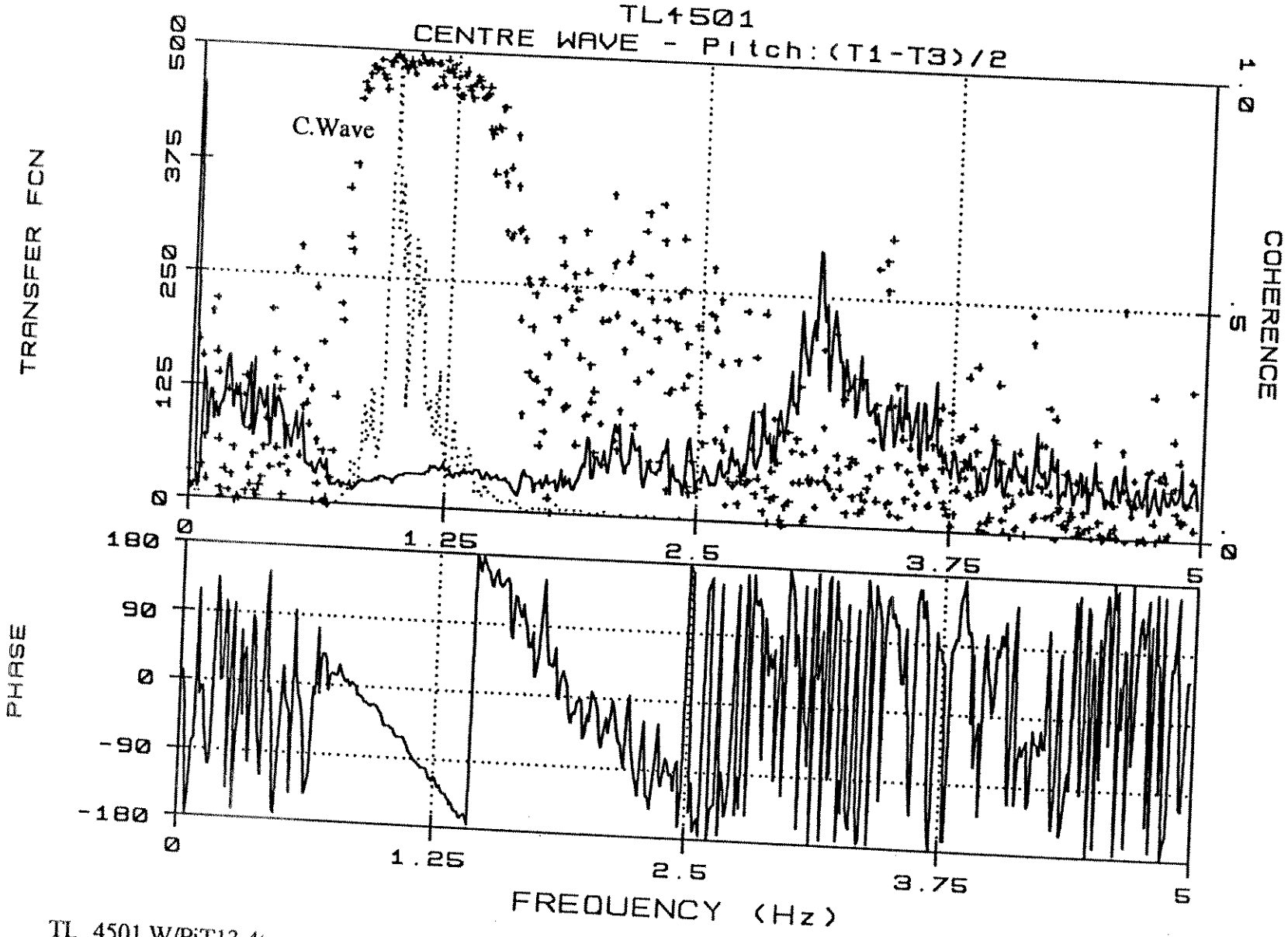

TL 4501.W/PiT13.4t

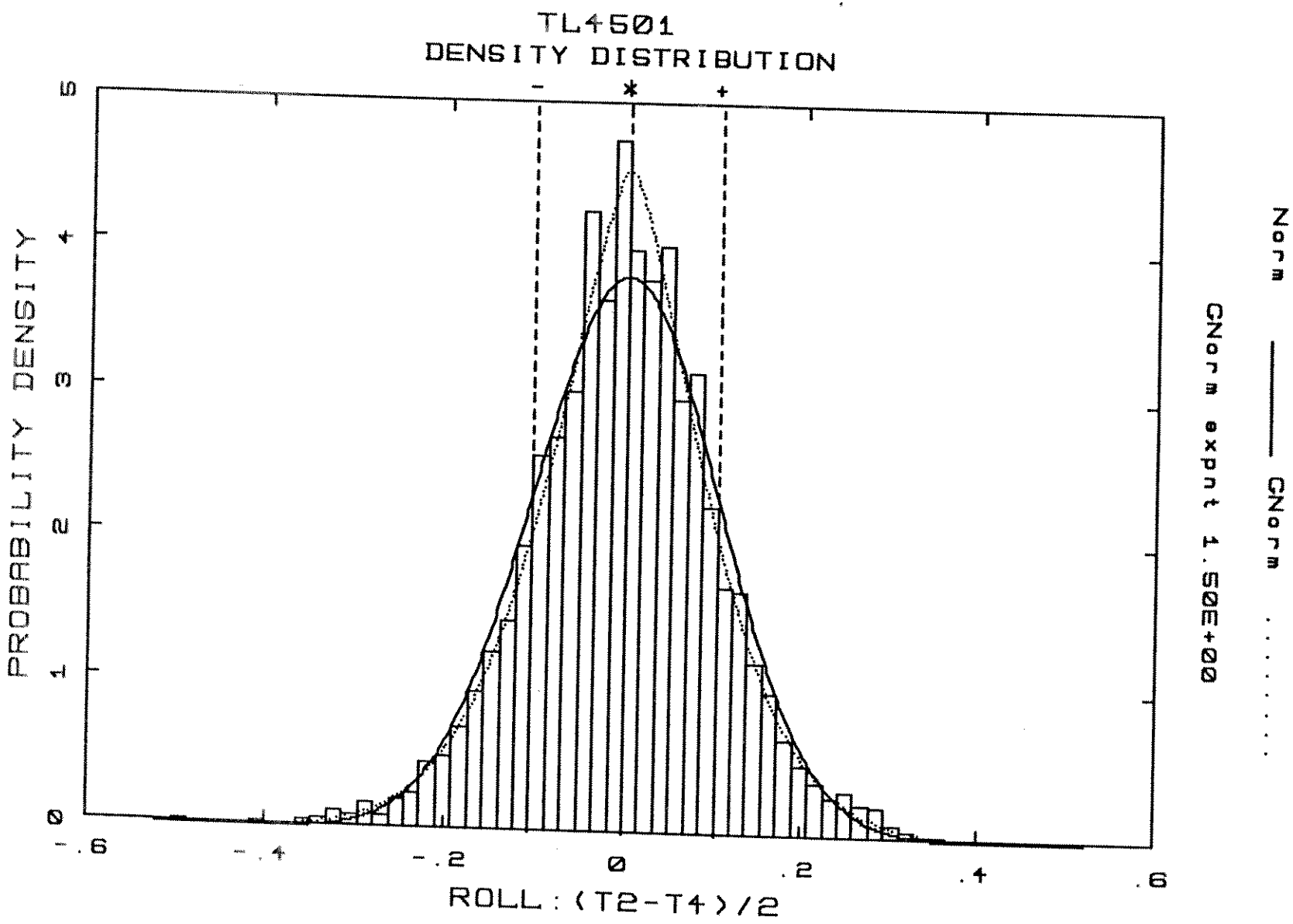

TL4501.RoT24.1

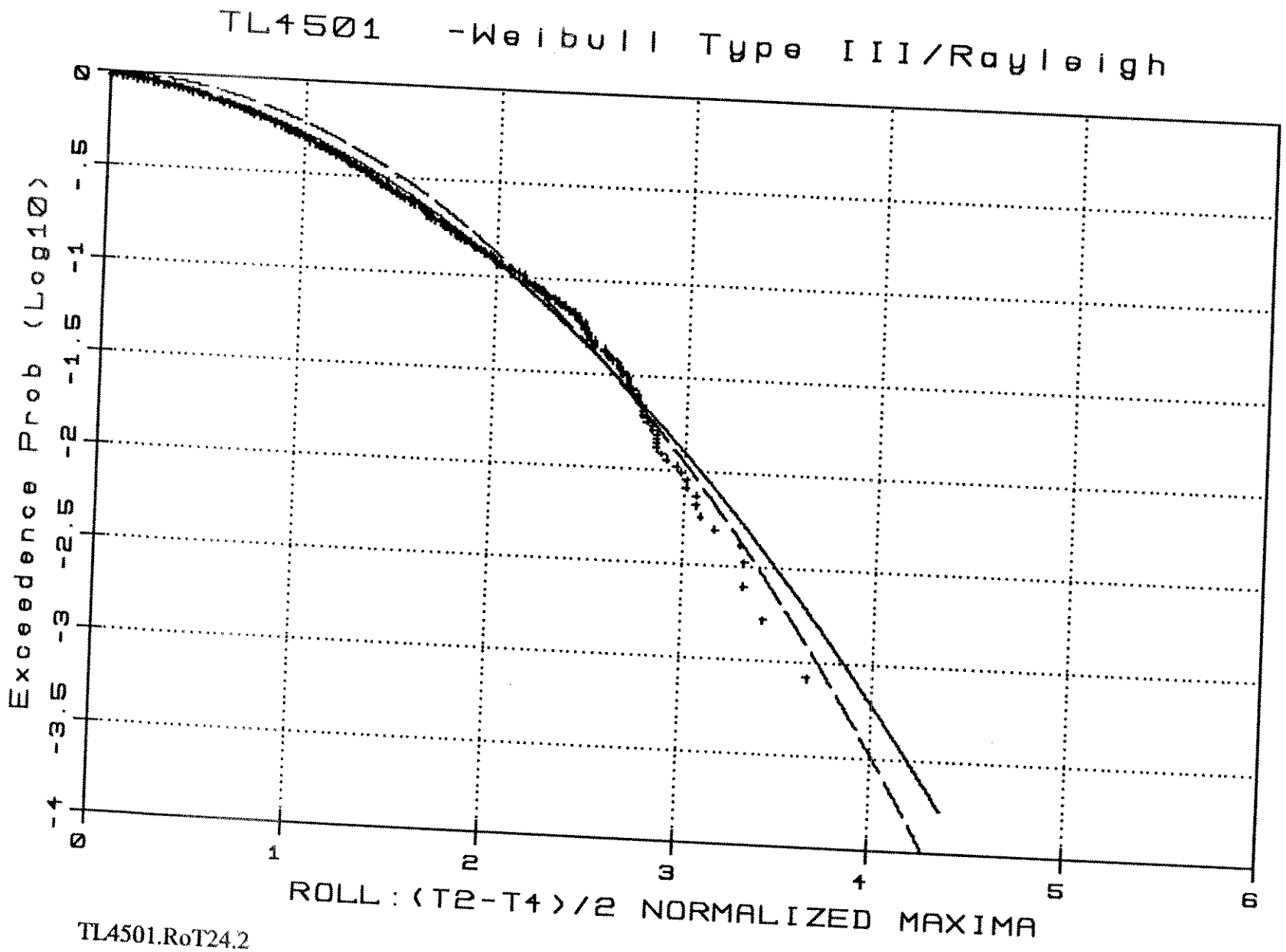

TL4501.RoT24.2

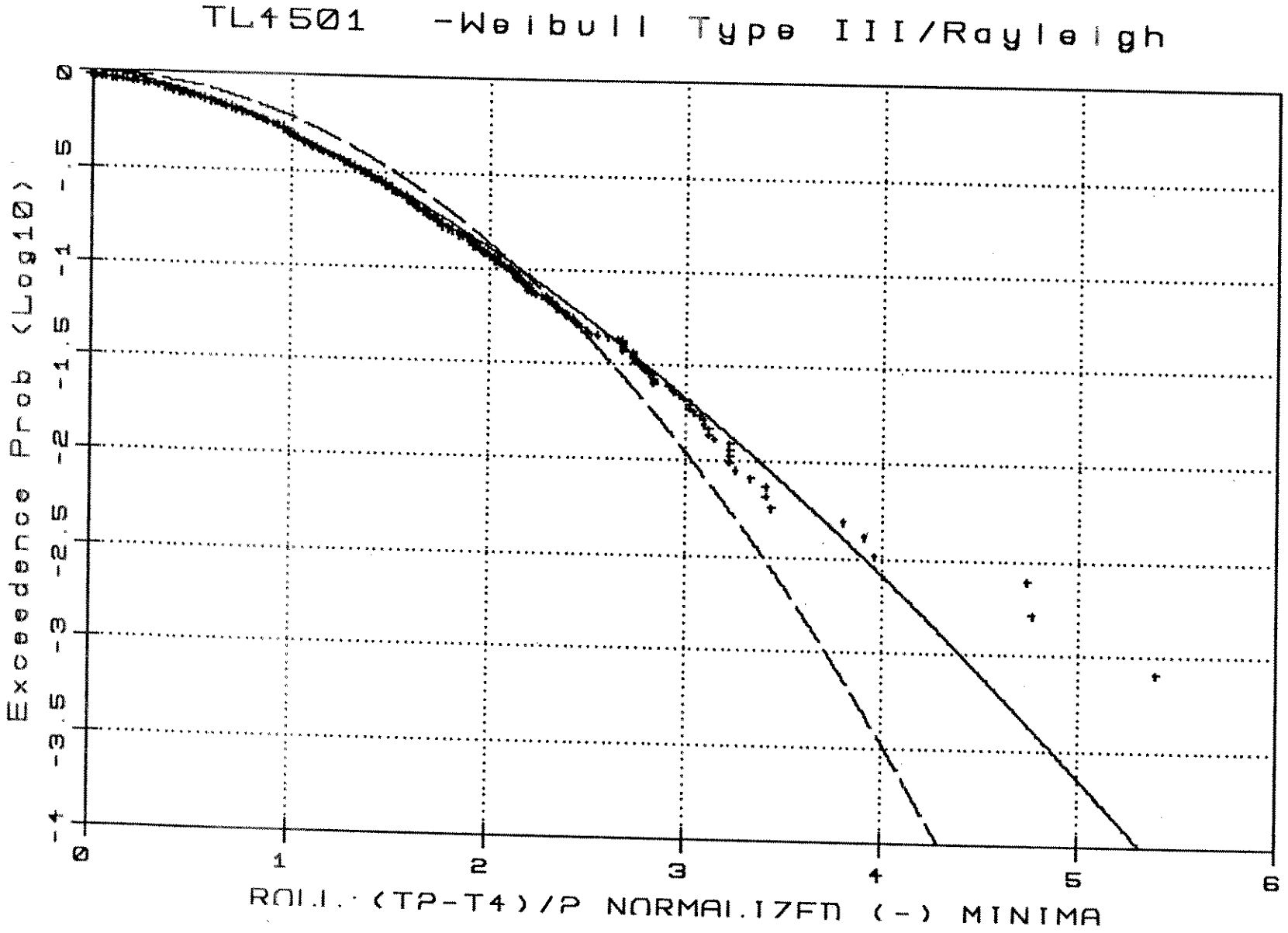

TL4501.RoT24.3

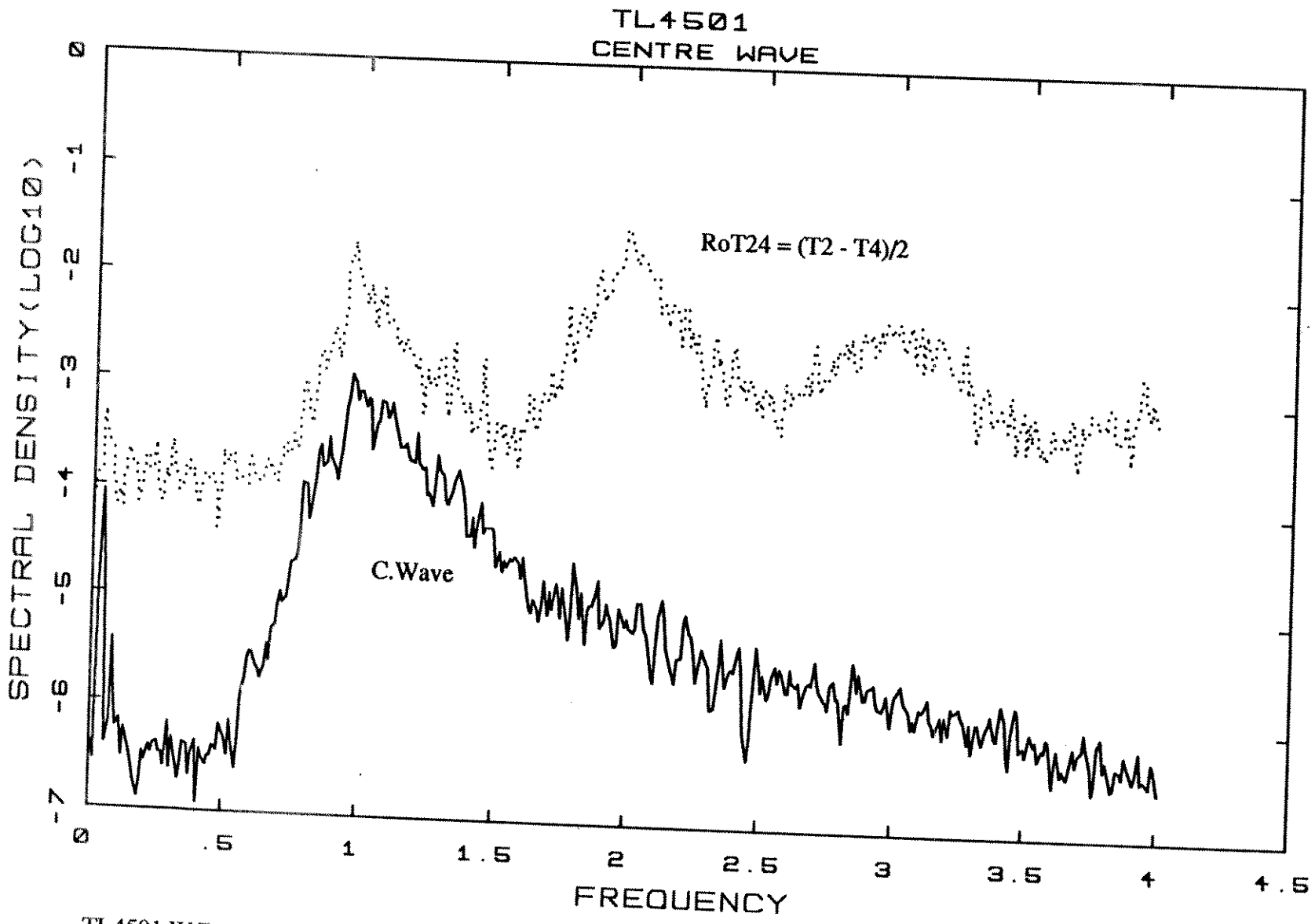

TL4501.W/RoT24.4

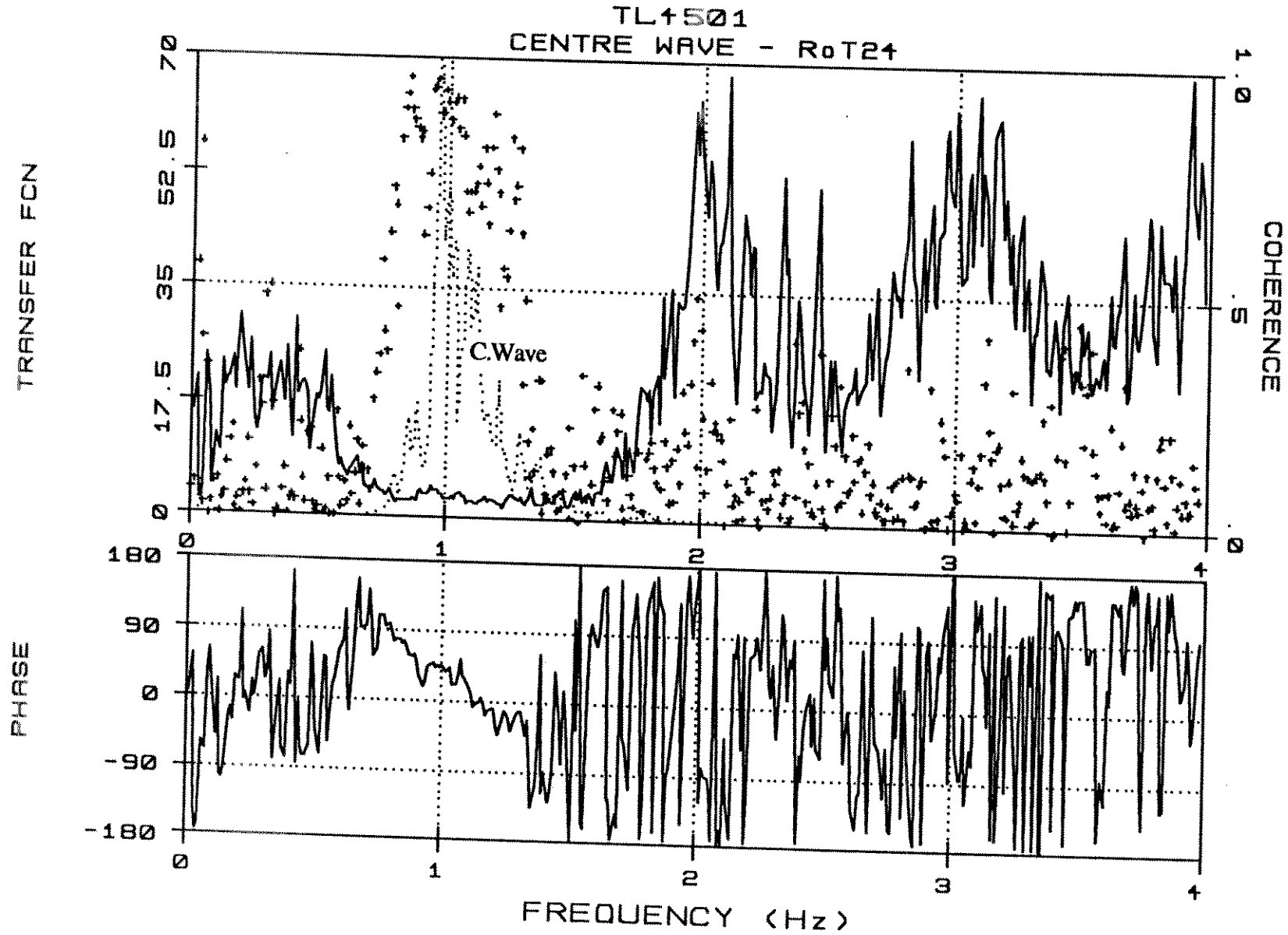

TL4501.W/RoT24.4t

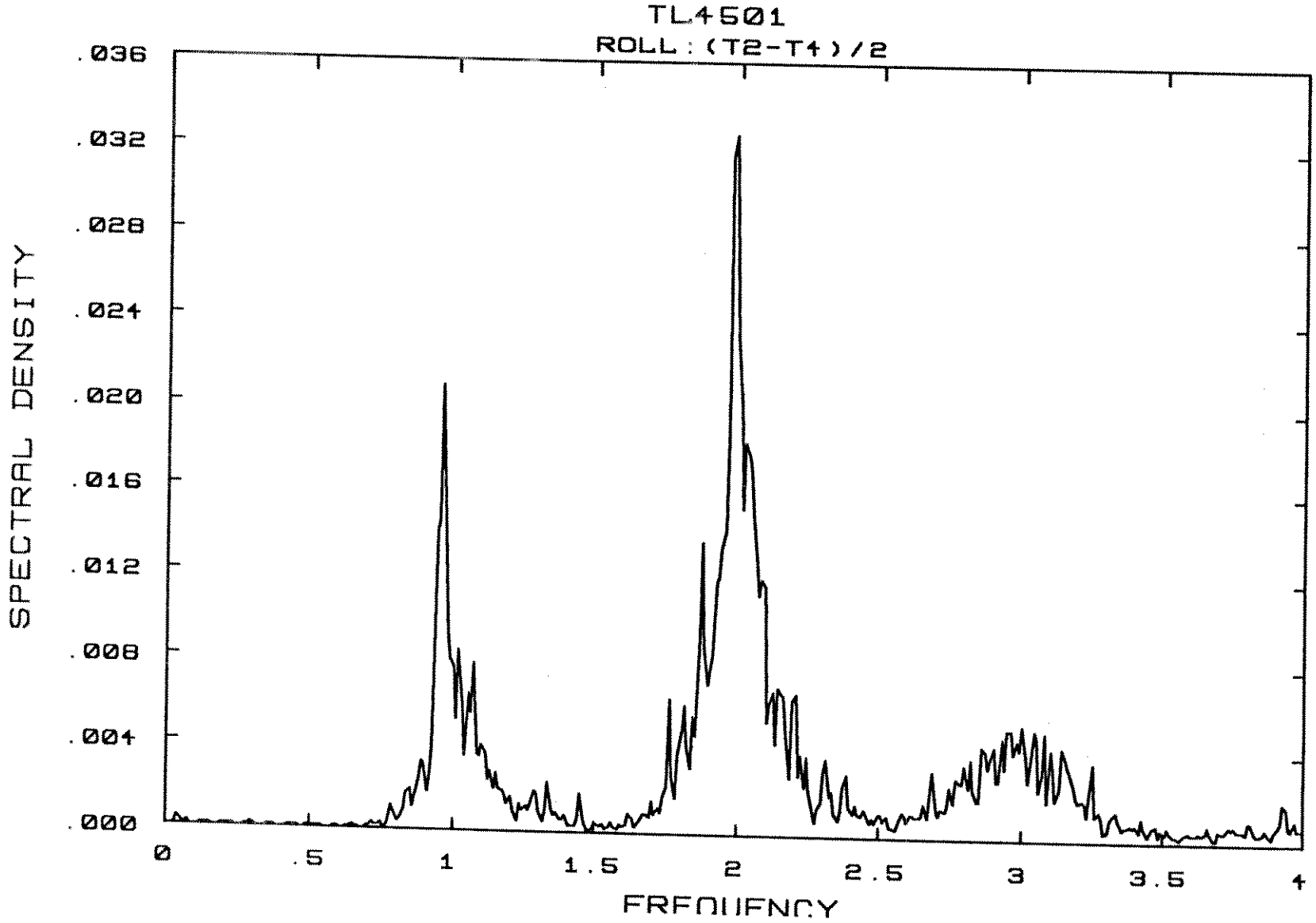

TL4501.RoT24.4

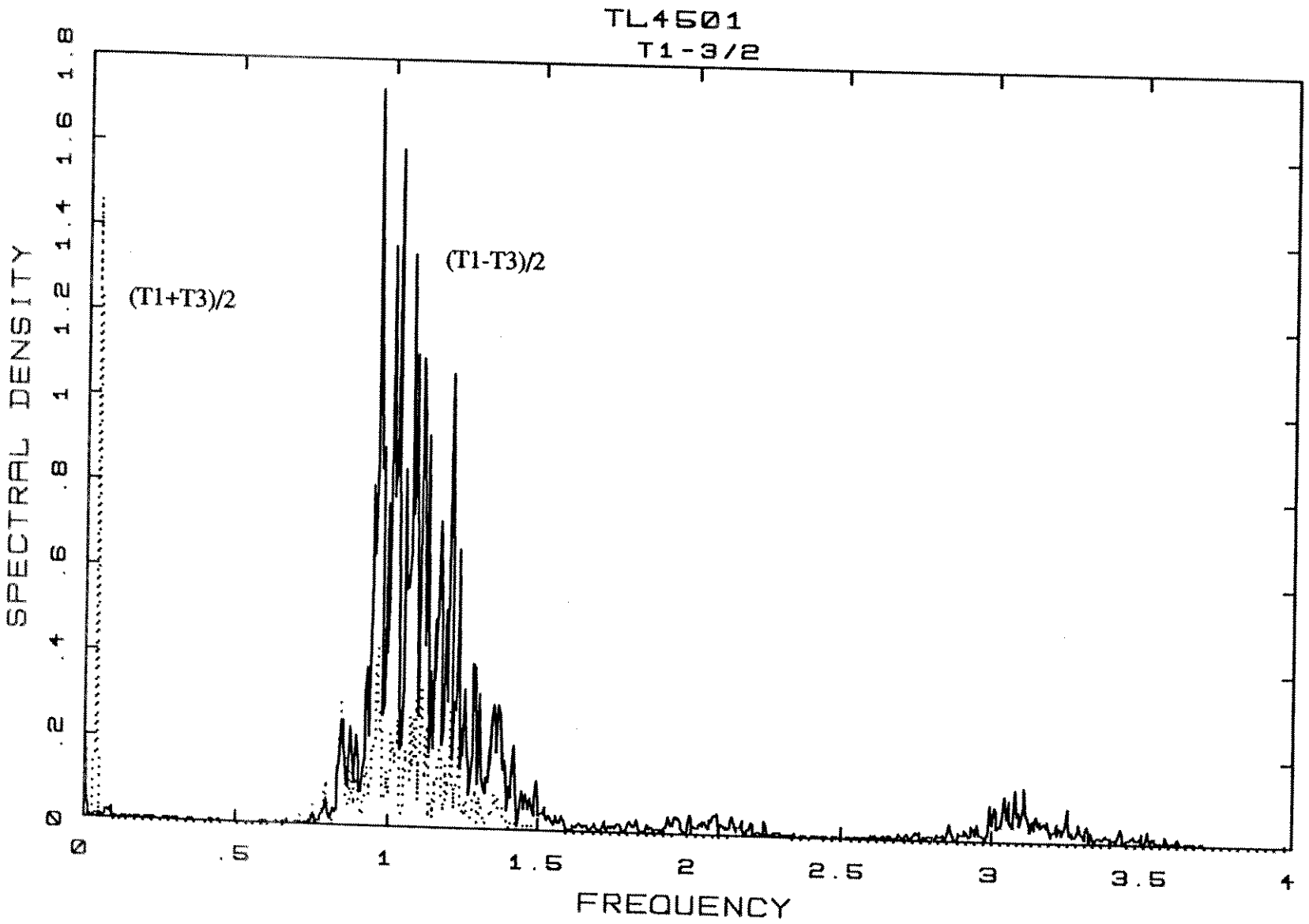

L4501.PI/HT13.4

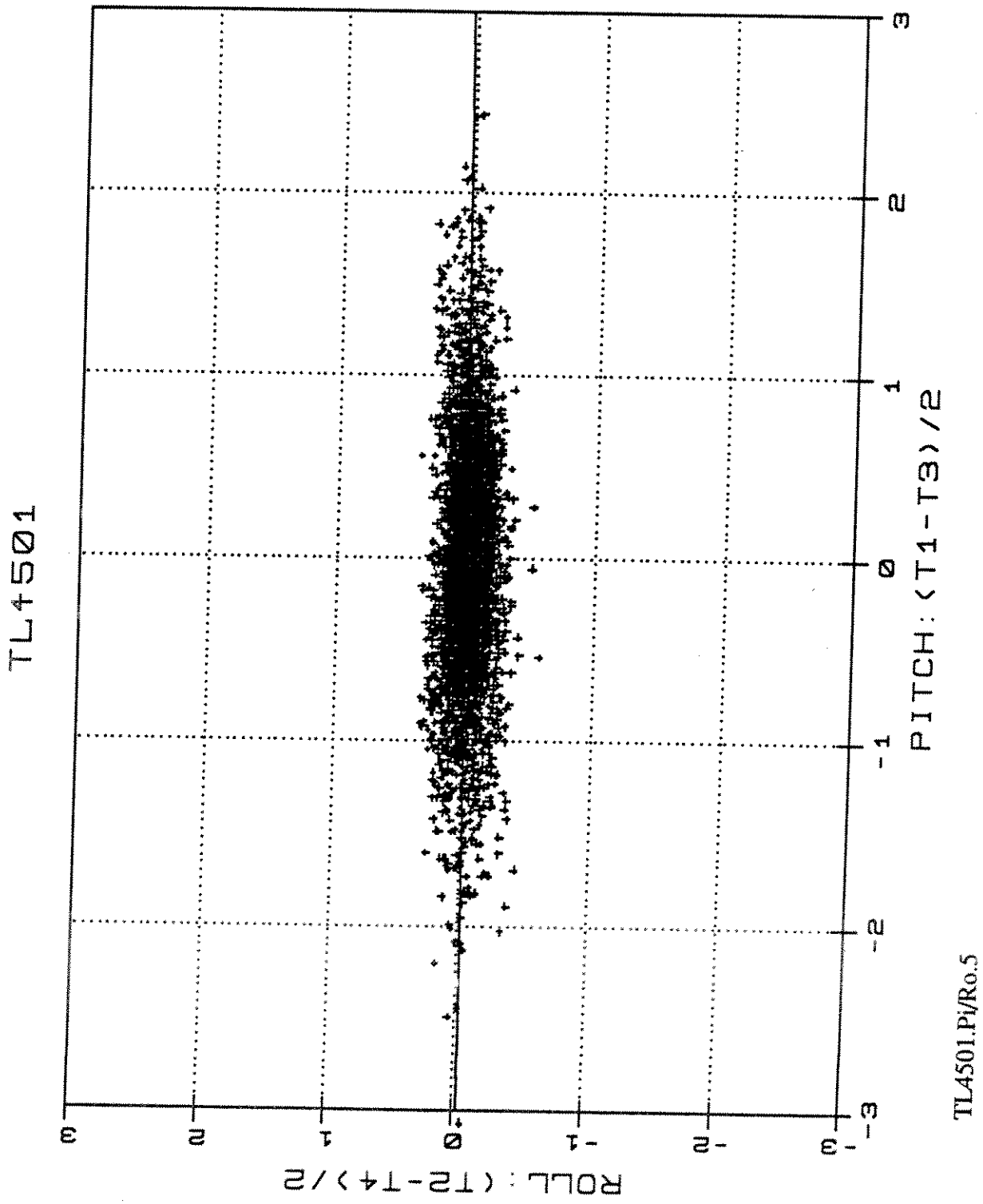

TL4501.Pi/Ro.5

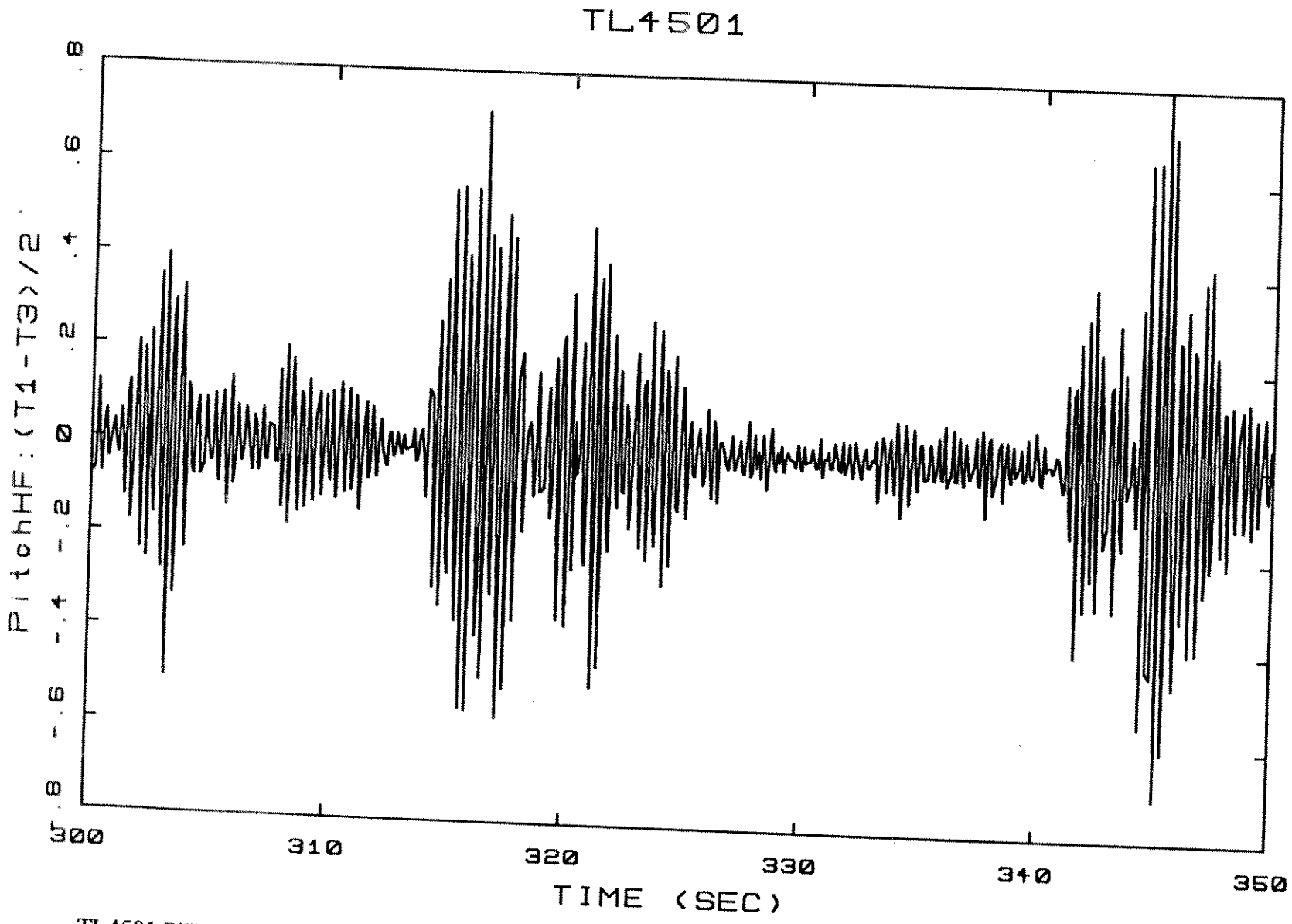

TL4501.PiT13HF.TIM

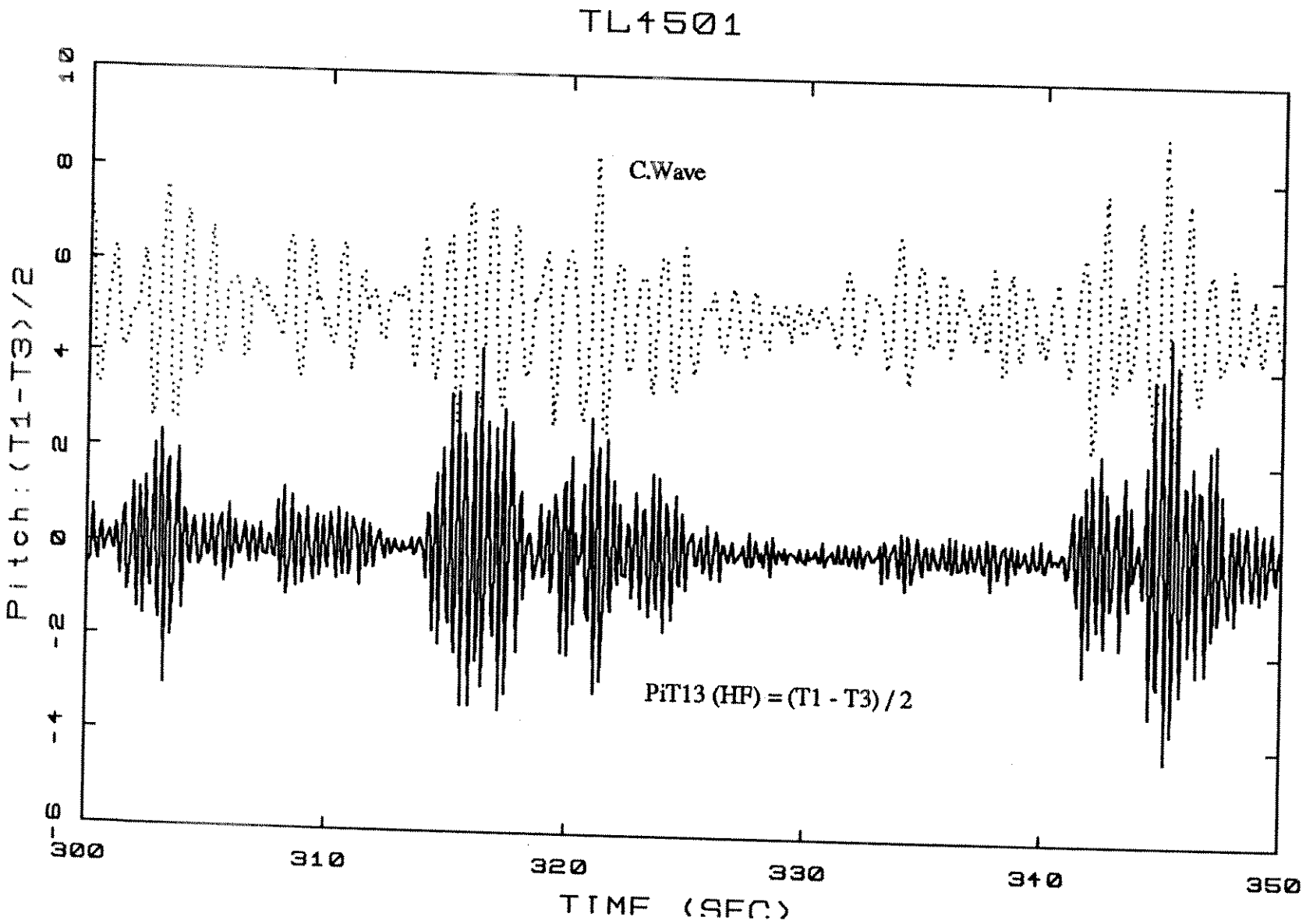

TL4501.W/PiT13HF.TIM

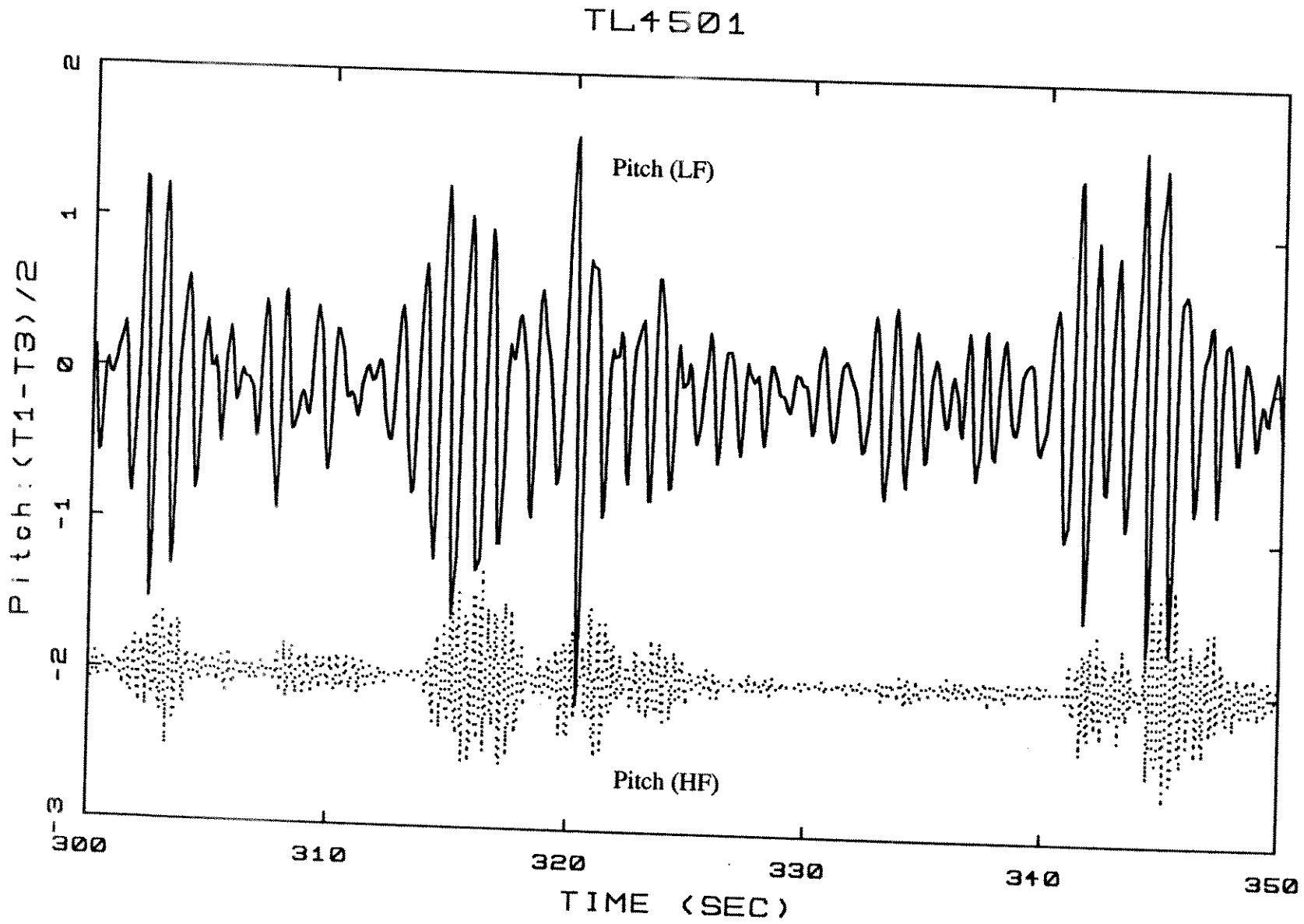

TL4501.PiT13HF/LF.TIM
High Frequency Pitch (HF) Offset = -2.0

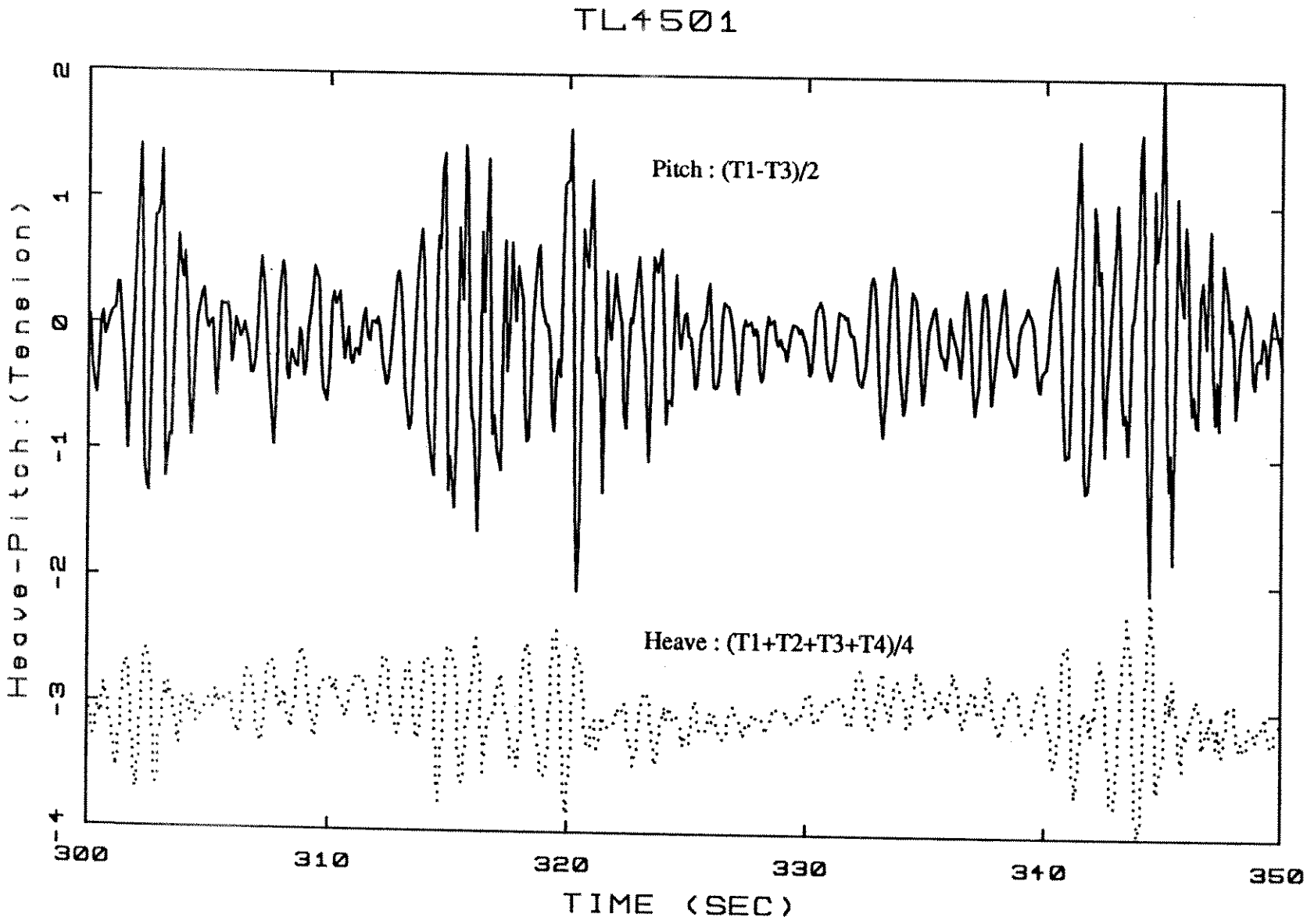

TL4501.HTavgPiT13.TIM
Heave (Averaged Tension) Offset -3.0

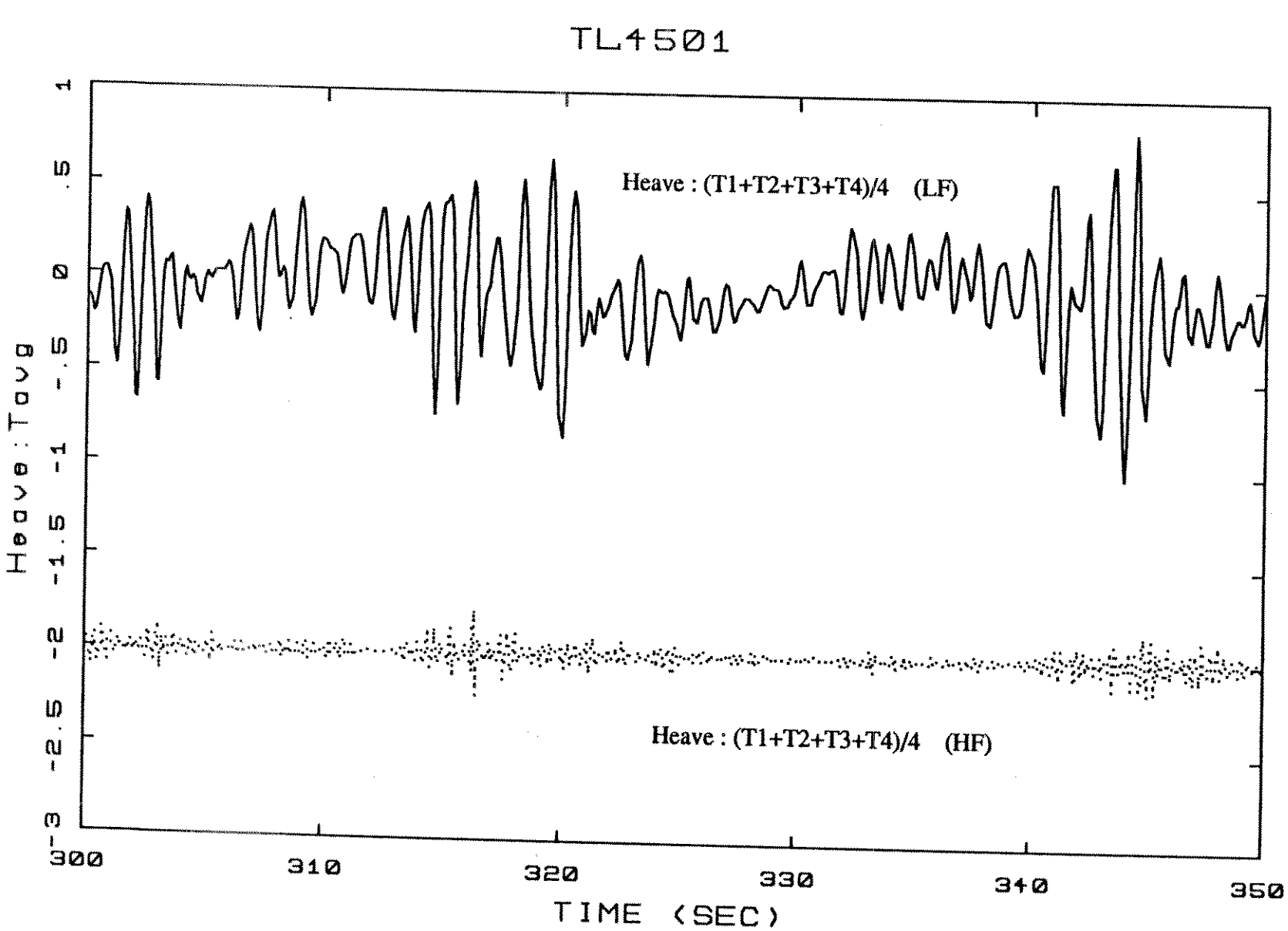

TL4501.HTavgHF/LF.TIM

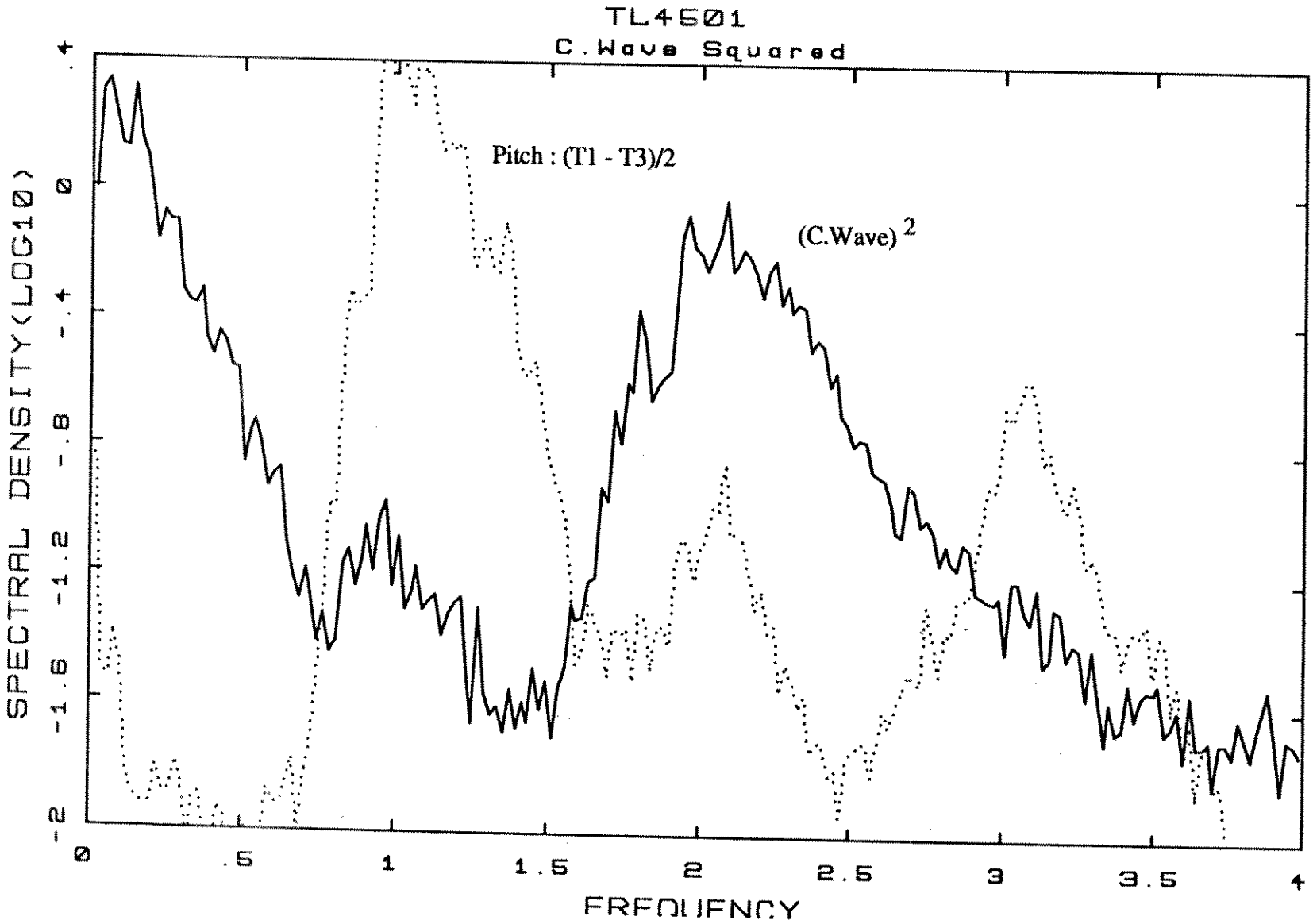

TL4501.WSQ/PiT13.4
C.Wave Squared and Pitch are normalized

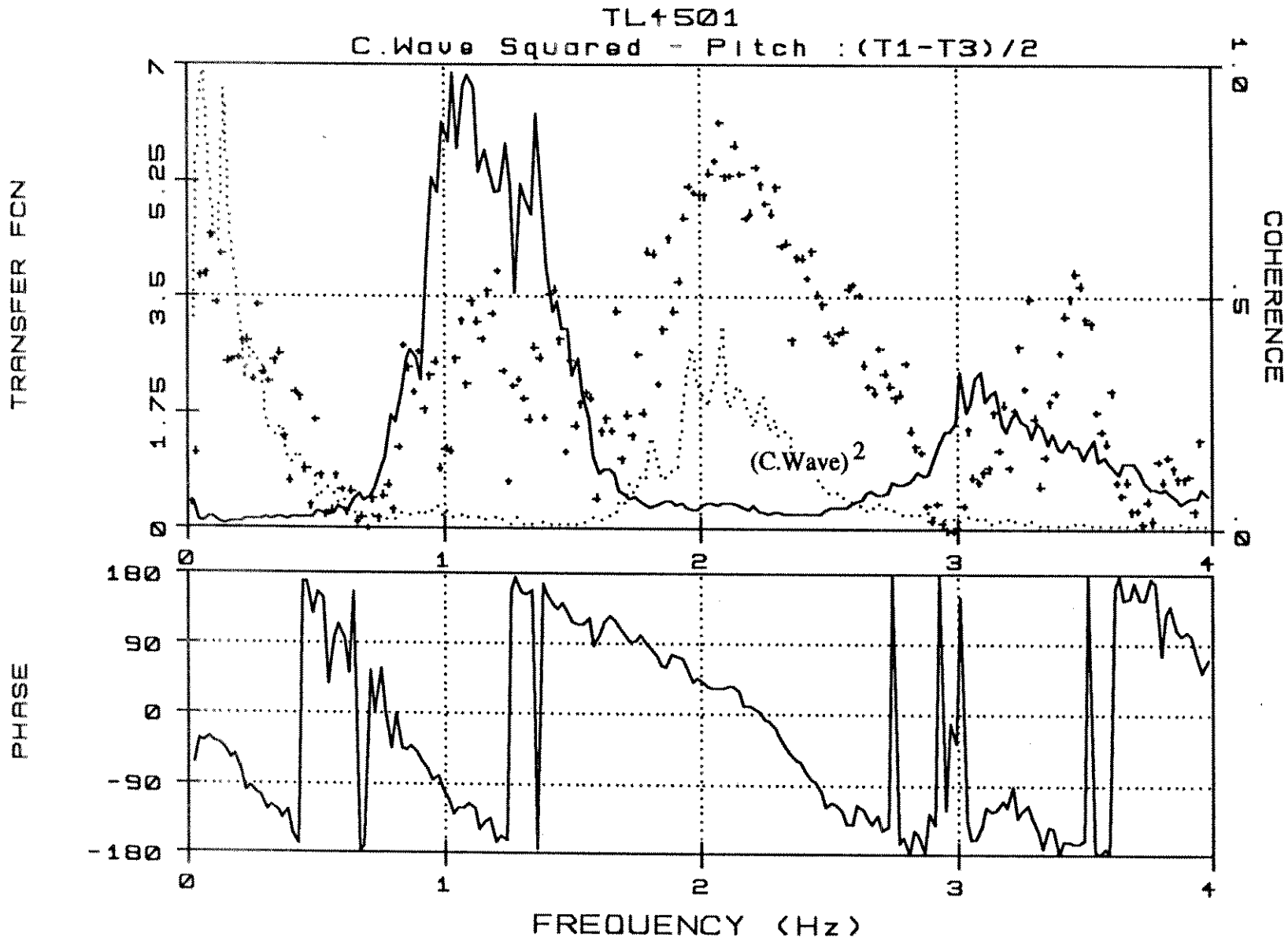

TL4501.WSQ/PiT13.4t
C.Wave Squared and Pitch are normalized.

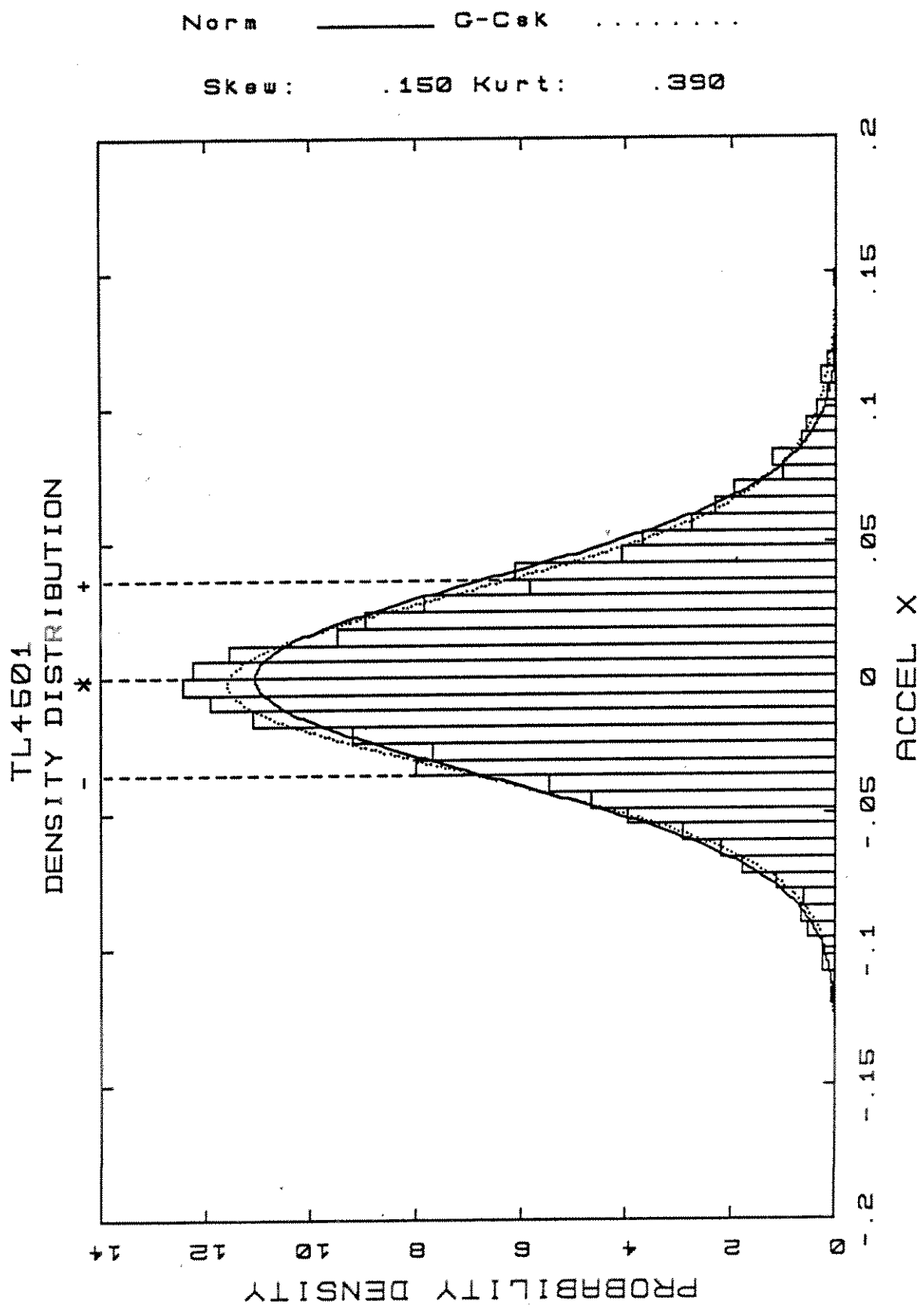
Norm
G-Csk
Skew: .150 Kurt: .390
TL4501
DENSITY DISTRIBUTION
+
*
-
PROBABILITY DENSITY
0
2
4
6
8
10
12
14
-.2
-.15
-.1
-.05
0
.05
.1
.15
.2
ACCEL X

TL4501.A.1

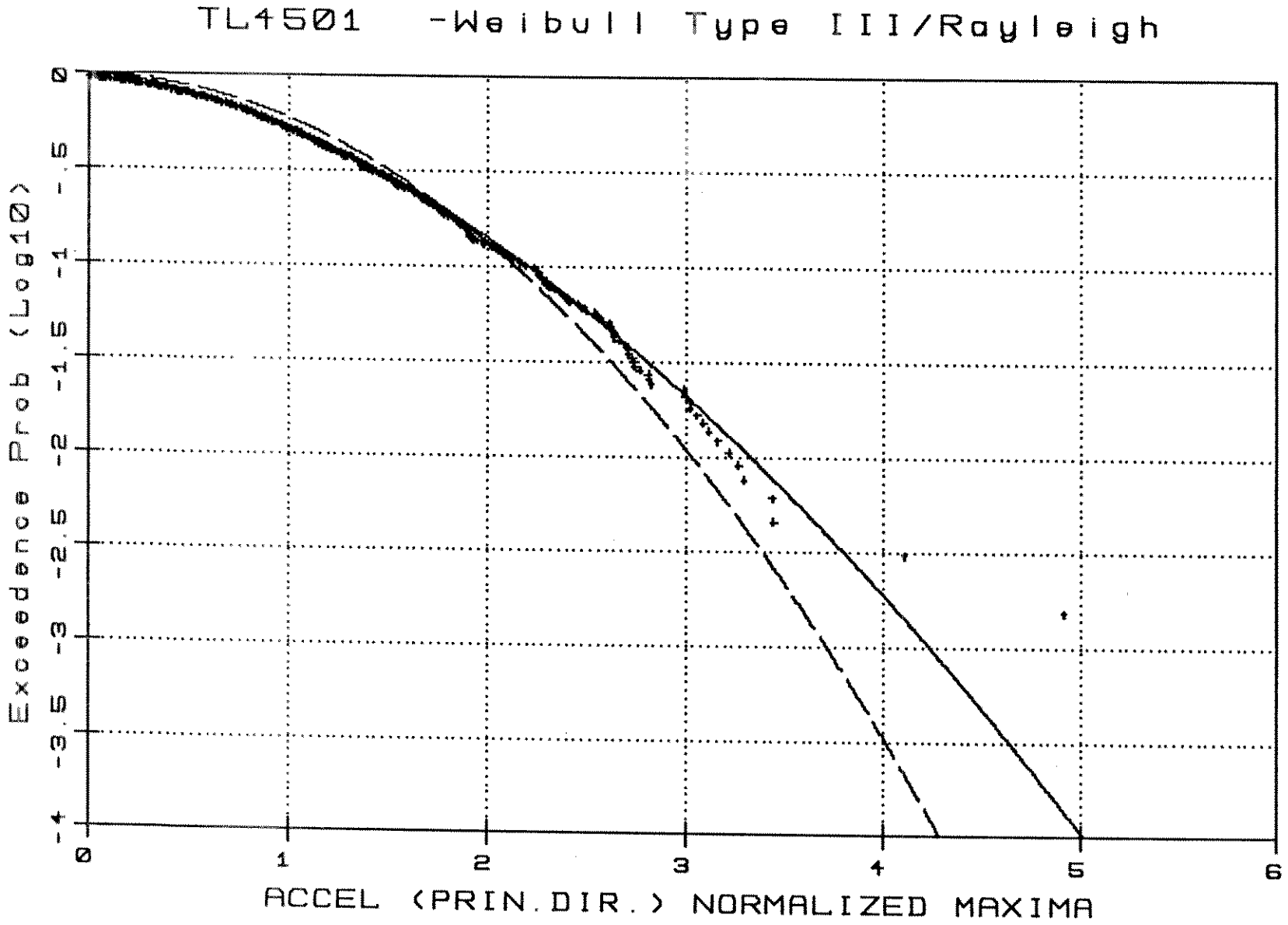
TL4501 -Weibull Type III/Rayleigh
Exceedence Prob (Log10)
0
-.5
-1
-1.5
-2
-2.5
-3
-3.5
-4
0
1
2
3
4
5
6
ACCEL (PRIN.DIR.) NORMALIZED MAXIMA

TL4501.A.2

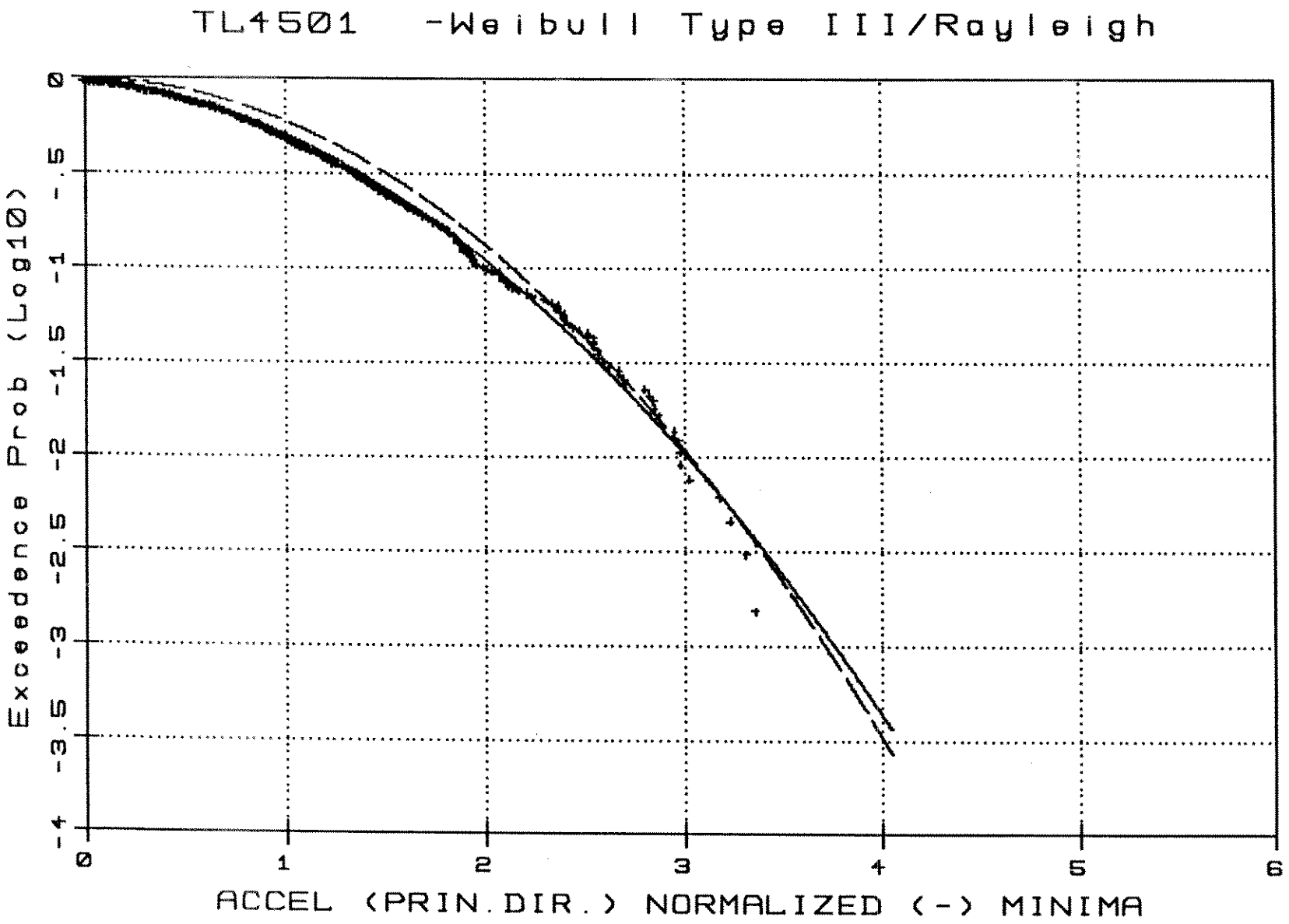
TL4501 -Weibull Type III/Rayleigh
Exceedence Prob (Log10)
0
-.5
-1
-1.5
-2
-2.5
-3
-3.5
-4
0
1
2
3
4
5
6
ACCEL (PRIN.DIR.) NORMALIZED (-) MINIMA

TL4501.A.3

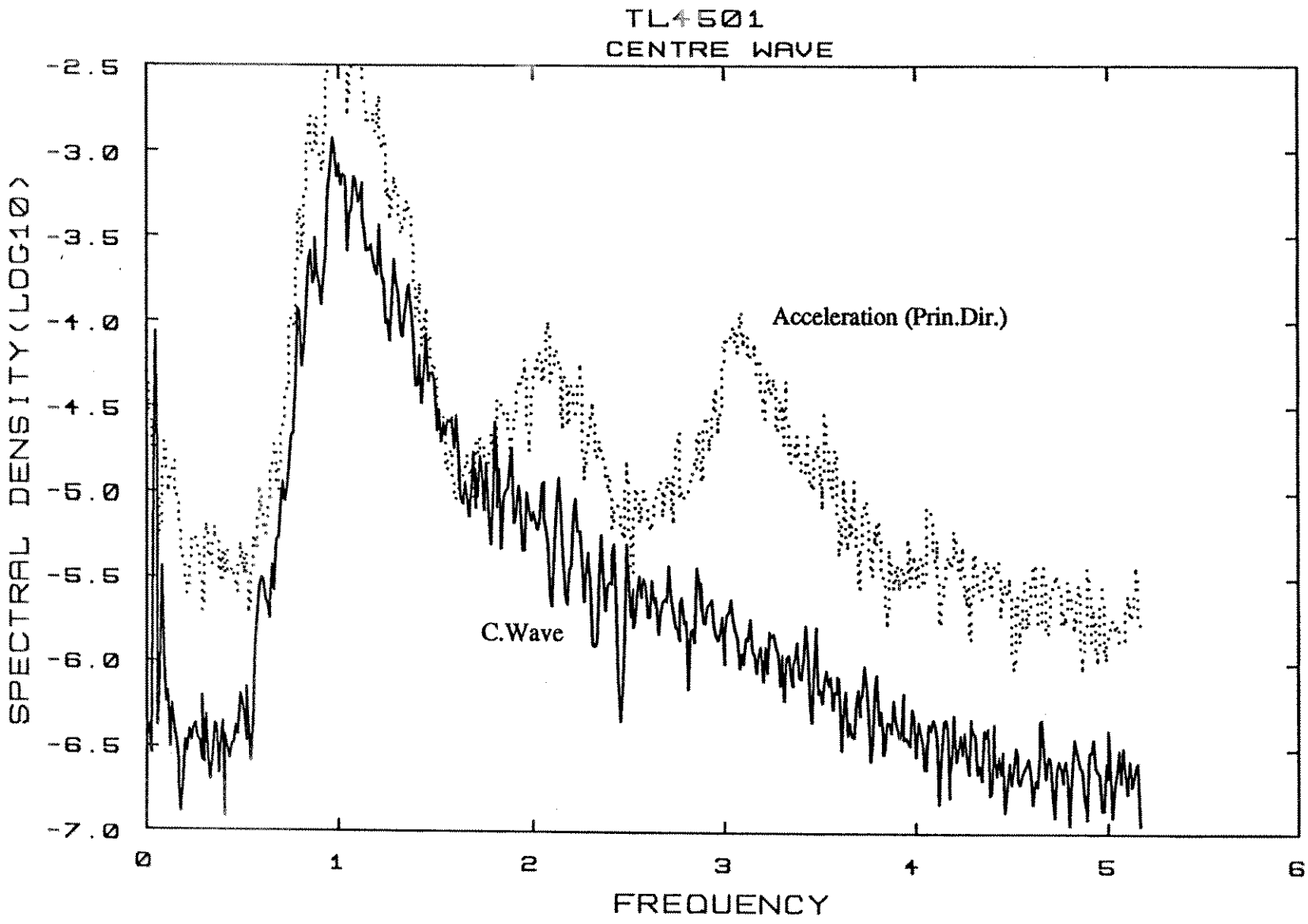
TL4501
CENTRE WAVE
SPECTRAL DENSITY(LOG10)
-2.5
-3.0
-3.5
-4.0
-4.5
-5.0
-5.5
-6.0
-6.5
-7.0
0
1
2
3
4
5
6
FREQUENCY
Acceleration (Prin.Dir.)
C.Wave

TL4501.W/A.4

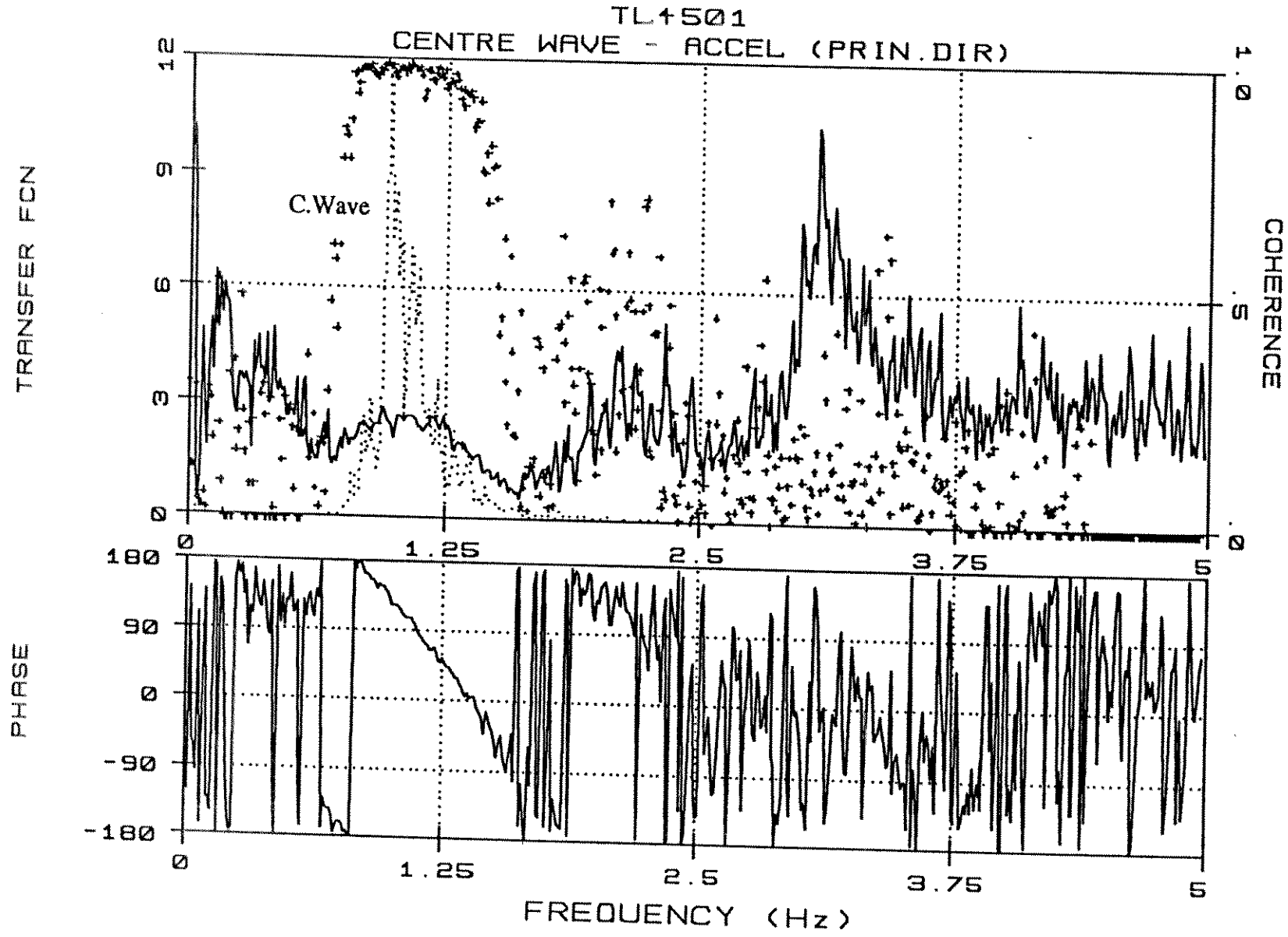
TL4501
CENTRE WAVE - ACCEL (PRIN.DIR)
TRANSFER FCN
12
9
6
3
0
C.Wave
COHERENCE
1.0
.5
0
0
1.25
2.5
3.75
5
PHASE
180
90
0
-90
-180
0
1.25
2.5
3.75
5
FREQUENCY (Hz)

TL4501.W/A.4t

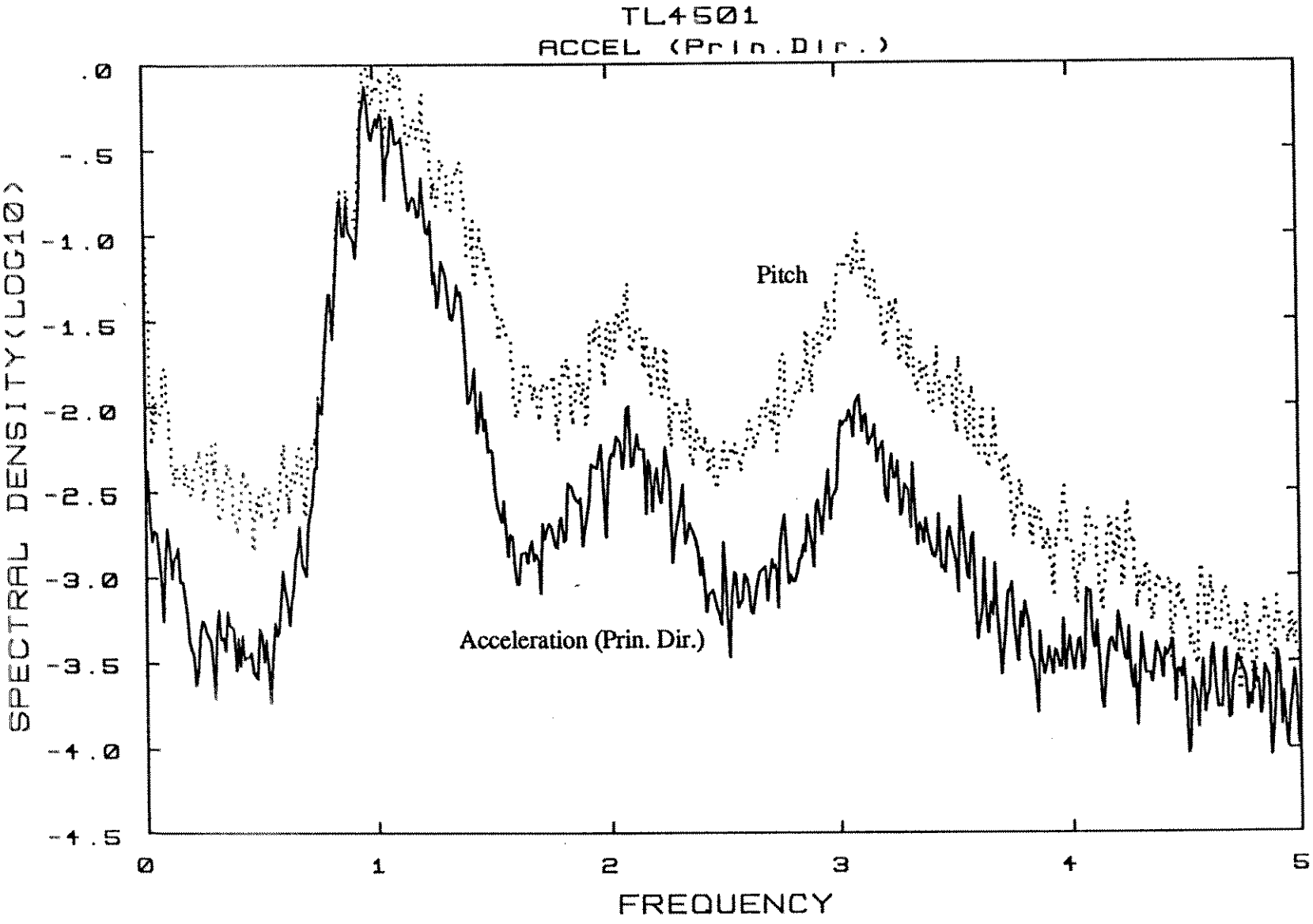

TL4501.A/PiT13.4

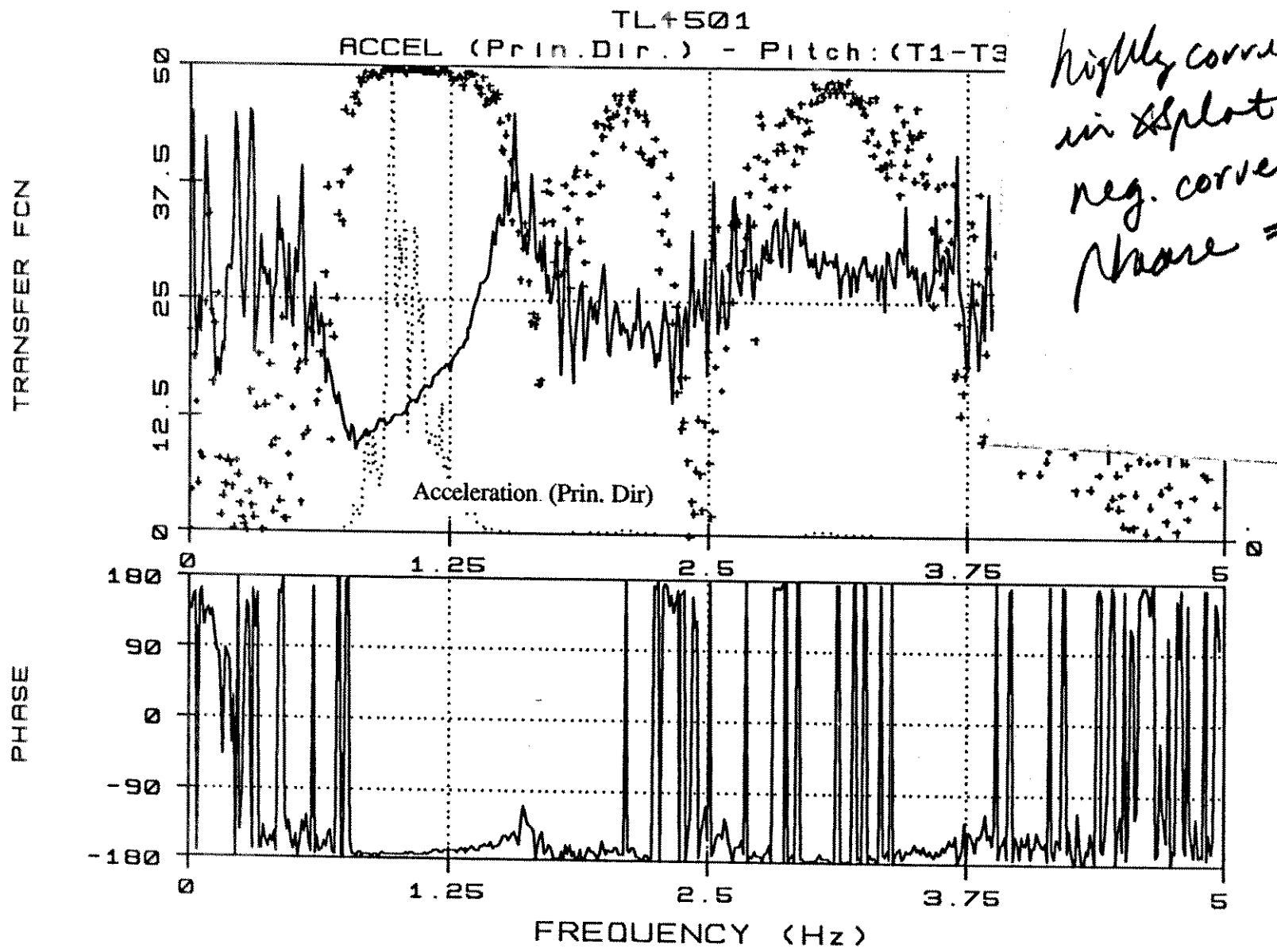

highly correl
in Xplot - 90
neg. correlation
phase = 180°

TL4501.A/PiT13.4t

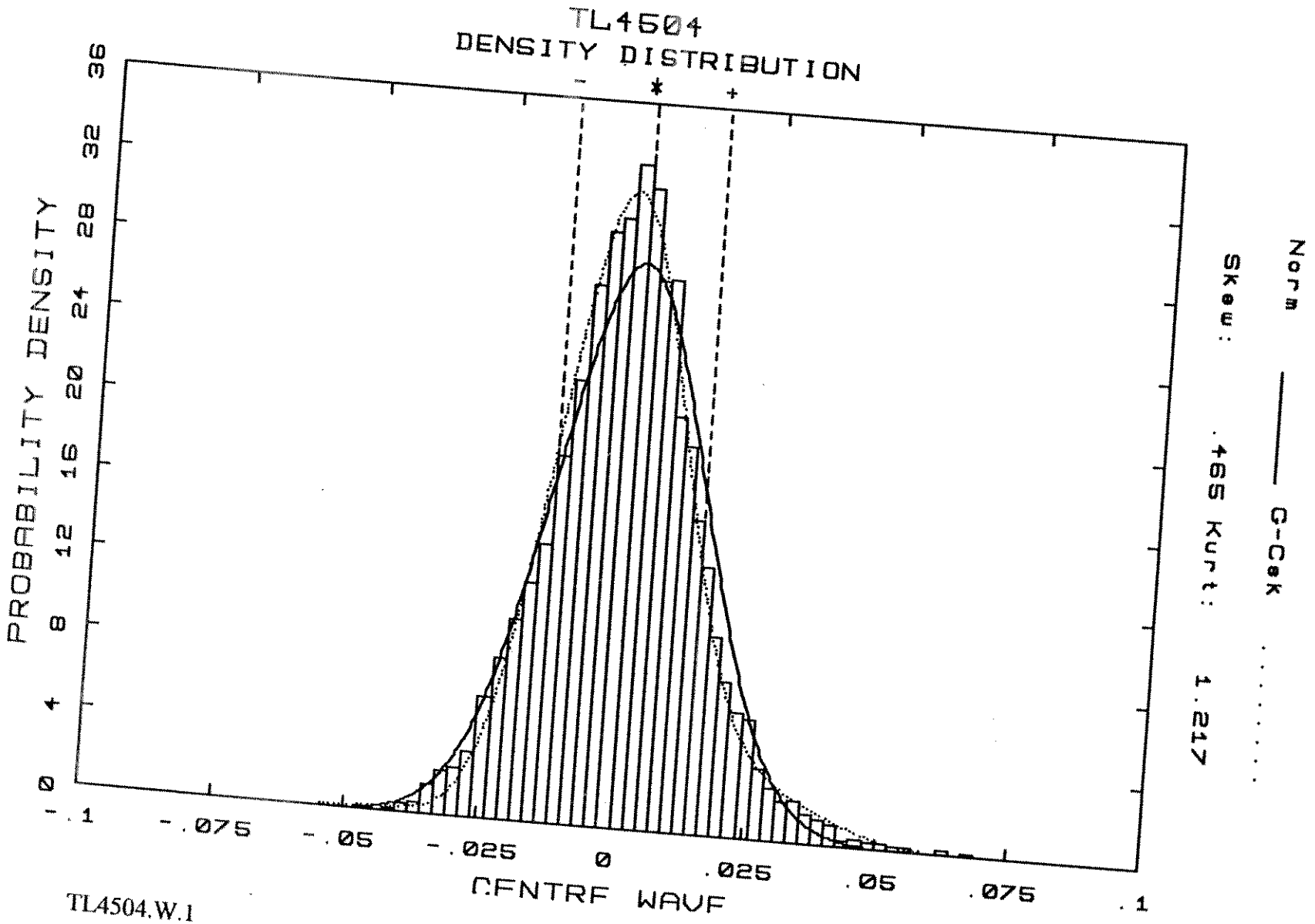
TL4504
DENSITY DISTRIBUTION
PROBABILITY DENSITY
0
4
8
12
16
20
24
28
32
36
-.1
-.075
-.05
-.025
0
.025
.05
.075
.1
CENTRE WAVE
Norm
G-Cak
Skew: .465 Kurt: 1.217

TL4504.W.1

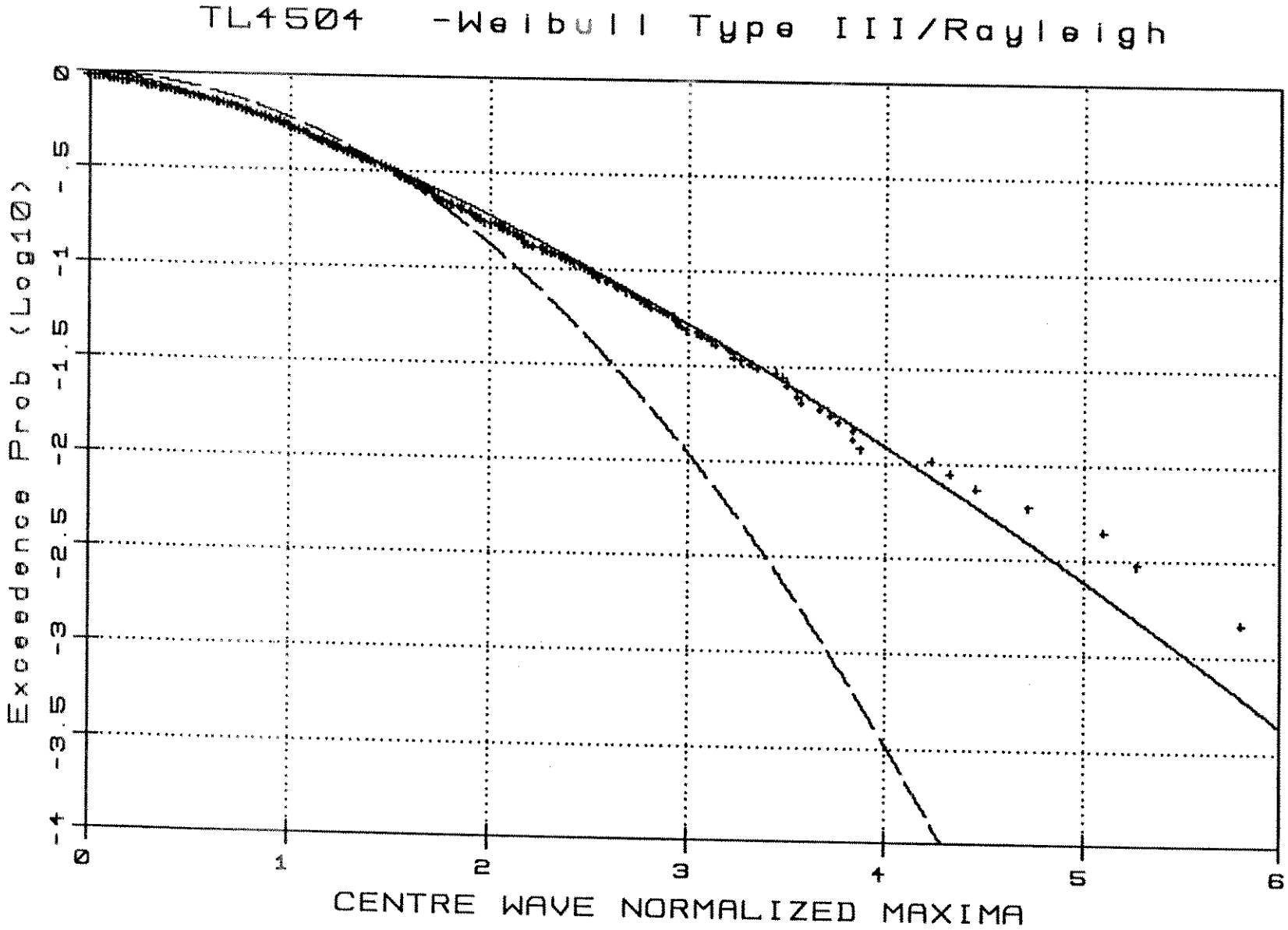
TL4504 -Weibull Type III/Rayleigh
Exceedence Prob (Log10)
0
-.5
-1
-1.5
-2
-2.5
-3
-3.5
-4
0
1
2
3
4
5
6
CENTRE WAVE NORMALIZED MAXIMA

TL4504.W.2

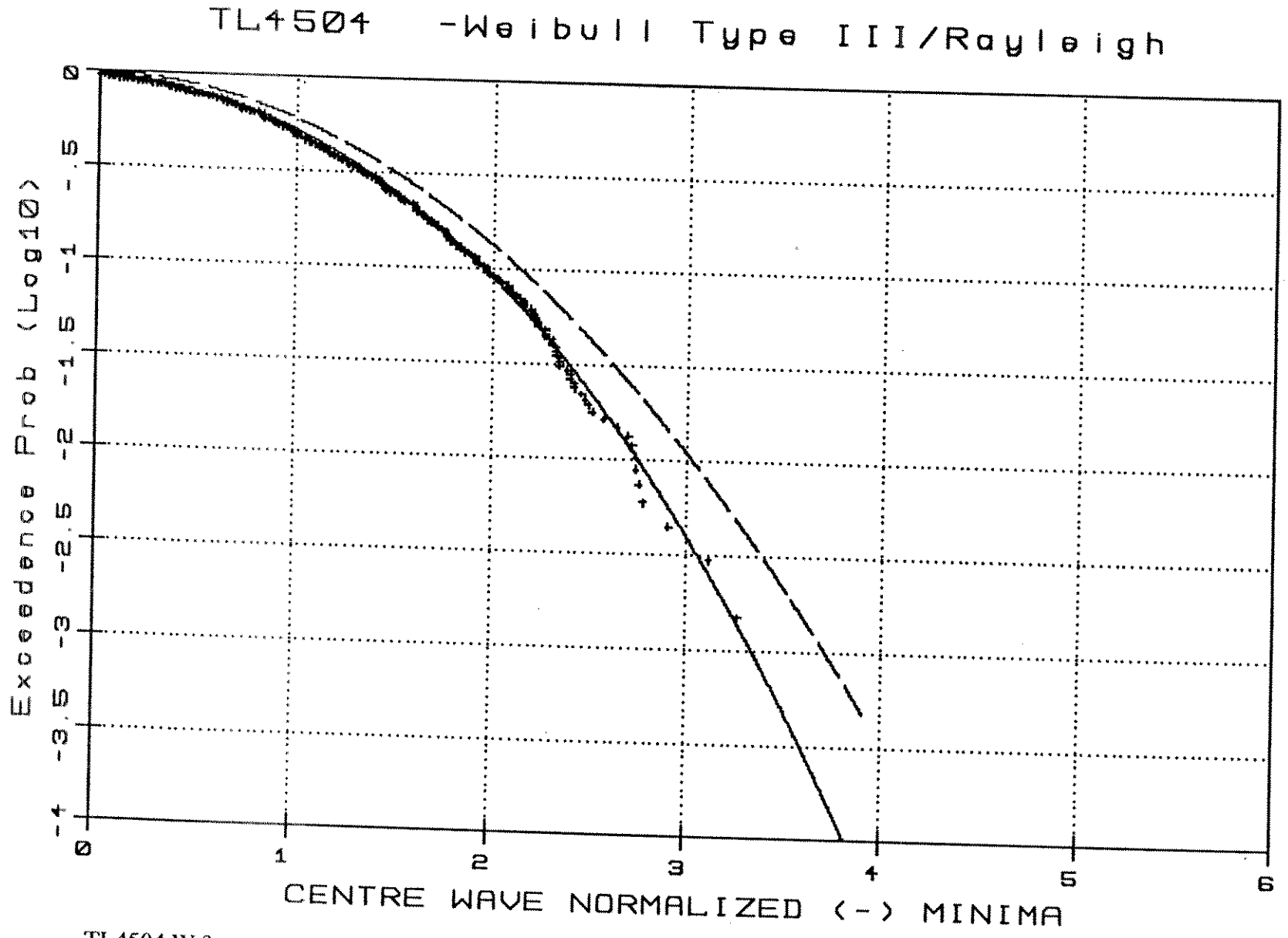
TL4504 -Weibull Type III/Rayleigh
Exceedence Prob (Log10)
0
-.5
-1
-1.5
-2
-2.5
-3
-3.5
-4
0
1
2
3
4
5
6
CENTRE WAVE NORMALIZED (-) MINIMA

TL4504.W.3

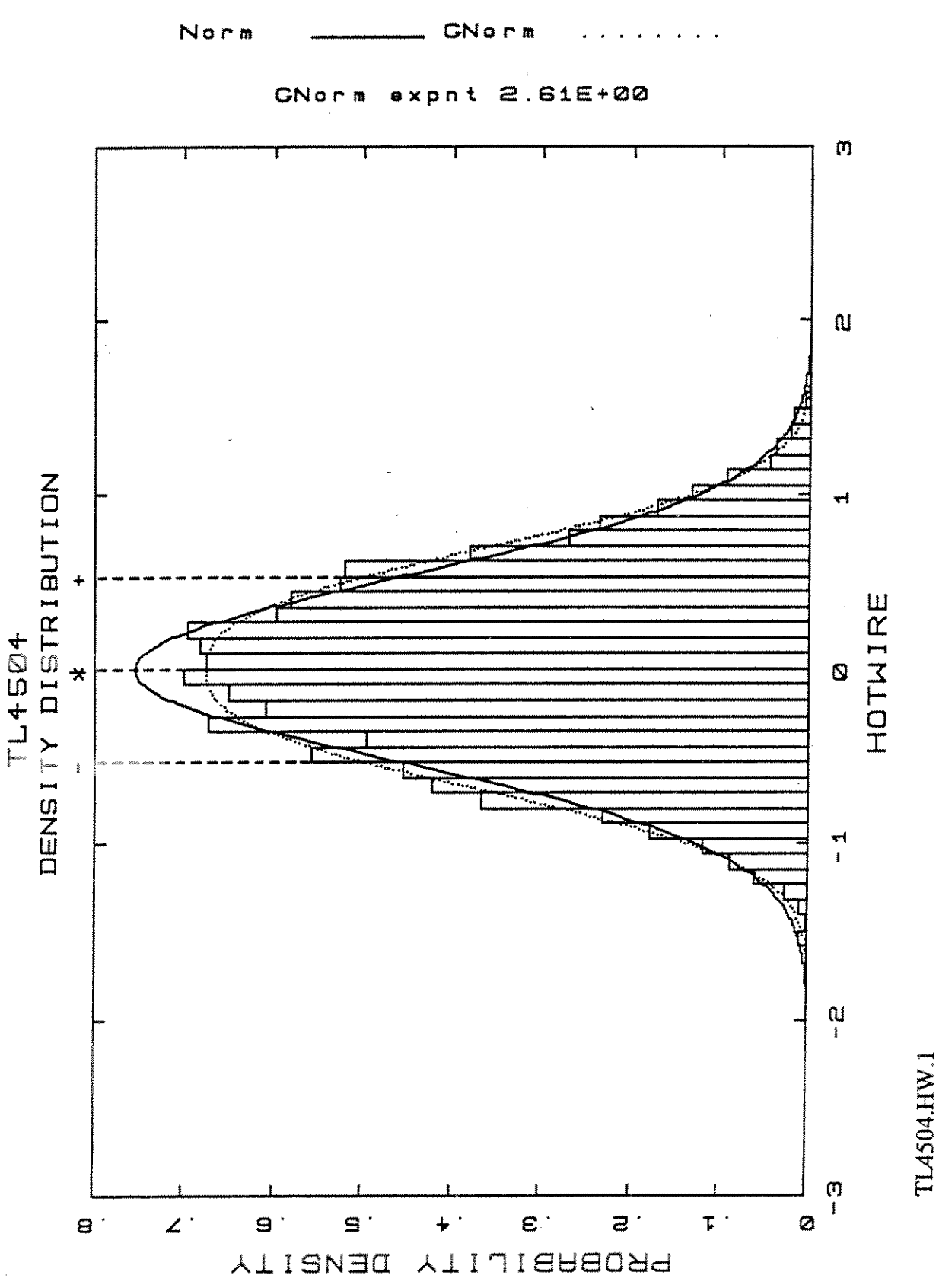
Norm
GNorm
GNorm expnt 2.61E+00
TL4504
DENSITY DISTRIBUTION
PROBABILITY DENSITY
HOTWIRE
TL4504.HW.1

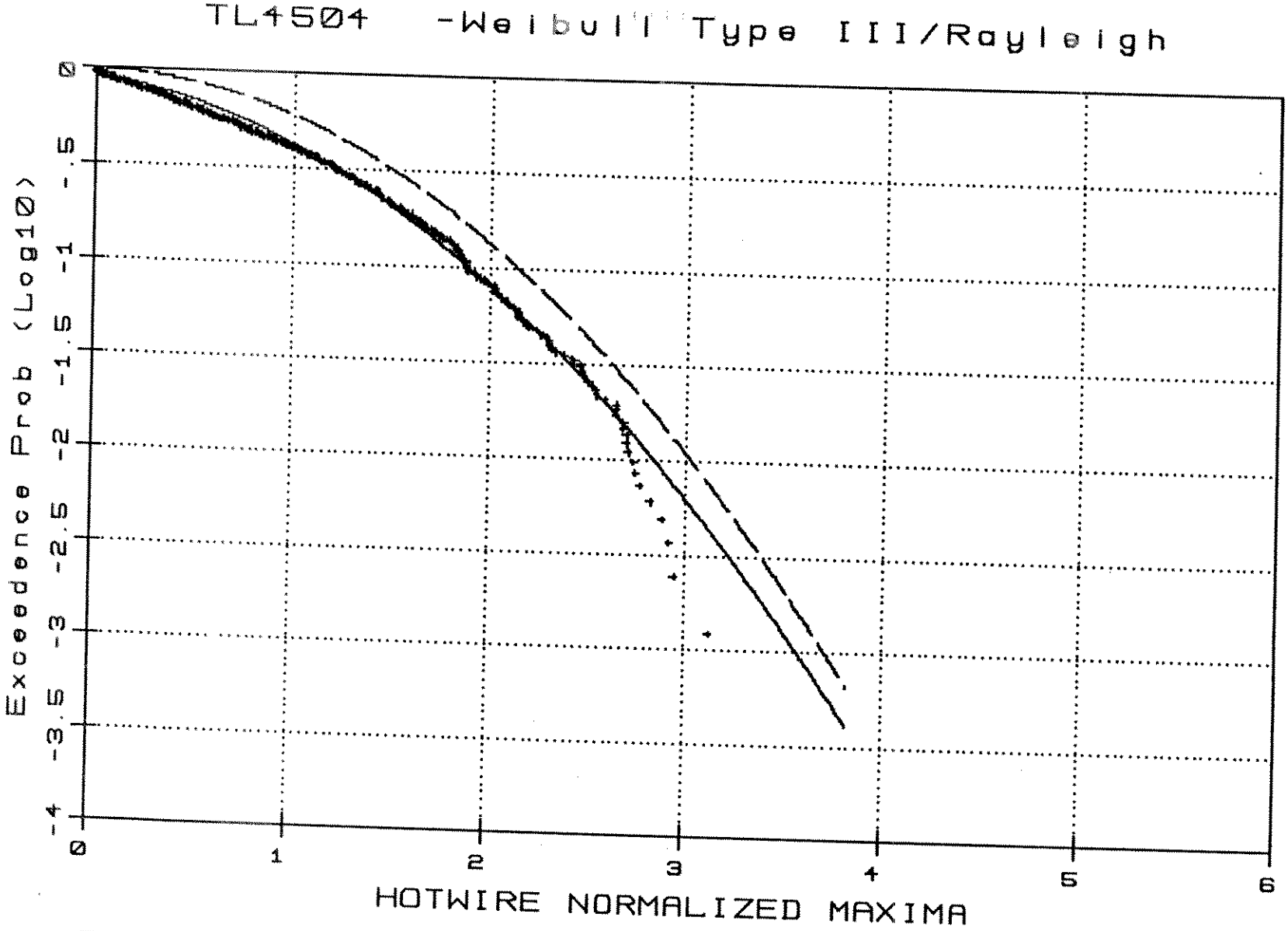
TL4504 -Weibull Type III/Rayleigh
Exceedence Prob (Log10)
0
-.5
-1
-1.5
-2
-2.5
-3
-3.5
-4
0
1
2
3
4
5
6
HOTWIRE NORMALIZED MAXIMA

TL4504.HW.2

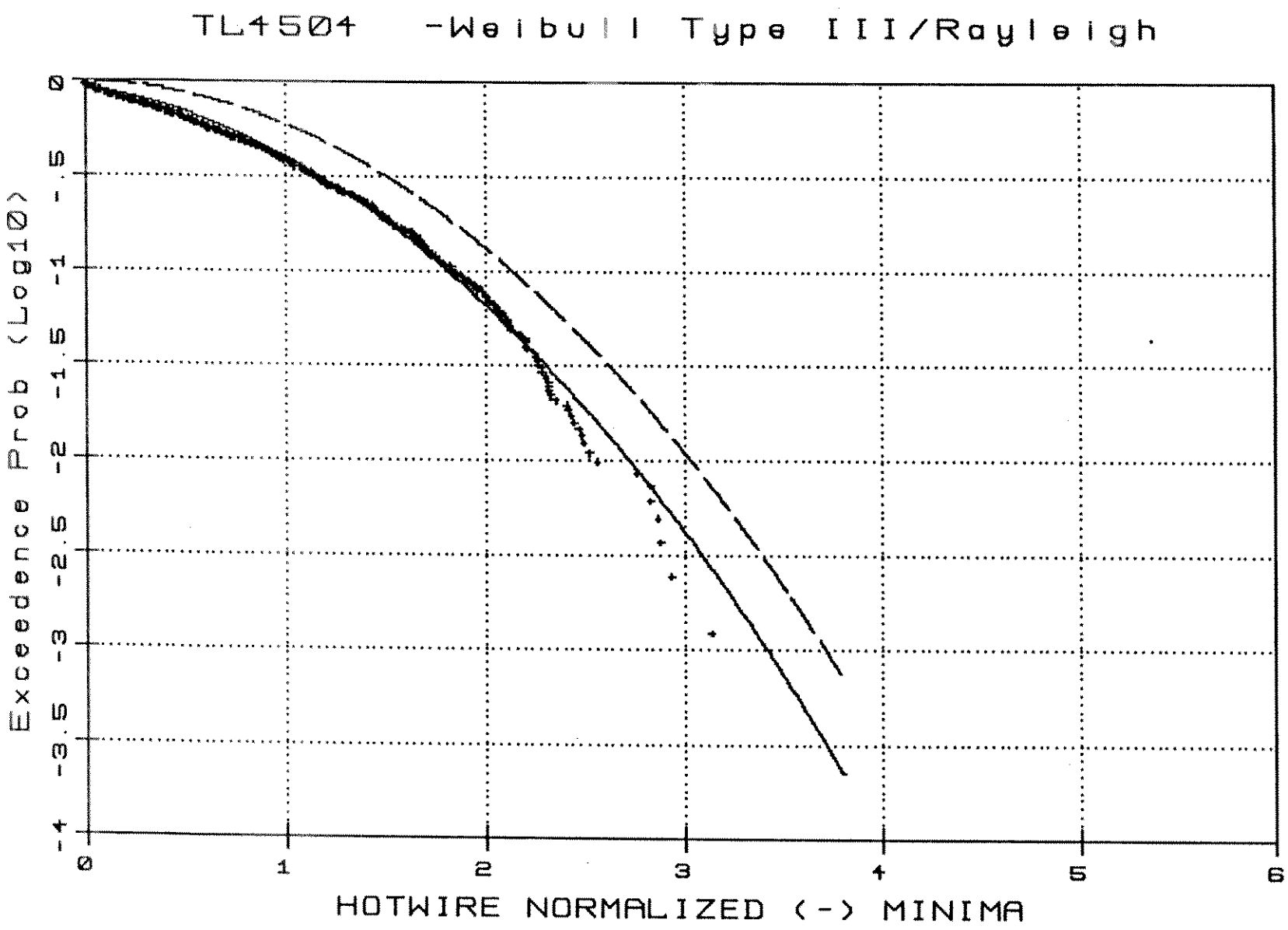
TL4504 -Weibull Type III/Rayleigh
Exceedence Prob (Log10)
0
-.5
-1
-1.5
-2
-2.5
-3
-3.5
-4
0
1
2
3
4
5
6
HOTWIRE NORMALIZED (-) MINIMA

TL4504.HW.3

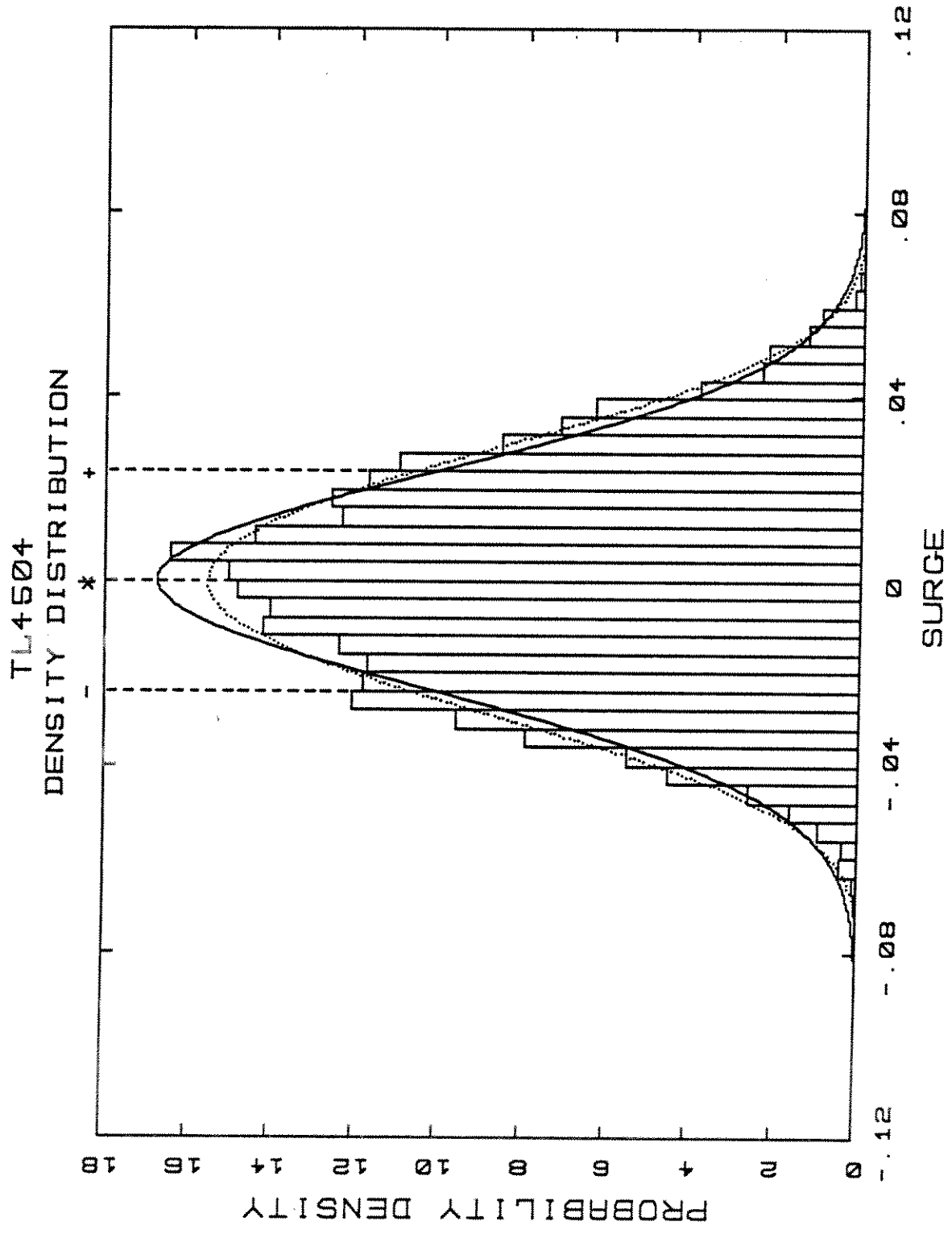
Norm
C-Cek
Skew: .014 Kurt: -.574
TL4504
DENSITY DISTRIBUTION
+
*
-
PROBABILITY DENSITY
0
2
4
6
8
10
12
14
16
18
.12
.08
.04
0
-.04
-.08
-.12
SURGE

TL4504.S.1

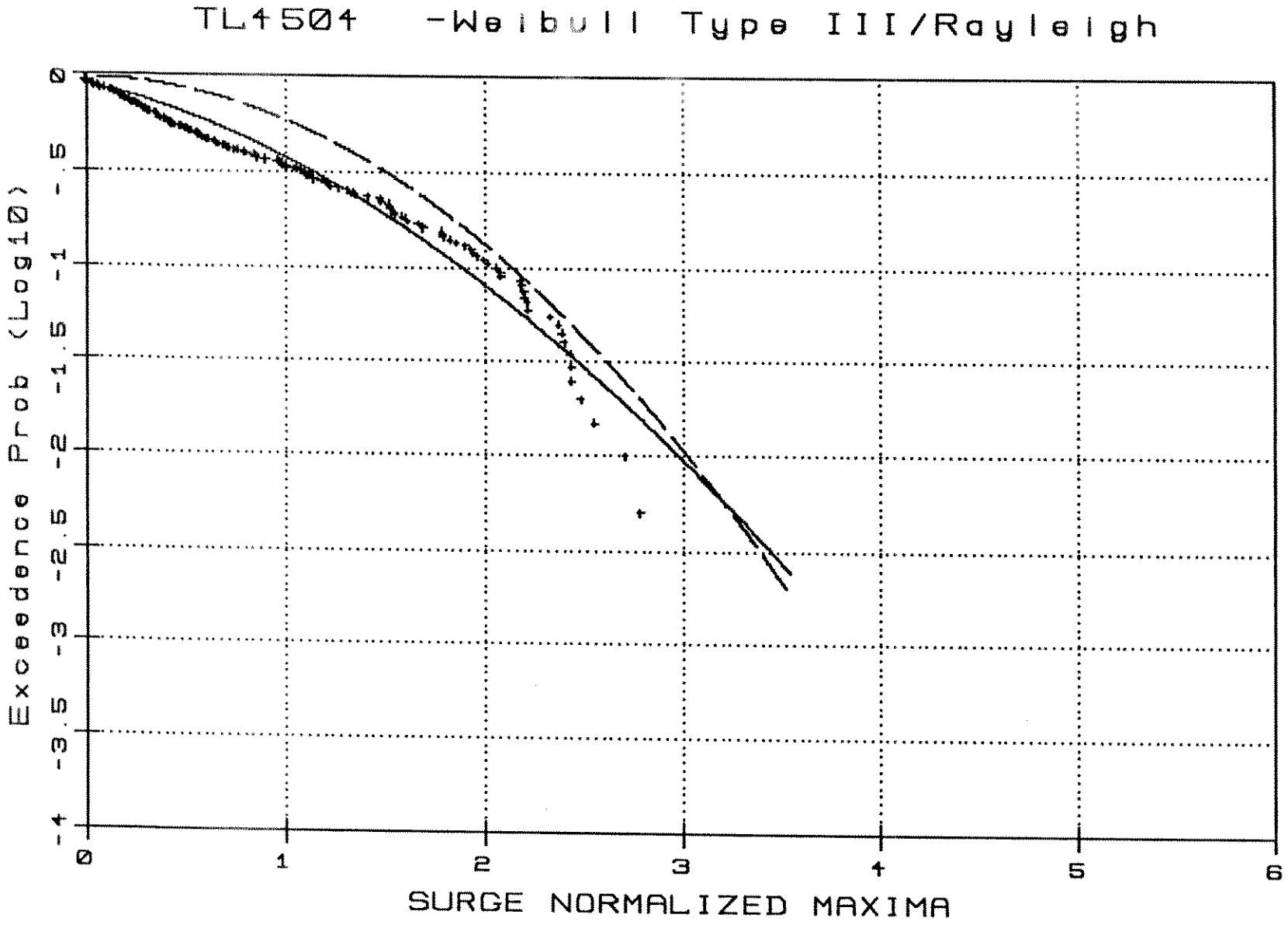
TL4504 -Weibull Type III/Rayleigh
Exceedence Prob (Log10)
0
-.5
-1
-1.5
-2
-2.5
-3
-3.5
-4
0
1
2
3
4
5
6
SURGE NORMALIZED MAXIMA

TL4504.S.2

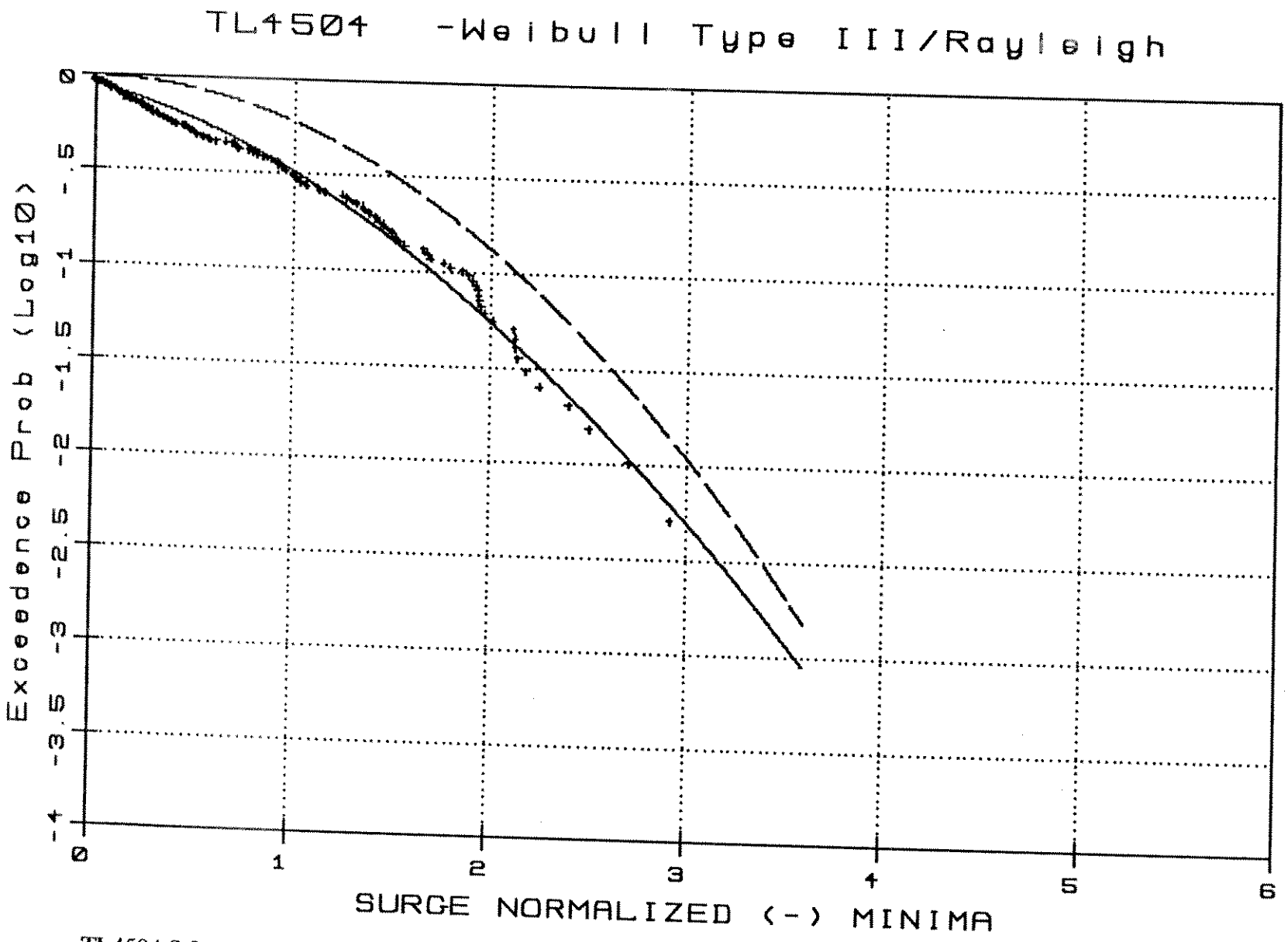
TL4504 -Weibull Type III/Rayleigh
Exceedence Prob (Log10)
0
-.5
-1
-1.5
-2
-2.5
-3
-3.5
-4
0
1
2
3
4
5
6
SURGE NORMALIZED (-) MINIMA

TL4504.S.3

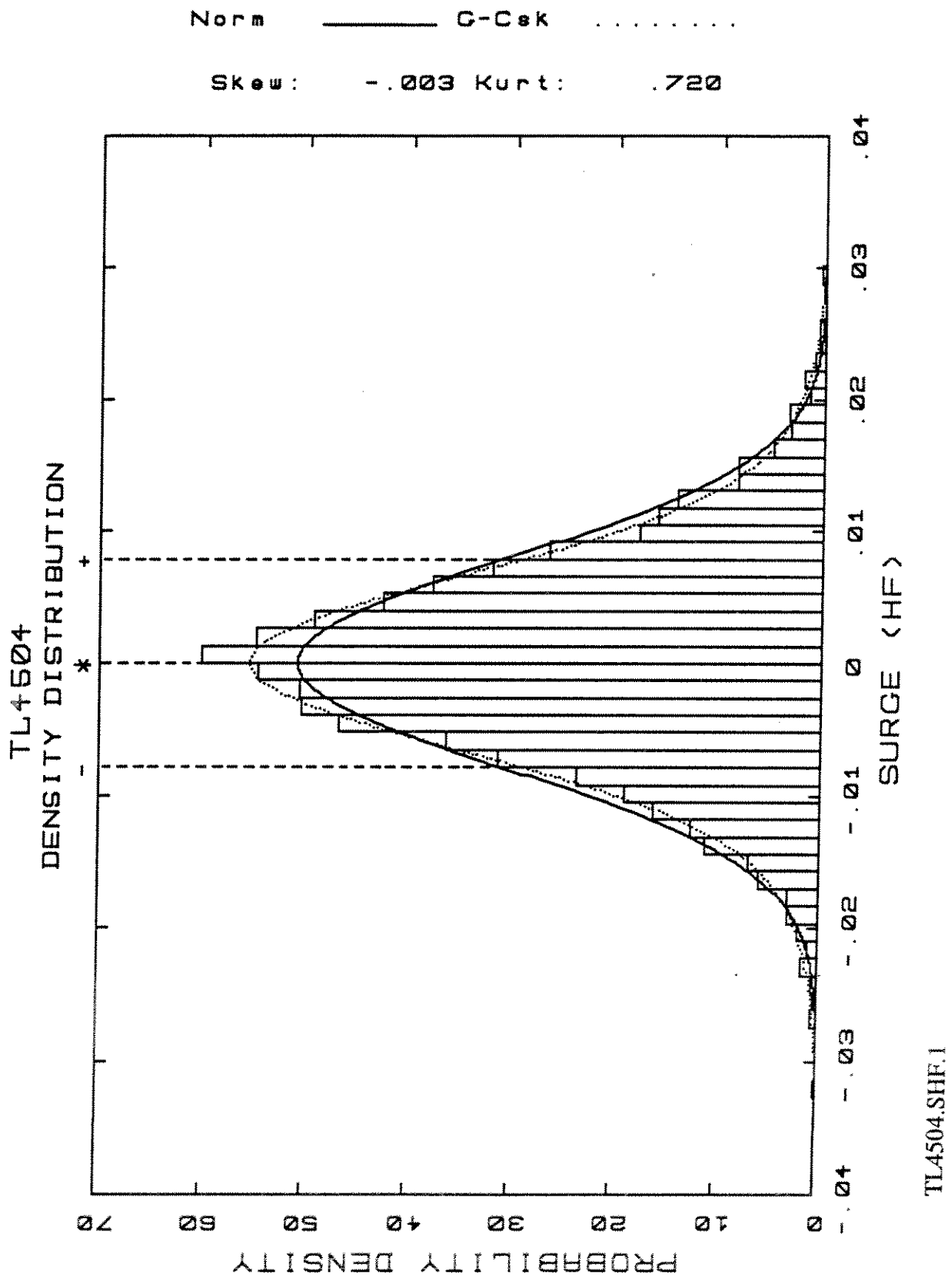
Norm
C-Csk
Skew: -.003 Kurt: .720
TL4504
DENSITY DISTRIBUTION
+
*
-
PROBABILITY DENSITY
0
10
20
30
40
50
60
70
-.04
-.03
-.02
-.01
0
.01
.02
.03
.04
SURGE (HF)

TL4504.SHF.1

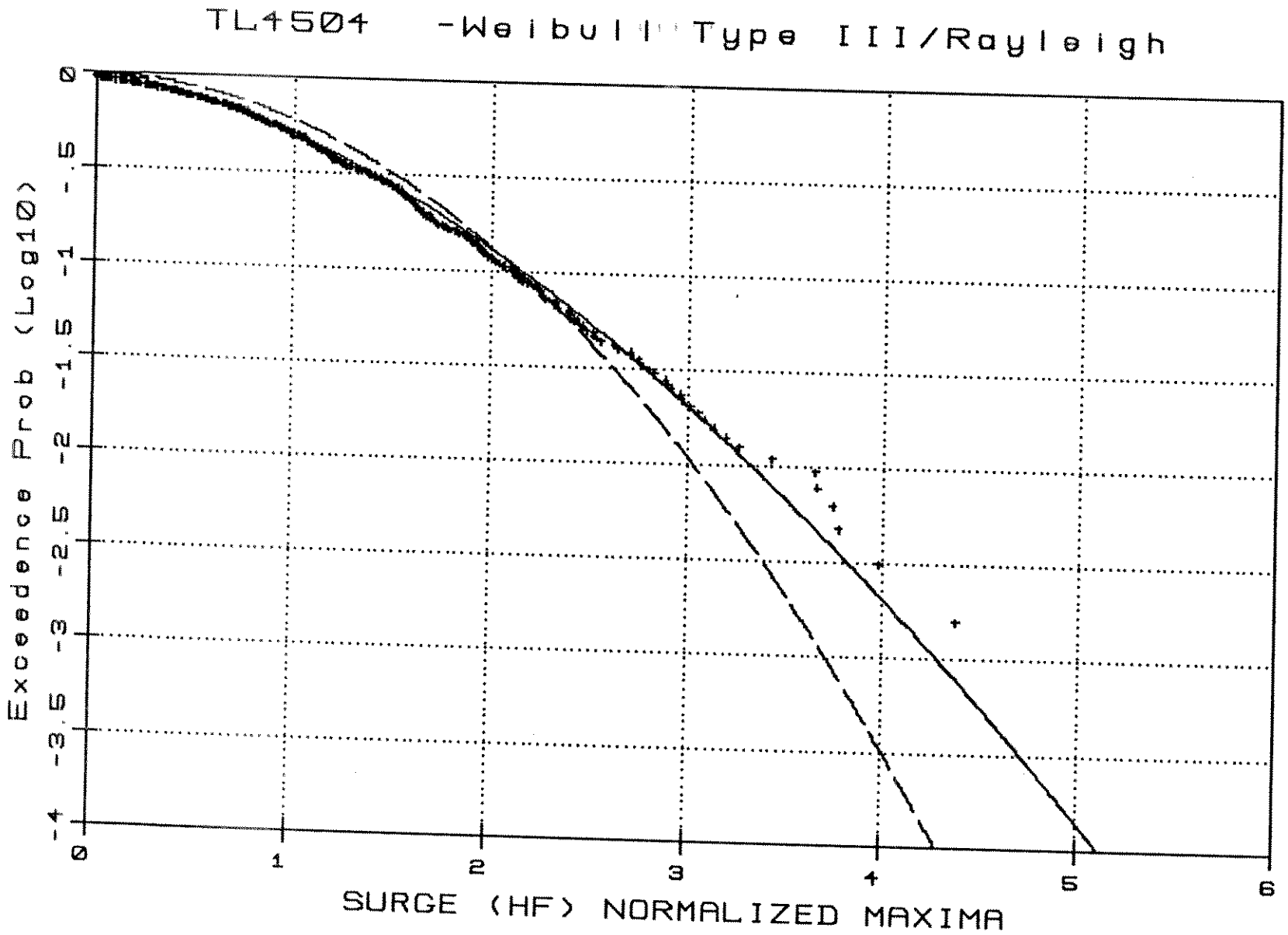
TL4504 -Weibull Type III/Rayleigh
Exceedence Prob (Log10)
0
-.5
-1
-1.5
-2
-2.5
-3
-3.5
-4
0
1
2
3
4
5
6
SURGE (HF) NORMALIZED MAXIMA

TL4504.SHF.2

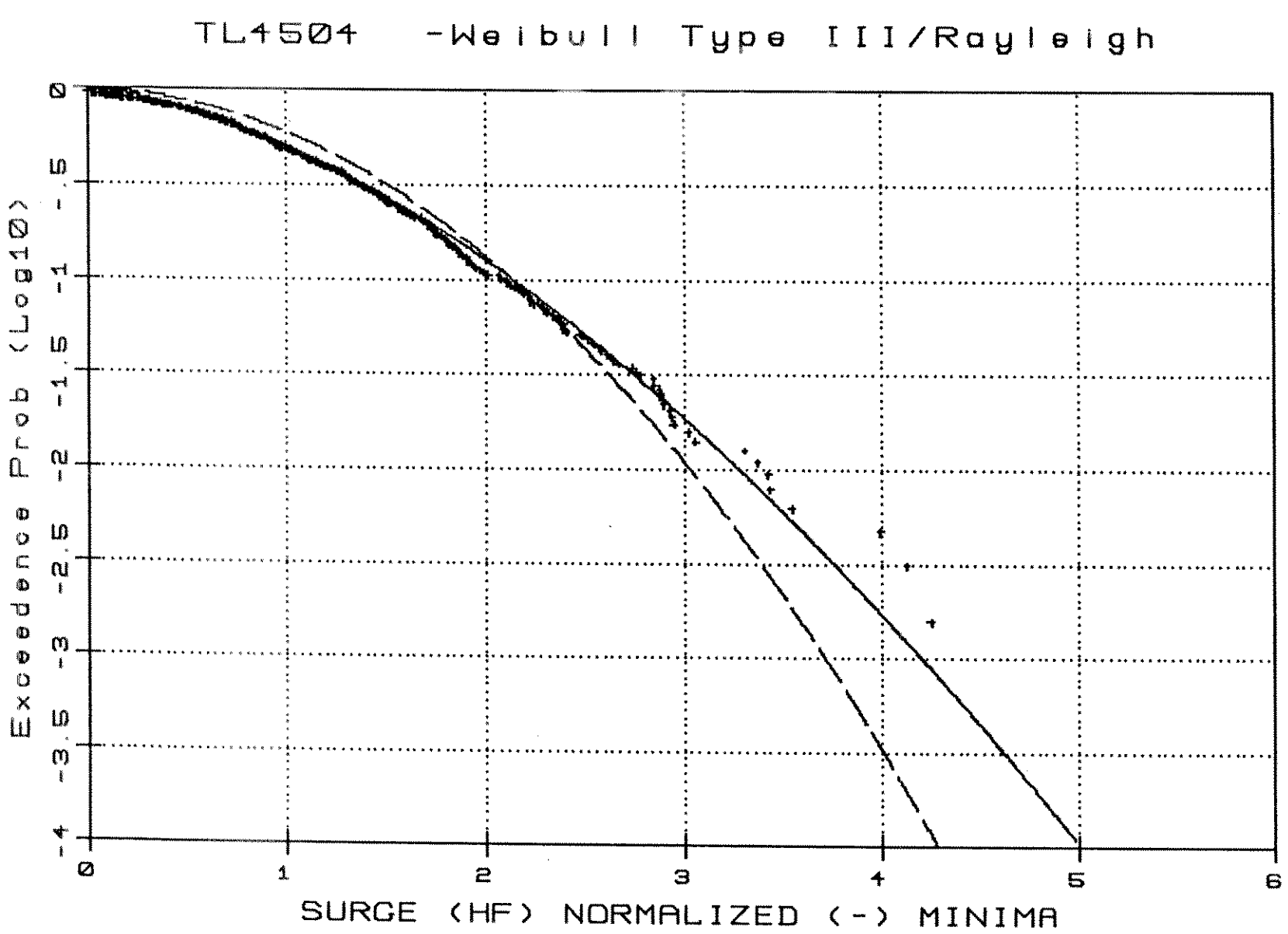
TL4504 -Weibull Type III/Rayleigh
Exceedence Prob (Log10)
0
-.5
-1
-1.5
-2
-2.5
-3
-3.5
-4
0
1
2
3
4
5
6
SURGE (HF) NORMALIZED (-) MINIMA

TL4504.SHF.3

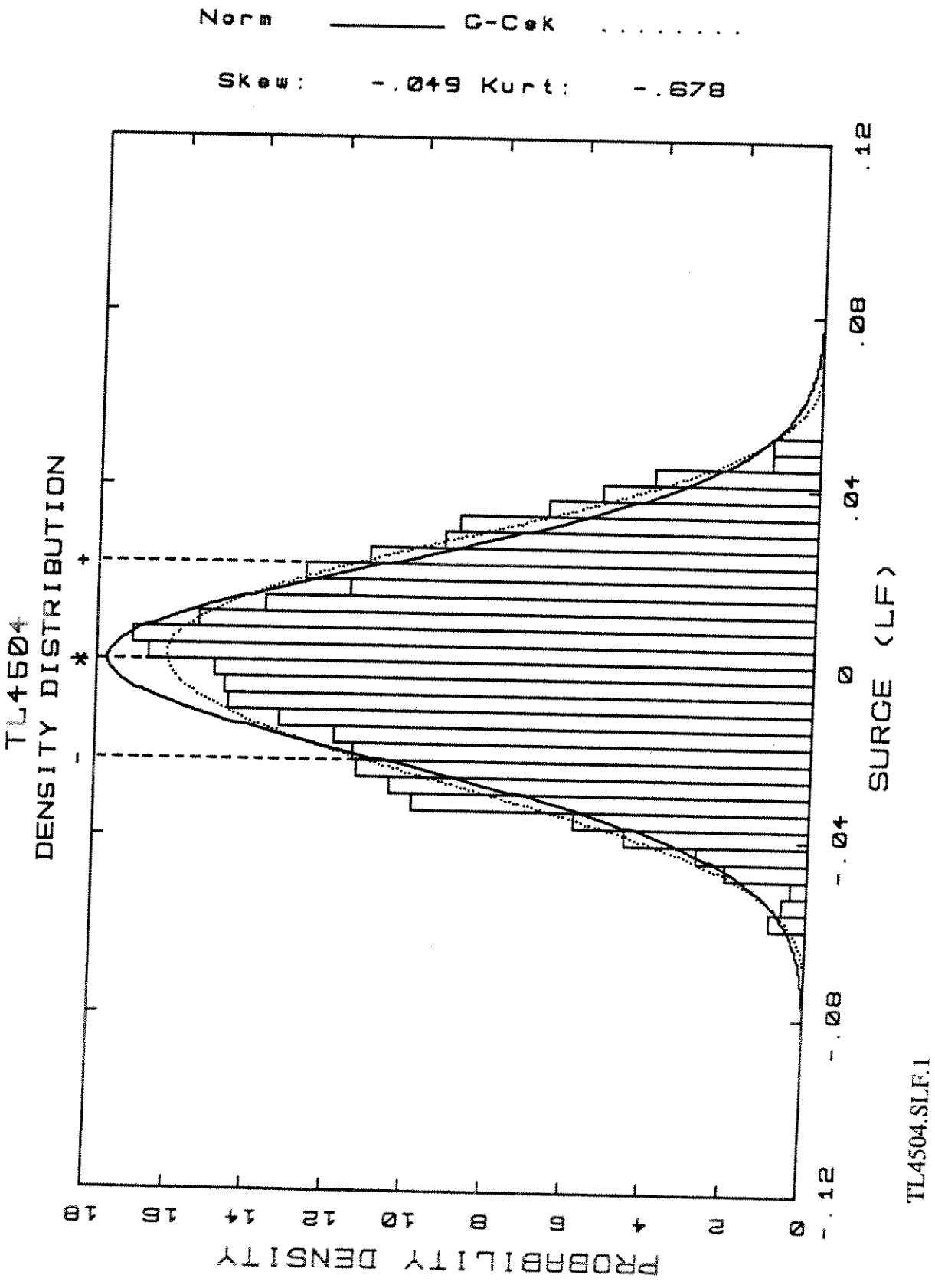
Norm
G-Cek
Skew: -.049 Kurt: -.678
TL4504
DENSITY DISTRIBUTION
+
*
-
PROBABILITY DENSITY
0 2 4 6 8 10 12 14 16 18
SURGE (LF)
.12 .08 .04 0 -.04 -.08 -.12

TL4504.SLF.1

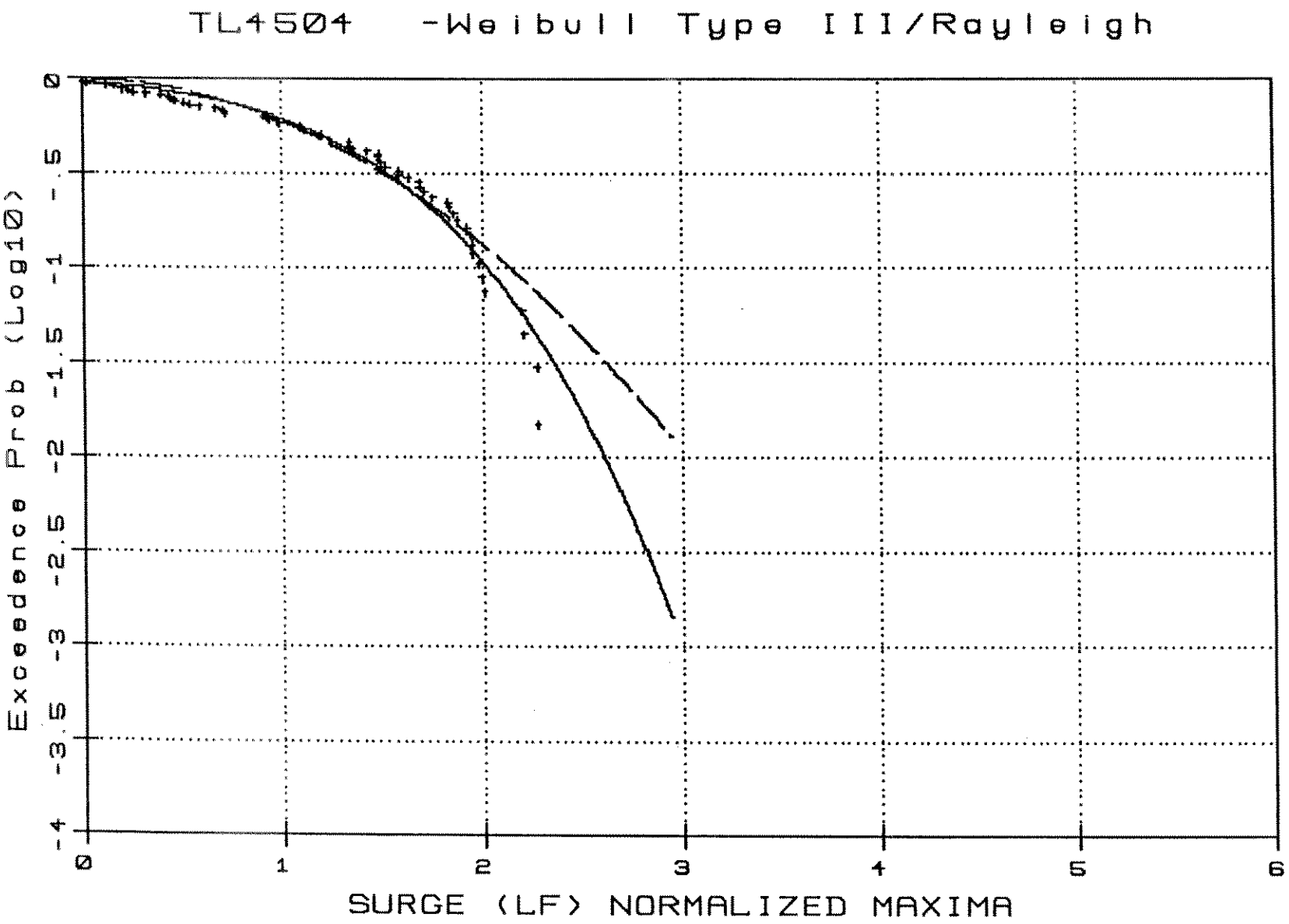
TL4504 -Weibull Type III/Rayleigh
Exceedence Prob (Log10)
0
-.5
-1
-1.5
-2
-2.5
-3
-3.5
-4
0
1
2
3
4
5
6
SURGE (LF) NORMALIZED MAXIMA

TL4504.SLF.2

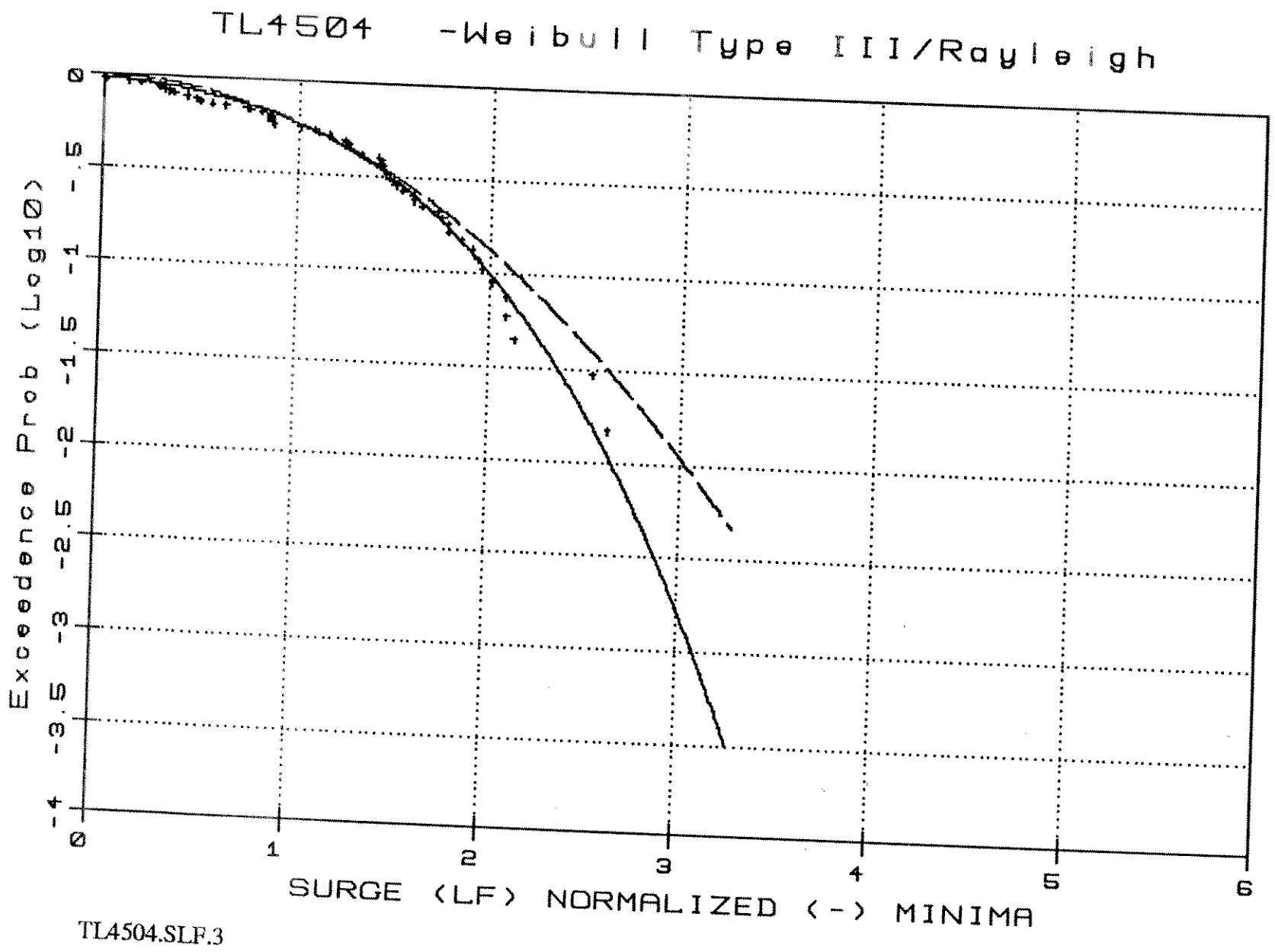
TL4504 -Weibull Type III/Rayleigh
Exceedence Prob (Log10)
0
-.5
-1
-1.5
-2
-2.5
-3
-3.5
-4
0
1
2
3
4
5
6
SURGE (LF) NORMALIZED (-) MINIMA

TL4504.SLF.3

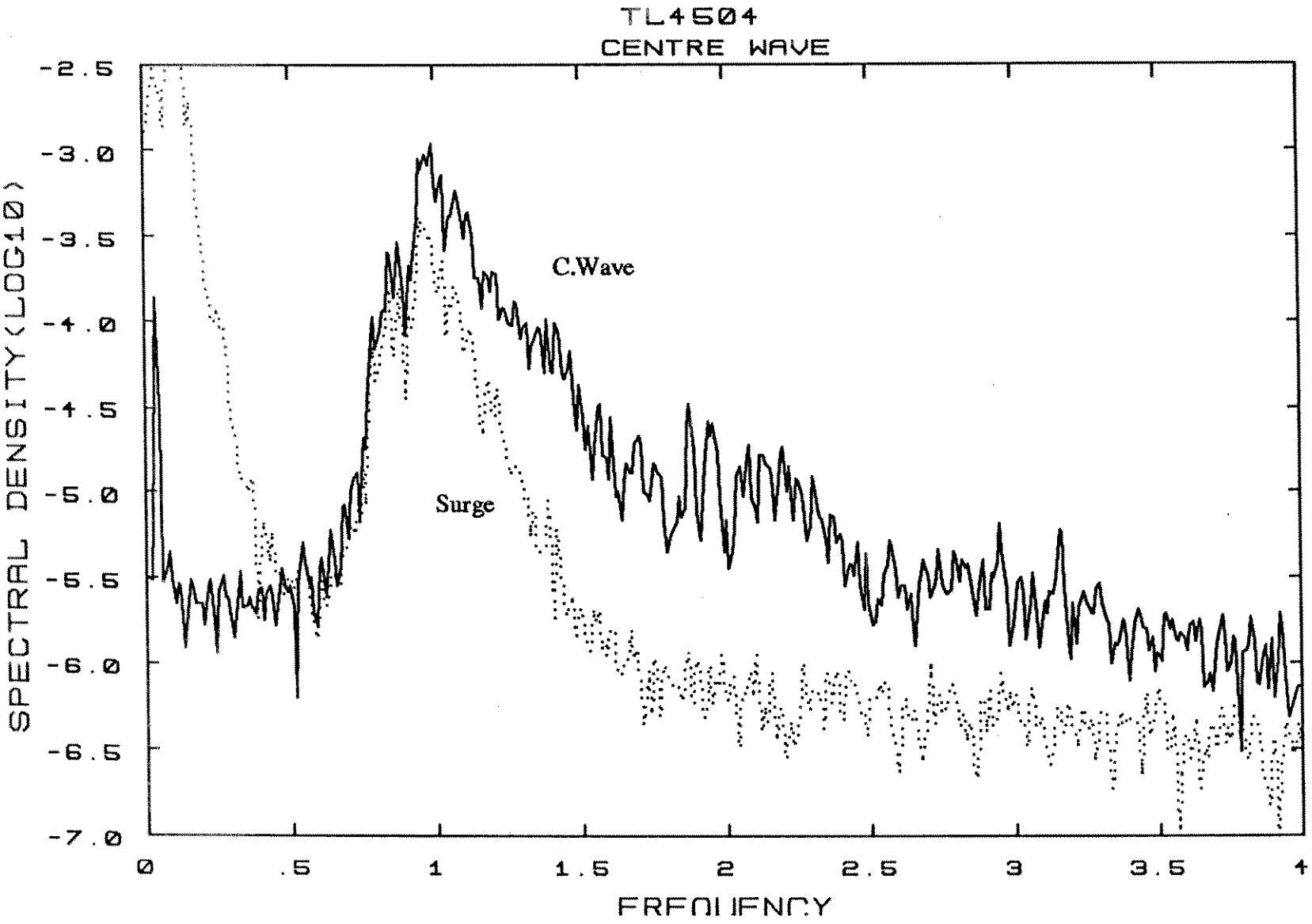
TL4504
CENTRE WAVE
SPECTRAL DENSITY(LOG10)
-2.5
-3.0
-3.5
-4.0
-4.5
-5.0
-5.5
-6.0
-6.5
-7.0
0
.5
1
1.5
2
2.5
3
3.5
4
FREQUENCY
C.Wave
Surge

TL4504.W/S.4

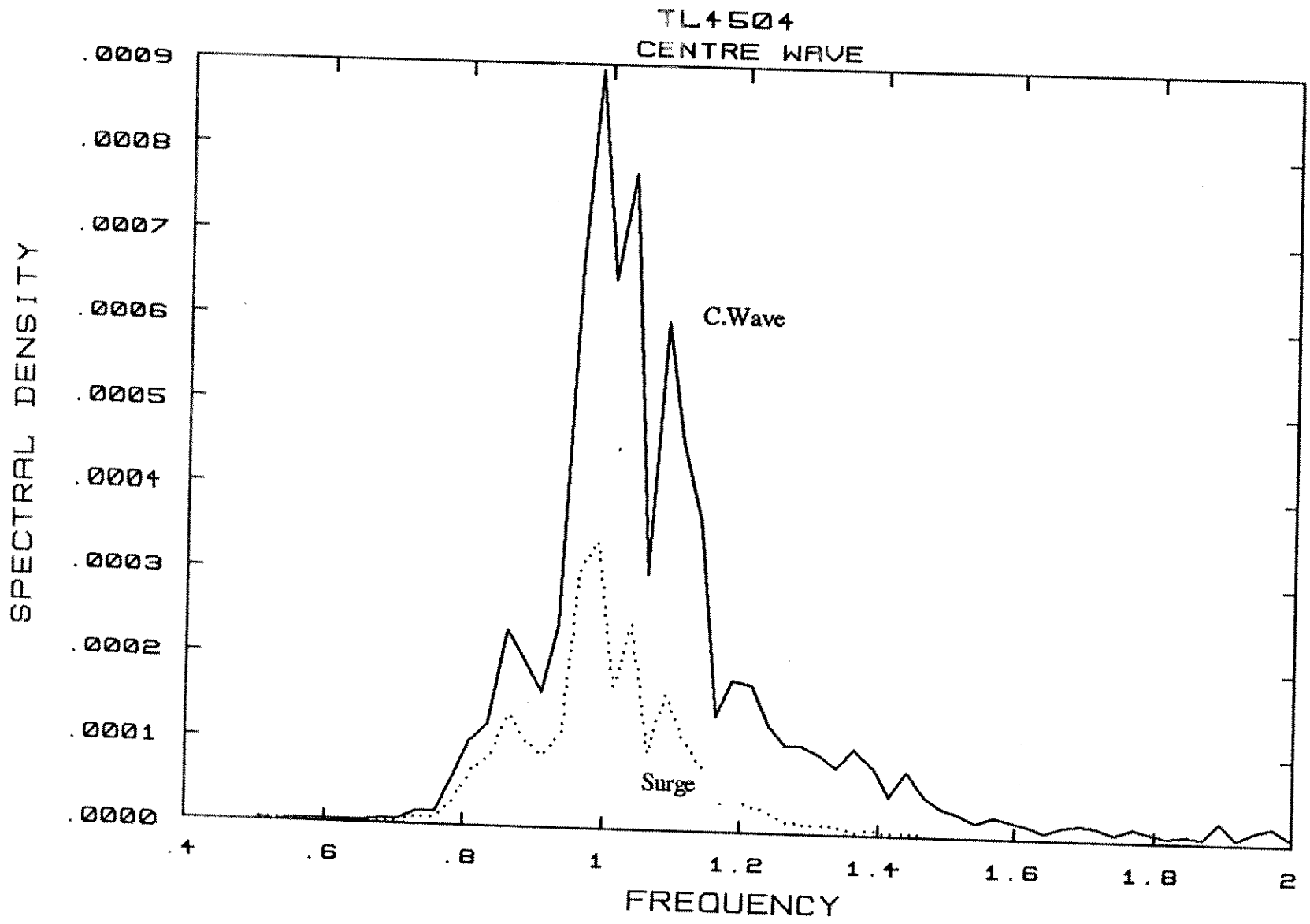
TL4504
CENTRE WAVE
SPECTRAL DENSITY
.0009
.0008
.0007
.0006
.0005
.0004
.0003
.0002
.0001
.0000
C.Wave
Surge
.4
.6
.8
1
1.2
1.4
1.6
1.8
2
FREQUENCY

TL4504.W/S.4*

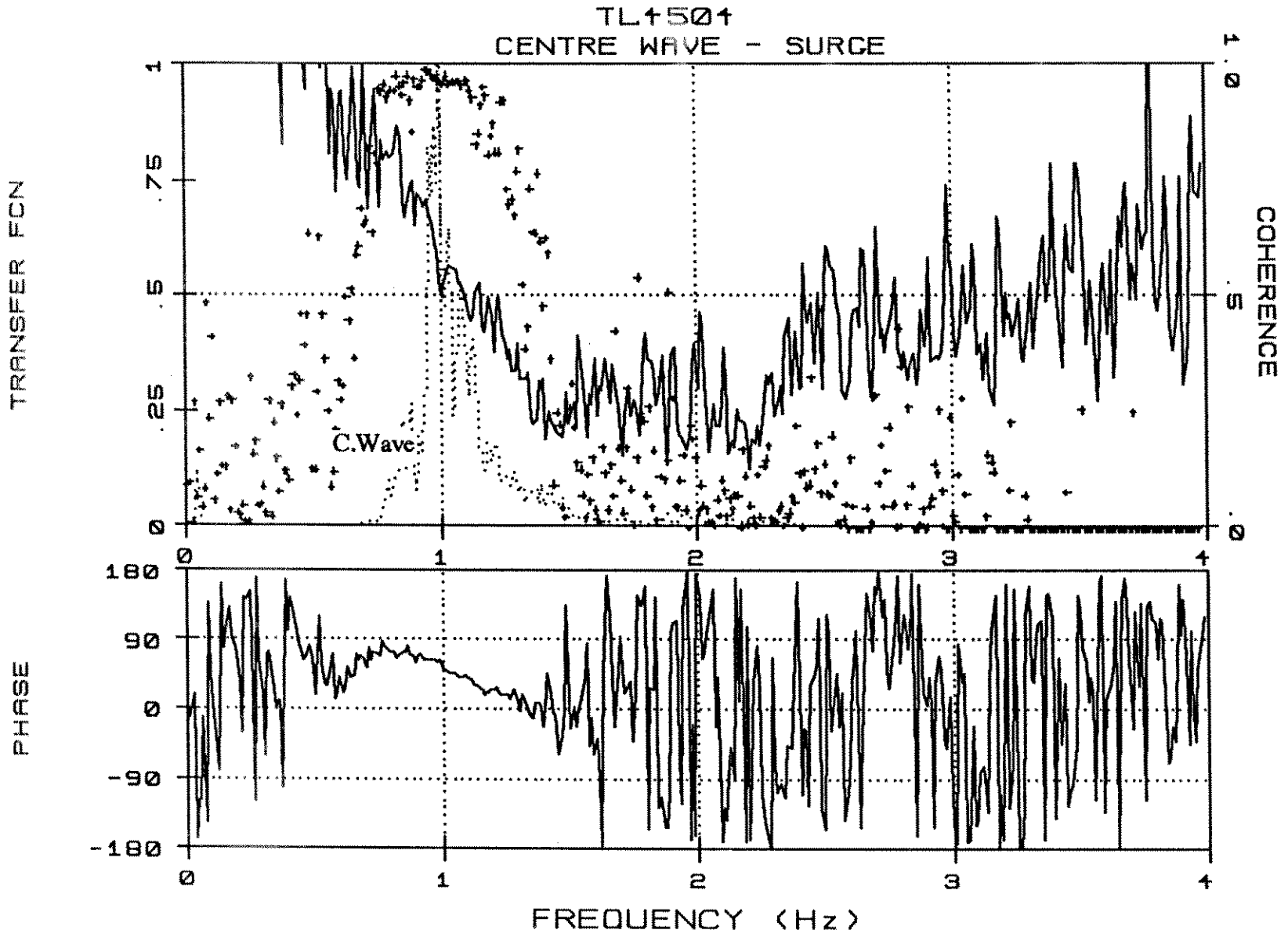
TL1501
CENTRE WAVE - SURGE
TRANSFER FCN
COHERENCE
C.Wave
PHASE
FREQUENCY (Hz)
0
.25
.5
.75
1
1.0
180
90
-90
-180
2
3
4

TL4504.W/S.4t

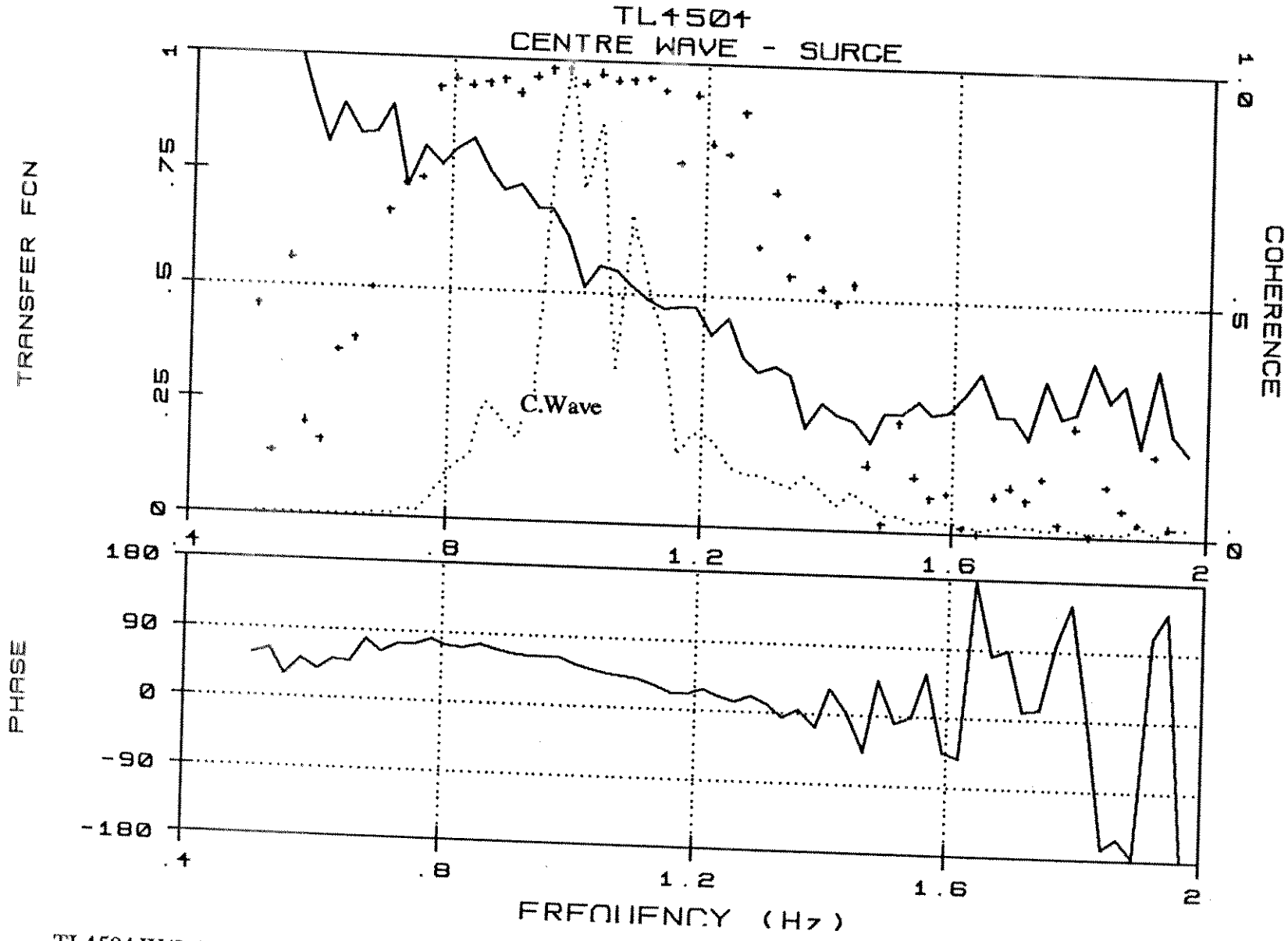
TL4501
CENTRE WAVE - SURGE
TRANSFER FCN
COHERENCE
C.Wave
PHASE
FREQUENCY (Hz)
1
.75
.5
.25
0
1.0
.5
0
180
90
0
-90
-180
.4
.8
1.2
1.6
2

TL4504.W/S.4t*

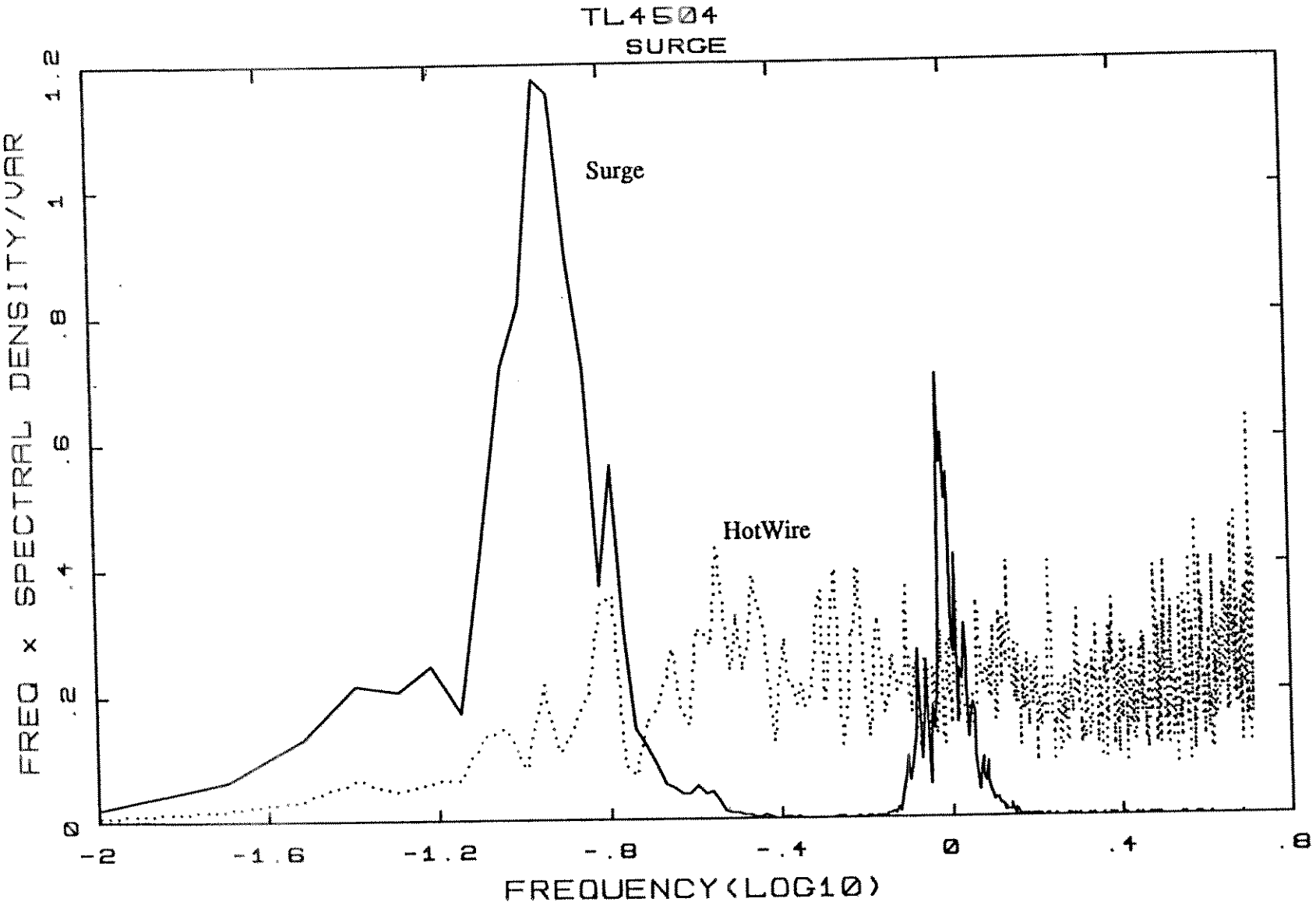
TL4504
SURGE
FREQ x SPECTRAL DENSITY/VAR
0
.2
.4
.6
.8
1
1.2
Surge
HotWire
-2
-1.6
-1.2
-.8
-.4
0
.4
.8
FREQUENCY(LOG10)

TL4504.HW/S.4

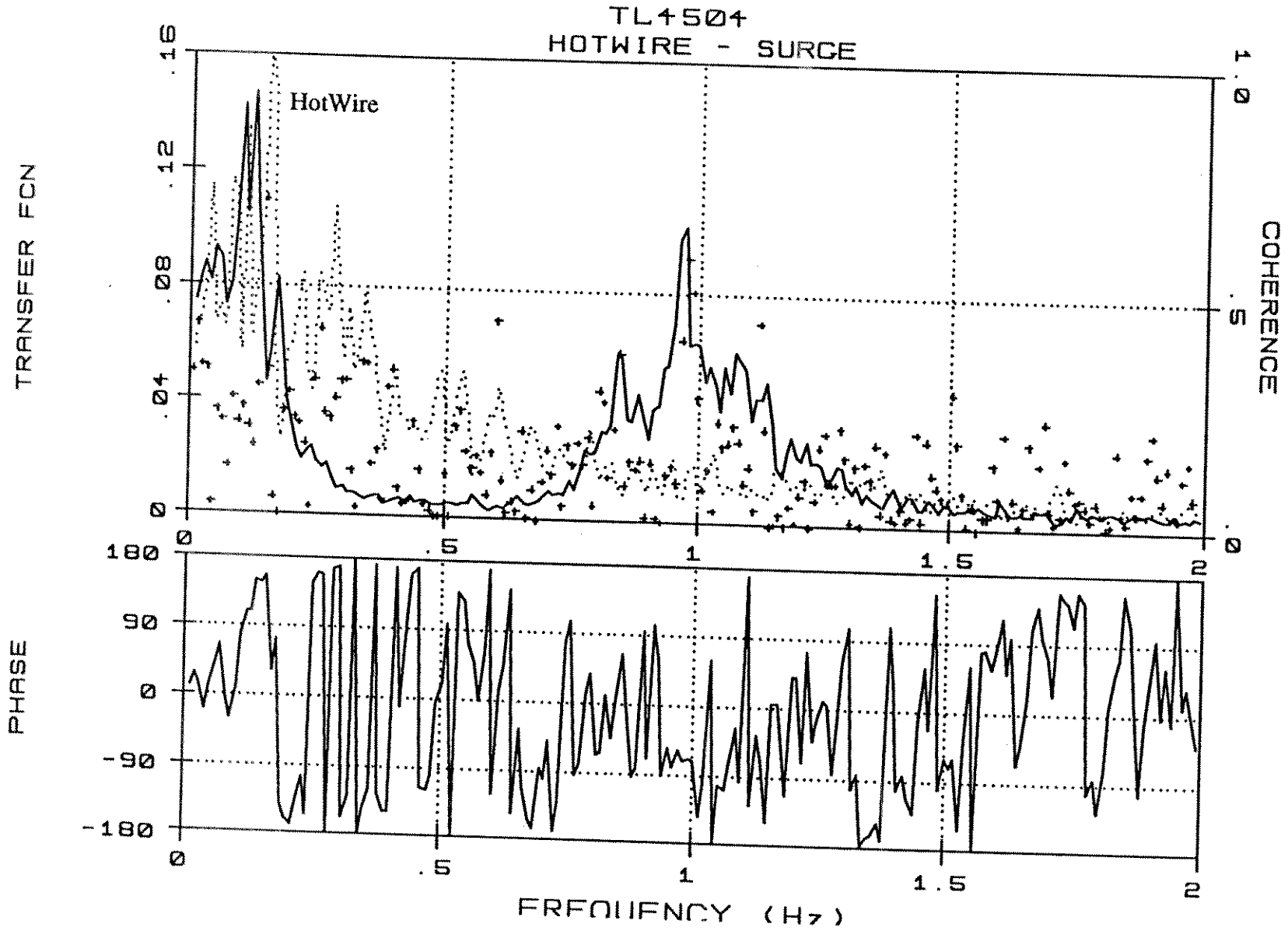

TL4504.HW/S.4t

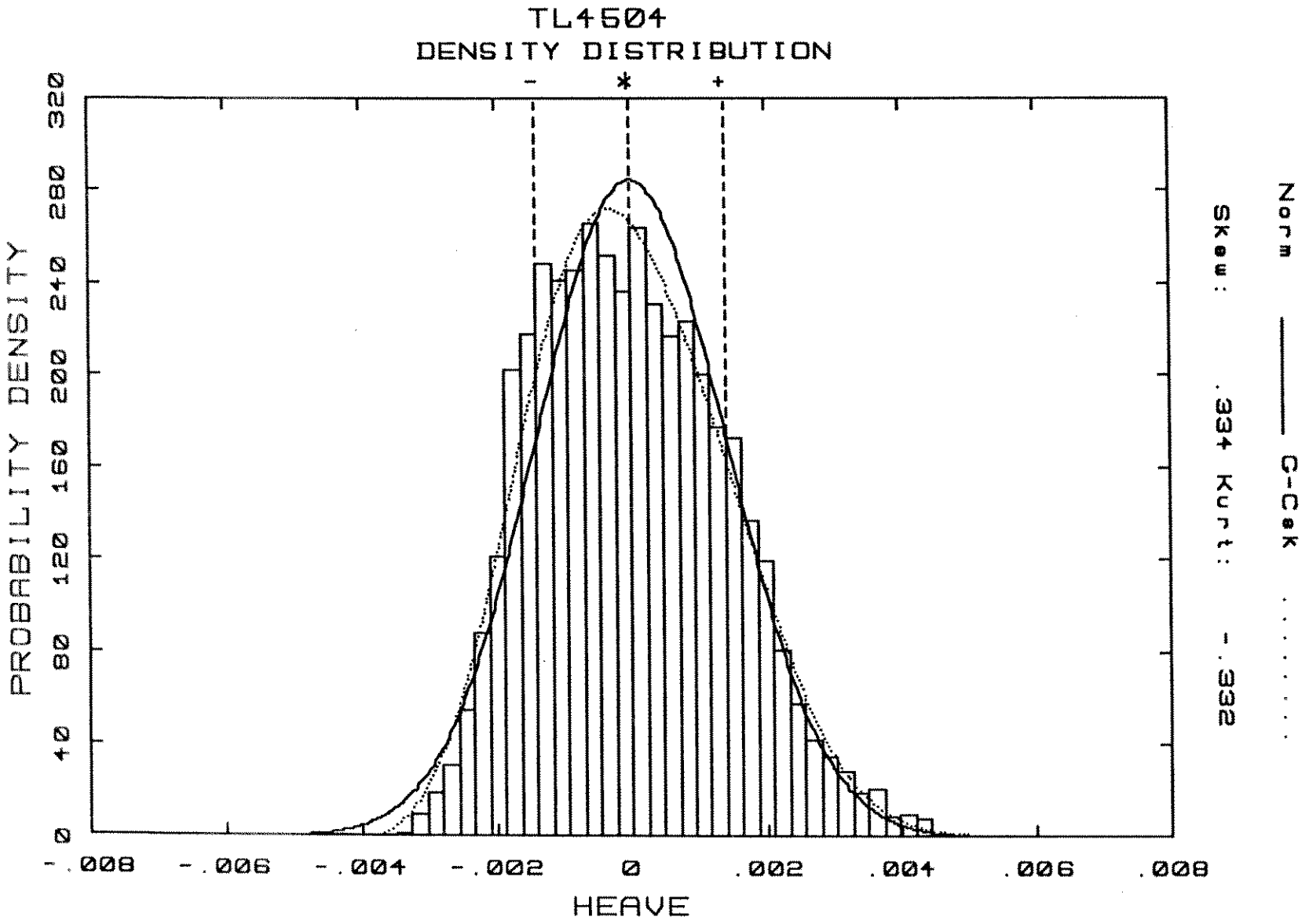
TL4504
DENSITY DISTRIBUTION
- * +
PROBABILITY DENSITY
0 40 80 120 160 200 240 280 320
-.008 -.006 -.004 -.002 0 .002 .004 .006 .008
HEAVE
Norm ——— C-Cek .....
Skew: .334 Kurt: -.332

TL4504.H.1

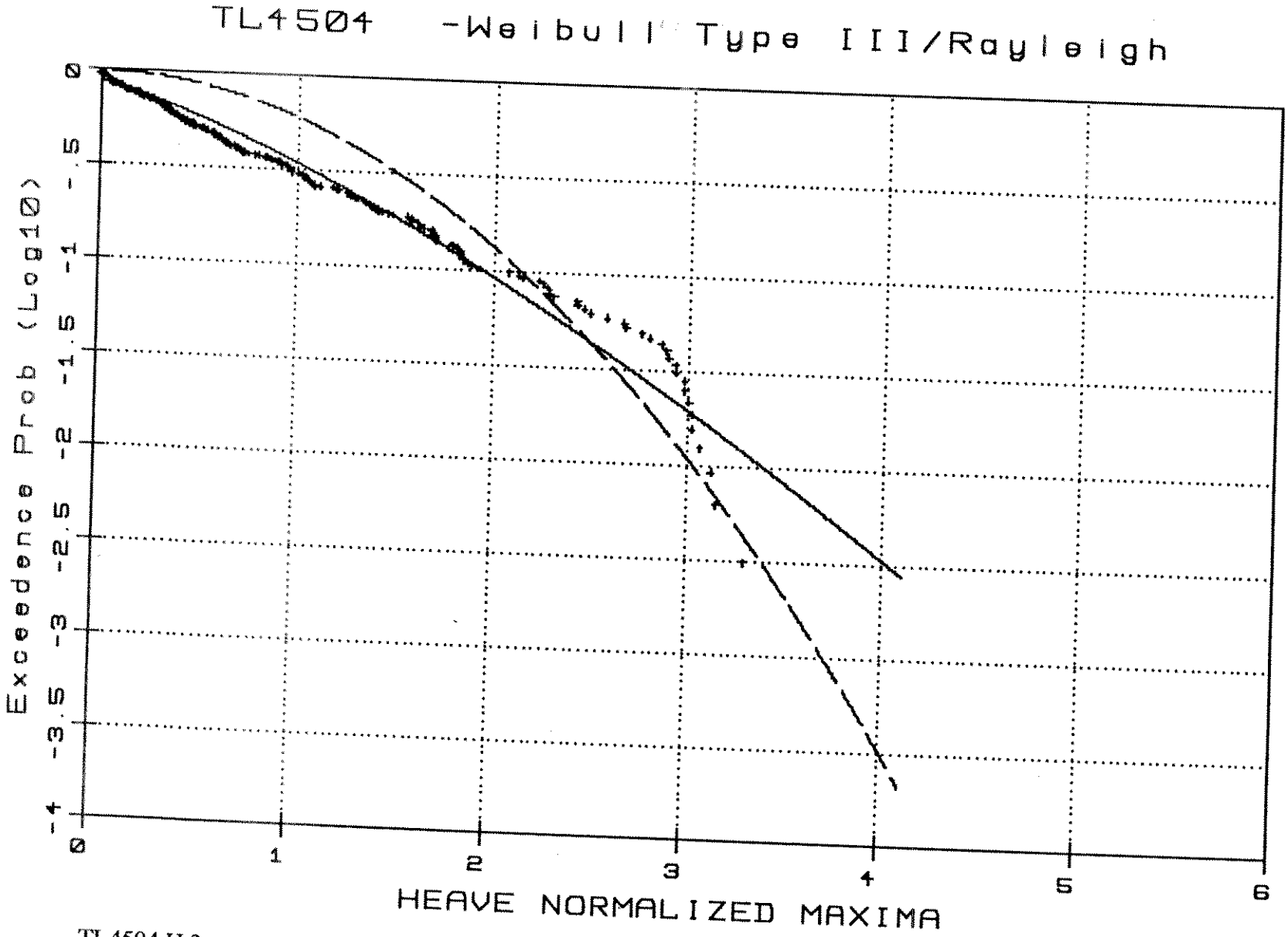
TL4504 -Weibull Type III/Rayleigh
Exceedence Prob (Log10)
0
-.5
-1
-1.5
-2
-2.5
-3
-3.5
-4
0
1
2
3
4
5
6
HEAVE NORMALIZED MAXIMA

TL4504.H.2

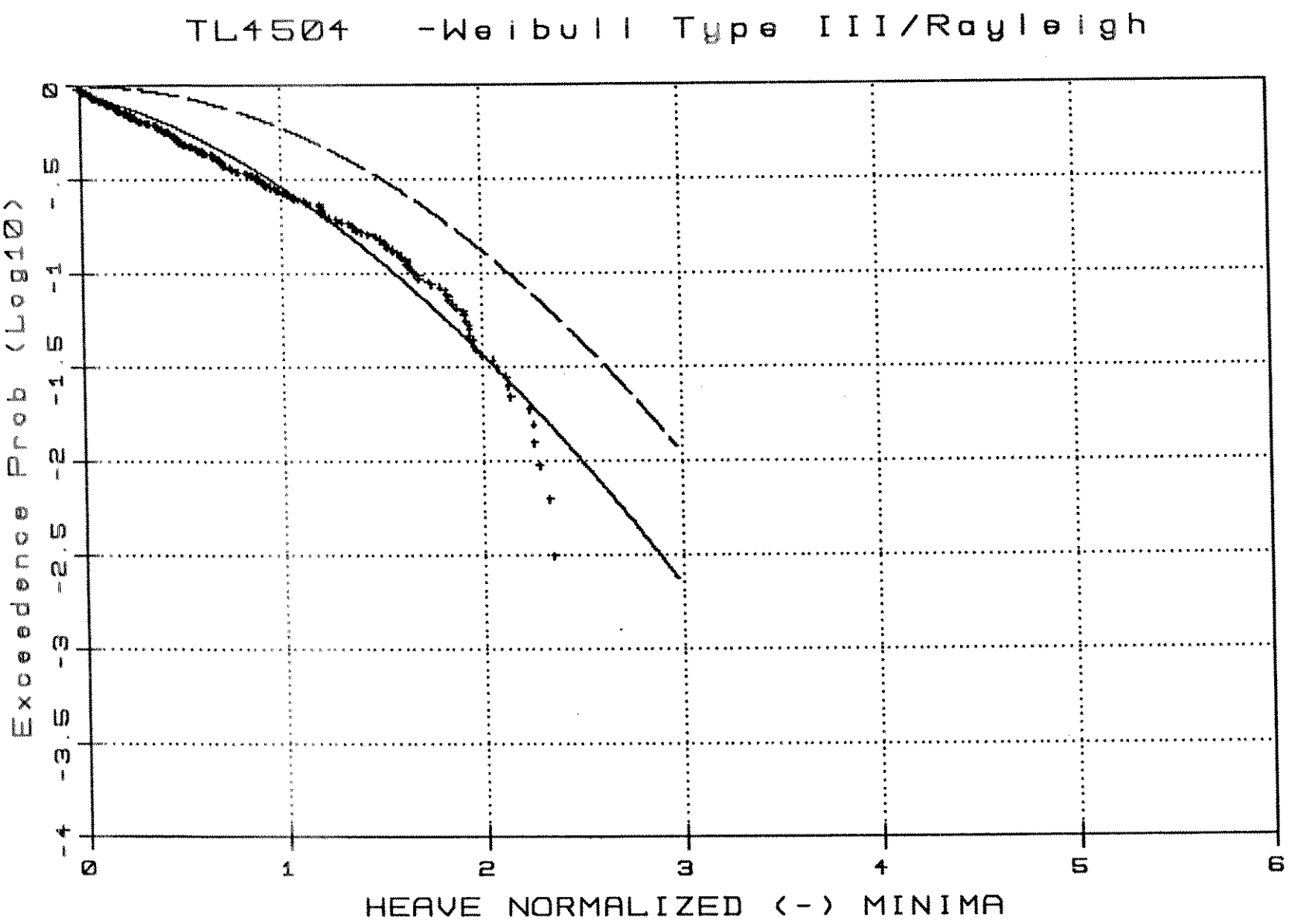
TL4504 -Weibull Type III/Rayleigh
Exceedence Prob (Log10)
0
-.5
-1
-1.5
-2
-2.5
-3
-3.5
-4
0
1
2
3
4
5
6
HEAVE NORMALIZED (-) MINIMA

TL4504.H.3

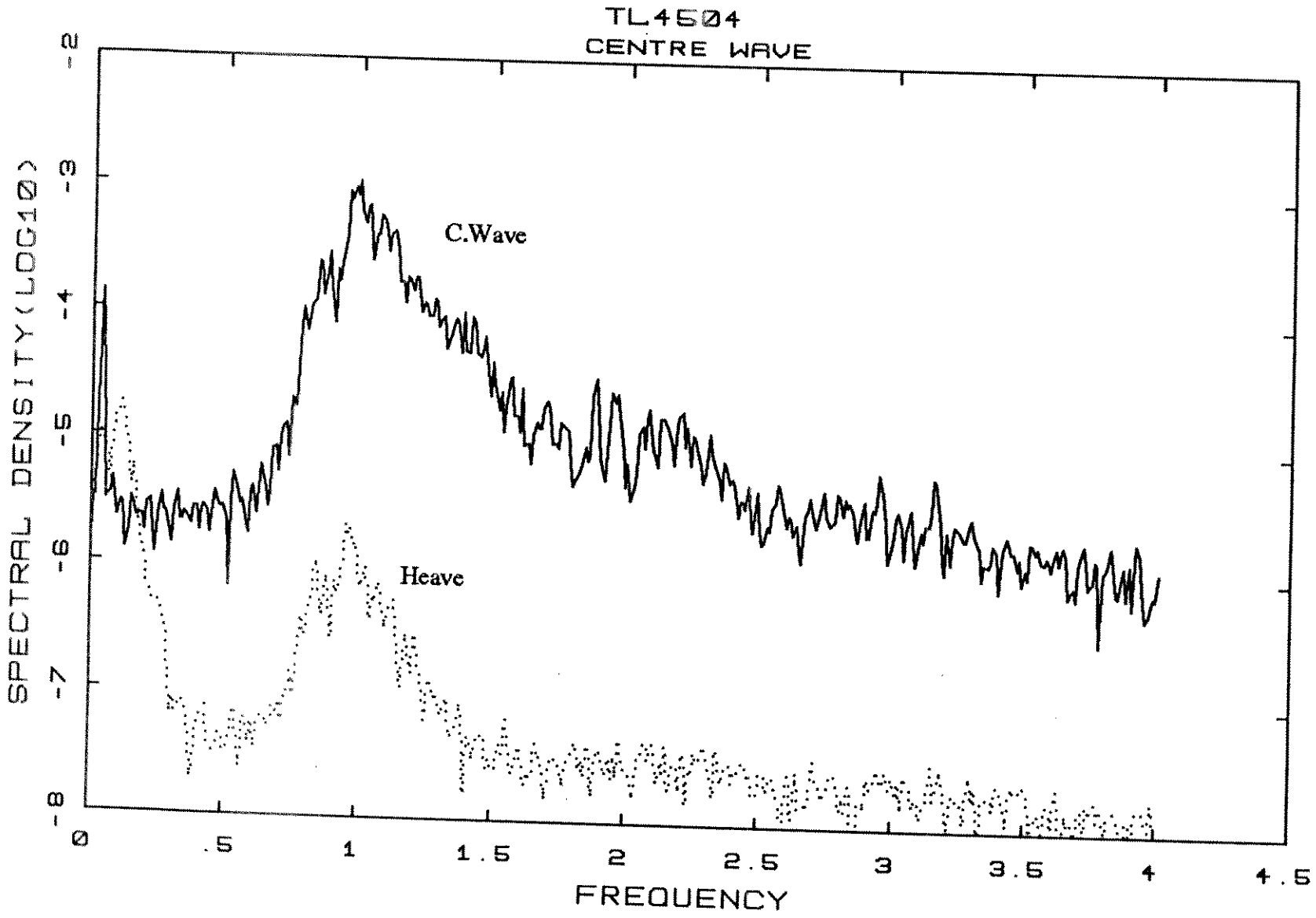
TL4504
CENTRE WAVE
SPECTRAL DENSITY(LOG10)
-2
-3
-4
-5
-6
-7
-8
C.Wave
Heave
0
.5
1
1.5
2
2.5
3
3.5
4
4.5
FREQUENCY

TL4504.W/H.4

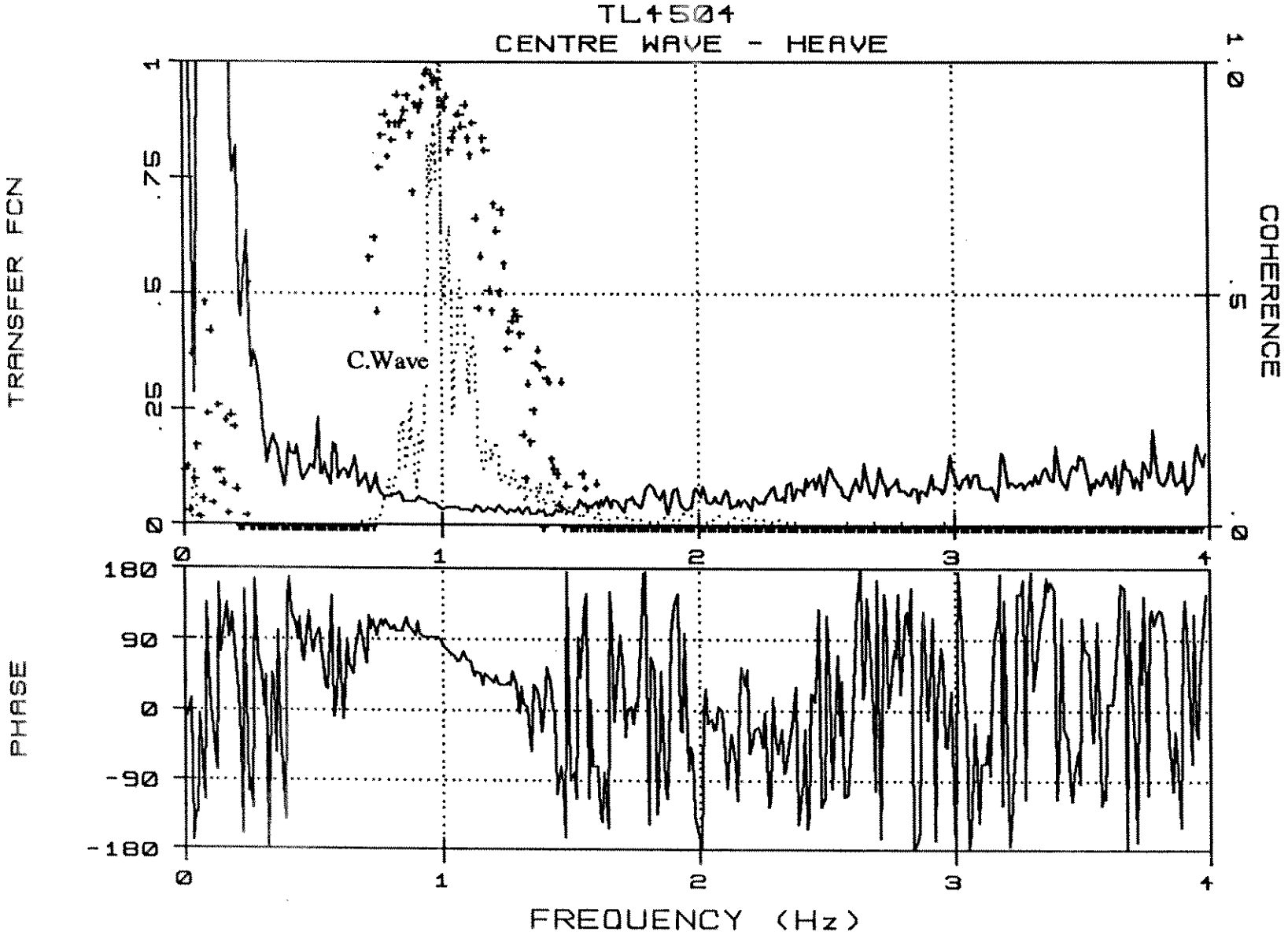
TL4504
CENTRE WAVE - HEAVE
TRANSFER FCN
COHERENCE
C.Wave
PHASE
FREQUENCY (Hz)
1
.75
.5
.25
0
1.0
.5
0
180
90
0
-90
-180
0
1
2
3
4

TL4504.W/H.4t

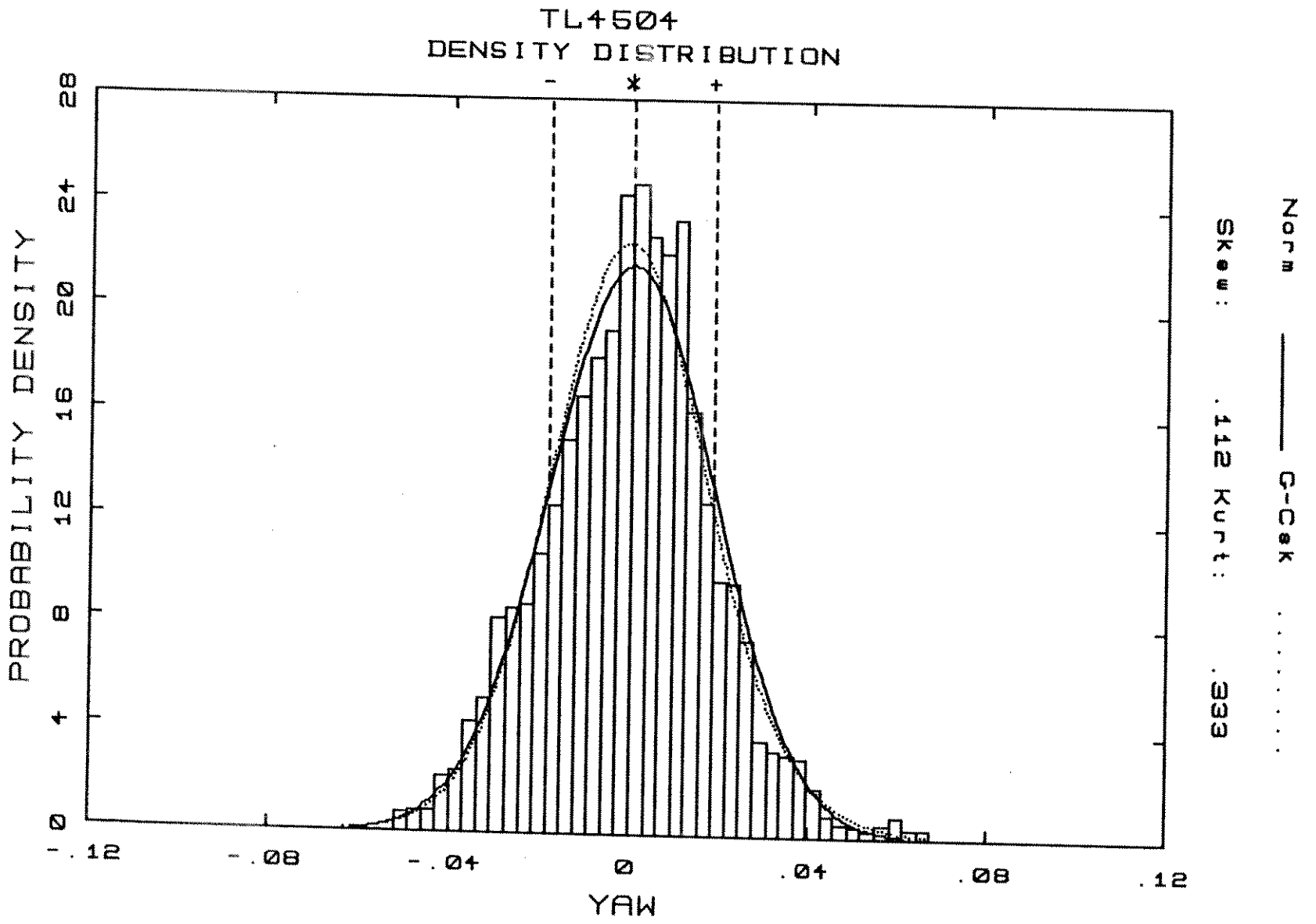
TL4504
DENSITY DISTRIBUTION
- * +
PROBABILITY DENSITY
0
4
8
12
16
20
24
28
-.12
-.08
-.04
0
.04
.08
.12
YAW
Norm
C-Cek
Skew: .112 Kurt: .333

TL4504.Y.1

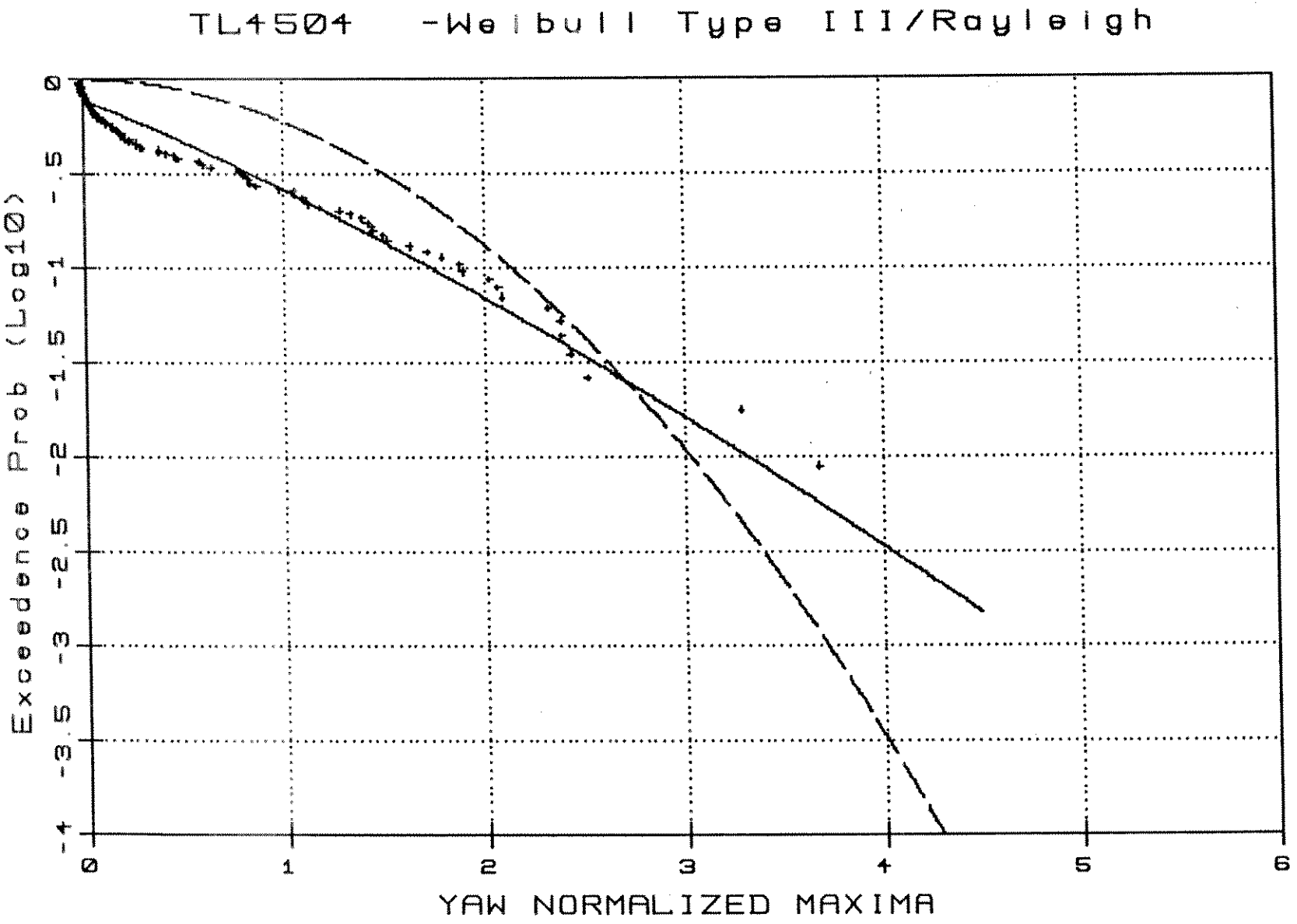
TL4504 -Weibull Type III/Rayleigh
Exceedence Prob (Log10)
0
-.5
-1
-1.5
-2
-2.5
-3
-3.5
-4
0
1
2
3
4
5
6
YAW NORMALIZED MAXIMA

TL4504.Y.2

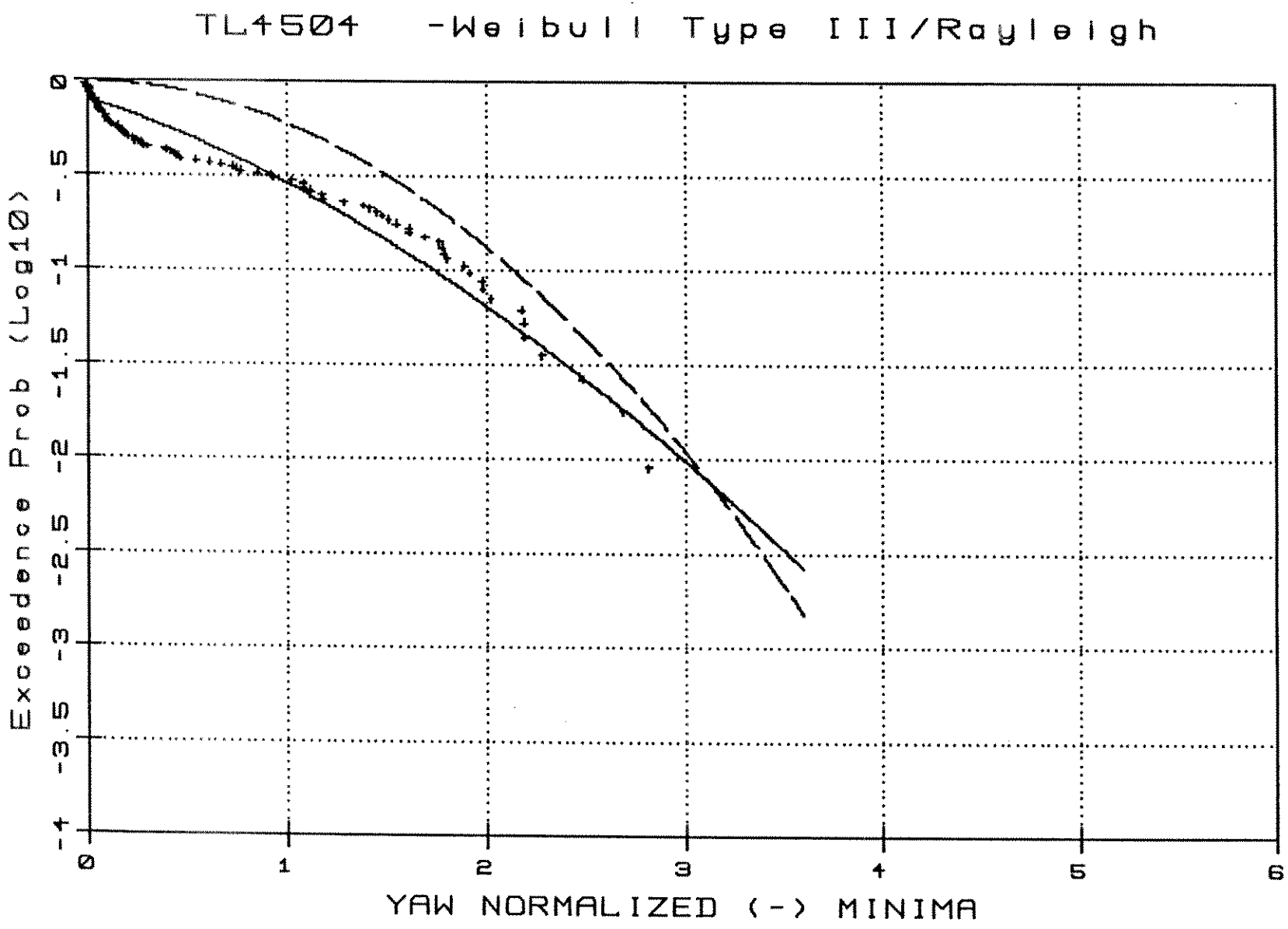
TL4504 -Weibull Type III/Rayleigh
Exceedence Prob (Log10)
0
-.5
-1
-1.5
-2
-2.5
-3
-3.5
-4
0
1
2
3
4
5
6
YAW NORMALIZED (-) MINIMA

TL4504.Y.3

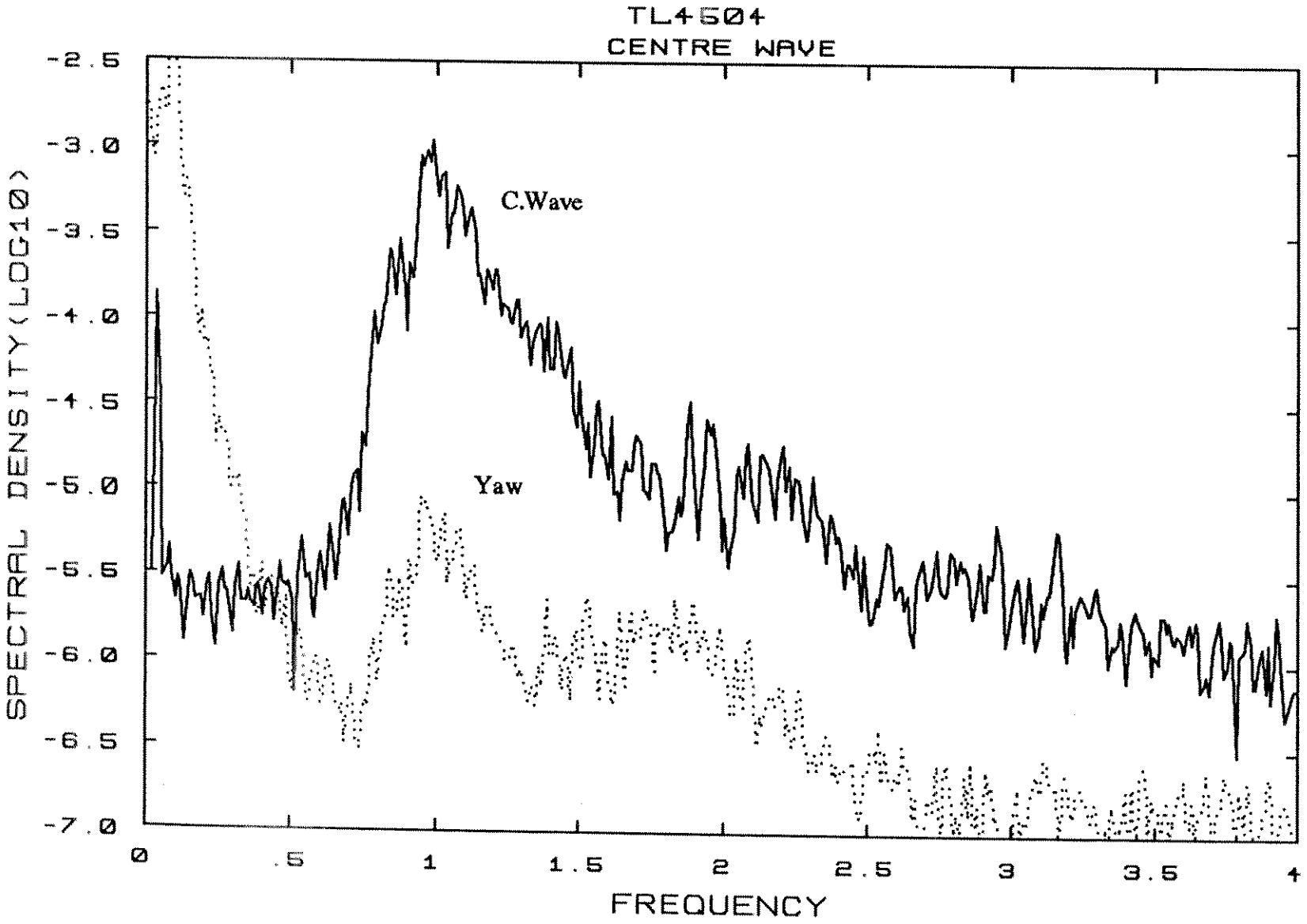
TL4504
CENTRE WAVE
SPECTRAL DENSITY(LOG10)
-2.5
-3.0
-3.5
-4.0
-4.5
-5.0
-5.5
-6.0
-6.5
-7.0
C.Wave
Yaw
0
.5
1
1.5
2
2.5
3
3.5
4
FREQUENCY

TL4504.W/Y.4

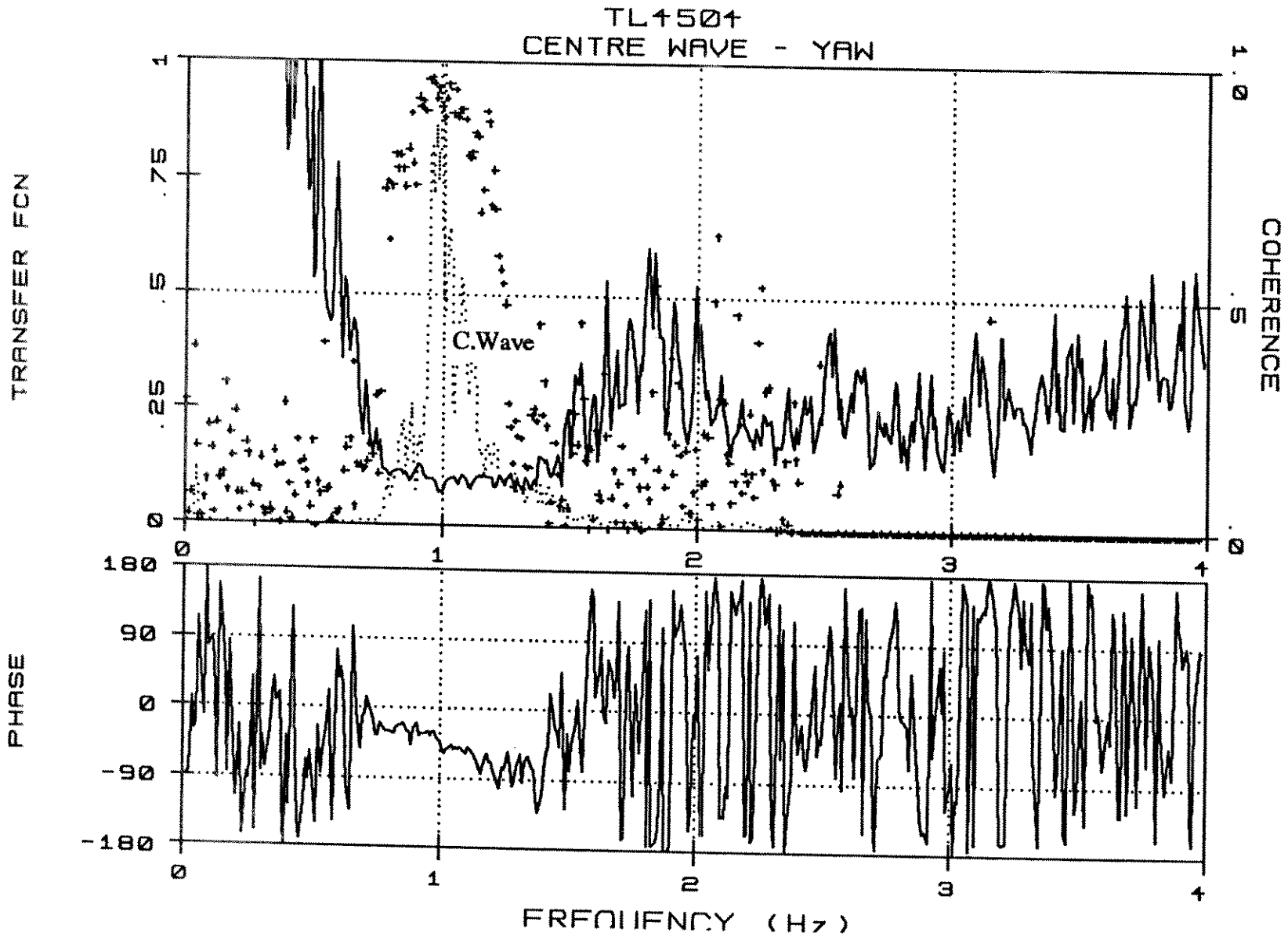
TL4501
CENTRE WAVE - YAW
TRANSFER FCN
COHERENCE
C.Wave
PHASE
FREQUENCY (Hz)
1.0
.75
.5
.25
0
180
90
0
-90
-180
1
2
3
4

TL4504.W/Y.4t

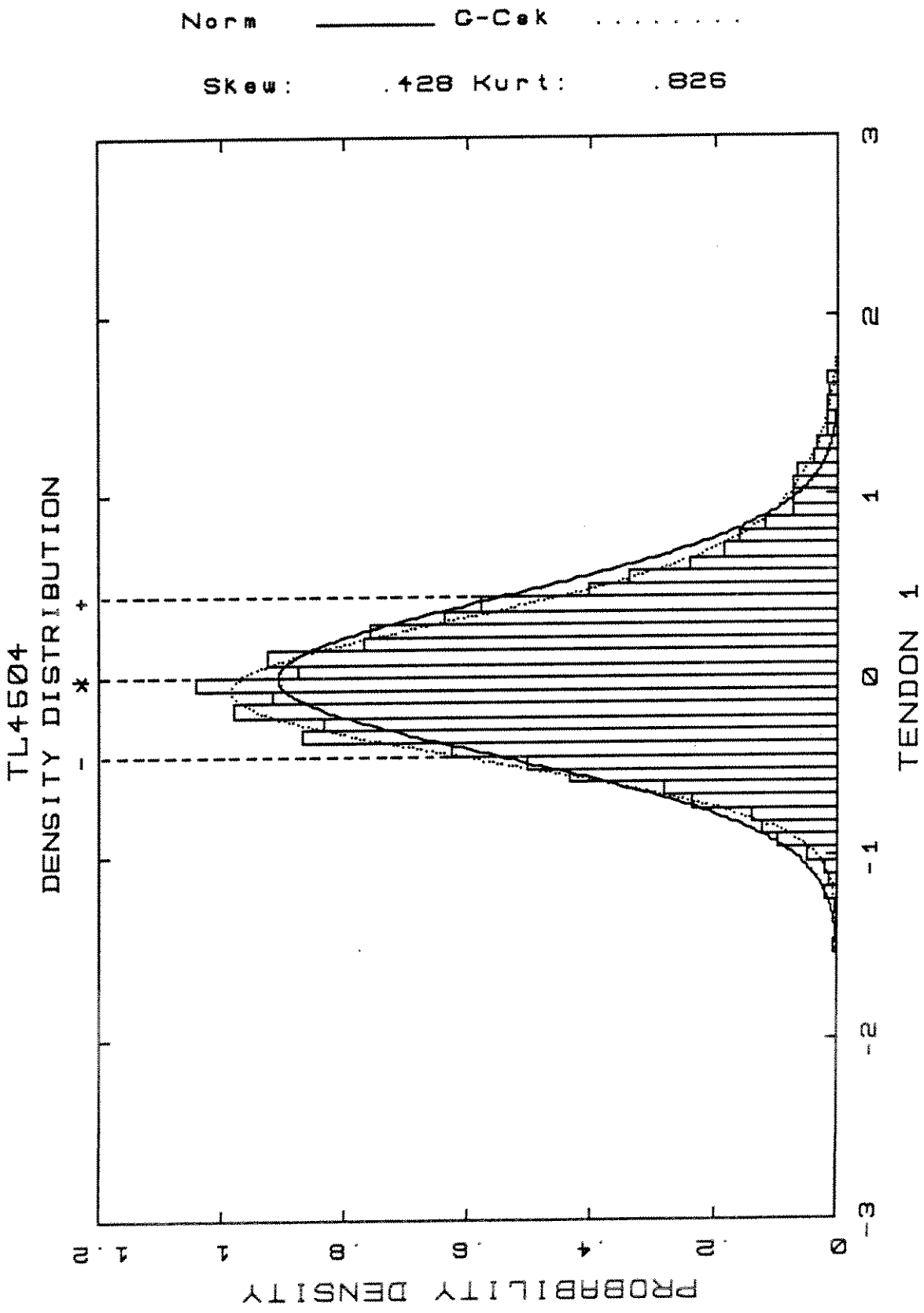
Norm
G-Cek
Skew: .428 Kurt: .826
TL4504
DENSITY DISTRIBUTION
TENDON 1
PROBABILITY DENSITY
3
2
1
0
-1
-2
-3
1.2
1
.8
.6
.4
.2
0

TL4504.T1.1

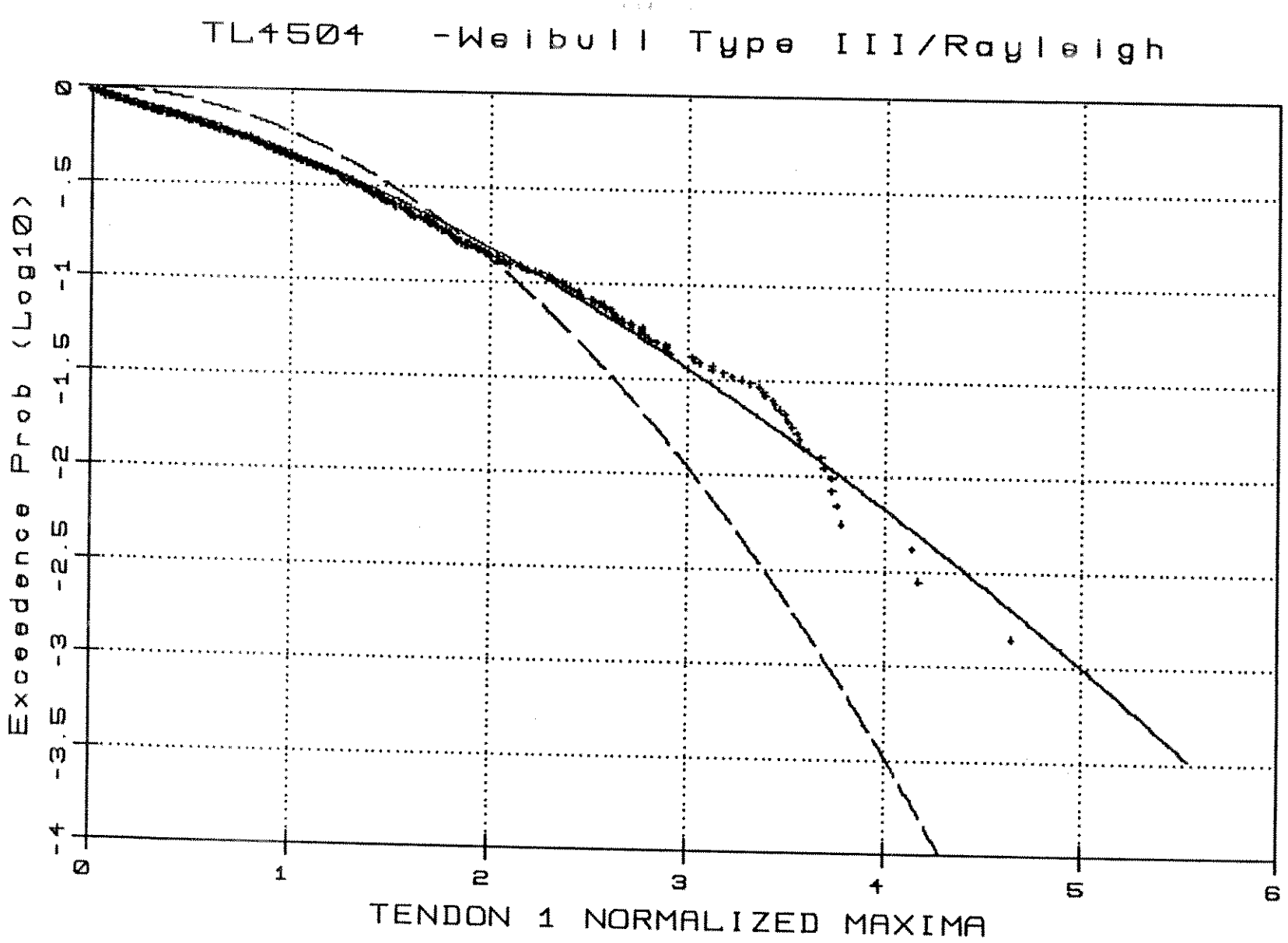
TL4504 -Weibull Type III/Rayleigh
Exceedence Prob (Log10)
0
-.5
-1
-1.5
-2
-2.5
-3
-3.5
-4
0
1
2
3
4
5
6
TENDON 1 NORMALIZED MAXIMA

TL4504.T1.2

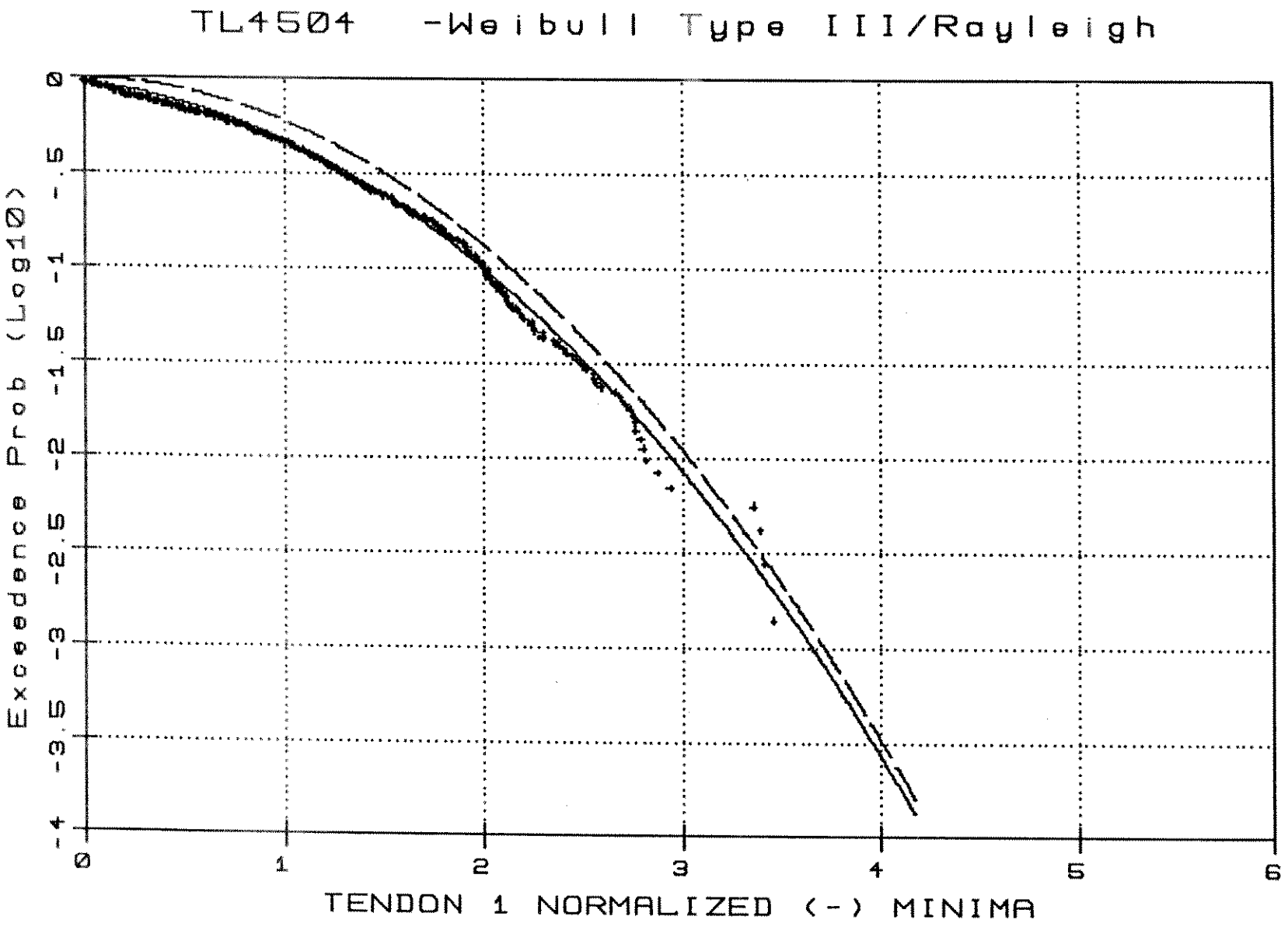
TL4504 -Weibull Type III/Rayleigh
Exceedence Prob (Log10)
0
-.5
-1
-1.5
-2
-2.5
-3
-3.5
-4
0
1
2
3
4
5
6
TENDON 1 NORMALIZED (-) MINIMA

TL4504.T1.3

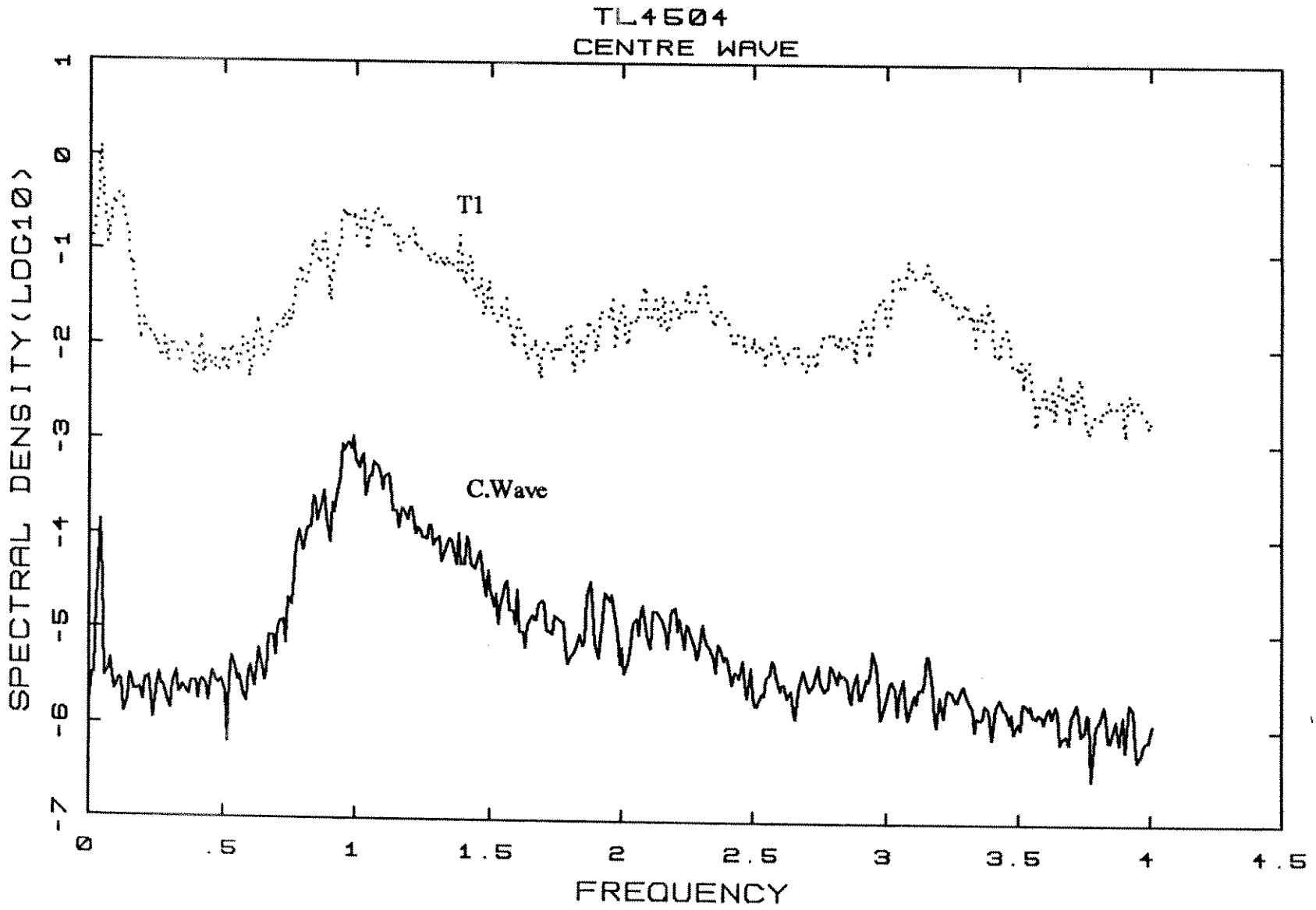
TL4504
CENTRE WAVE
SPECTRAL DENSITY(LOG10)
1
0
-1
-2
-3
-4
-5
-6
-7
T1
C.Wave
0
.5
1
1.5
2
2.5
3
3.5
4
4.5
FREQUENCY

TL4504.W/T1.4

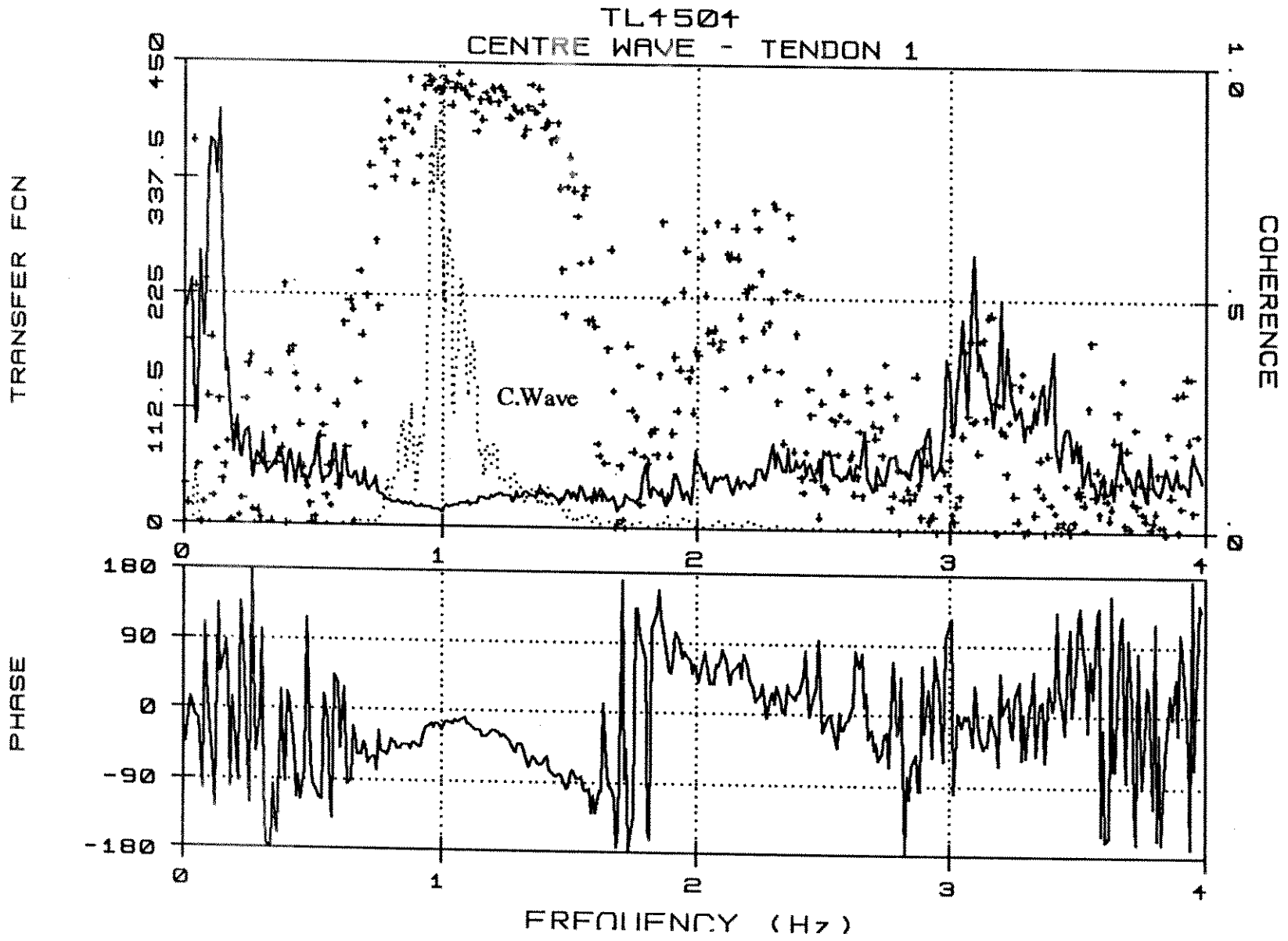

TL4504.W/T1.4t

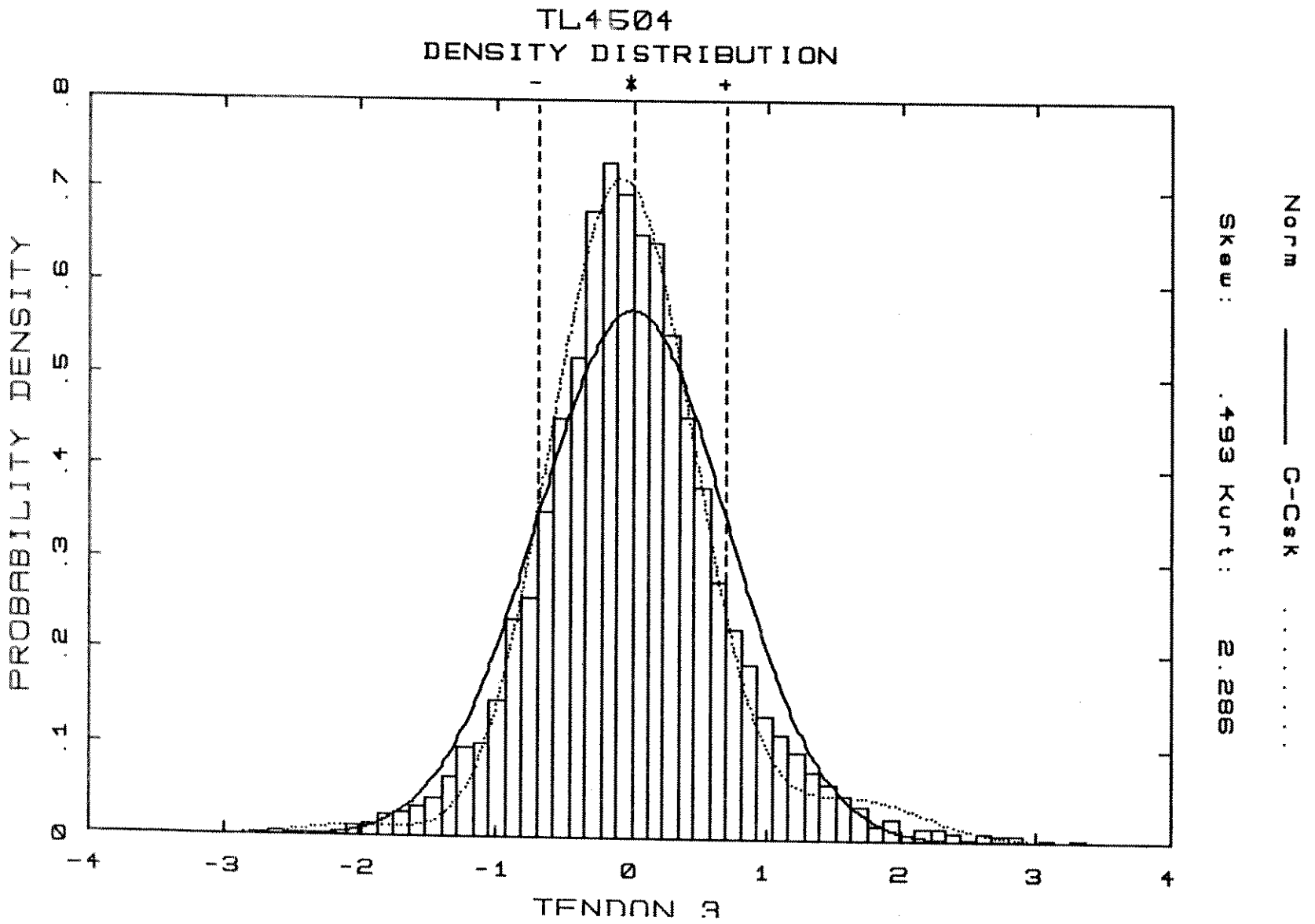
TL4504
DENSITY DISTRIBUTION
- * +
PROBABILITY DENSITY
0 .1 .2 .3 .4 .5 .6 .7 .8
-4 -3 -2 -1 0 1 2 3 4
TENDON 3
Norm
C-Csk
Skew: .493 Kurt: 2.286

TL4504.T3.1

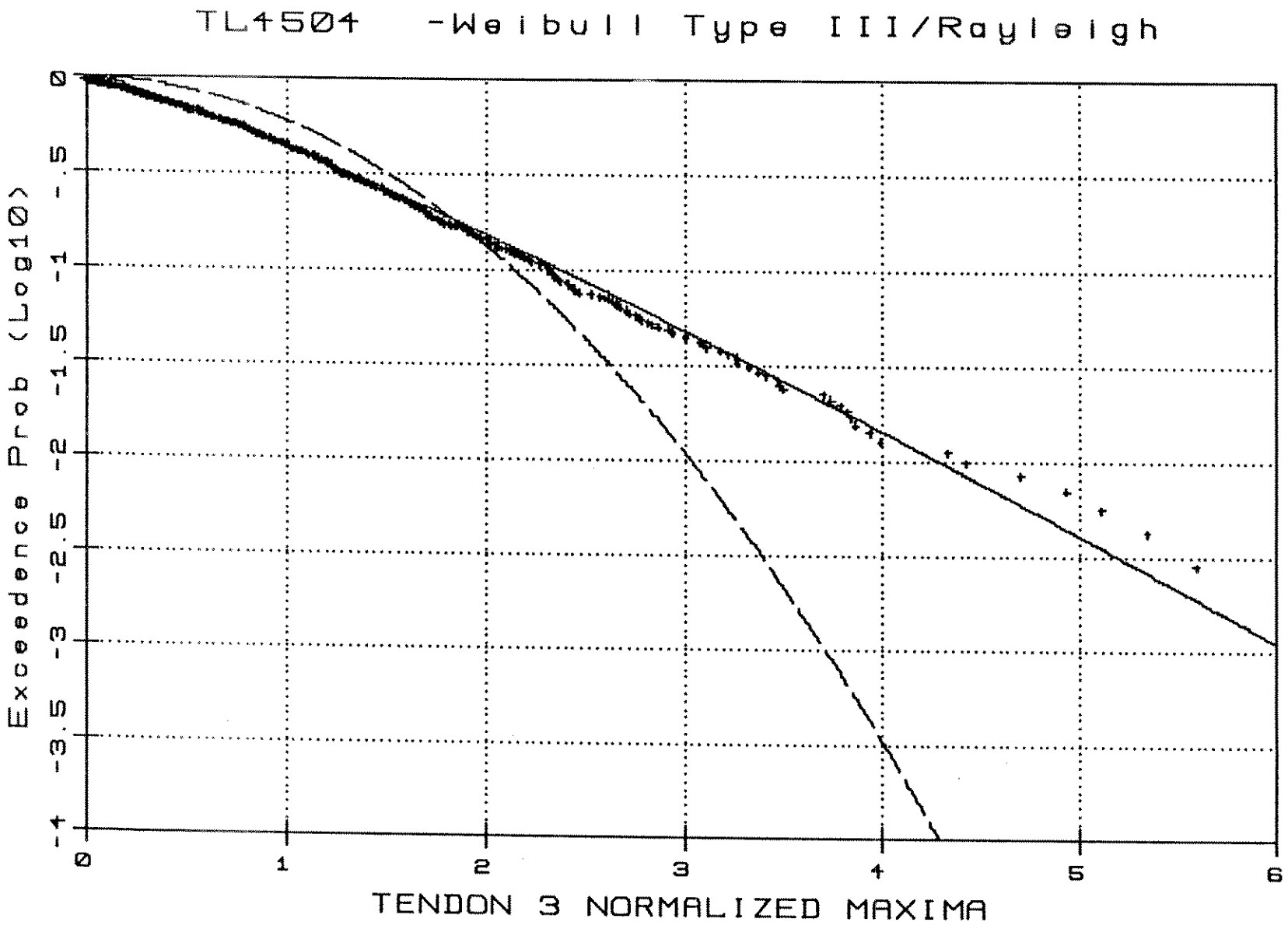
TL4504 -Weibull Type III/Rayleigh
Exceedence Prob (Log10)
0
-.5
-1
-1.5
-2
-2.5
-3
-3.5
-4
0
1
2
3
4
5
6
TENDON 3 NORMALIZED MAXIMA

TL4504.T3.2

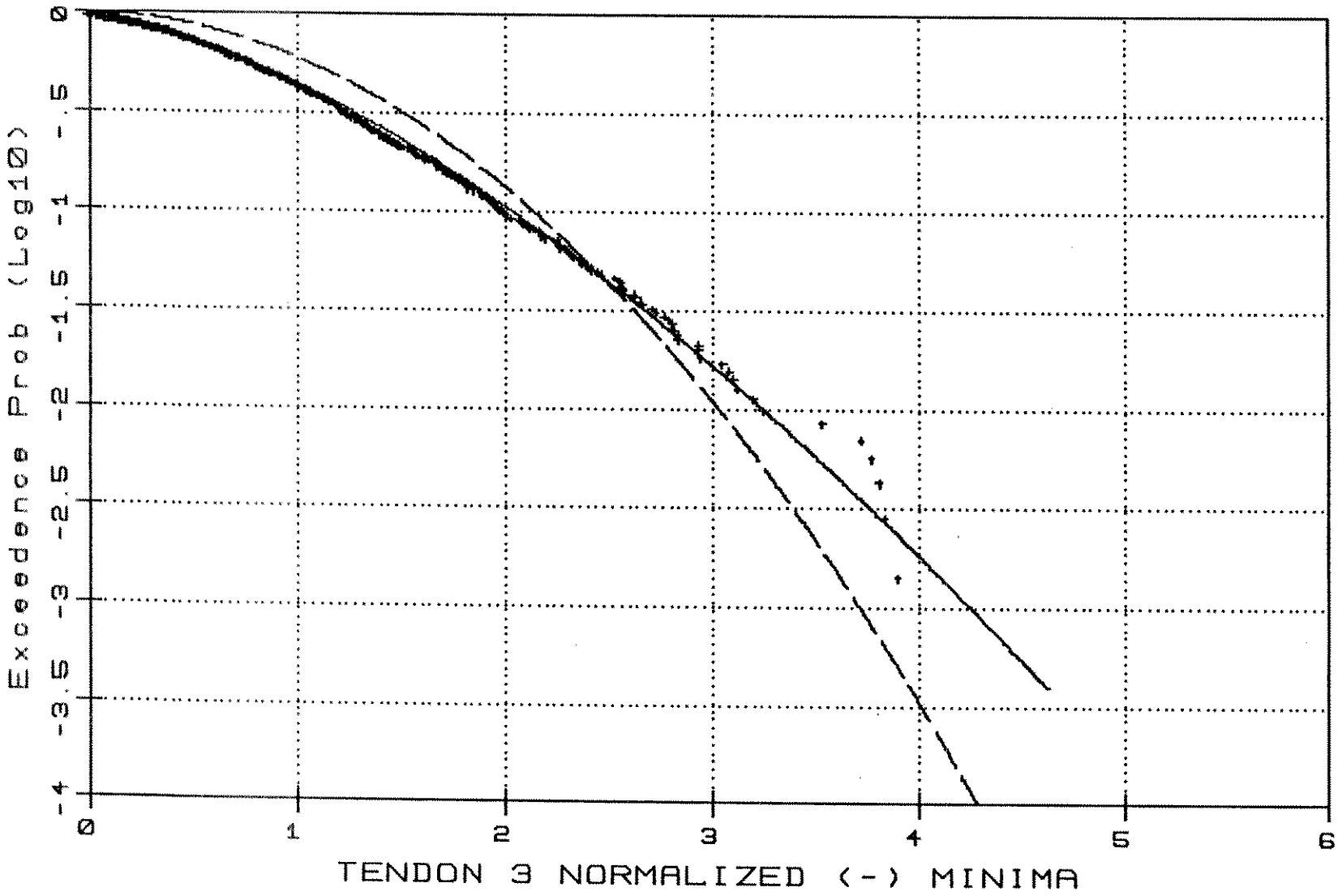
TL4504 -Weibull Type III/Rayleigh
Exceedence Prob (Log10)
0
-.5
-1
-1.5
-2
-2.5
-3
-3.5
-4
0
1
2
3
4
5
6
TENDON 3 NORMALIZED (-) MINIMA

TL4504.T3.3

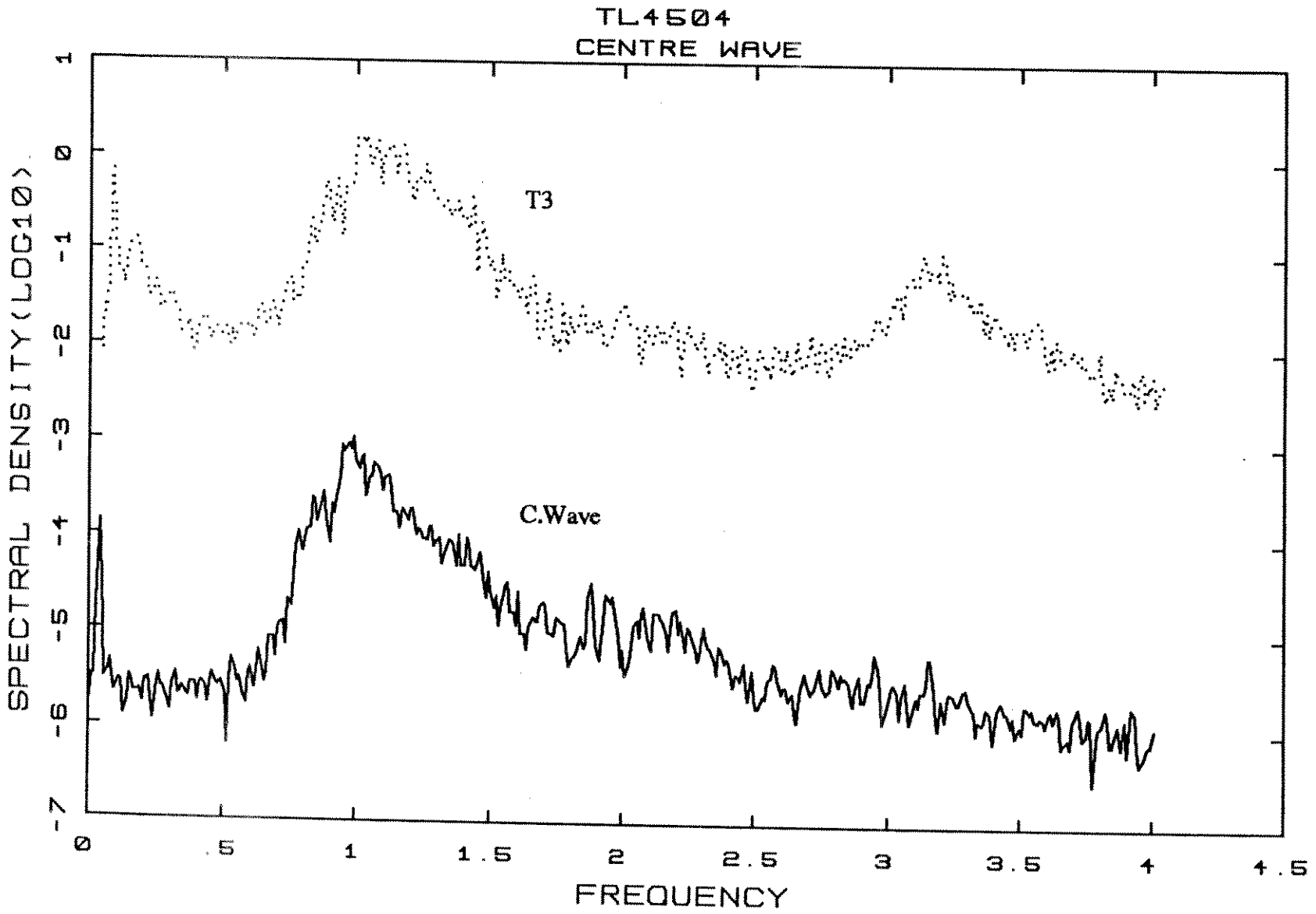
TL4504
CENTRE WAVE
SPECTRAL DENSITY(LOG10)
1
0
-1
-2
-3
-4
-5
-6
-7
T3
C.Wave
0
.5
1
1.5
2
2.5
3
3.5
4
4.5
FREQUENCY

TL4504.W/T3.4

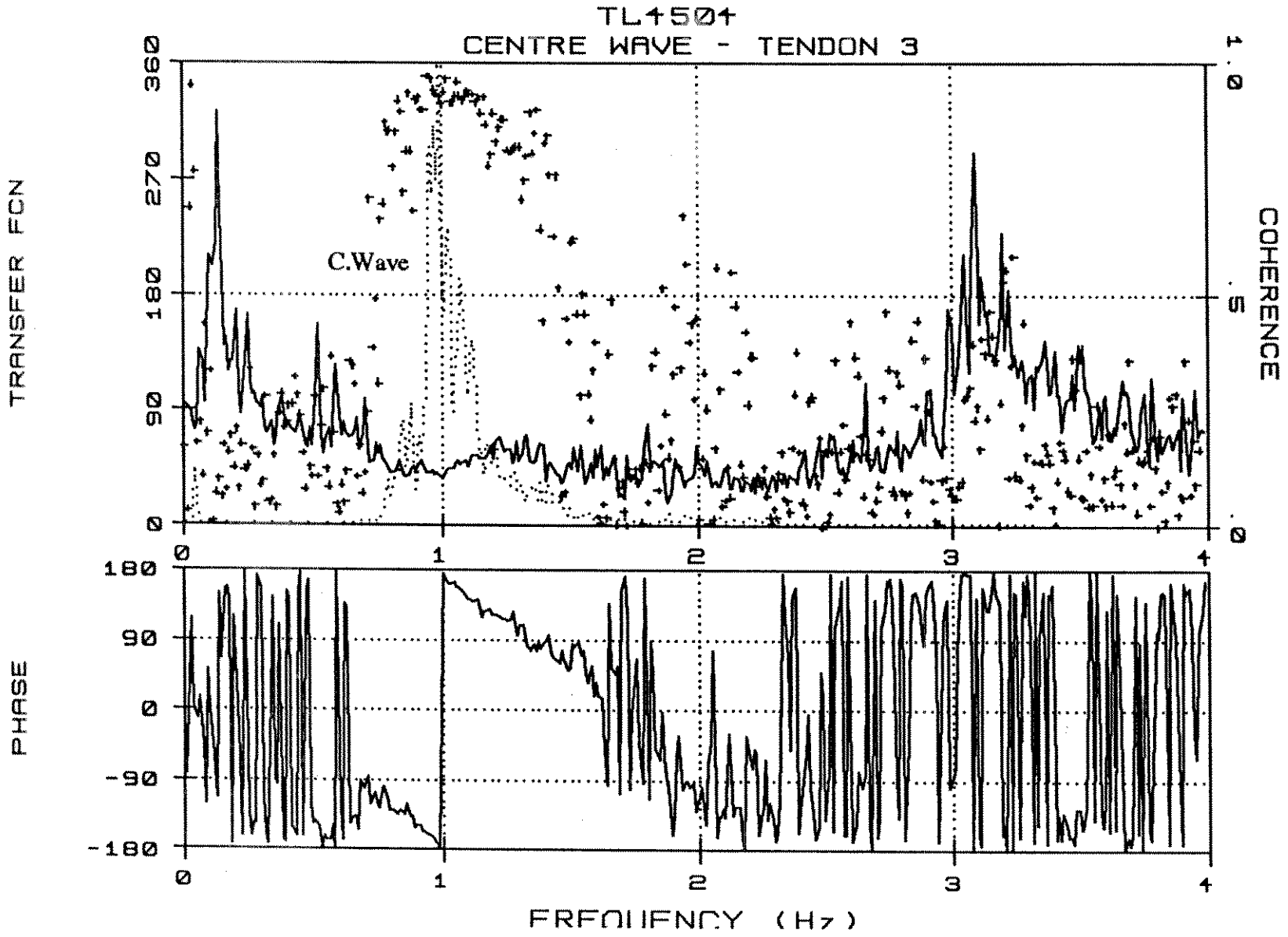

TL4504.W/T3.4t

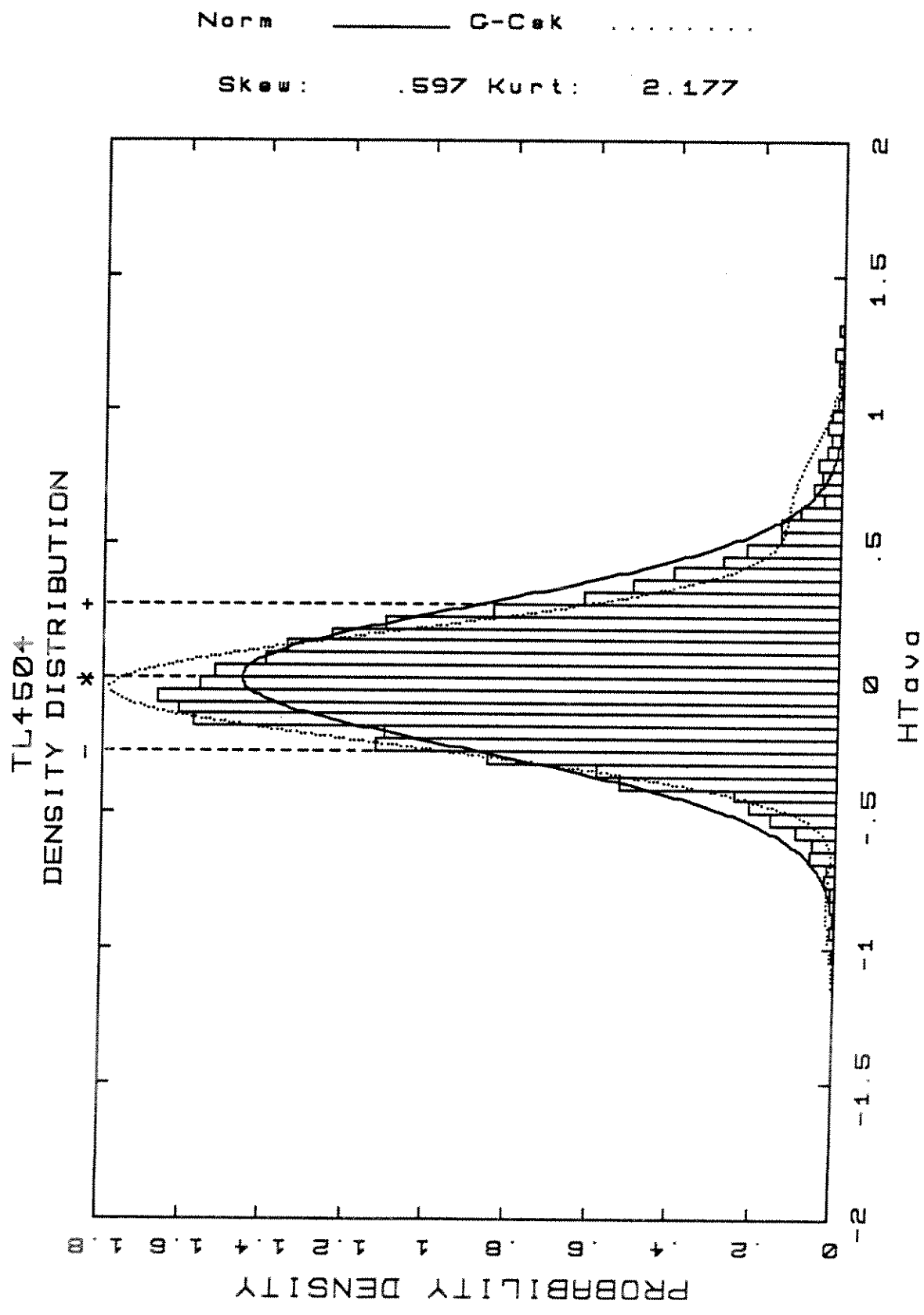

TL4504.HTavg.1

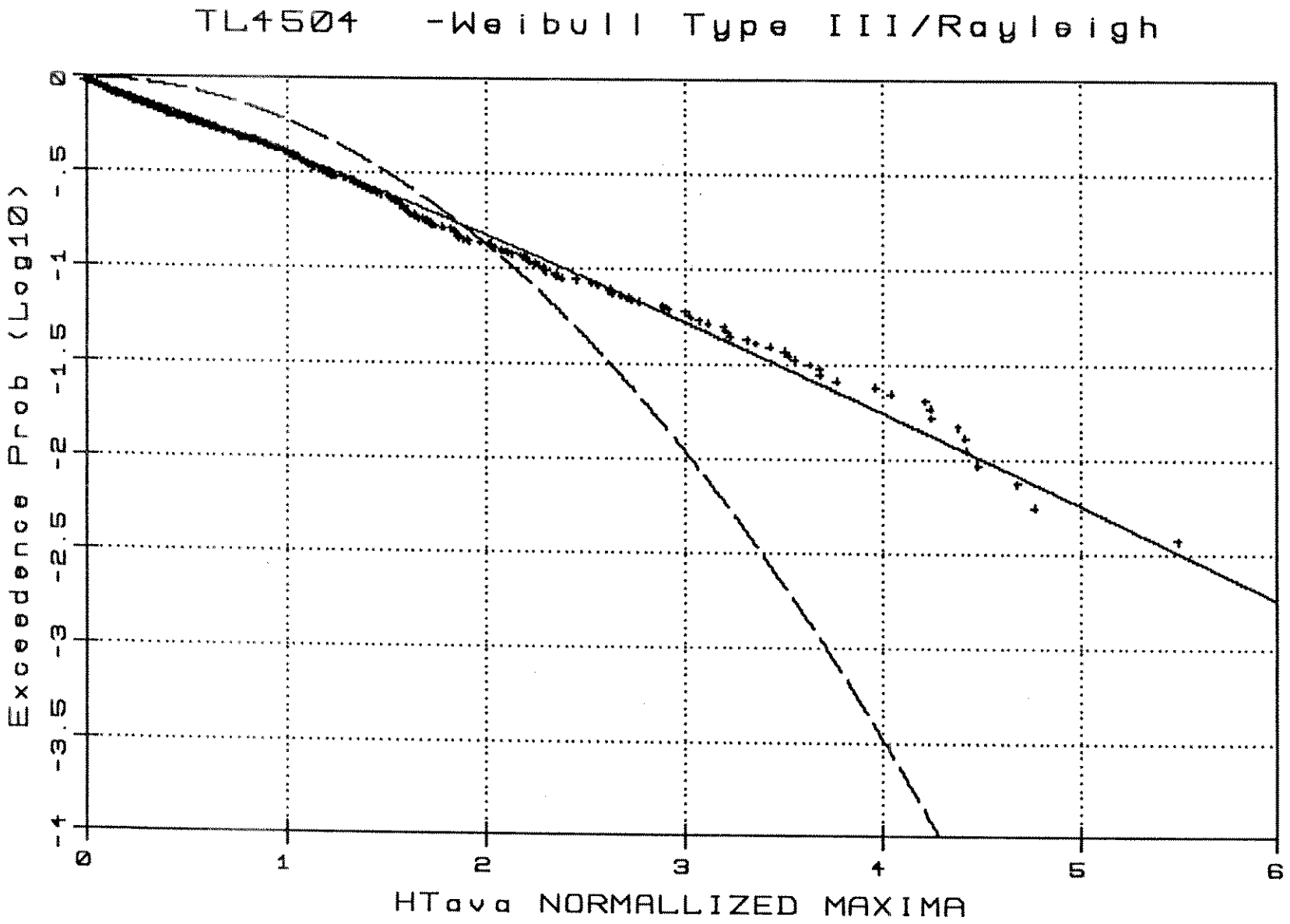

TL4504.HTavg.2

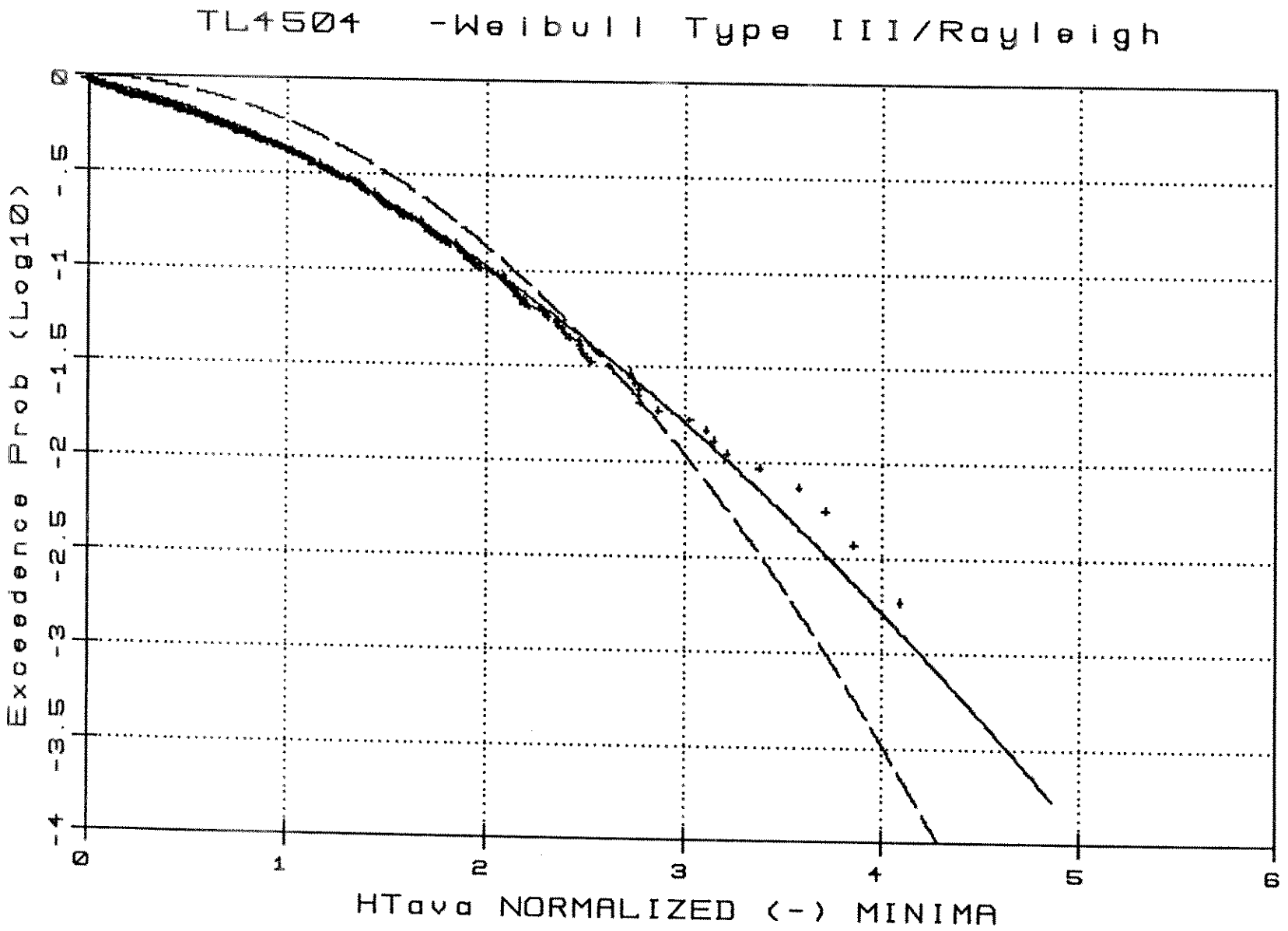

TL4504.HTavg.3

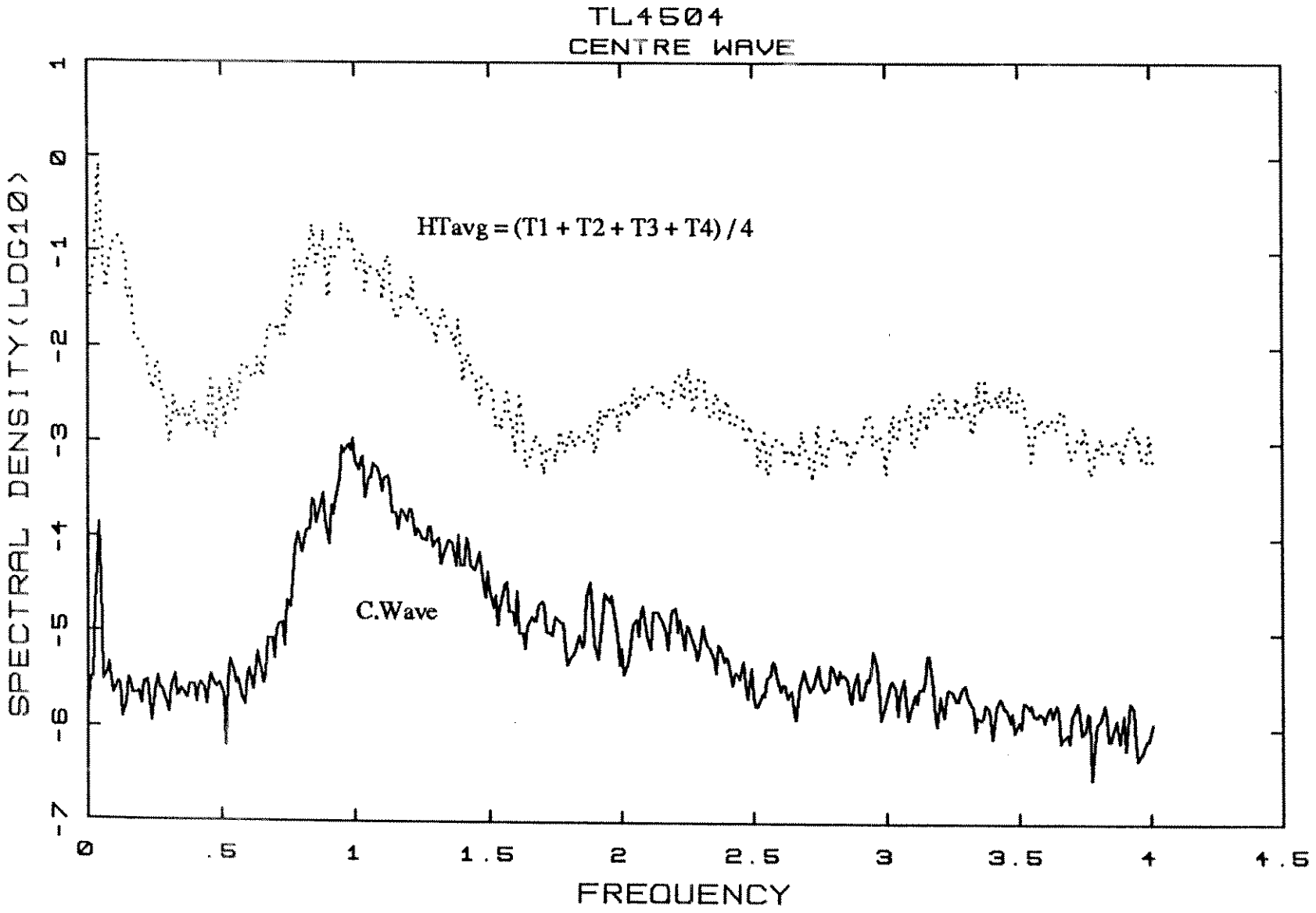

TL4504.W/HTavg.4

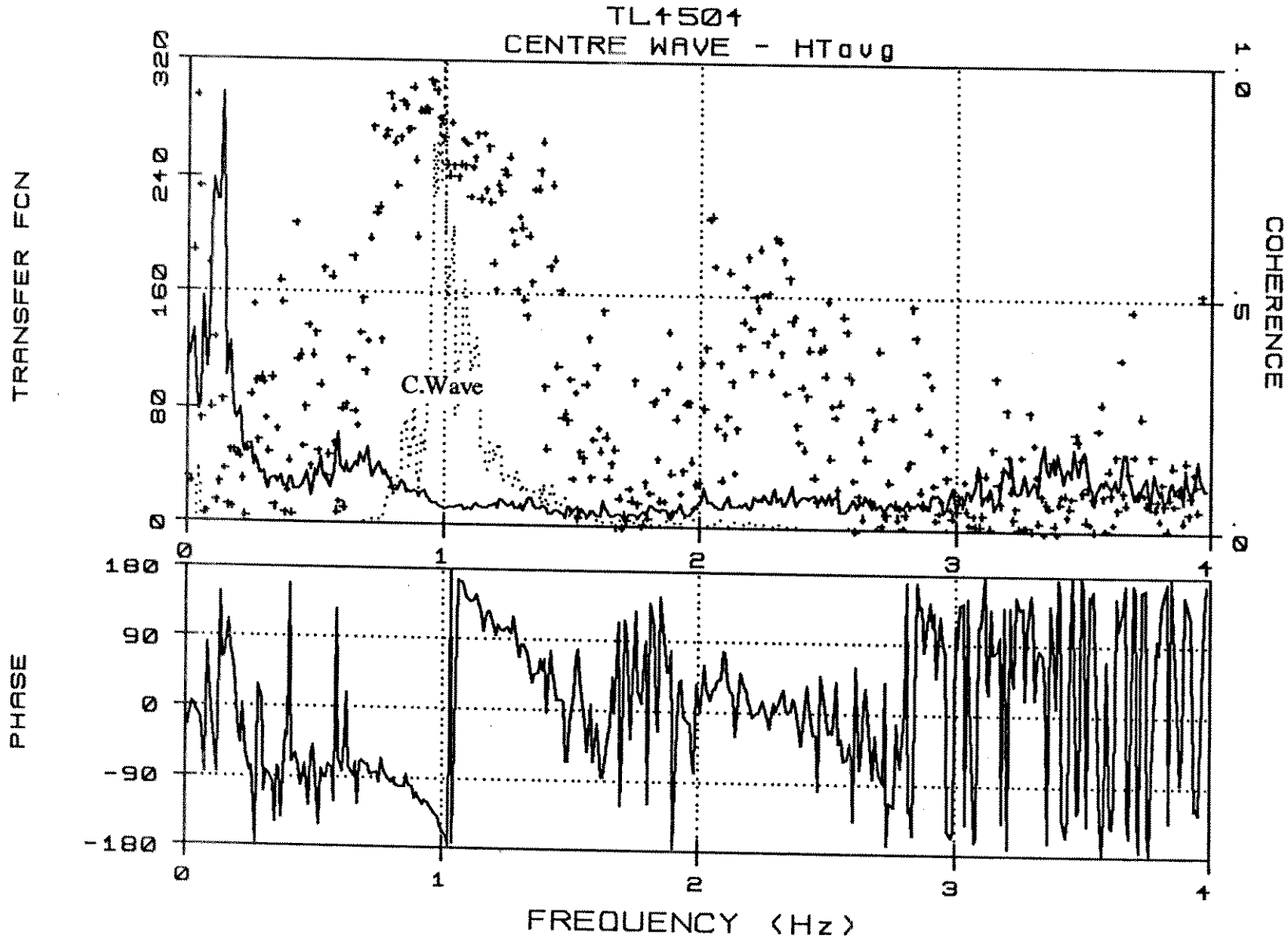

TL4504.W/HTavg.4t

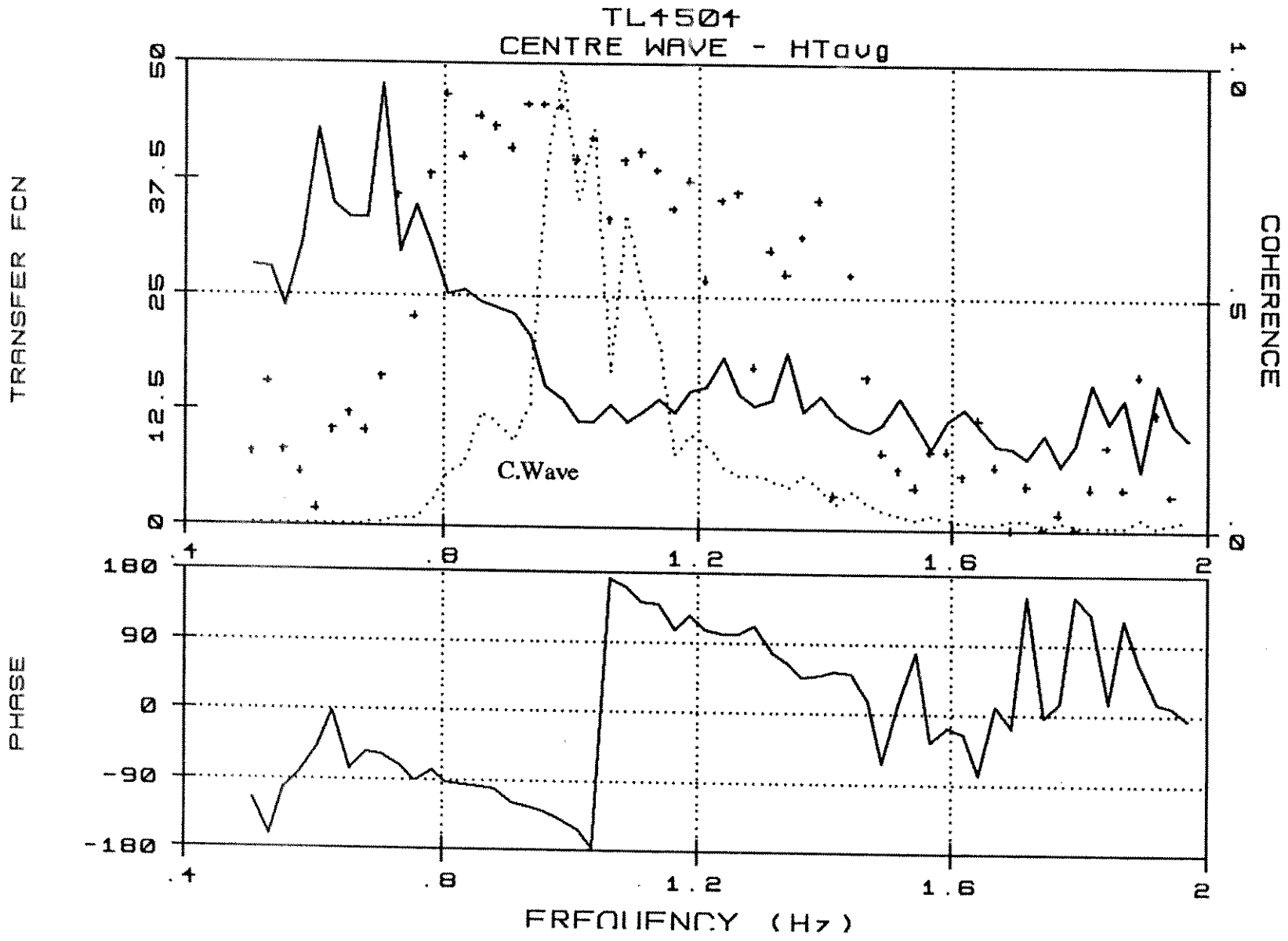

TL4504.W/HTavg.4t*

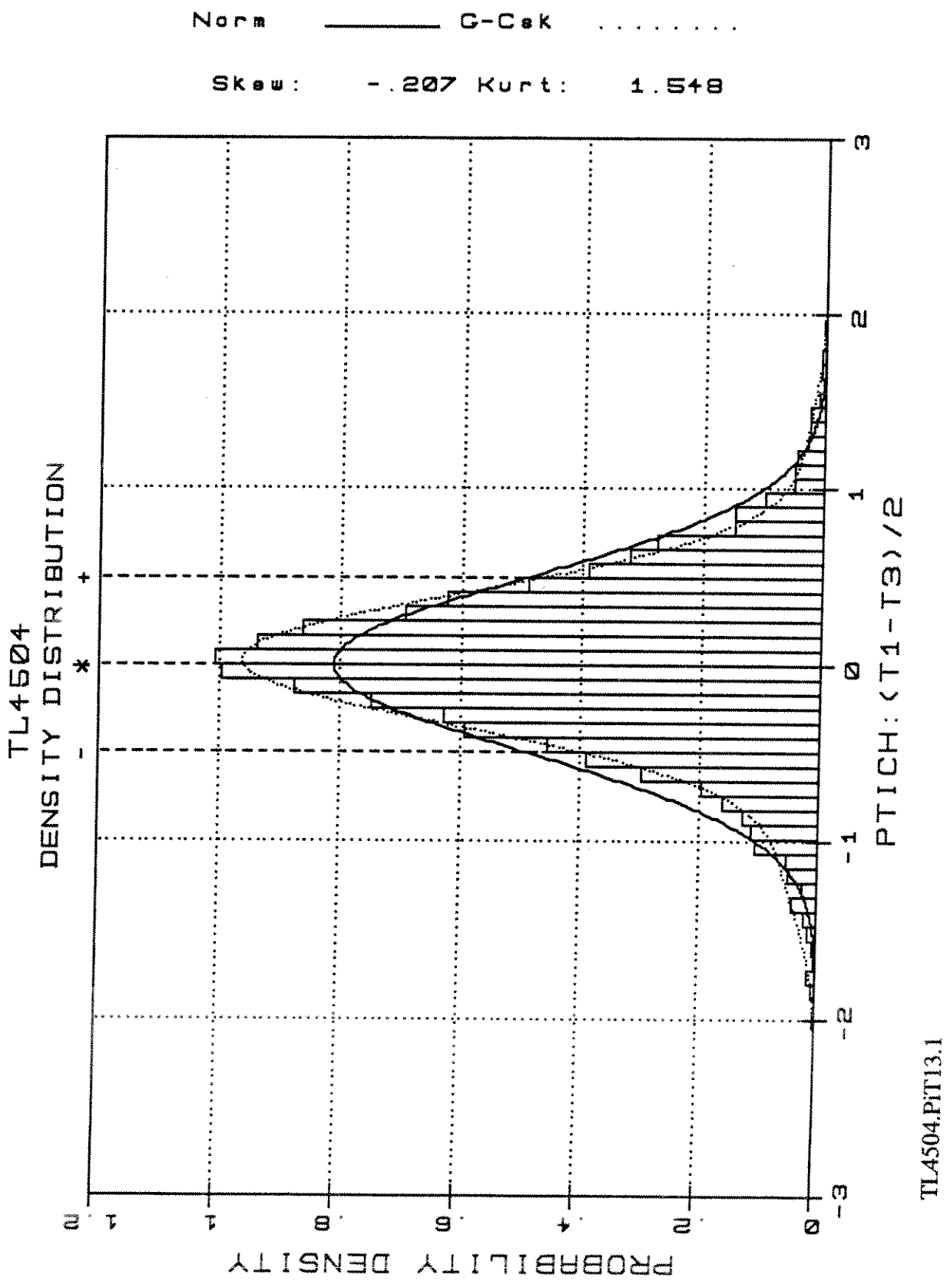

TL4504.PIT13.1

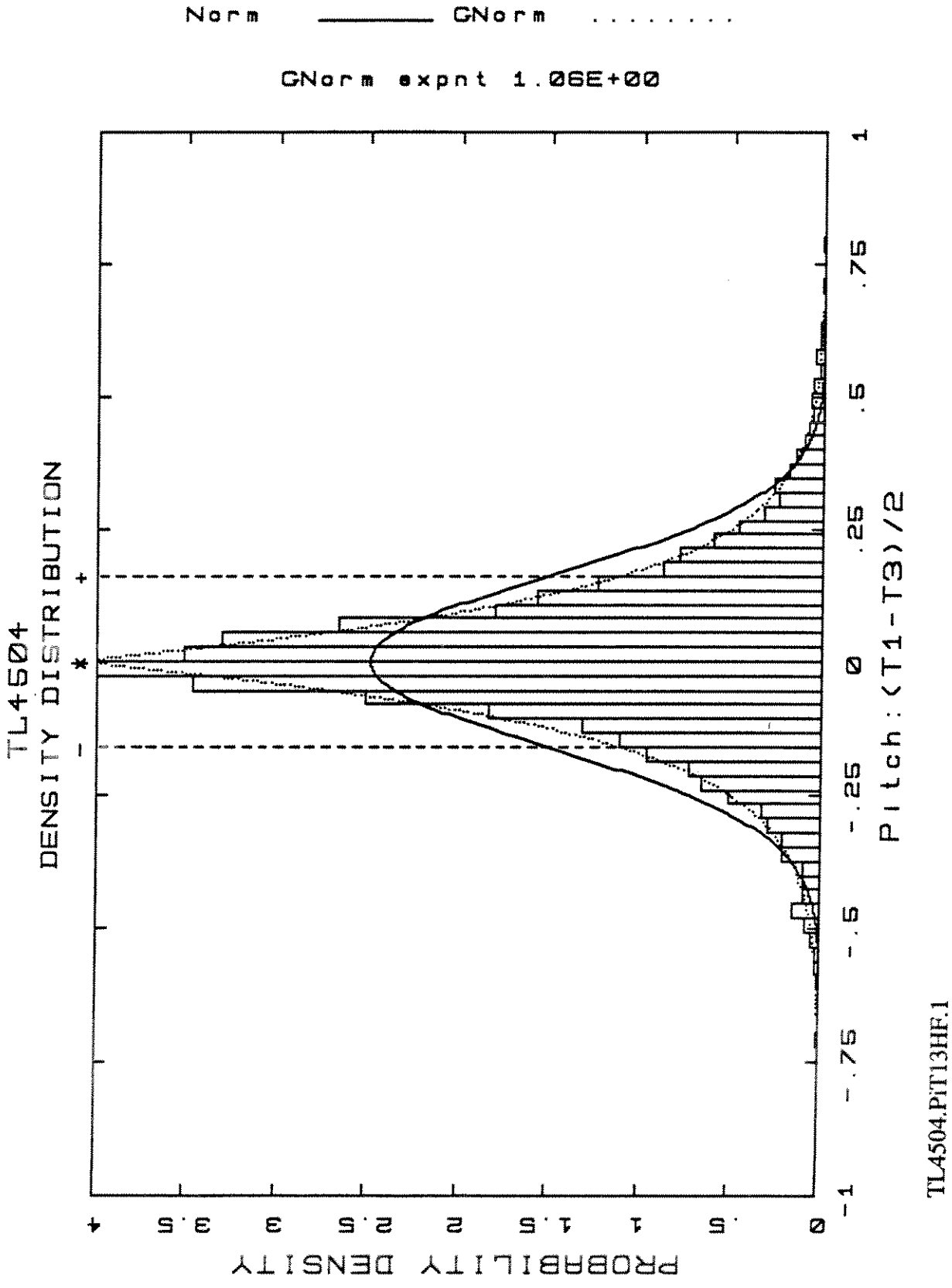

TL4504.PiT13HF.1

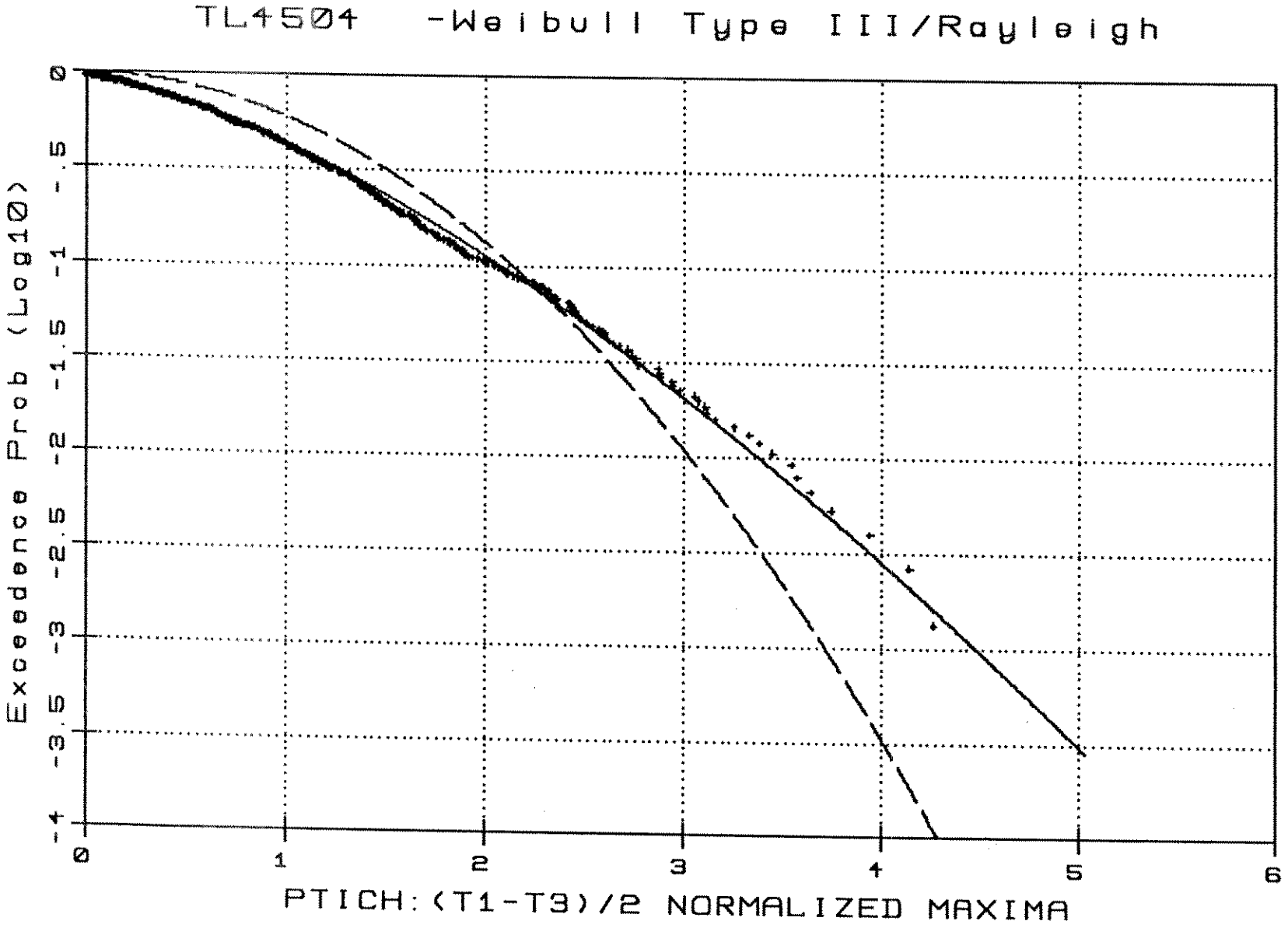

TL4504.PiT13.2

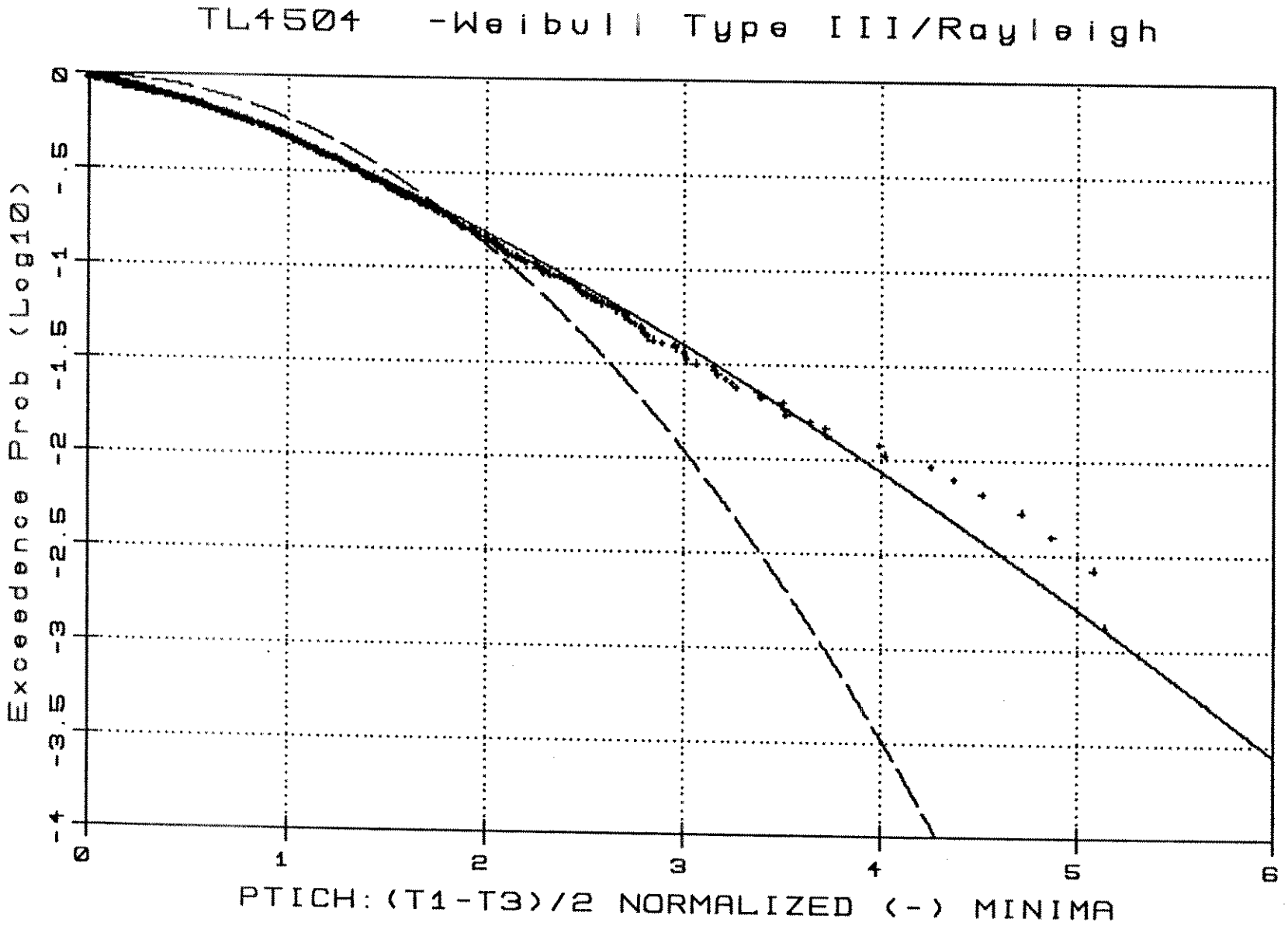

TL4504.PiT13.3

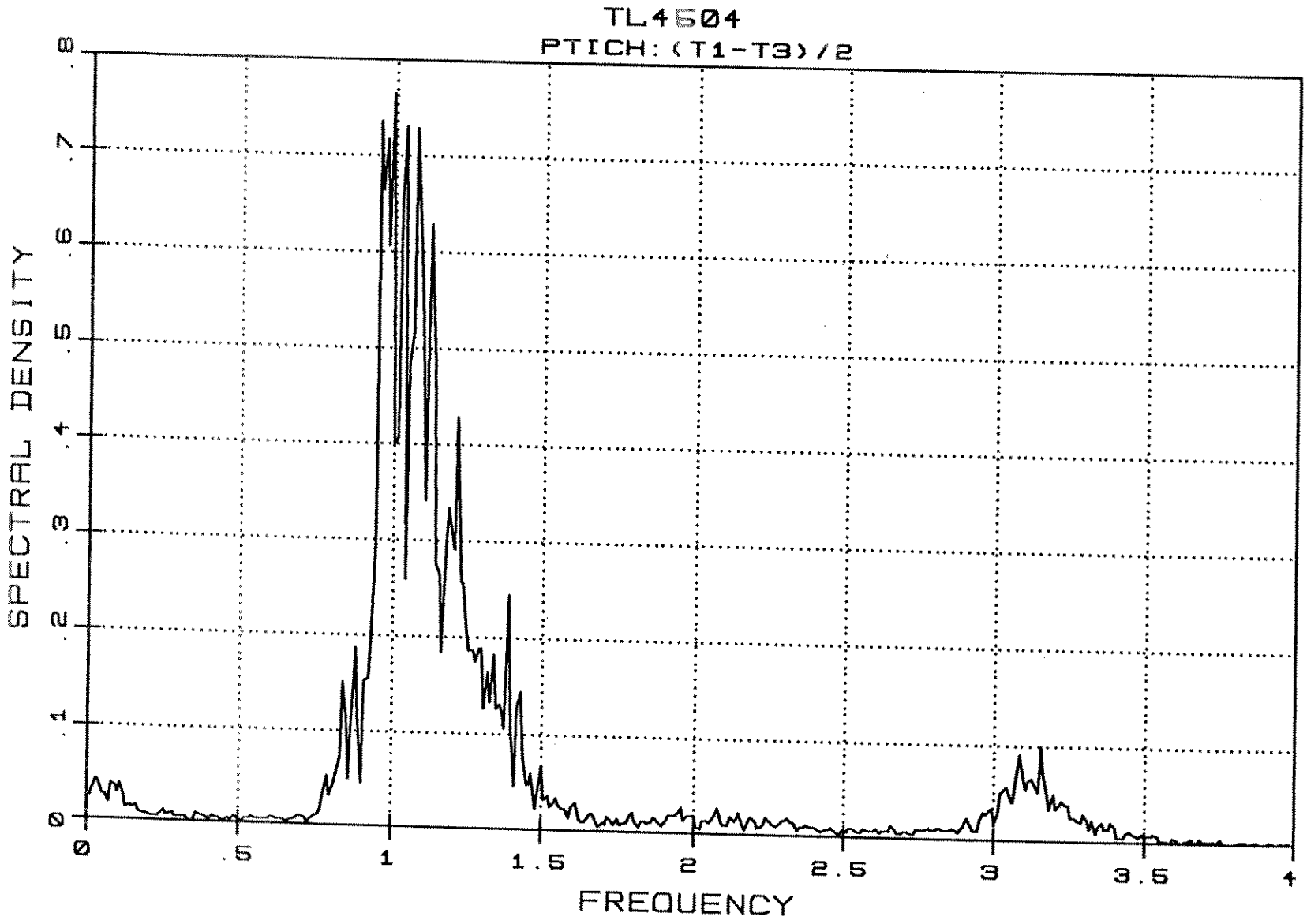

TL4504.PiT13.4

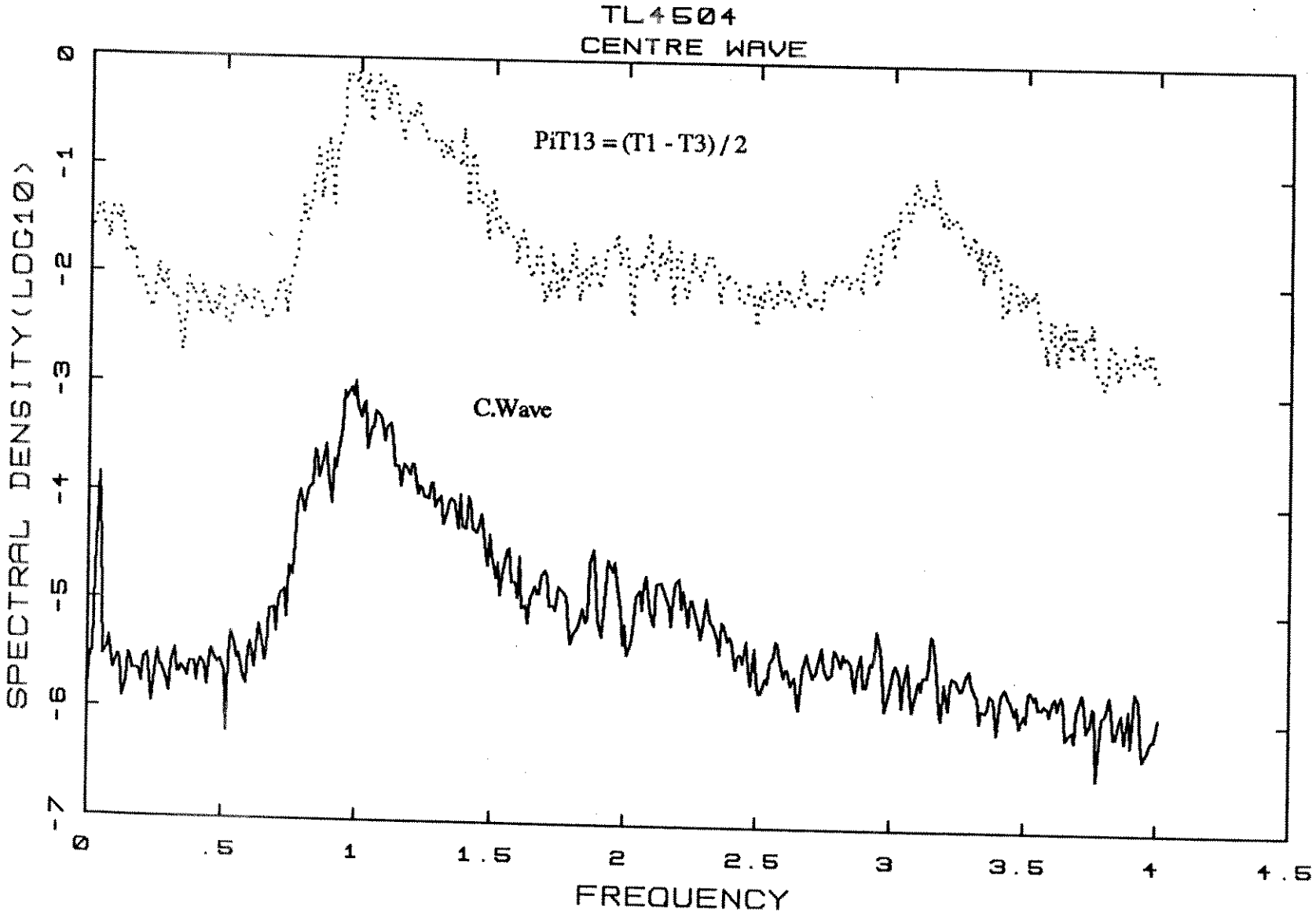

TL4504.W/PiT13.4

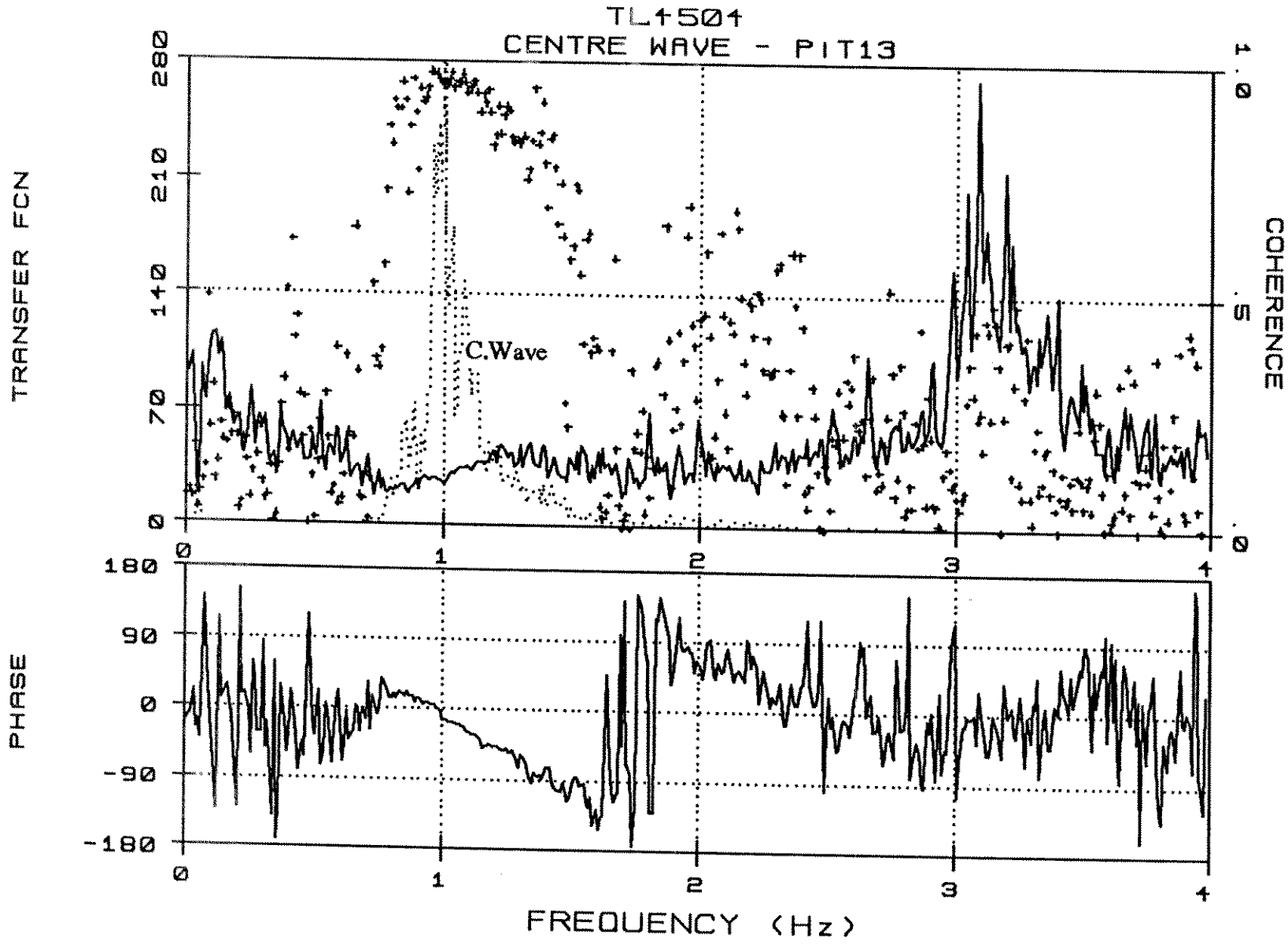

TL4504.W/PiT13.4t

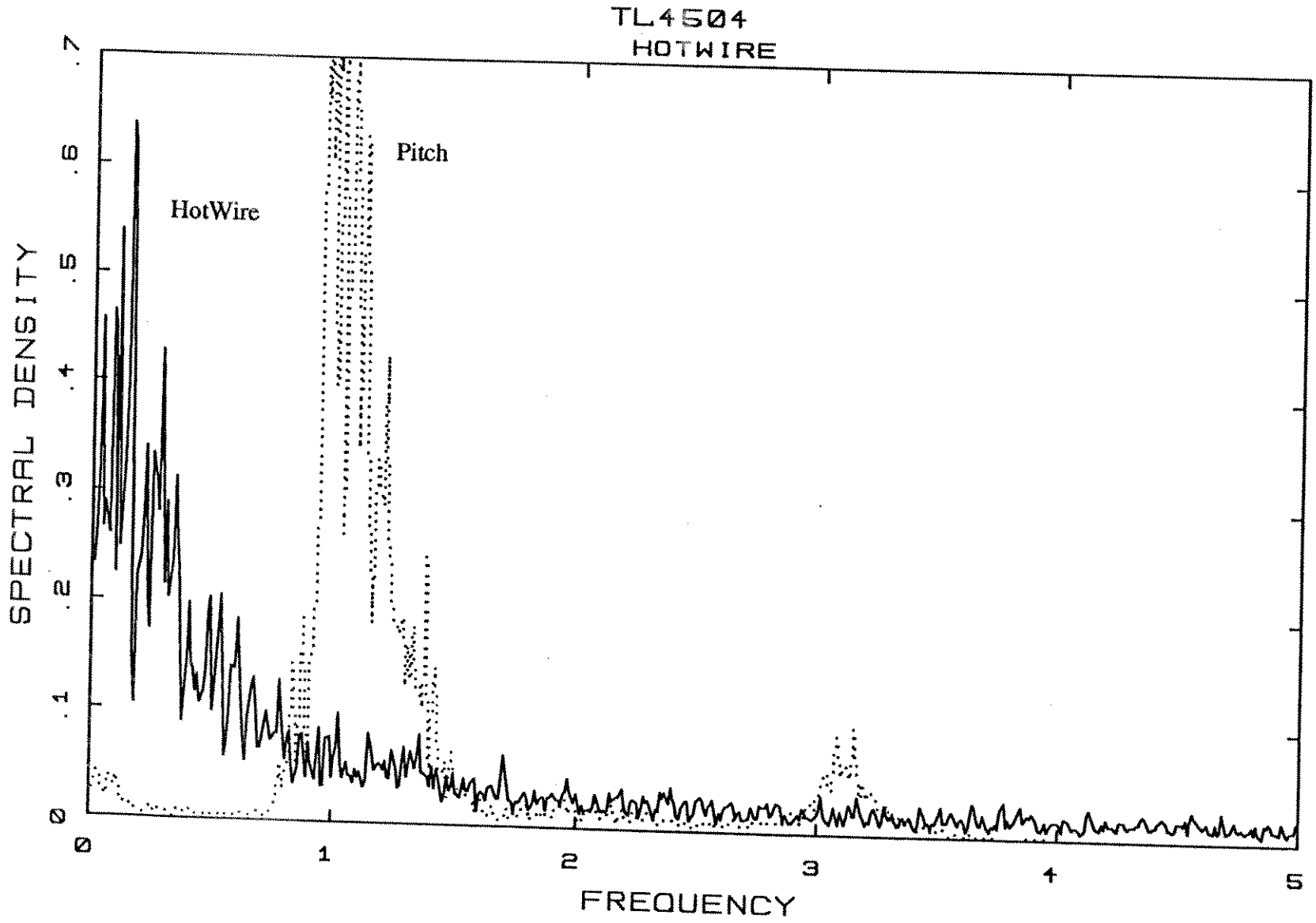

TL4504.HW/PiT13.4

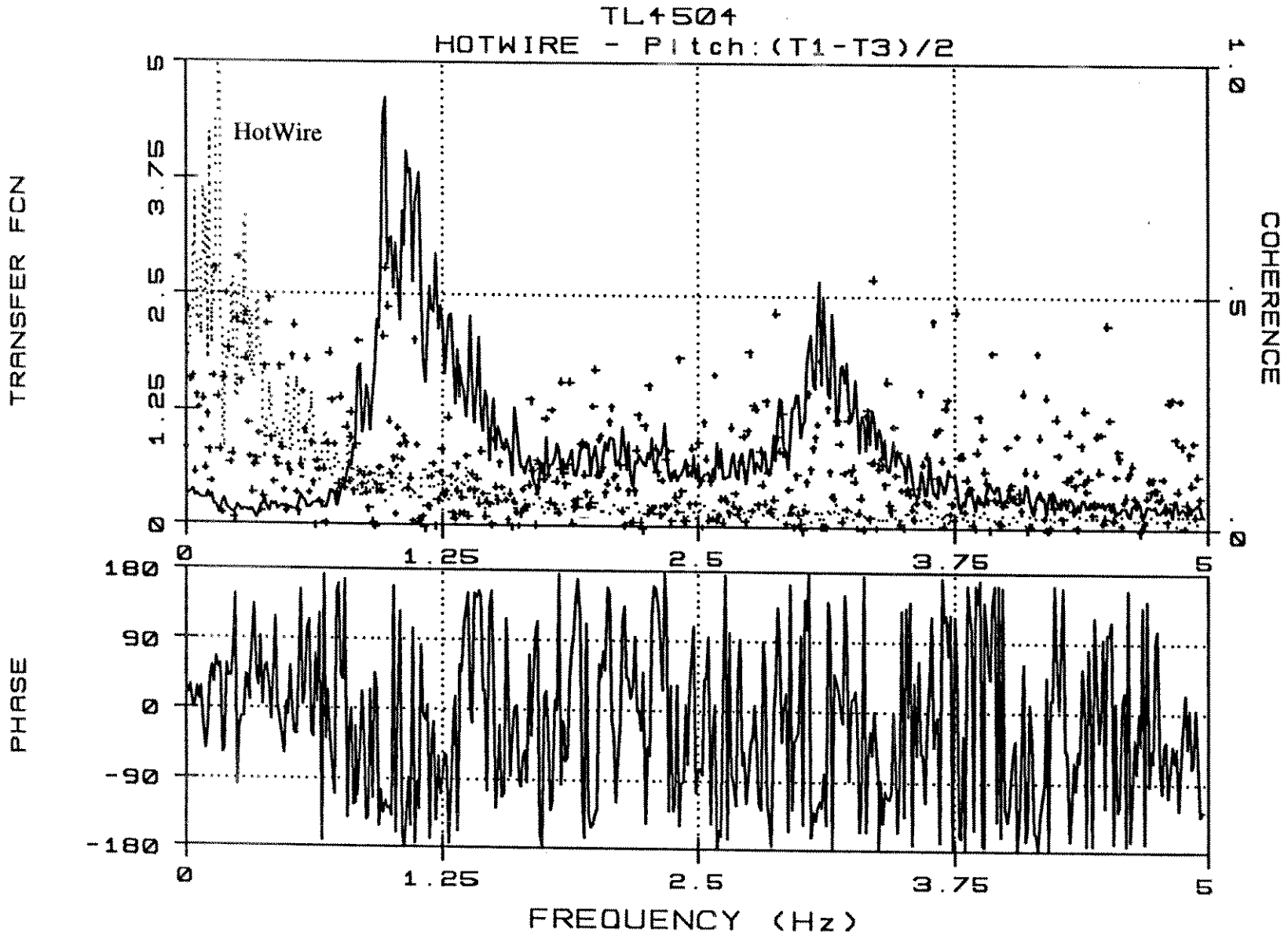

TL4504.HW/PiT13.4t

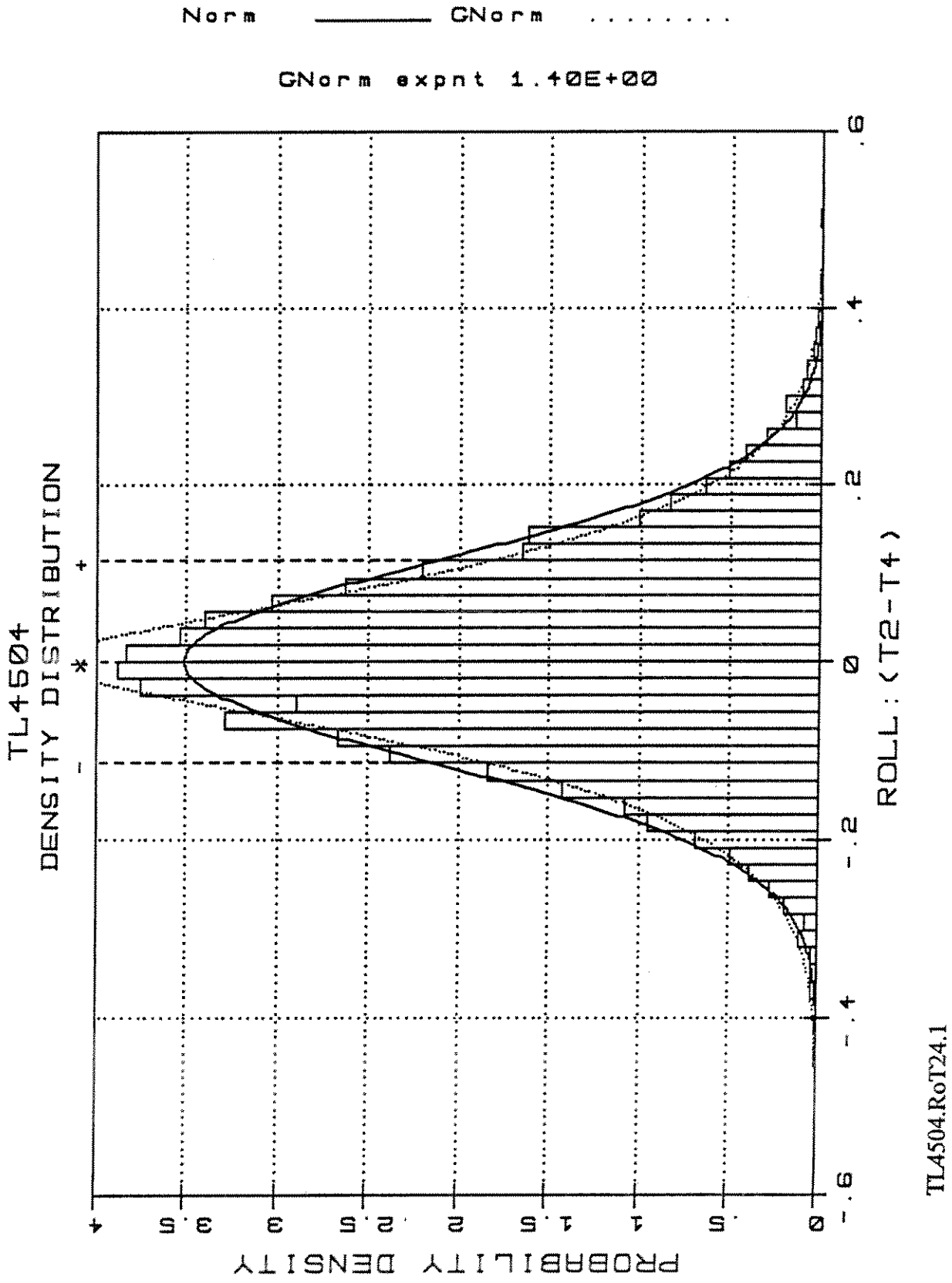
Norm
GNorm
GNorm expnt 1.40E+00
TL4504
DENSITY DISTRIBUTION
PROBABILITY DENSITY
ROLL: (T2-T4)
TL4504.RoT24.1

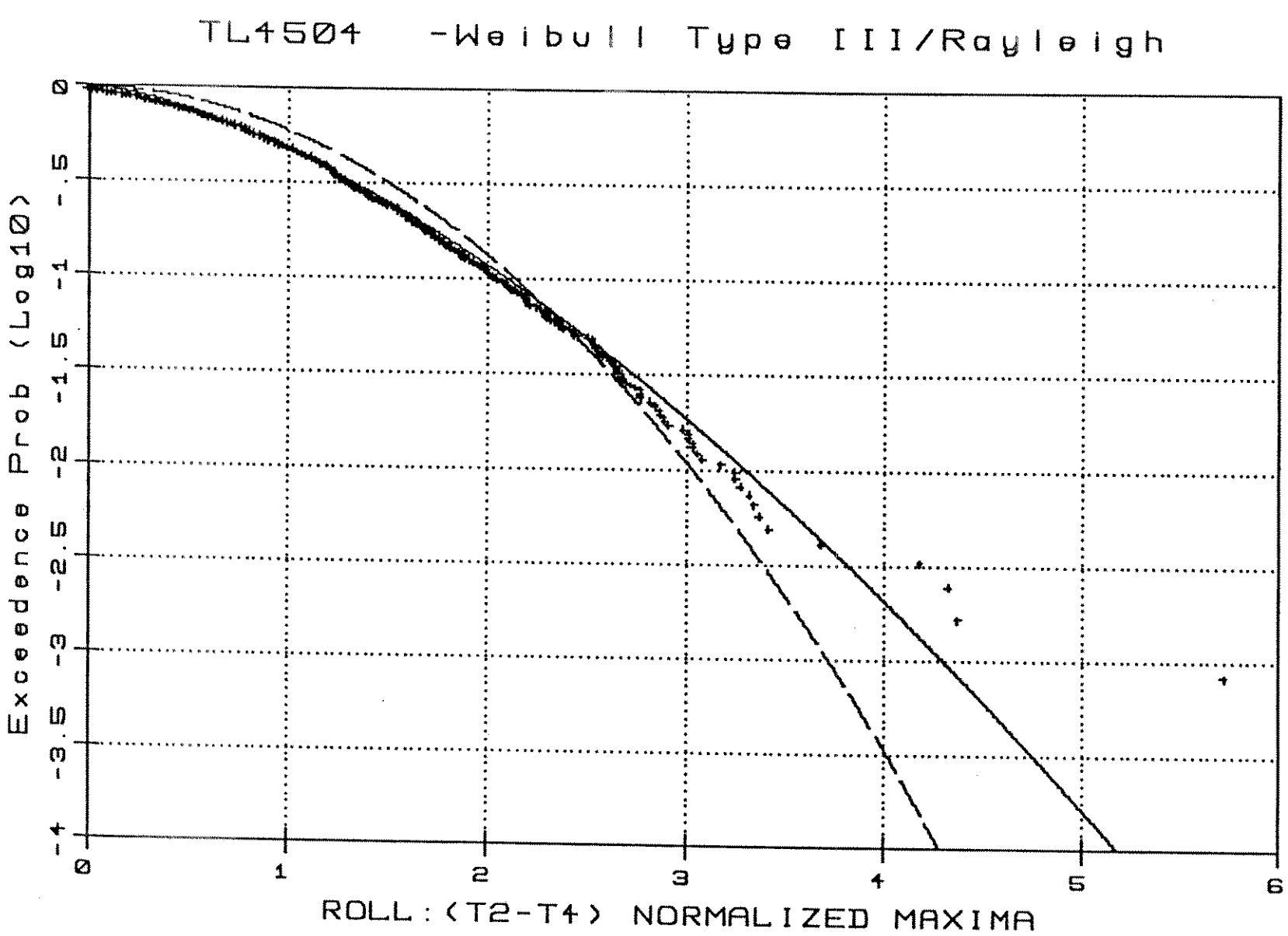

TL4504.RoT24.2

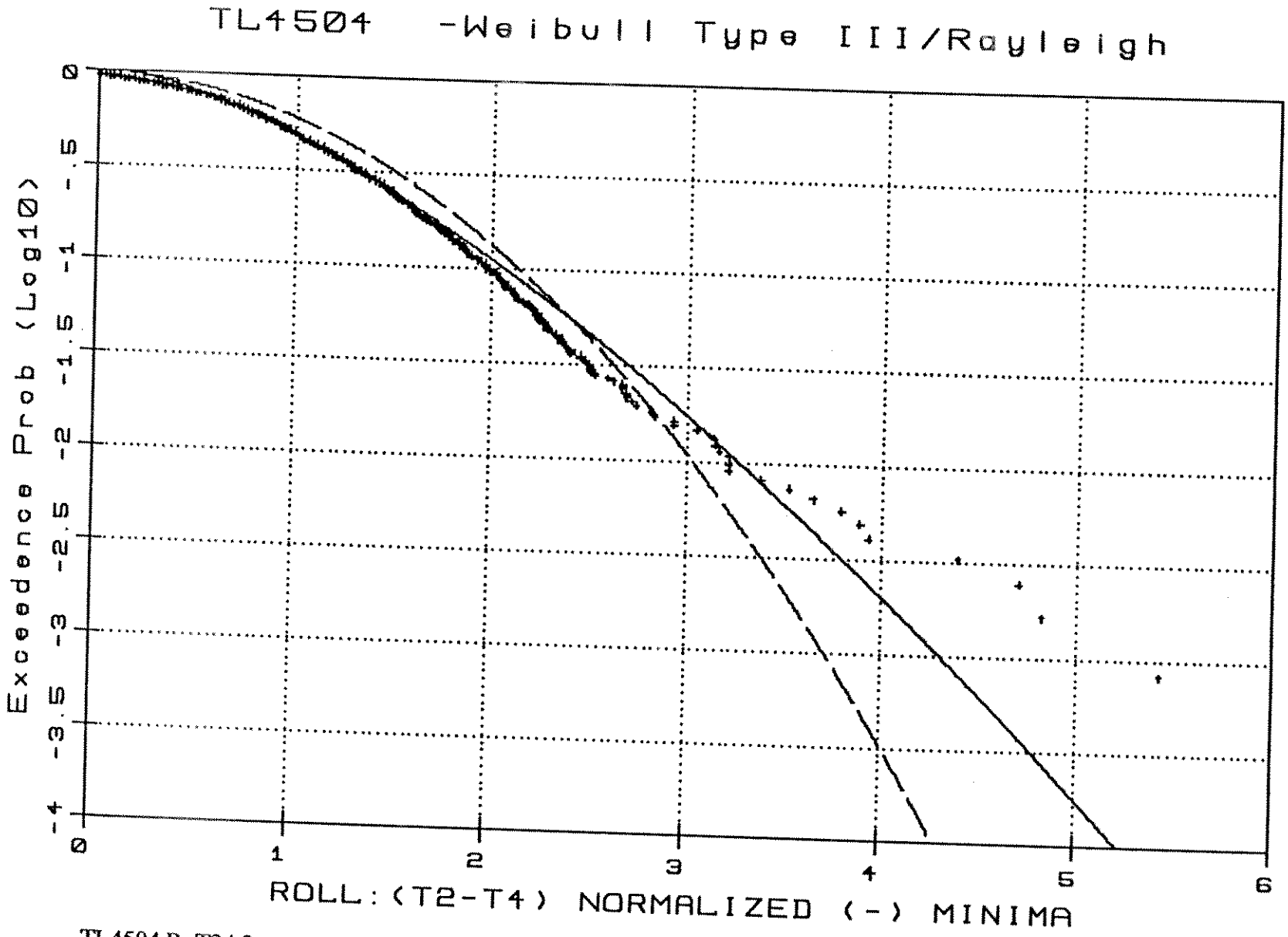

TL4504.RoT24.3

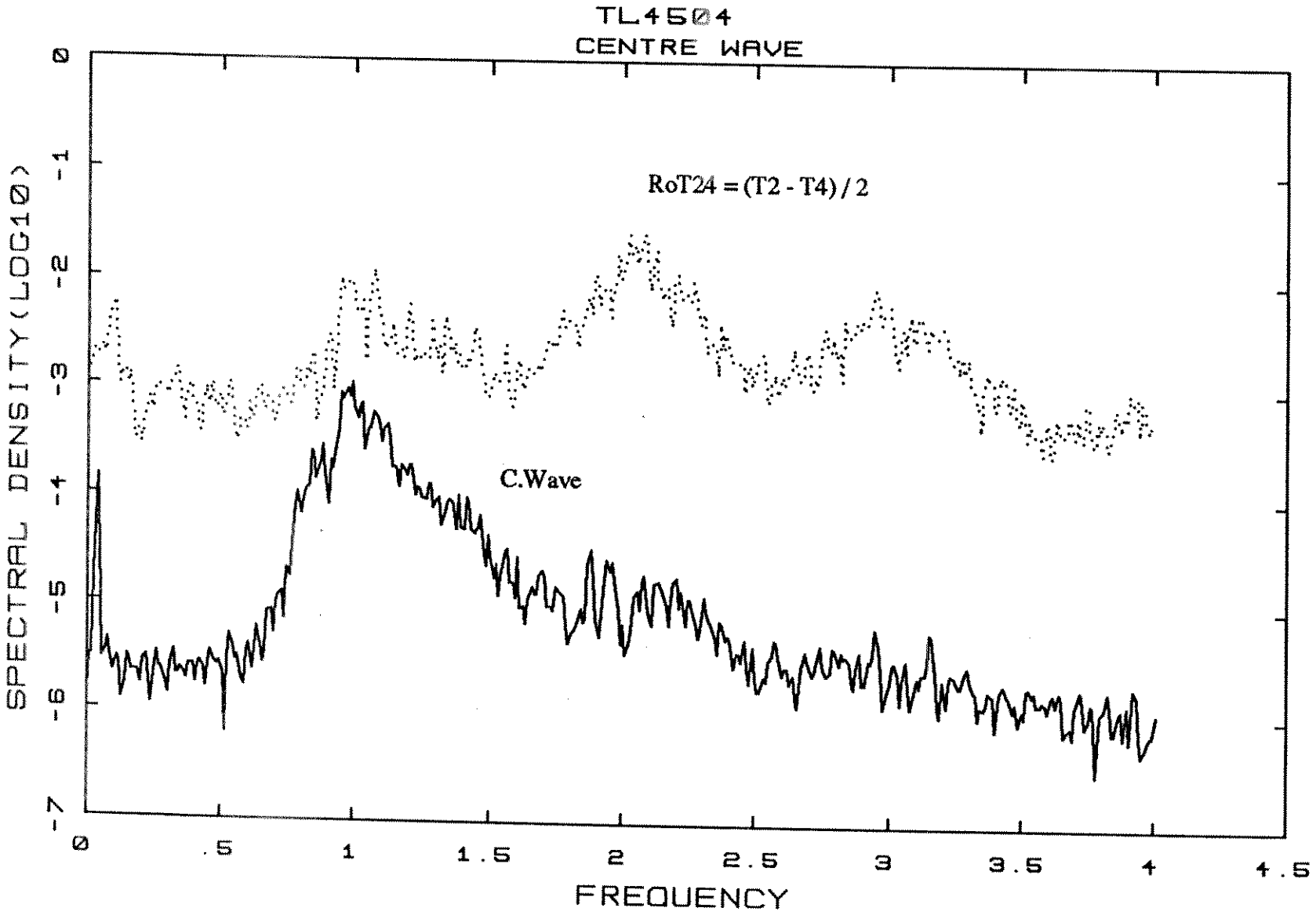

TL4504.W/RoT24.4

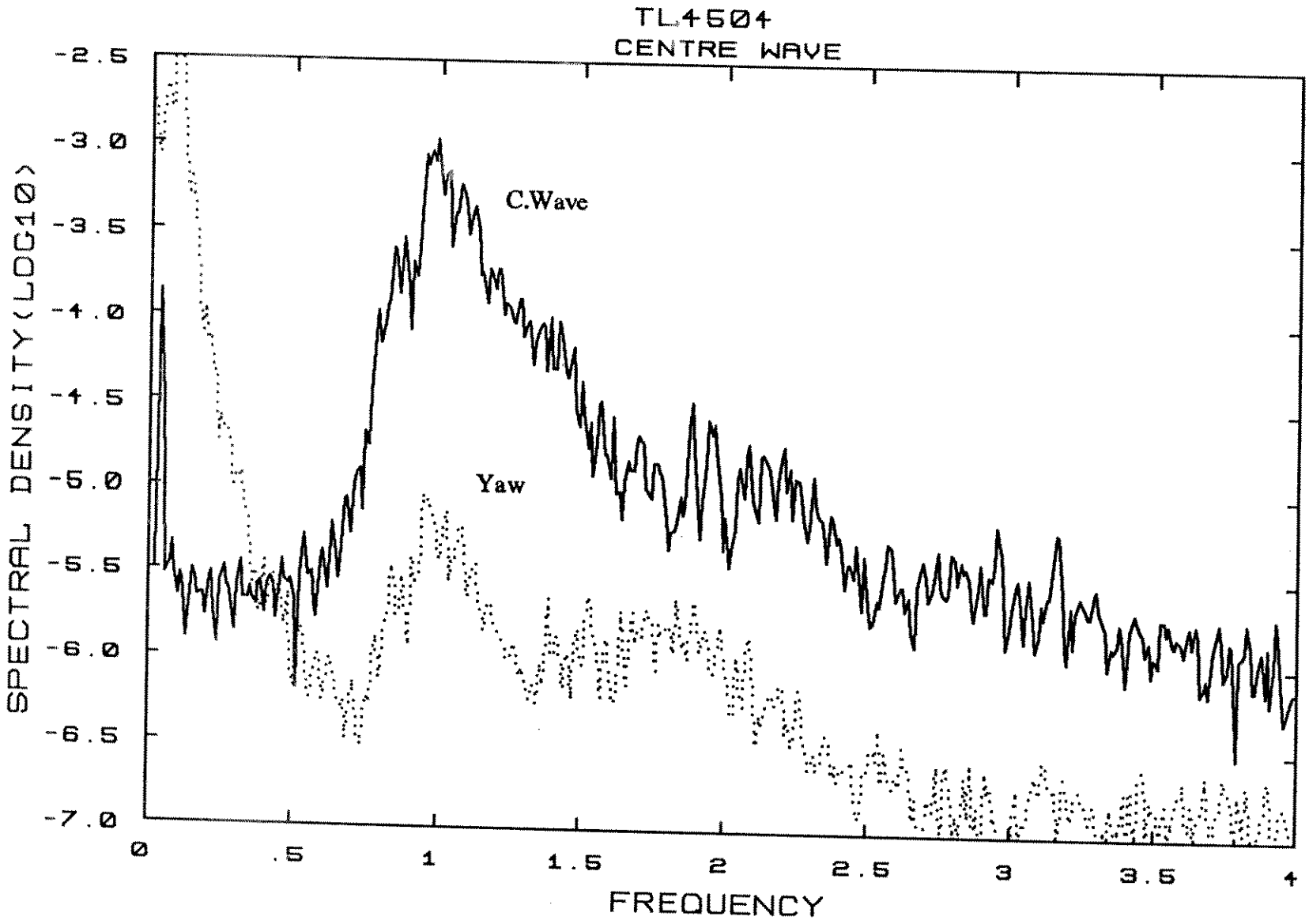
TL4504
CENTRE WAVE
SPECTRAL DENSITY(LOG10)
-2.5
-3.0
-3.5
-4.0
-4.5
-5.0
-5.5
-6.0
-6.5
-7.0
C.Wave
Yaw
0
.5
1
1.5
2
2.5
3
3.5
4
FREQUENCY

TL4504.W/Y.4

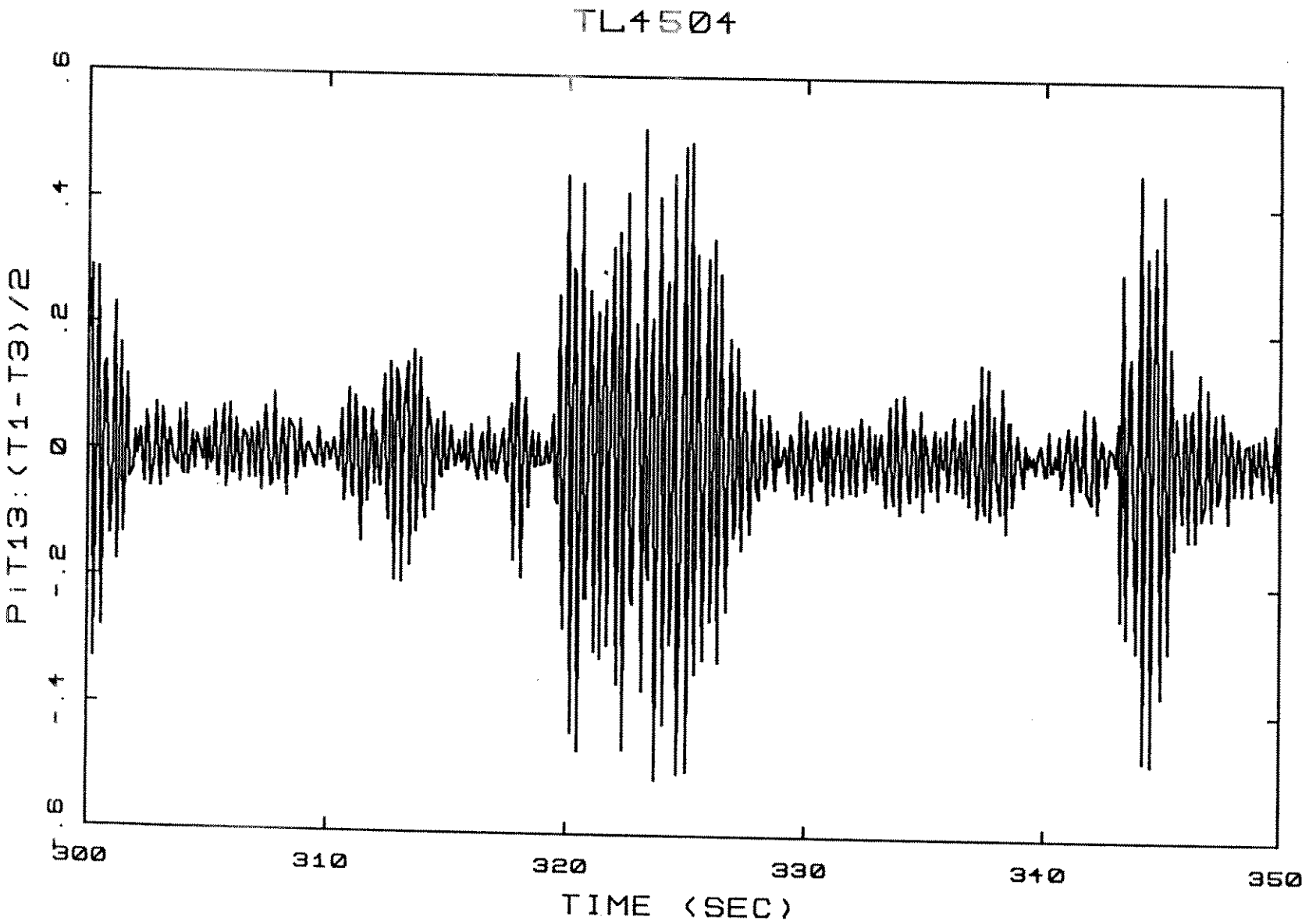

TL4504.PiT13HF.TIM

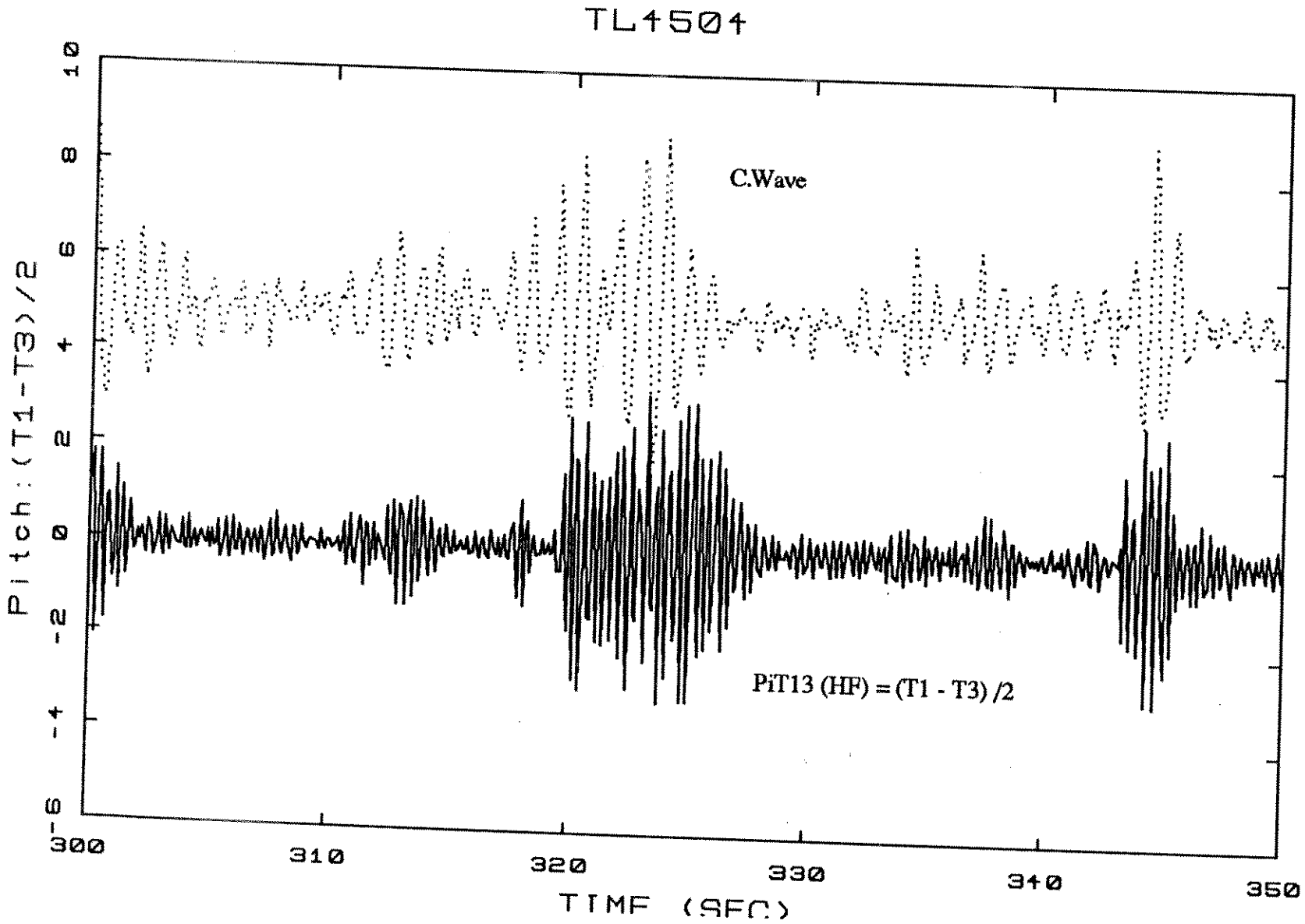

TL4504.W/PiT13HF.TIM

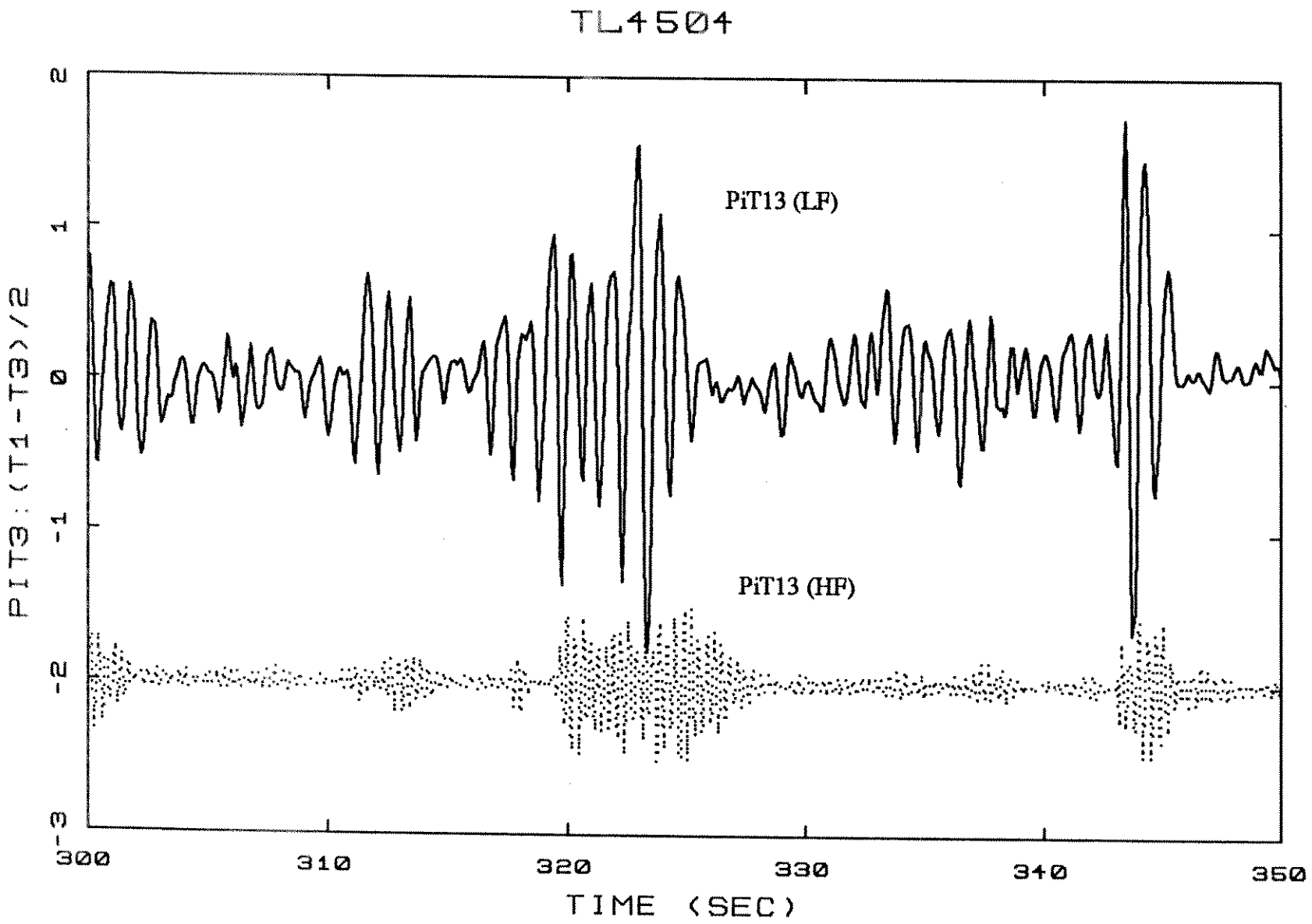

TL4504.PiT13HF/LF.TIM

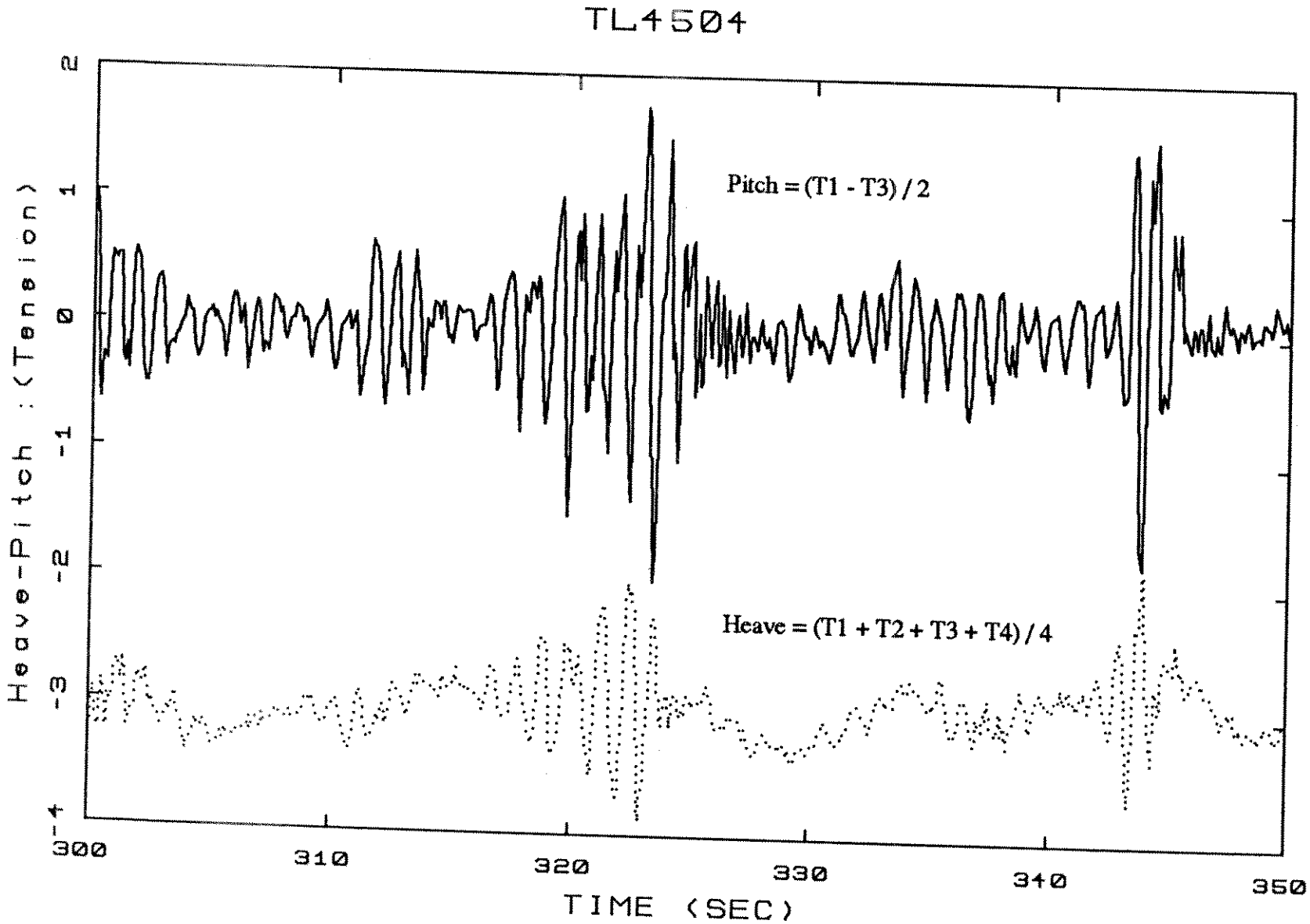

TL4504.HTavg/PiT13.TIM

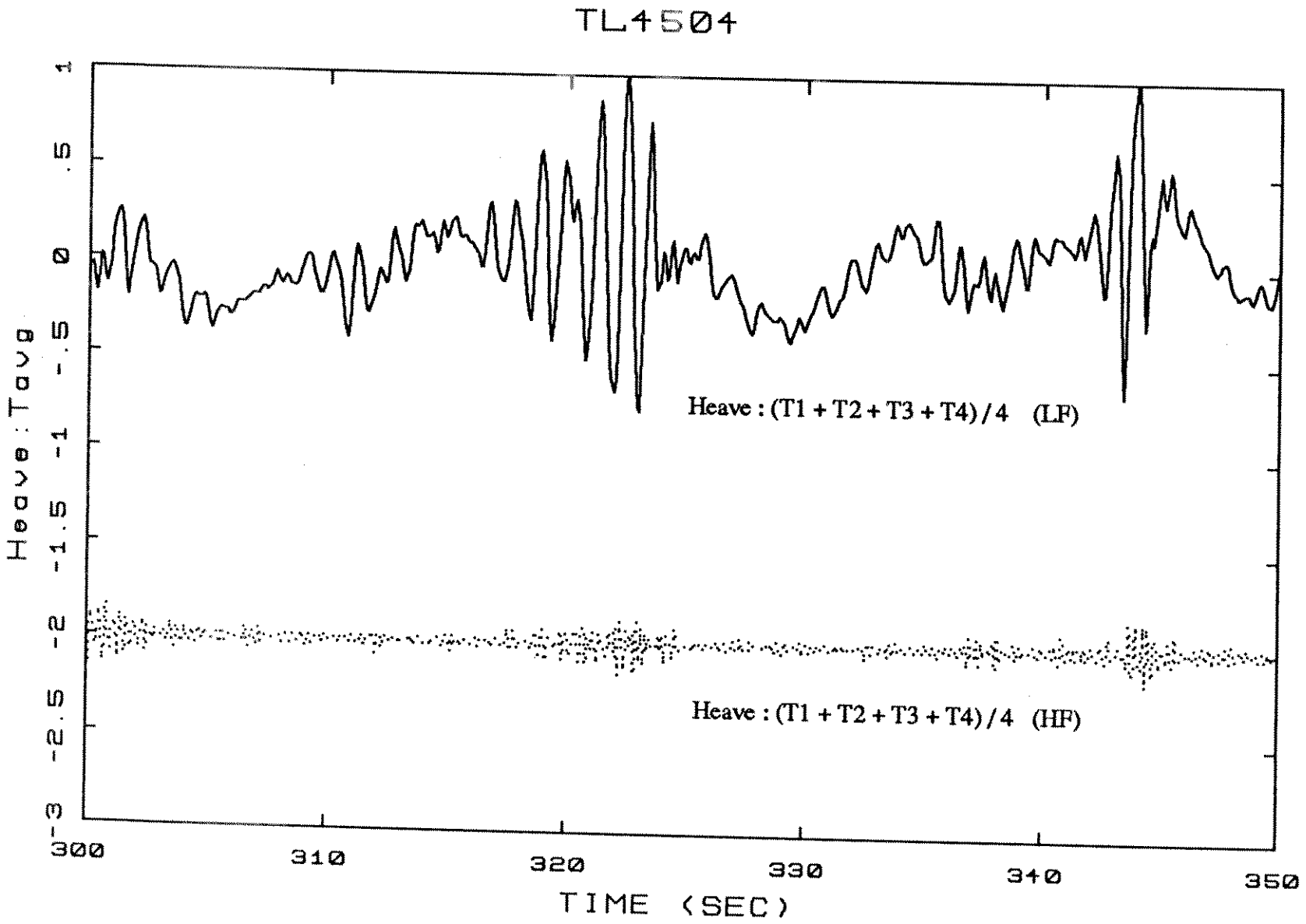

TL4504.HTavgHF/LF.TIM

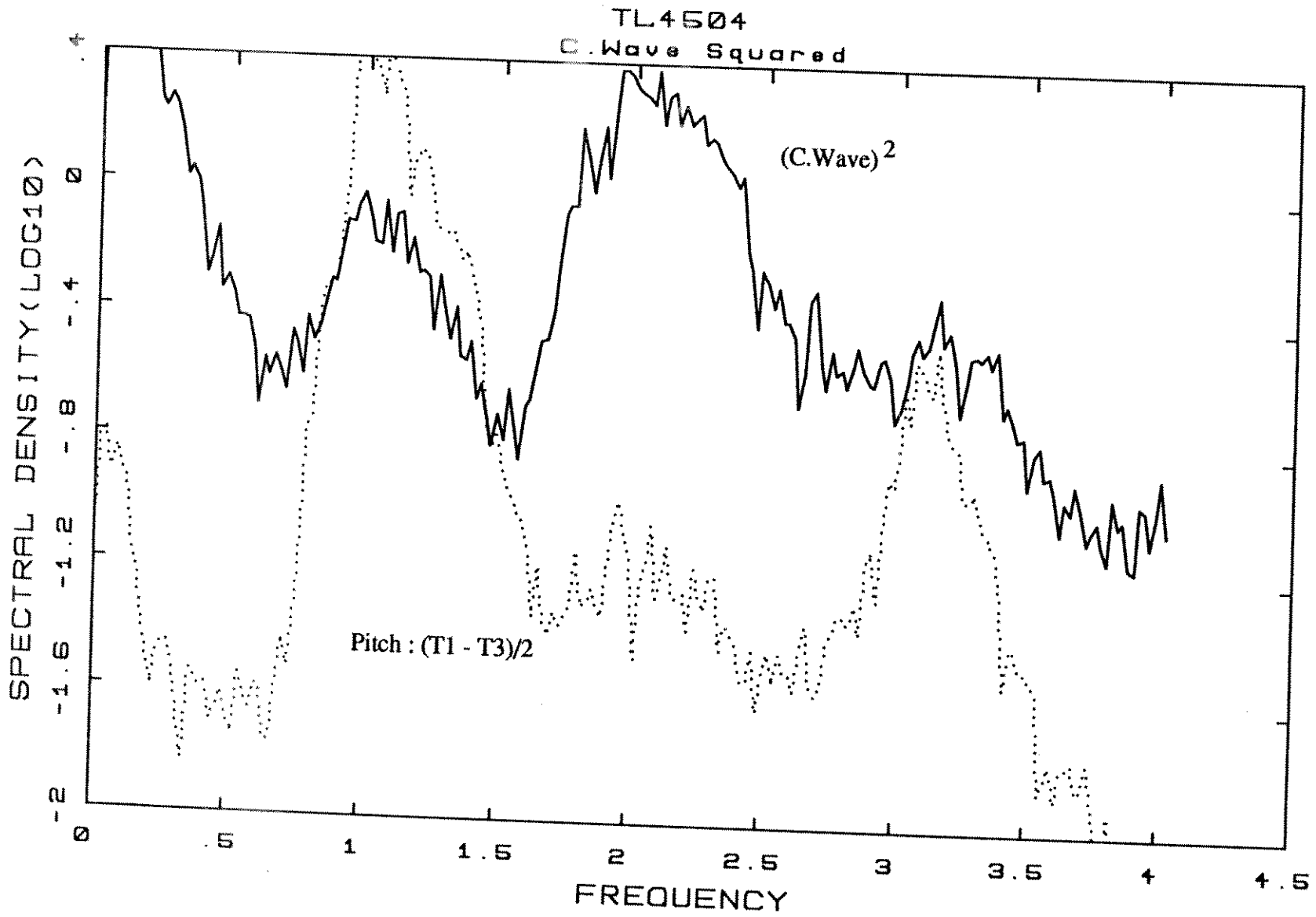

TL4504.WSQ/PiT13.4
C.Wave Squared and Pitch are normalized

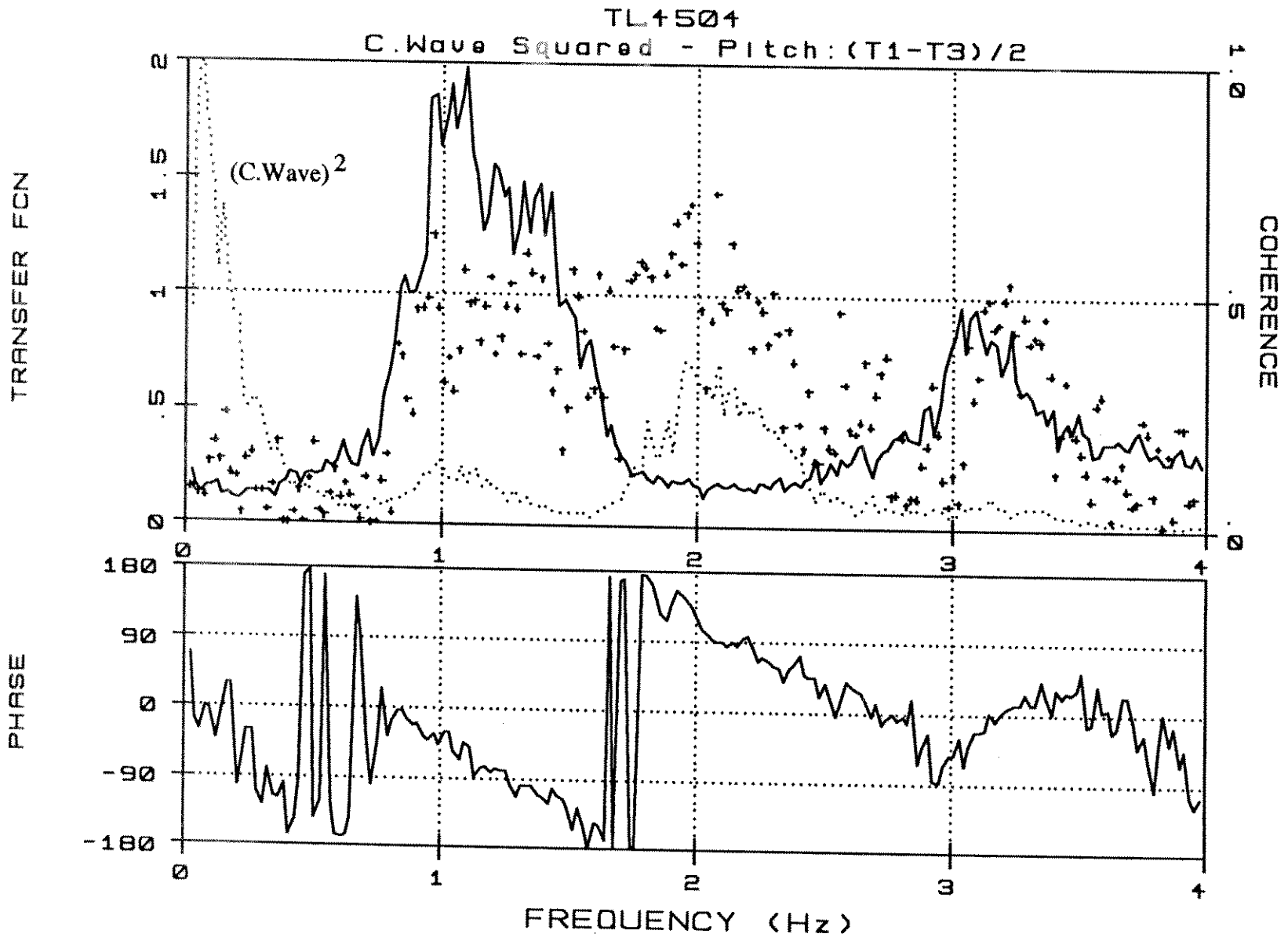

TL4504.WSQ/PiT13.4t
C.Wave Squared and Pitch are normalized

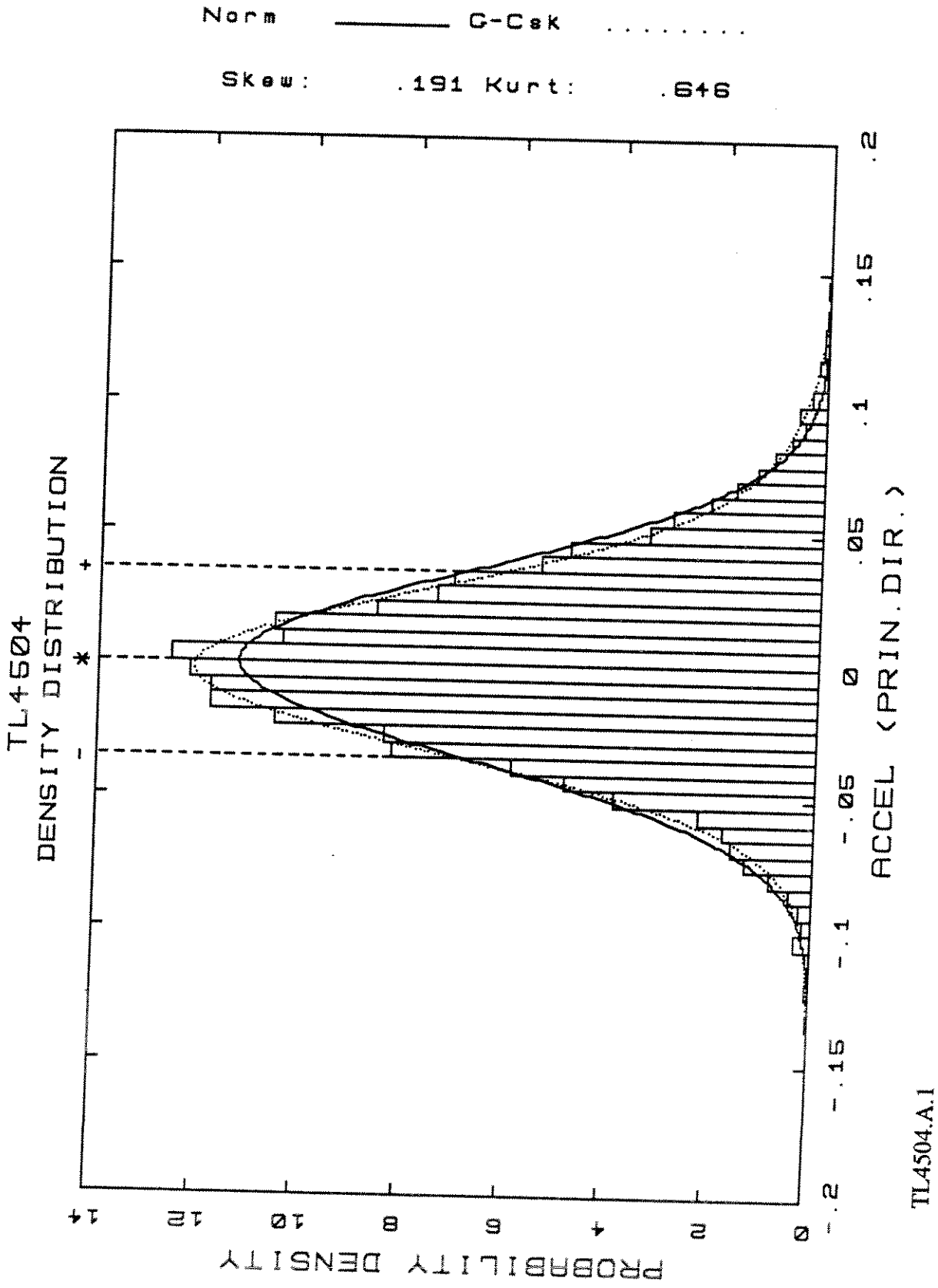
Norm ——— G-Csk .....
Skew: .191 Kurt: .646
TL4504
DENSITY DISTRIBUTION
+
*
-
PROBABILITY DENSITY
0
2
4
6
8
10
12
14
-.2
-.15
-.1
-.05
0
.05
.1
.15
.2
ACCEL (PRIN.DIR.)

TL4504.A.1

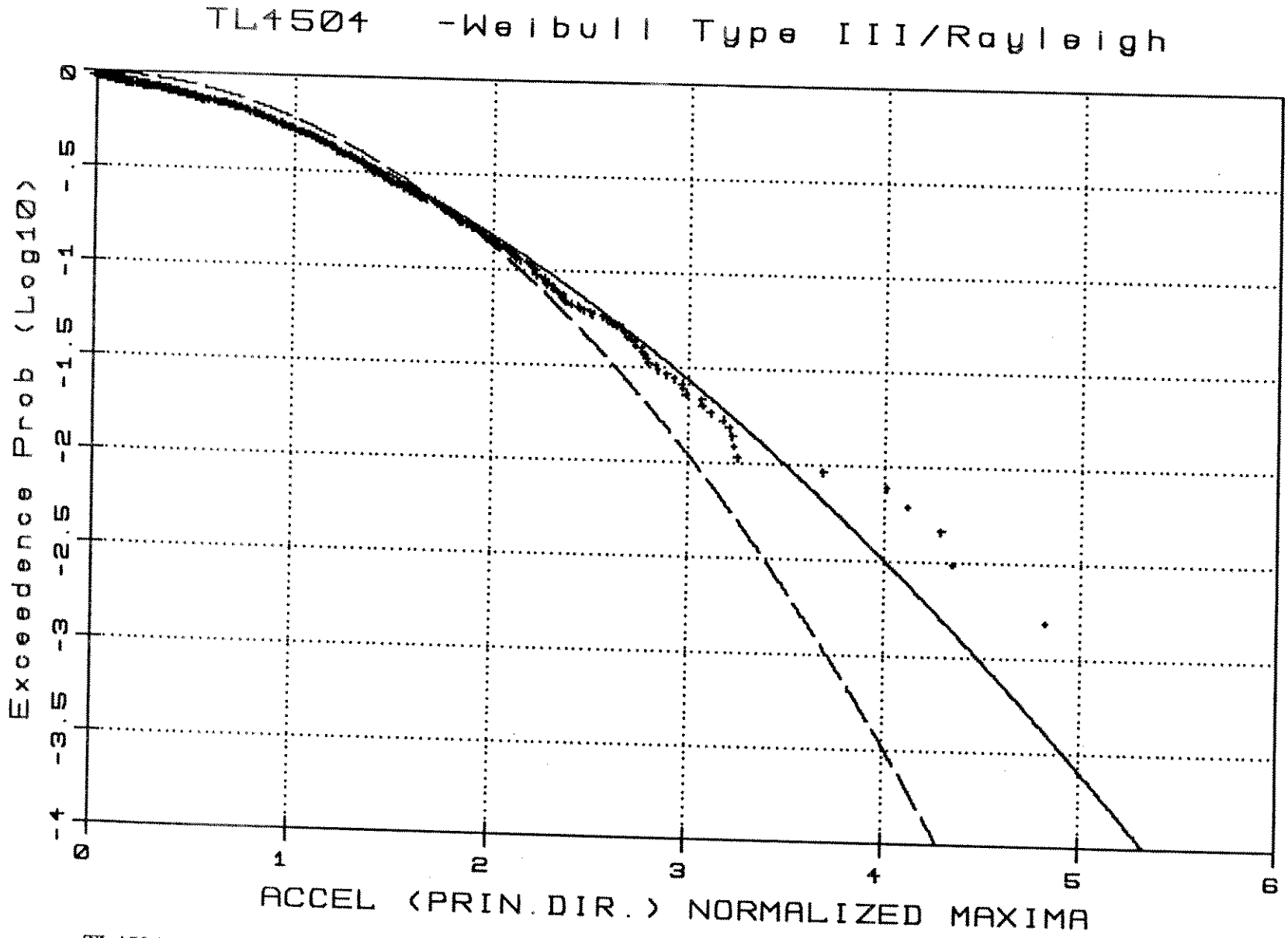
TL4504 -Weibull Type III/Rayleigh
Exceedence Prob (Log10)
0
-.5
-1
-1.5
-2
-2.5
-3
-3.5
-4
0
1
2
3
4
5
6
ACCEL (PRIN.DIR.) NORMALIZED MAXIMA

TL4504.A.2

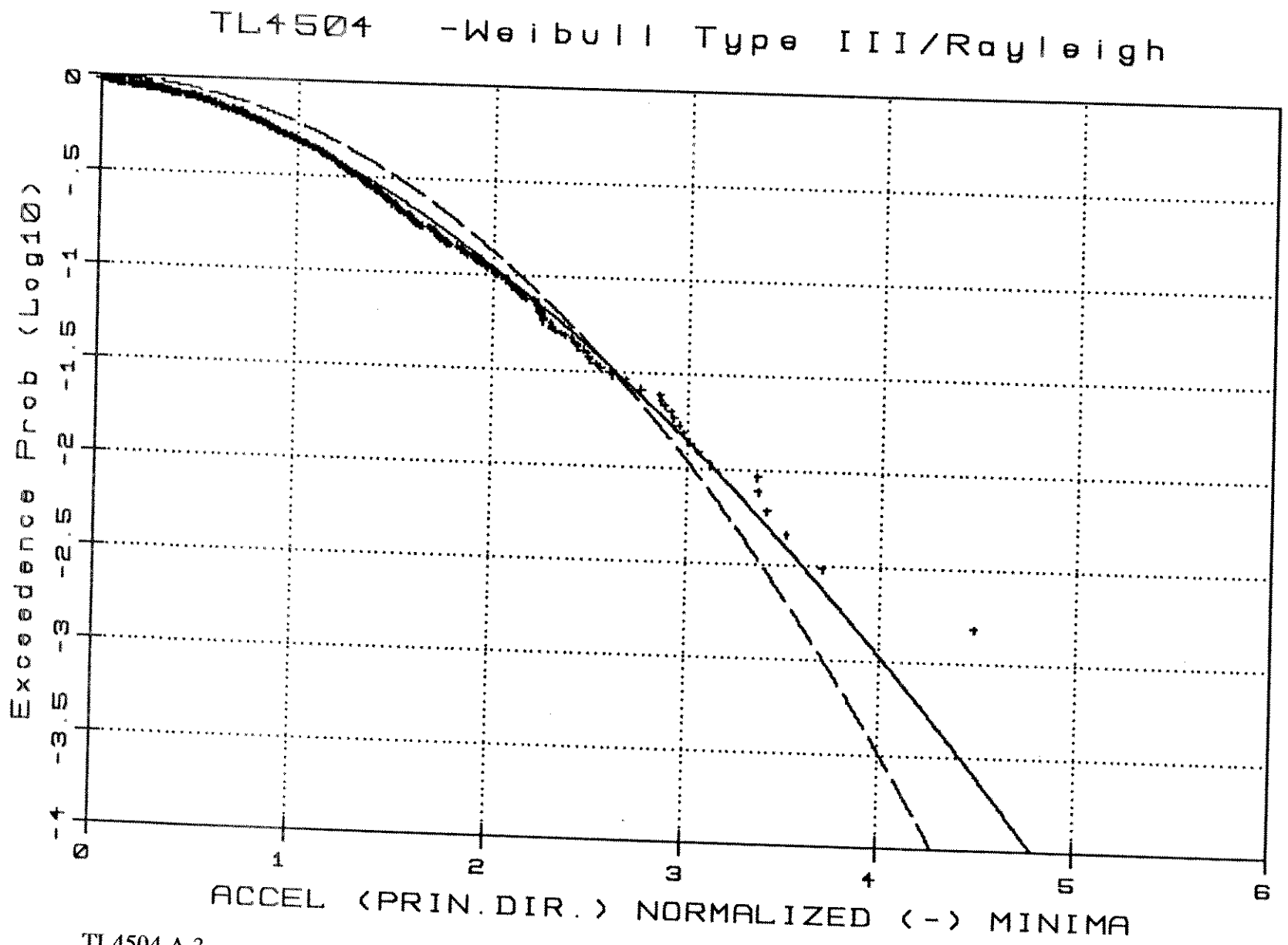
TL4504 -Weibull Type III/Rayleigh
Exceedence Prob (Log10)
0
-.5
-1
-1.5
-2
-2.5
-3
-3.5
-4
0
1
2
3
4
5
6
ACCEL (PRIN.DIR.) NORMALIZED (-) MINIMA

TL4504.A.3

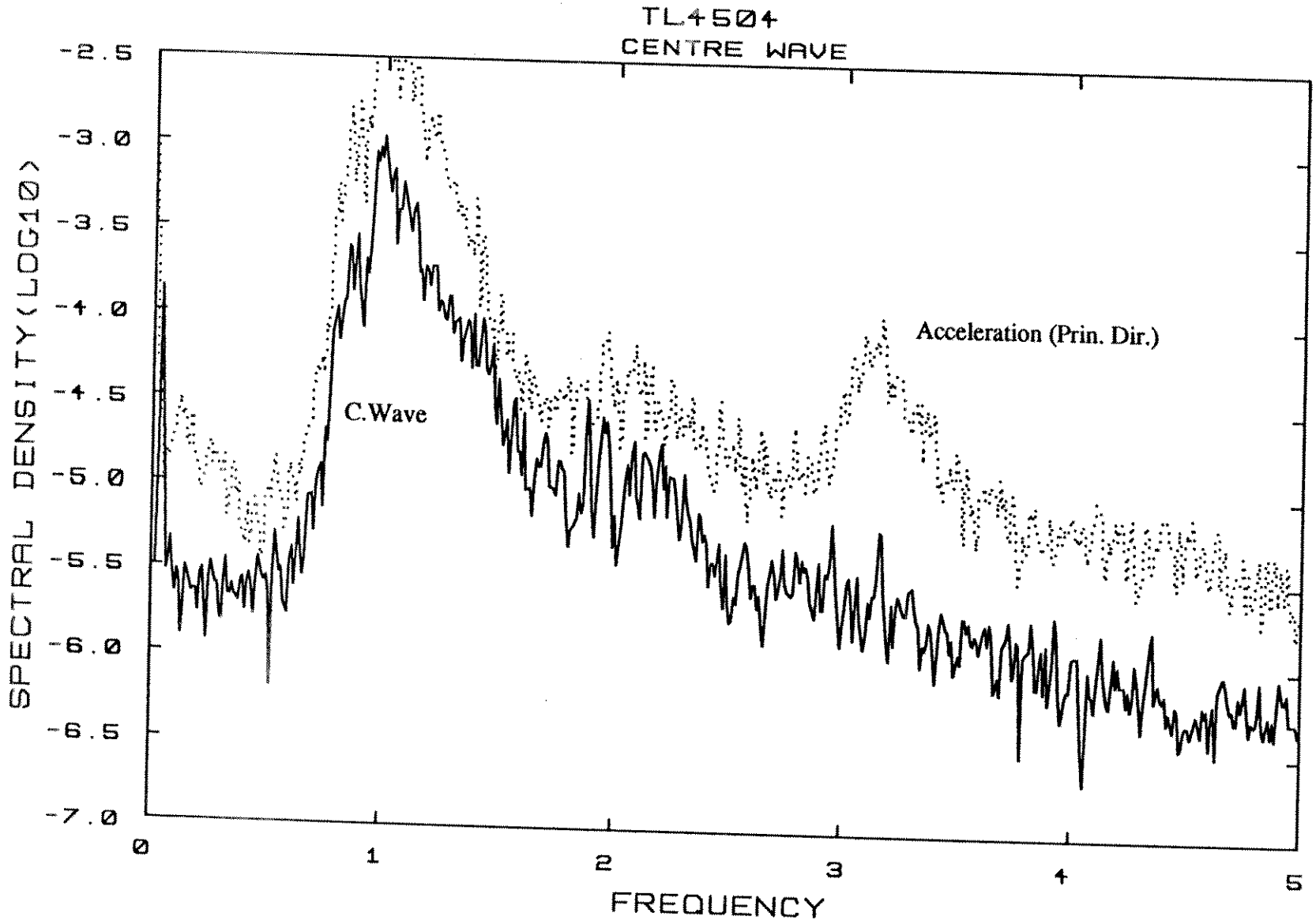
TL4504
CENTRE WAVE
SPECTRAL DENSITY(LOG10)
-2.5
-3.0
-3.5
-4.0
-4.5
-5.0
-5.5
-6.0
-6.5
-7.0
0
1
2
3
4
5
FREQUENCY
C.Wave
Acceleration (Prin. Dir.)

TL4504.W/A.4

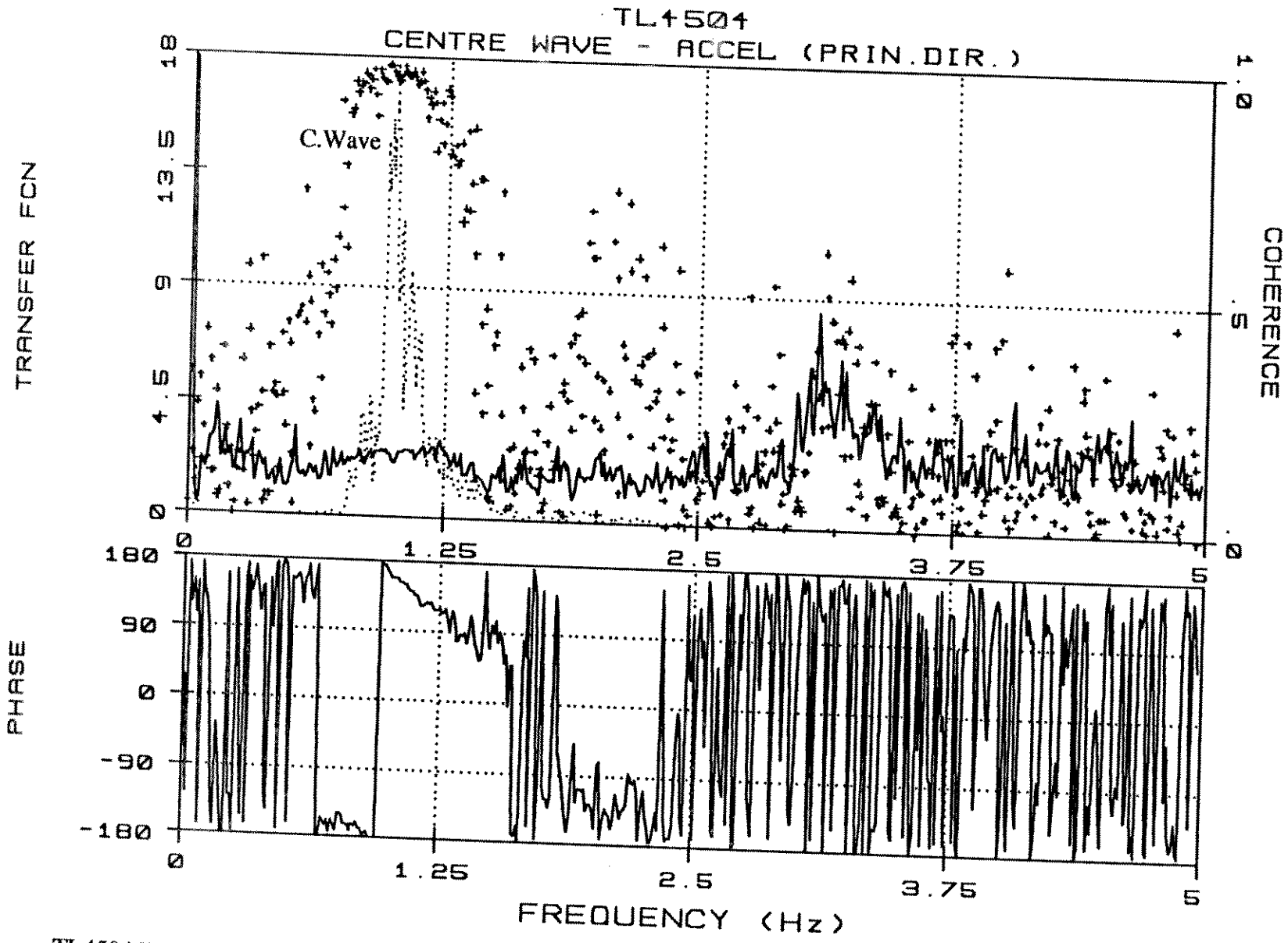
TL4504
CENTRE WAVE - ACCEL (PRIN.DIR.)
C.Wave
TRANSFER FCN
COHERENCE
PHASE
FREQUENCY (Hz)
18
13.5
9
4.5
0
1.0
.5
.0
180
90
0
-90
-180
0
1.25
2.5
3.75
5

TL4504.W/A.4t

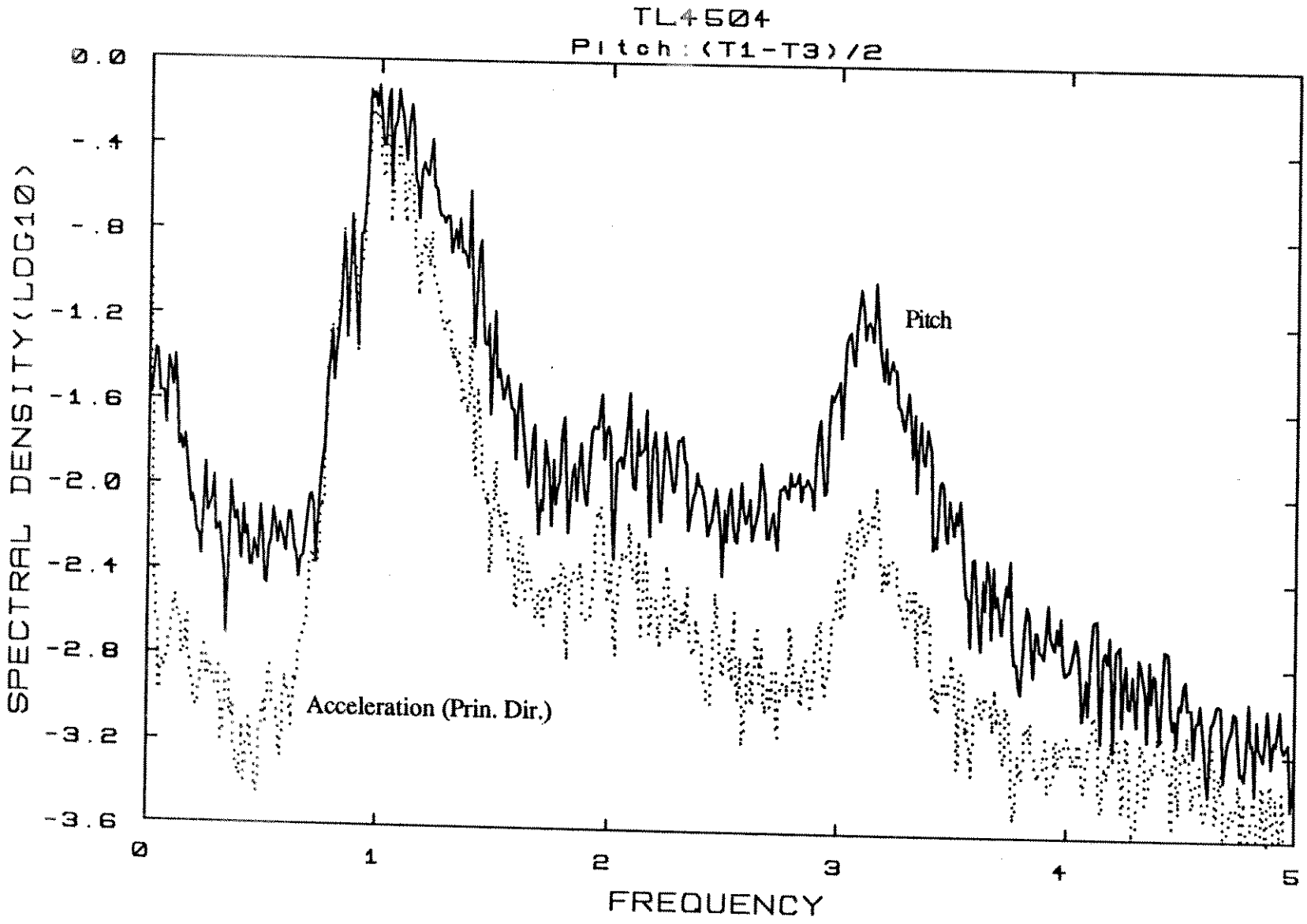

TL4504.A/PiT13.4

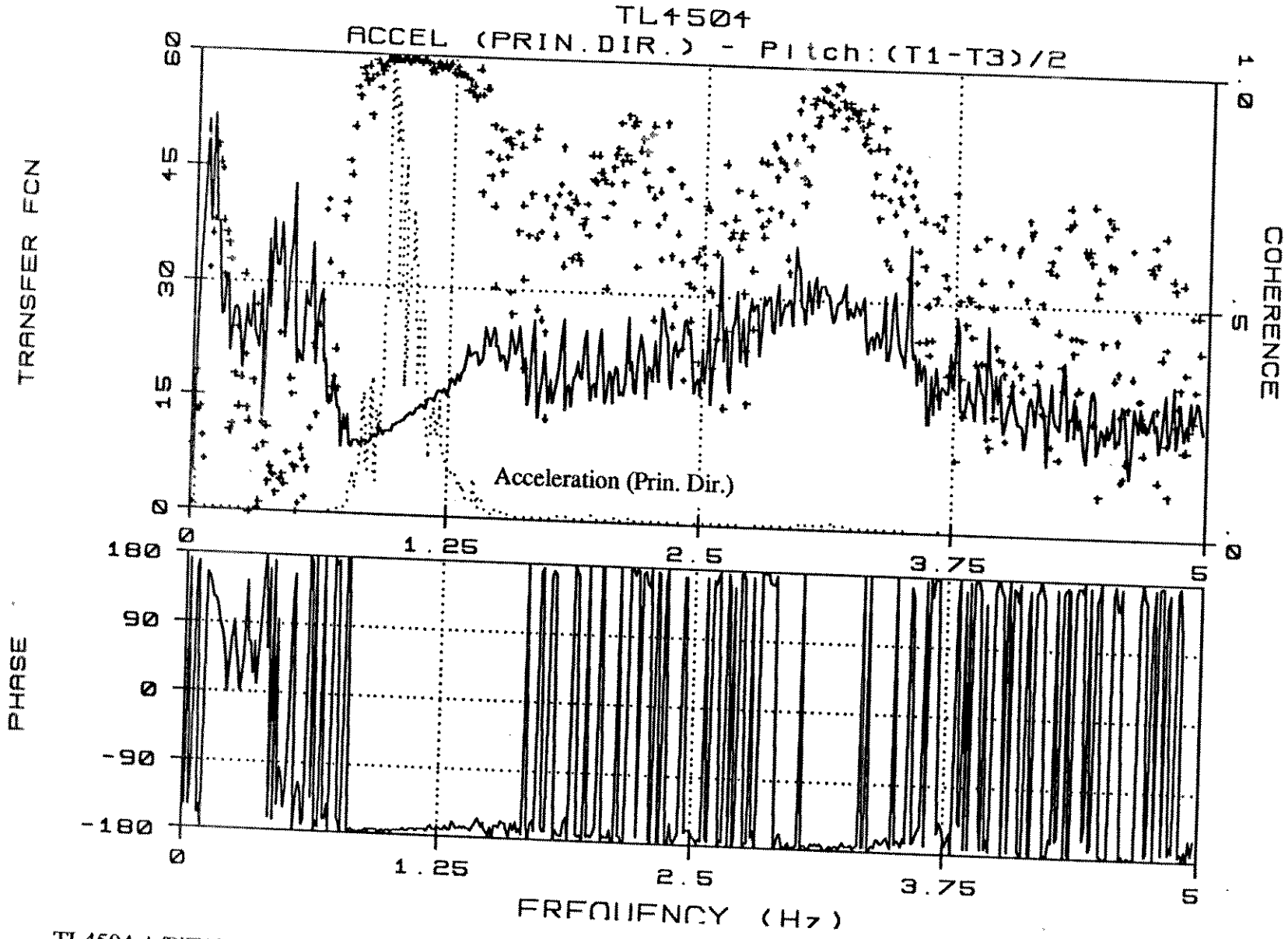

TL4504.A/PiT13.4t

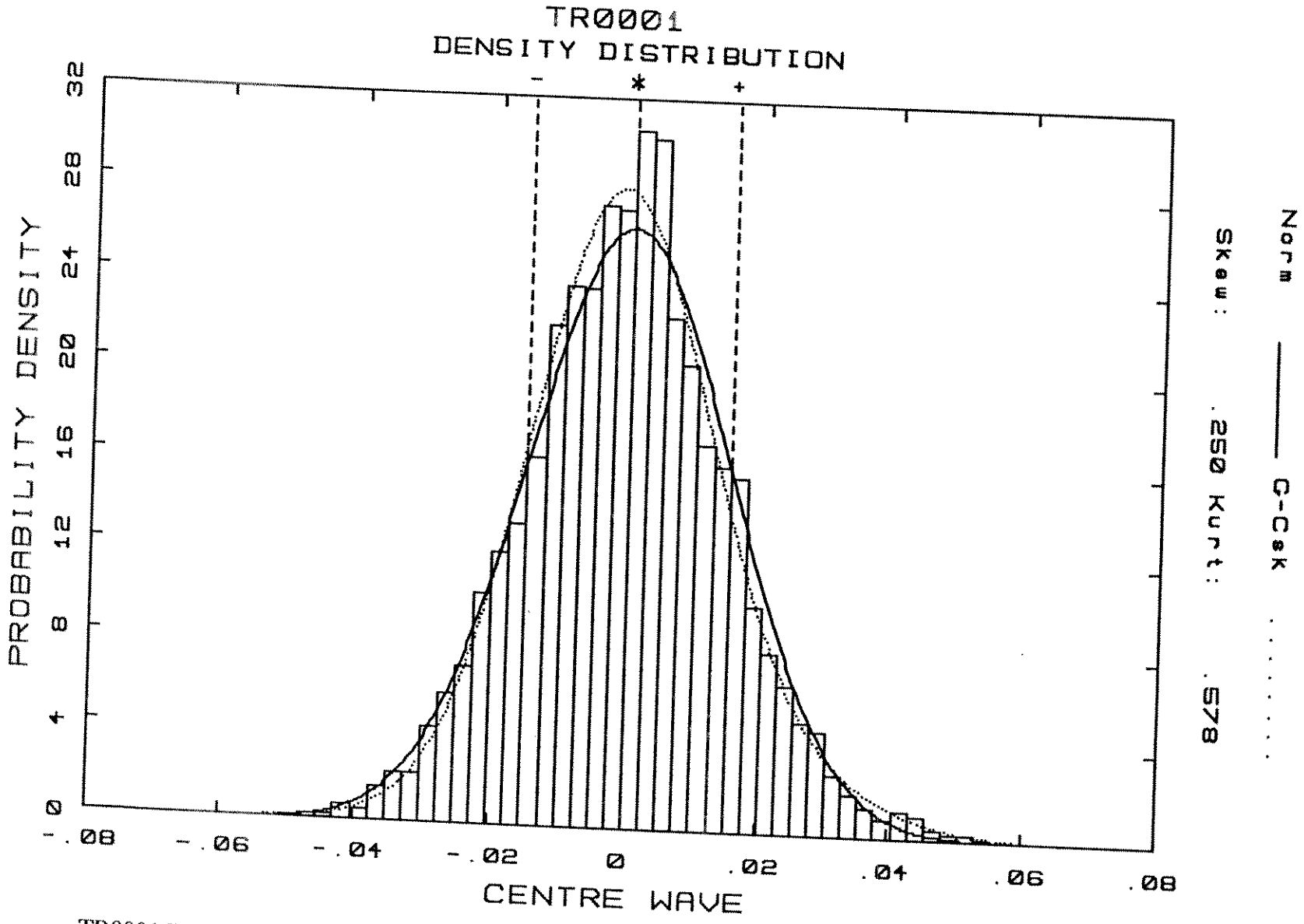
TR0001
DENSITY DISTRIBUTION
PROBABILITY DENSITY
0
4
8
12
16
20
24
28
32
-.08
-.06
-.04
-.02
0
.02
.04
.06
.08
CENTRE WAVE
Norm
C-Cek
Skew: .250 Kurt: .578

TR0001.W.1

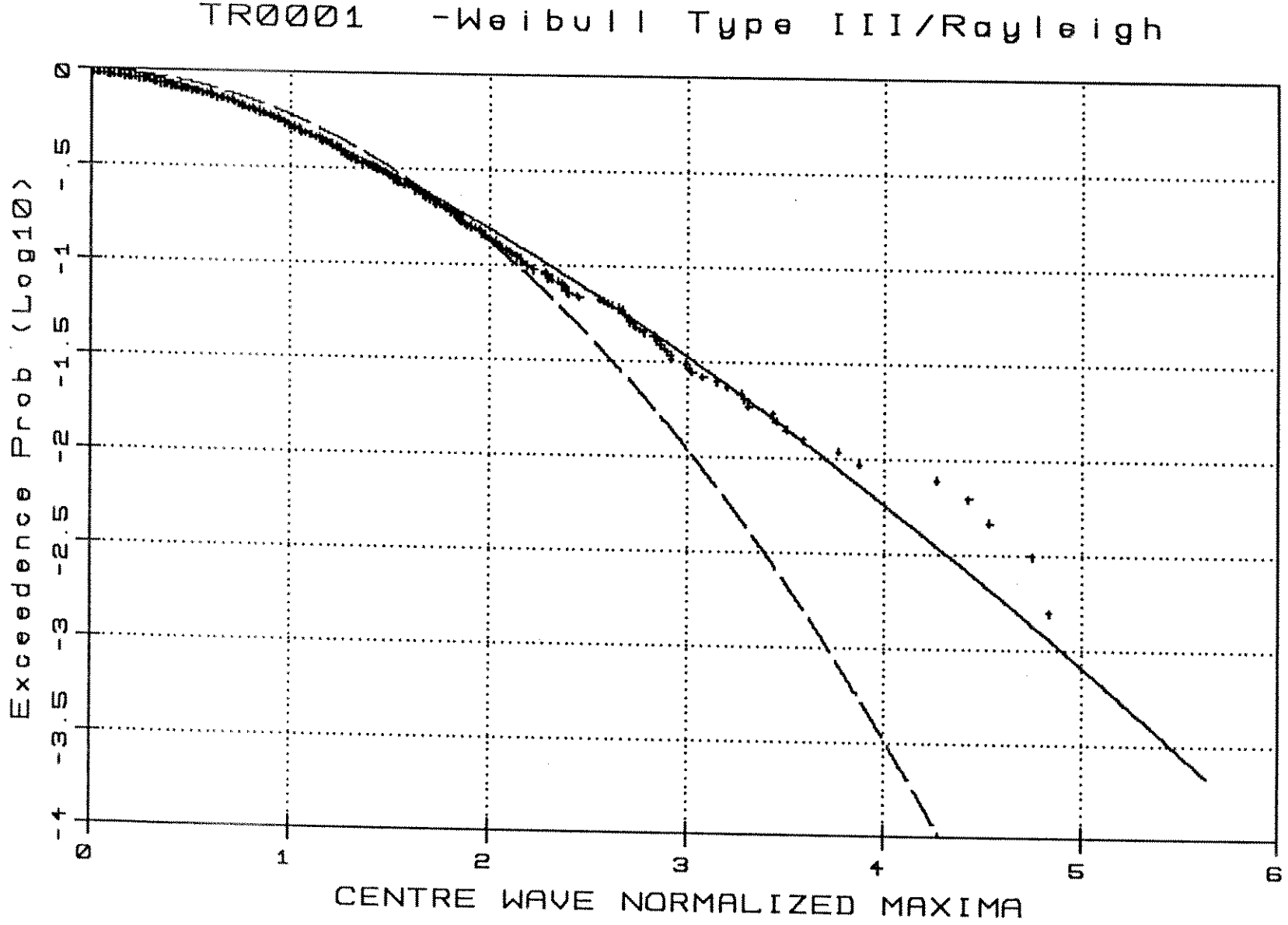
TR0001 -Weibull Type III/Rayleigh
Exceedence Prob (Log10)
0
-.5
-1
-1.5
-2
-2.5
-3
-3.5
-4
0
1
2
3
4
5
6
CENTRE WAVE NORMALIZED MAXIMA

TR0001.W.2

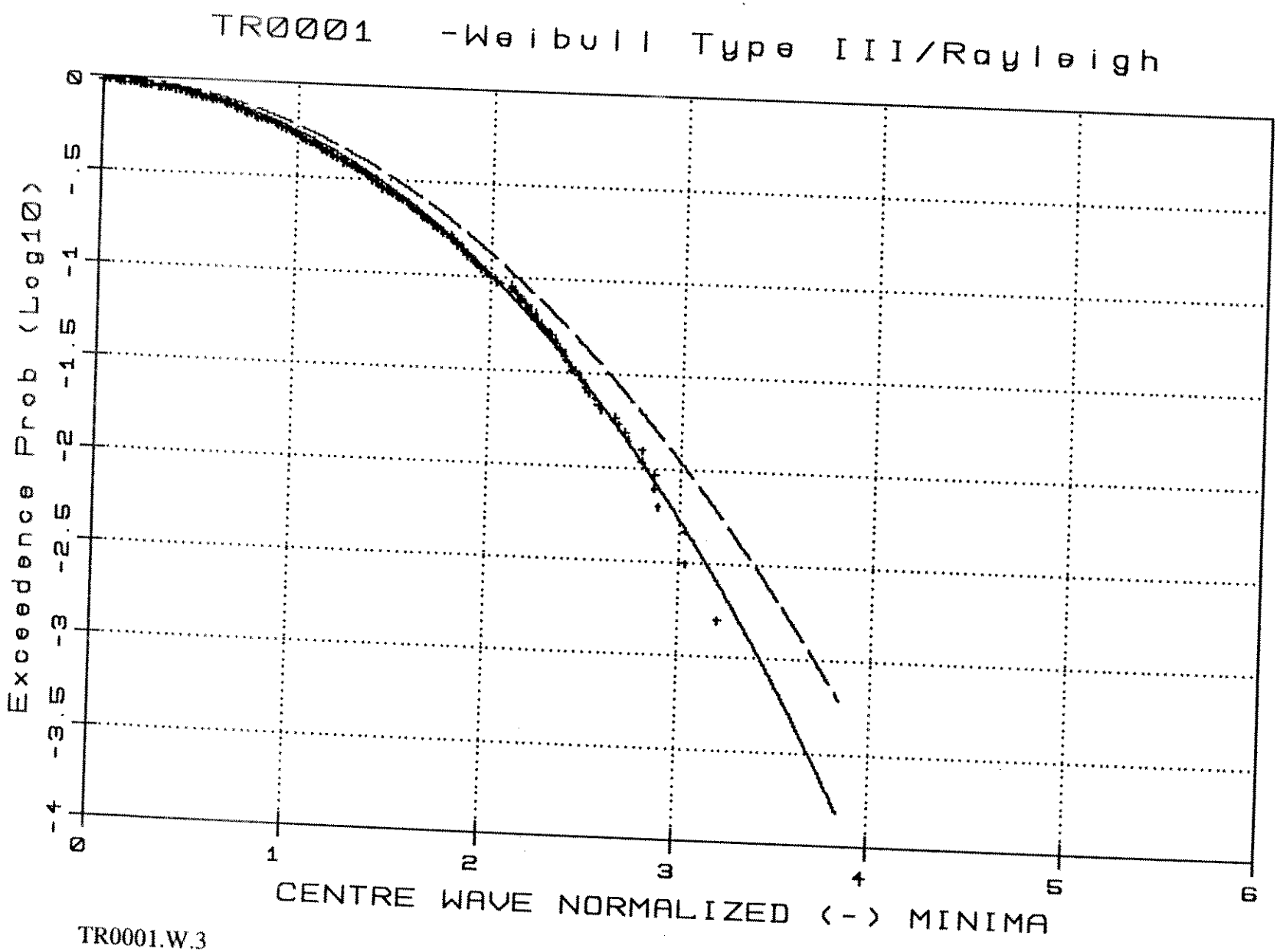
TR0001 -Weibull Type III/Rayleigh
Exceedence Prob (Log10)
0
-.5
-1
-1.5
-2
-2.5
-3
-3.5
-4
0
1
2
3
4
5
6
CENTRE WAVE NORMALIZED (-) MINIMA

TR0001.W.3

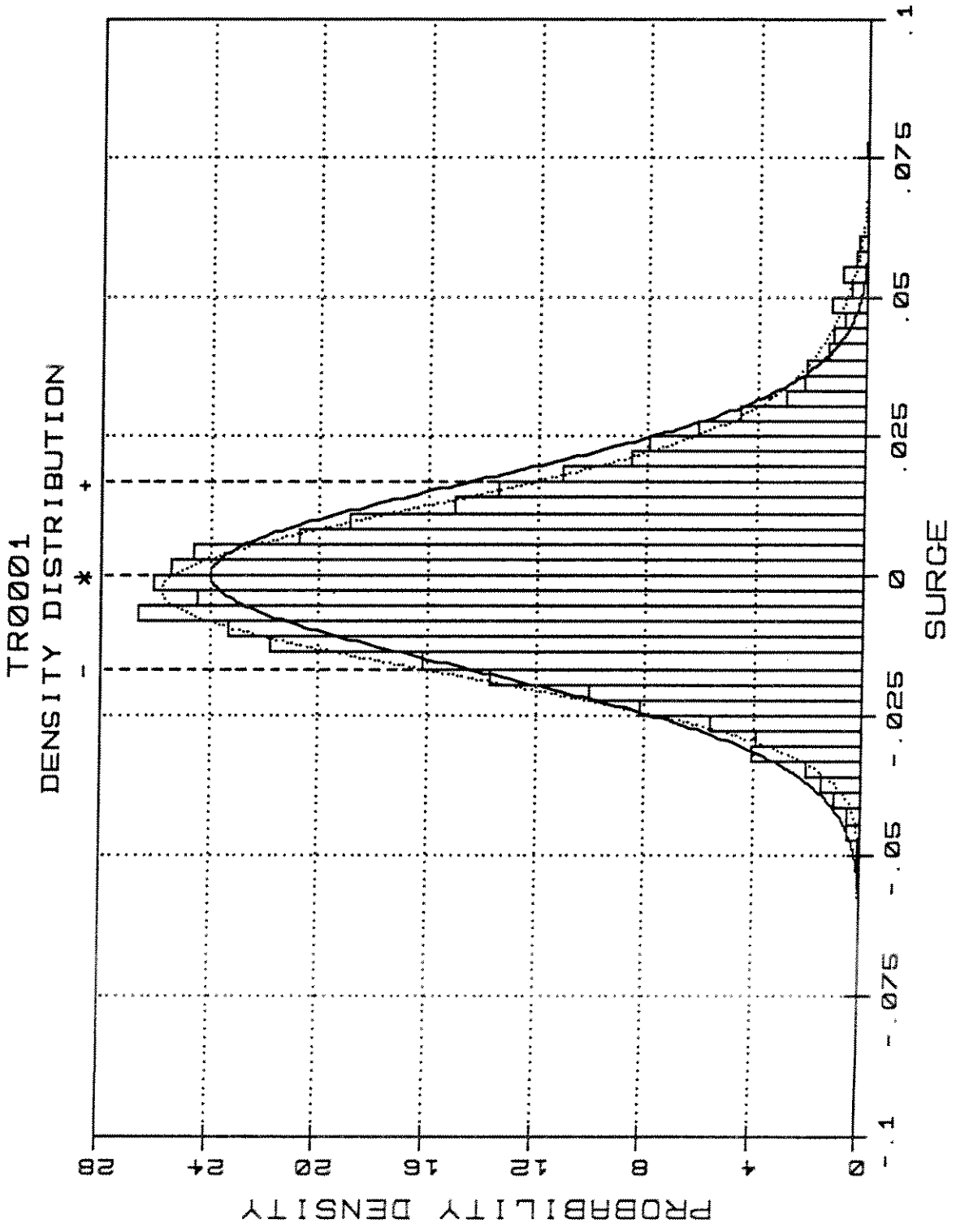
Norm ——— G-Csk .....
Skew: .427 Kurt: .746
TR0001
DENSITY DISTRIBUTION
+
*
-
PROBABILITY DENSITY
0
4
8
12
16
20
24
28
SURGE
.1
.075
.05
.025
0
-.025
-.05
-.075
-.1

TR001.S.1

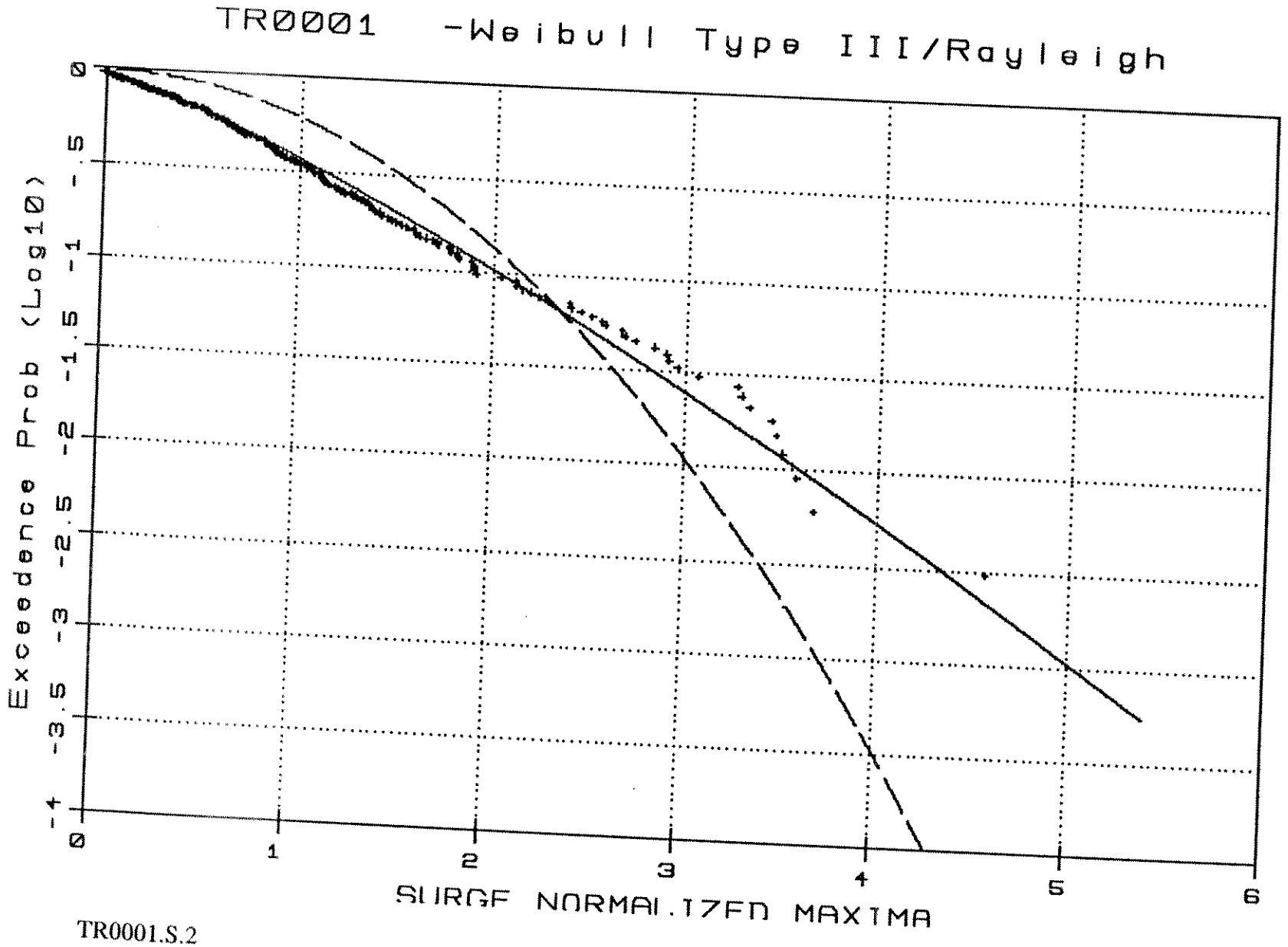
TR0001 -Weibull Type III/Rayleigh
Exceedence Prob (Log10)
0
-.5
-1
-1.5
-2
-2.5
-3
-3.5
-4
0
1
2
3
4
5
6
SURGE NORMALIZED MAXIMA

TR0001.S.2

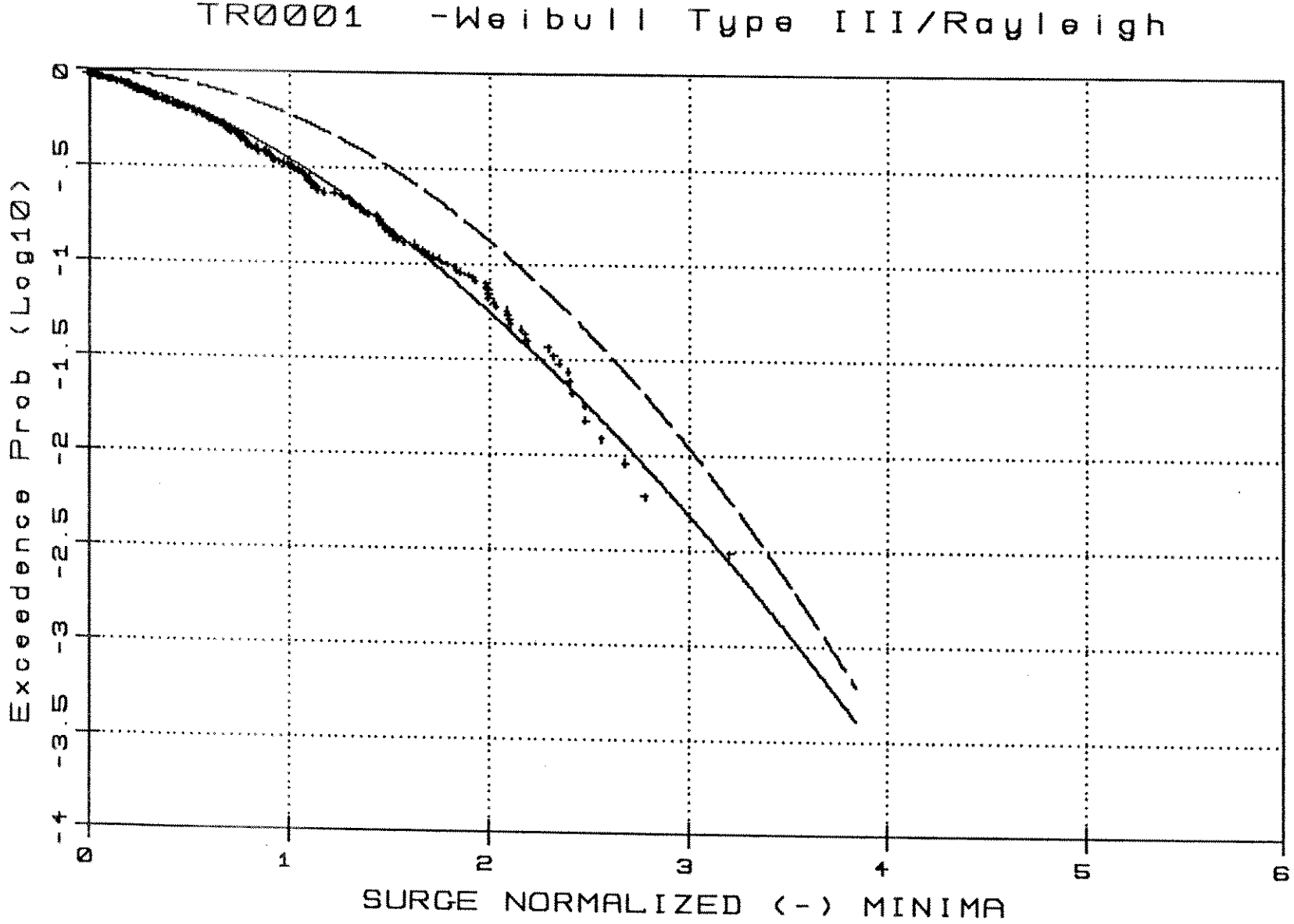
TR0001 -Weibull Type III/Rayleigh
Exceedence Prob (Log10)
0
-.5
-1
-1.5
-2
-2.5
-3
-3.5
-4
0
1
2
3
4
5
6
SURGE NORMALIZED (-) MINIMA

TR0001.S.3

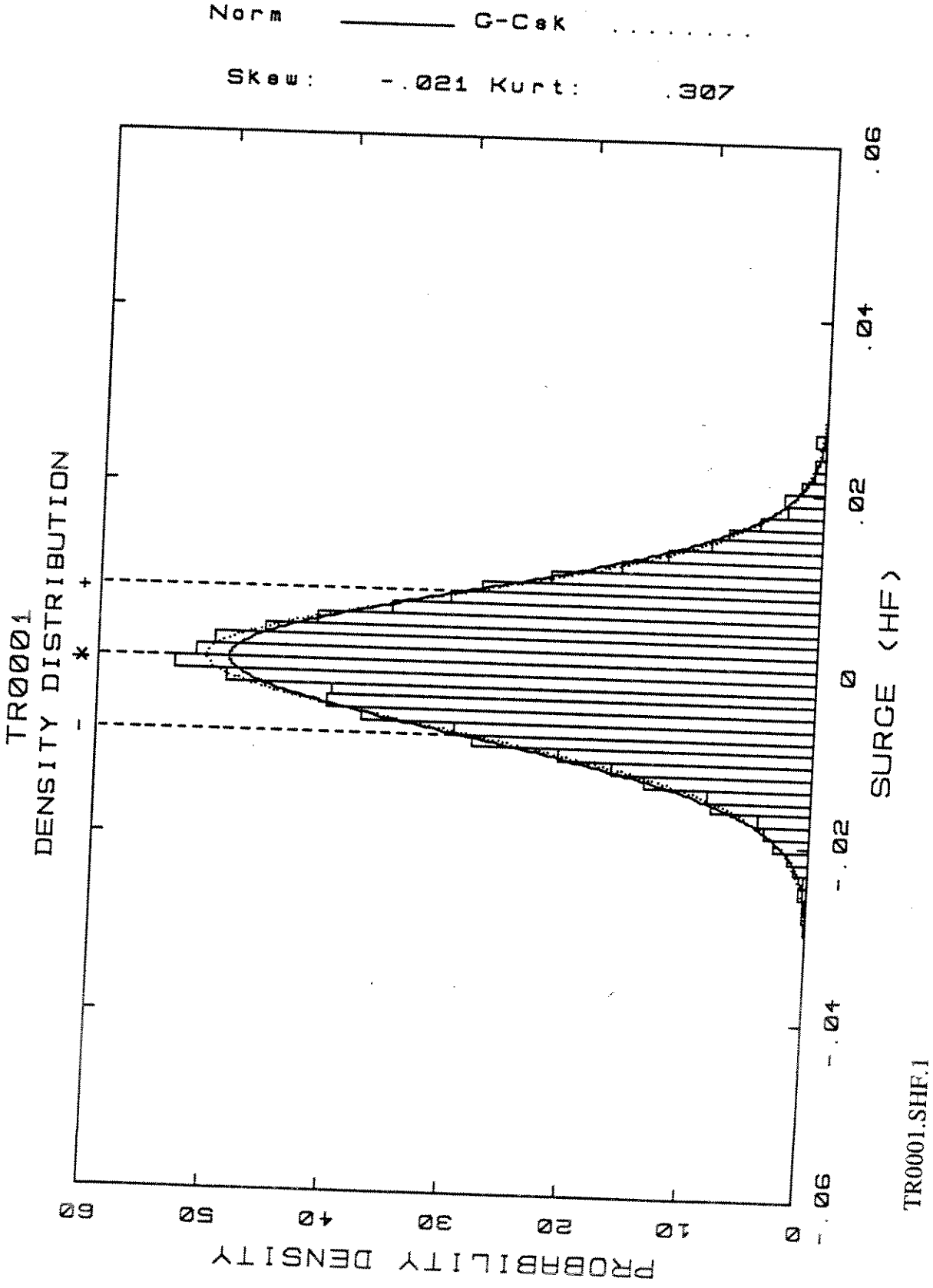
Norm ——— G-Csk .....
Skew: -.021 Kurt: .307
TR0001
DENSITY DISTRIBUTION
PROBABILITY DENSITY
SURGE (HF)
TR0001.SHF.1

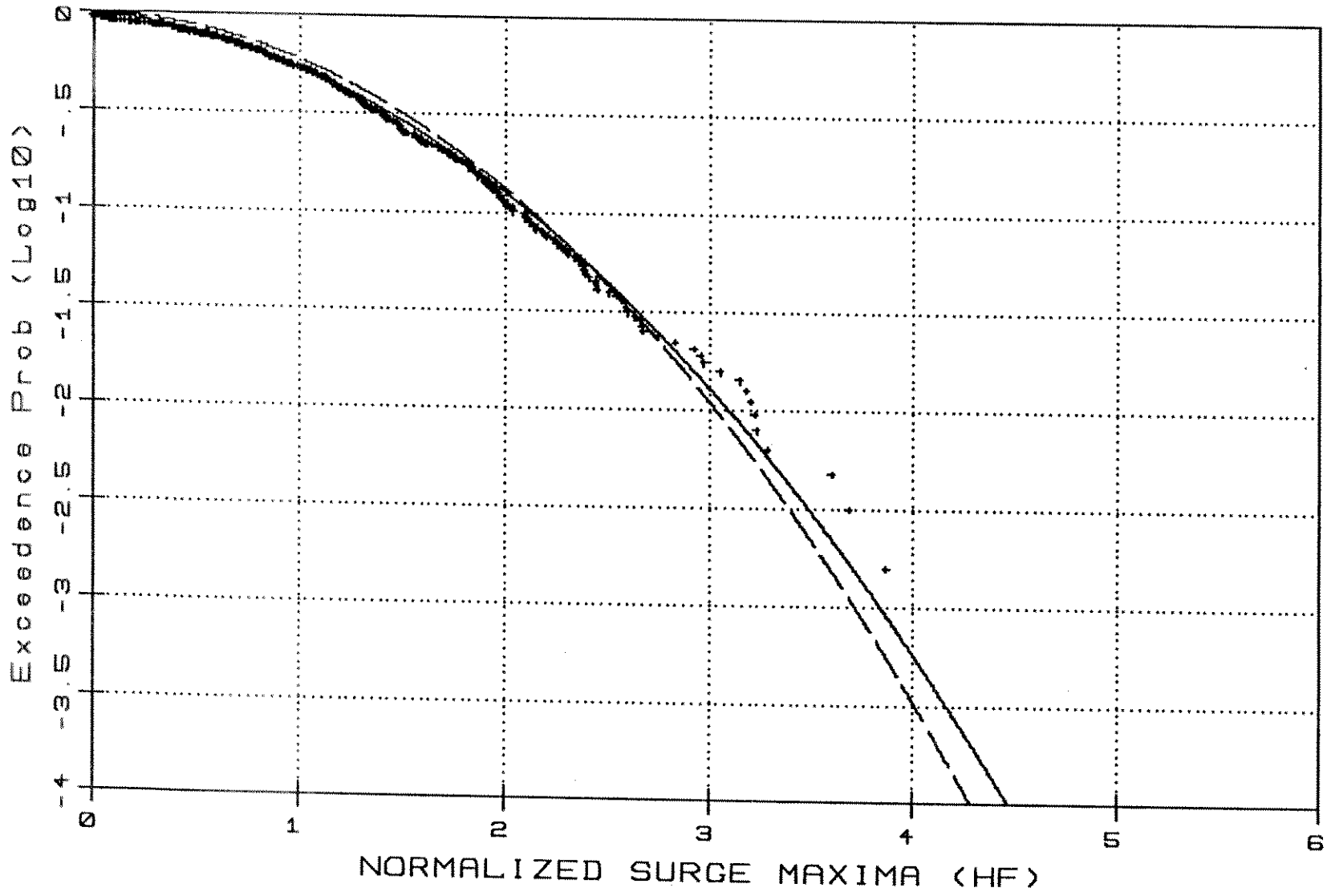
TR0001 -Weibull Type III/Rayleigh
Exceedence Prob (Log10)
0
-.5
-1
-1.5
-2
-2.5
-3
-3.5
-4
0
1
2
3
4
5
6
NORMALIZED SURGE MAXIMA (HF)

TR0001.SHF.2

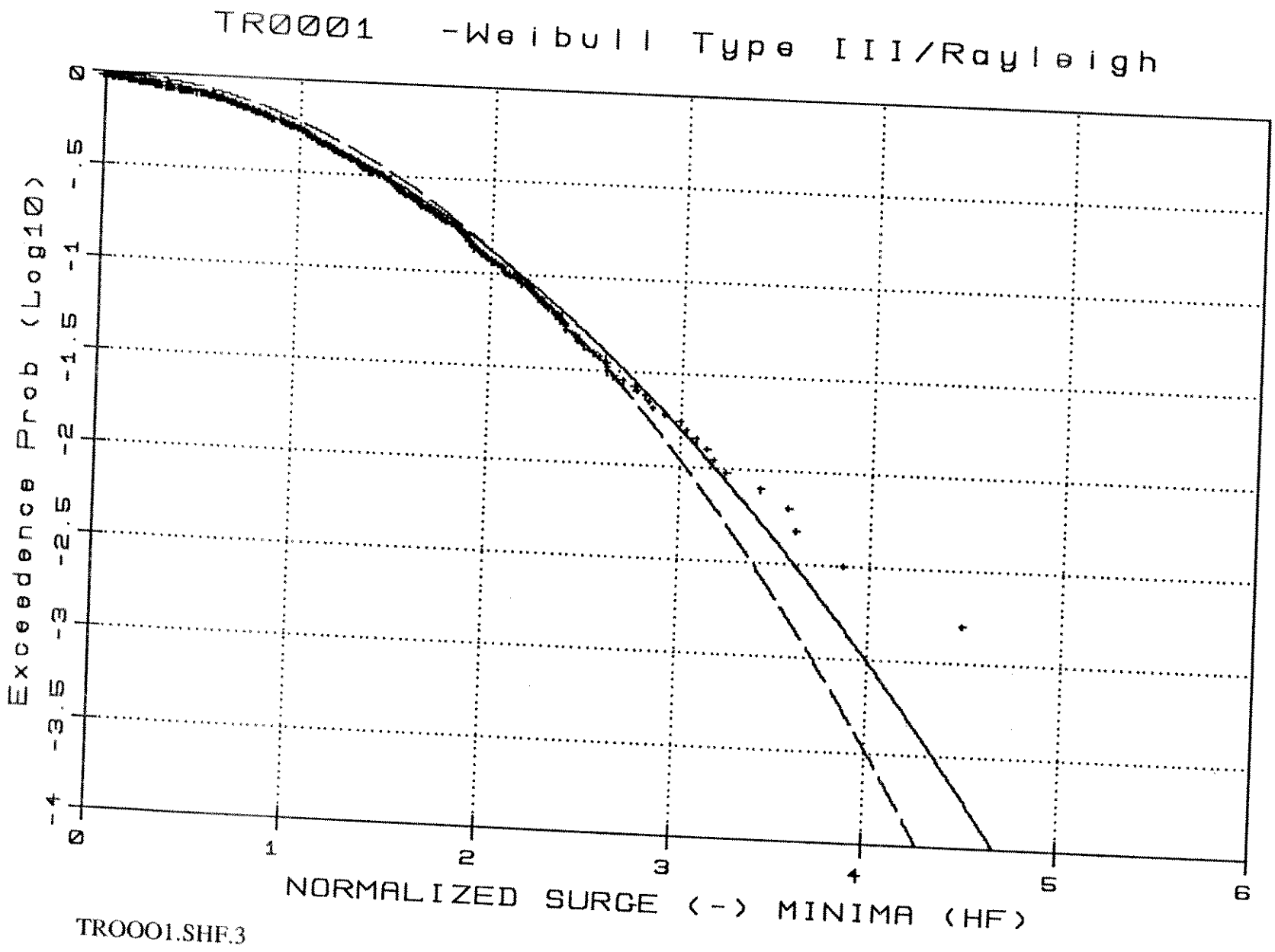
TR0001 -Weibull Type III/Rayleigh
Exceedence Prob (Log10)
0
-.5
-1
-1.5
-2
-2.5
-3
-3.5
-4
0
1
2
3
4
5
6
NORMALIZED SURGE (-) MINIMA (HF)

TROOO1.SHF.3

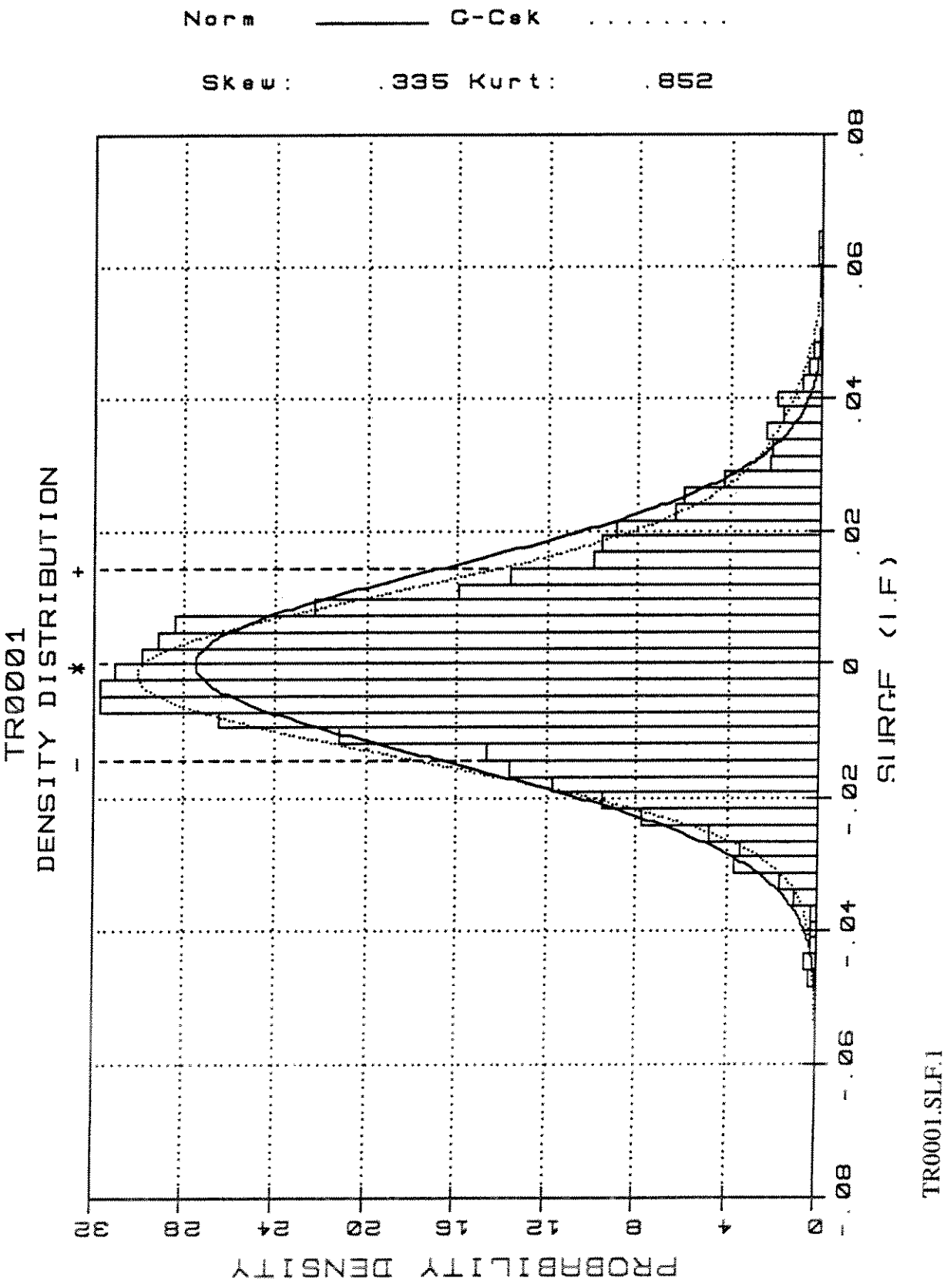
Norm
G-Cek
Skew: .335 Kurt: .852
TR0001
DENSITY DISTRIBUTION
PROBABILITY DENSITY
SURGE (I.F.)
32
28
24
20
16
12
8
4
0
.08
.06
.04
.02
0
-.02
-.04
-.06
-.08

TR0001.SLF1

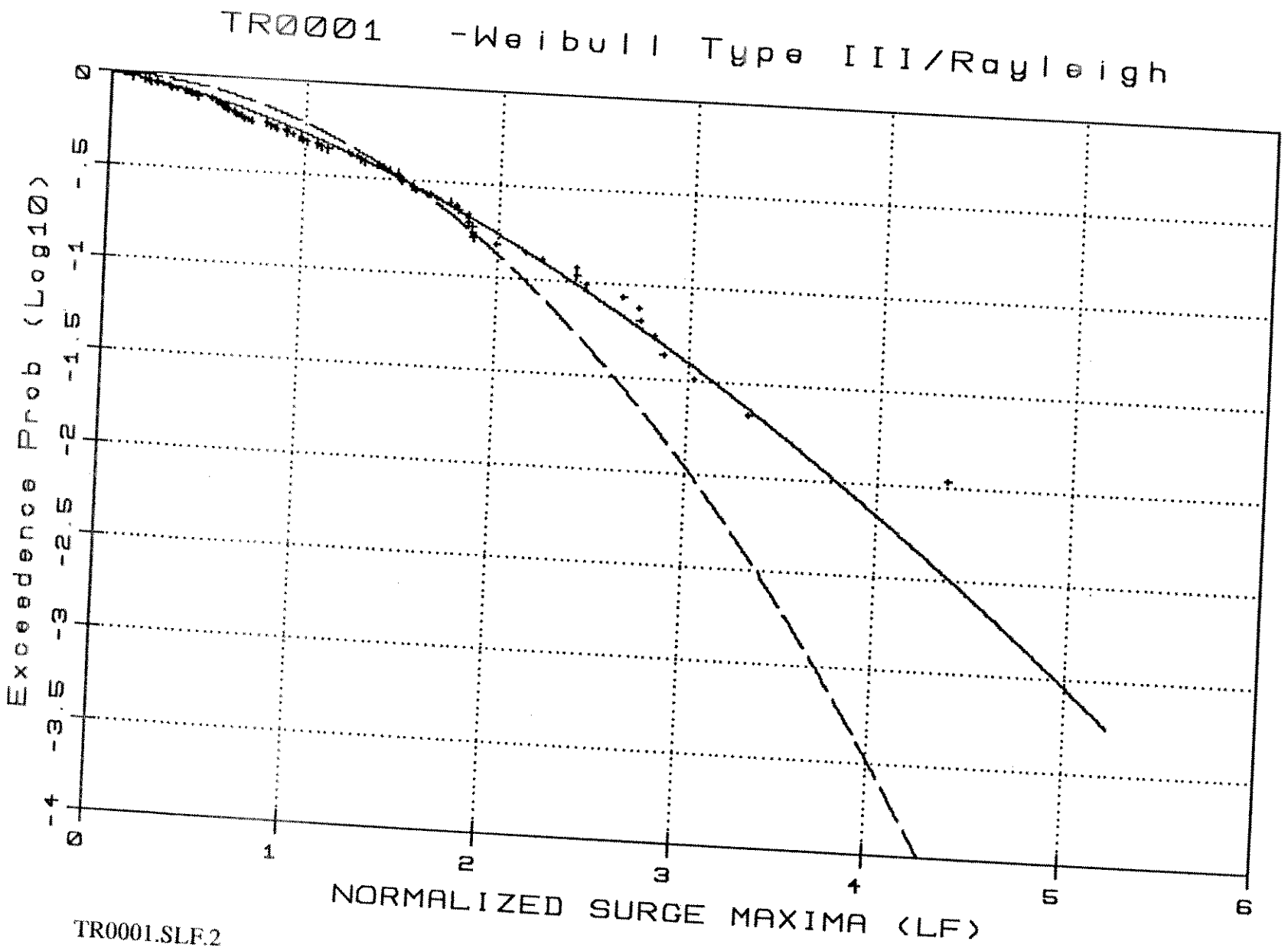
TR0001 -Weibull Type III/Rayleigh
Exceedence Prob (Log10)
0
-.5
-1
-1.5
-2
-2.5
-3
-3.5
-4
0
1
2
3
4
5
6
NORMALIZED SURGE MAXIMA (LF)

TR0001.SLF.2

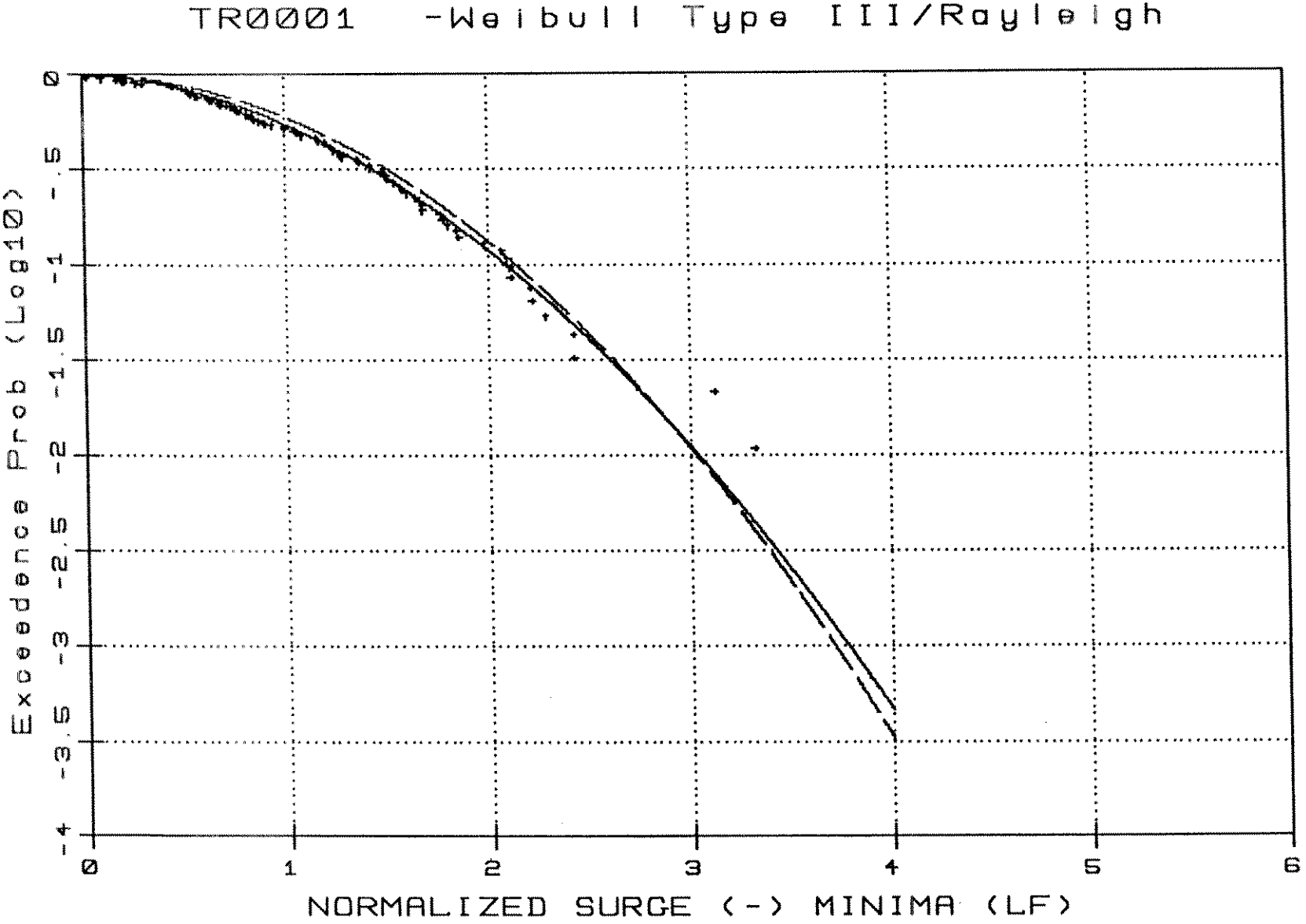
TR0001 -Weibull Type III/Rayleigh
Exceedence Prob (Log10)
0
-.5
-1
-1.5
-2
-2.5
-3
-3.5
-4
0
1
2
3
4
5
6
NORMALIZED SURGE (-) MINIMA (LF)

TR0001.SLF.3

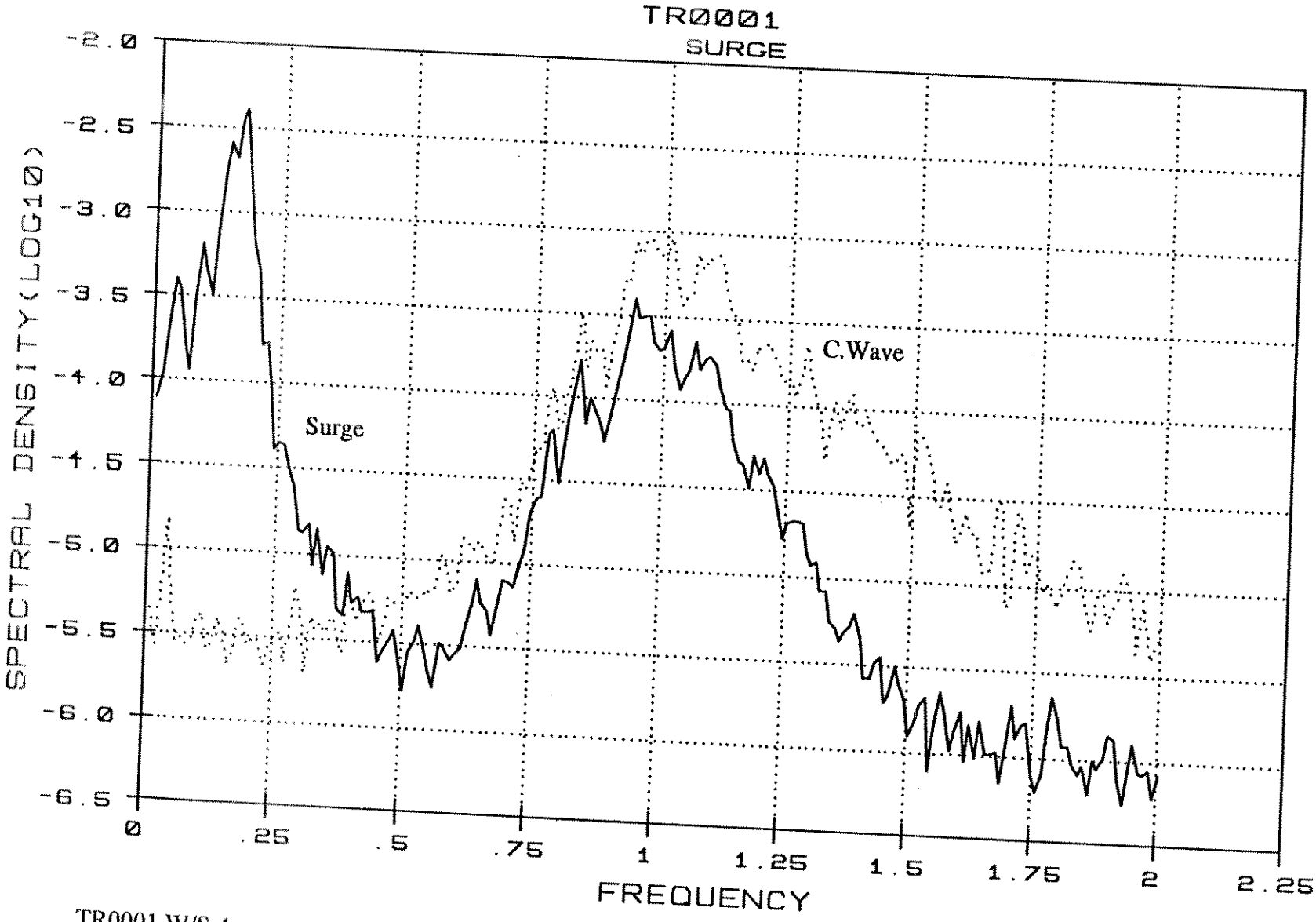
TR0001
SURGE
SPECTRAL DENSITY(LOG10)
-2.0
-2.5
-3.0
-3.5
-4.0
-4.5
-5.0
-5.5
-6.0
-6.5
0
.25
.5
.75
1
1.25
1.5
1.75
2
2.25
FREQUENCY
Surge
C.Wave

TR0001.W/S.4

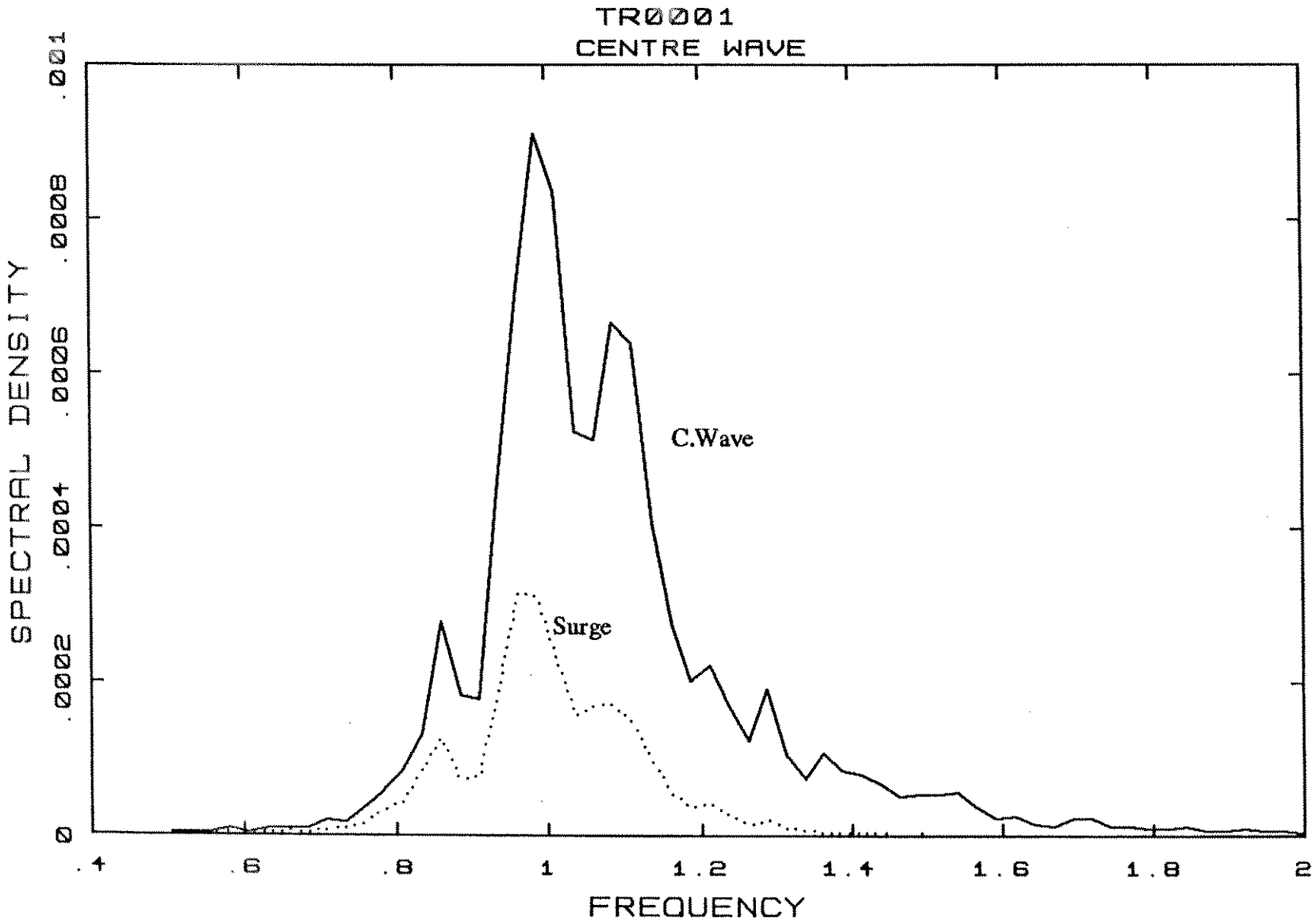
TR0001
CENTRE WAVE
SPECTRAL DENSITY
.001
.0008
.0006
.0004
.0002
0
C.Wave
Surge
.4
.6
.8
1
1.2
1.4
1.6
1.8
2
FREQUENCY

TR0001.W/S.4*

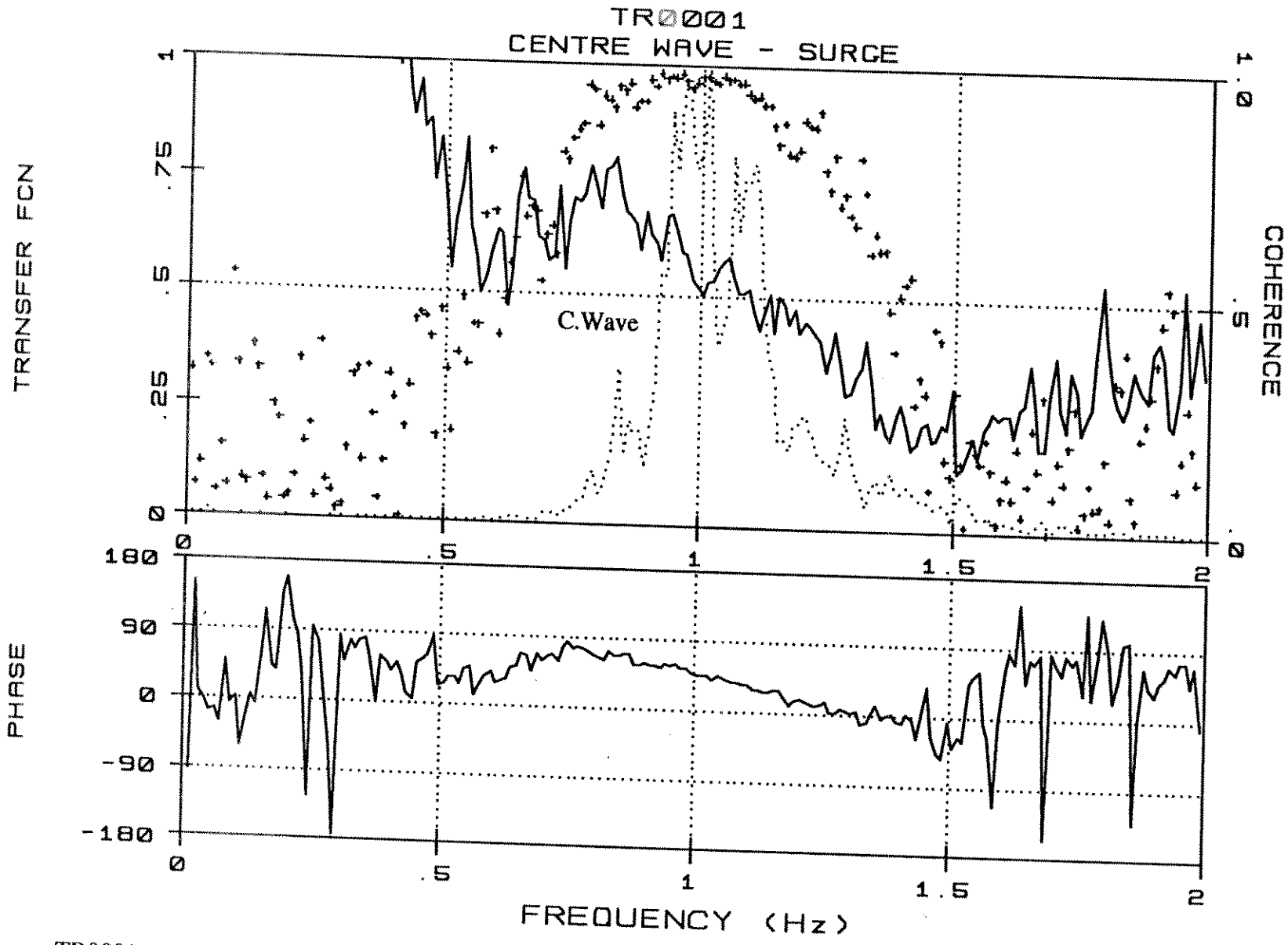
TR0001
CENTRE WAVE - SURCE
TRANSFER FCN
COHERENCE
C.Wave
PHASE
FREQUENCY (Hz)
0
.25
.5
.75
1
1.5
2
180
90
-90
-180

TR0001.W/S.4t

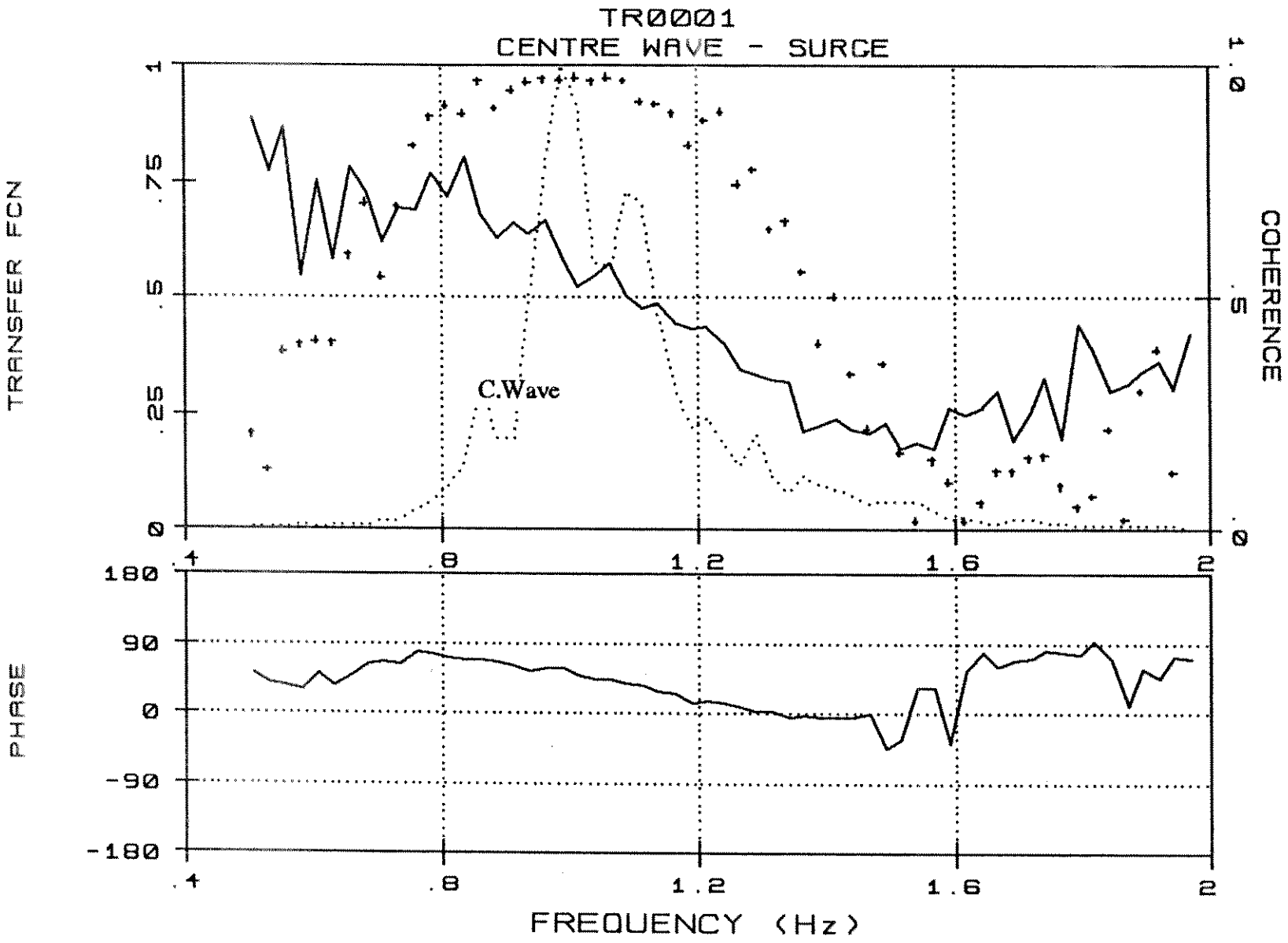
TR0001
CENTRE WAVE - SURGE
TRANSFER FCN
COHERENCE
C.Wave
1
.75
.5
.25
0
1.0
.5
0
.4
.8
1.2
1.6
2
180
90
0
-90
-180
PHASE
FREQUENCY (Hz)

TR0001/W/S.4t*

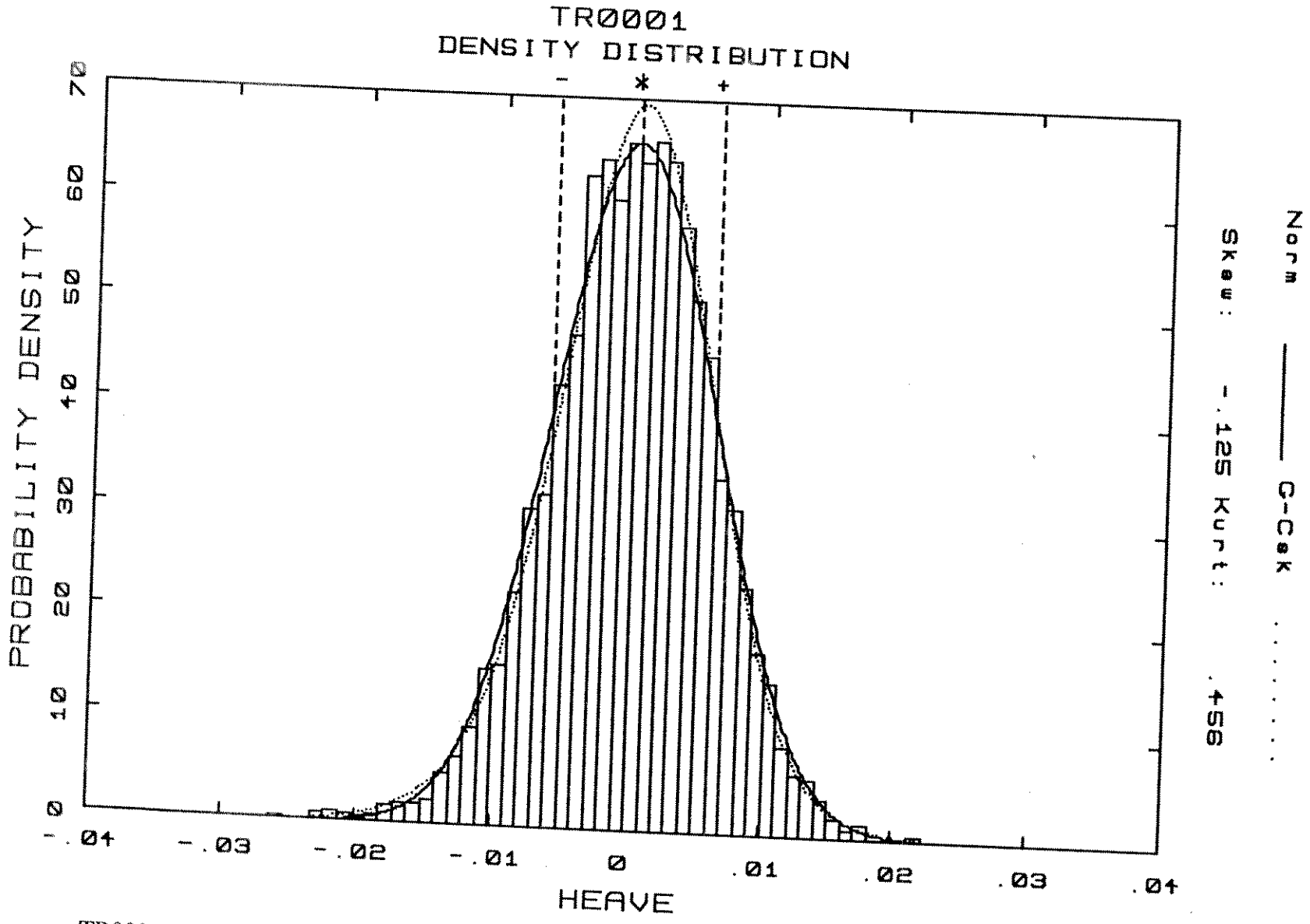
TR0001
DENSITY DISTRIBUTION
PROBABILITY DENSITY
0
10
20
30
40
50
60
70
-.04
-.03
-.02
-.01
0
.01
.02
.03
.04
HEAVE
Norm
C-Cek
Skew: -.125 Kurt: .456

TR0001.H.1

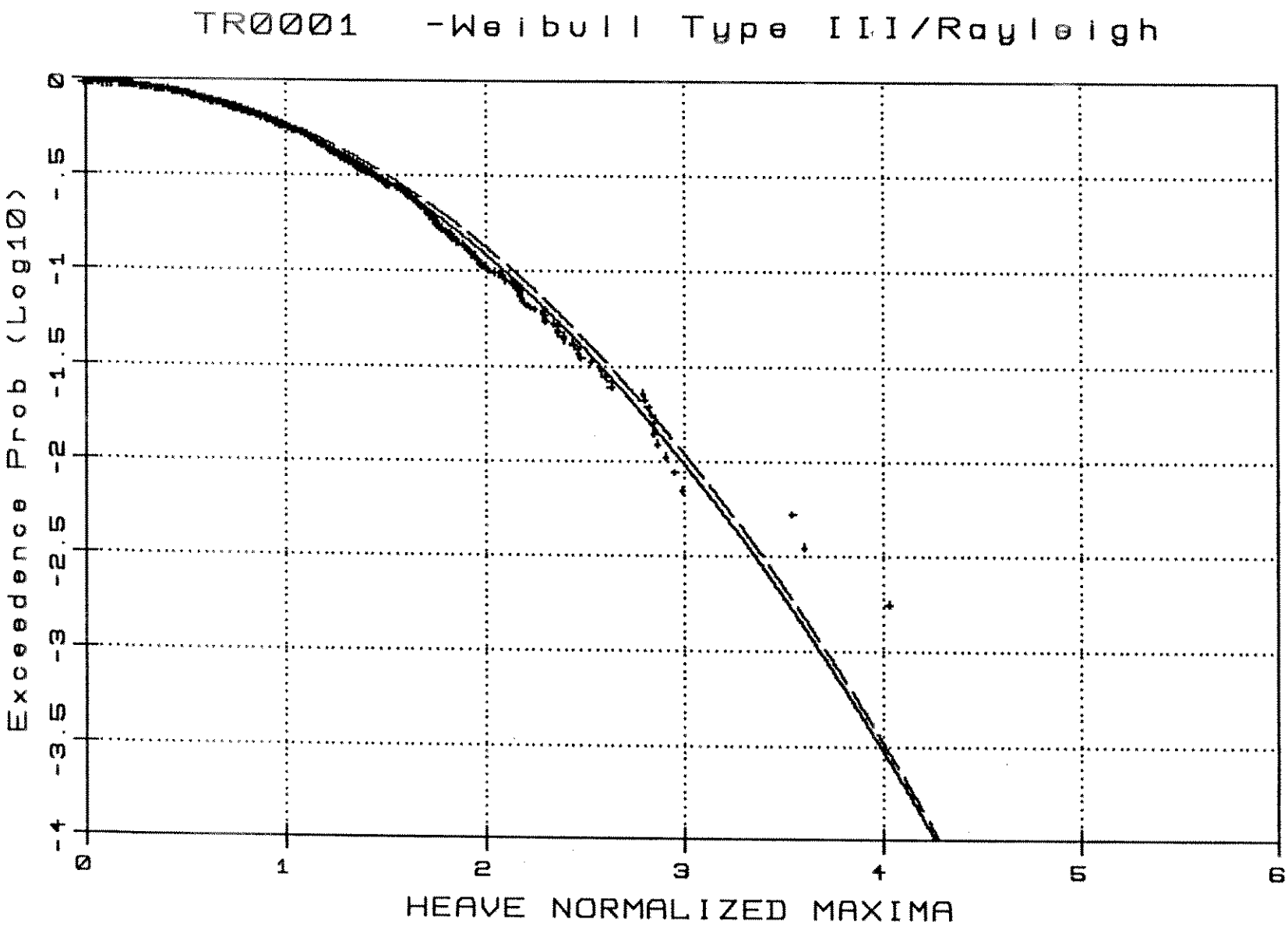
TR0001 -Weibull Type III/Rayleigh
Exceedence Prob (Log10)
0
-.5
-1
-1.5
-2
-2.5
-3
-3.5
-4
0
1
2
3
4
5
6
HEAVE NORMALIZED MAXIMA

TR0001.H.2

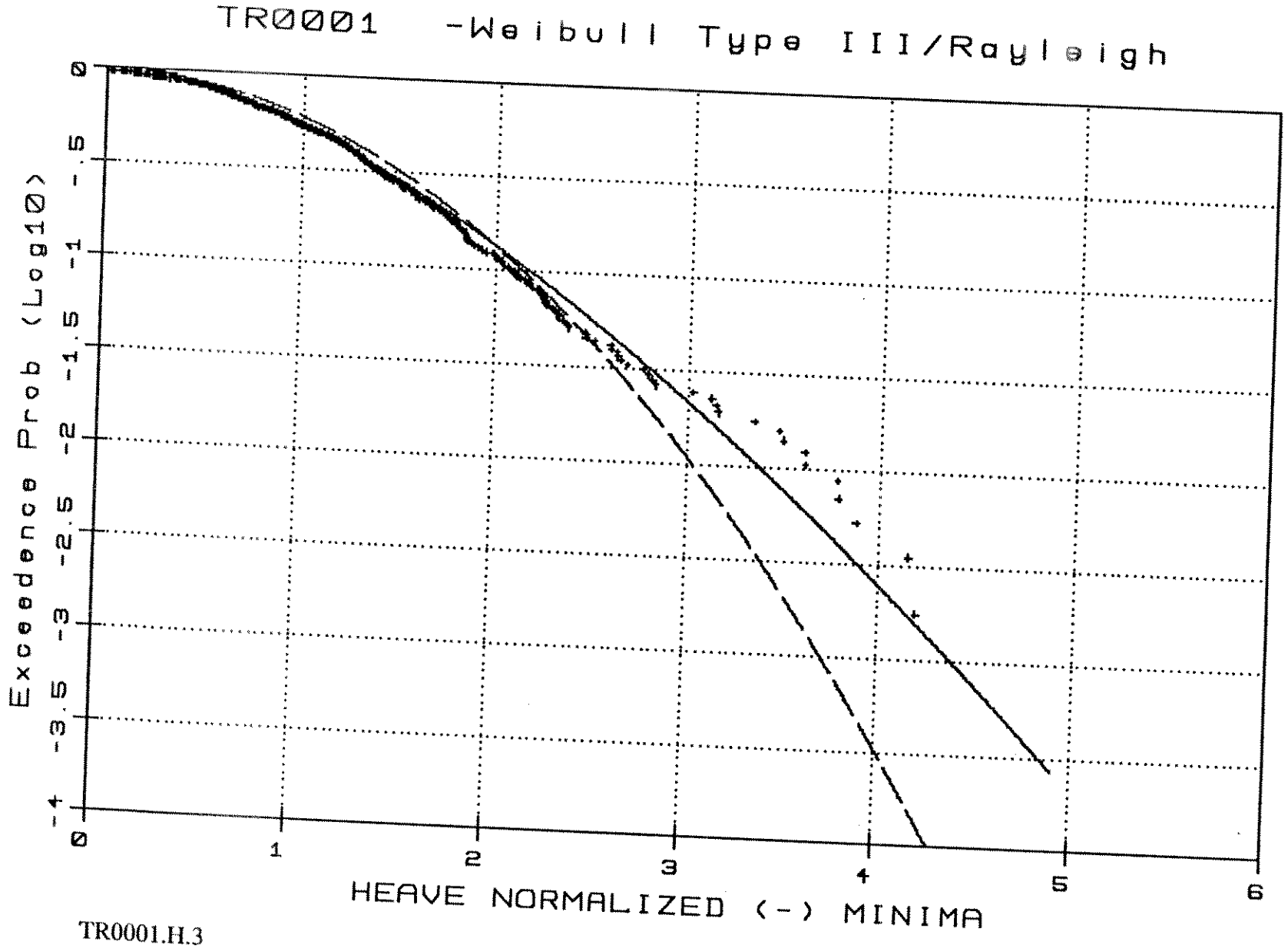
TR0001 -Weibull Type III/Rayleigh
Exceedence Prob (Log10)
0
-.5
-1
-1.5
-2
-2.5
-3
-3.5
-4
0
1
2
3
4
5
6
HEAVE NORMALIZED (-) MINIMA

TR0001.H.3

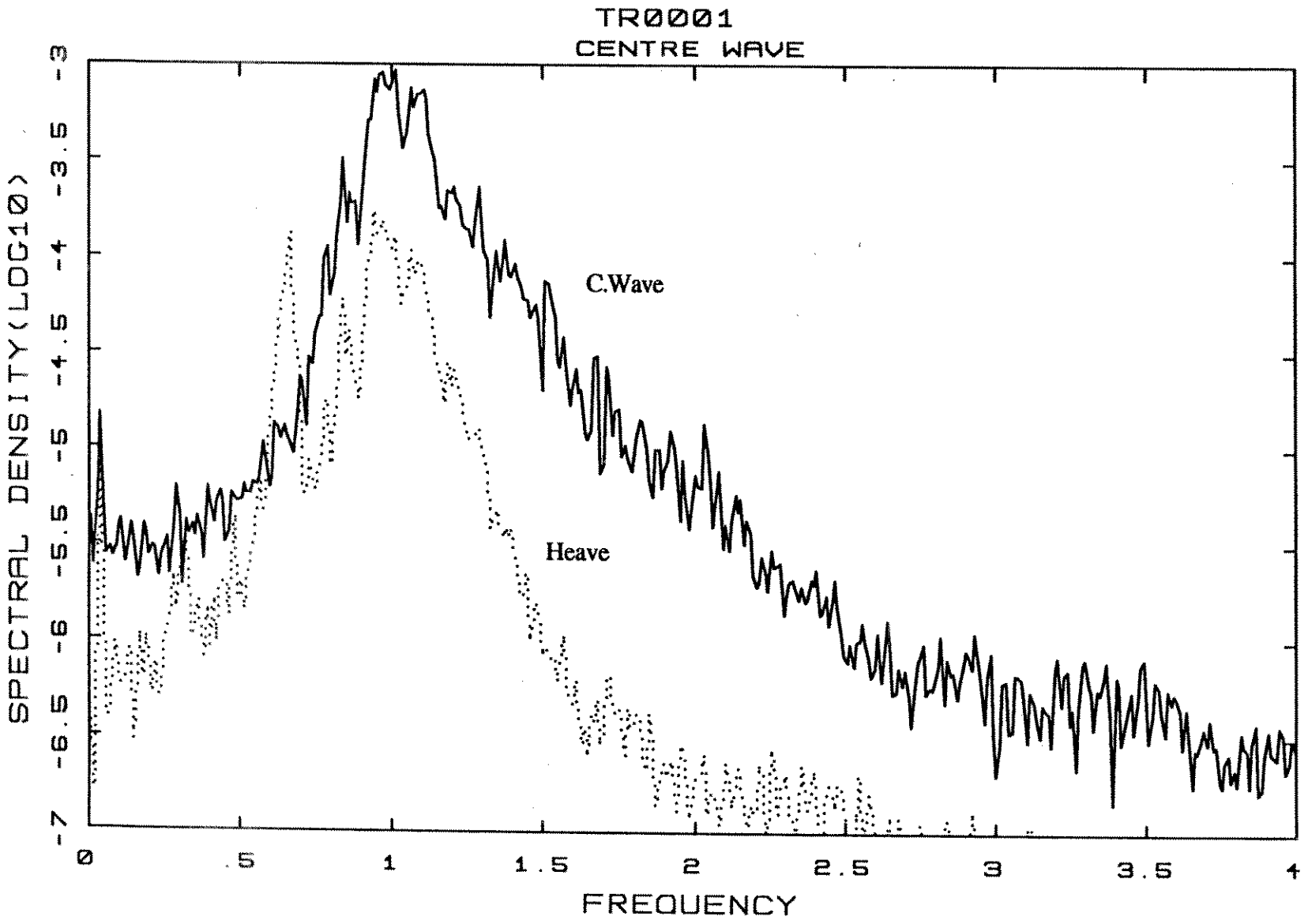
TR0001
CENTRE WAVE
SPECTRAL DENSITY(LOG10)
-3
-3.5
-4
-4.5
-5
-5.5
-6
-6.5
-7
C.Wave
Heave
0
.5
1
1.5
2
2.5
3
3.5
4
FREQUENCY

TR0001.W/H.4

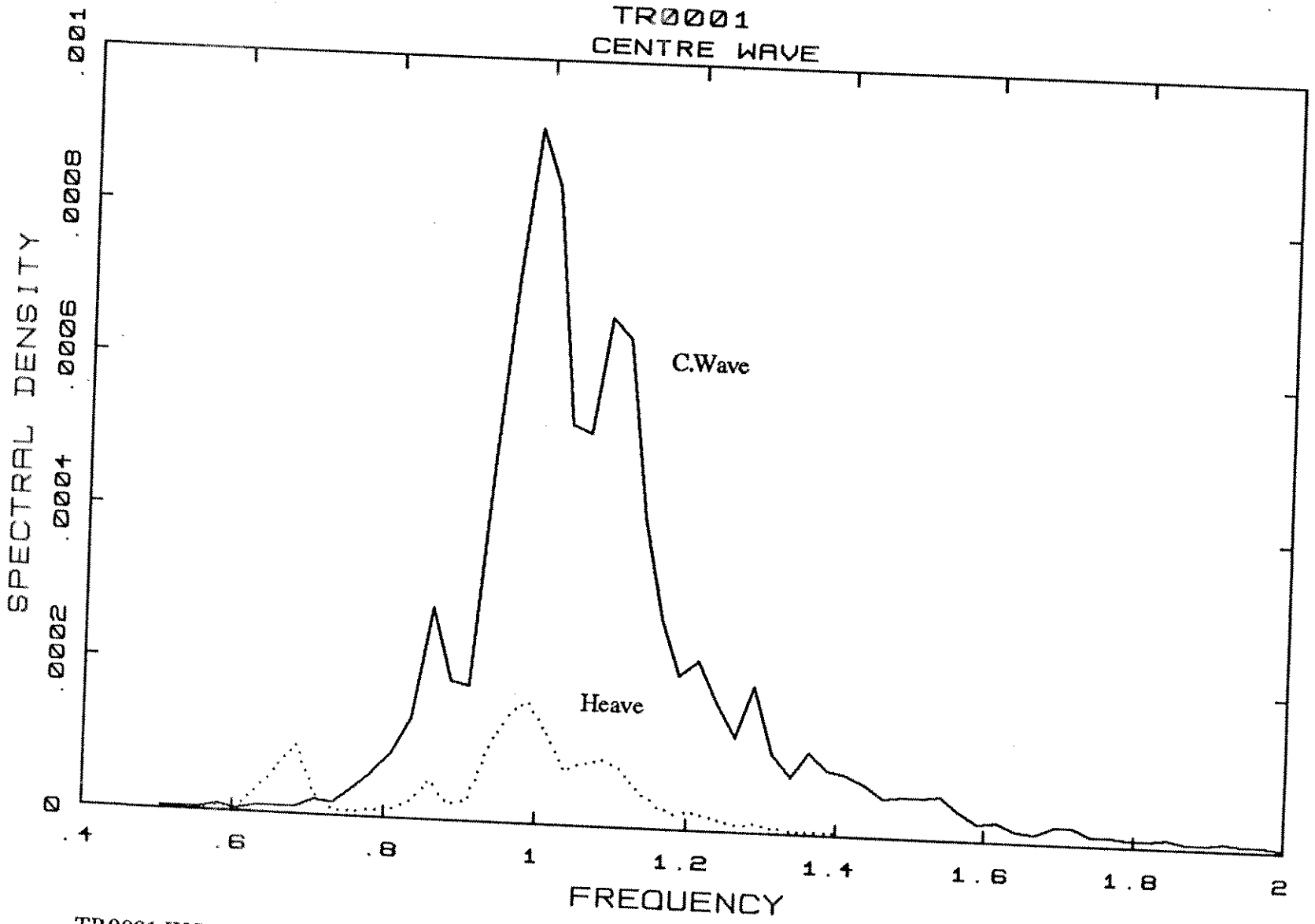
TR0001
CENTRE WAVE
SPECTRAL DENSITY
.001
.0008
.0006
.0004
.0002
0
C.Wave
Heave
.4
.6
.8
1
1.2
1.4
1.6
1.8
2
FREQUENCY

TR0001.W/H.4*

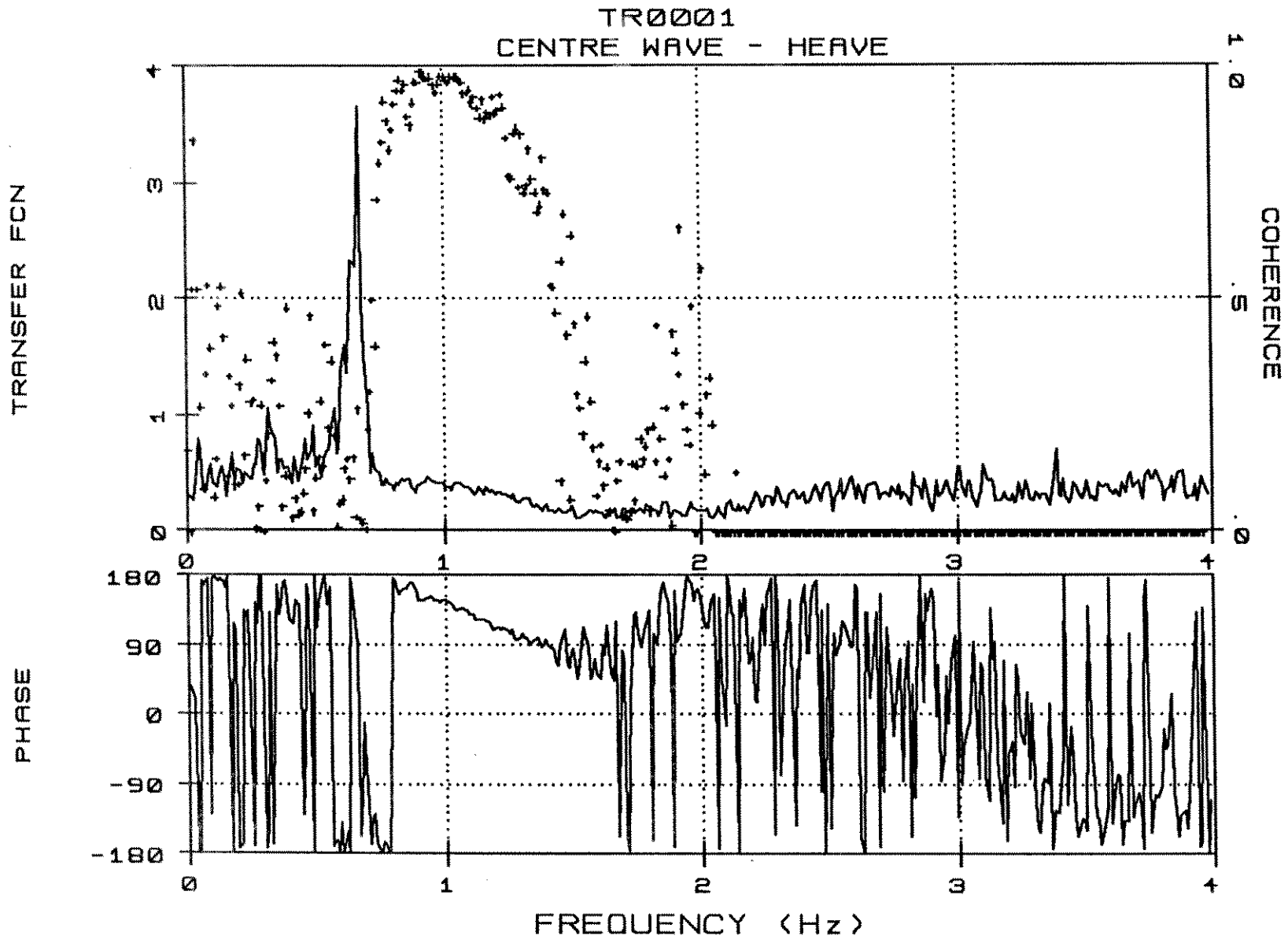
TR0001
CENTRE WAVE - HEAVE
TRANSFER FCN
COHERENCE
PHASE
FREQUENCY (Hz)
0
1
2
3
4
.5
1.0
180
90
-90
-180

TR0001.W/H.4t

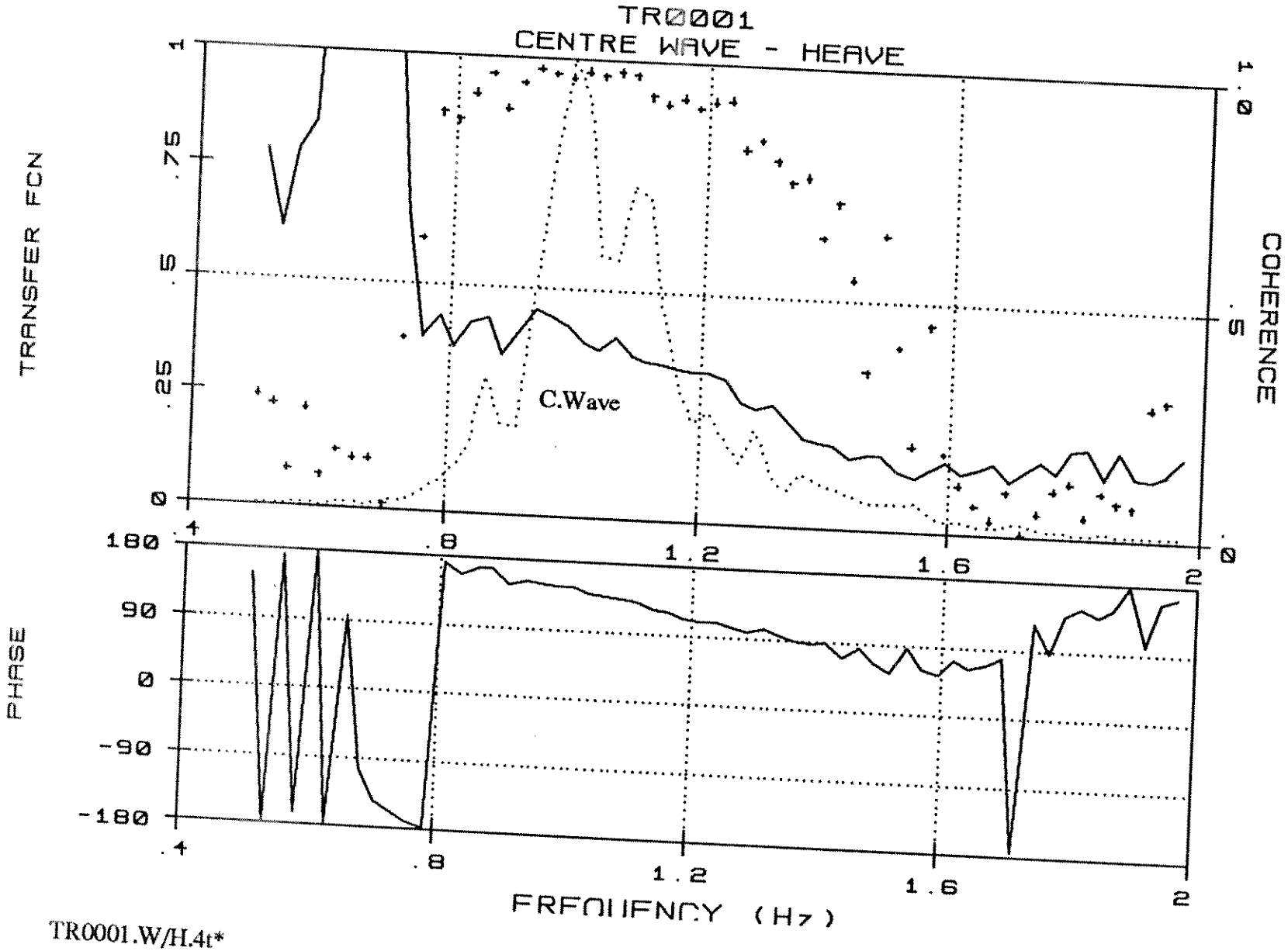
TR0001
CENTRE WAVE - HEAVE
TRANSFER FCN
COHERENCE
C.Wave
1
.75
.5
.25
0
1.0
.5
0
180
90
0
-90
-180
.4
.8
1.2
1.6
2
PHASE
FREQUENCY (Hz)

TR0001.W/H.4t*

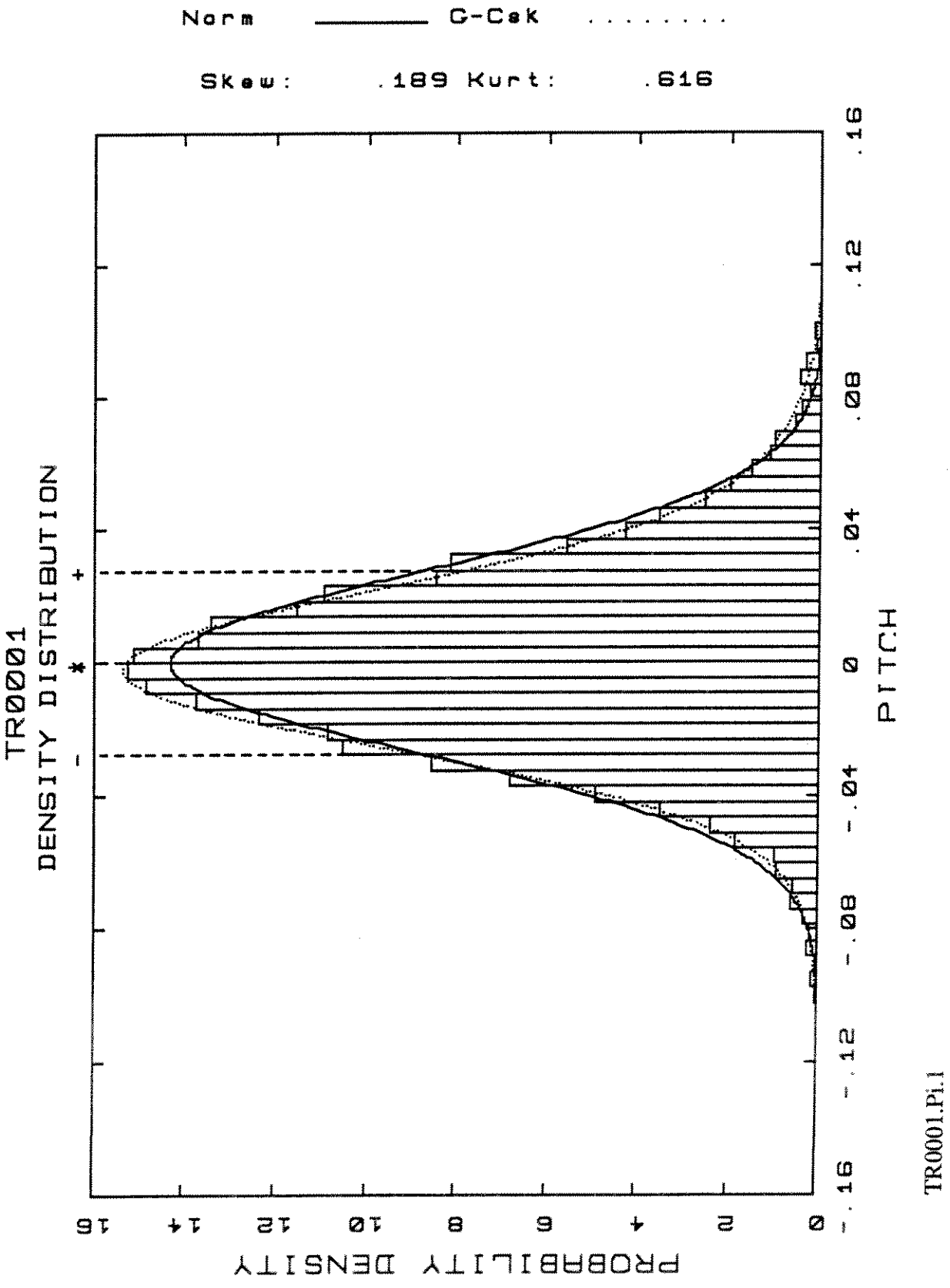
Norm
C-Cek
Skew: .189 Kurt: .616
TR0001
DENSITY DISTRIBUTION
PROBABILITY DENSITY
PITCH
0
2
4
6
8
10
12
14
16
-.16
-.12
-.08
-.04
0
.04
.08
.12
.16

TR0001.Pi.1

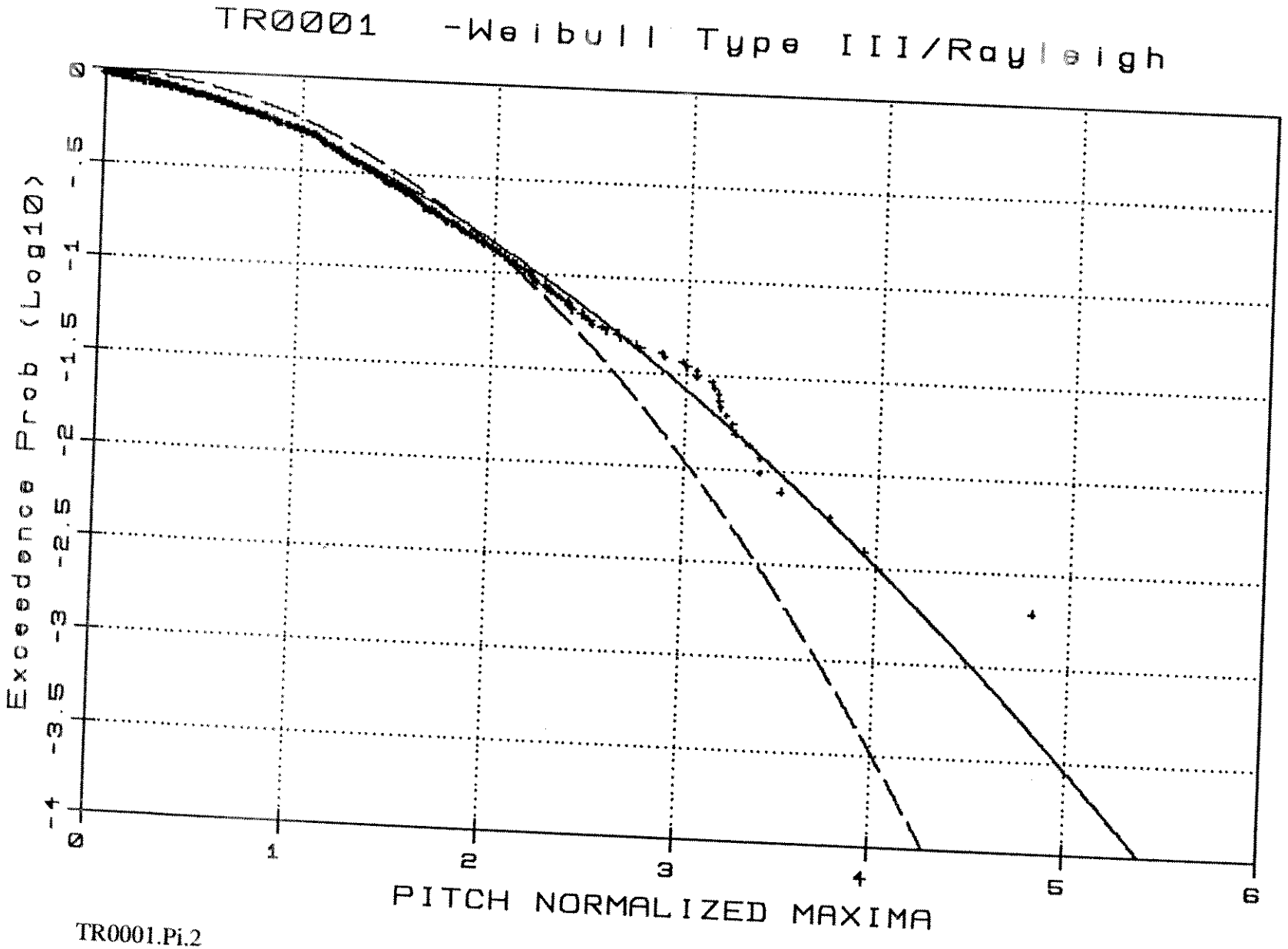
TR0001 -Weibull Type III/Rayleigh
Exceedence Prob (Log10)
0
-.5
-1
-1.5
-2
-2.5
-3
-3.5
-4
0
1
2
3
4
5
6
PITCH NORMALIZED MAXIMA

TR0001.Pi.2

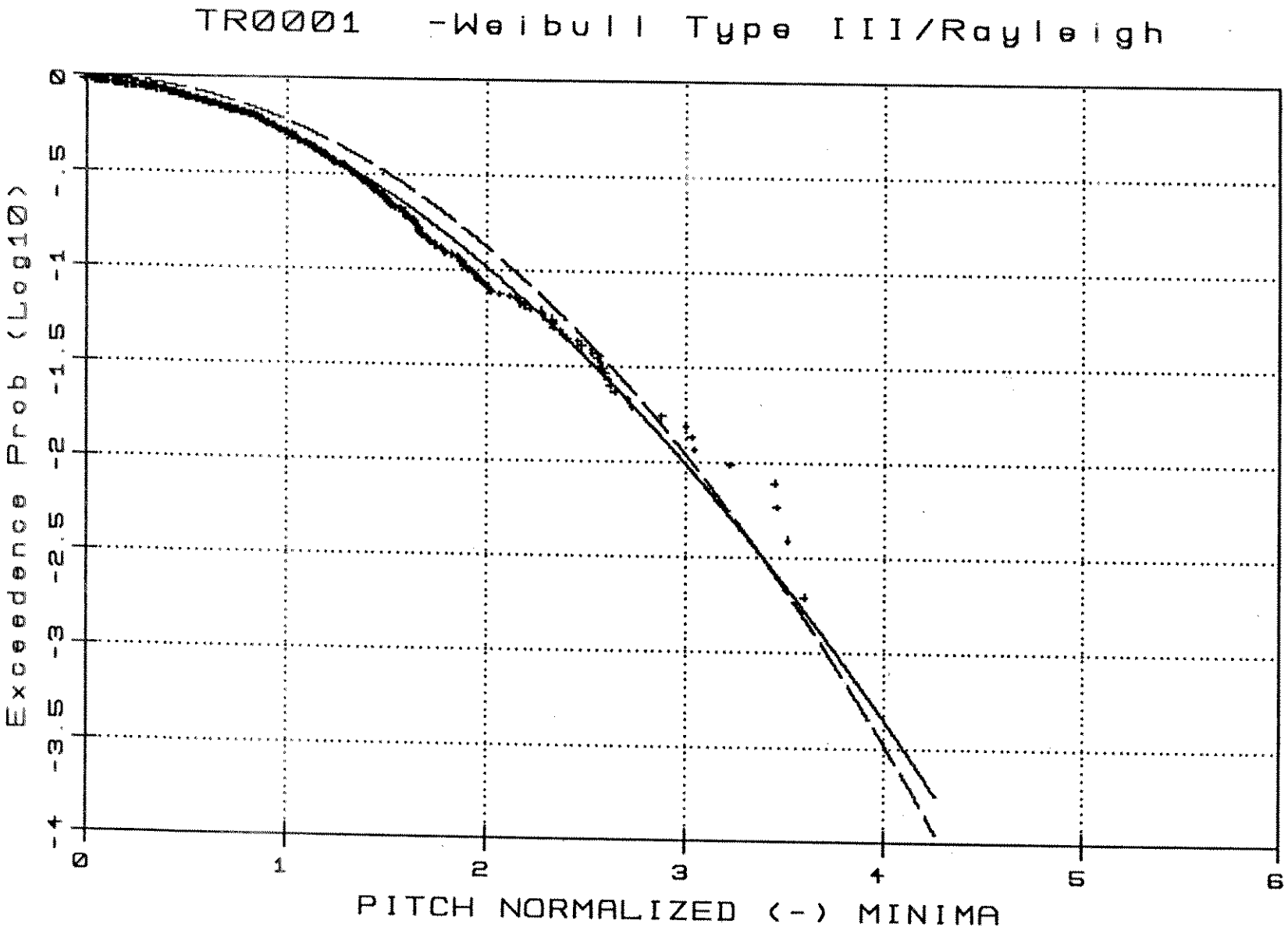
TR0001 -Weibull Type III/Rayleigh
Exceedence Prob (Log10)
0
-.5
-1
-1.5
-2
-2.5
-3
-3.5
-4
0
1
2
3
4
5
6
PITCH NORMALIZED (-) MINIMA

STR0001.Pi.3

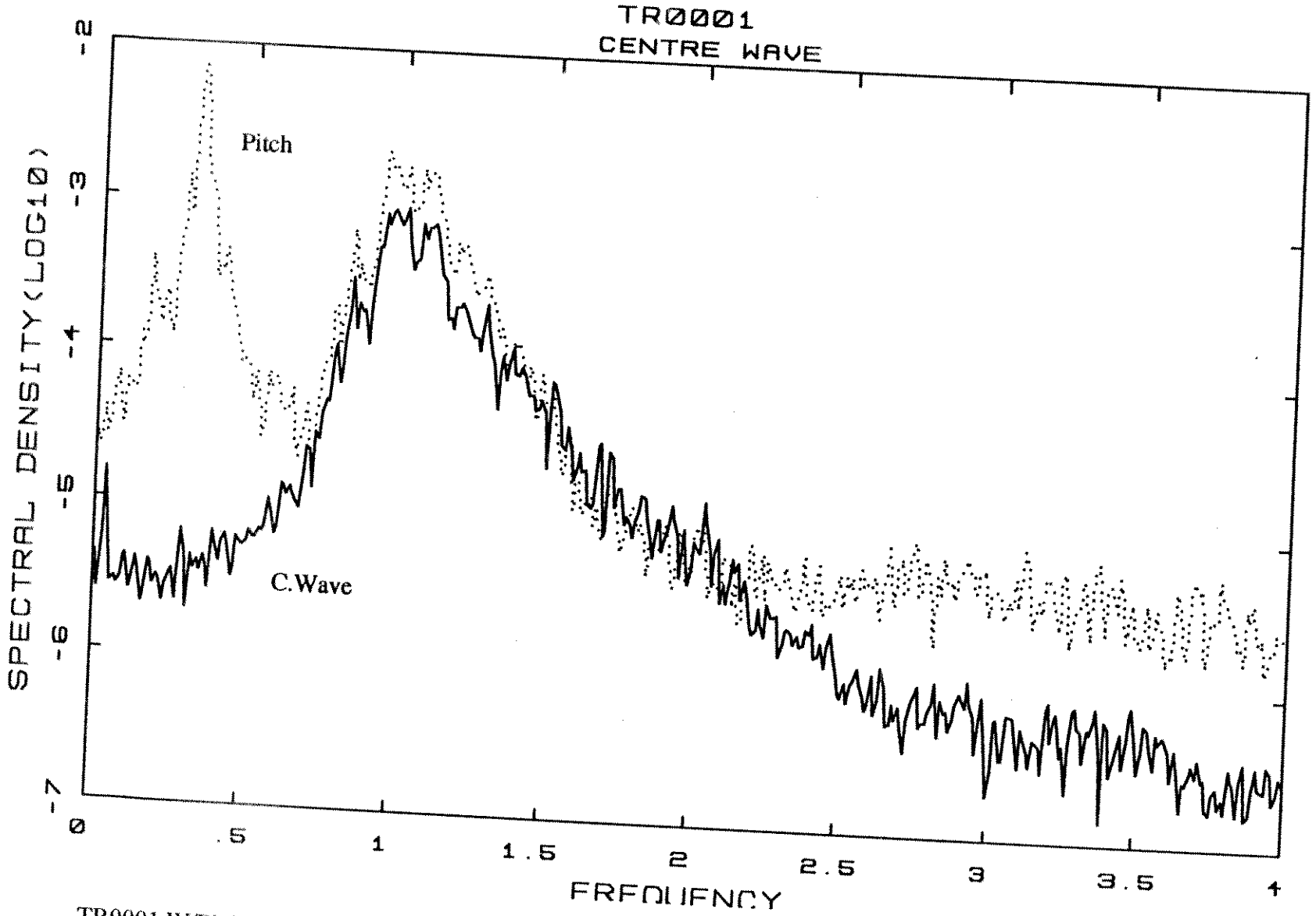
TR0001
CENTRE WAVE
Pitch
C.Wave
SPECTRAL DENSITY(LOG10)
-2
-3
-4
-5
-6
-7
0
.5
1
1.5
2
2.5
3
3.5
4
FREQUENCY

TR0001.W/Pi.4

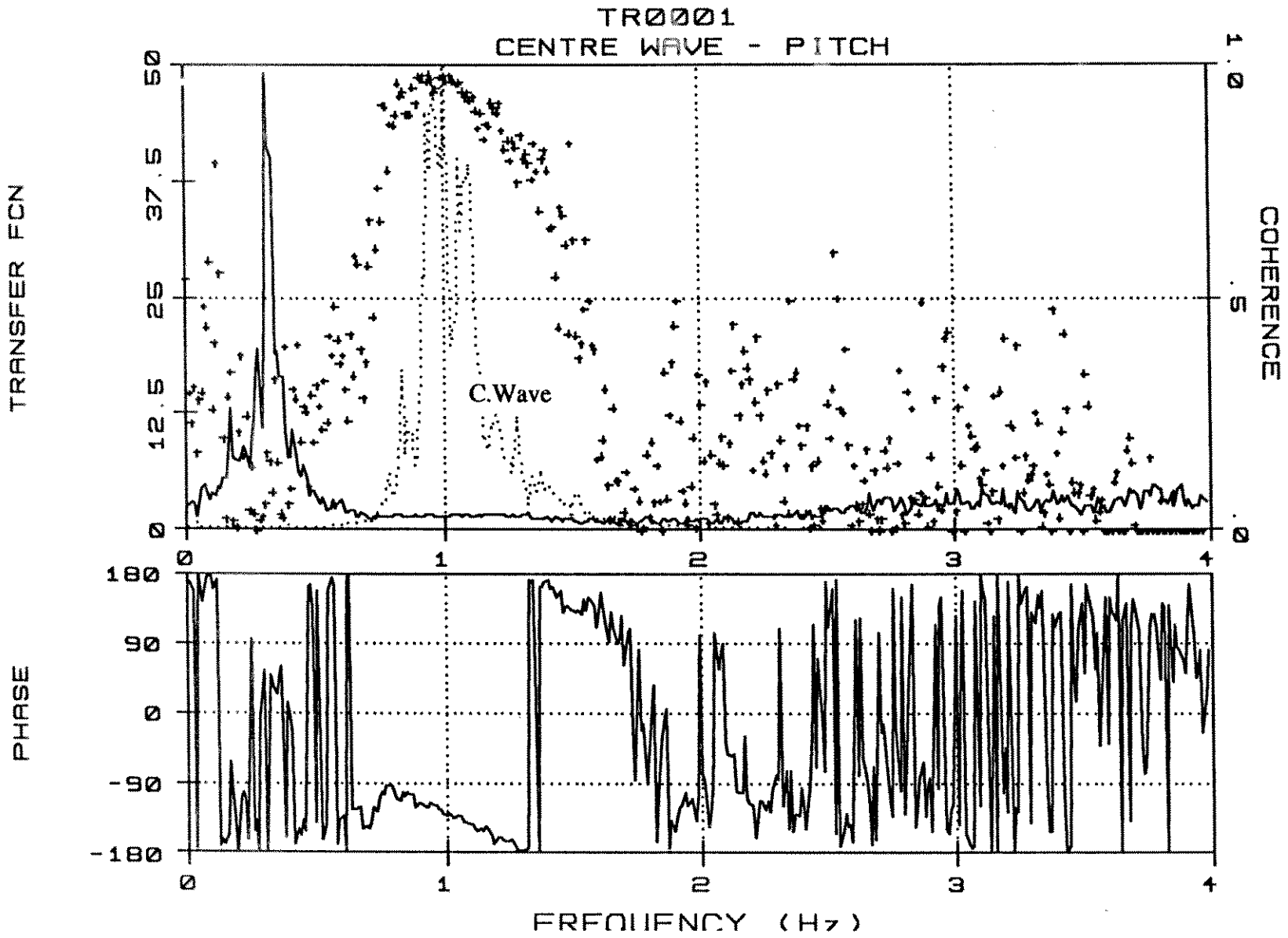

TR0001.W/Pi.4t

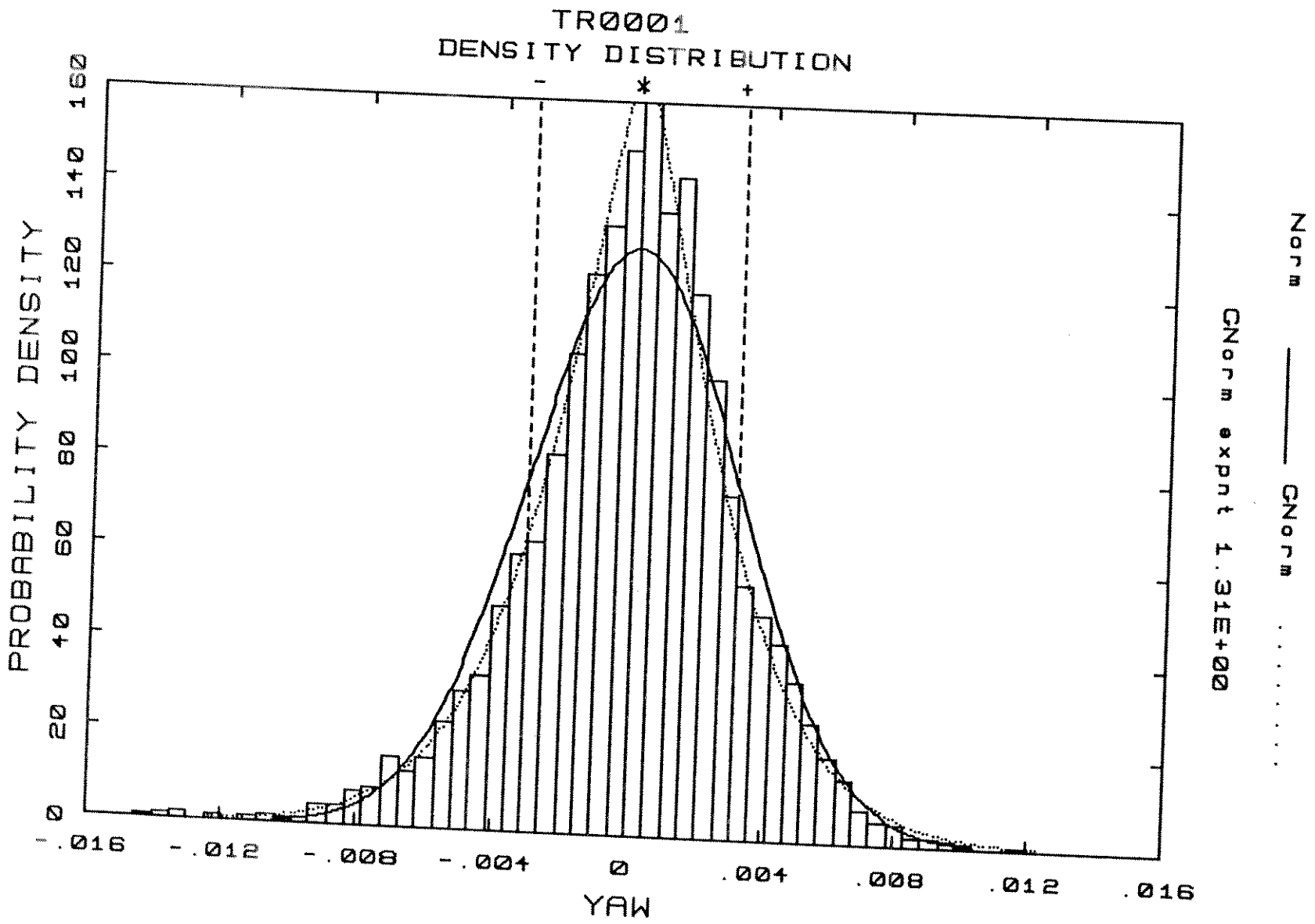
TR0001
DENSITY DISTRIBUTION
PROBABILITY DENSITY
0
20
40
60
80
100
120
140
160
-.016
-.012
-.008
-.004
0
.004
.008
.012
.016
YAW
CNorm expnt 1.31E+00
Norm
CNorm

TR0001.Y.1

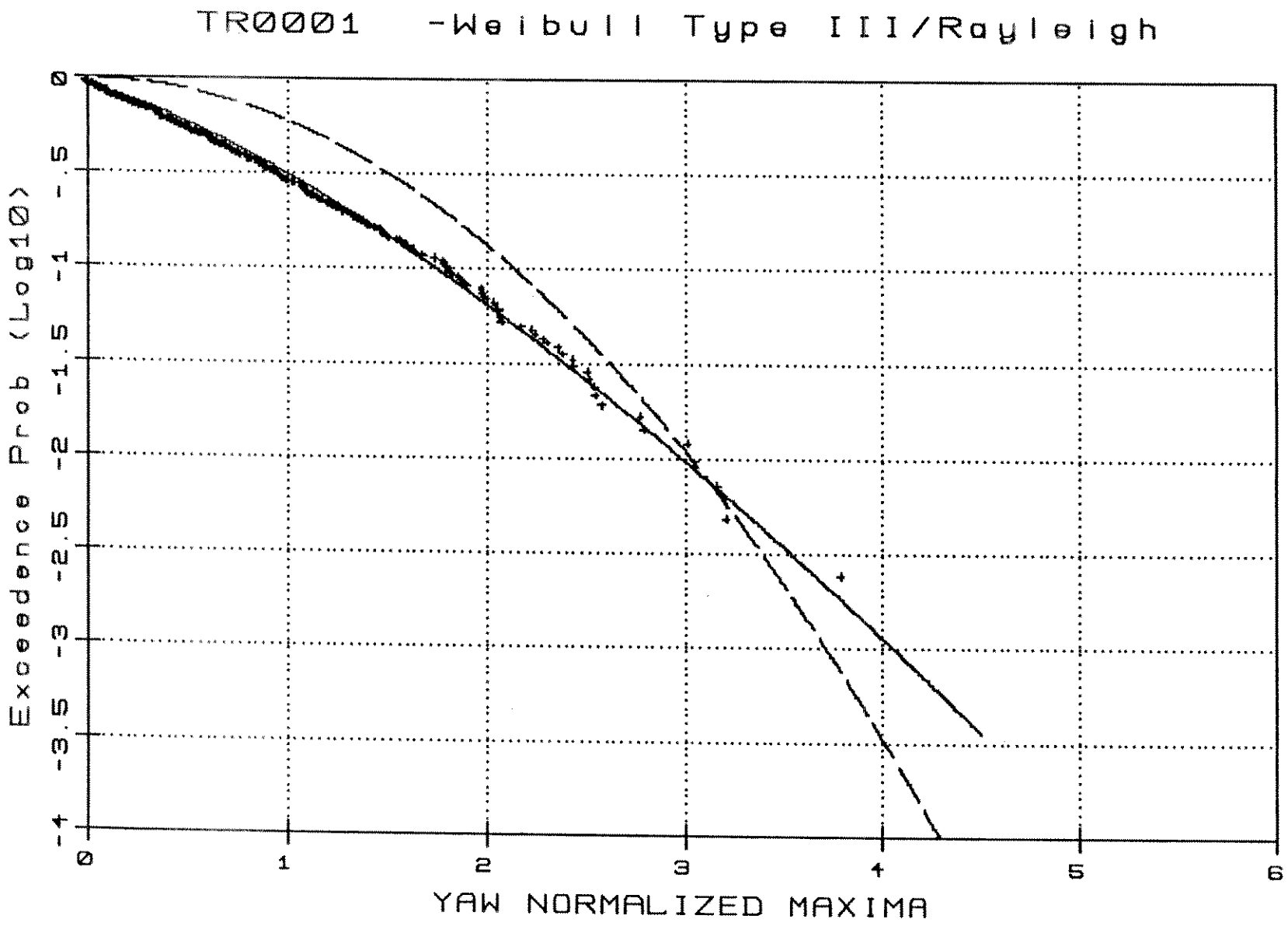
TR0001 -Weibull Type III/Rayleigh
Exceedence Prob (Log10)
0
-.5
-1
-1.5
-2
-2.5
-3
-3.5
-4
0
1
2
3
4
5
6
YAW NORMALIZED MAXIMA

TR0001.Y.2

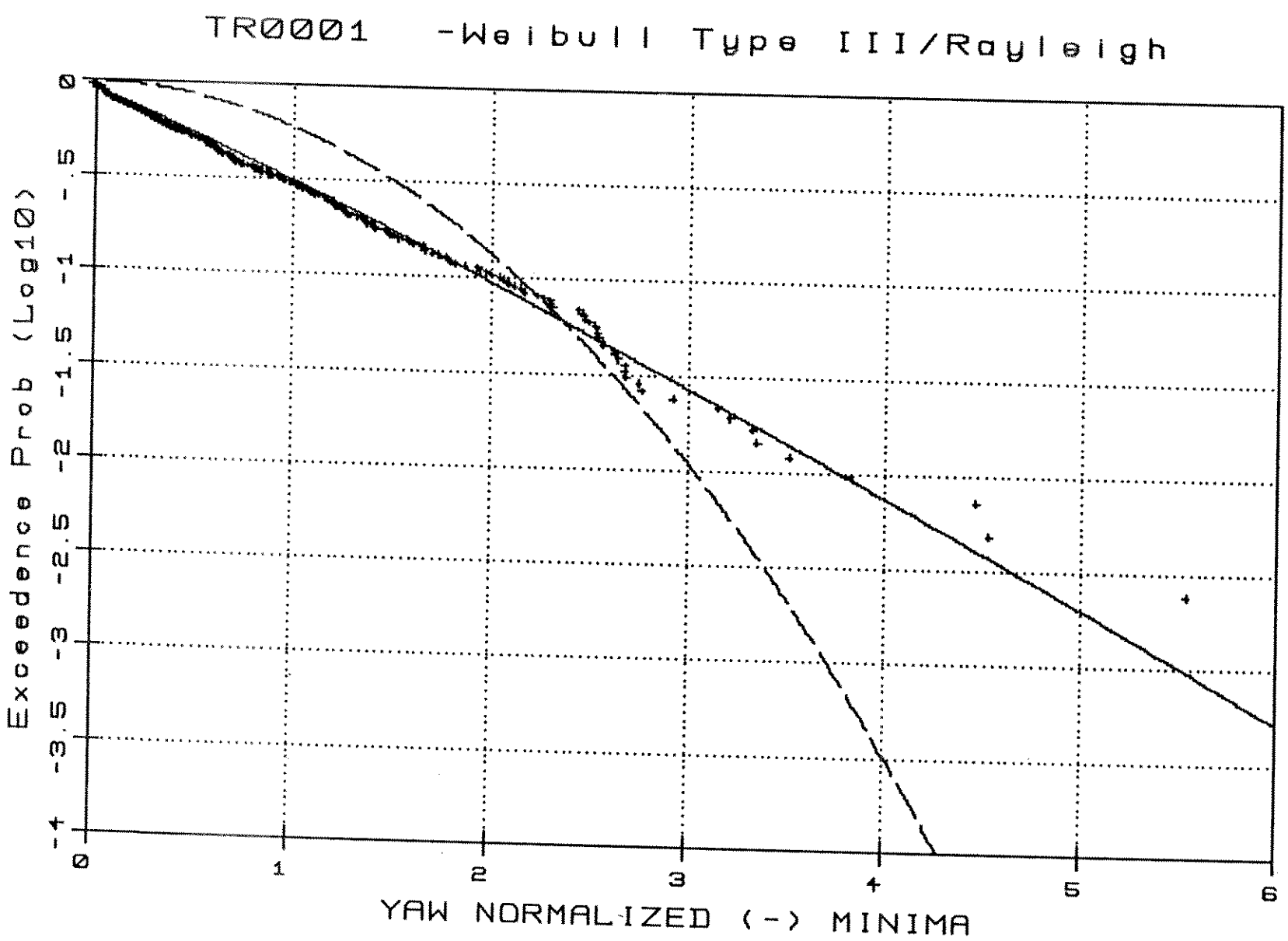
TR0001 -Weibull Type III/Rayleigh
Exceedence Prob (Log10)
0
-.5
-1
-1.5
-2
-2.5
-3
-3.5
-4
0
1
2
3
4
5
6
YAW NORMALIZED (-) MINIMA

TR0001.Y.3

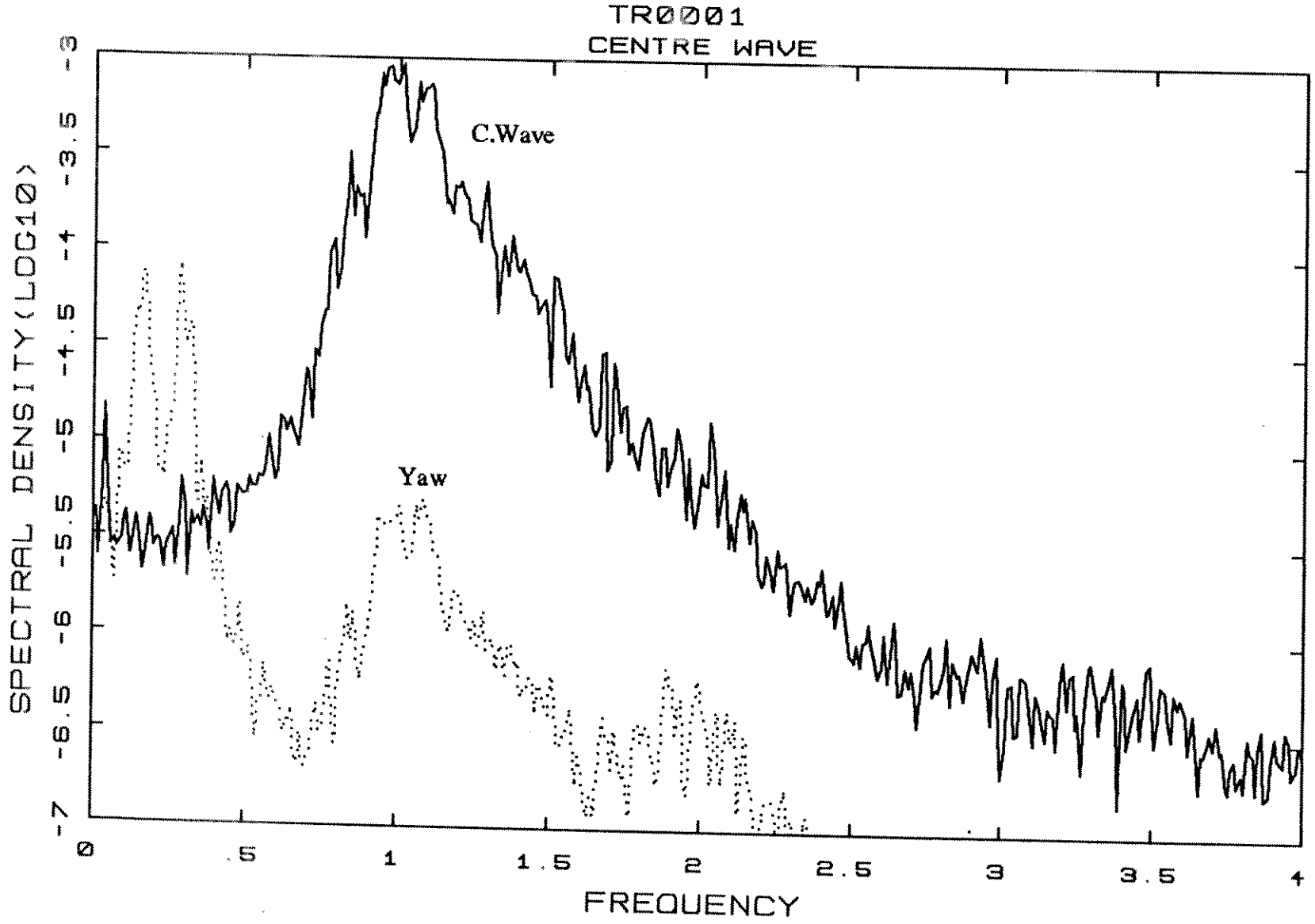
TR0001
CENTRE WAVE
C.Wave
Yaw
SPECTRAL DENSITY(LOG10)
-3
-3.5
-4
-4.5
-5
-5.5
-6
-6.5
-7
0
.5
1
1.5
2
2.5
3
3.5
4
FREQUENCY

TR0001.W/Y.4

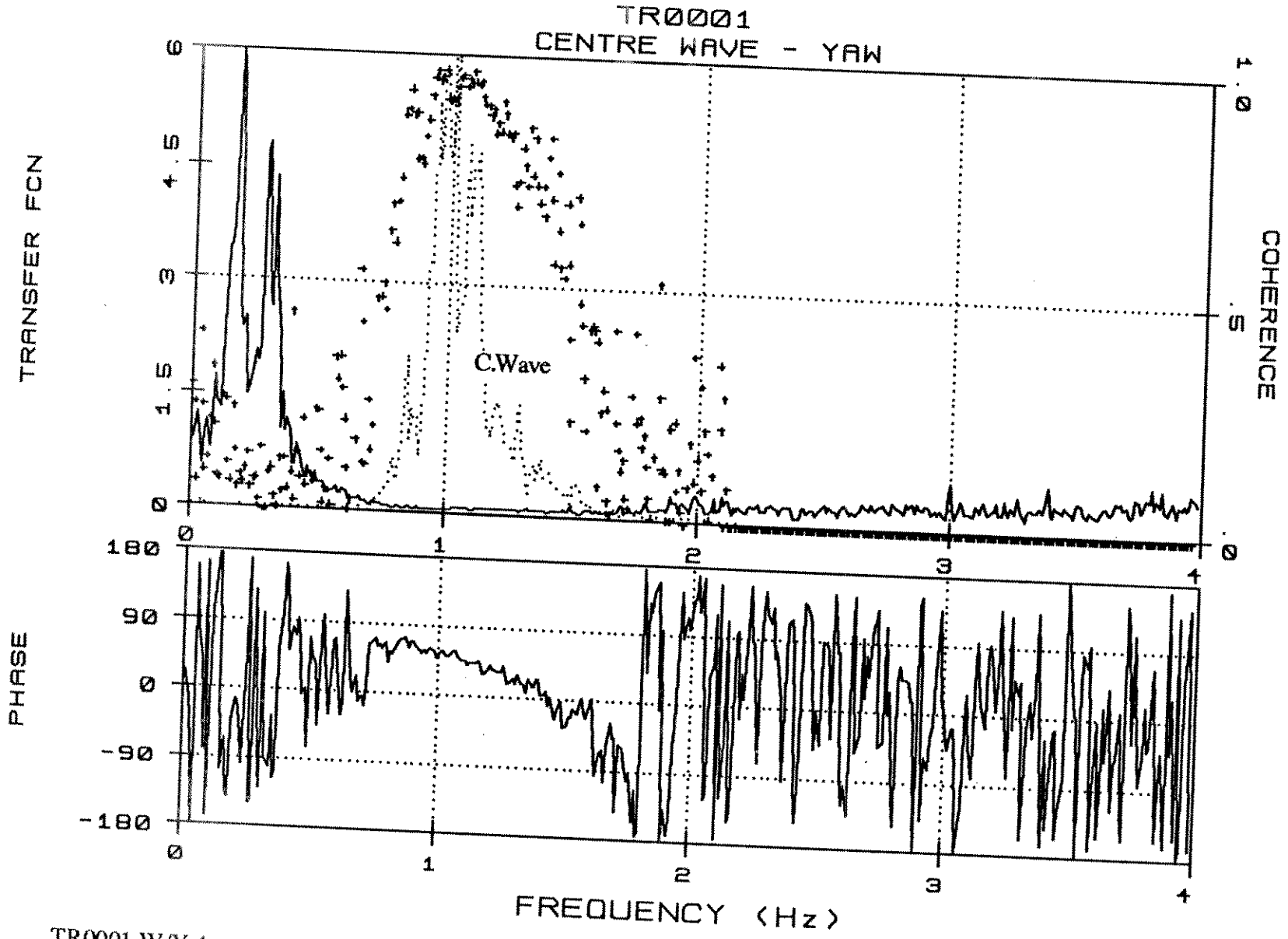
TR0001
CENTRE WAVE - YAW
TRANSFER FCN
COHERENCE
C.Wave
PHASE
FREQUENCY (Hz)
6
4.5
3
1.5
0
1.0
.5
0
180
90
0
-90
-180
0
1
2
3
4

TR0001.W/Y.4t

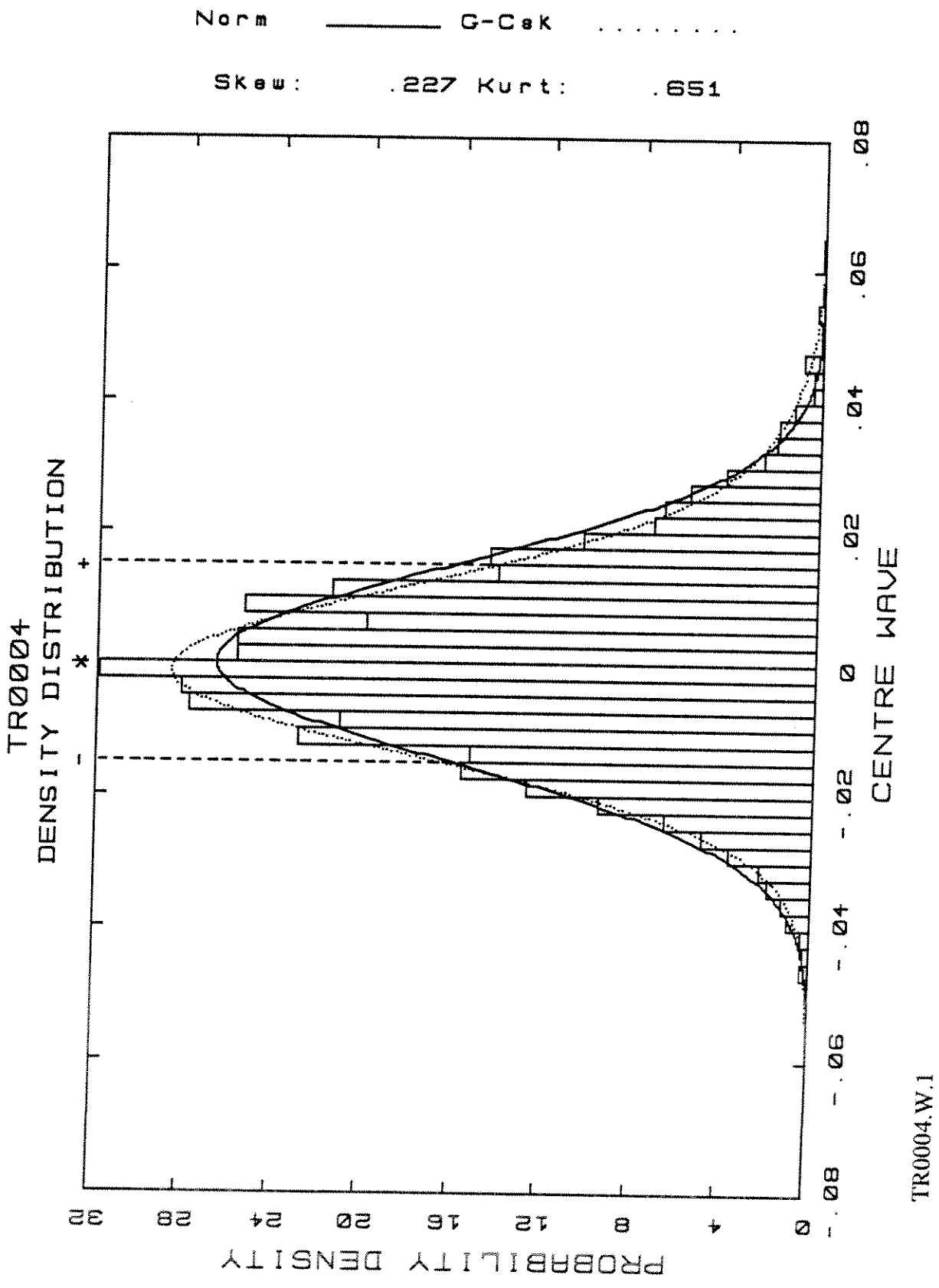
Norm
G-Cek
Skew: .227 Kurt: .651
TR0004
DENSITY DISTRIBUTION
+
*
-
PROBABILITY DENSITY
0
4
8
12
16
20
24
28
32
-.08
-.06
-.04
-.02
0
.02
.04
.06
.08
CENTRE WAVE

TR0004.W.1

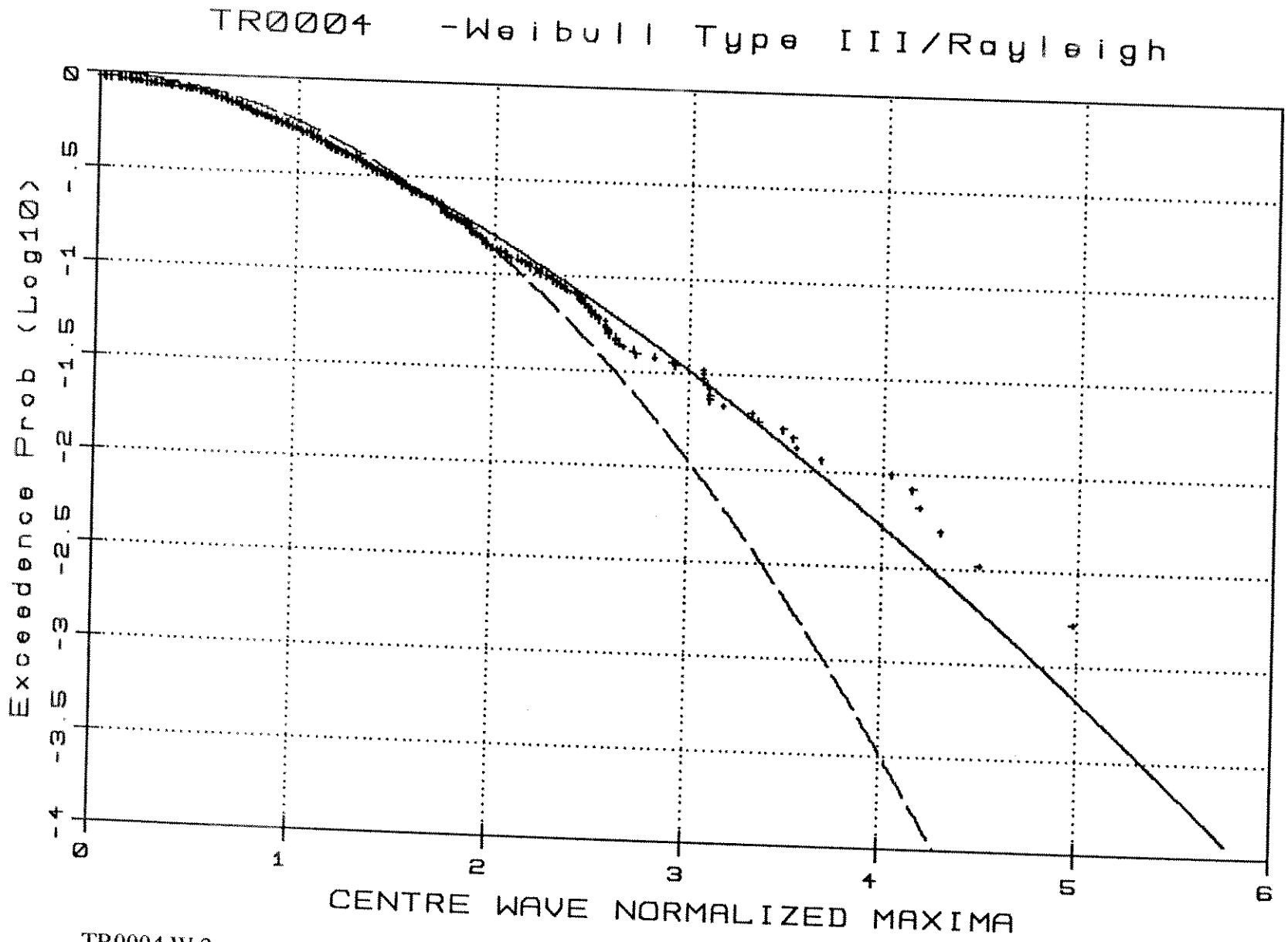
TR0004 -Weibull Type III/Rayleigh
Exceedence Prob (Log10)
0
-.5
-1
-1.5
-2
-2.5
-3
-3.5
-4
0
1
2
3
4
5
6
CENTRE WAVE NORMALIZED MAXIMA

TR0004.W.2

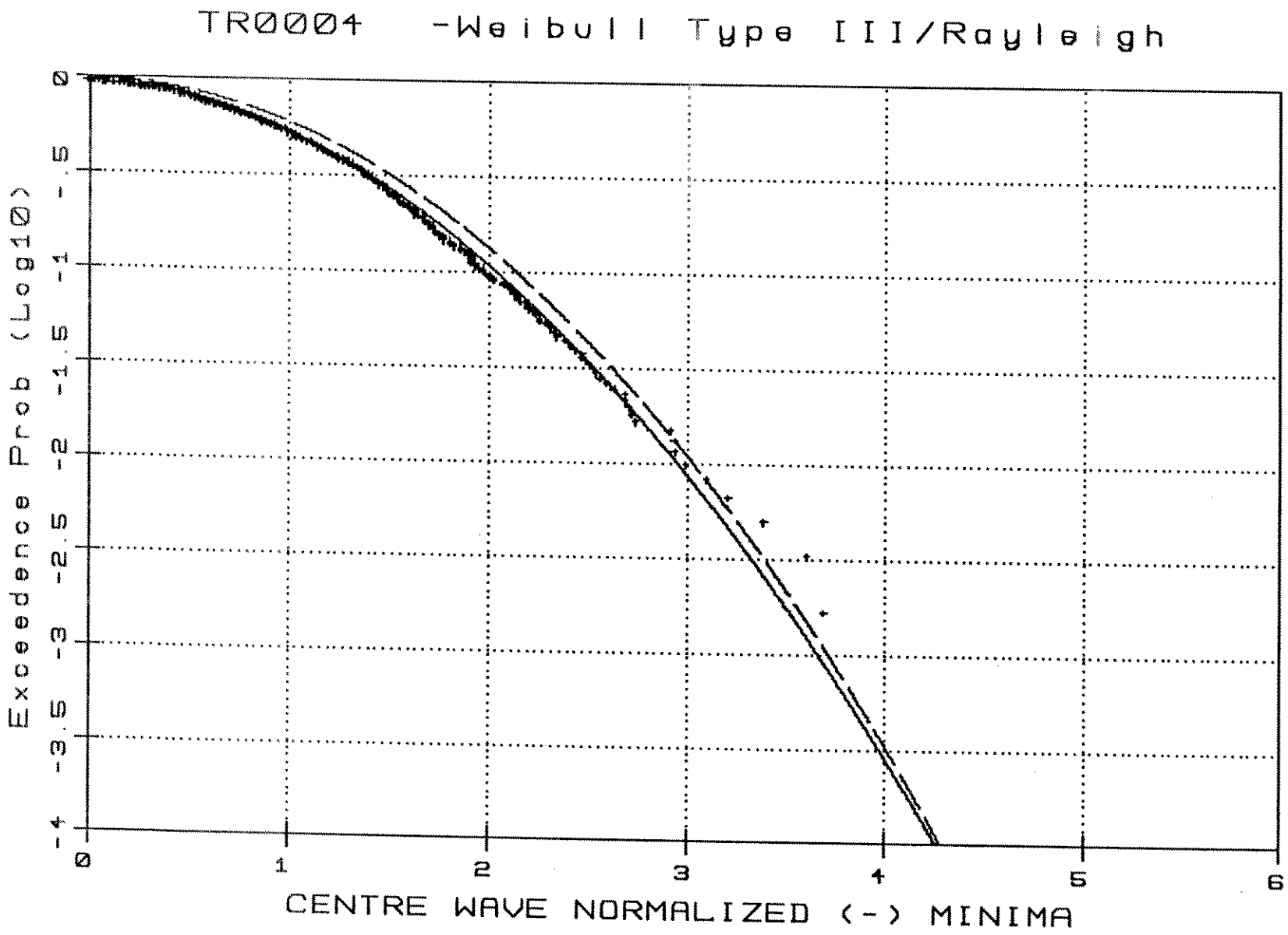
TR0004 -Weibull Type III/Rayleigh
Exceedence Prob (Log10)
0
-.5
-1
-1.5
-2
-2.5
-3
-3.5
-4
0
1
2
3
4
5
6
CENTRE WAVE NORMALIZED (-) MINIMA

TR0004.W.3

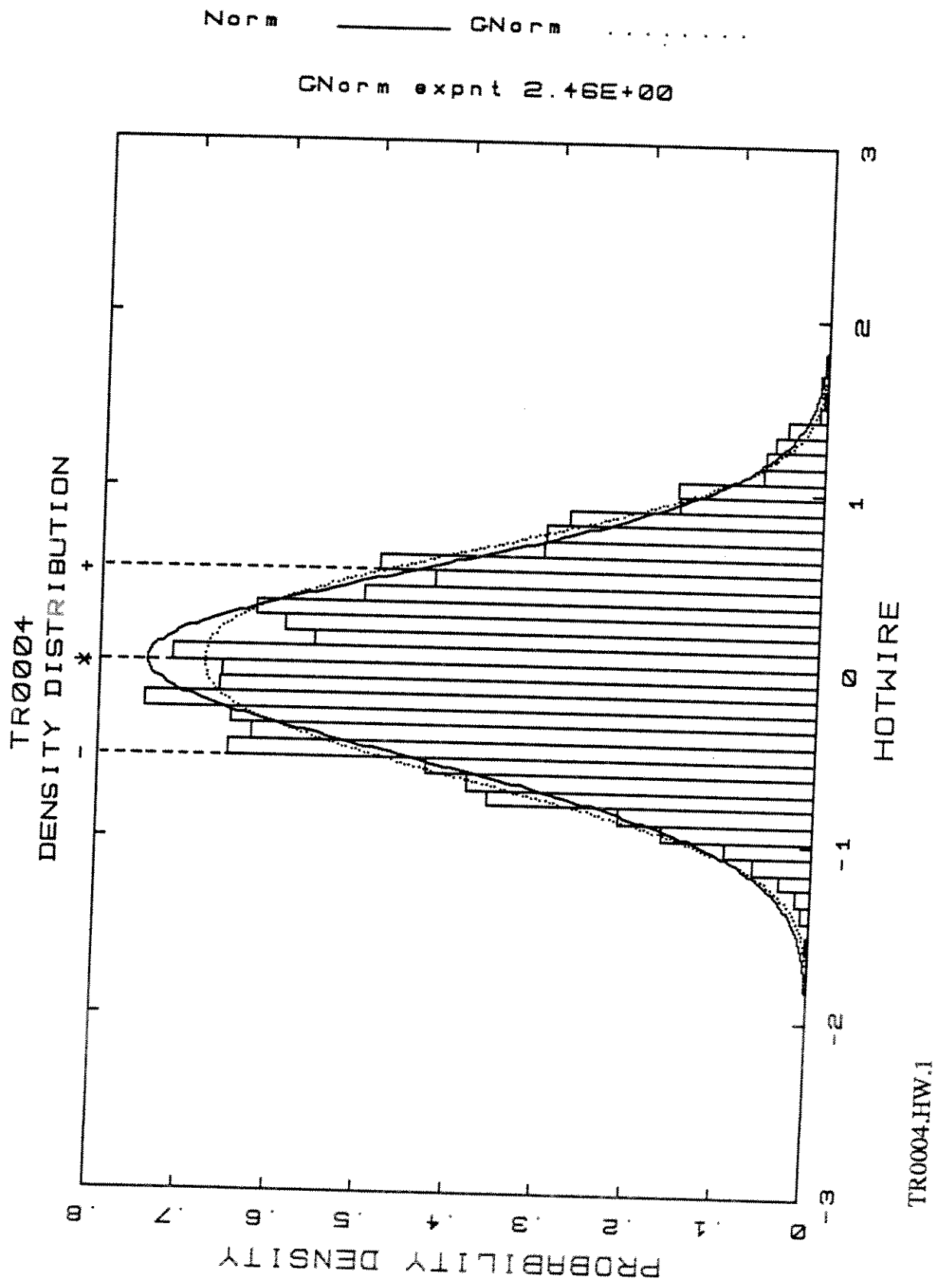
Norm ——— CNorm .....
CNorm expnt 2.46E+00
TR0004
DENSITY DISTRIBUTION
PROBABILITY DENSITY
HOTWIRE
TR0004.HW.1

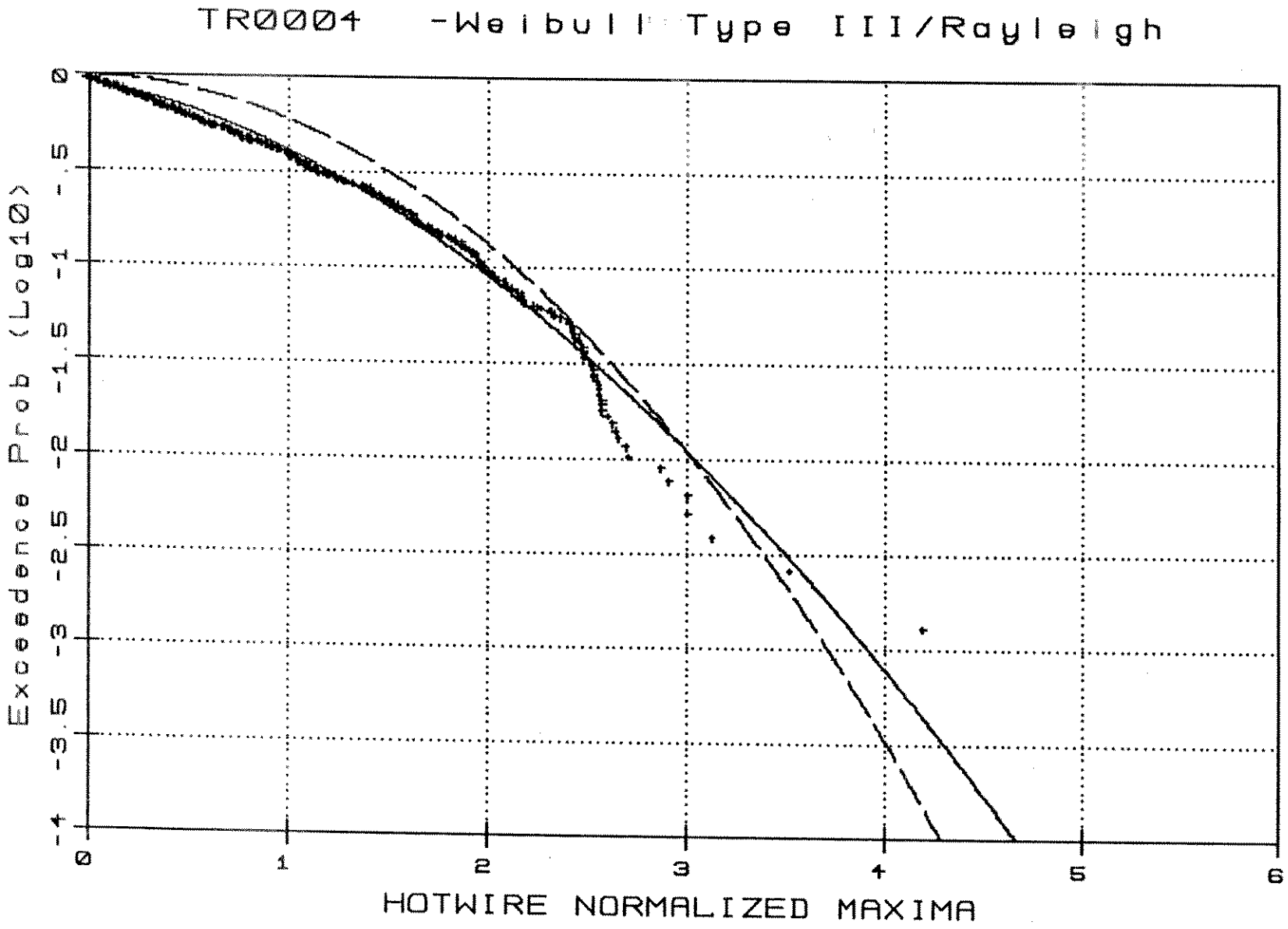
TR0004 -Weibull Type III/Rayleigh
Exceedence Prob (Log10)
0
-.5
-1
-1.5
-2
-2.5
-3
-3.5
-4
0
1
2
3
4
5
6
HOTWIRE NORMALIZED MAXIMA

TR0004.HW.2

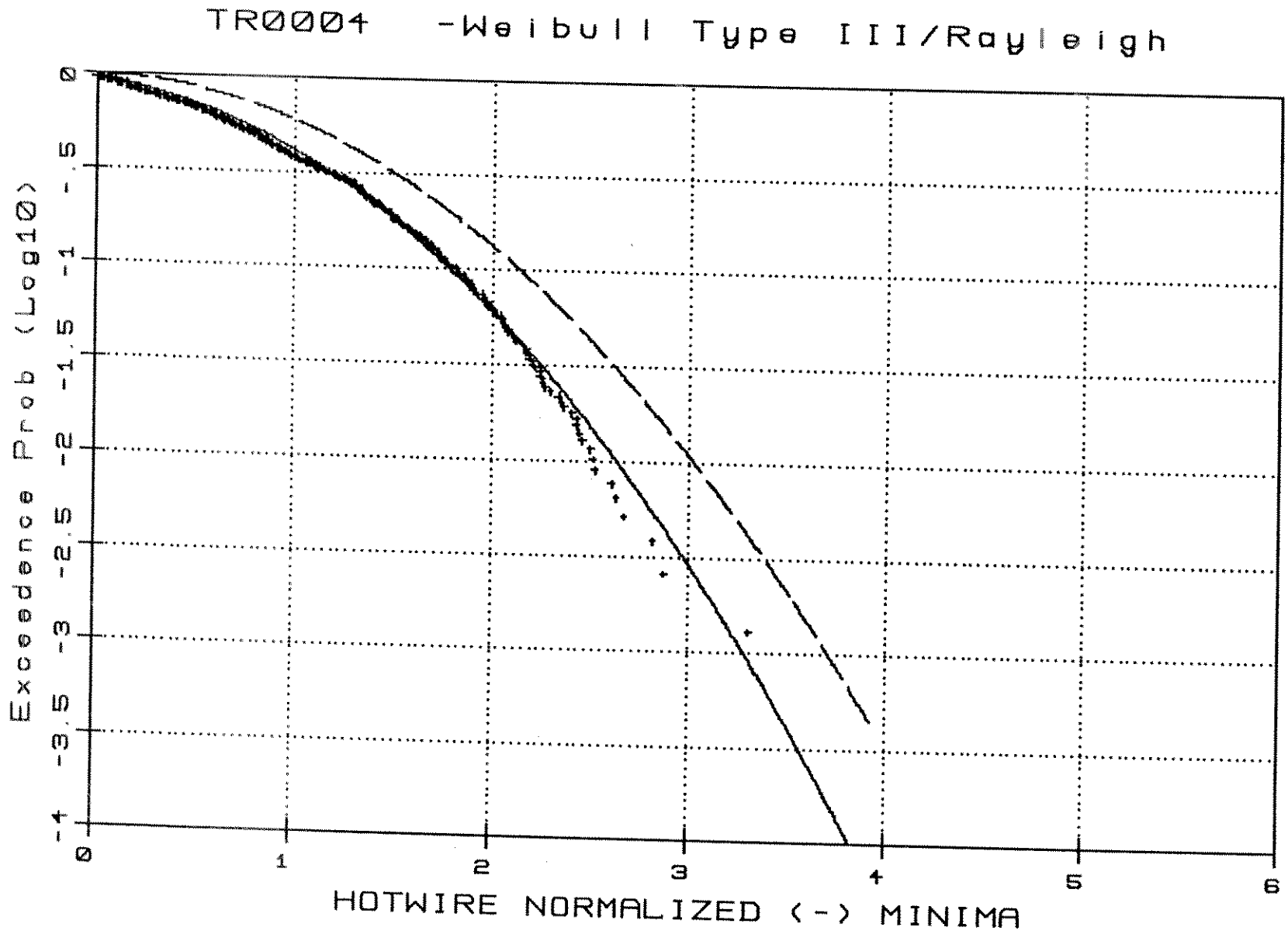
TR0004 -Weibull Type III/Rayleigh
Exceedence Prob (Log10)
0
-.5
-1
-1.5
-2
-2.5
-3
-3.5
-4
0
1
2
3
4
5
6
HOTWIRE NORMALIZED (-) MINIMA

TR0004.HW.3

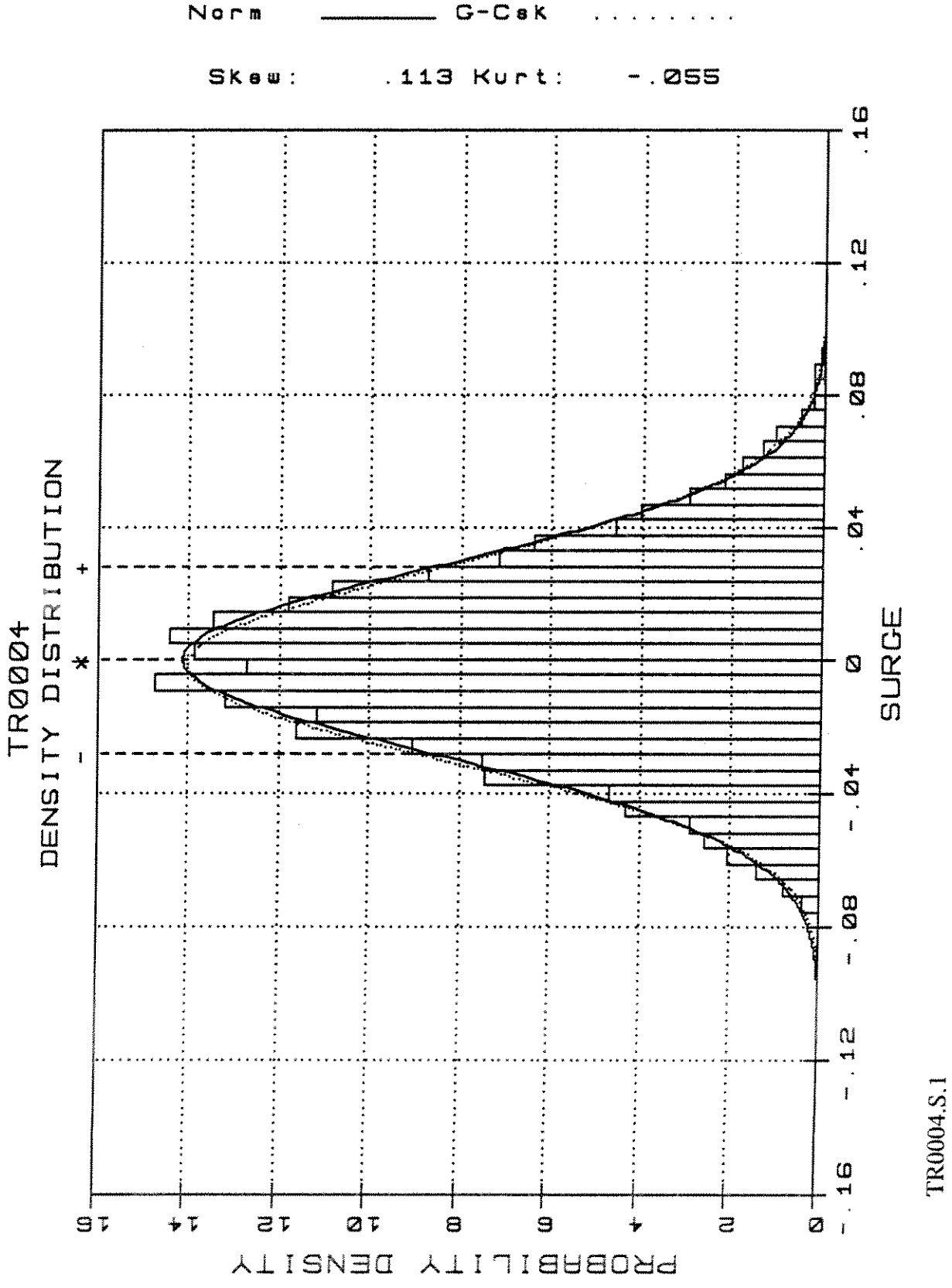
Norm
G-Cak
Skew: .113 Kurt: -.055
TR0004
DENSITY DISTRIBUTION
+
*
-
PROBABILITY DENSITY
0
2
4
6
8
10
12
14
16
-.16
-.12
-.08
-.04
0
.04
.08
.12
.16
SURGE

TR0004.S.1

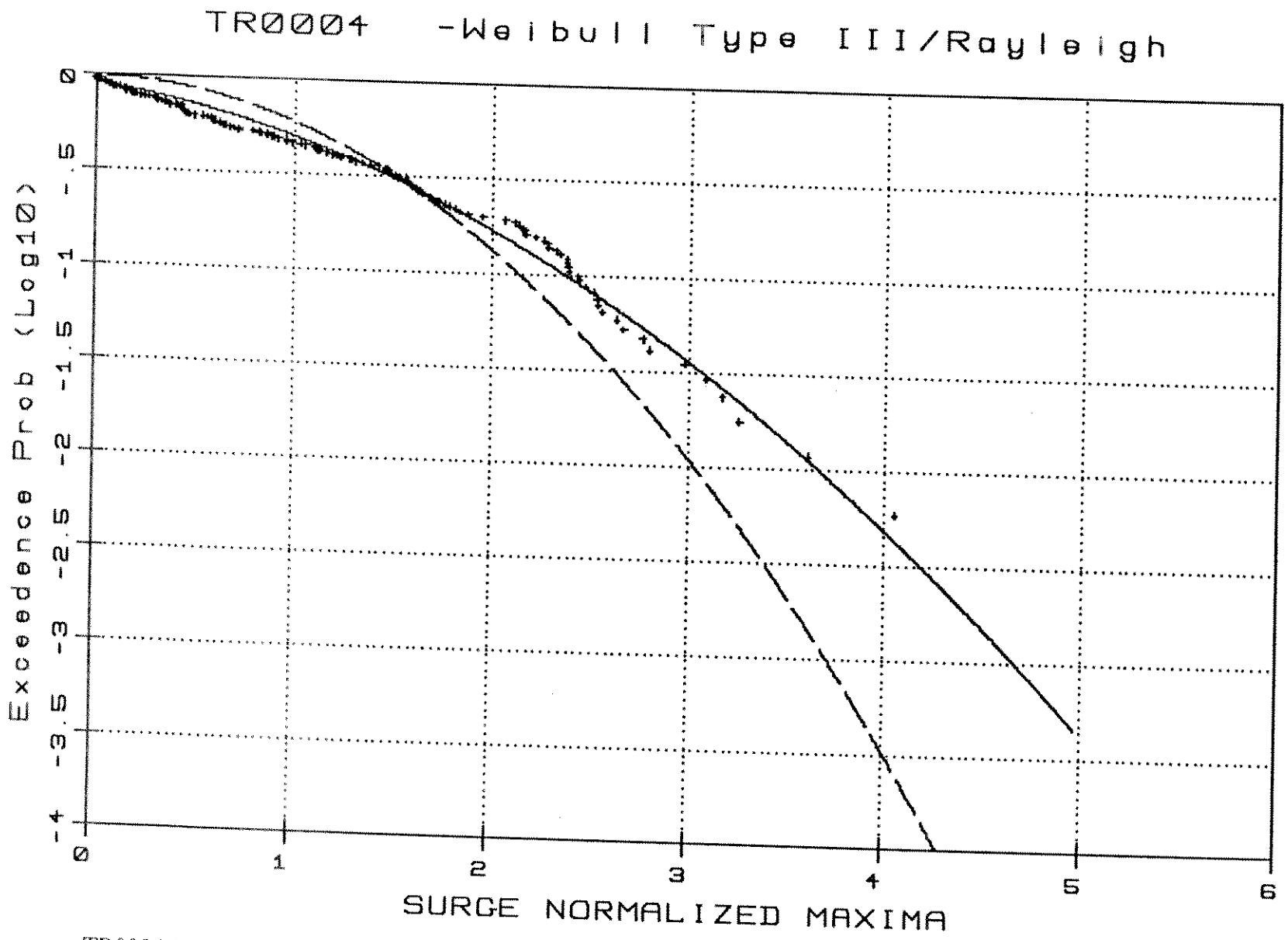
TR0004 -Weibull Type III/Rayleigh
Exceedence Prob (Log10)
0
-.5
-1
-1.5
-2
-2.5
-3
-3.5
-4
0
1
2
3
4
5
6
SURGE NORMALIZED MAXIMA

TR0004.S.2

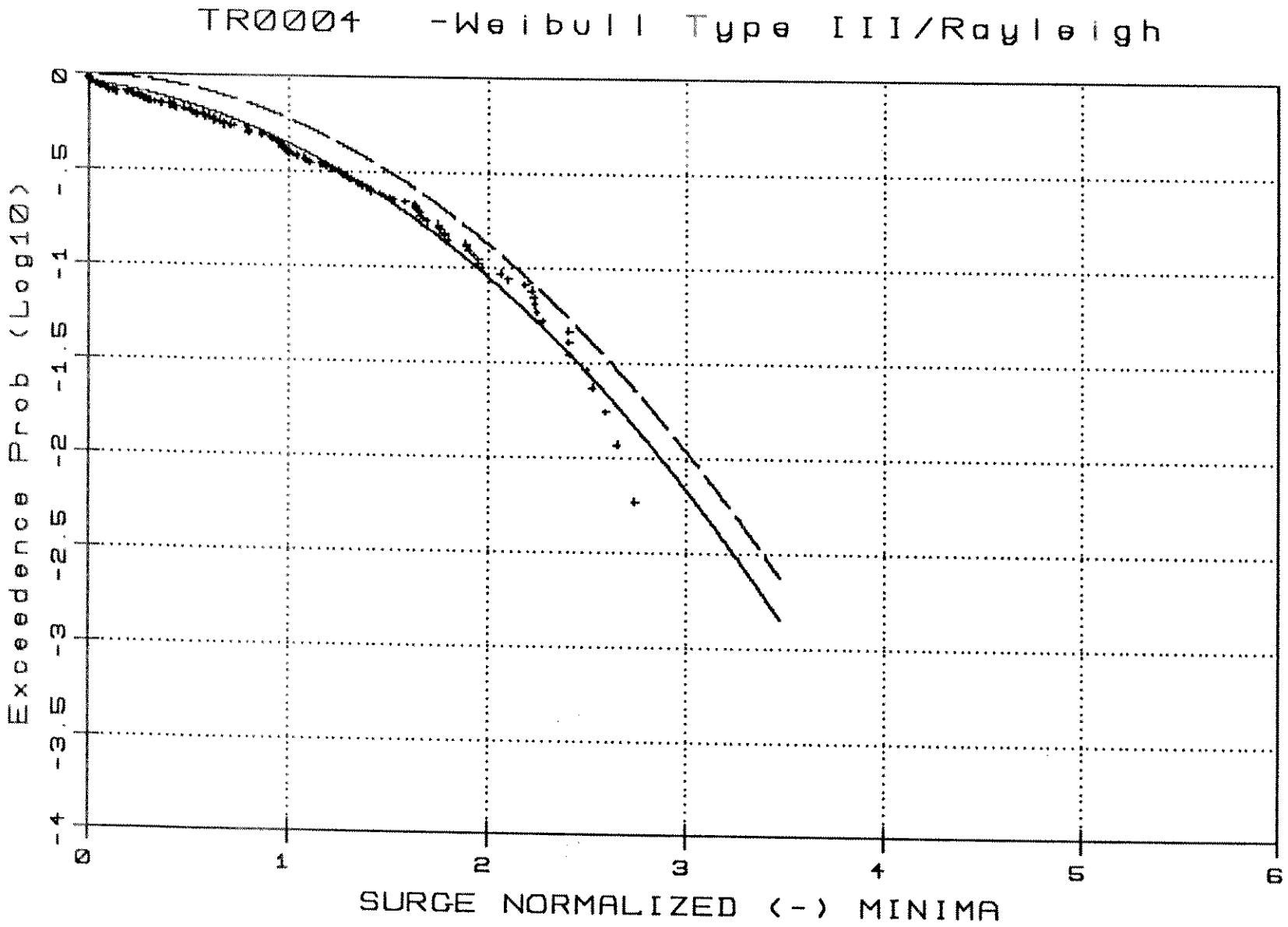
TR0004 -Weibull Type III/Rayleigh
Exceedence Prob (Log10)
0
-.5
-1
-1.5
-2
-2.5
-3
-3.5
-4
0
1
2
3
4
5
6
SURGE NORMALIZED (-) MINIMA

TR0004.S.3

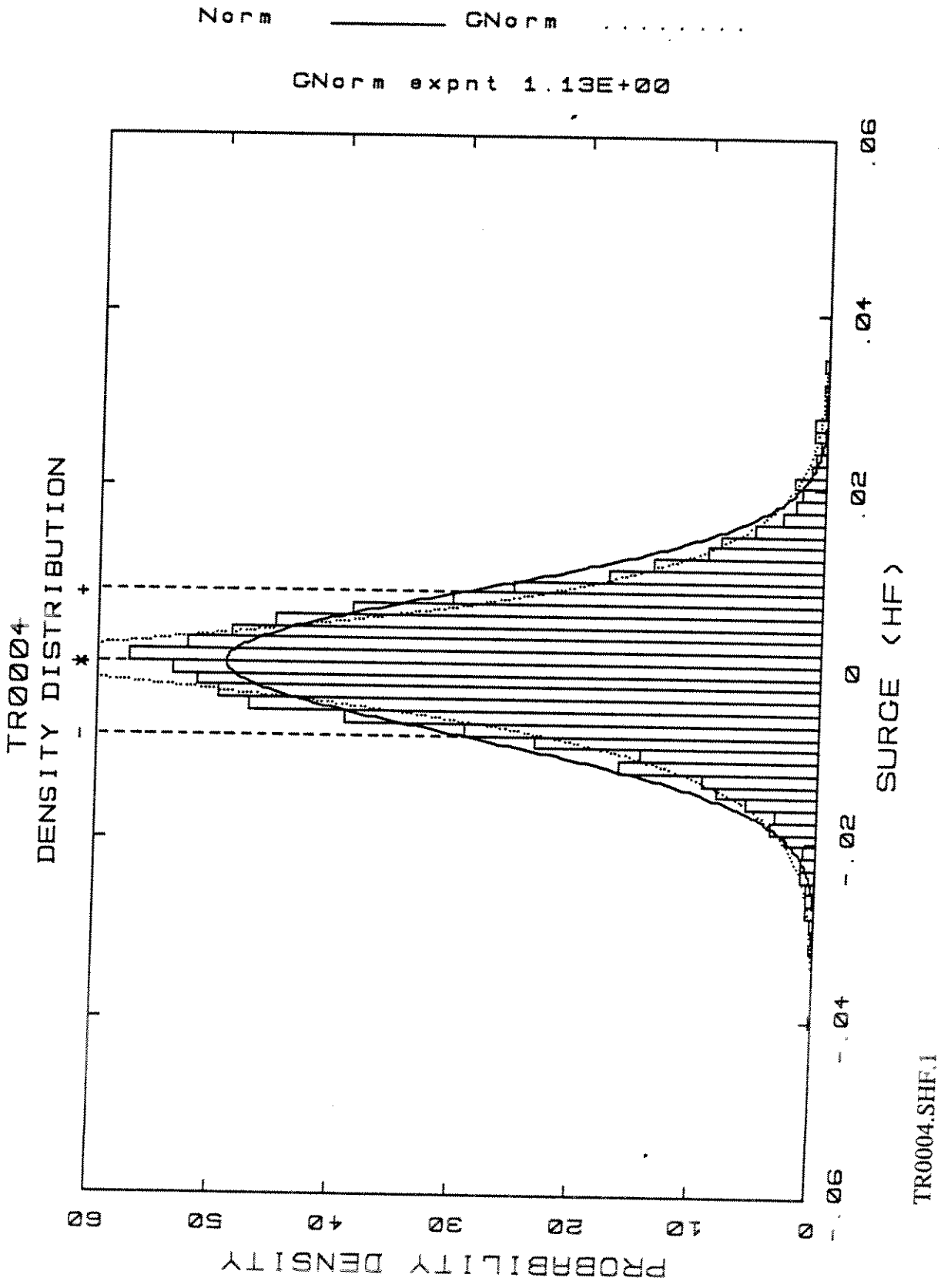
Norm
GNorm
GNorm expnt 1.13E+00
TR0004
DENSITY DISTRIBUTION
PROBABILITY DENSITY
SURGE (HF)
0
10
20
30
40
50
60
.06
.04
.02
0
-.02
-.04
-.06

TR0004.SHF.1

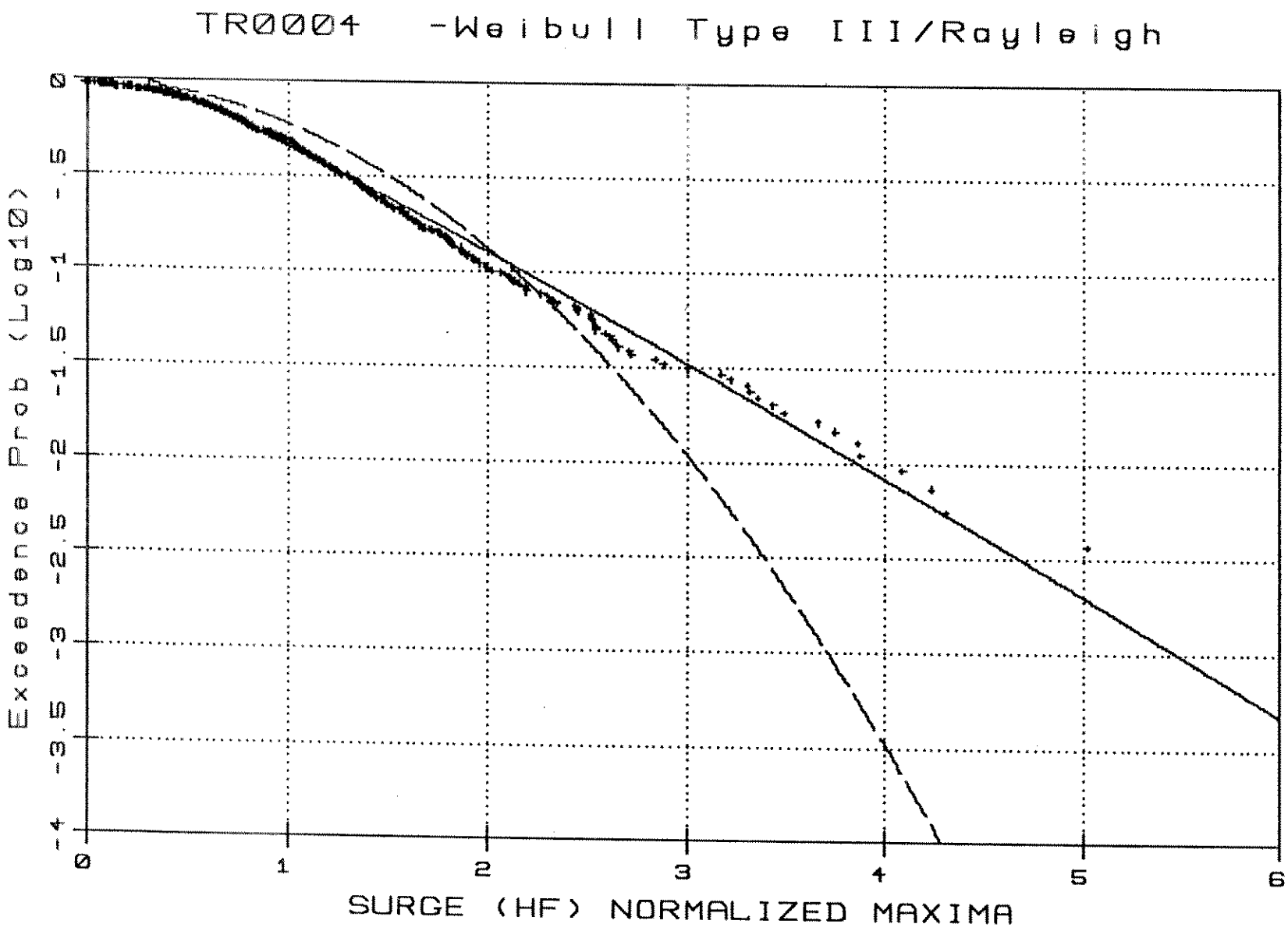
TR0004 -Weibull Type III/Rayleigh
Exceedence Prob (Log10)
0
-.5
-1
-1.5
-2
-2.5
-3
-3.5
-4
0
1
2
3
4
5
6
SURGE (HF) NORMALIZED MAXIMA

TR0004.SHF.2

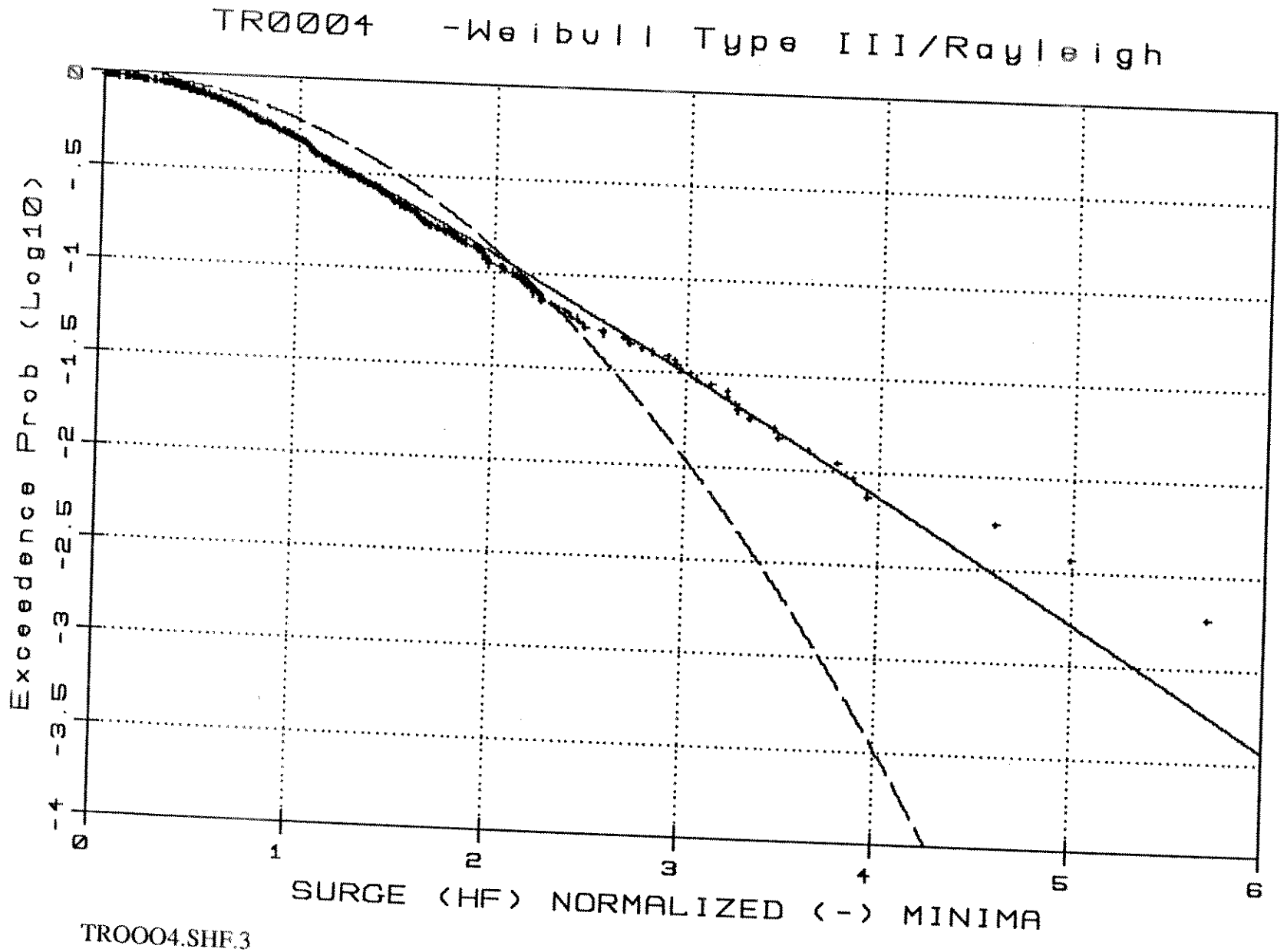
TR0004 -Weibull Type III/Rayleigh
Exceedence Prob (Log10)
0
-.5
-1
-1.5
-2
-2.5
-3
-3.5
-4
0
1
2
3
4
5
6
SURGE (HF) NORMALIZED (-) MINIMA

TROOO4.SHF.3

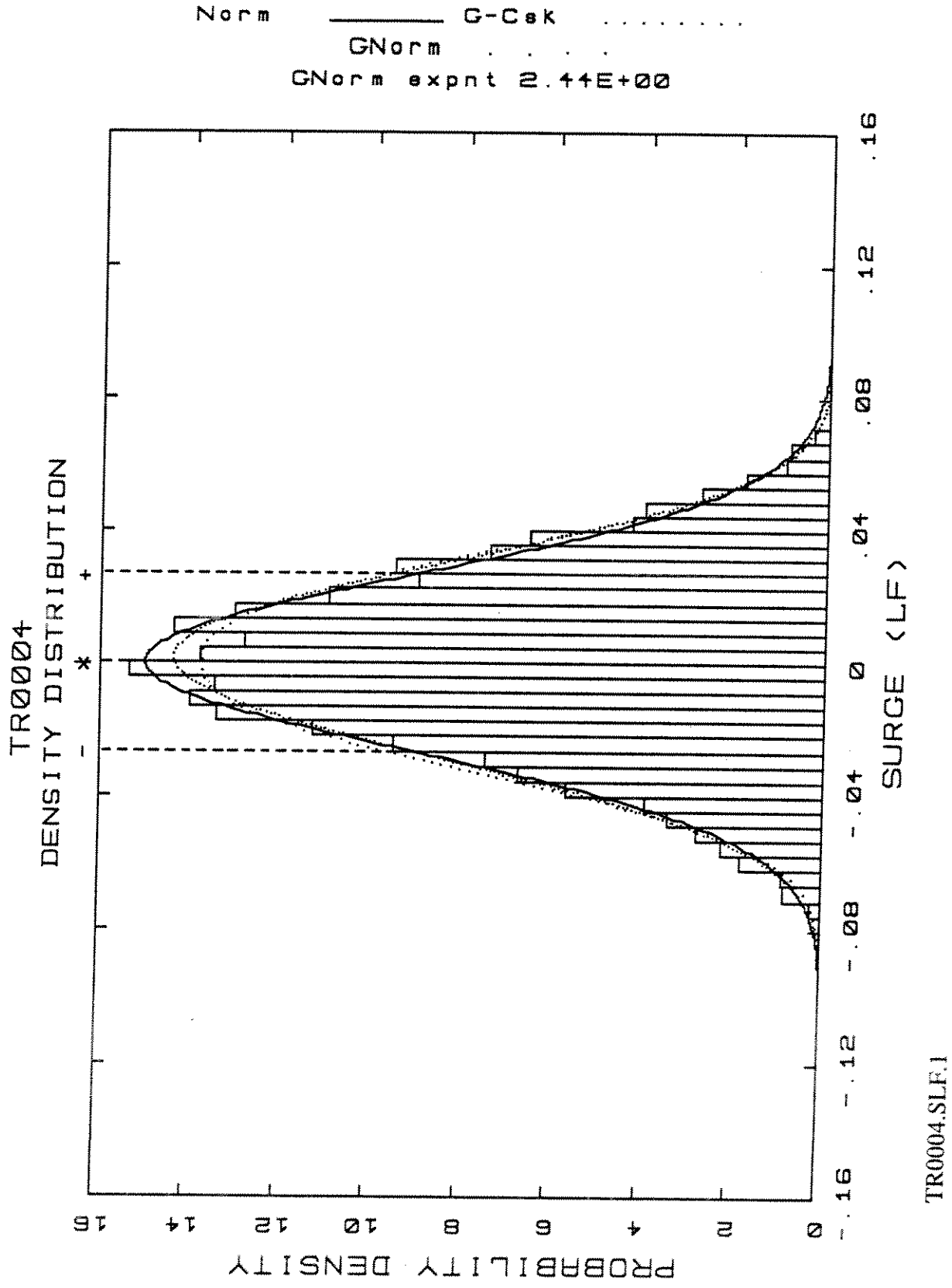
Norm _____ G-Csk .....
GNorm . . . .
GNorm expnt 2.44E+00
TR0004
DENSITY DISTRIBUTION
+
*
-
PROBABILITY DENSITY
0
2
4
6
8
10
12
14
16
SURGE (LF)
.16
.12
.08
.04
0
-.04
-.08
-.12
-.16

TR0004.SLF1

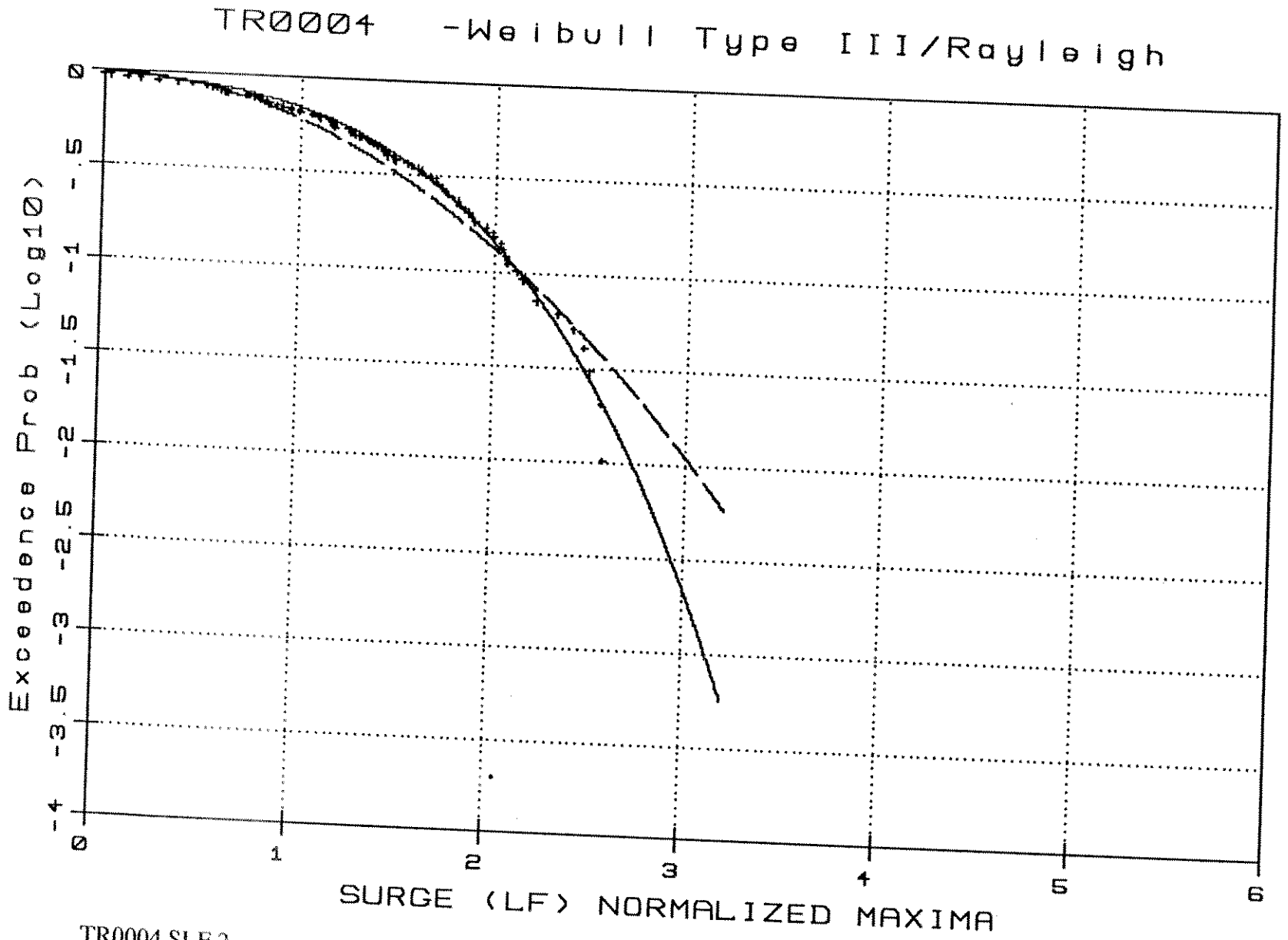
TR0004 -Weibull Type III/Rayleigh
Exceedence Prob (Log10)
0
-.5
-1
-1.5
-2
-2.5
-3
-3.5
-4
0
1
2
3
4
5
6
SURGE (LF) NORMALIZED MAXIMA

TR0004.SLF.2

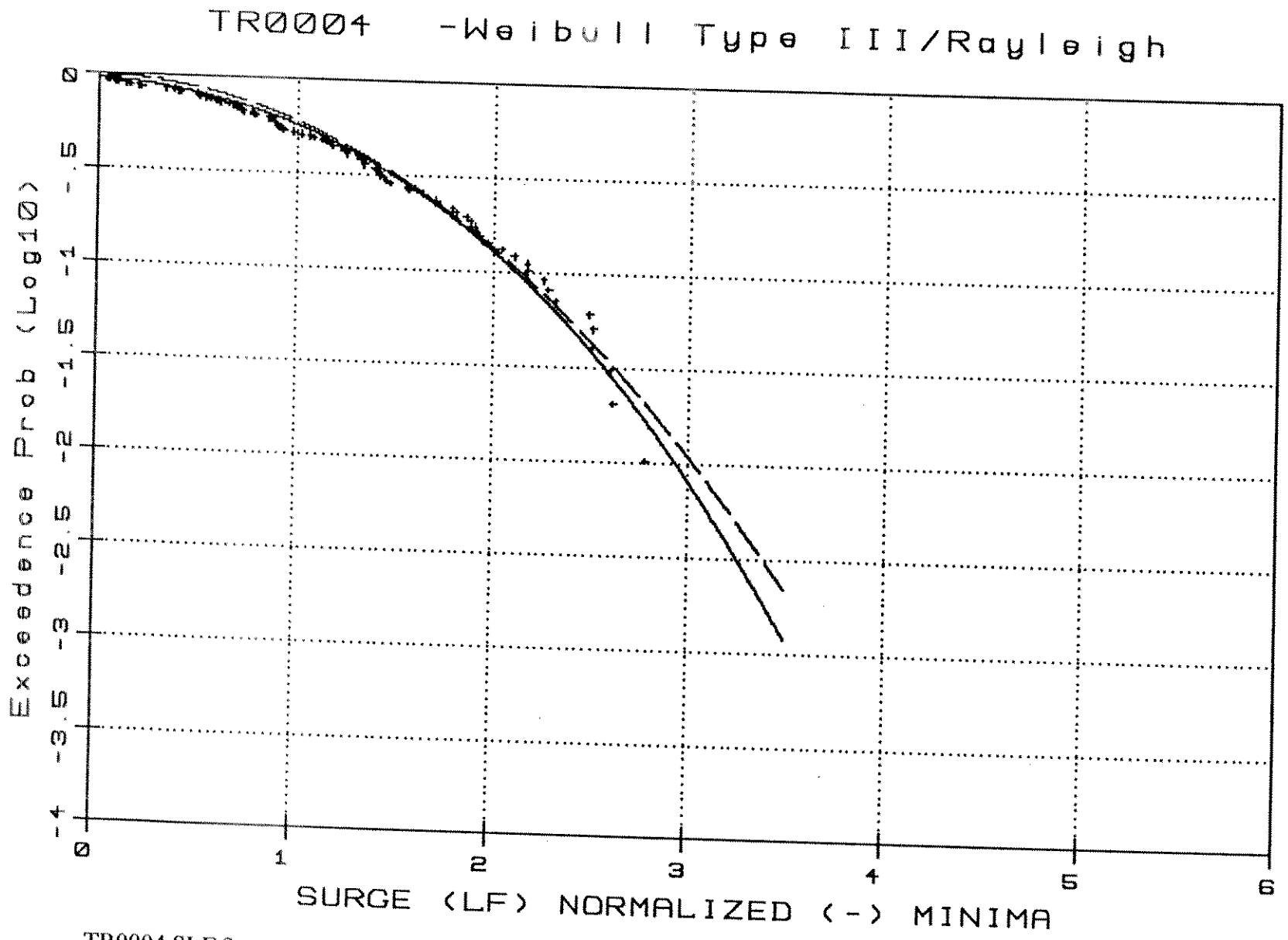
TR0004 -Weibull Type III/Rayleigh
Exceedence Prob (Log10)
0
-.5
-1
-1.5
-2
-2.5
-3
-3.5
-4
0
1
2
3
4
5
6
SURGE (LF) NORMALIZED (-) MINIMA

TR0004.SLF.3

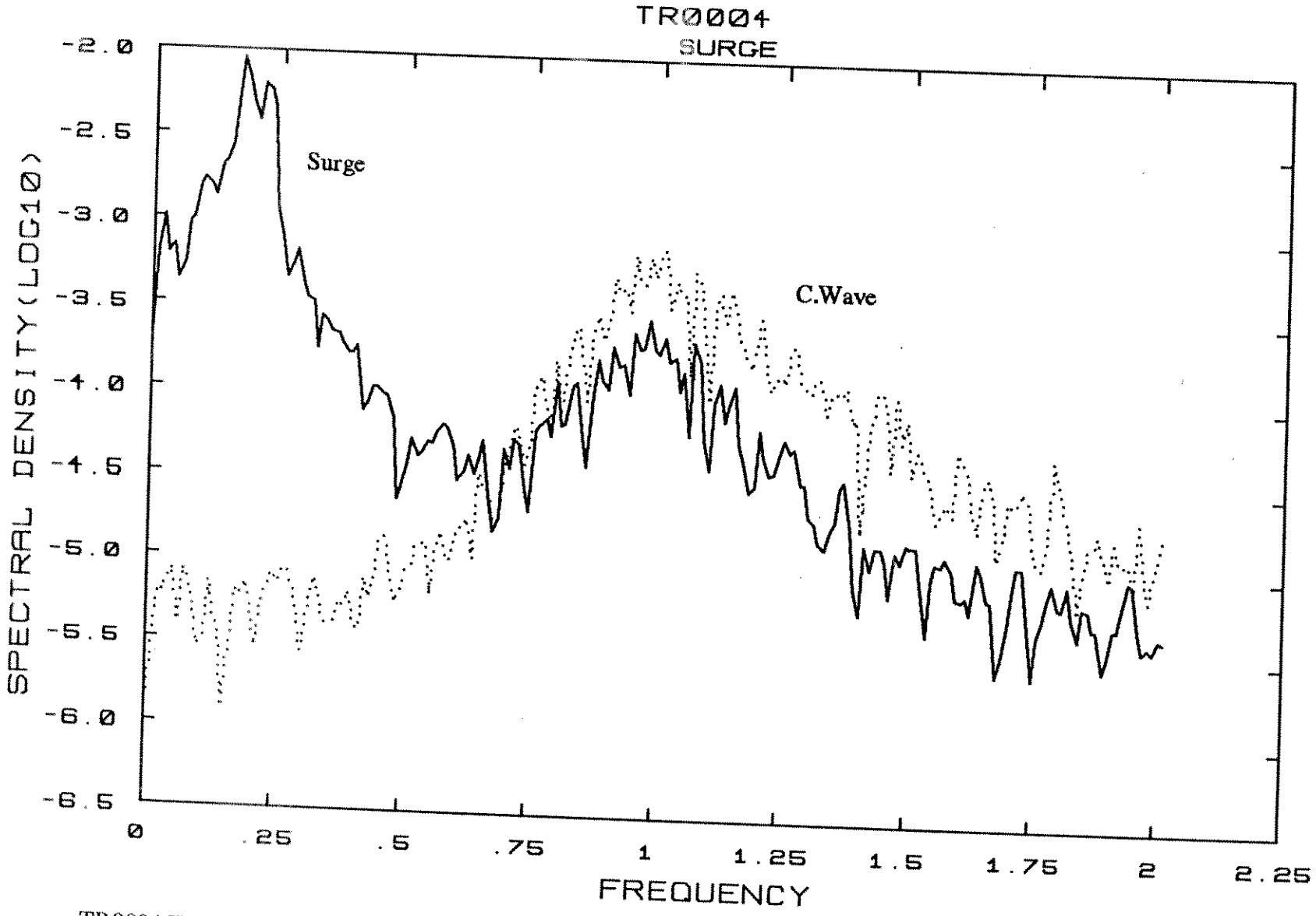
TR0004
SURGE
SPECTRAL DENSITY(LOG10)
-2.0
-2.5
-3.0
-3.5
-4.0
-4.5
-5.0
-5.5
-6.0
-6.5
Surge
C.Wave
0
.25
.5
.75
1
1.25
1.5
1.75
2
2.25
FREQUENCY

TR0004.W/S.4

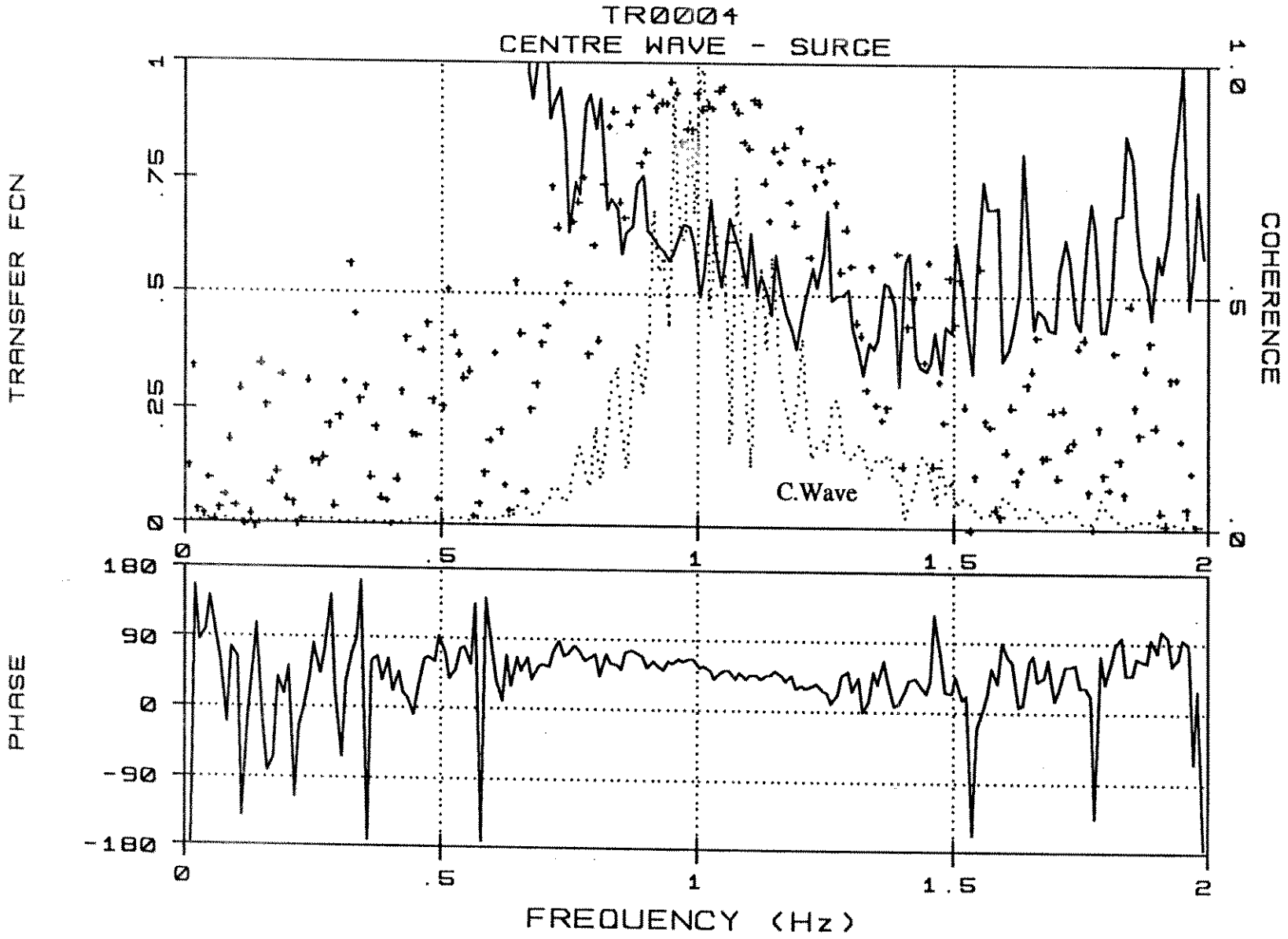
TR0004
CENTRE WAVE - SURGE
TRANSFER FCN
COHERENCE
C.Wave
PHASE
FREQUENCY (Hz)
0
.25
.5
.75
1
1.5
2
180
90
-90
-180

TR0004.W/S.4t

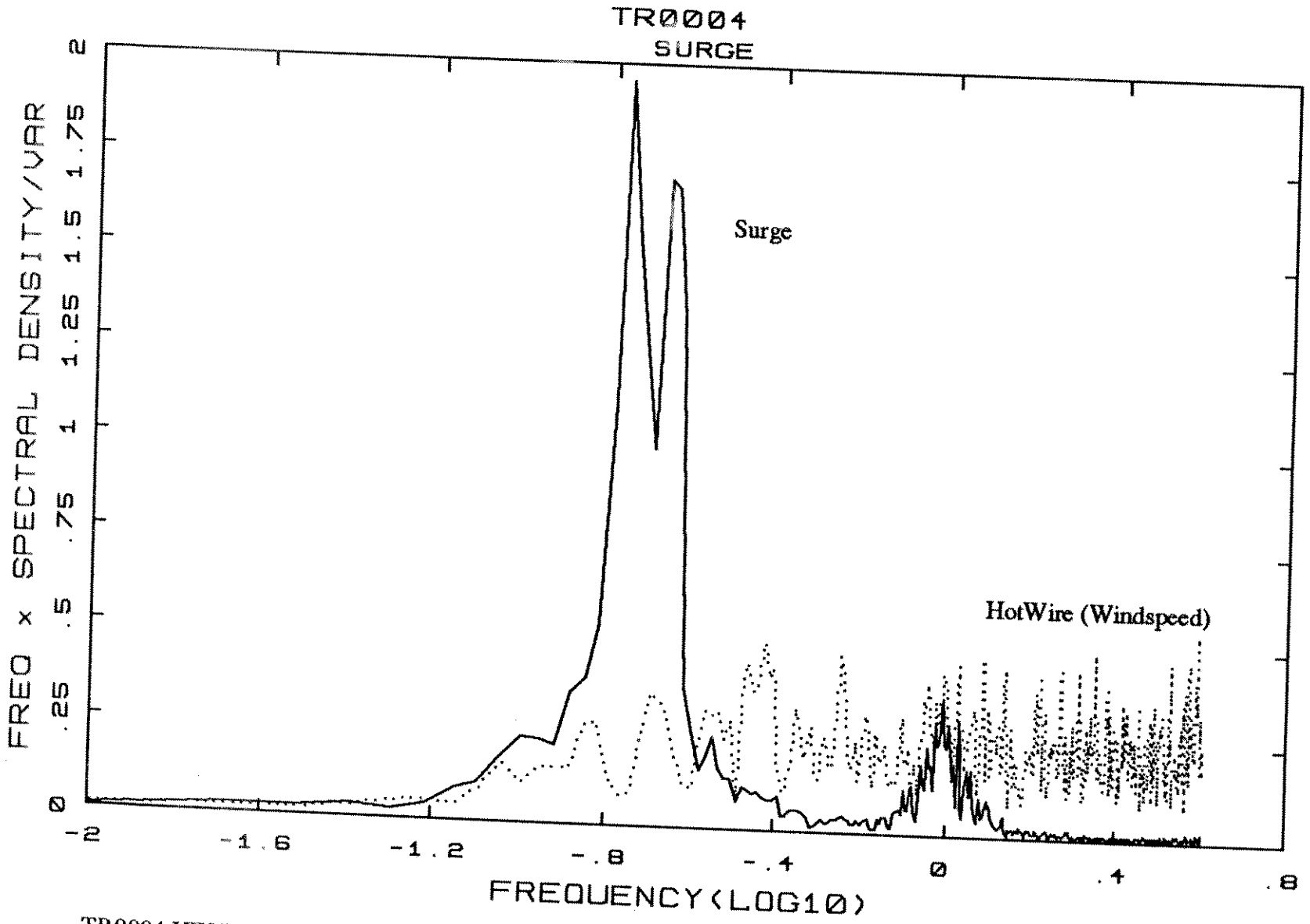
TR0004
SURGE
FREQ x SPECTRAL DENSITY/VAR
0
.25
.5
.75
1
1.25
1.5
1.75
2
Surge
HotWire (Windspeed)
-2
-1.6
-1.2
-.8
-.4
0
.4
.8
FREQUENCY(LOG10)

TR0004.HW/S.4

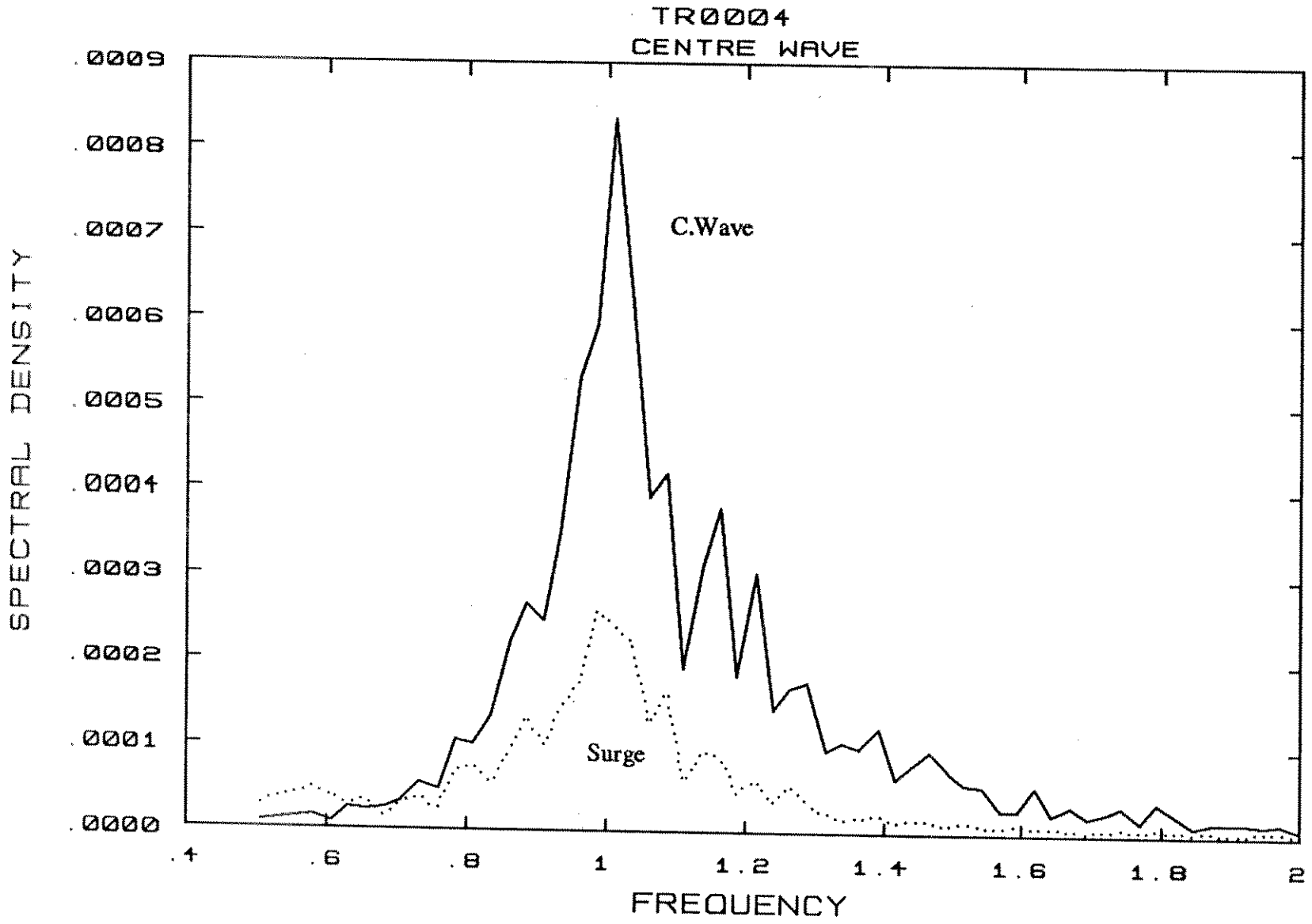
TR0004
CENTRE WAVE
.0009
.0008
.0007
.0006
.0005
.0004
.0003
.0002
.0001
.0000
SPECTRAL DENSITY
C.Wave
Surge
.4
.6
.8
1
1.2
1.4
1.6
1.8
2
FREQUENCY

TR0004.W/S.4*

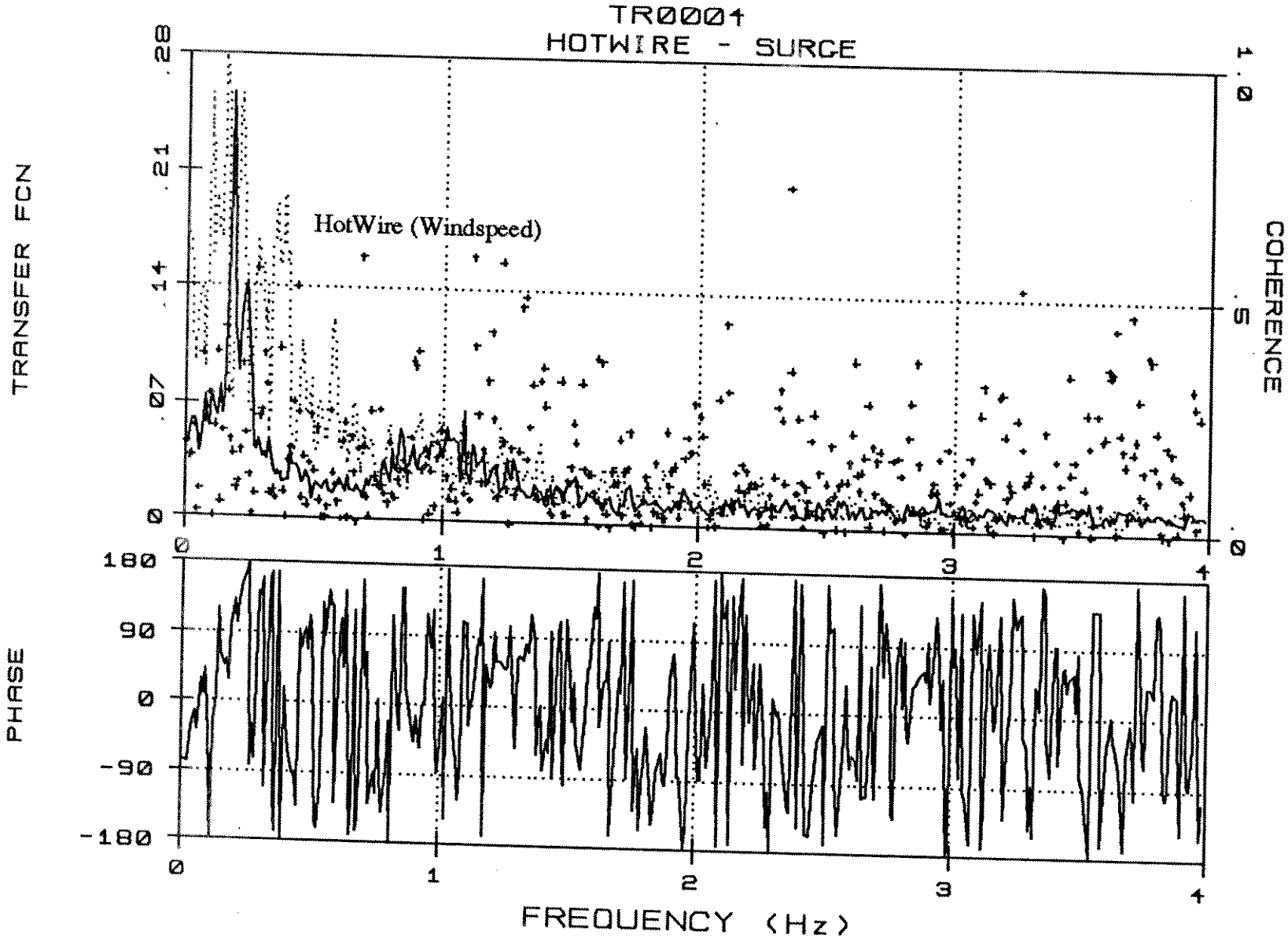

TR0004.HW/S.4t

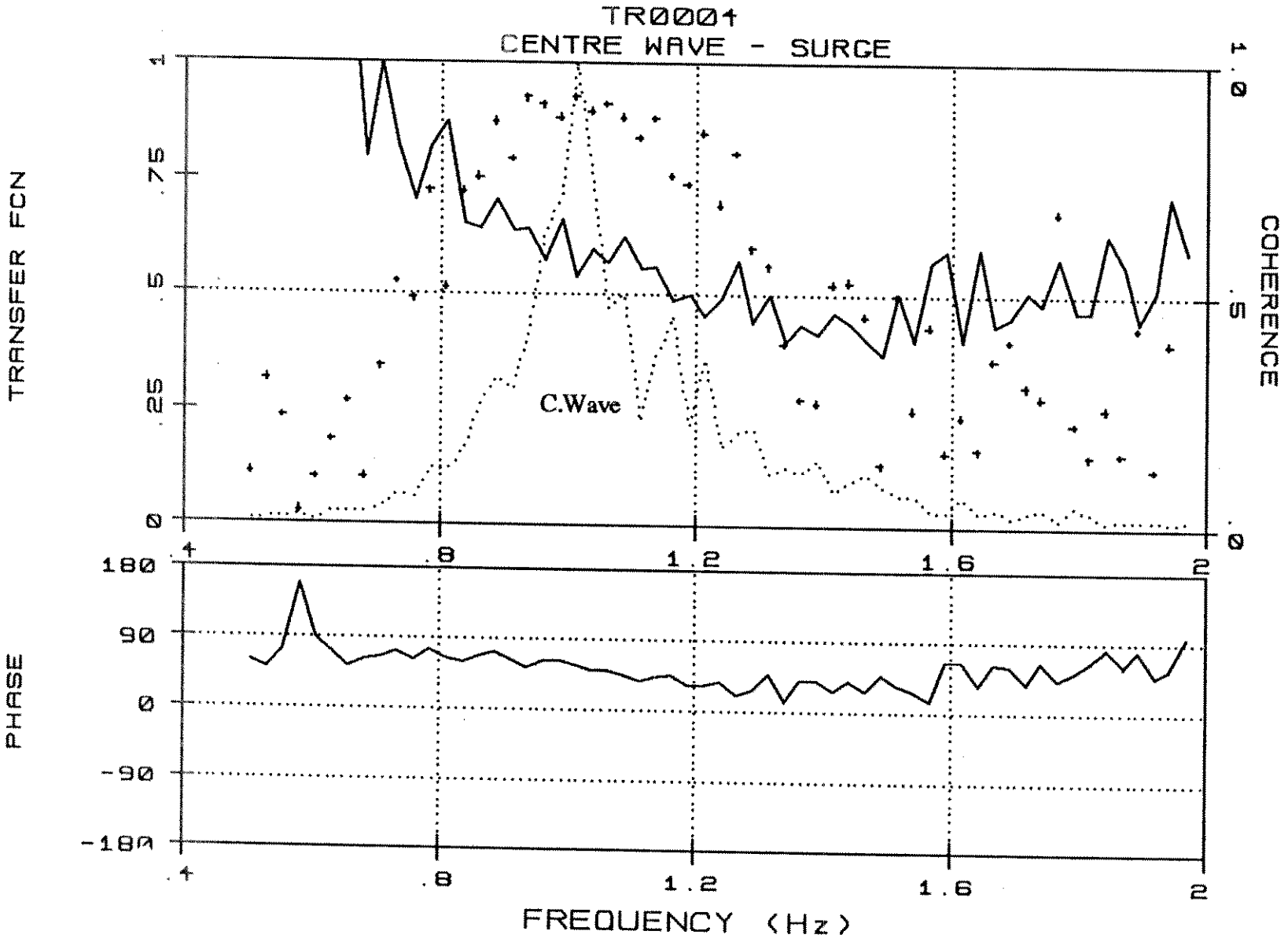
TR0001
CENTRE WAVE - SURGE
TRANSFER FCN
COHERENCE
PHASE
C.Wave
1.0
.75
.5
.25
0
.4
.8
1.2
1.6
2
180
90
0
-90
-180
FREQUENCY (Hz)

TR0004.W/S.4t*

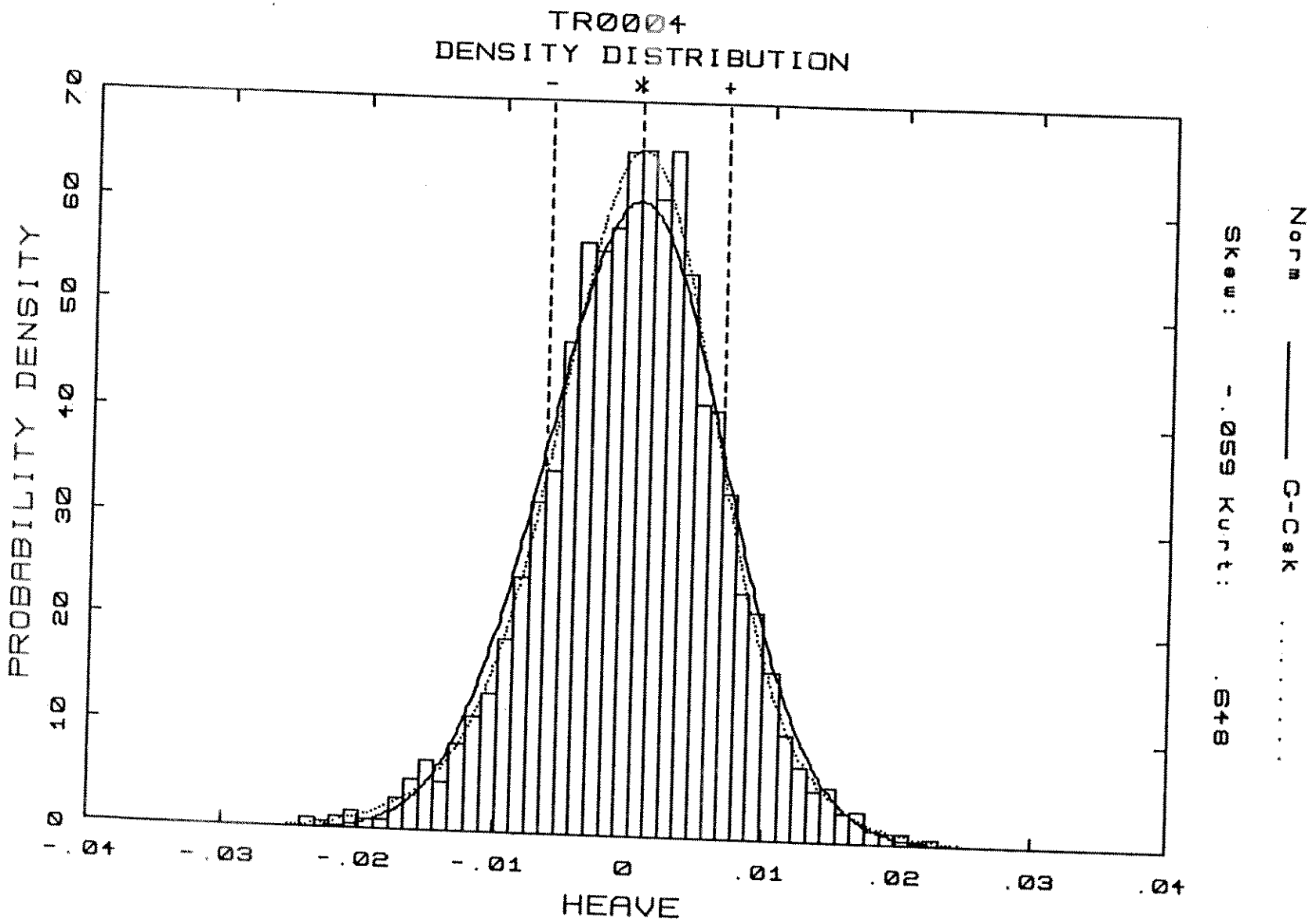
TR0004
DENSITY DISTRIBUTION
- * +
PROBABILITY DENSITY
0
10
20
30
40
50
60
70
-.04
-.03
-.02
-.01
0
.01
.02
.03
.04
HEAVE
Norm
Q-Qsk
Skew: -.059 Kurt: .648

TR0004.H.1

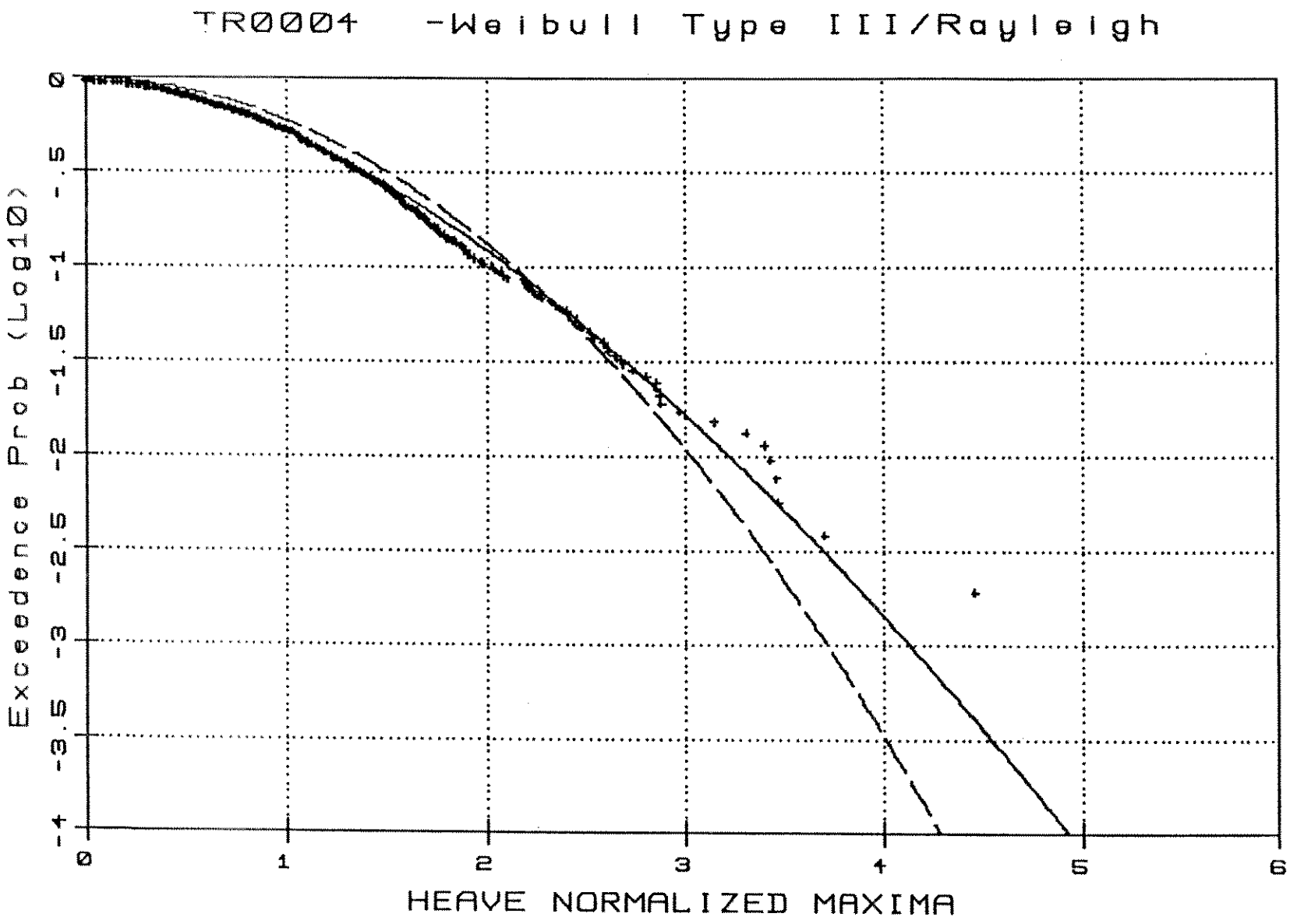
TR0004 -Weibull Type III/Rayleigh
Exceedence Prob (Log10)
0
-.5
-1
-1.5
-2
-2.5
-3
-3.5
-4
0
1
2
3
4
5
6
HEAVE NORMALIZED MAXIMA

TR0004.H.2

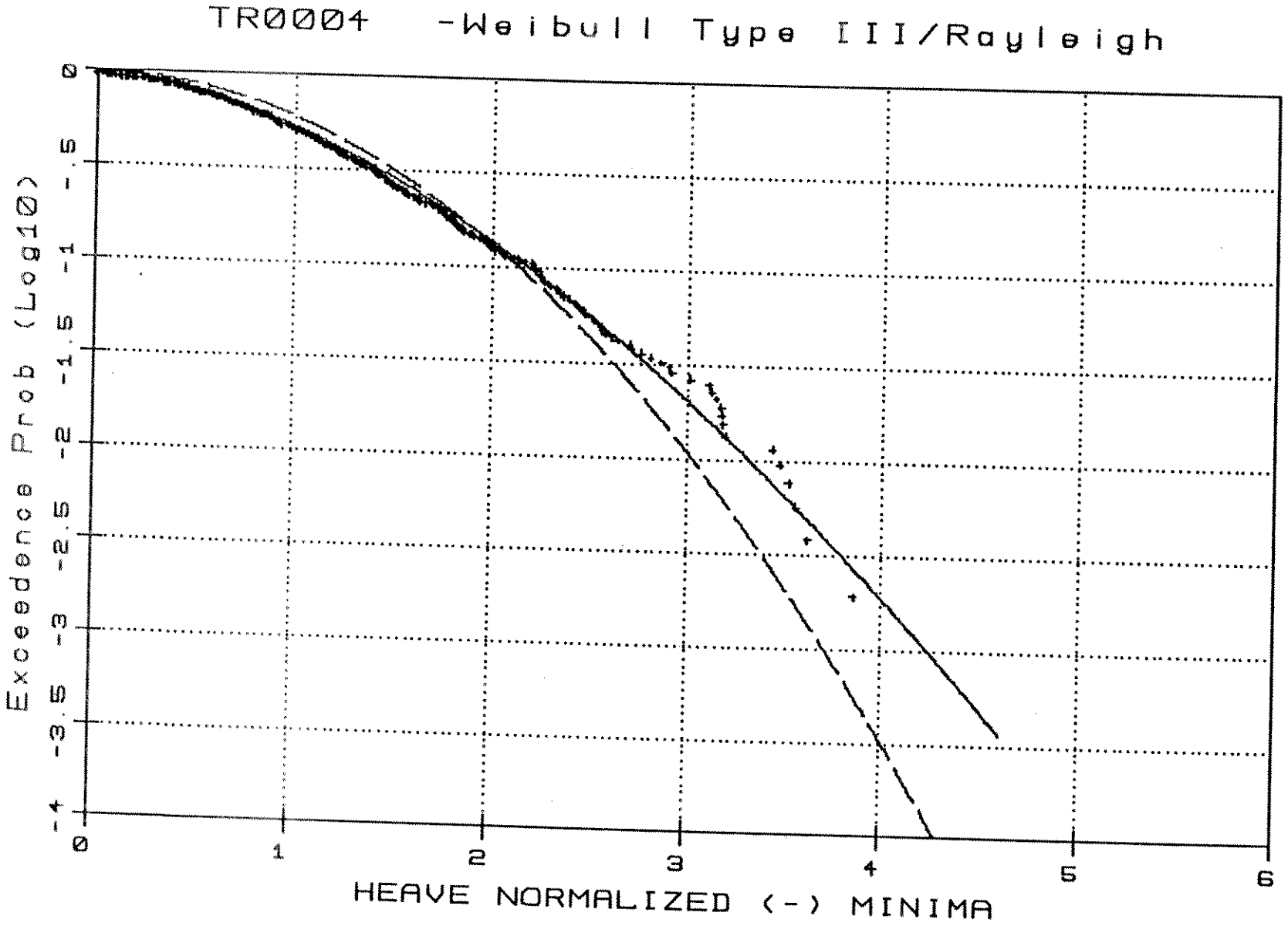
TR0004 -Weibull Type III/Rayleigh
Exceedence Prob (Log10)
0
-.5
-1
-1.5
-2
-2.5
-3
-3.5
-4
0
1
2
3
4
5
6
HEAVE NORMALIZED (-) MINIMA

TR0004.H.3

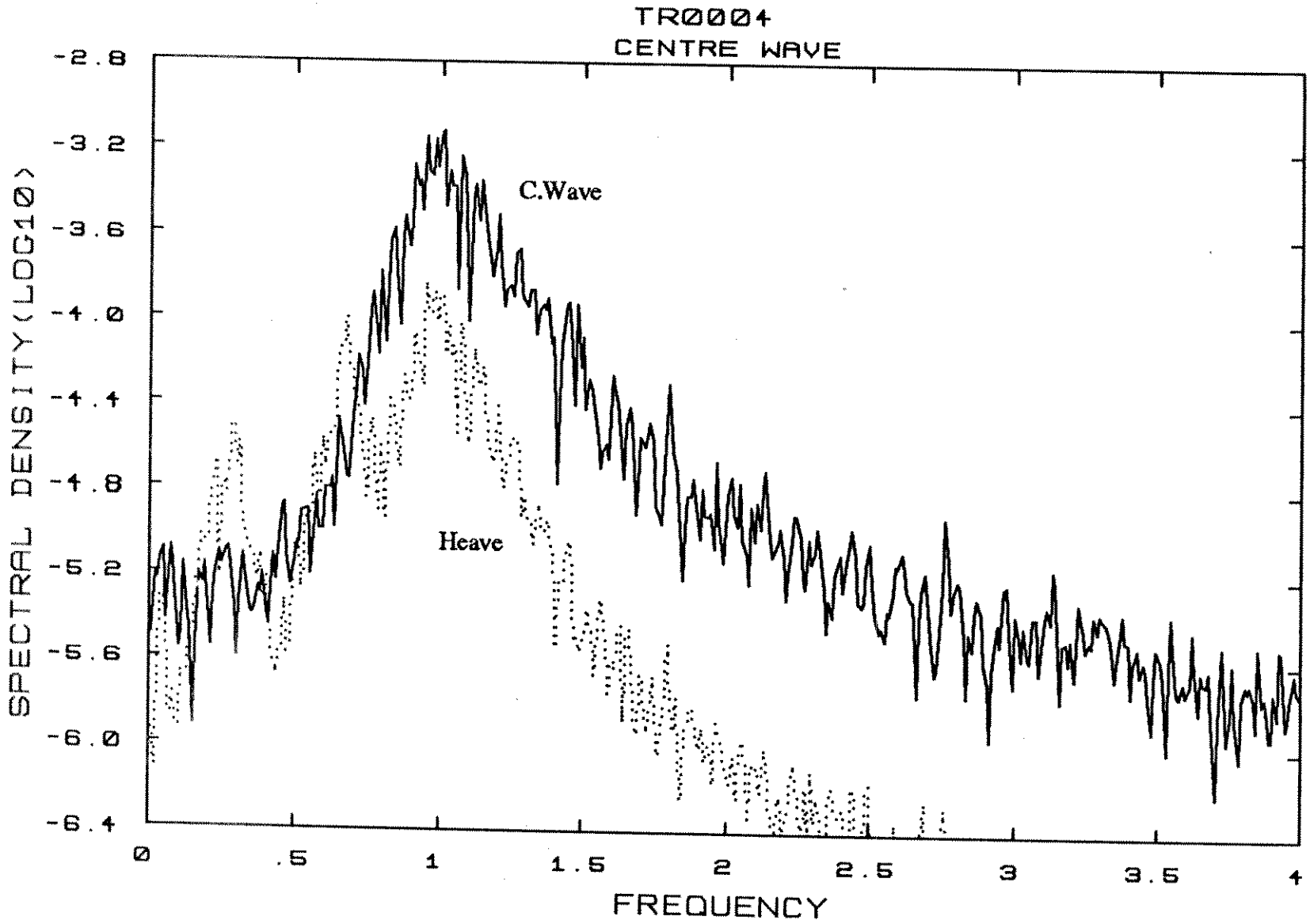
TR0004
CENTRE WAVE
SPECTRAL DENSITY(LOG10)
-2.8
-3.2
-3.6
-4.0
-4.4
-4.8
-5.2
-5.6
-6.0
-6.4
C.Wave
Heave
0
.5
1
1.5
2
2.5
3
3.5
4
FREQUENCY

TR0004.W/H.4

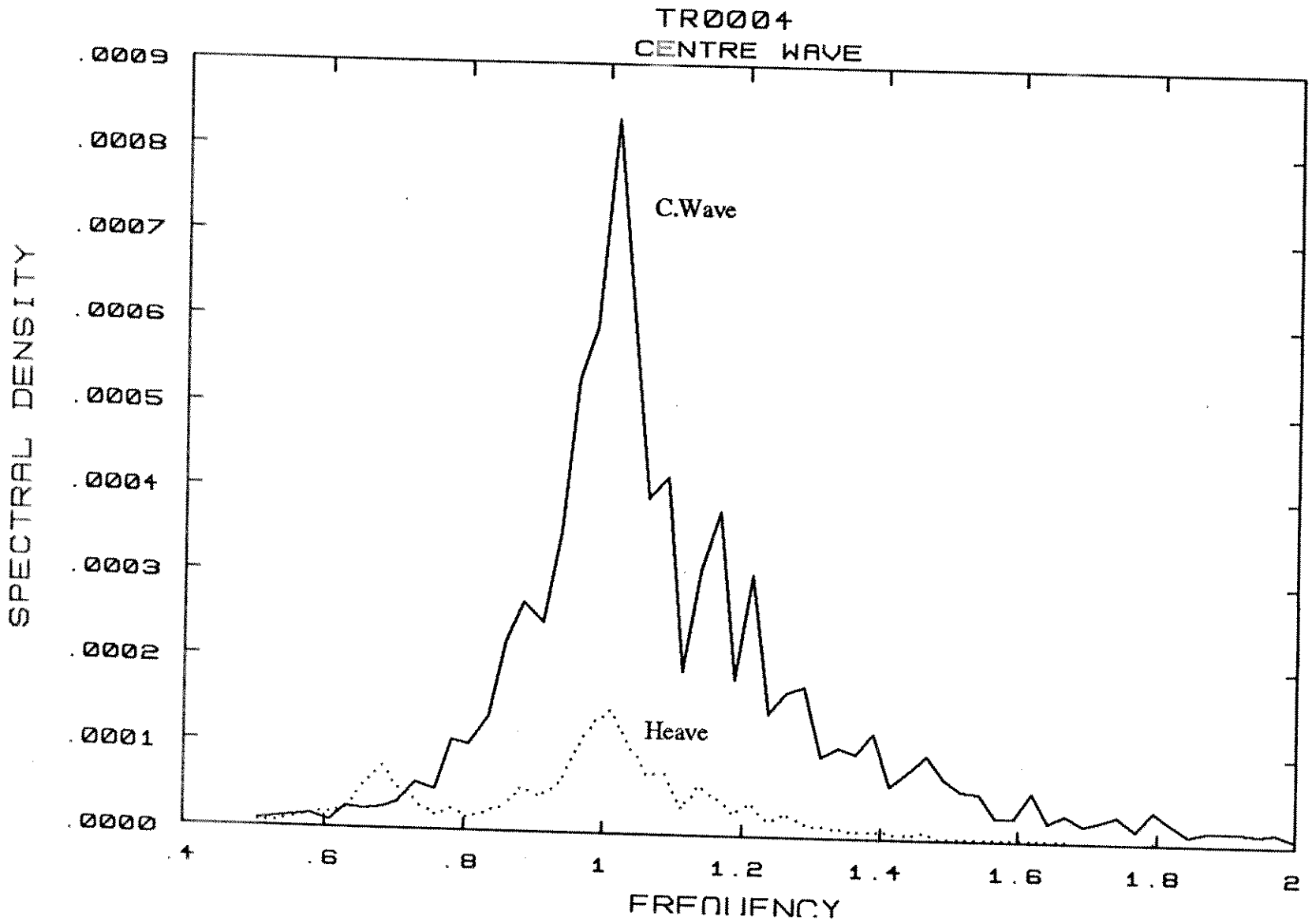
TR0004
CENTRE WAVE
SPECTRAL DENSITY
.0009
.0008
.0007
.0006
.0005
.0004
.0003
.0002
.0001
.0000
C.Wave
Heave
.4
.6
.8
1
1.2
1.4
1.6
1.8
2
FREQUENCY

TR0004.W/H.4*

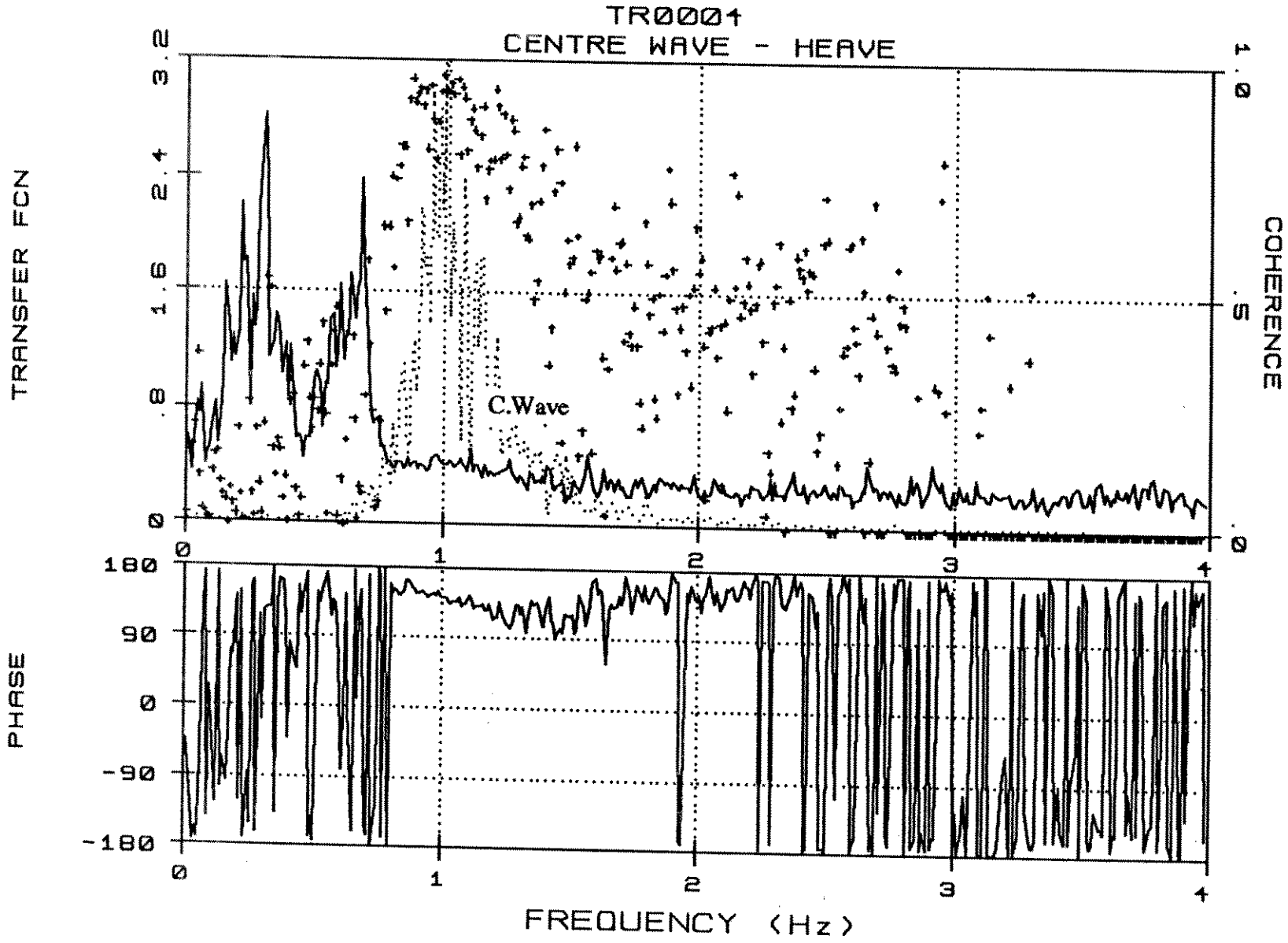
TR0004
CENTRE WAVE - HEAVE
TRANSFER FCN
3.2
2.4
1.6
.8
0
COHERENCE
1.0
.5
0
C.Wave
0
1
2
3
4
PHASE
180
90
0
-90
-180
FREQUENCY (Hz)

TR0004.W/H.4t

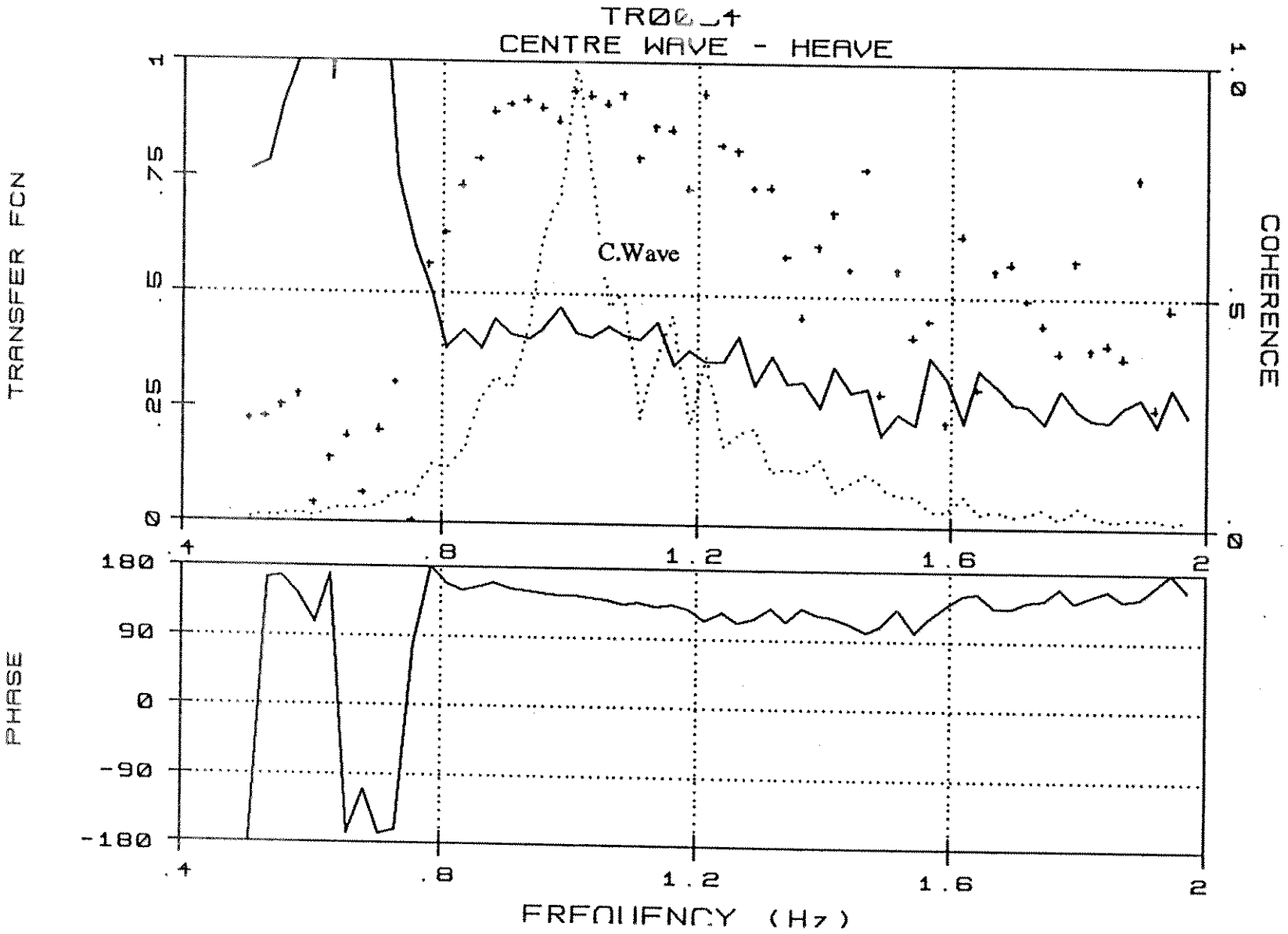
TR0[illegible]4
CENTRE WAVE - HEAVE
TRANSFER FCN
COHERENCE
C.Wave
1
.75
.5
.25
0
1.0
.5
0
.4
.8
1.2
1.6
2
180
90
0
-90
-180
PHASE
FREQUENCY (Hz)

TROOO4.W/H.4t*

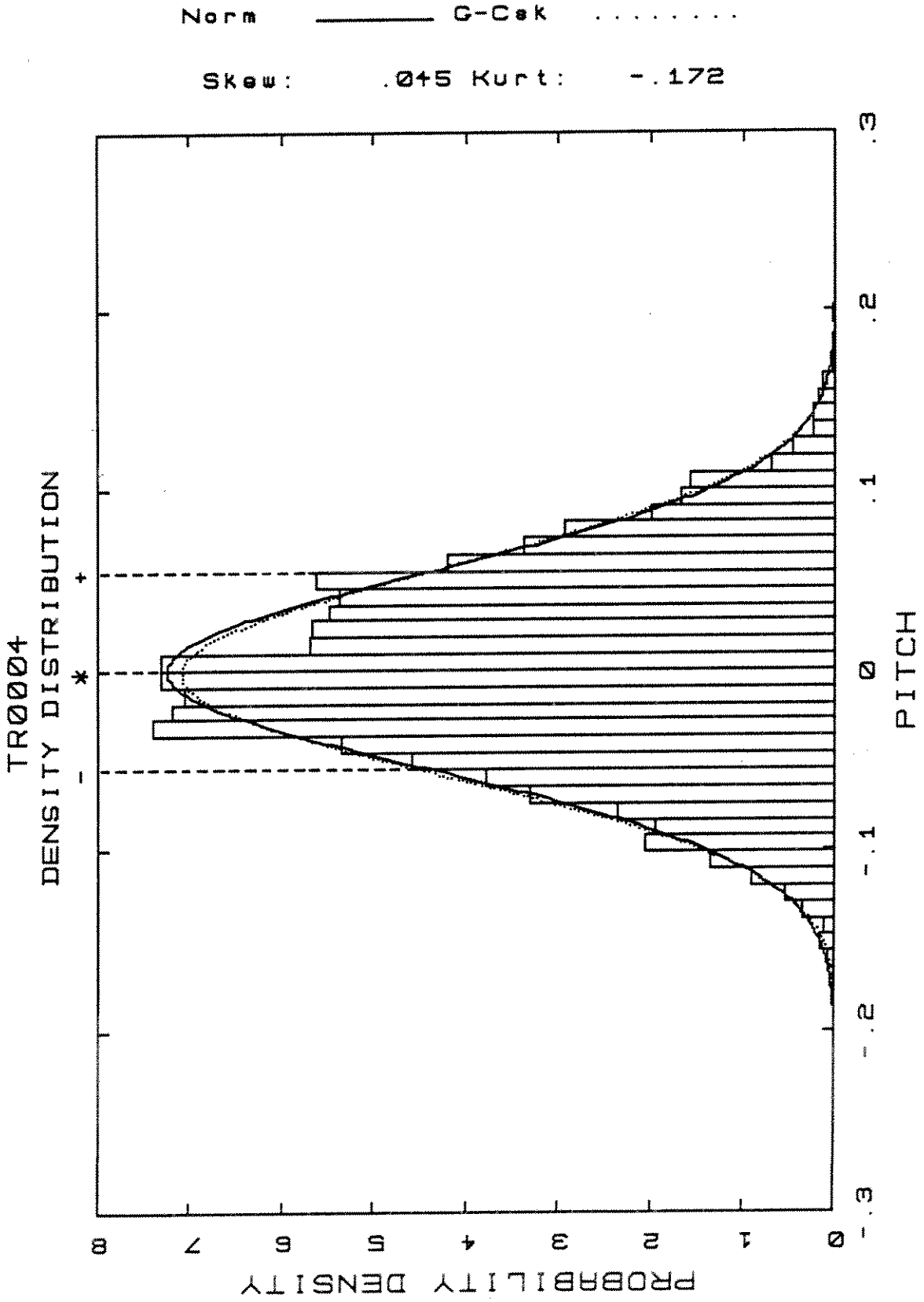
Norm ——— G-Cek .....
Skew: .045 Kurt: -.172
TR0004
DENSITY DISTRIBUTION
+
*
-
PROBABILITY DENSITY
0
1
2
3
4
5
6
7
8
.3
.2
.1
0
-.1
-.2
-.3
PITCH

TR0004.Pi.1

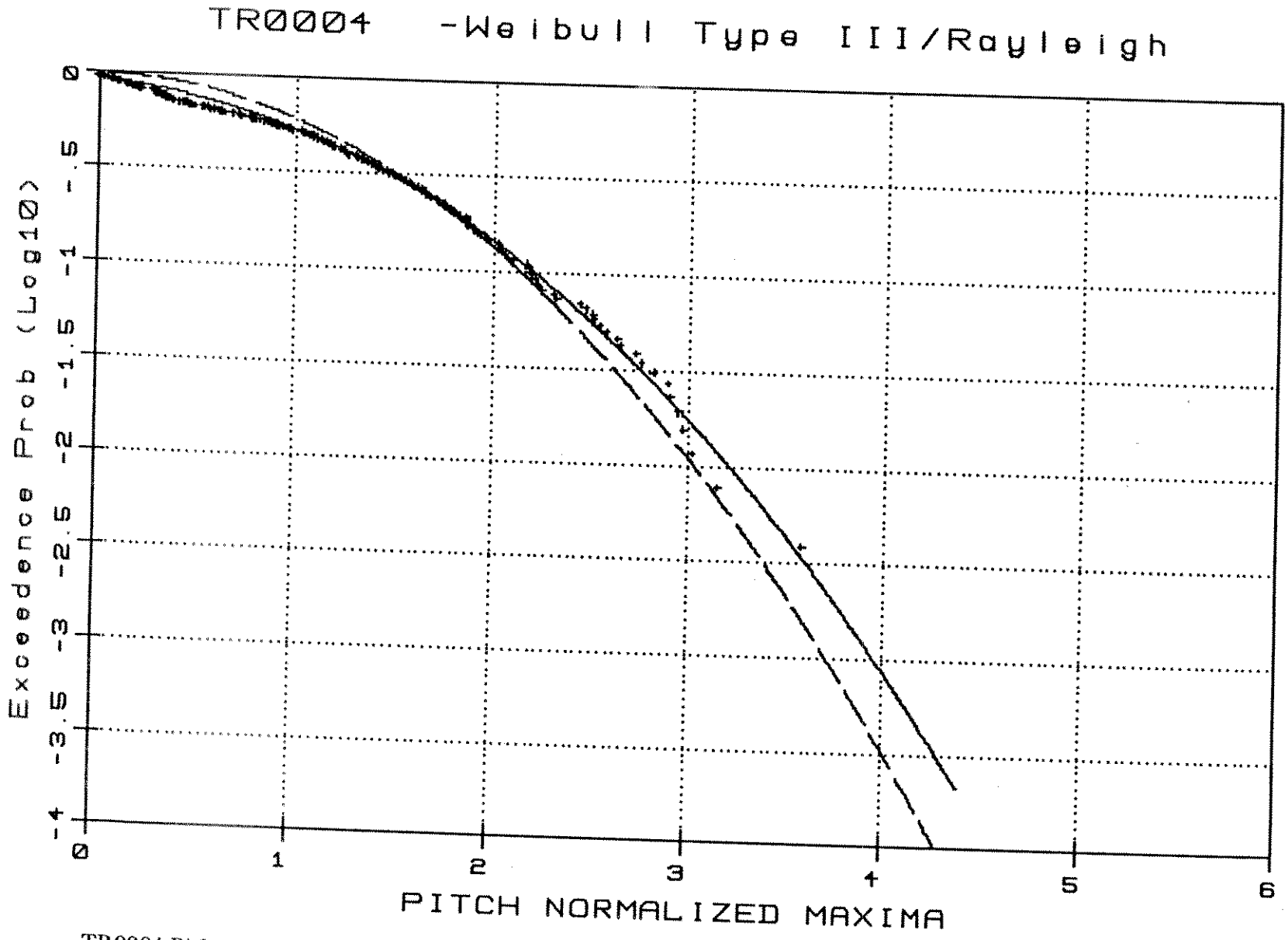
TR0004 -Weibull Type III/Rayleigh
Exceedence Prob (Log10)
0
-.5
-1
-1.5
-2
-2.5
-3
-3.5
-4
0
1
2
3
4
5
6
PITCH NORMALIZED MAXIMA

TR0004.Pi.2

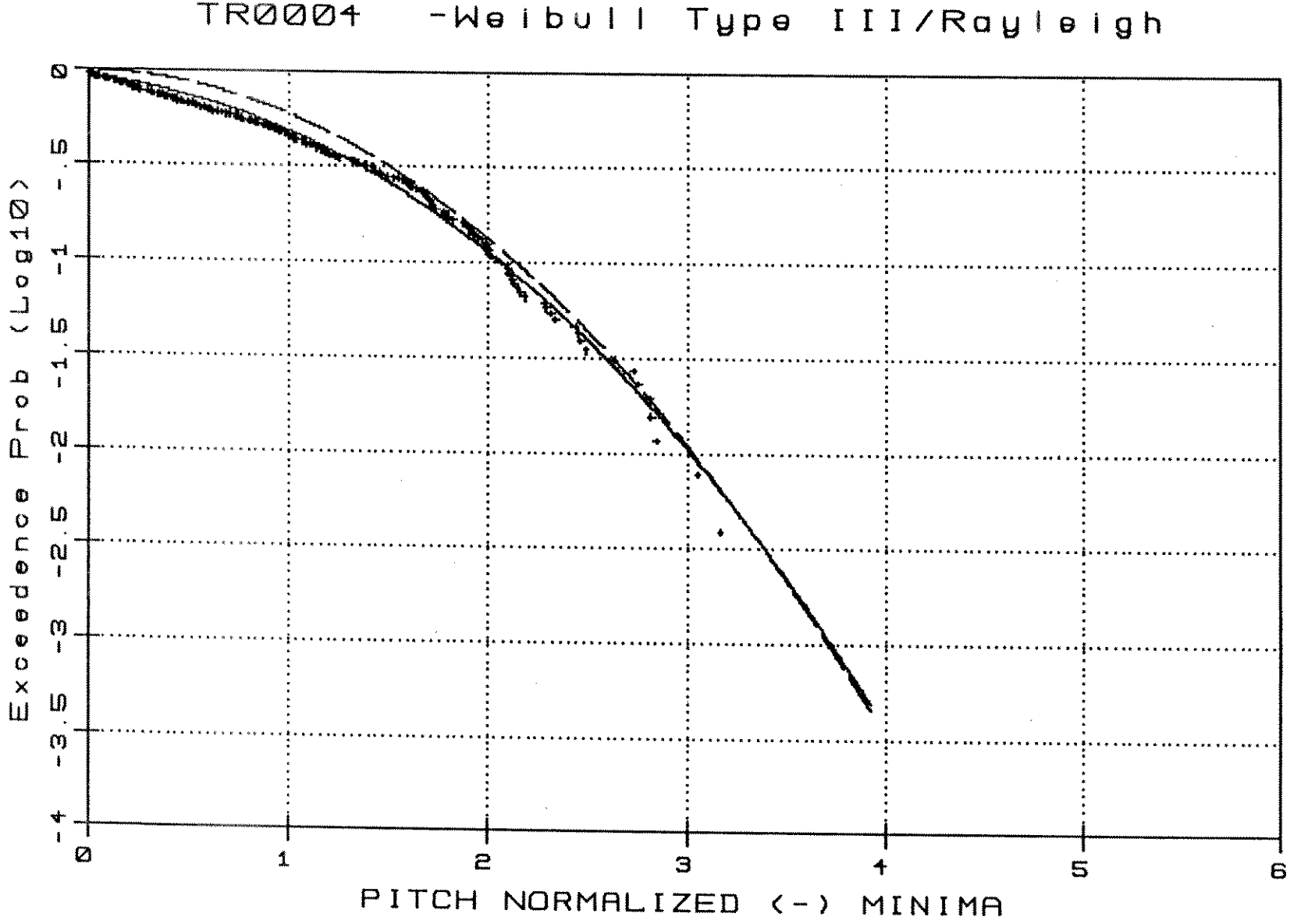
TR0004 -Weibull Type III/Rayleigh
Exceedence Prob (Log10)
0
-.5
-1
-1.5
-2
-2.5
-3
-3.5
-4
0
1
2
3
4
5
6
PITCH NORMALIZED (-) MINIMA

TR0004.Pi.3

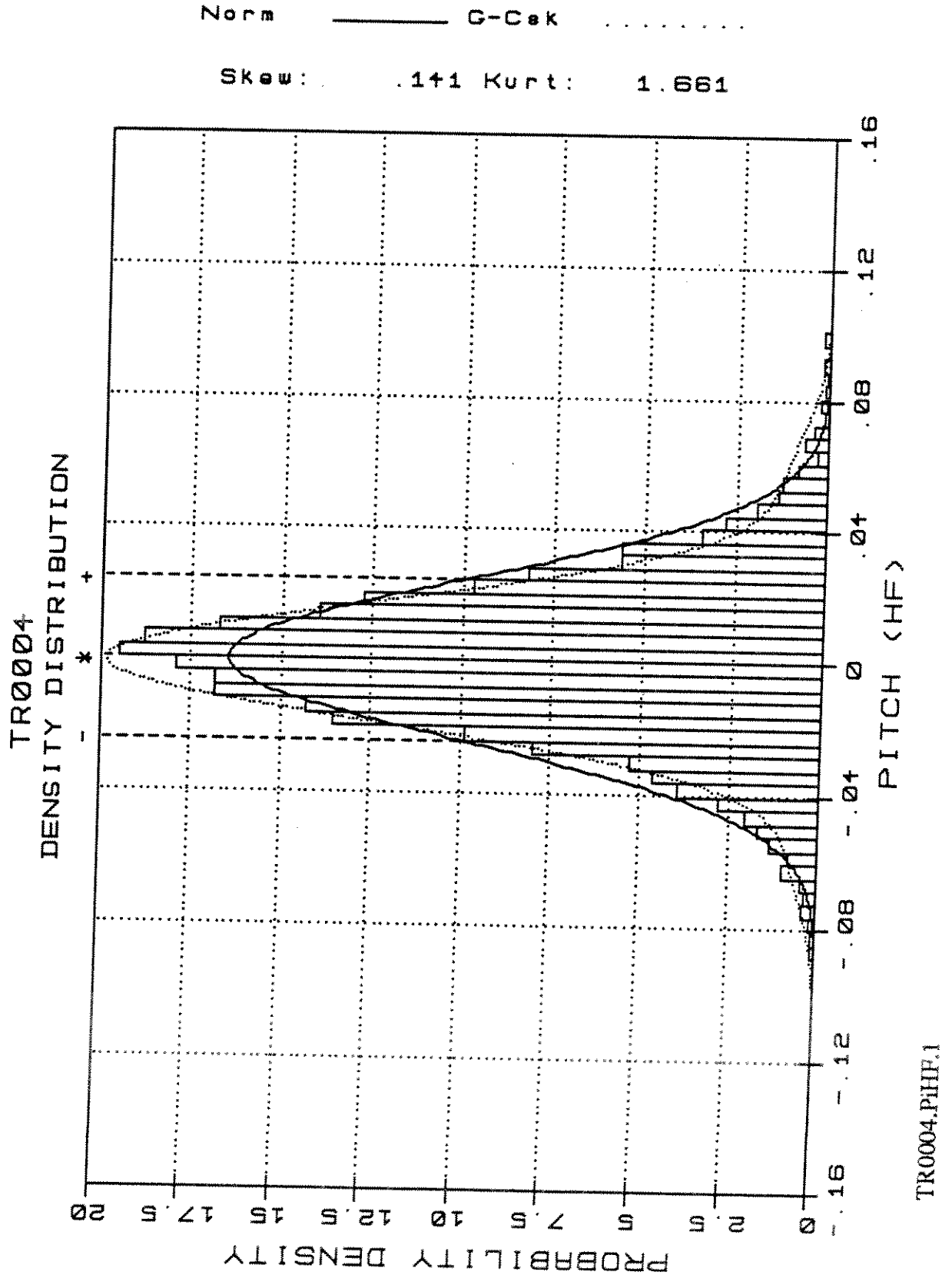
Norm
C-Cak
Skew: .141 Kurt: 1.661
TR0004
DENSITY DISTRIBUTION
PROBABILITY DENSITY
0
2.5
5
7.5
10
12.5
15
17.5
20
PITCH (HF)
.16
.12
.08
.04
0
-.04
-.08
-.12
-.16

TR0004.PHF.1

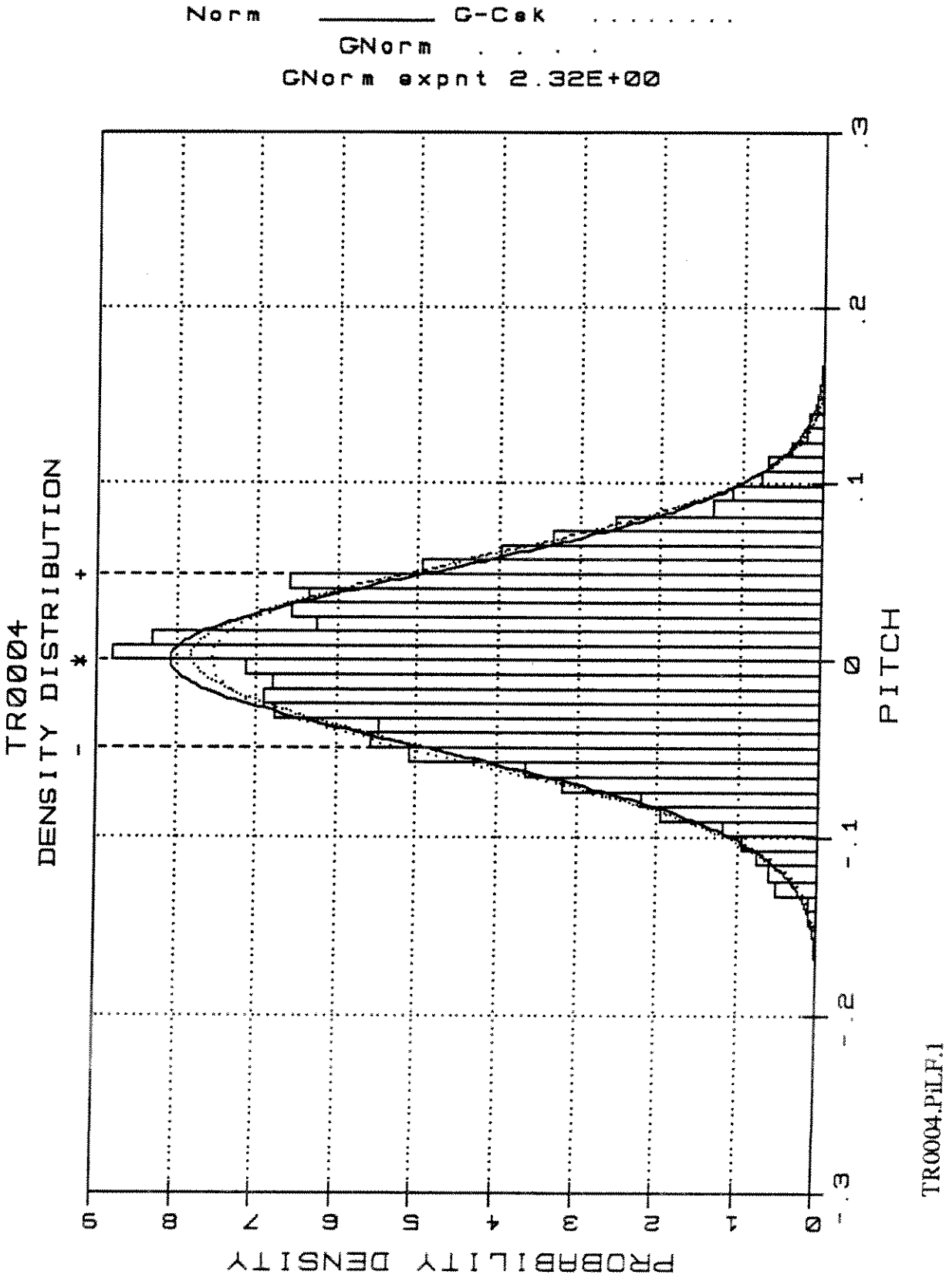
Norm
G-Cek
GNorm
GNorm expnt 2.32E+00
TR0004
DENSITY DISTRIBUTION
+
*
-
PROBABILITY DENSITY
0
1
2
3
4
5
6
7
8
9
PITCH
.3
.2
.1
0
-.1
-.2
-.3

TR0004.PLF1

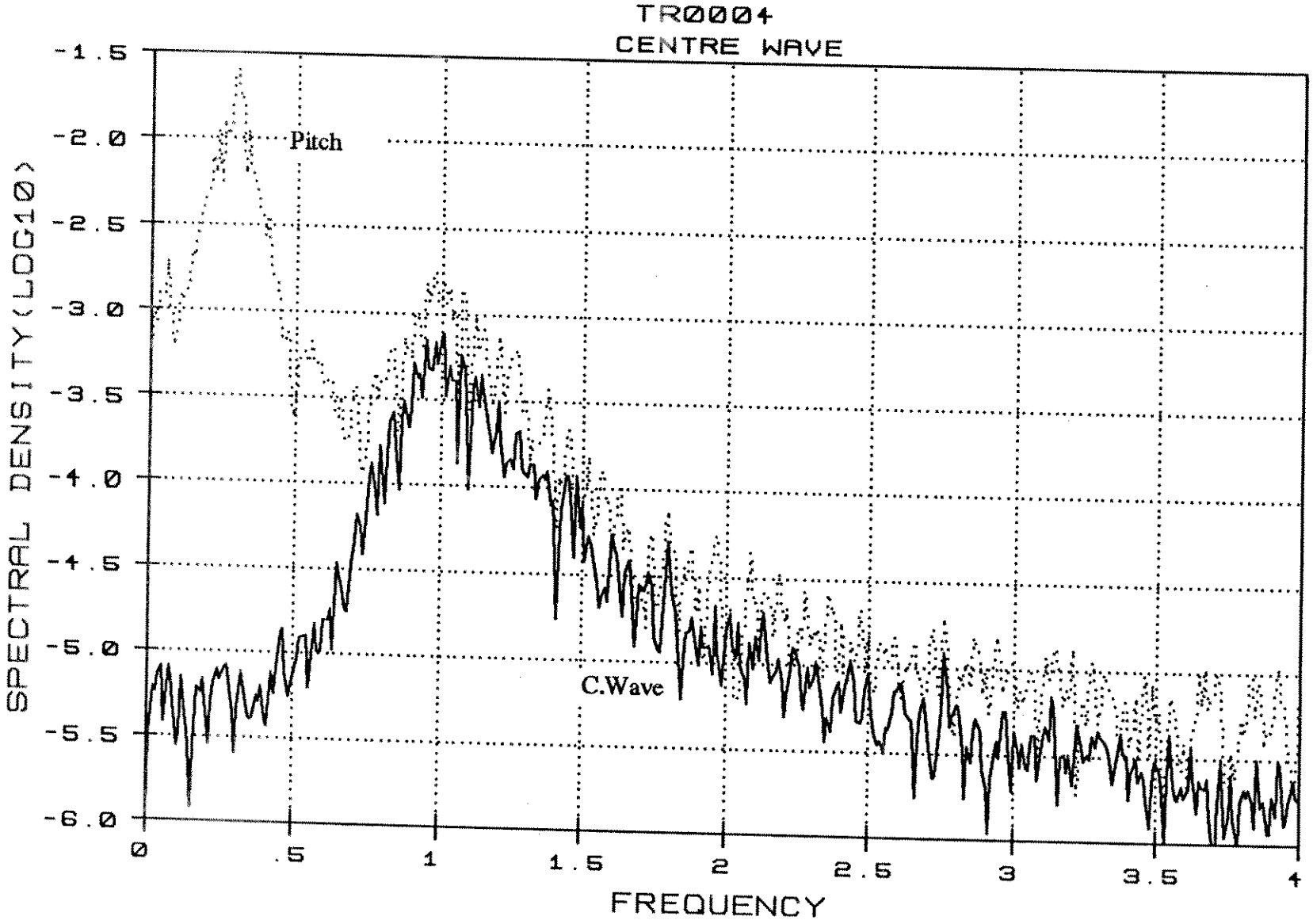
TR0004
CENTRE WAVE
SPECTRAL DENSITY(LOG10)
-1.5
-2.0
-2.5
-3.0
-3.5
-4.0
-4.5
-5.0
-5.5
-6.0
Pitch
C.Wave
0
.5
1
1.5
2
2.5
3
3.5
4
FREQUENCY

TR0004.W/Pi.4

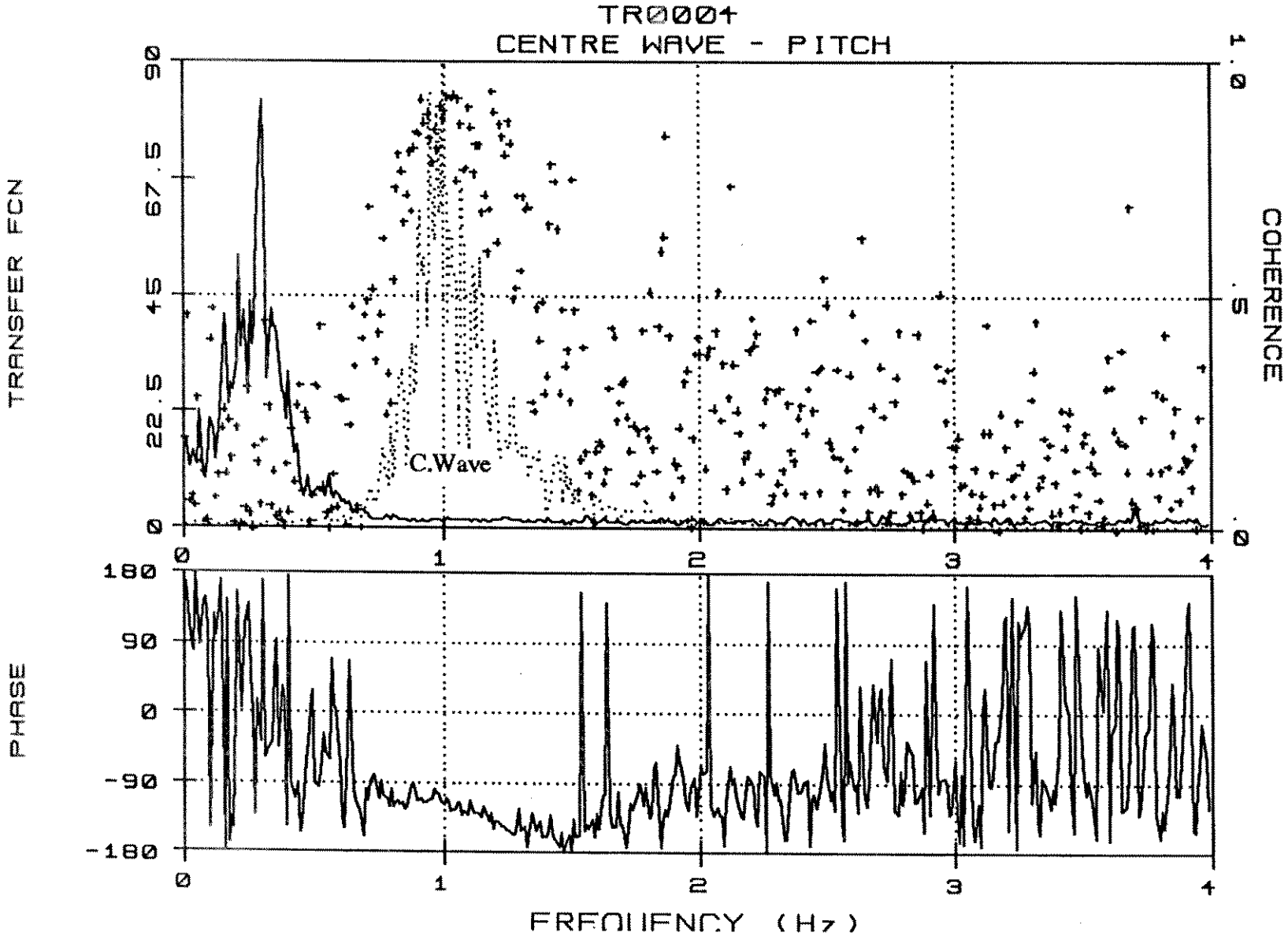

TR0004.W/Pi.4t

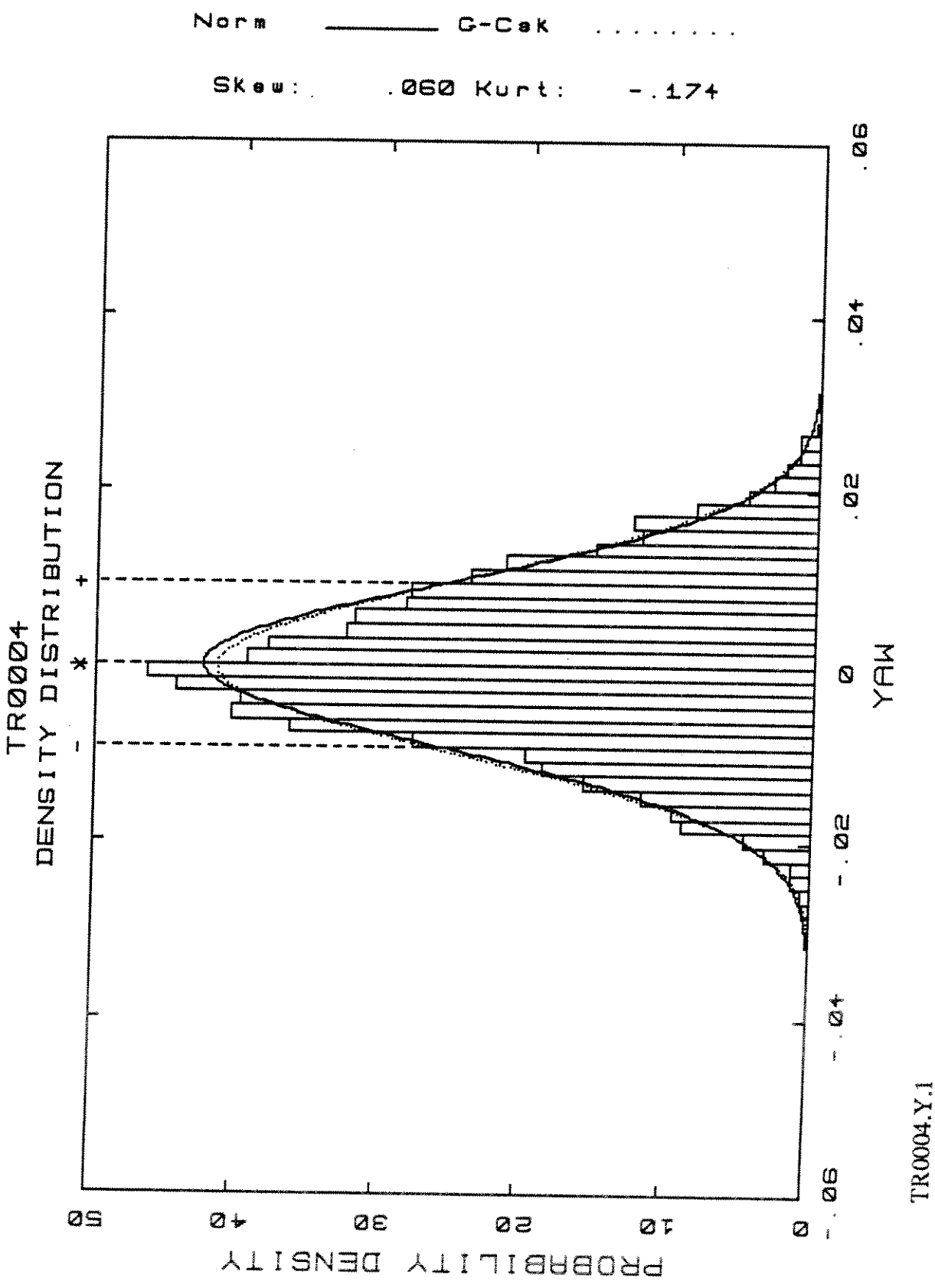
Norm
G-Cak
Skew: .060 Kurt: -.174
TR0004
DENSITY DISTRIBUTION
+
*
-
PROBABILITY DENSITY
0
10
20
30
40
50
-.06
-.04
-.02
0
.02
.04
.06
YAW
TR0004.Y.1

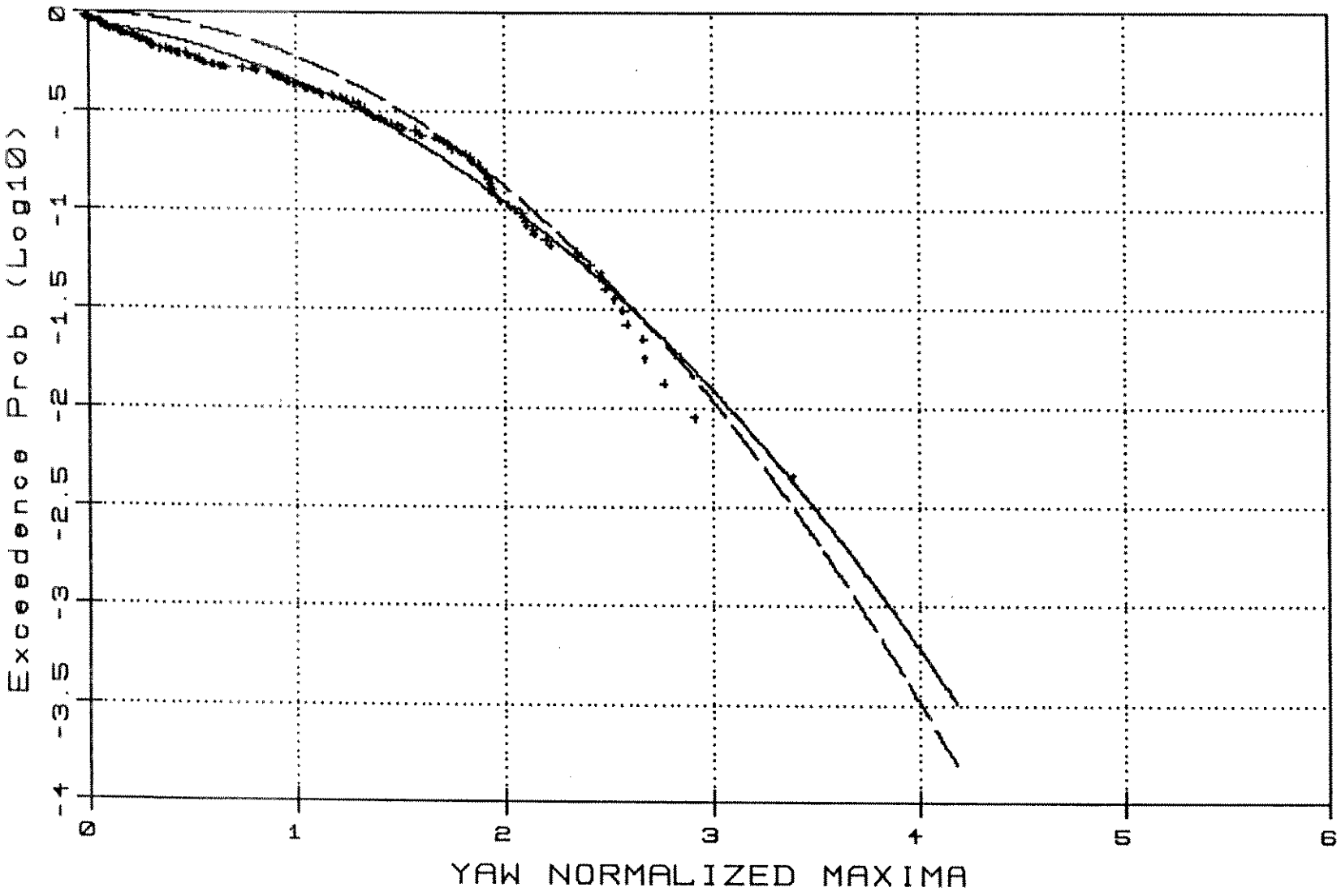
TR0004 -Weibull Type III/Rayleigh
Exceedence Prob (Log10)
0
-.5
-1
-1.5
-2
-2.5
-3
-3.5
-4
0
1
2
3
4
5
6
YAW NORMALIZED MAXIMA

TR0004.Y.2

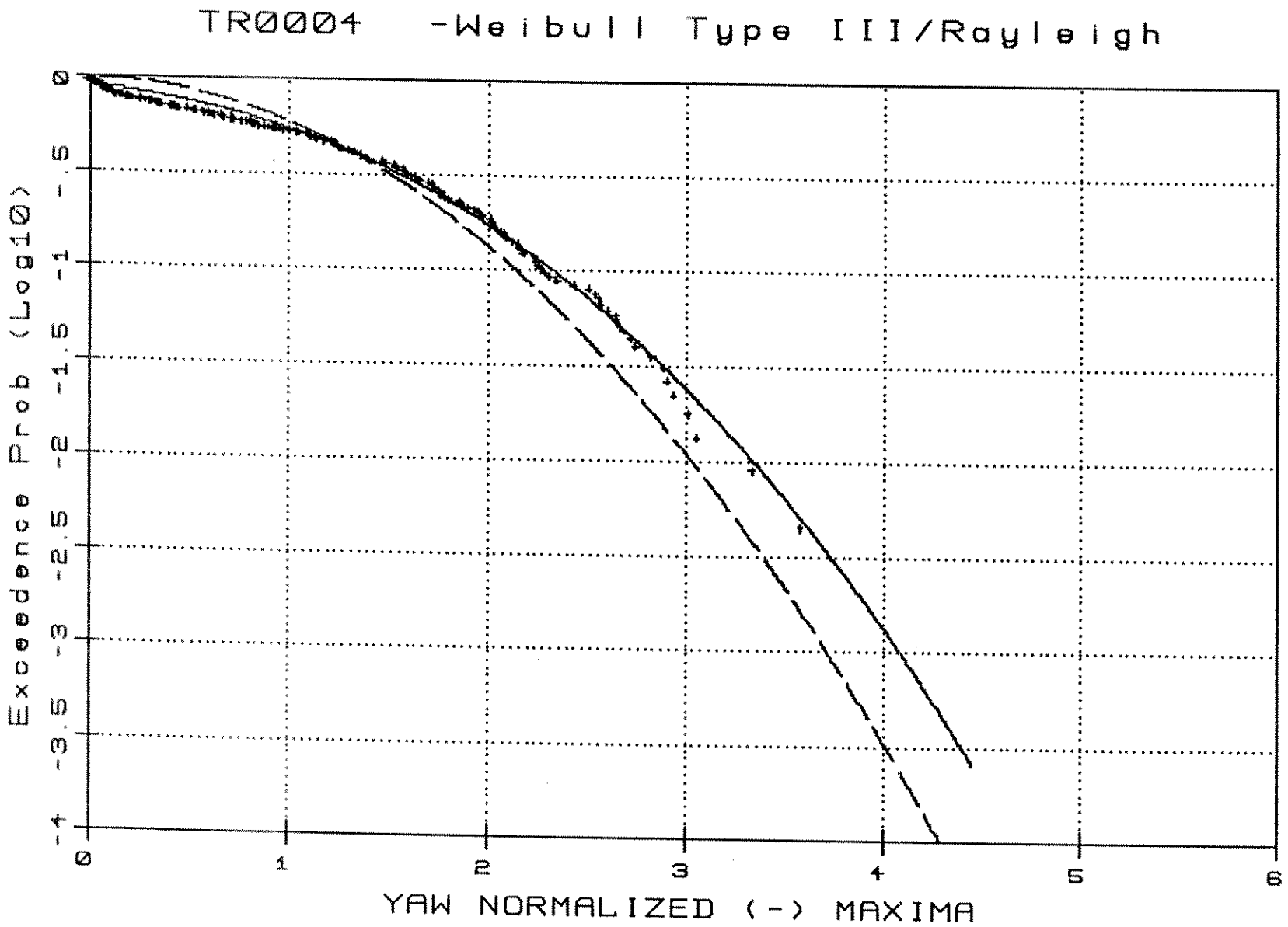
TR0004 -Weibull Type III/Rayleigh
Exceedence Prob (Log10)
0
-.5
-1
-1.5
-2
-2.5
-3
-3.5
-4
0
1
2
3
4
5
6
YAW NORMALIZED (-) MAXIMA

TR0004.Y.3

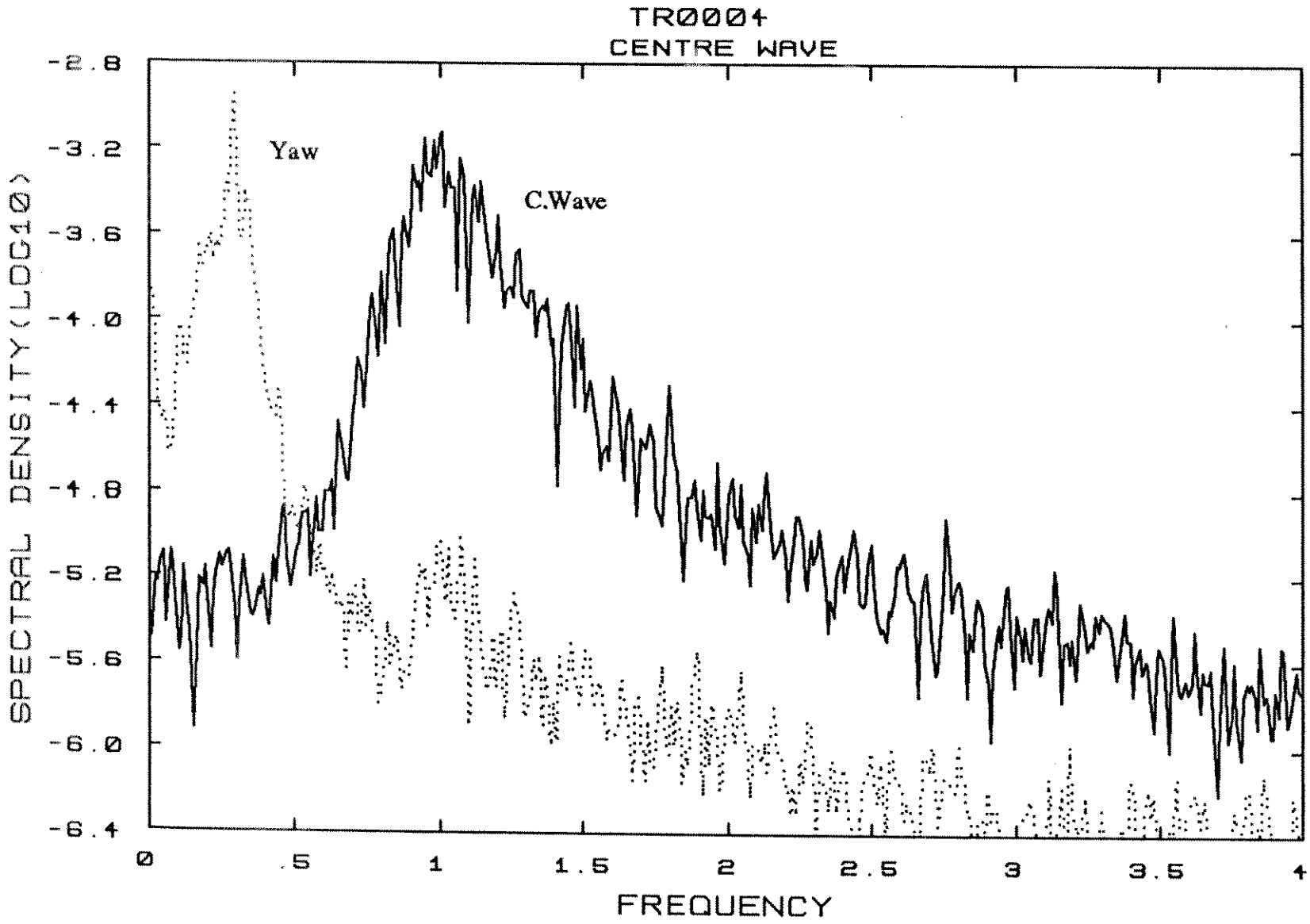
TR0004
CENTRE WAVE
SPECTRAL DENSITY(LOG10)
-2.8
-3.2
-3.6
-4.0
-4.4
-4.8
-5.2
-5.6
-6.0
-6.4
Yaw
C.Wave
0
.5
1
1.5
2
2.5
3
3.5
4
FREQUENCY

TR0004.W/Y.4

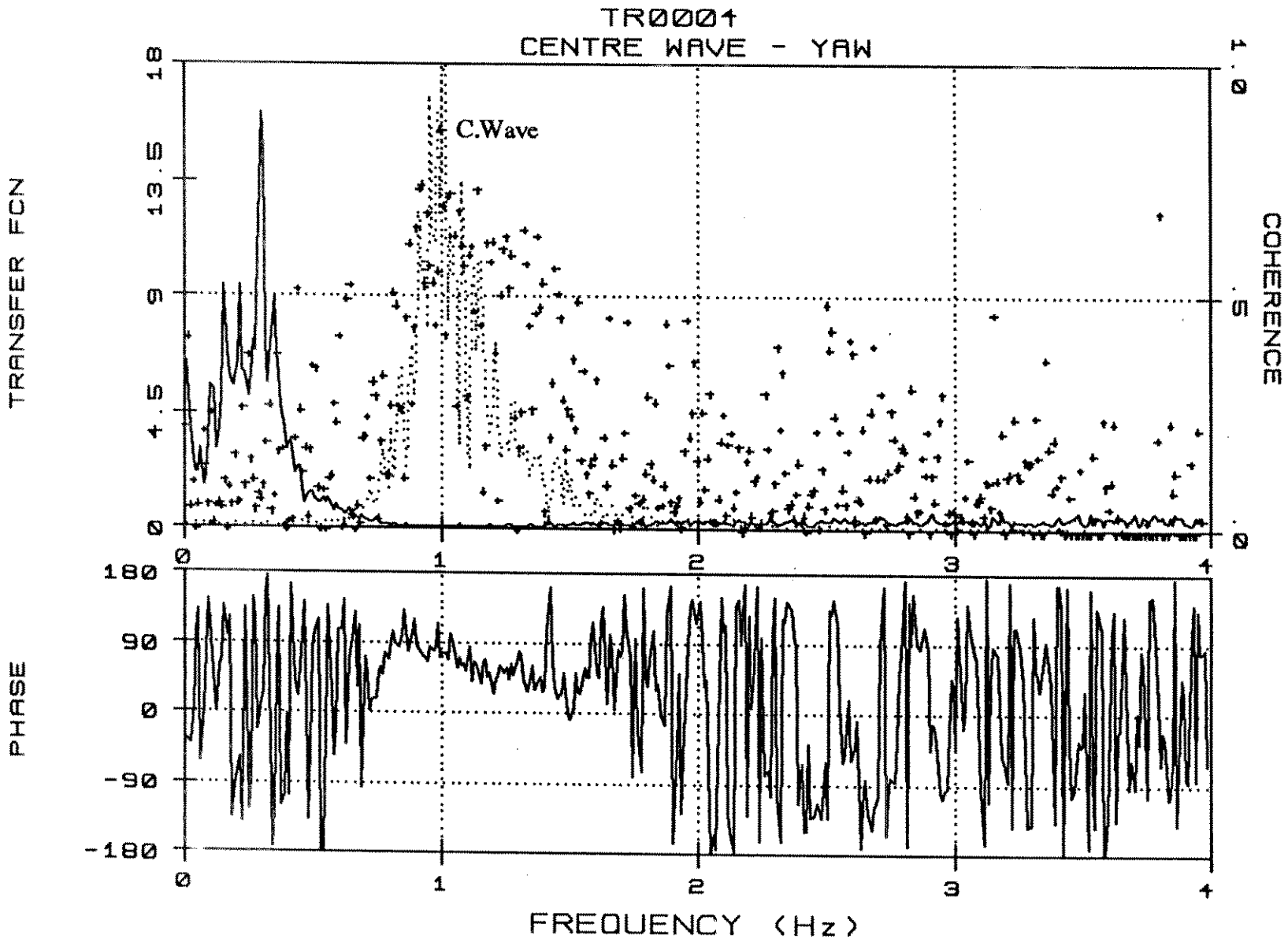
TR0004
CENTRE WAVE - YAW
C.Wave
TRANSFER FCN
COHERENCE
PHASE
FREQUENCY (Hz)
18
13.5
9
4.5
0
1.0
.5
0
180
90
0
-90
-180
0
1
2
3
4

TR0004.W/Y.4t

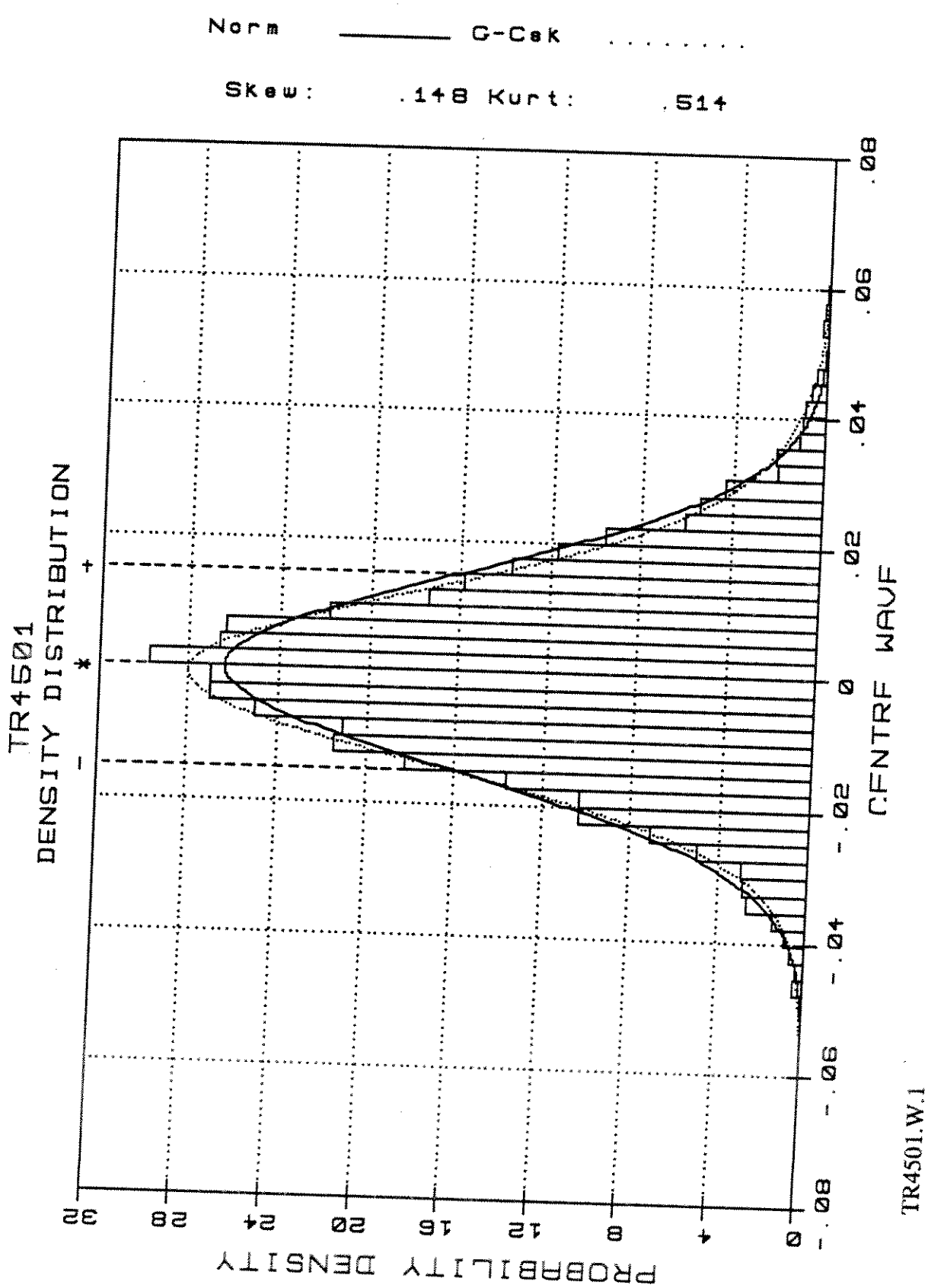
Norm
G-Cak
Skew: .148 Kurt: .514
TR4501
DENSITY DISTRIBUTION
+
*
-
PROBABILITY DENSITY
0
4
8
12
16
20
24
28
32
CENTRF WAVF
.08
.06
.04
.02
0
-.02
-.04
-.06
-.08

TR4501.W.1

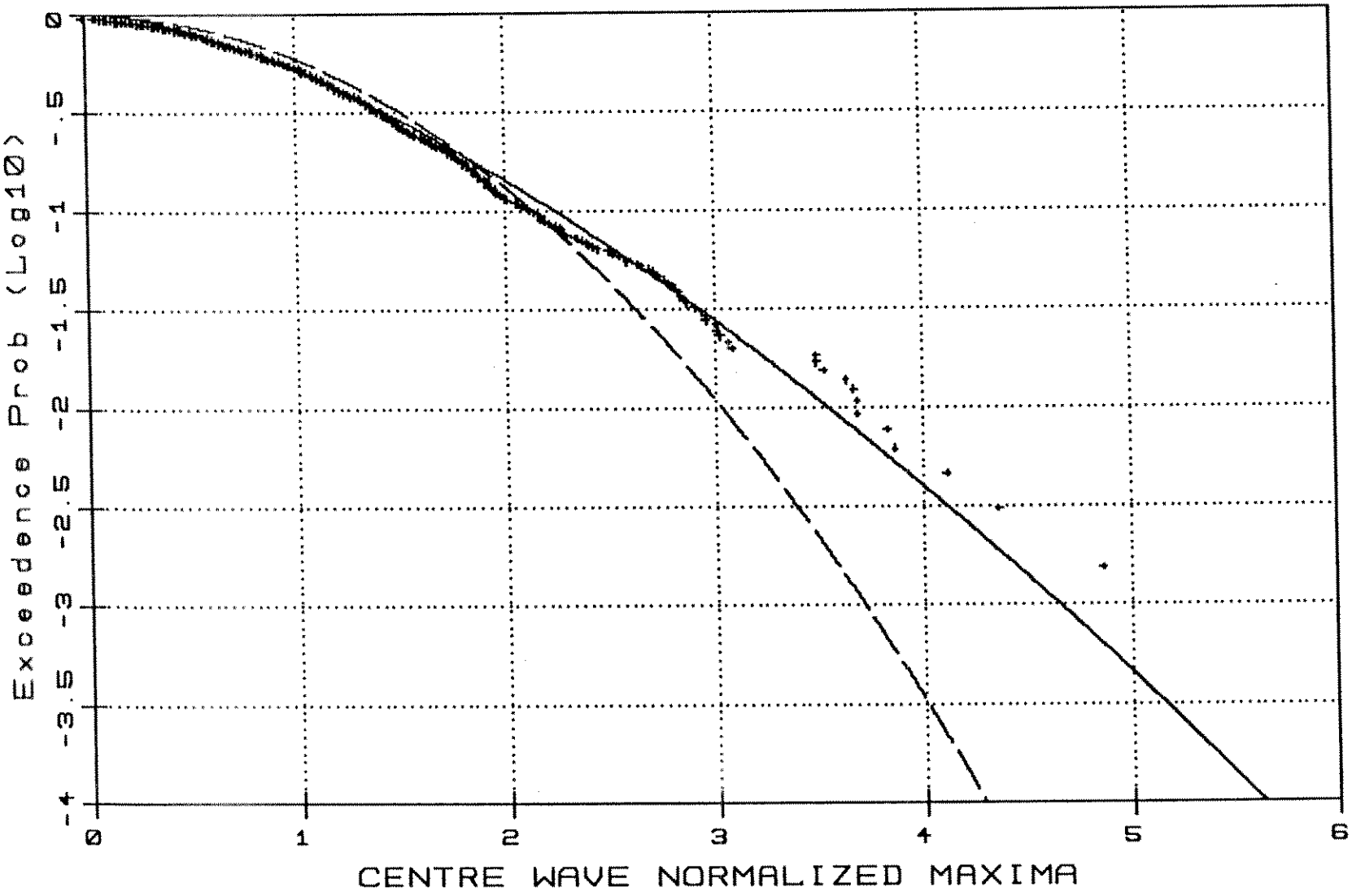
TR4501 -Weibull Type III/Rayleigh
Exceedence Prob (Log10)
0
-.5
-1
-1.5
-2
-2.5
-3
-3.5
-4
0
1
2
3
4
5
6
CENTRE WAVE NORMALIZED MAXIMA

TR4501.W.2

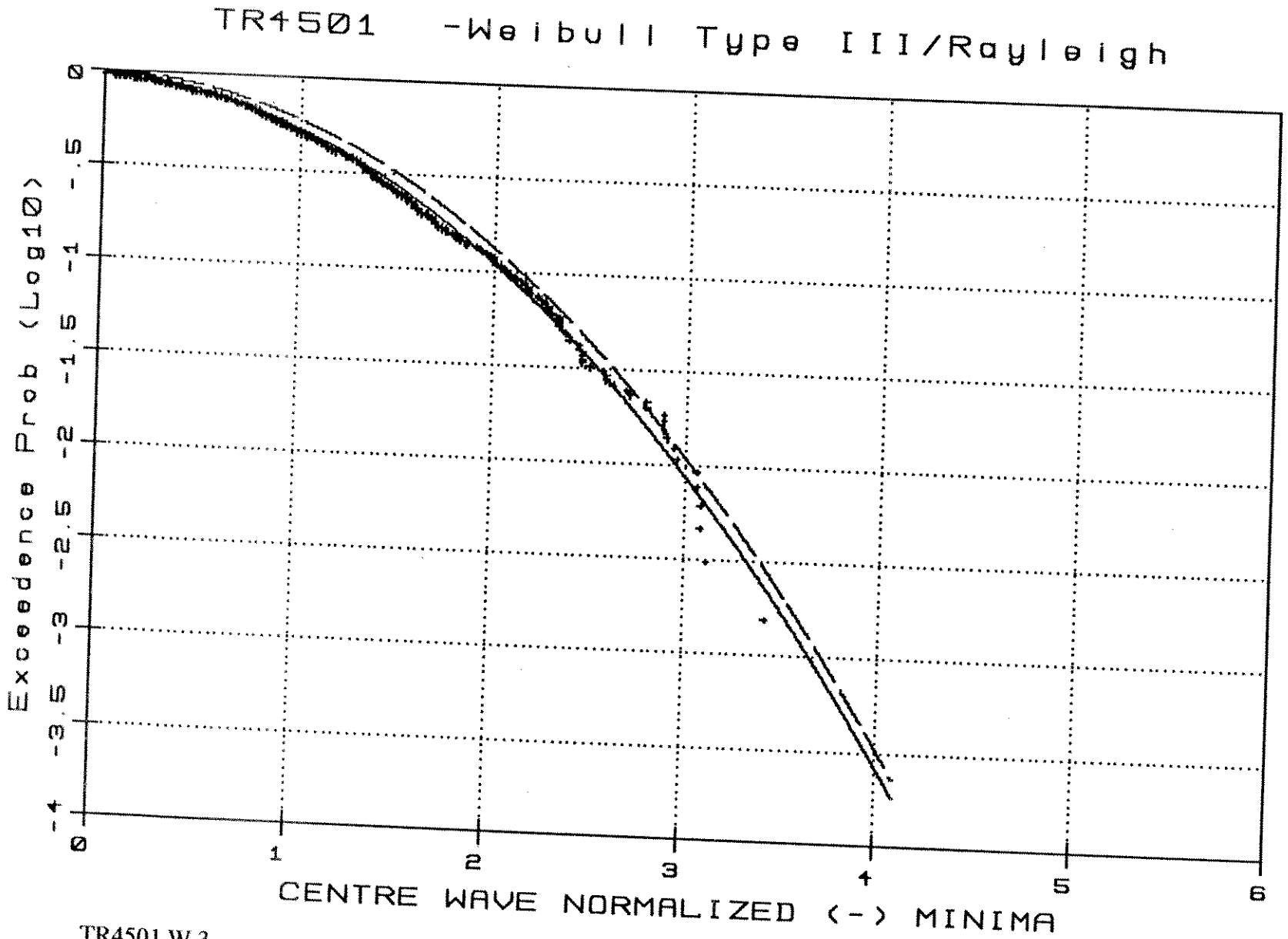
TR4501 -Weibull Type III/Rayleigh
Exceedence Prob (Log10)
0
-.5
-1
-1.5
-2
-2.5
-3
-3.5
-4
0
1
2
3
4
5
6
CENTRE WAVE NORMALIZED (-) MINIMA

TR4501.W.3

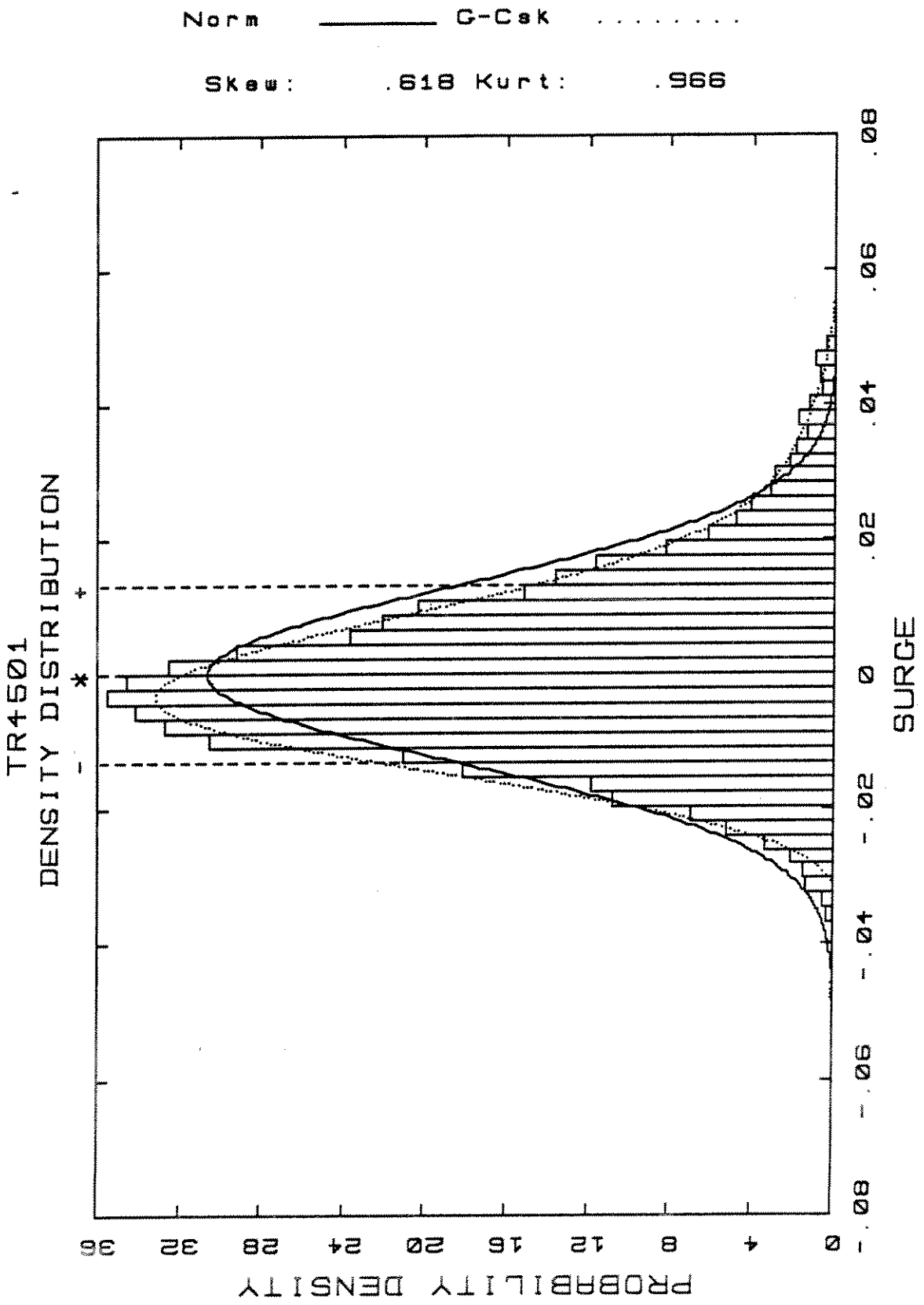
Norm
G-Csk
Skew: .618 Kurt: .966
TR4501
DENSITY DISTRIBUTION
PROBABILITY DENSITY
0 4 8 12 16 20 24 28 32 36
.08 .06 .04 .02 0 -.02 -.04 -.06 -.08
SURGE

TR4501.S.1

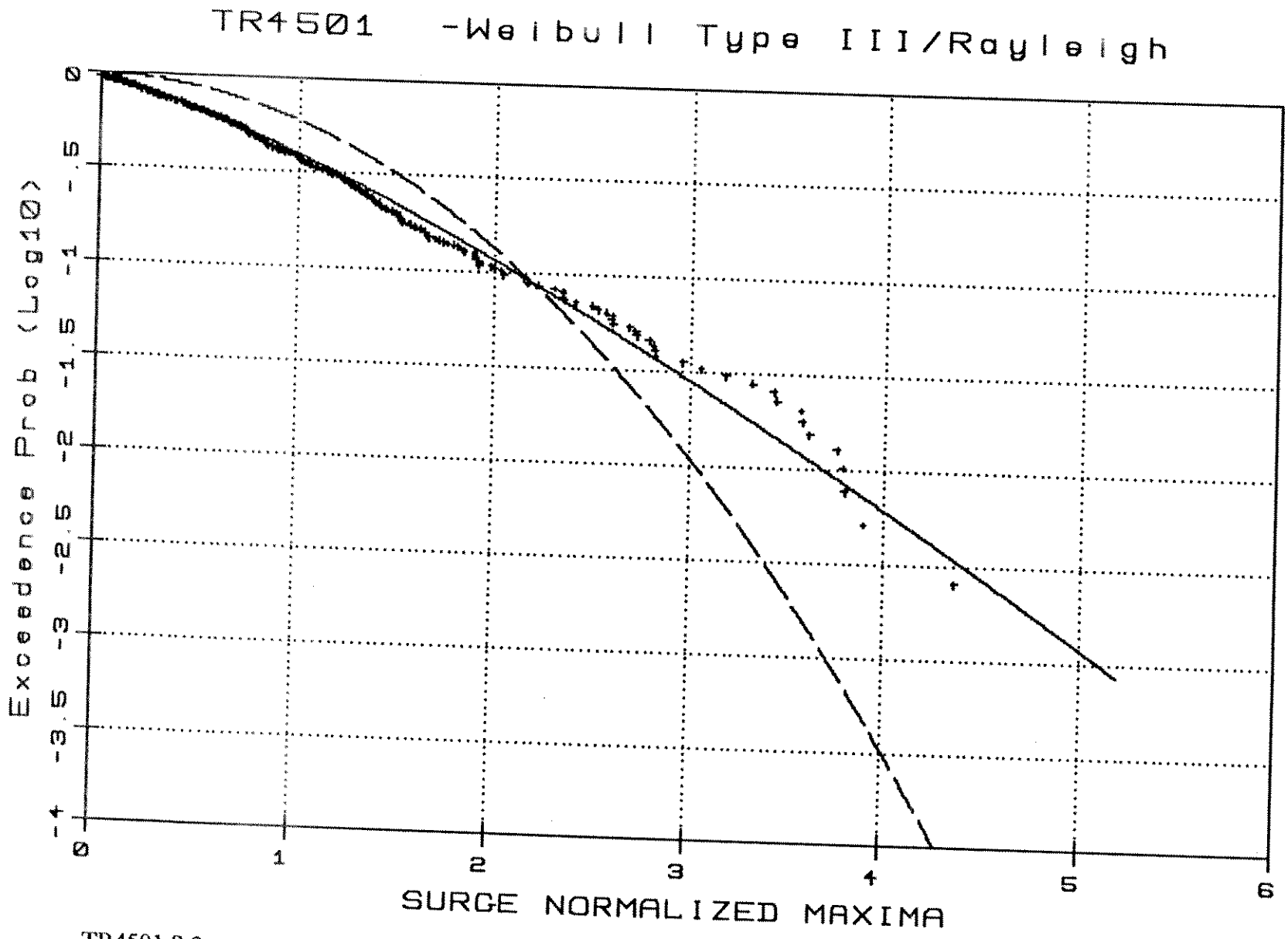
TR4501 -Weibull Type III/Rayleigh
Exceedence Prob (Log10)
0
-.5
-1
-1.5
-2
-2.5
-3
-3.5
-4
0
1
2
3
4
5
6
SURGE NORMALIZED MAXIMA

TR4501.S.2

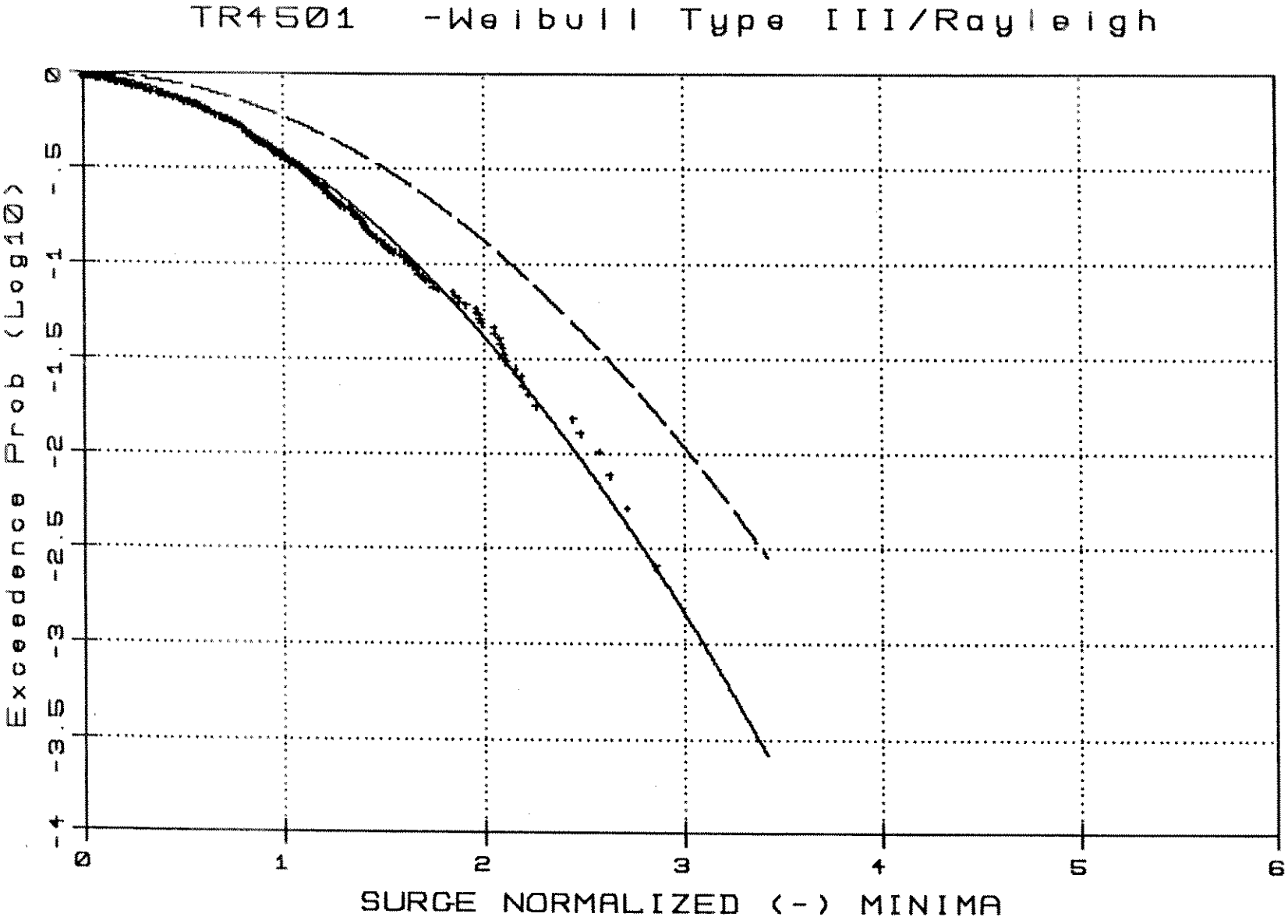
TR4501 -Weibull Type III/Rayleigh
Exceedence Prob (Log10)
0
-.5
-1
-1.5
-2
-2.5
-3
-3.5
-4
0
1
2
3
4
5
6
SURGE NORMALIZED (-) MINIMA

TR4501.S.3

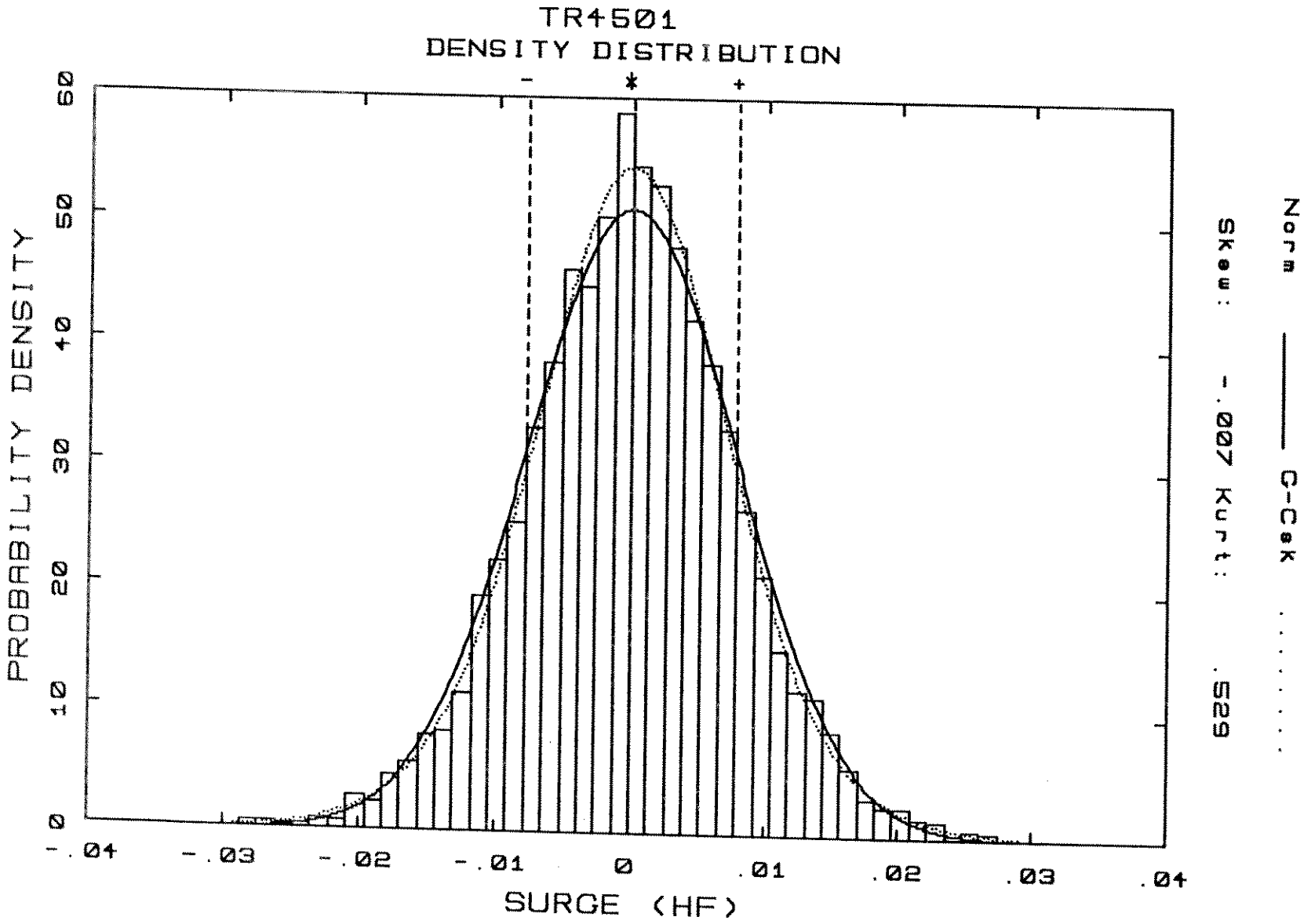
TR4501
DENSITY DISTRIBUTION
PROBABILITY DENSITY
0
10
20
30
40
50
60
-.04
-.03
-.02
-.01
0
.01
.02
.03
.04
SURGE (HF)
Norm
C-Csk
Skew: -.007 Kurt: .529

TR4501.SHF.1

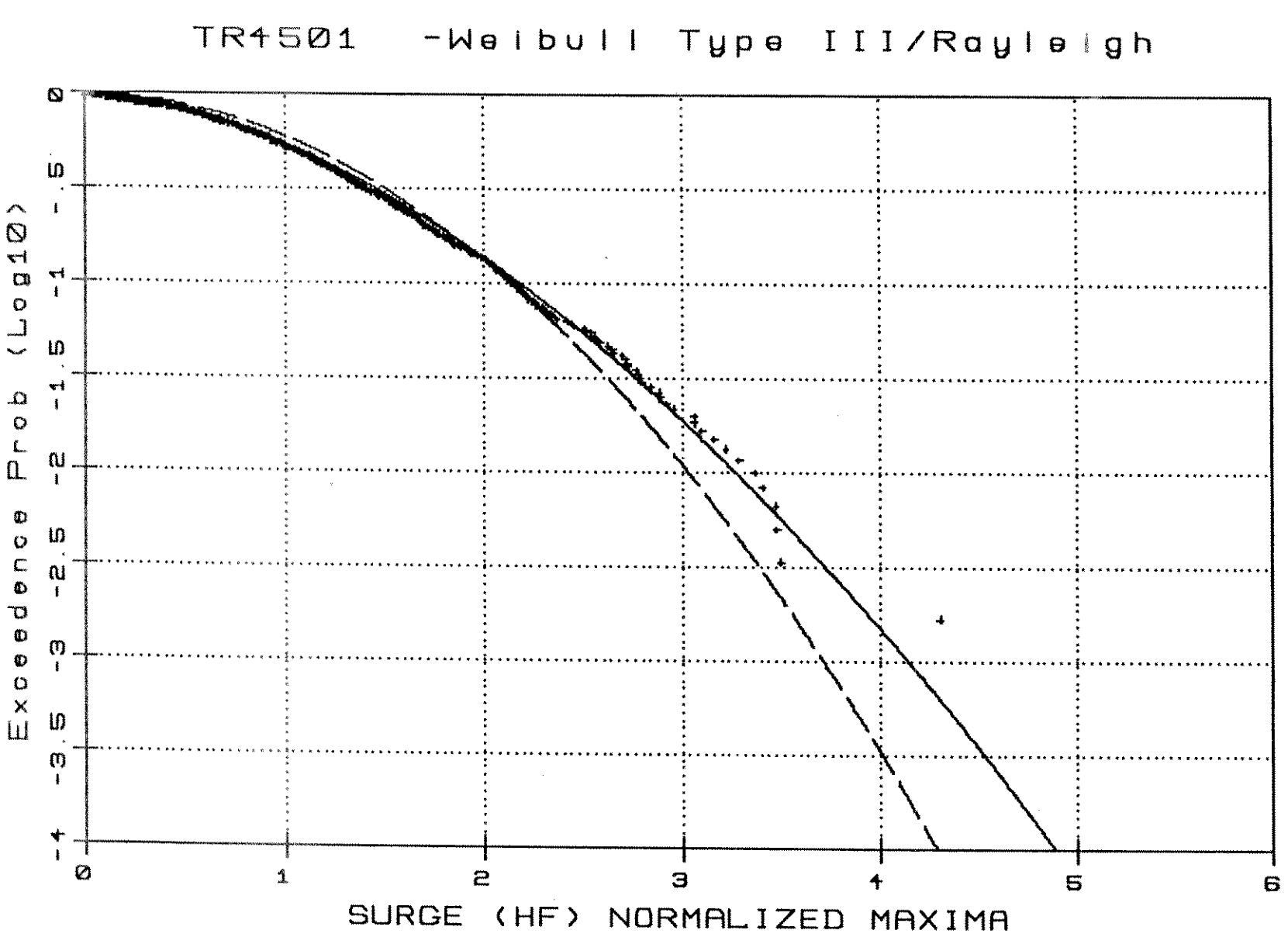
TR4501 -Weibull Type III/Rayleigh
Exceedence Prob (Log10)
0
-.5
-1
-1.5
-2
-2.5
-3
-3.5
-4
0
1
2
3
4
5
6
SURGE (HF) NORMALIZED MAXIMA

TR4501.SHF.2

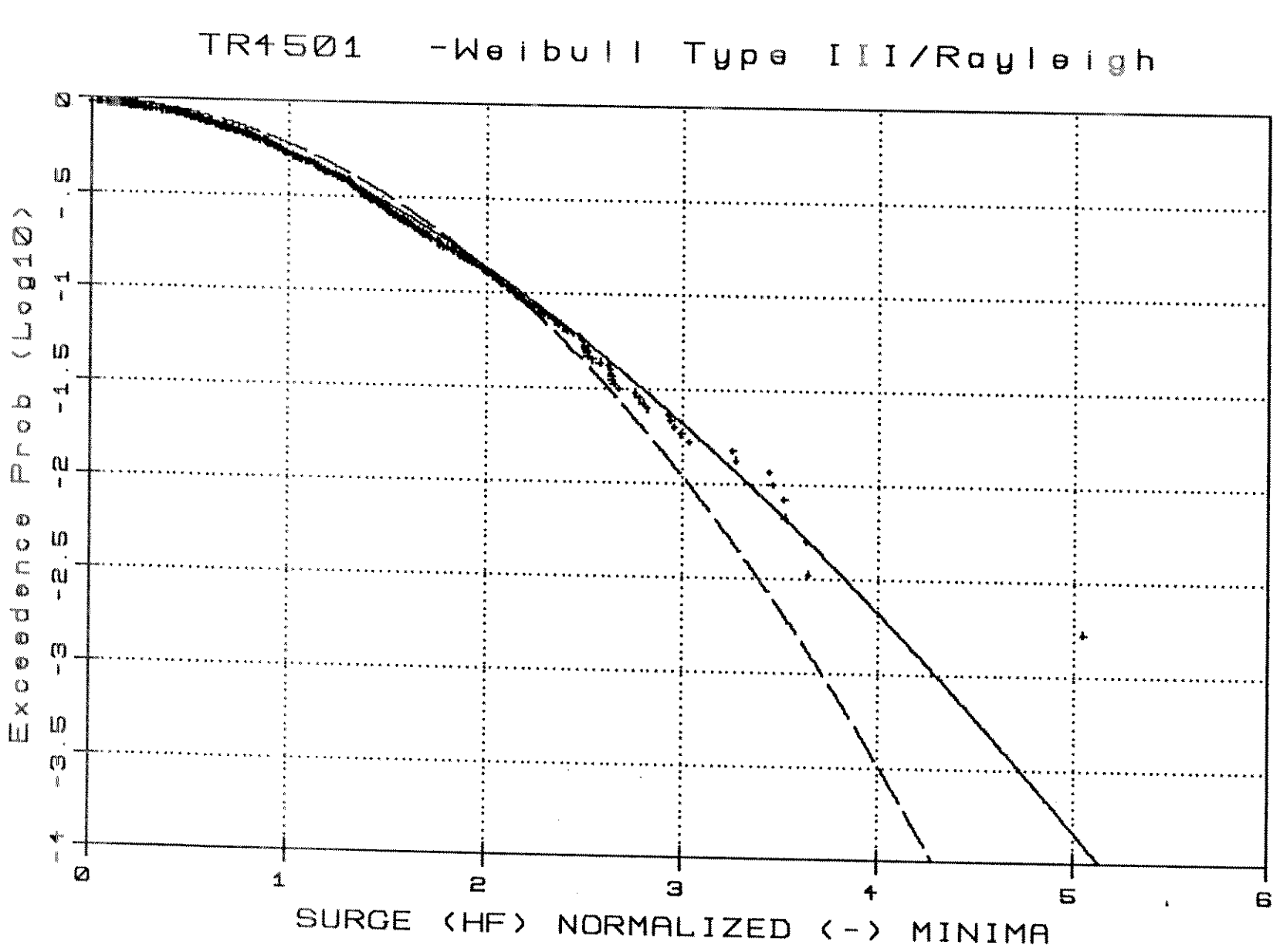
TR4501 -Weibull Type III/Rayleigh
Exceedence Prob (Log10)
0
-.5
-1
-1.5
-2
-2.5
-3
-3.5
-4
0
1
2
3
4
5
6
SURGE (HF) NORMALIZED (-) MINIMA

TR4501.SHF.3

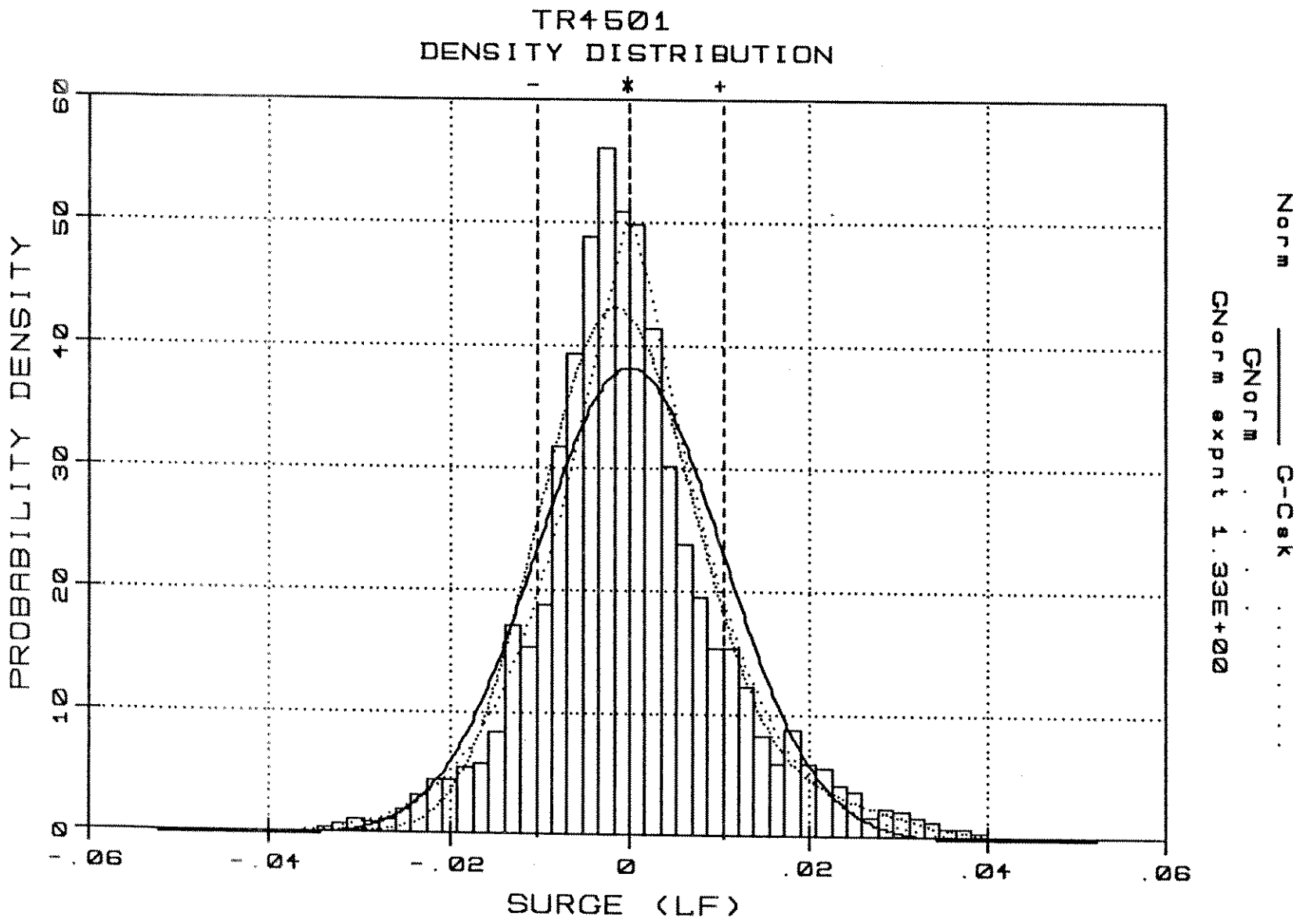
TR4501
DENSITY DISTRIBUTION
PROBABILITY DENSITY
0
10
20
30
40
50
60
-.06
-.04
-.02
0
.02
.04
.06
SURGE (LF)
Norm
GNorm
Q-Csk
GNorm expnt 1.33E+00

TR4501.SLF.1

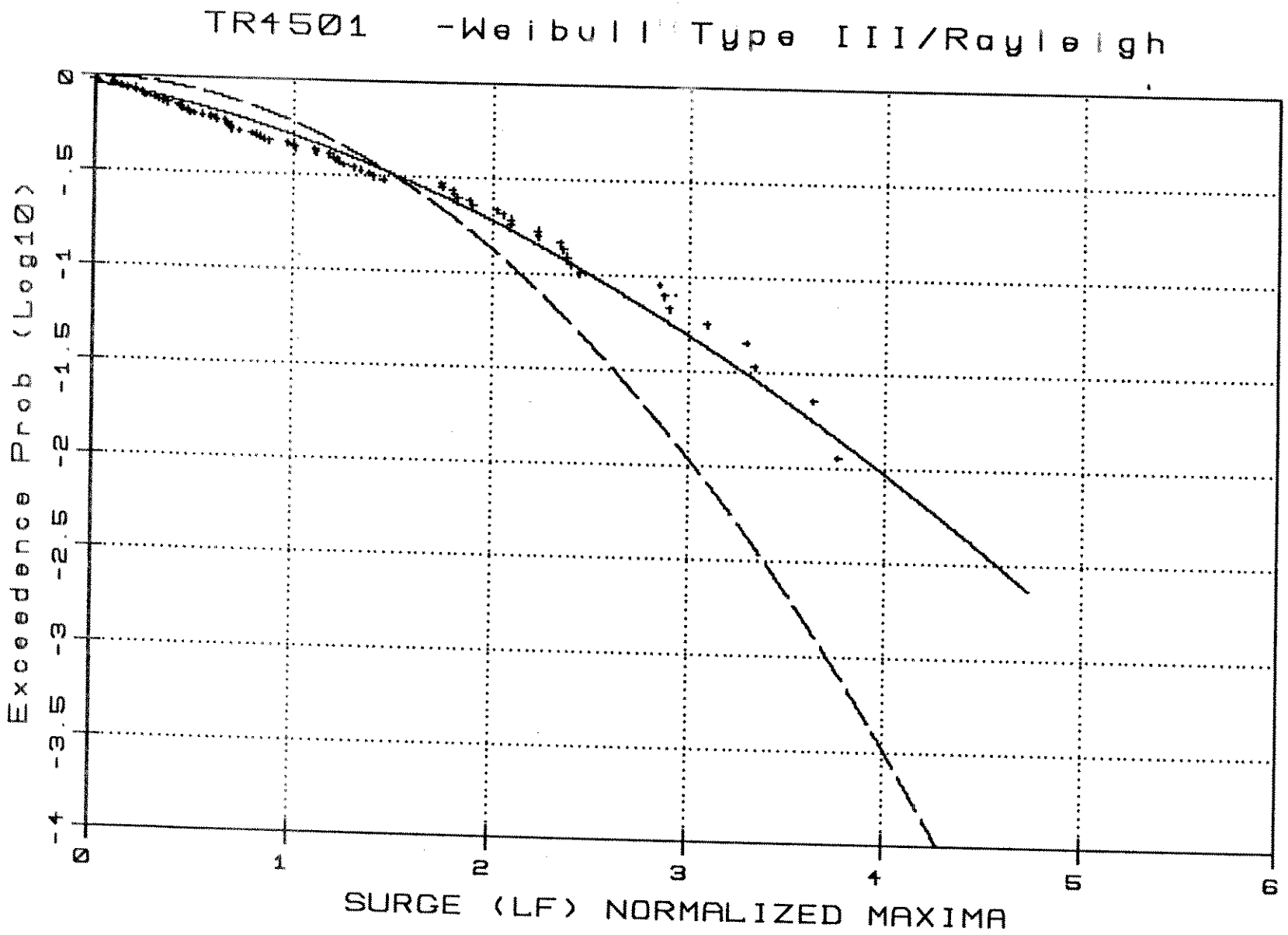
TR4501 -Weibull Type III/Rayleigh
Exceedence Prob (Log10)
0
-.5
-1
-1.5
-2
-2.5
-3
-3.5
-4
0
1
2
3
4
5
6
SURGE (LF) NORMALIZED MAXIMA

TR4501.SLF.2

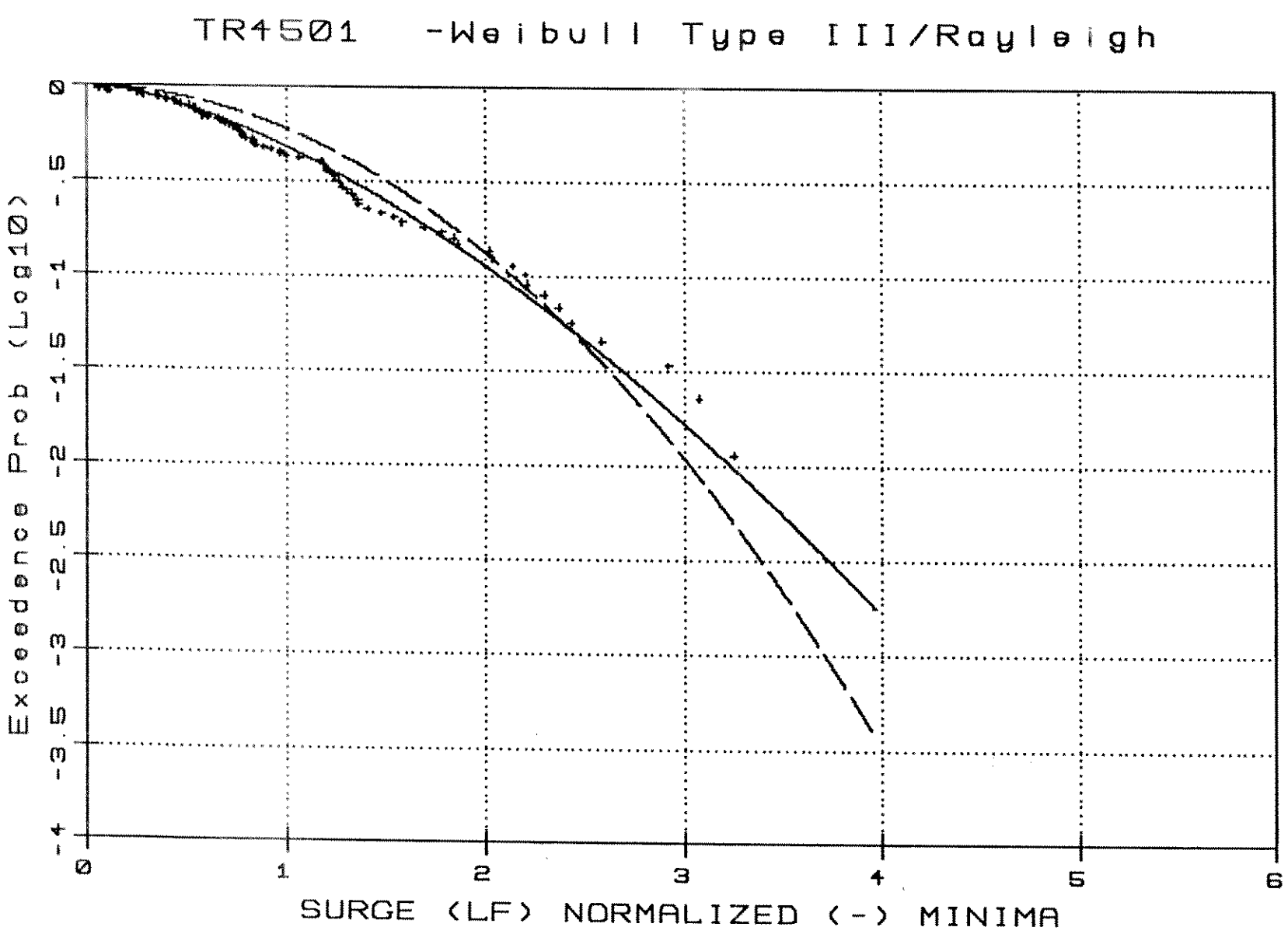
TR4501 -Weibull Type III/Rayleigh
Exceedence Prob (Log10)
0
-.5
-1
-1.5
-2
-2.5
-3
-3.5
-4
0
1
2
3
4
5
6
SURGE (LF) NORMALIZED (-) MINIMA

TR4501.SLF.3

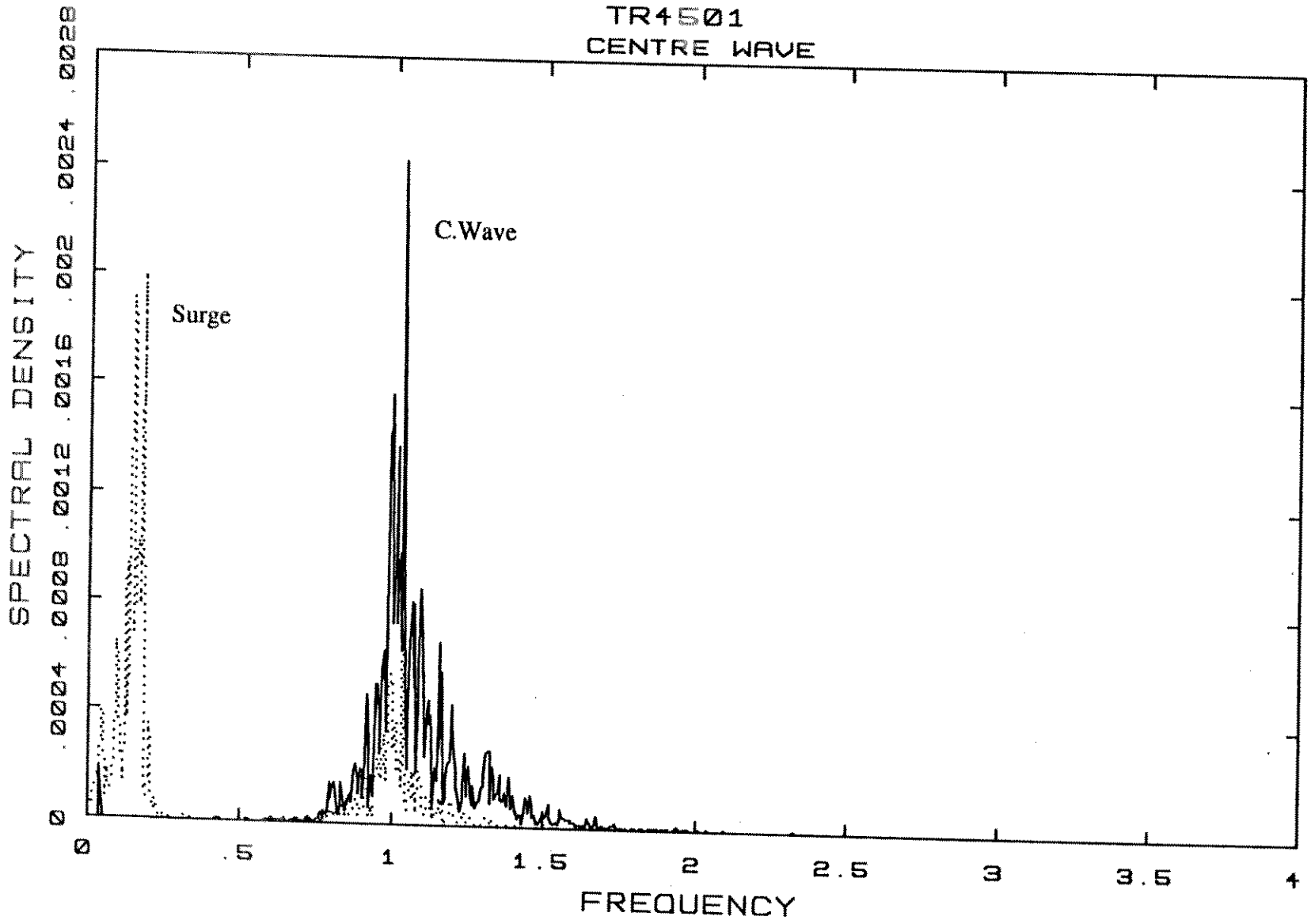
TR4501
CENTRE WAVE
SPECTRAL DENSITY
0
.0004
.0008
.0012
.0016
.002
.0024
.0028
C.Wave
Surge
0
.5
1
1.5
2
2.5
3
3.5
4
FREQUENCY

TR4501.W/S.4

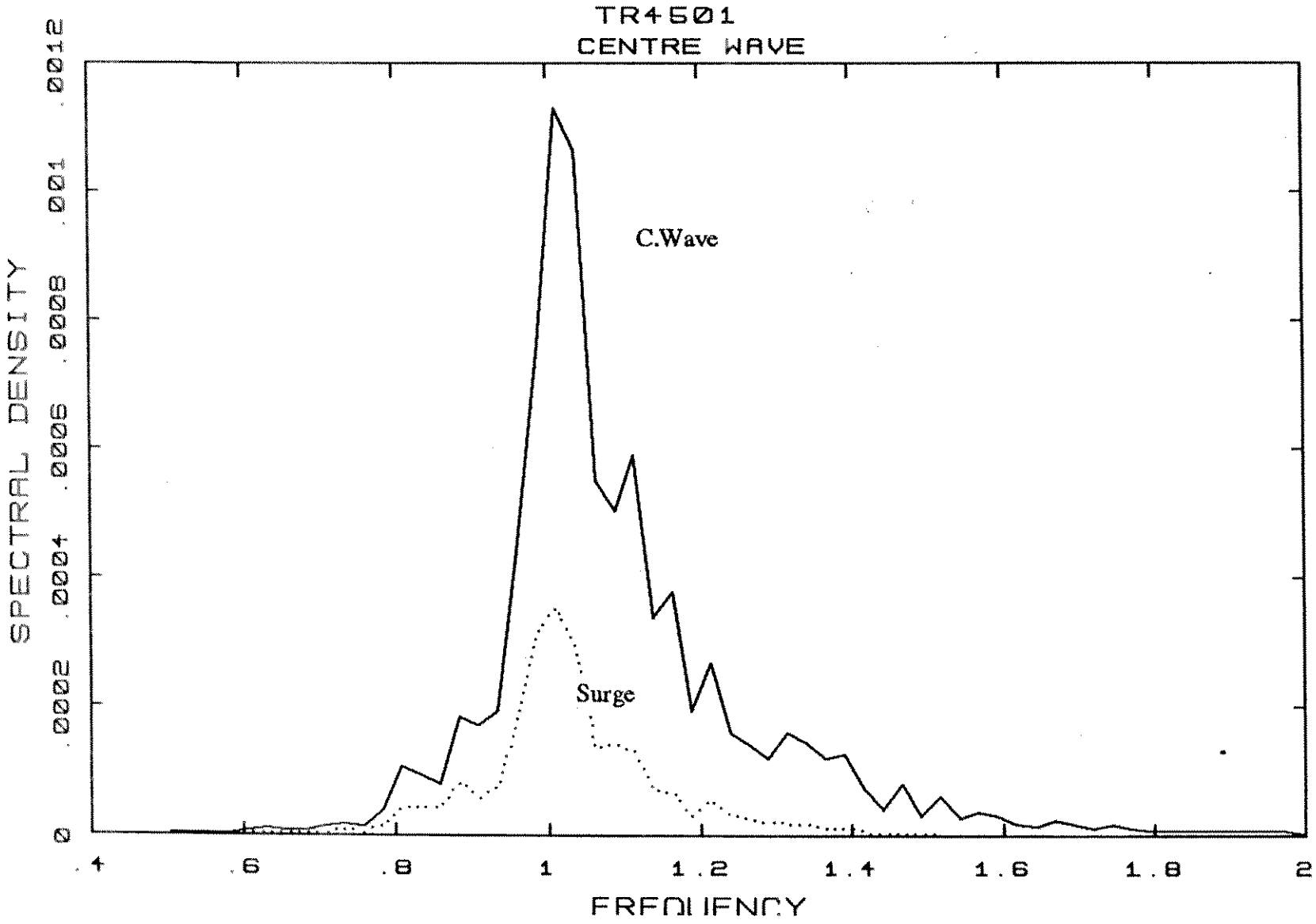
TR4501
CENTRE WAVE
SPECTRAL DENSITY
0
.0002
.0004
.0006
.0008
.001
.0012
C.Wave
Surge
.4
.6
.8
1
1.2
1.4
1.6
1.8
2
FREQUENCY

TR4501.W/S.4*

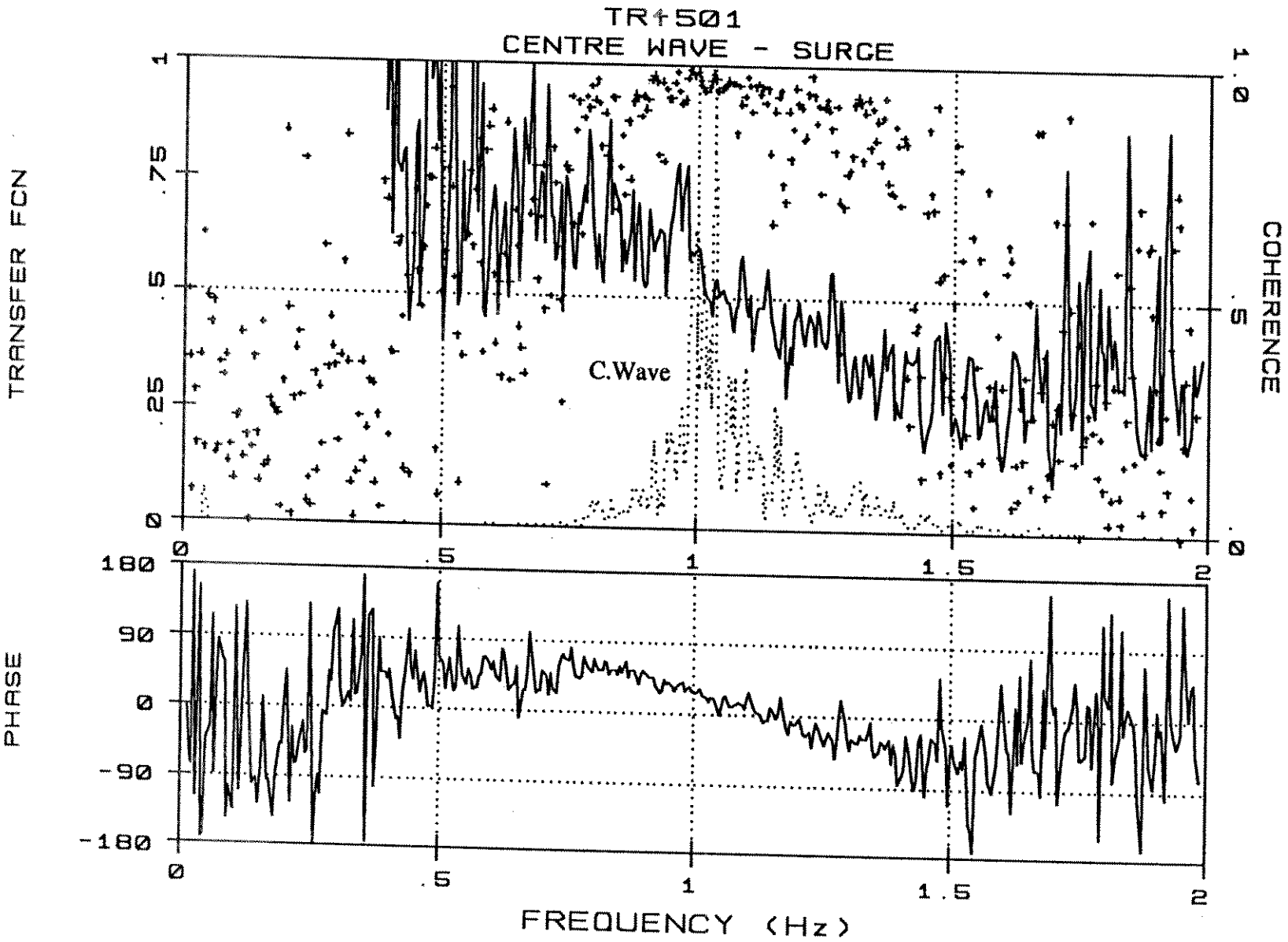
TR4501
CENTRE WAVE - SURGE
TRANSFER FCN
COHERENCE
C.Wave
PHASE
FREQUENCY (Hz)
1
.75
.5
.25
0
1.0
.5
0
180
90
0
-90
-180
.5
1
1.5
2

TR4501.W/S.4t

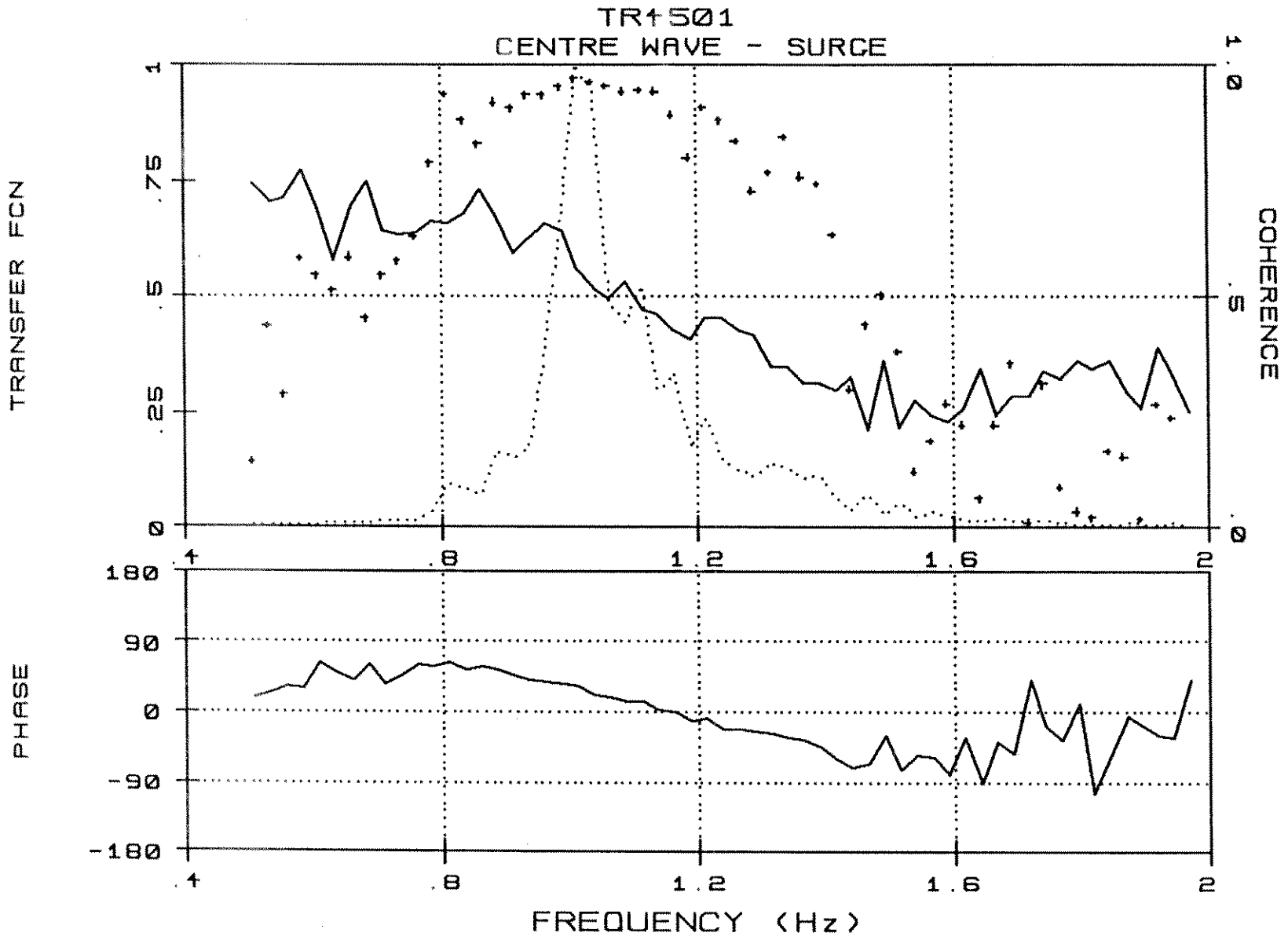
TR4501
CENTRE WAVE - SURGE
TRANSFER FCN
COHERENCE
PHASE
FREQUENCY (Hz)
1
.75
.5
.25
0
1.0
.5
0
180
90
0
-90
-180
.4
.8
1.2
1.6
2

TR4501.W/S.4t*

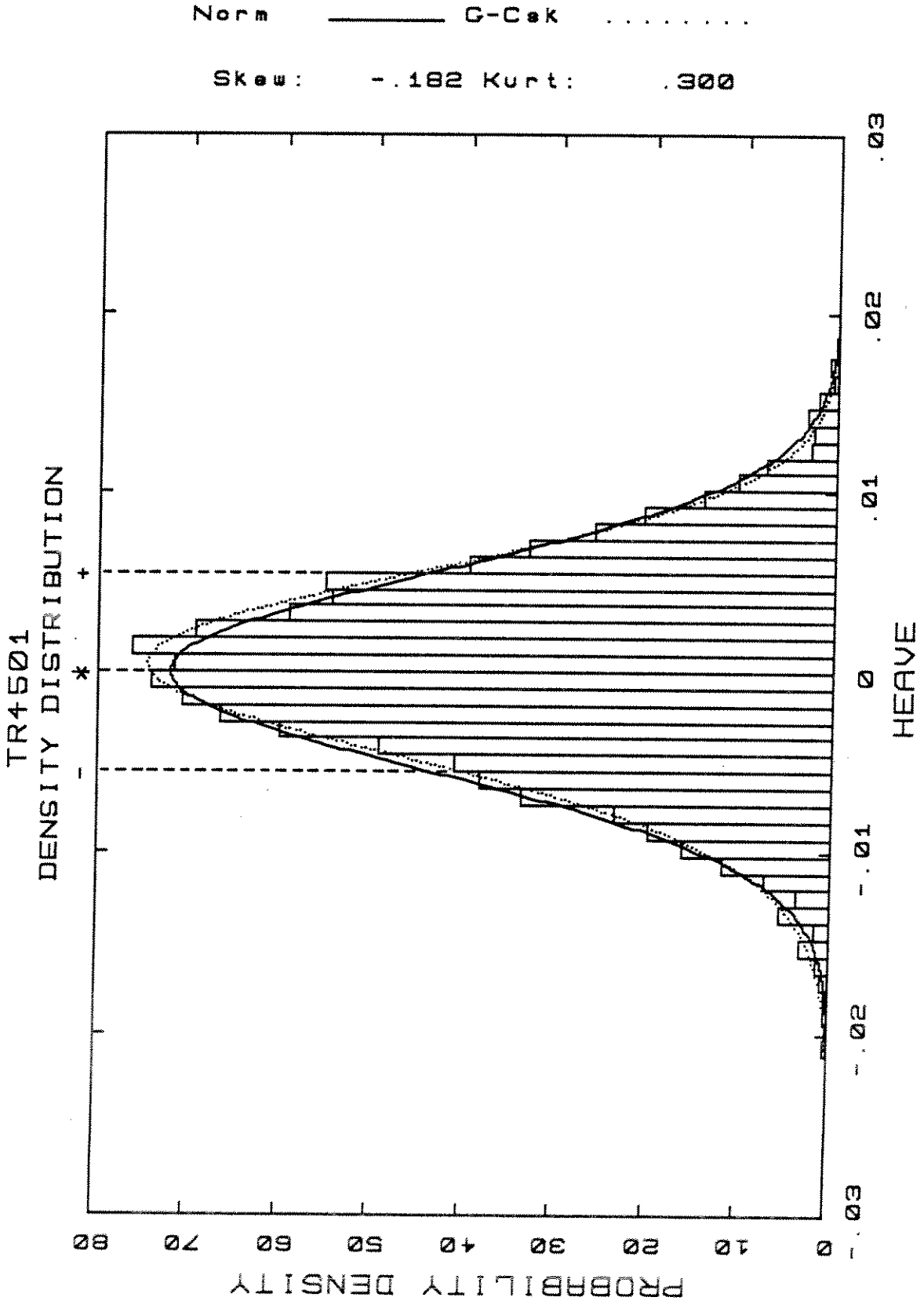
Norm _____ G-Cak .....
Skew: -.182 Kurt: .300
TR4501
DENSITY DISTRIBUTION
+
*
-
PROBABILITY DENSITY
0
10
20
30
40
50
60
70
80
-.03
-.02
-.01
0
.01
.02
.03
HEAVE

TR4501.H.1

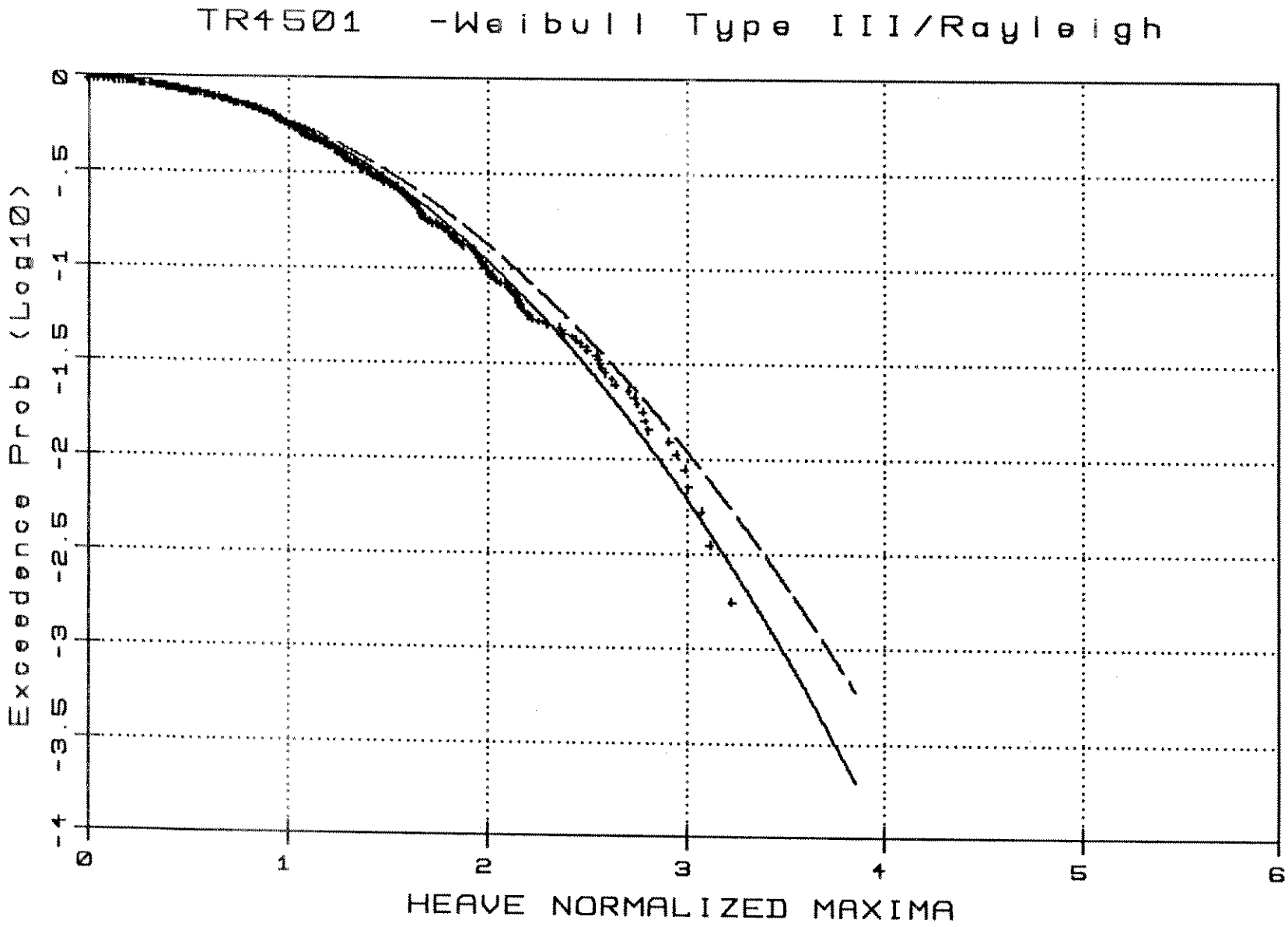

TR4501.H.2

Heave + down.

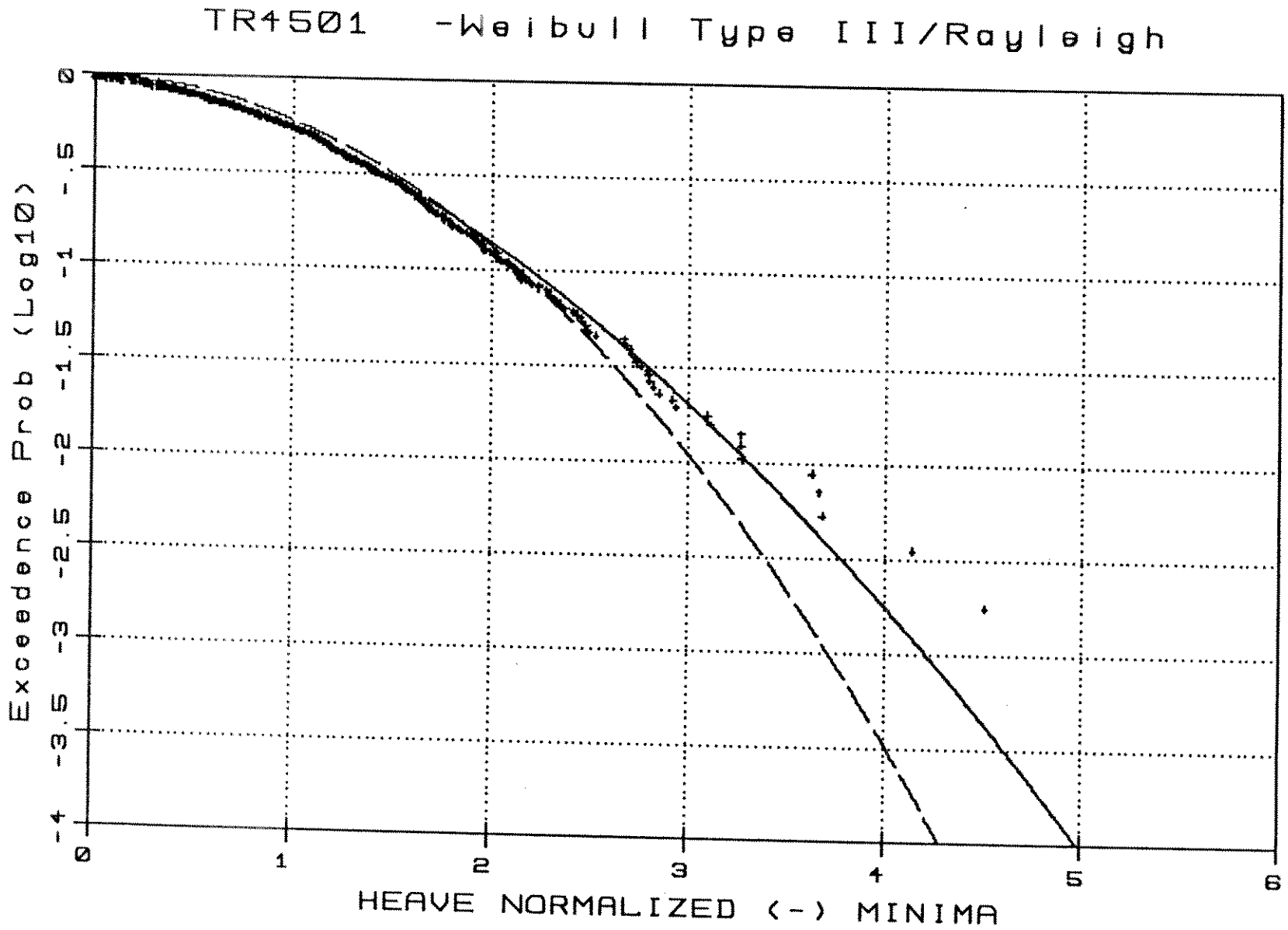

TR4501.H.3
Heave + down.

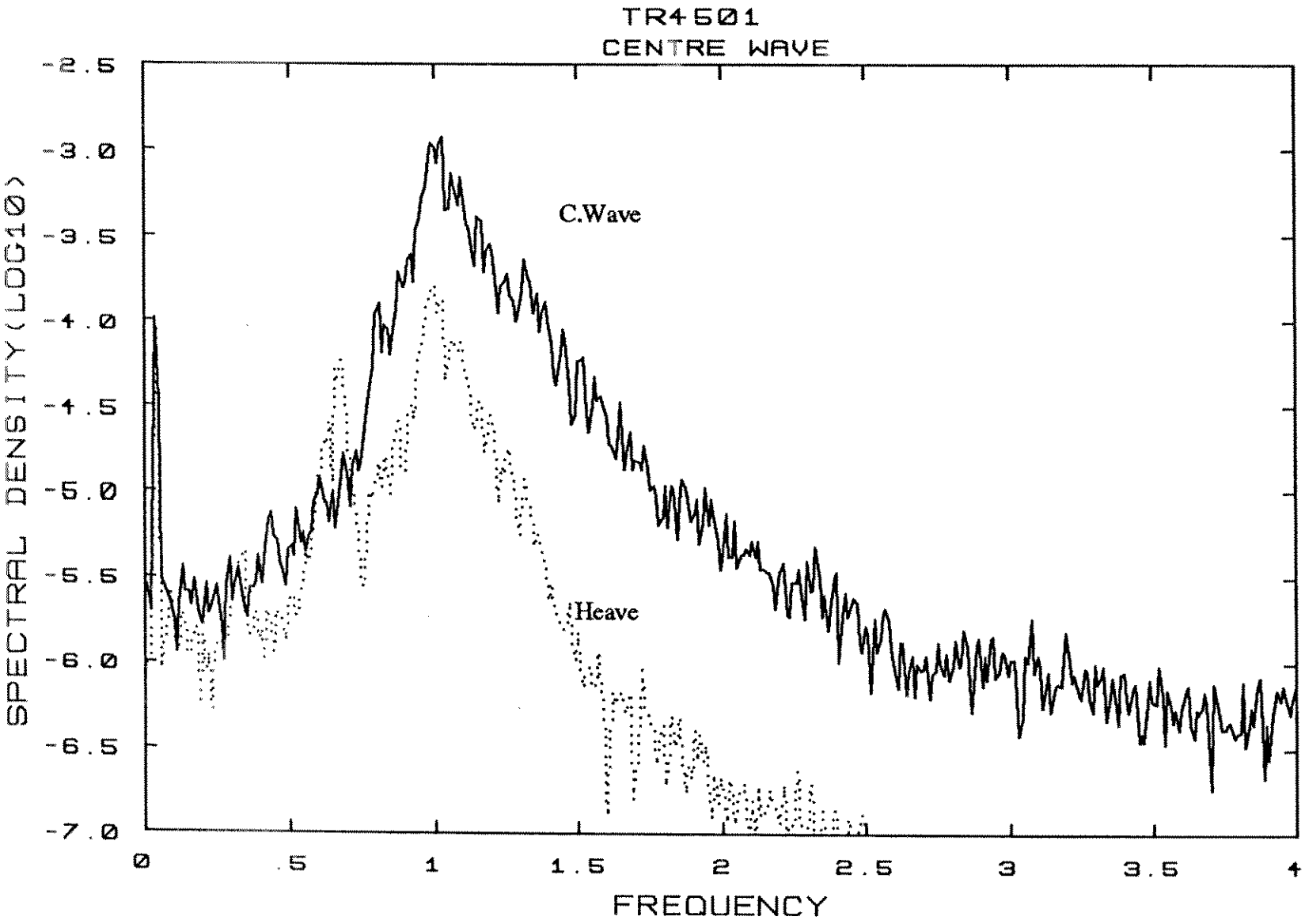
TR4501
CENTRE WAVE
SPECTRAL DENSITY(LOG10)
-2.5
-3.0
-3.5
-4.0
-4.5
-5.0
-5.5
-6.0
-6.5
-7.0
C.Wave
Heave
0
.5
1
1.5
2
2.5
3
3.5
4
FREQUENCY

TR4501.W/H.4

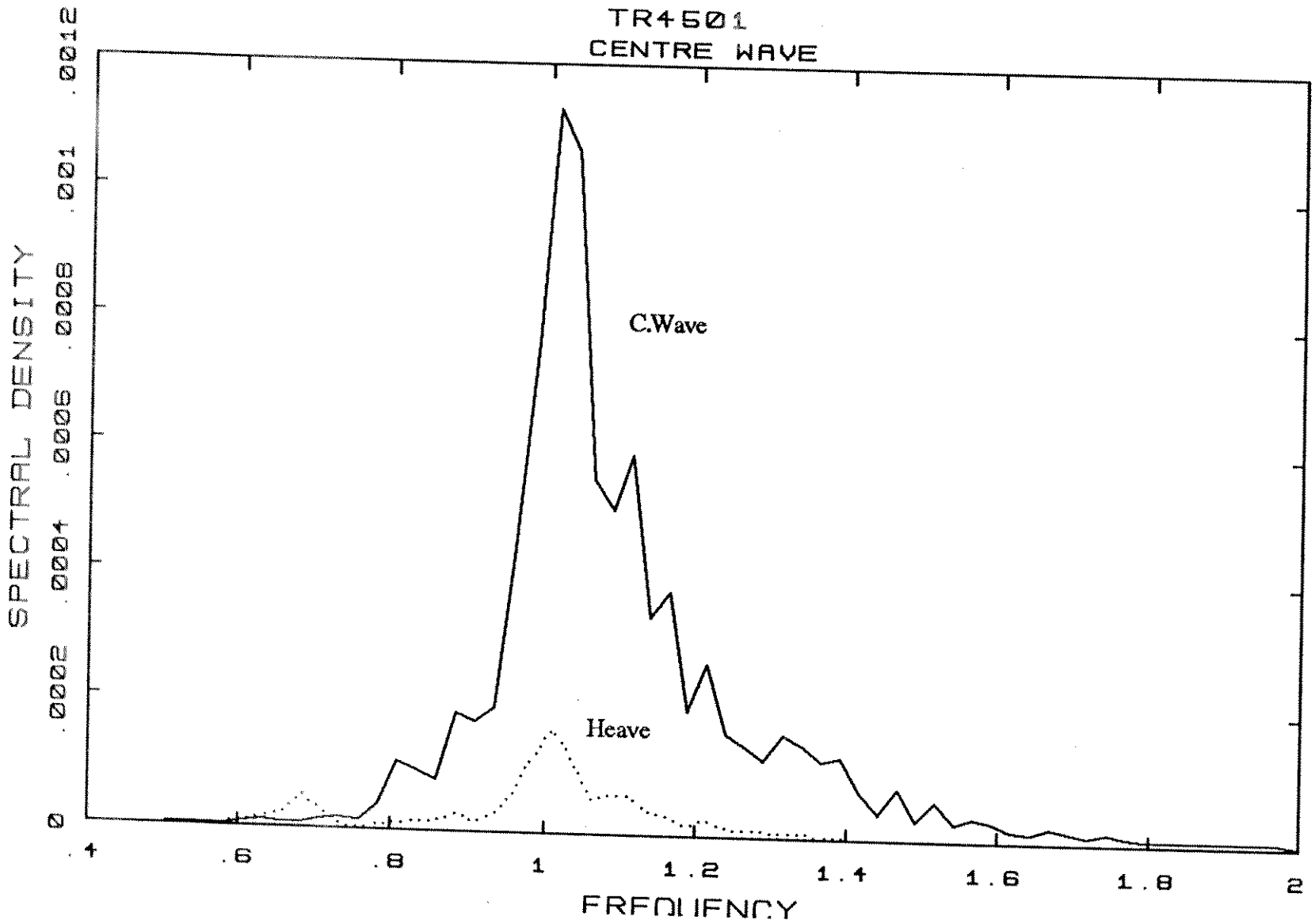
TR4501
CENTRE WAVE
SPECTRAL DENSITY
0
.0002
.0004
.0006
.0008
.001
.0012
C.Wave
Heave
.4
.6
.8
1
1.2
1.4
1.6
1.8
2
FREQUENCY

TR4501.W/H.4*

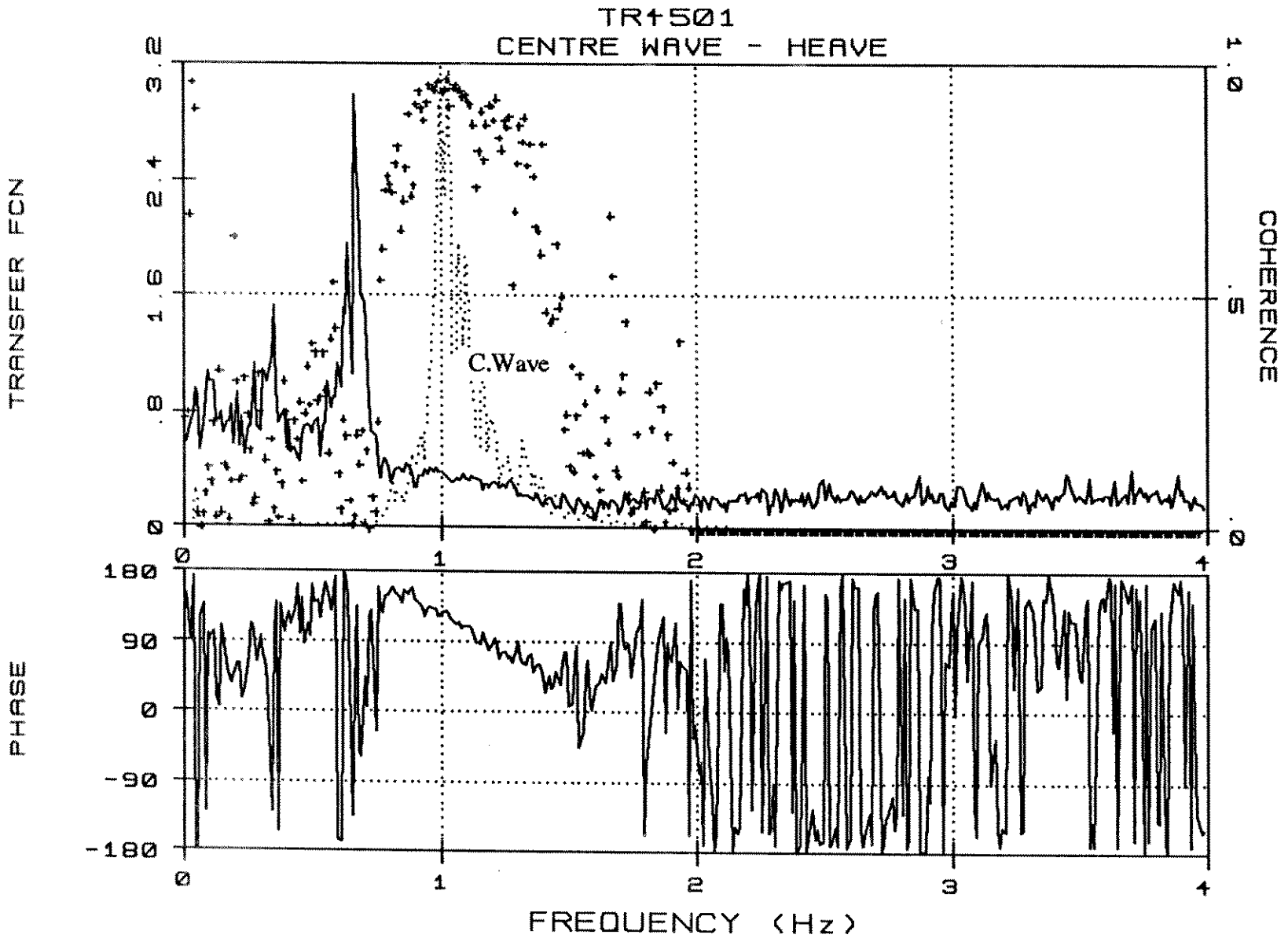
TR1501
CENTRE WAVE - HEAVE
TRANSFER FCN
3.2
2.4
1.6
.8
0
COHERENCE
1.0
.5
0
C.Wave
0
1
2
3
4
PHASE
180
90
0
-90
-180
FREQUENCY (Hz)

TR4501.W/H.4t

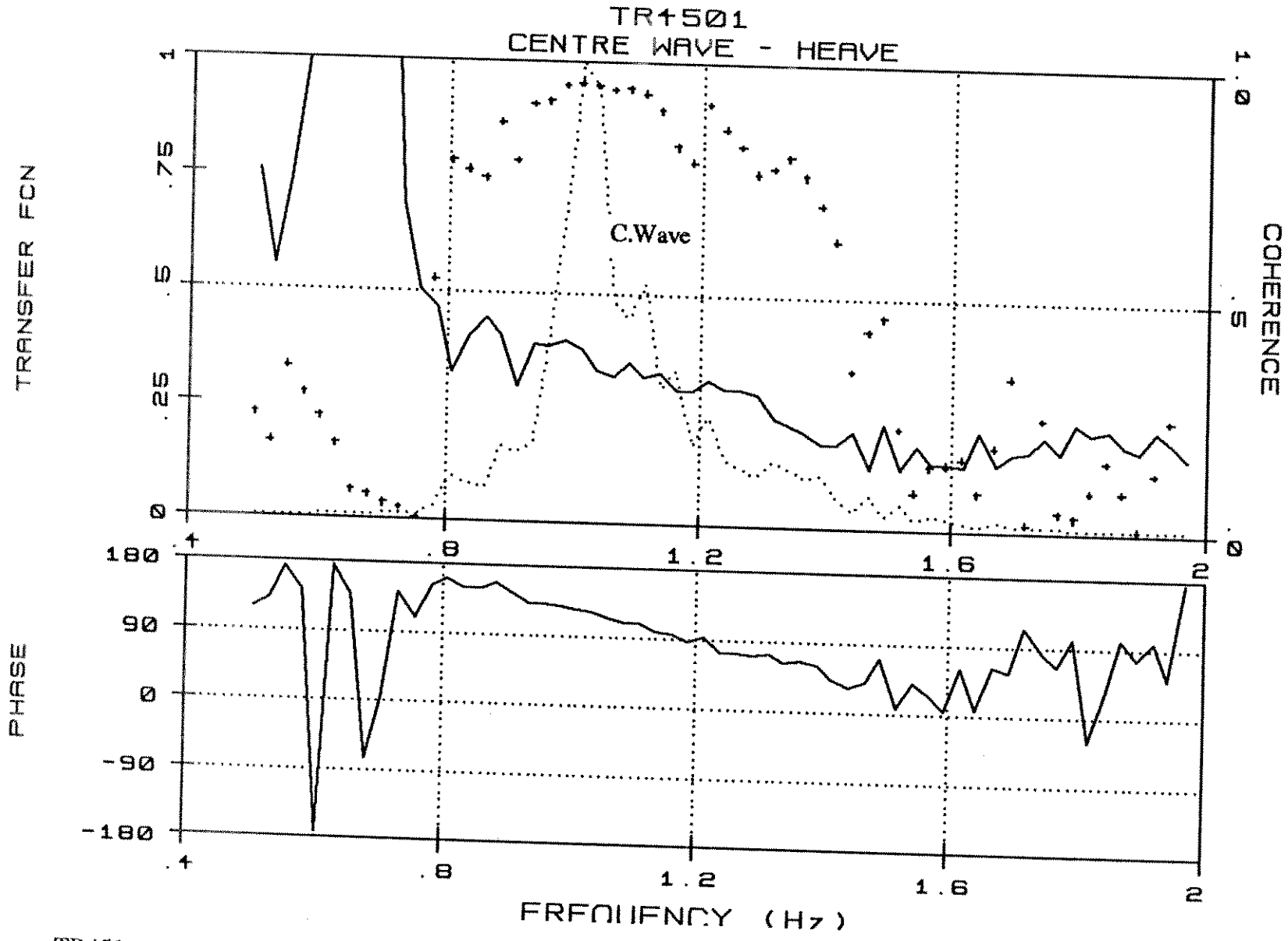
TR4501
CENTRE WAVE - HEAVE
TRANSFER FCN
COHERENCE
C.Wave
1
.75
.5
.25
0
1.0
.5
0
180
90
0
-90
-180
PHASE
.4
.8
1.2
1.6
2
FREQUENCY (Hz)

TR4501.W/H.4t*

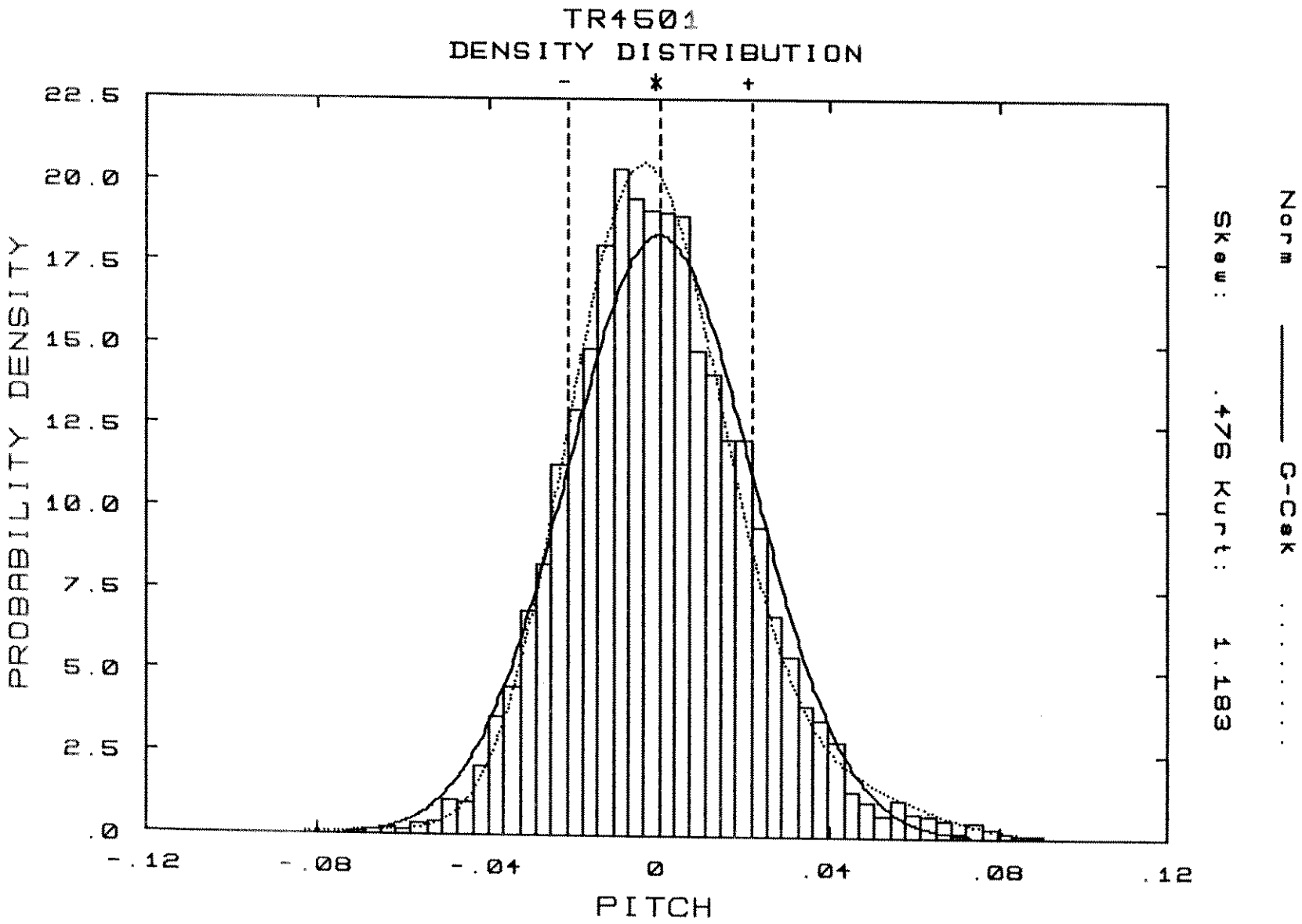
TR4501
DENSITY DISTRIBUTION
- * +
22.5
20.0
17.5
15.0
12.5
10.0
7.5
5.0
2.5
.0
PROBABILITY DENSITY
-.12
-.08
-.04
0
.04
.08
.12
PITCH
Norm
C-Cek
Skew: .476 Kurt: 1.183

TR4501.Pi.1

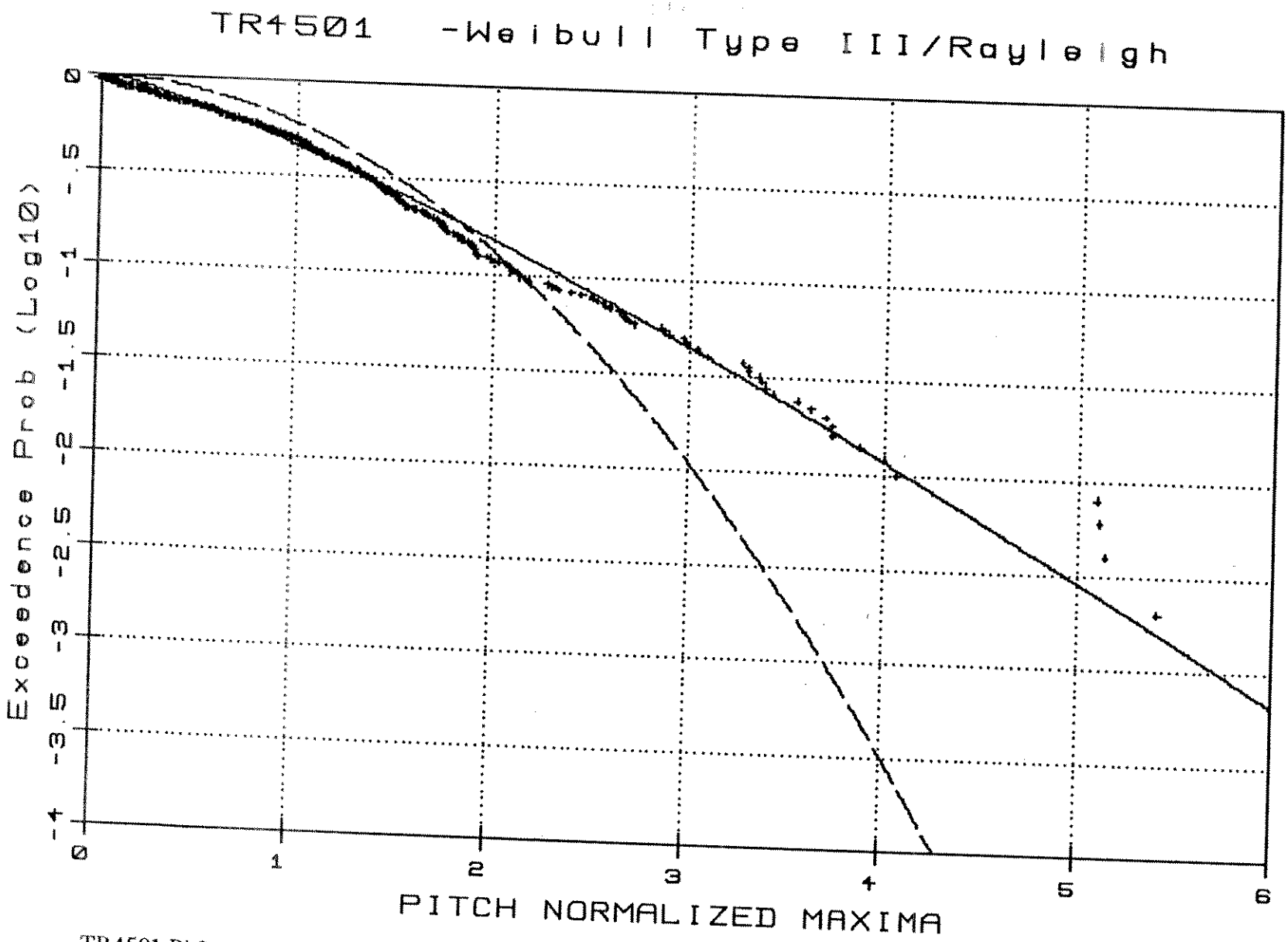
TR4501 -Weibull Type III/Rayleigh
Exceedence Prob (Log10)
0
-.5
-1
-1.5
-2
-2.5
-3
-3.5
-4
0
1
2
3
4
5
6
PITCH NORMALIZED MAXIMA

TR4501.Pi.2

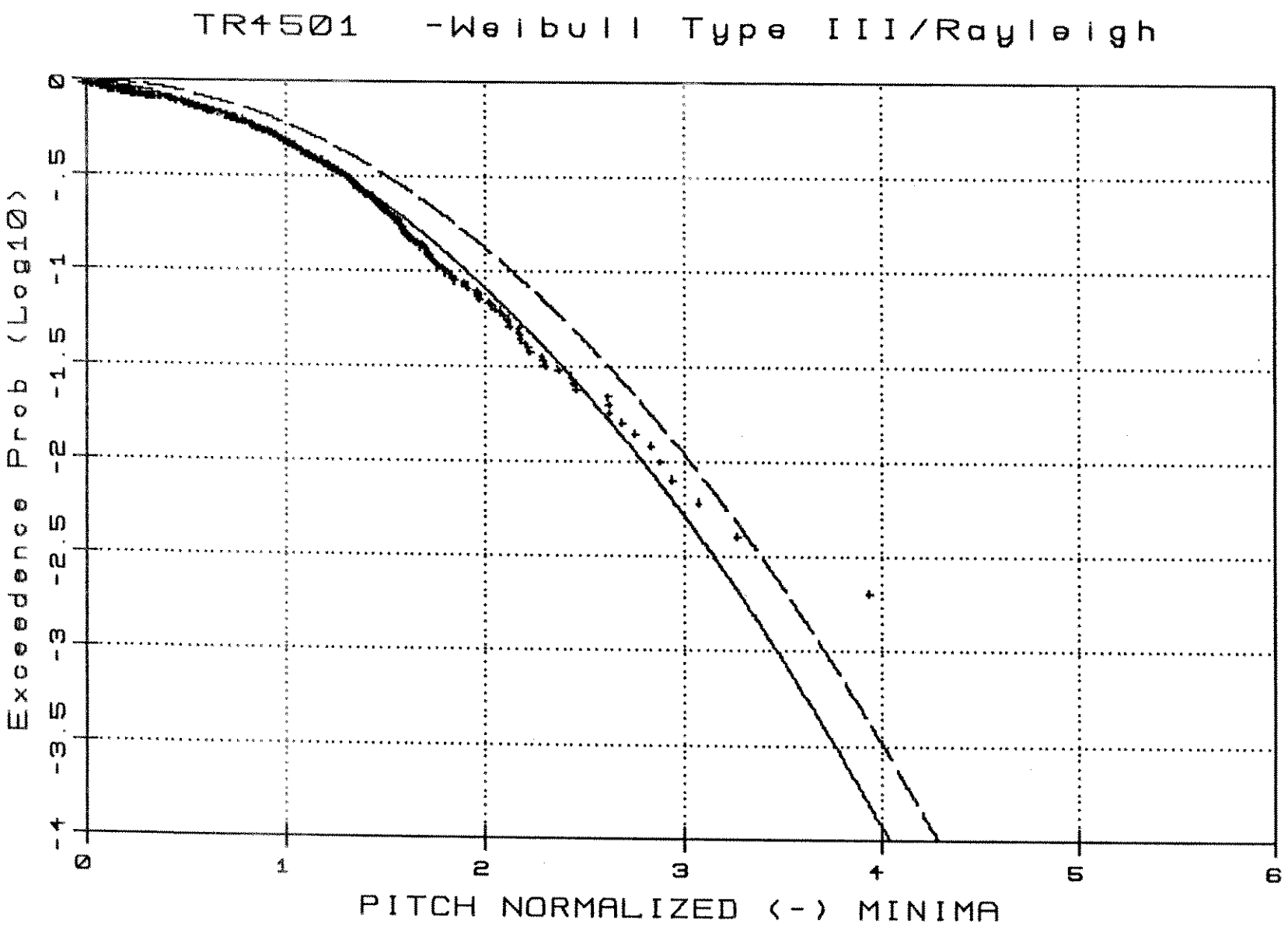
TR4501 -Weibull Type III/Rayleigh
Exceedence Prob (Log10)
0
-.5
-1
-1.5
-2
-2.5
-3
-3.5
-4
0
1
2
3
4
5
6
PITCH NORMALIZED (-) MINIMA

TR4501.Pi.3

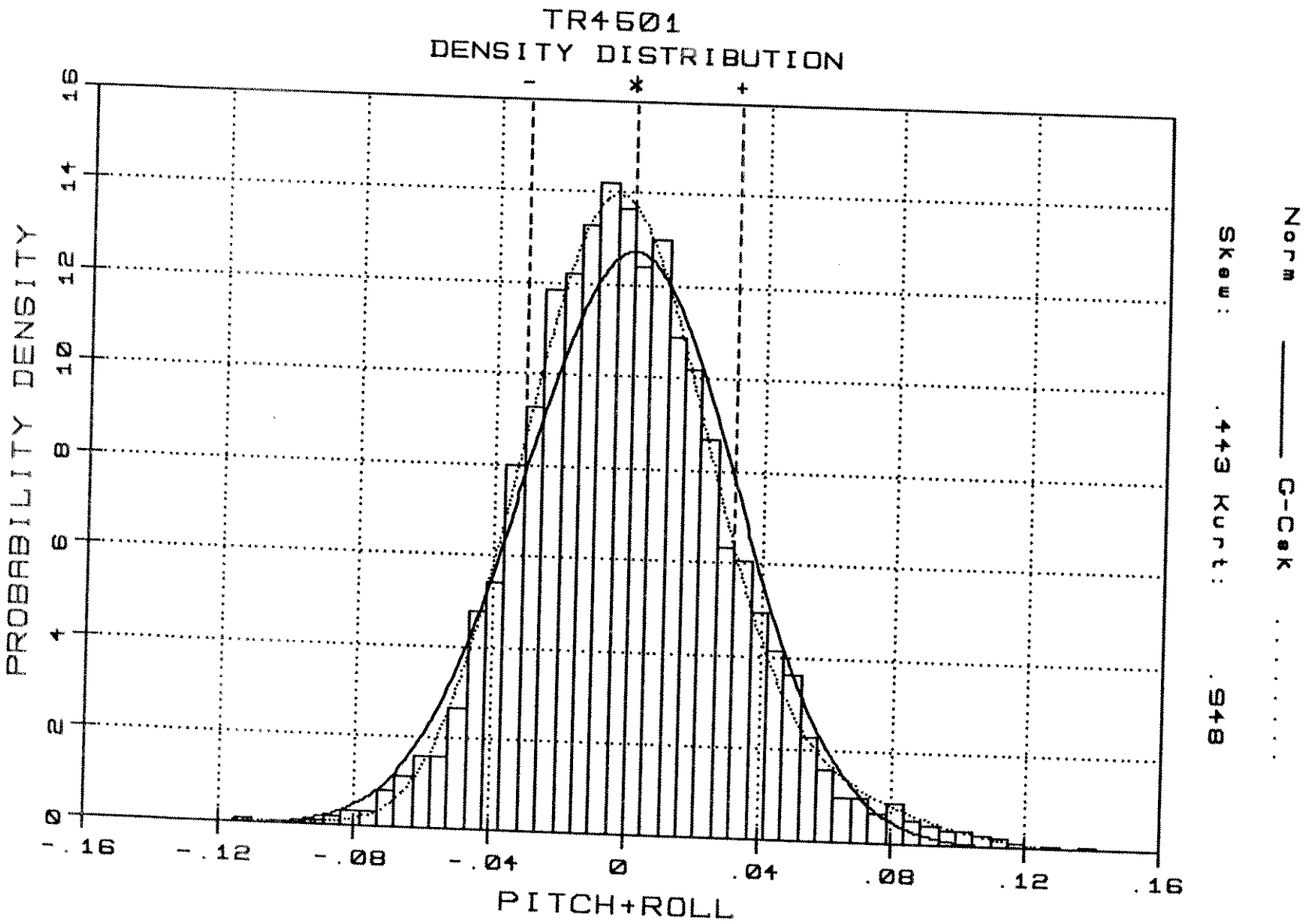

TR4501.Pi+Ro.1

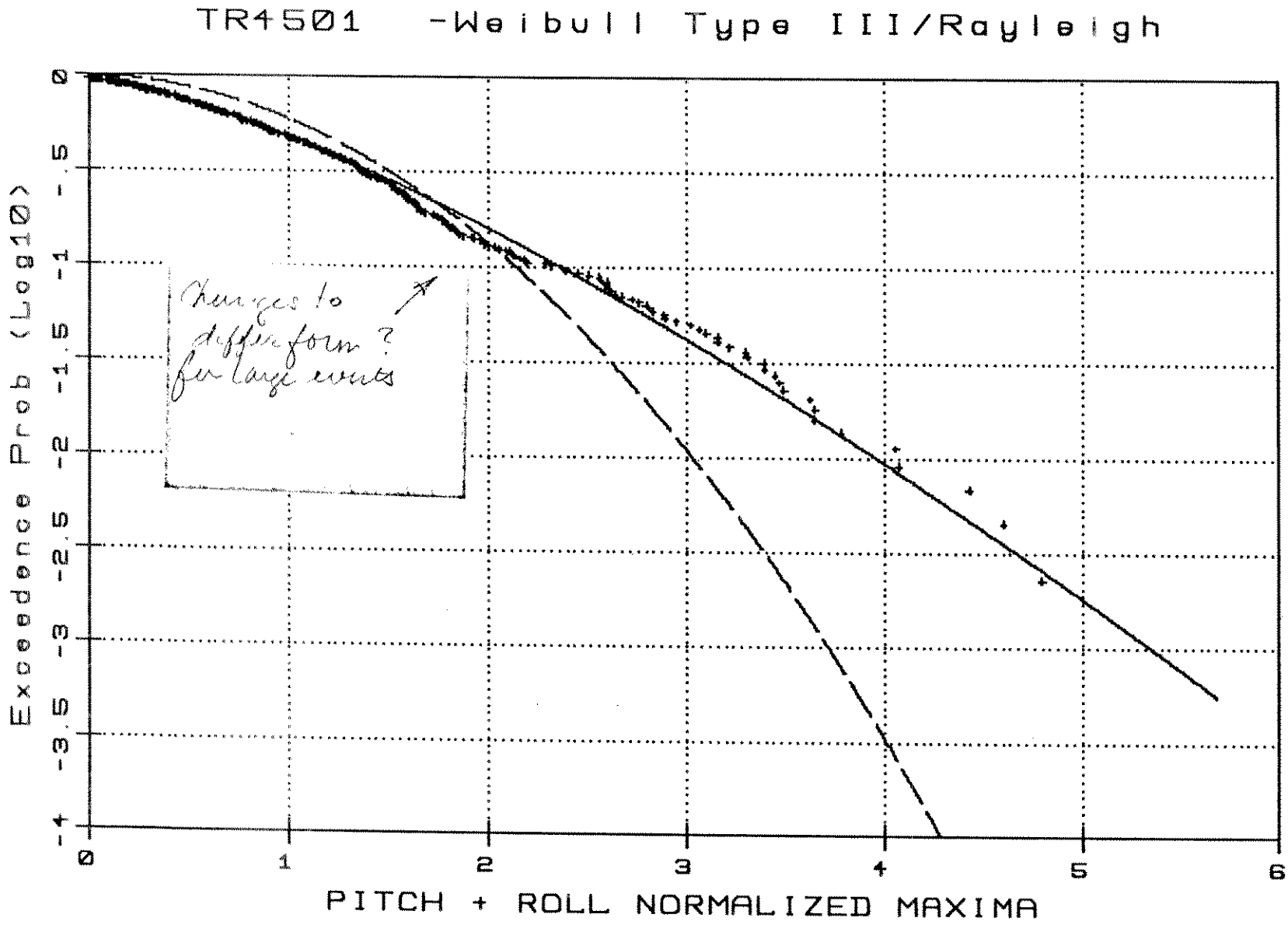

TR4501.Pi+Ro.2

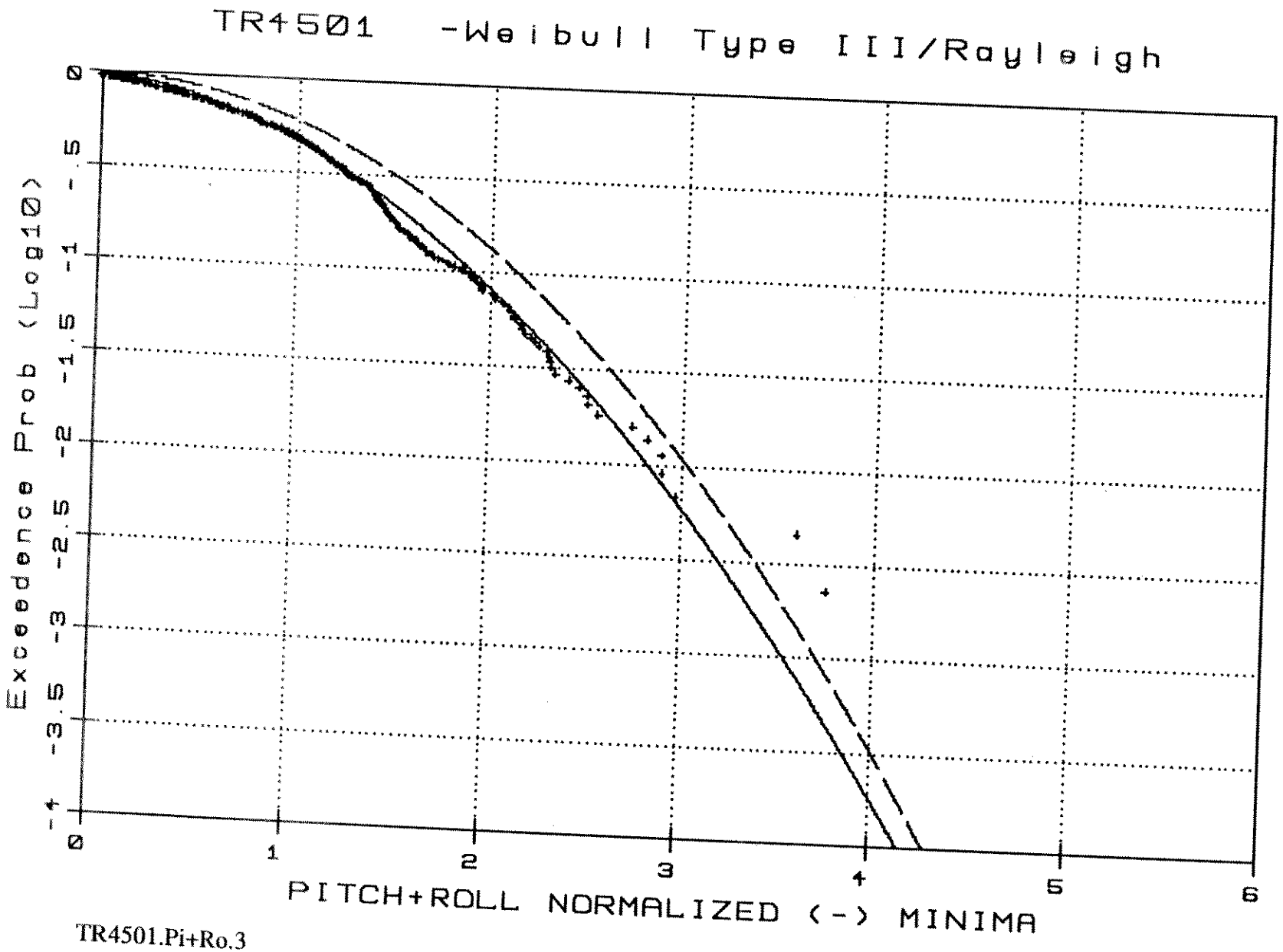

TR4501.Pi+Ro.3

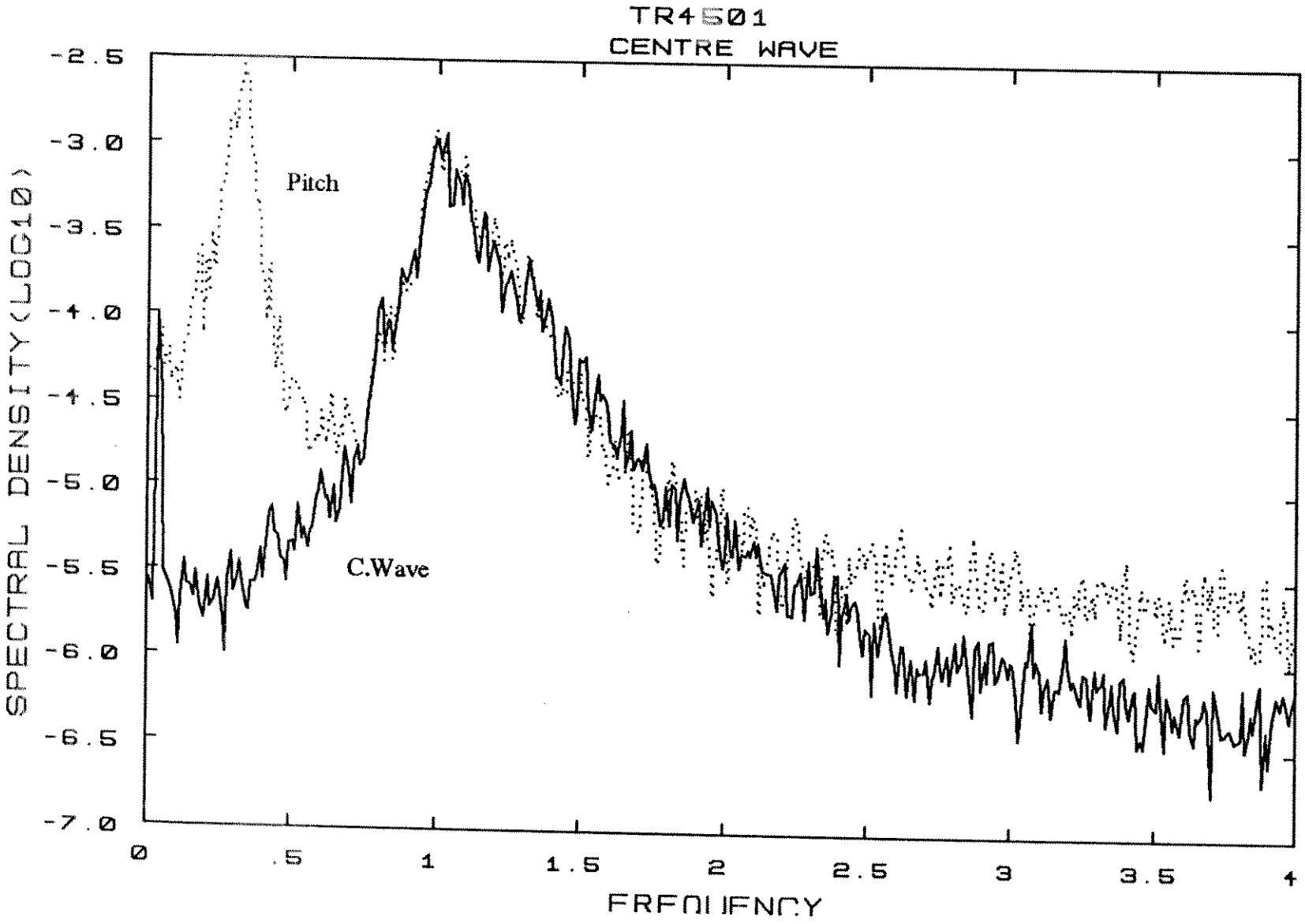
TR4501
CENTRE WAVE
SPECTRAL DENSITY(LOG10)
-2.5
-3.0
-3.5
-4.0
-4.5
-5.0
-5.5
-6.0
-6.5
-7.0
Pitch
C.Wave
0
.5
1
1.5
2
2.5
3
3.5
4
FREQUENCY

TR4501.W/Pi.4

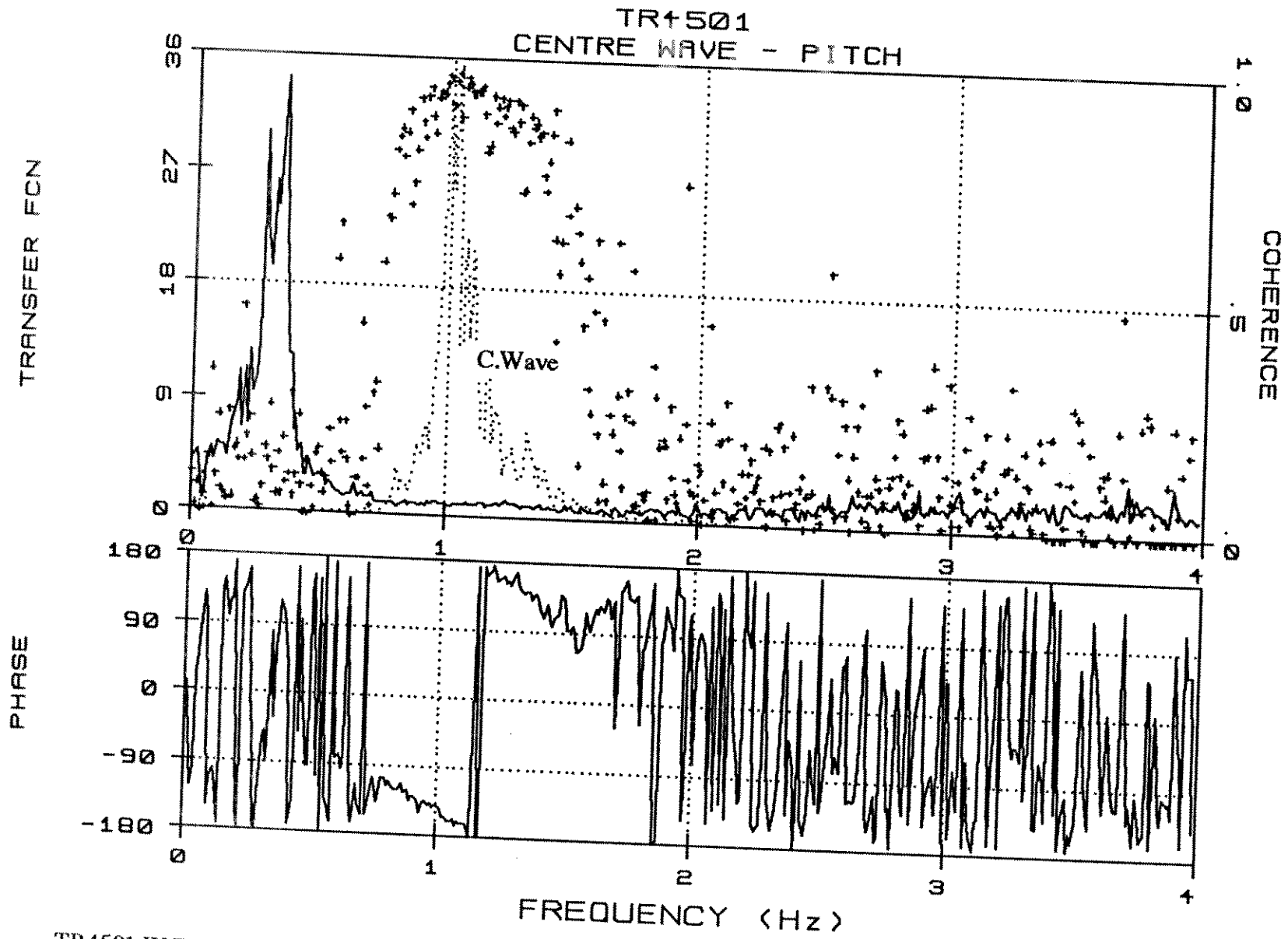

TR4501.W/Pi.4t

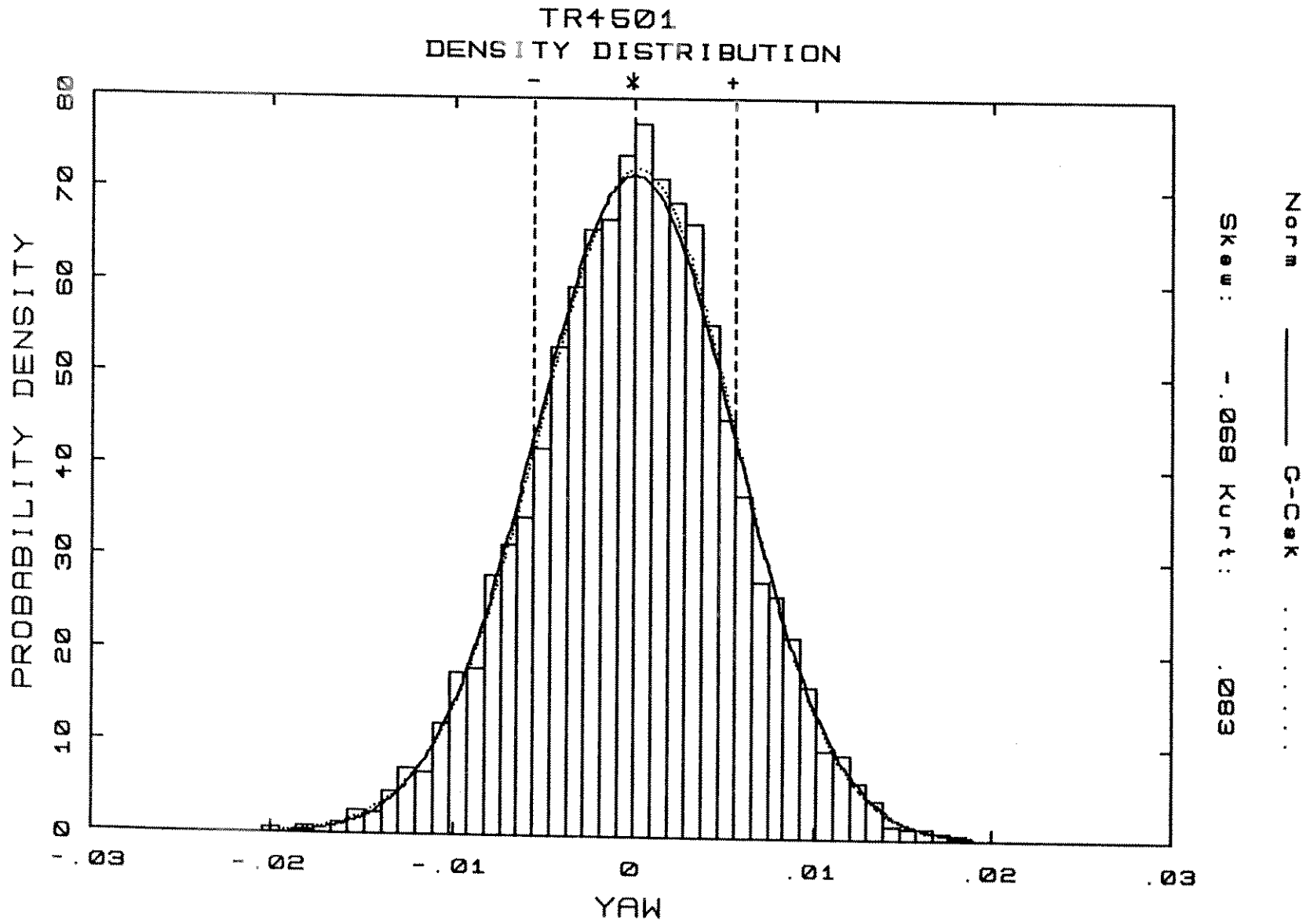
TR4501
DENSITY DISTRIBUTION
- * +
PROBABILITY DENSITY
0 10 20 30 40 50 60 70 80
-.03 -.02 -.01 0 .01 .02 .03
YAW
Norm ——— C-Cek .....
Skew: -.068 Kurt: .083

TR4501.Y.1

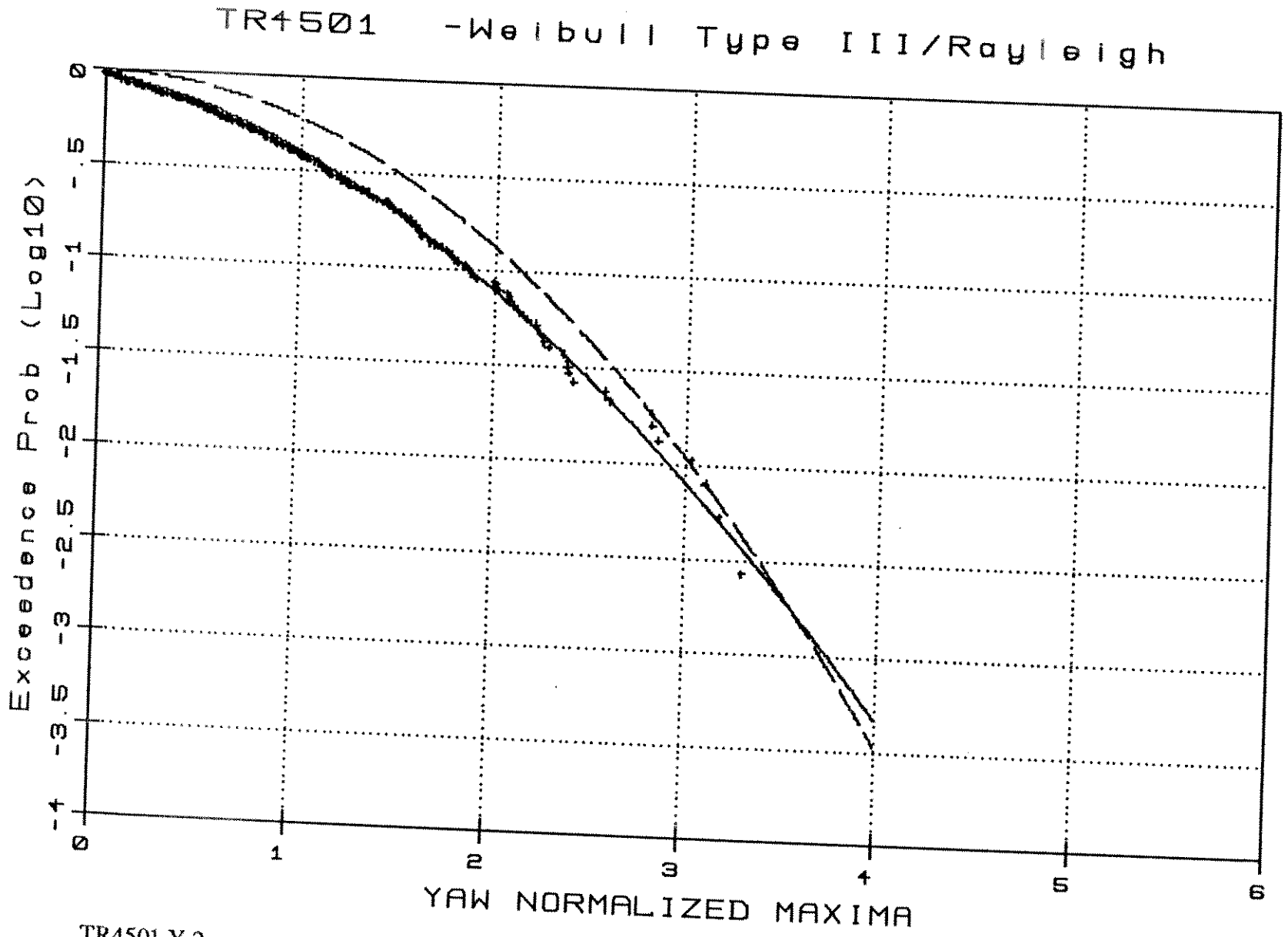
TR4501 -Weibull Type III/Rayleigh
Exceedence Prob (Log10)
0
-.5
-1
-1.5
-2
-2.5
-3
-3.5
-4
0
1
2
3
4
5
6
YAW NORMALIZED MAXIMA

TR4501.Y.2

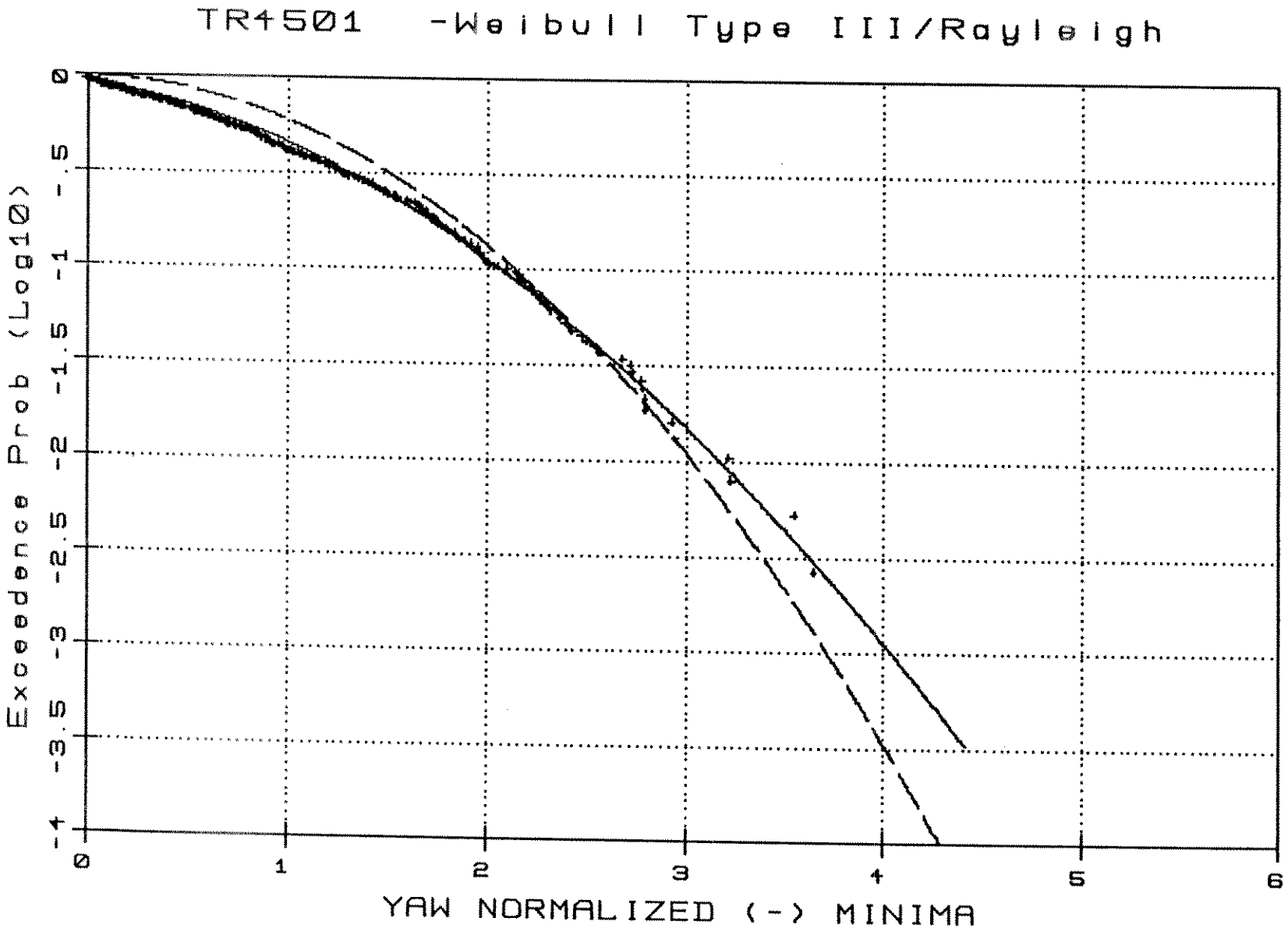
TR4501 -Weibull Type III/Rayleigh
Exceedence Prob (Log10)
0
-.5
-1
-1.5
-2
-2.5
-3
-3.5
-4
0
1
2
3
4
5
6
YAW NORMALIZED (-) MINIMA

TR4501.Y.3

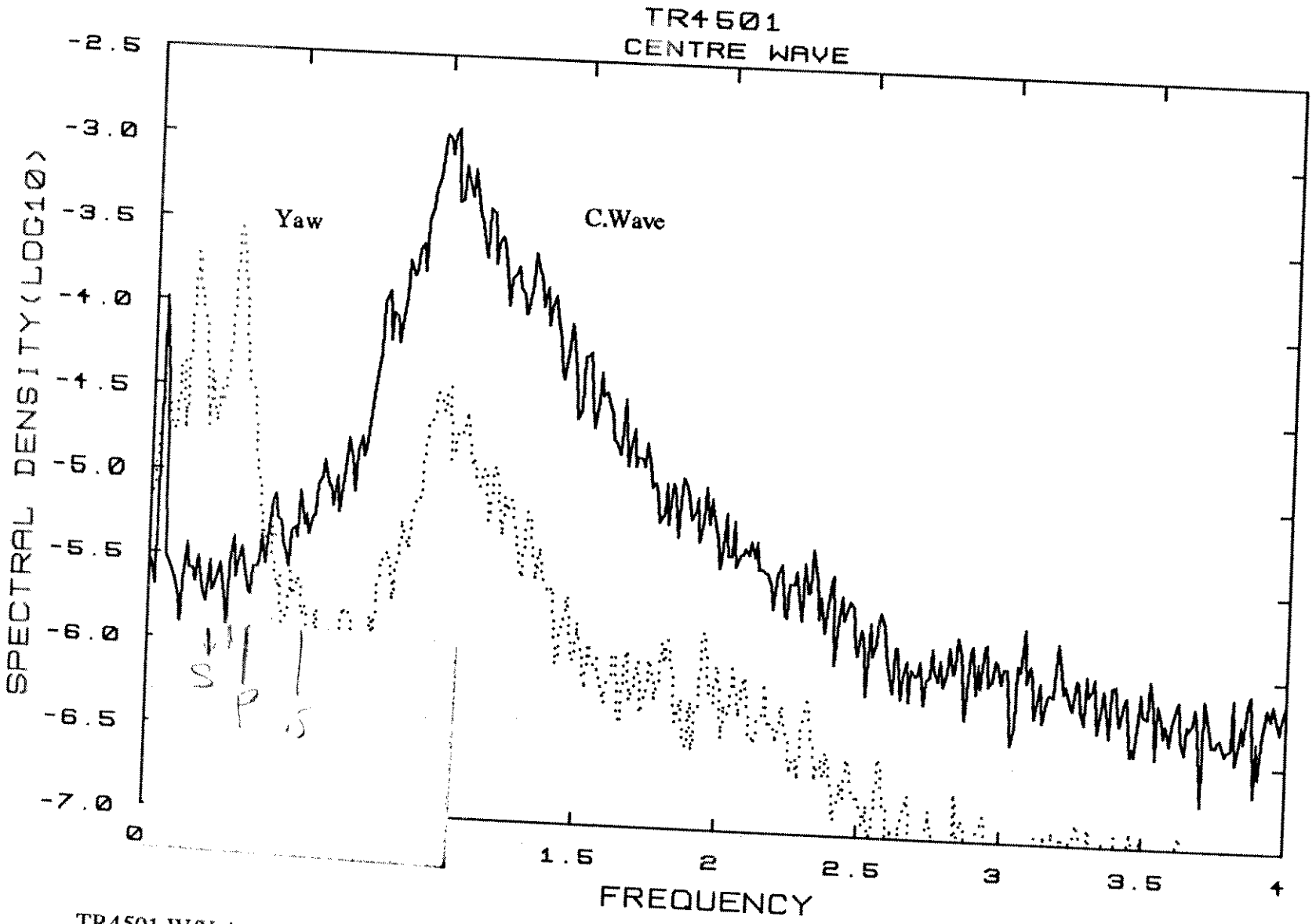
TR4501
CENTRE WAVE
SPECTRAL DENSITY(LOG10)
-2.5
-3.0
-3.5
-4.0
-4.5
-5.0
-5.5
-6.0
-6.5
-7.0
Yaw
C.Wave
0
1.5
2
2.5
3
3.5
4
FREQUENCY

TR4501.W/Y.4

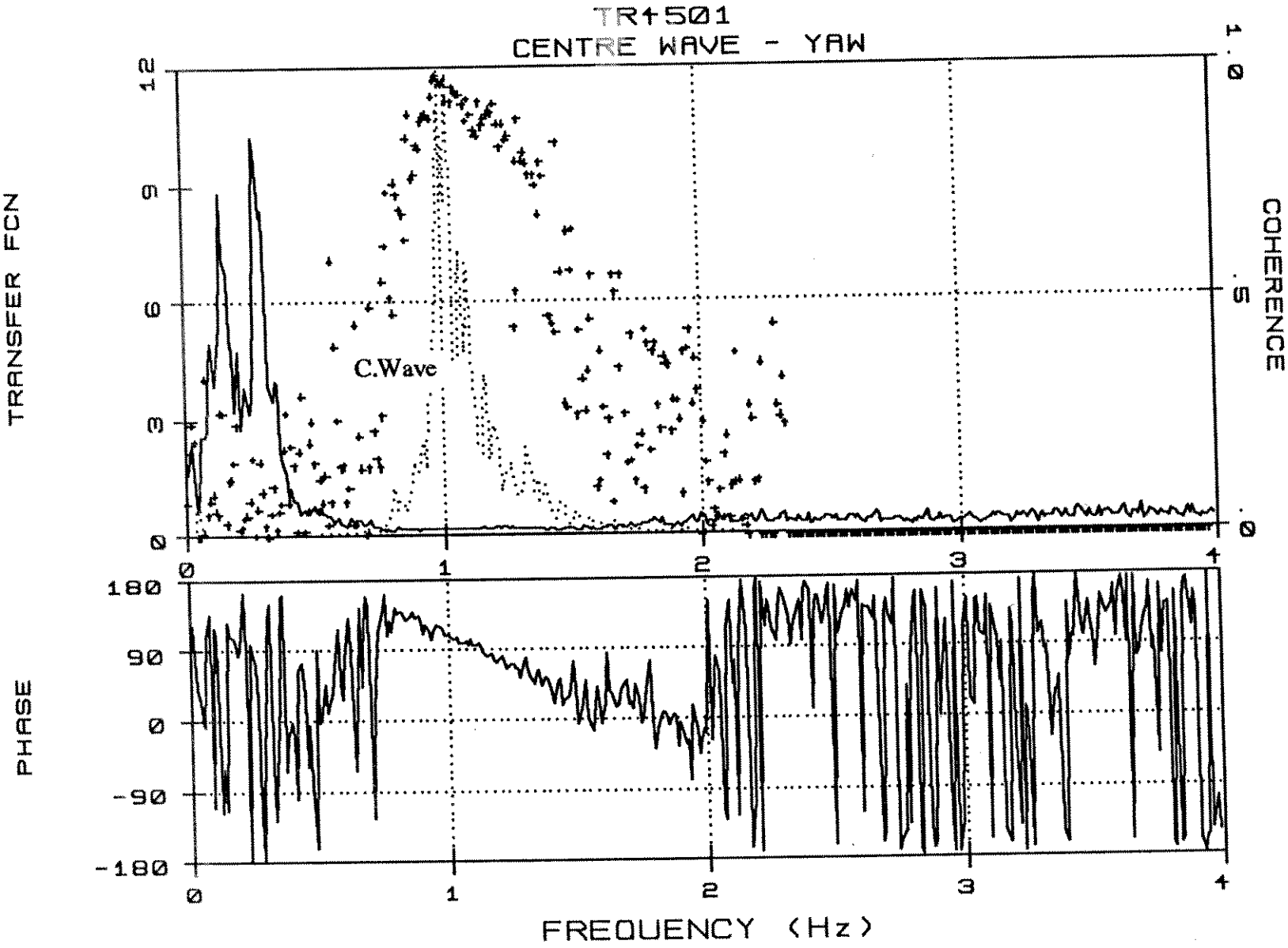
TR1501
CENTRE WAVE - YAW
TRANSFER FCN
COHERENCE
C.Wave
PHASE
FREQUENCY (Hz)

TR4501.W/Y.4t

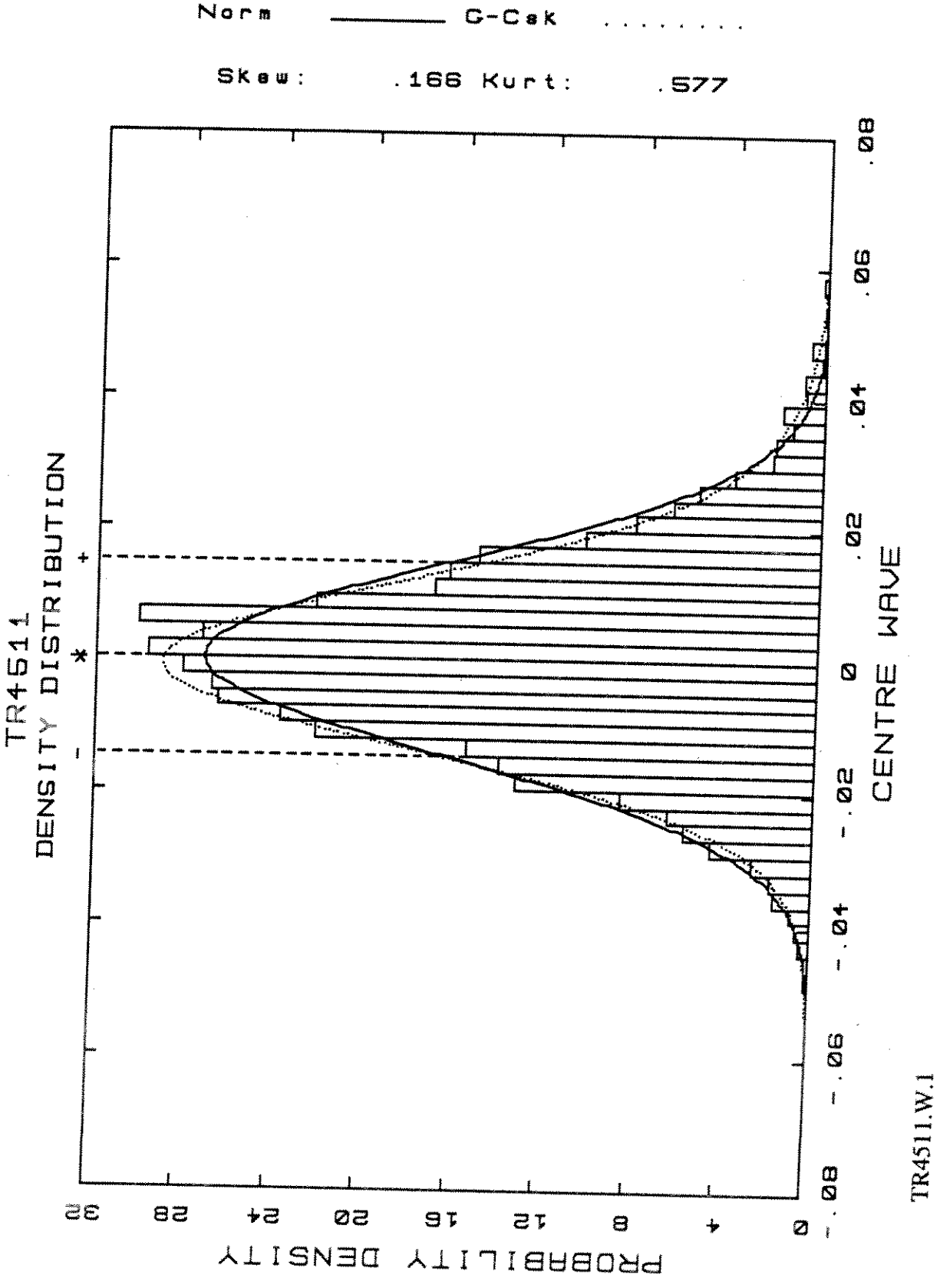
Norm ——— G-Cak .....
Skew: .166 Kurt: .577
TR4511
DENSITY DISTRIBUTION
+
*
-
PROBABILITY DENSITY
0
4
8
12
16
20
24
28
32
-.08
-.06
-.04
-.02
0
.02
.04
.06
.08
CENTRE WAVE

TR4511.W.1

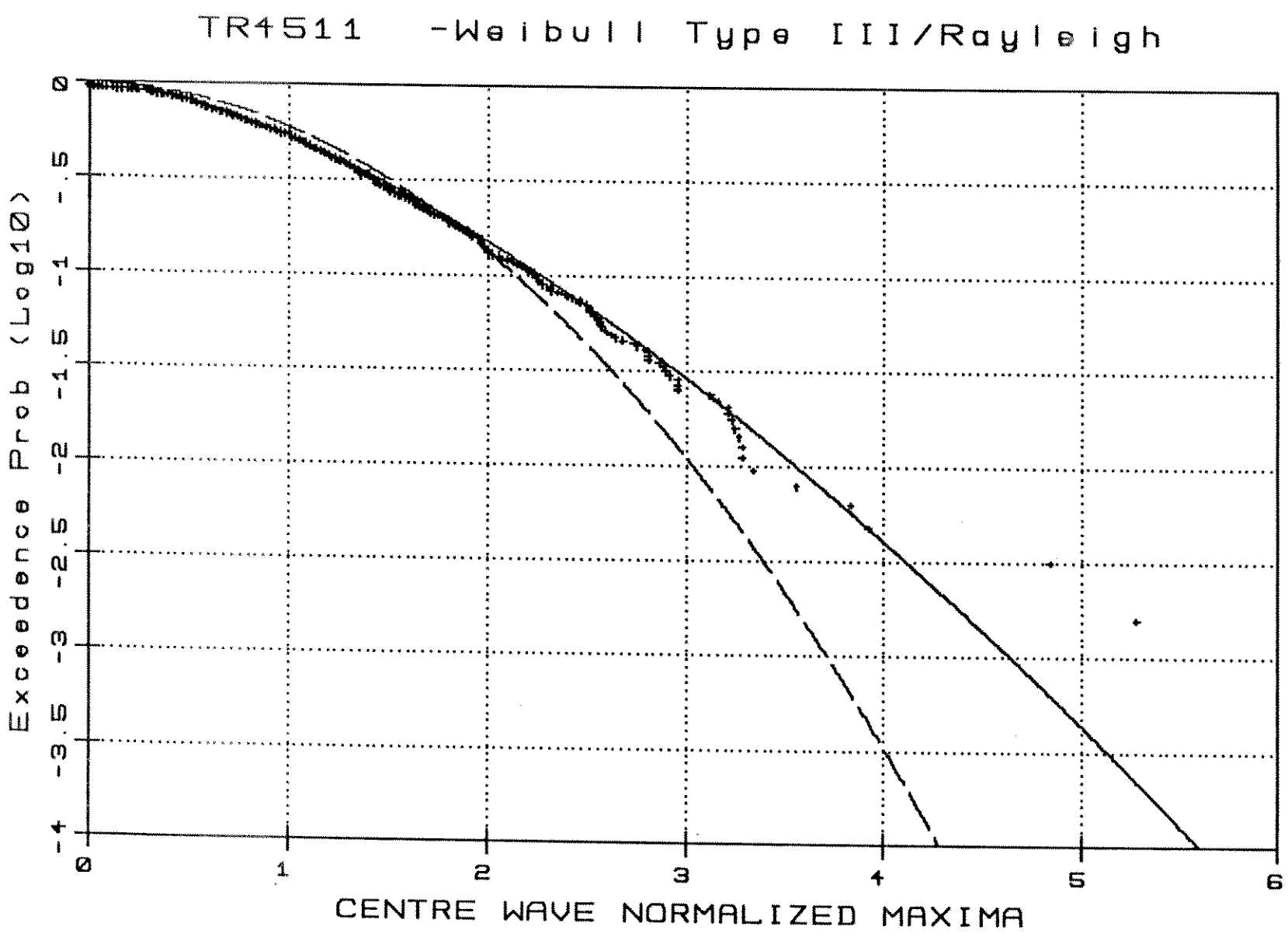
TR4511 -Weibull Type III/Rayleigh
Exceedence Prob (Log10)
0
-.5
-1
-1.5
-2
-2.5
-3
-3.5
-4
0
1
2
3
4
5
6
CENTRE WAVE NORMALIZED MAXIMA

TR4511.W.2

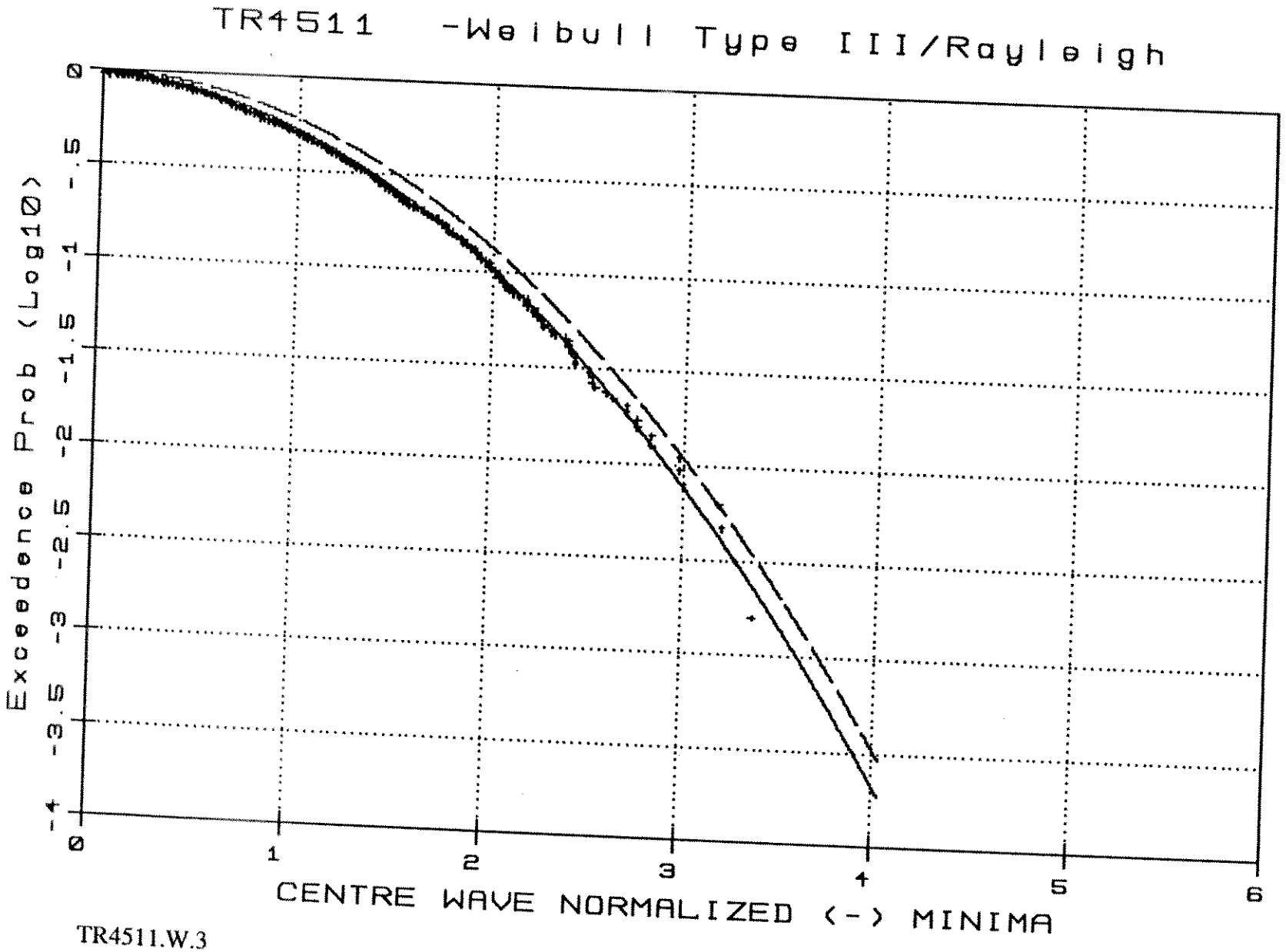
TR4511 -Weibull Type III/Rayleigh
Exceedence Prob (Log10)
0
-.5
-1
-1.5
-2
-2.5
-3
-3.5
-4
0
1
2
3
4
5
6
CENTRE WAVE NORMALIZED (-) MINIMA

TR4511.W.3

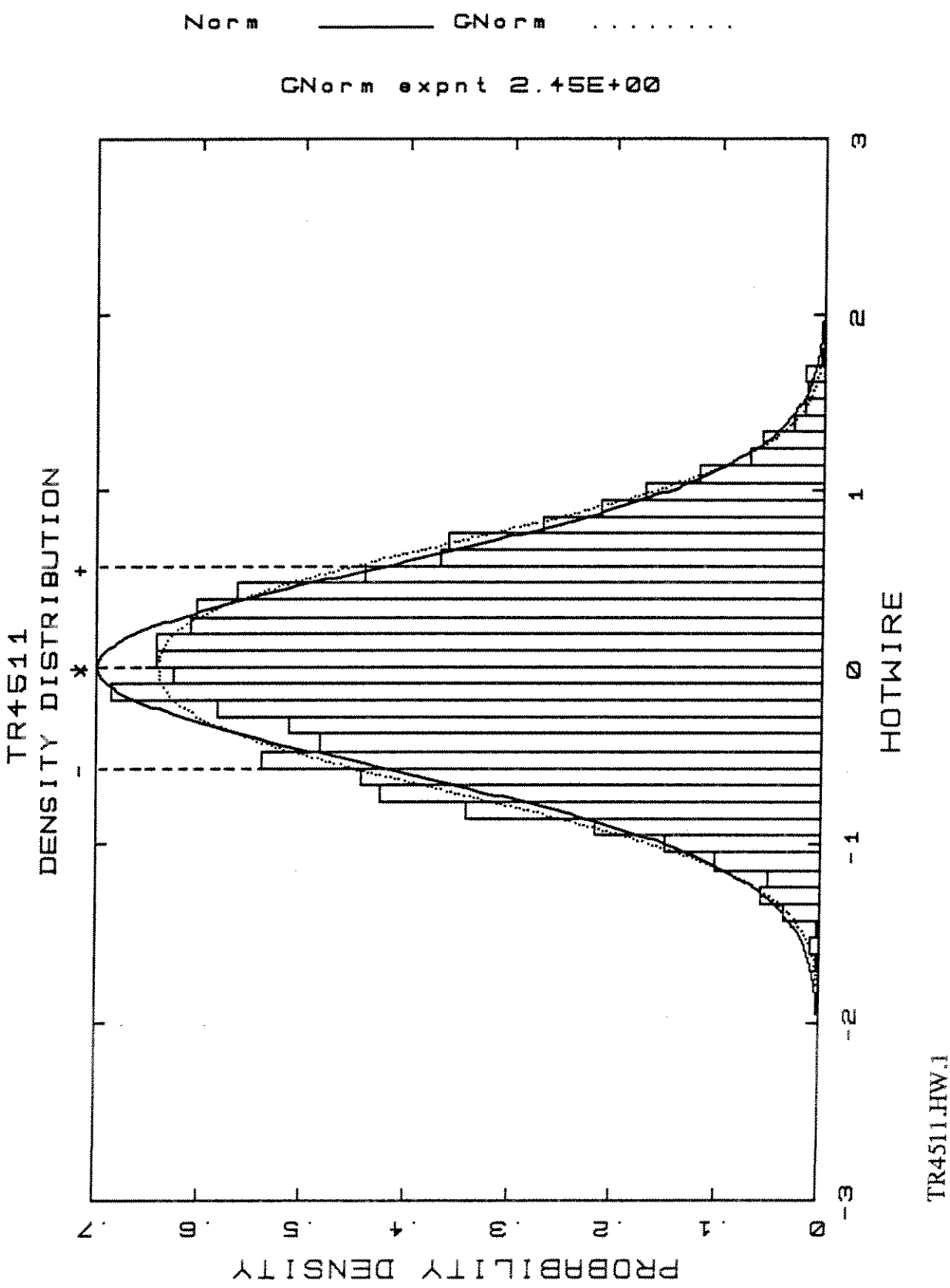
Norm
GNorm
GNorm expnt 2.45E+00
TR4511
DENSITY DISTRIBUTION
PROBABILITY DENSITY
HOTWIRE
TR4511.HW.1

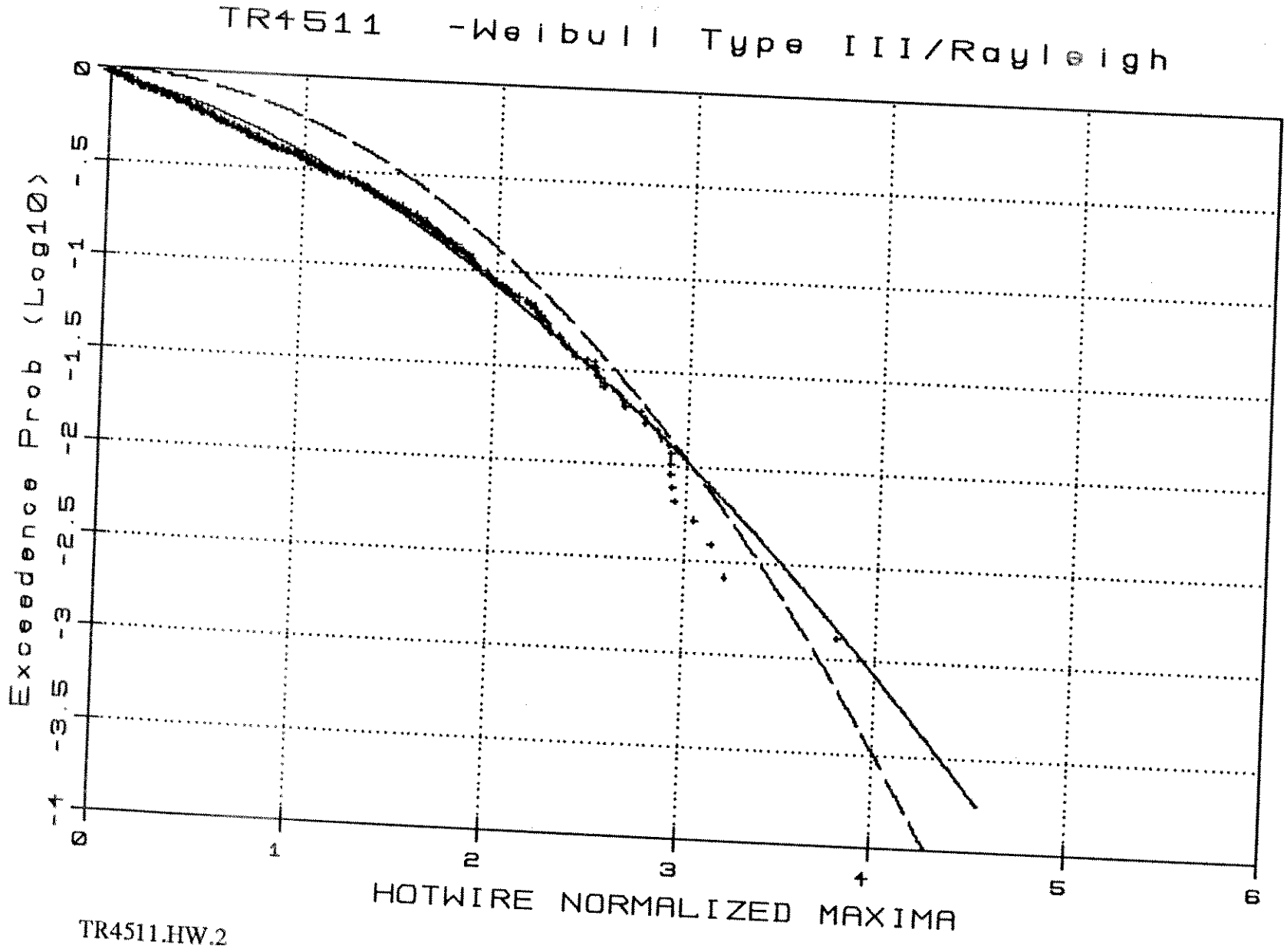
TR4511 -Weibull Type III/Rayleigh
Exceedence Prob (Log10)
0
-.5
-1
-1.5
-2
-2.5
-3
-3.5
-4
0
1
2
3
4
5
6
HOTWIRE NORMALIZED MAXIMA

TR4511.HW.2

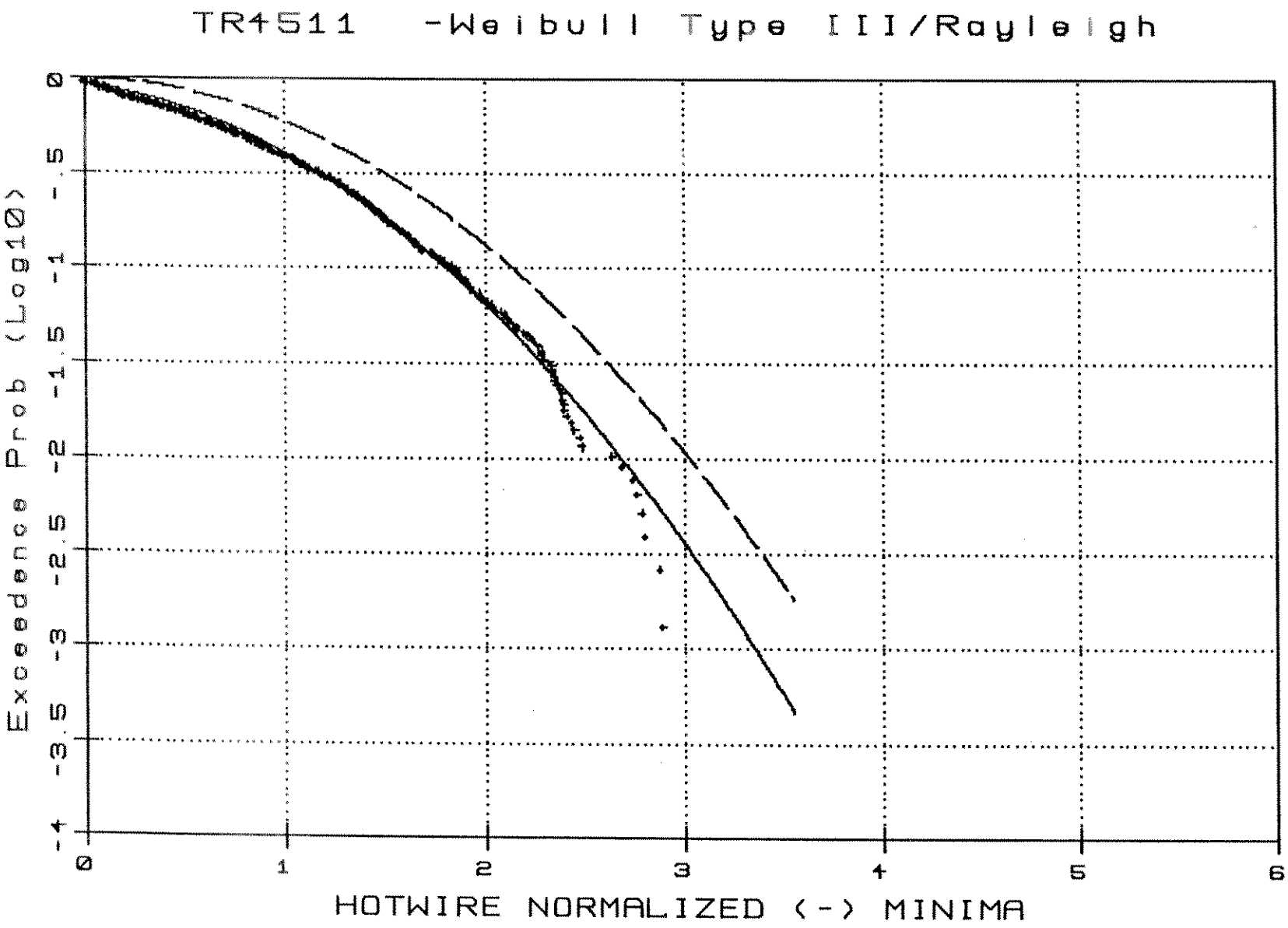
TR4511 -Weibull Type III/Rayleigh
Exceedence Prob (Log10)
0
-.5
-1
-1.5
-2
-2.5
-3
-3.5
-4
0
1
2
3
4
5
6
HOTWIRE NORMALIZED (-) MINIMA

TR4511.HW.3

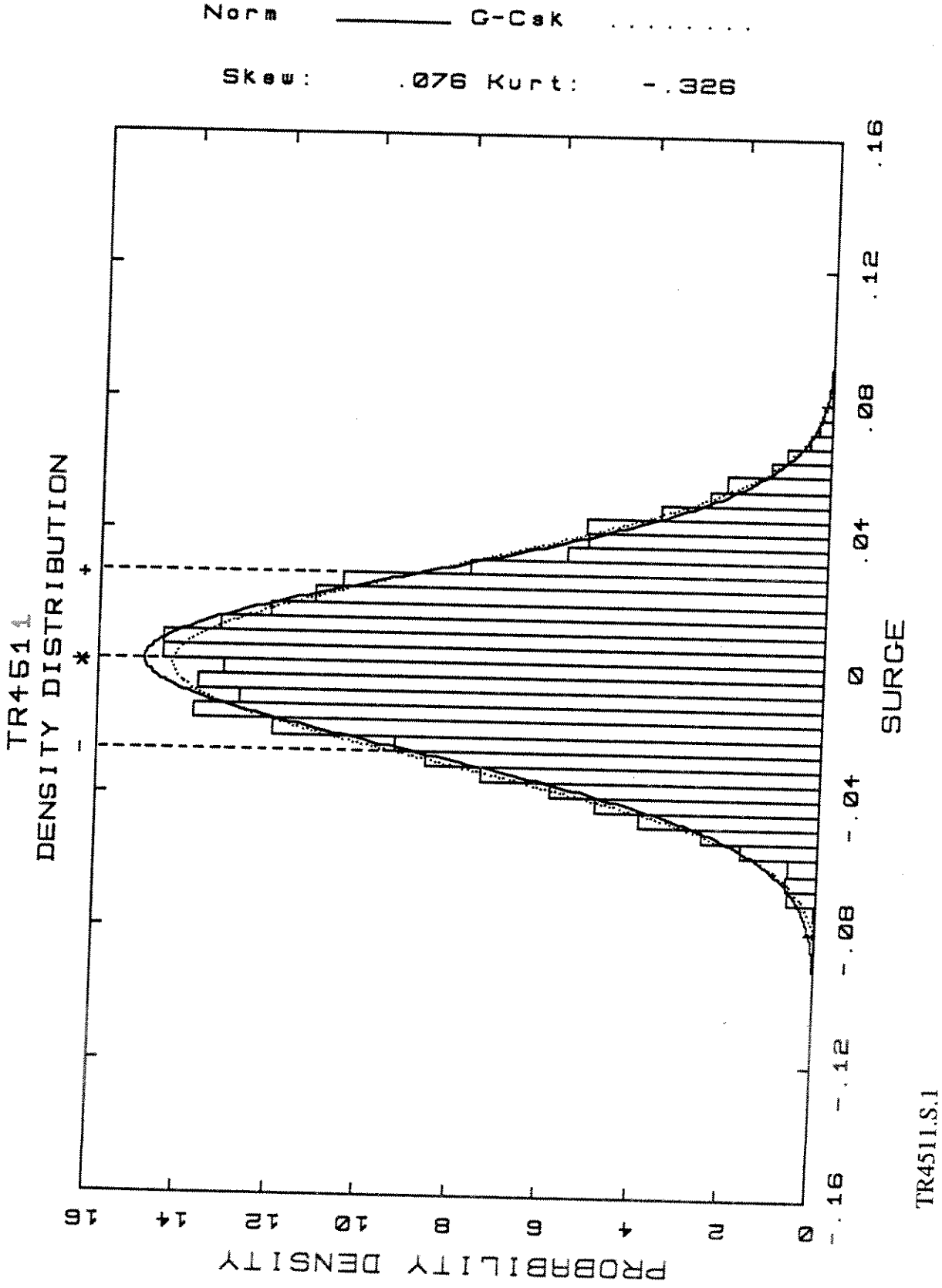
Norm
G-Cak
Skew: .076 Kurt: -.326
TR4511
DENSITY DISTRIBUTION
+
*
-
PROBABILITY DENSITY
0
2
4
6
8
10
12
14
16
SURGE
.16
.12
.08
.04
0
-.04
-.08
-.12
-.16

TR4511.S.1

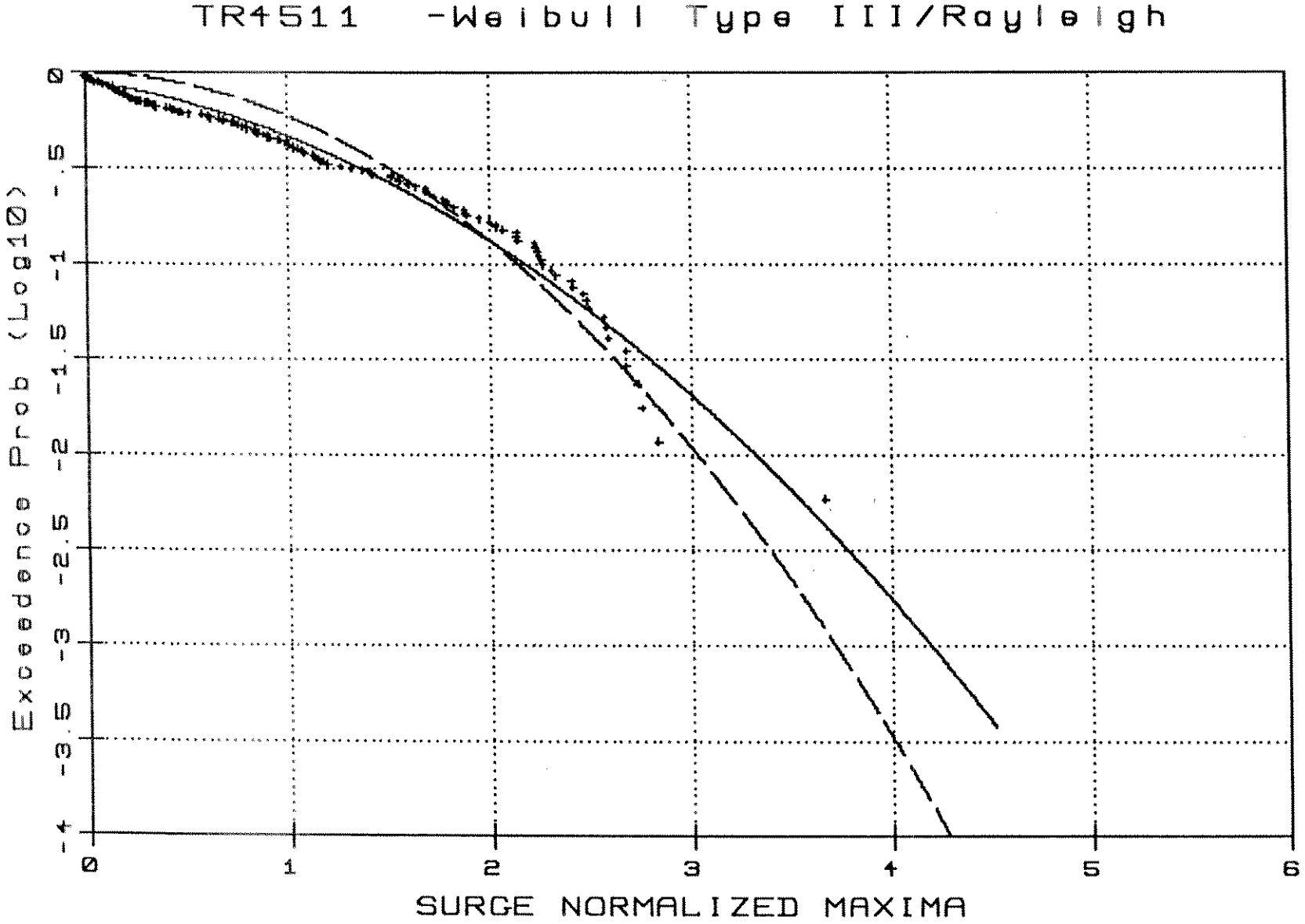
TR4511 -Weibull Type III/Rayleigh
Exceedence Prob (Log10)
0
-.5
-1
-1.5
-2
-2.5
-3
-3.5
-4
0
1
2
3
4
5
6
SURGE NORMALIZED MAXIMA

TR4511.S.2

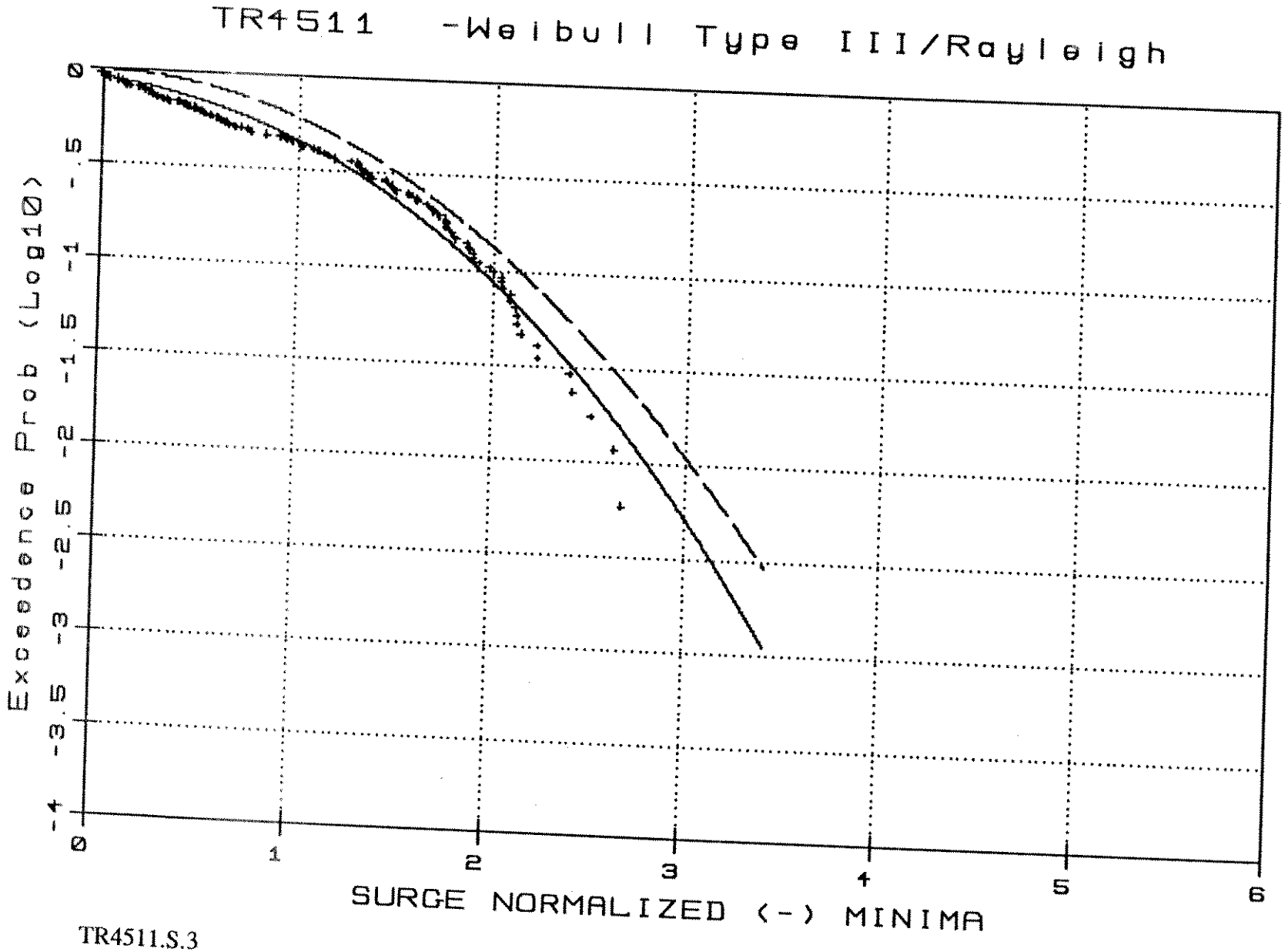
TR4511 -Weibull Type III/Rayleigh
Exceedence Prob (Log10)
0
-.5
-1
-1.5
-2
-2.5
-3
-3.5
-4
0
1
2
3
4
5
6
SURGE NORMALIZED (-) MINIMA

TR4511.S.3

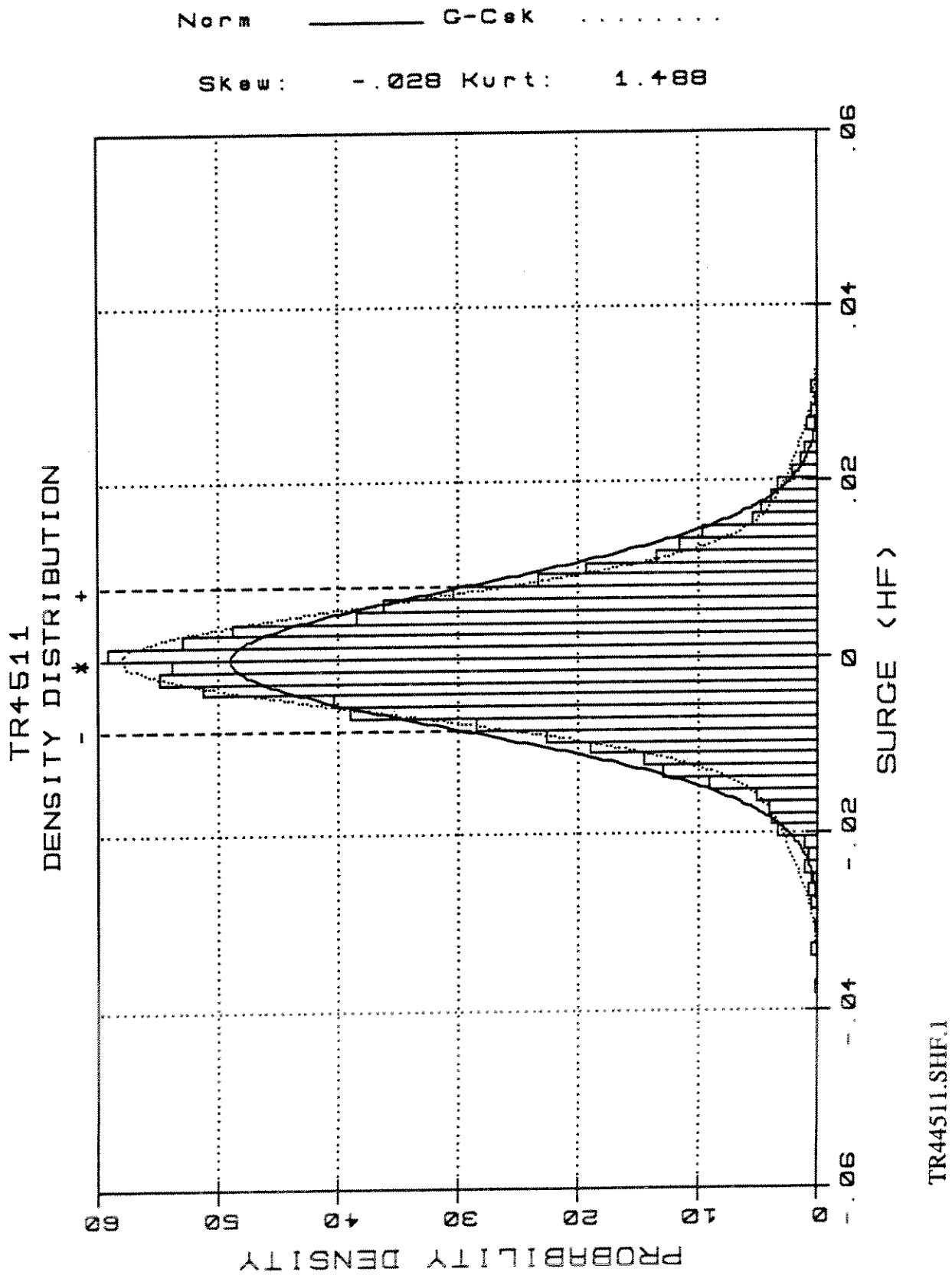

TR44511.SHF.1

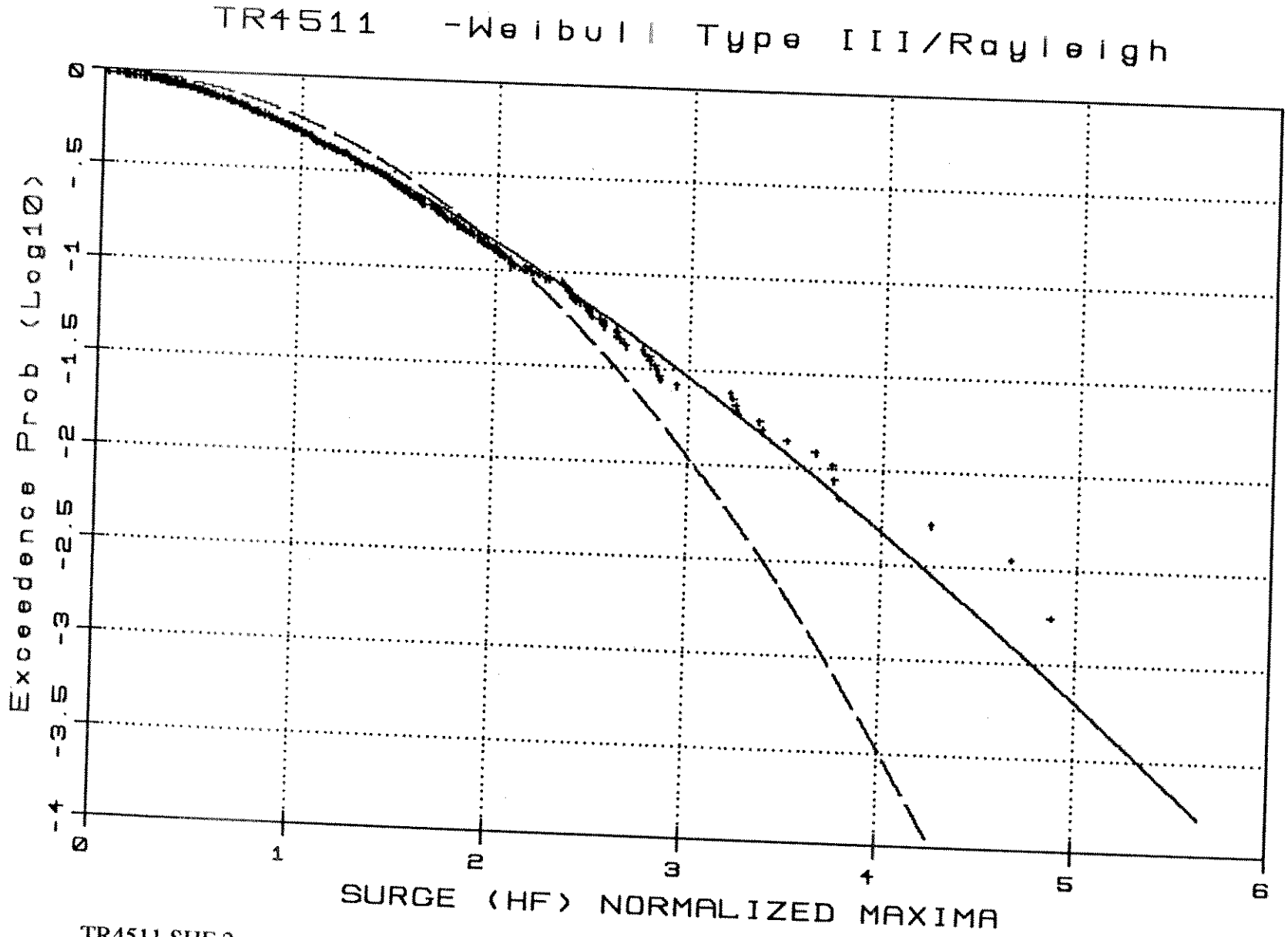
TR4511 -Weibull Type III/Rayleigh
Exceedence Prob (Log10)
0
-.5
-1
-1.5
-2
-2.5
-3
-3.5
-4
0
1
2
3
4
5
6
SURGE (HF) NORMALIZED MAXIMA

TR4511.SHF.2

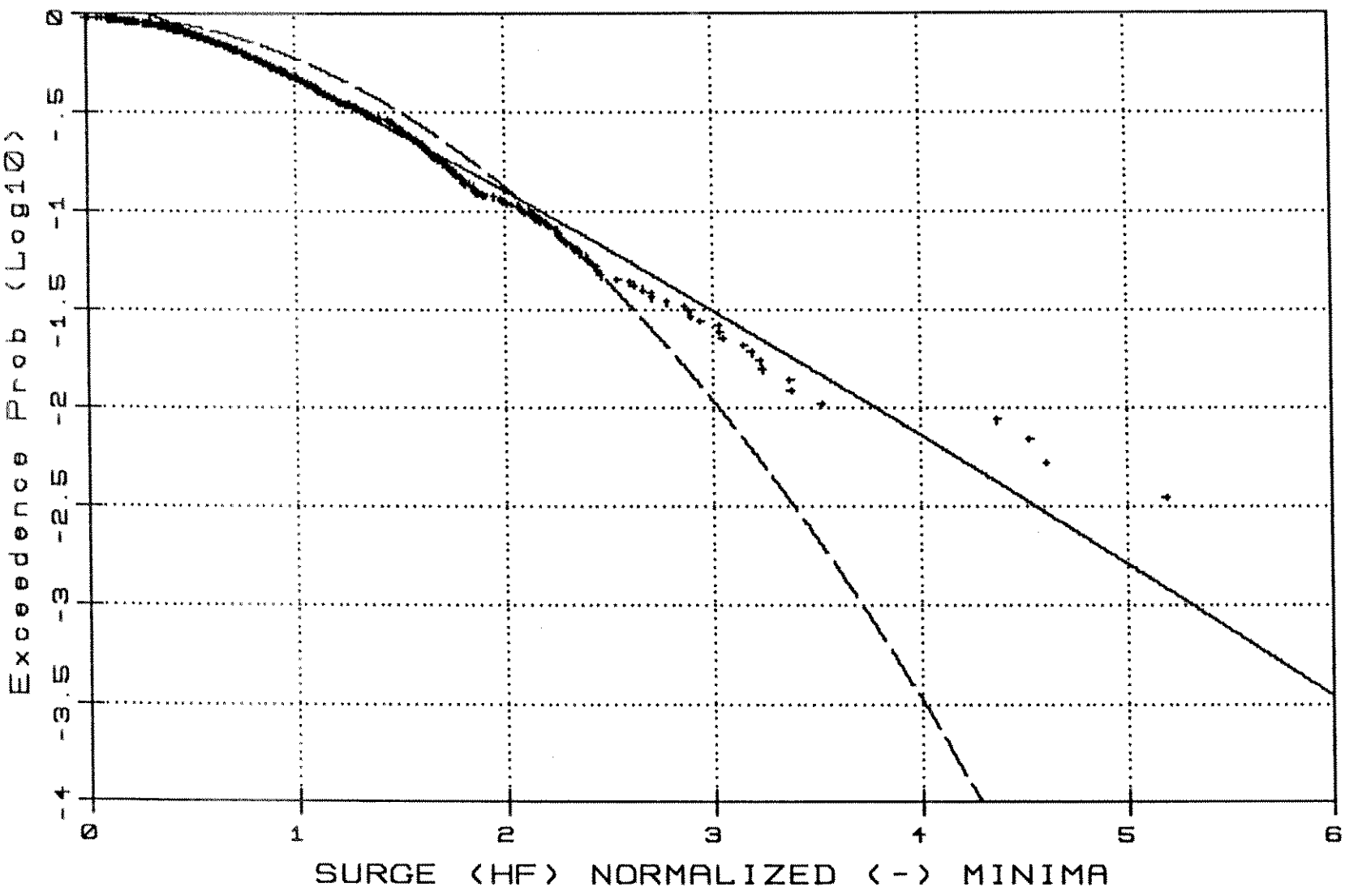
TR4511 -Weibull Type III/Rayleigh
Exceedence Prob (Log10)
0
-.5
-1
-1.5
-2
-2.5
-3
-3.5
-4
0
1
2
3
4
5
6
SURGE (HF) NORMALIZED (-) MINIMA

TR4511.SHF.3

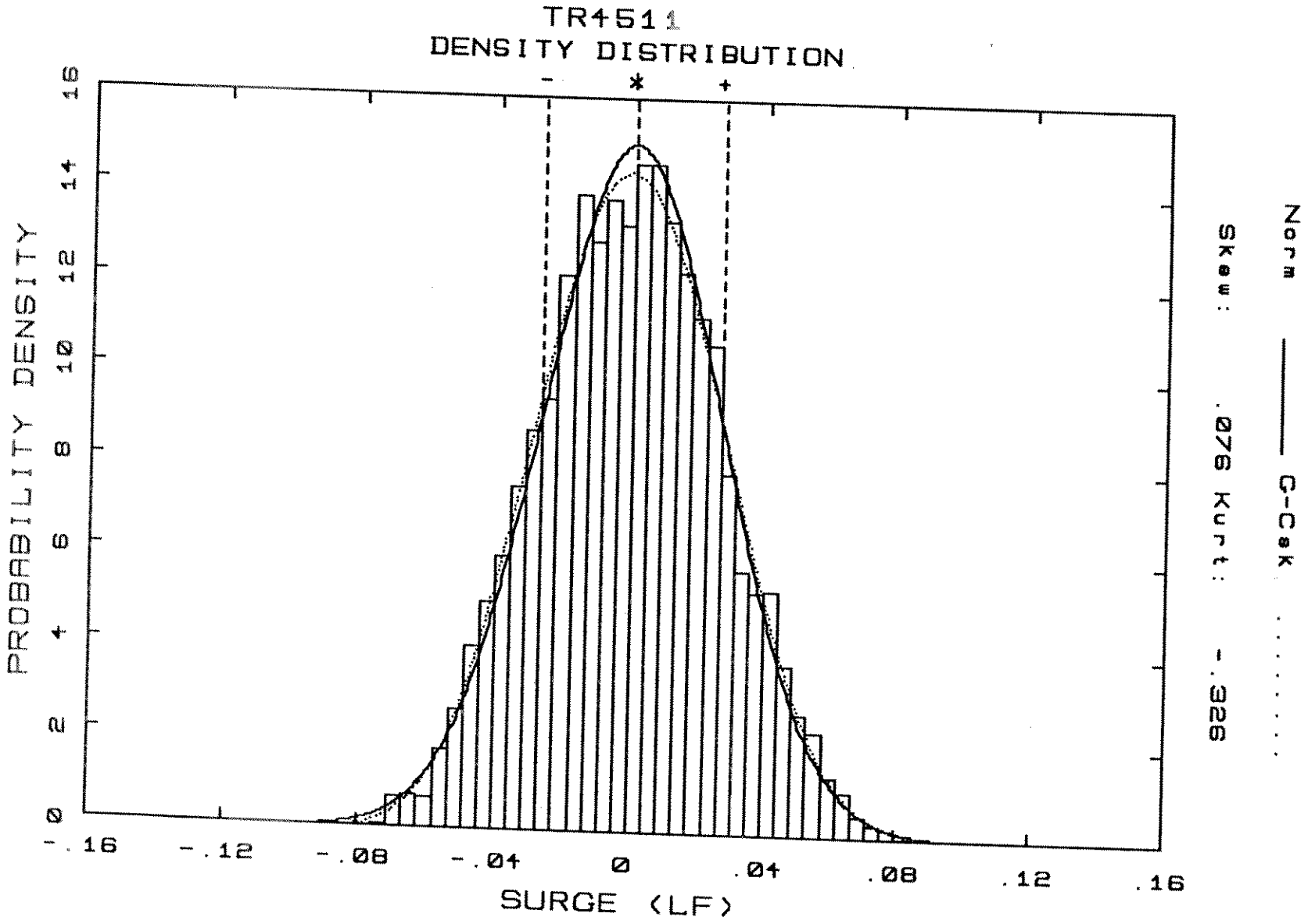
TR4511
DENSITY DISTRIBUTION
- * +
PROBABILITY DENSITY
0
2
4
6
8
10
12
14
16
-.16
-.12
-.08
-.04
0
.04
.08
.12
.16
SURGE (LF)
Norm
C-Cek
Skew: .076 Kurt: -.326

TR4511.SLF.1

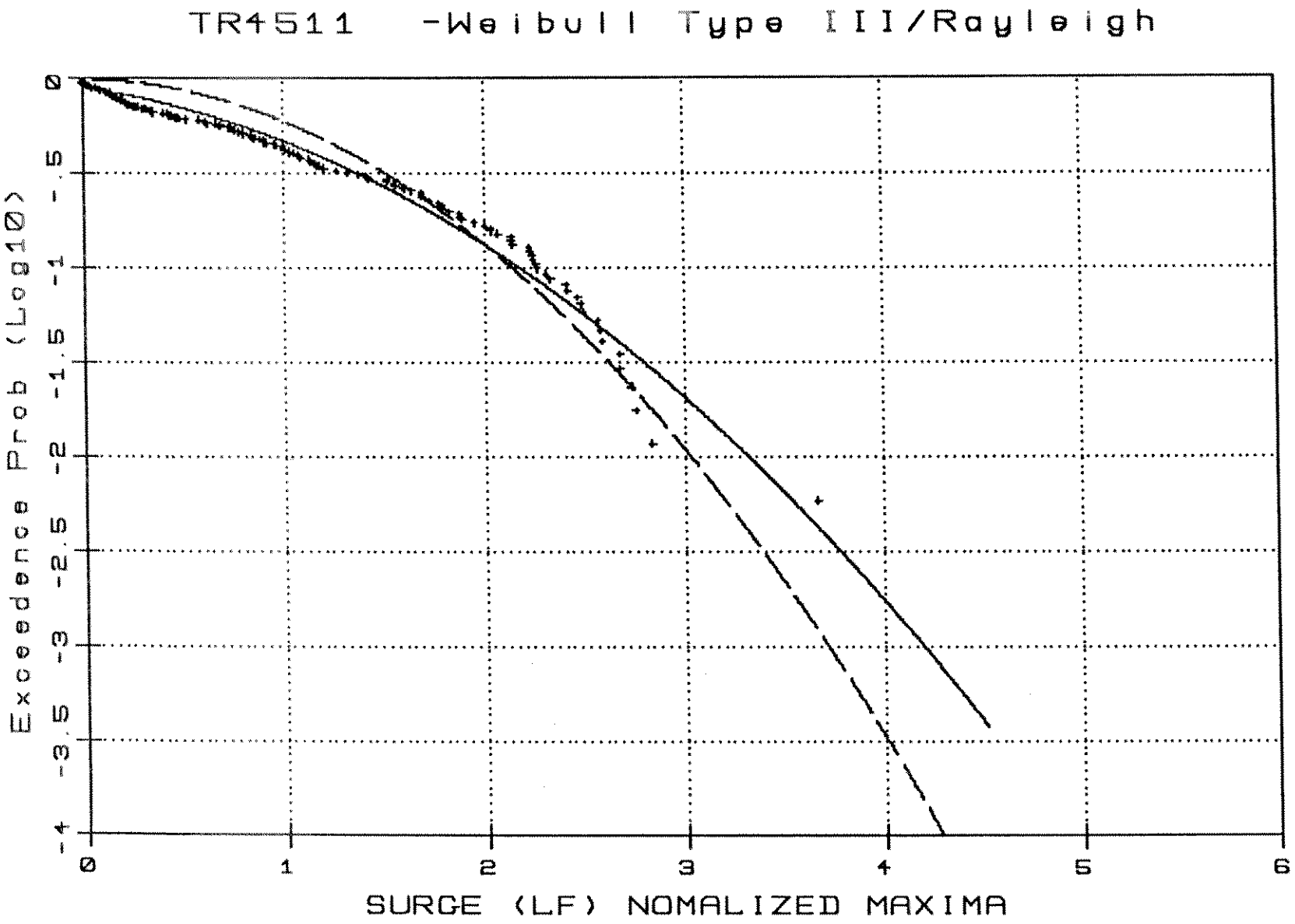
TR4511 -Weibull Type III/Rayleigh
Exceedence Prob (Log10)
0
-.5
-1
-1.5
-2
-2.5
-3
-3.5
-4
0
1
2
3
4
5
6
SURGE (LF) NOMALIZED MAXIMA

TR4511.SLF.2

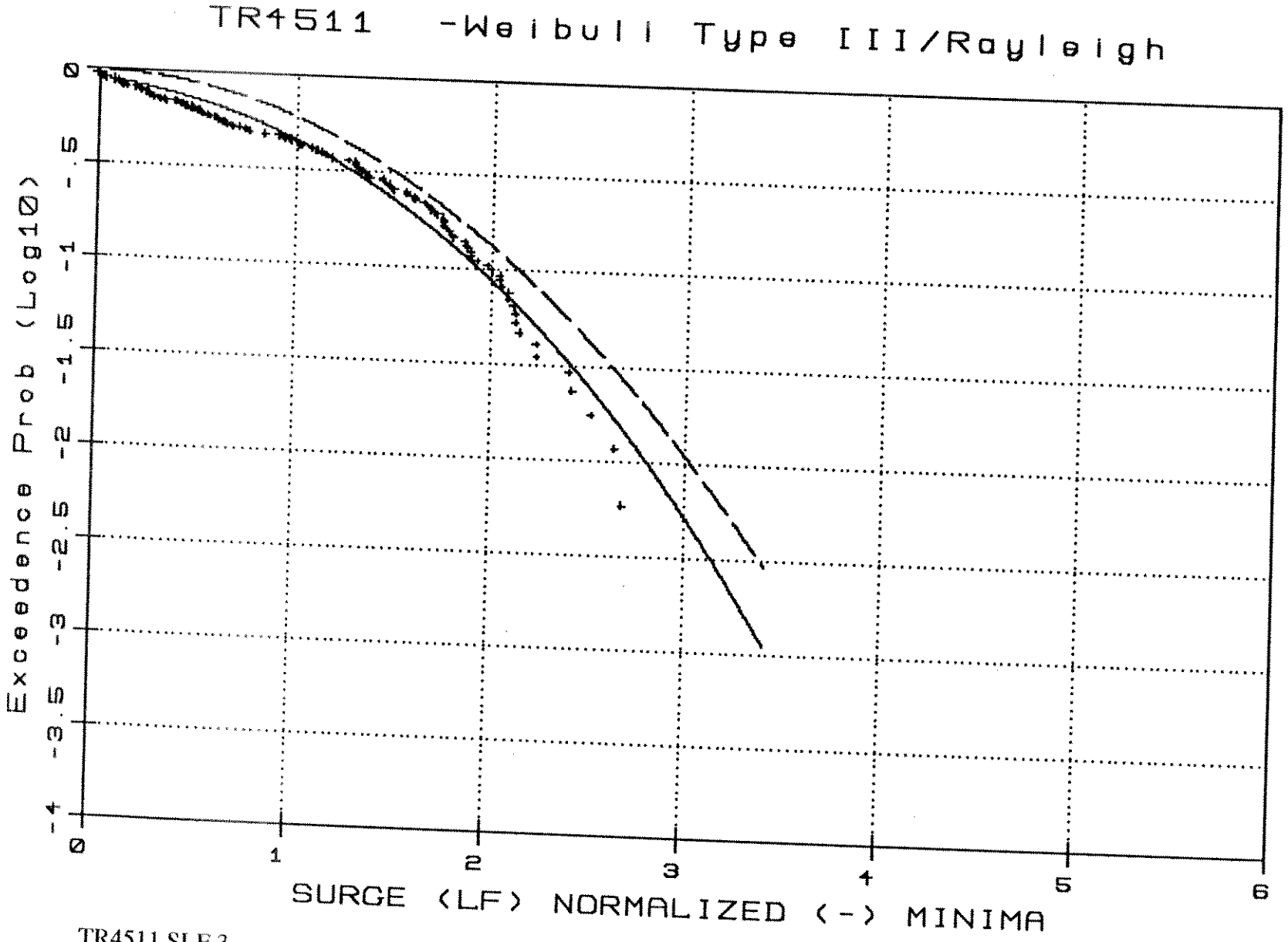
TR4511 -Weibull Type III/Rayleigh
Exceedence Prob (Log10)
0
-.5
-1
-1.5
-2
-2.5
-3
-3.5
-4
0
1
2
3
4
5
6
SURGE (LF) NORMALIZED (-) MINIMA

TR4511.SLF.3

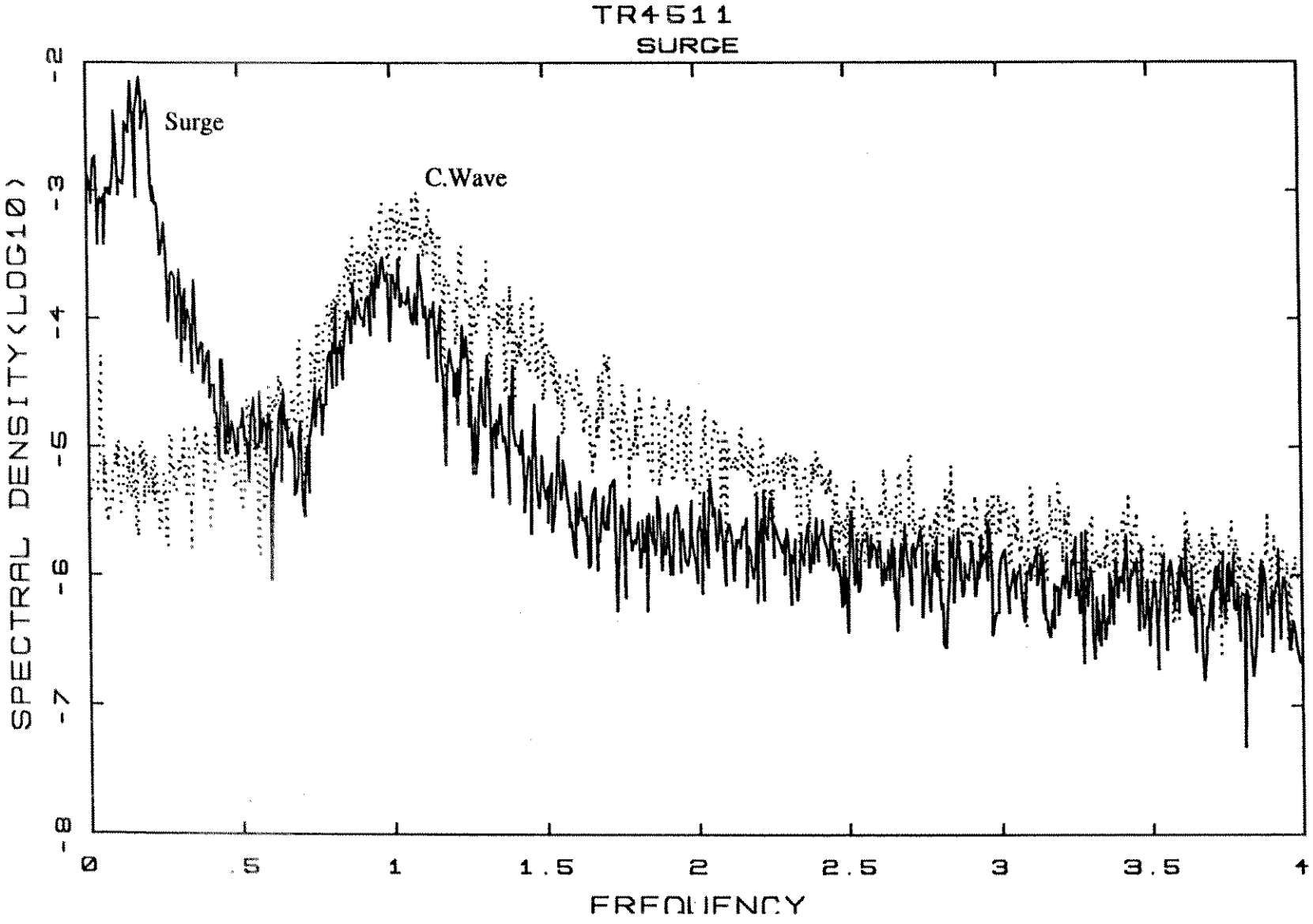
TR4511
SURGE
Surge
C.Wave
SPECTRAL DENSITY(LOG10)
-2
-3
-4
-5
-6
-7
-8
0
.5
1
1.5
2
2.5
3
3.5
4
FREQUENCY

TR4511.W/S.4

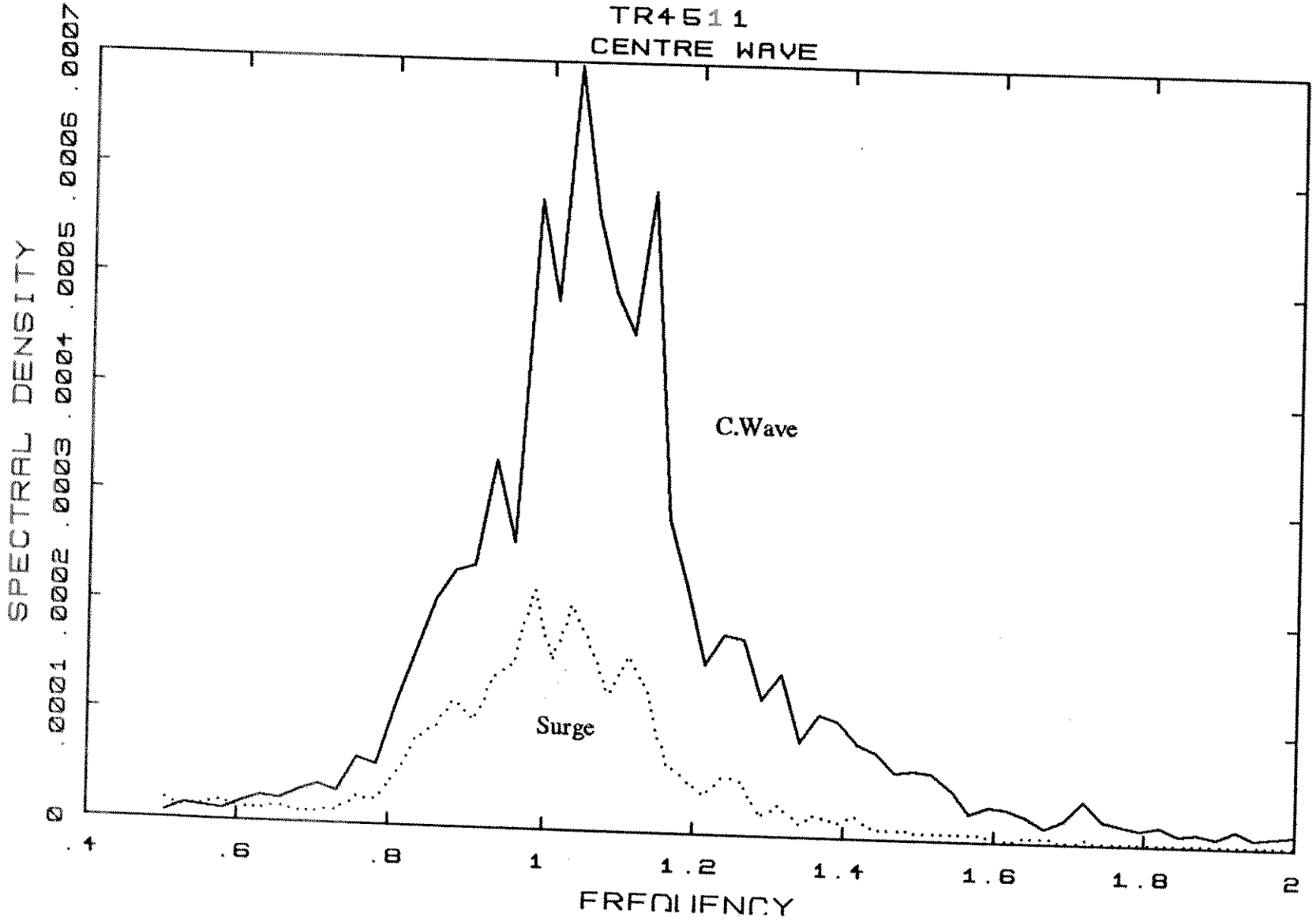
TR4511
CENTRE WAVE
SPECTRAL DENSITY
0
.0001
.0002
.0003
.0004
.0005
.0006
.0007
C.Wave
Surge
.4
.6
.8
1
1.2
1.4
1.6
1.8
2
FREQUENCY

TR4511.W/S.4*

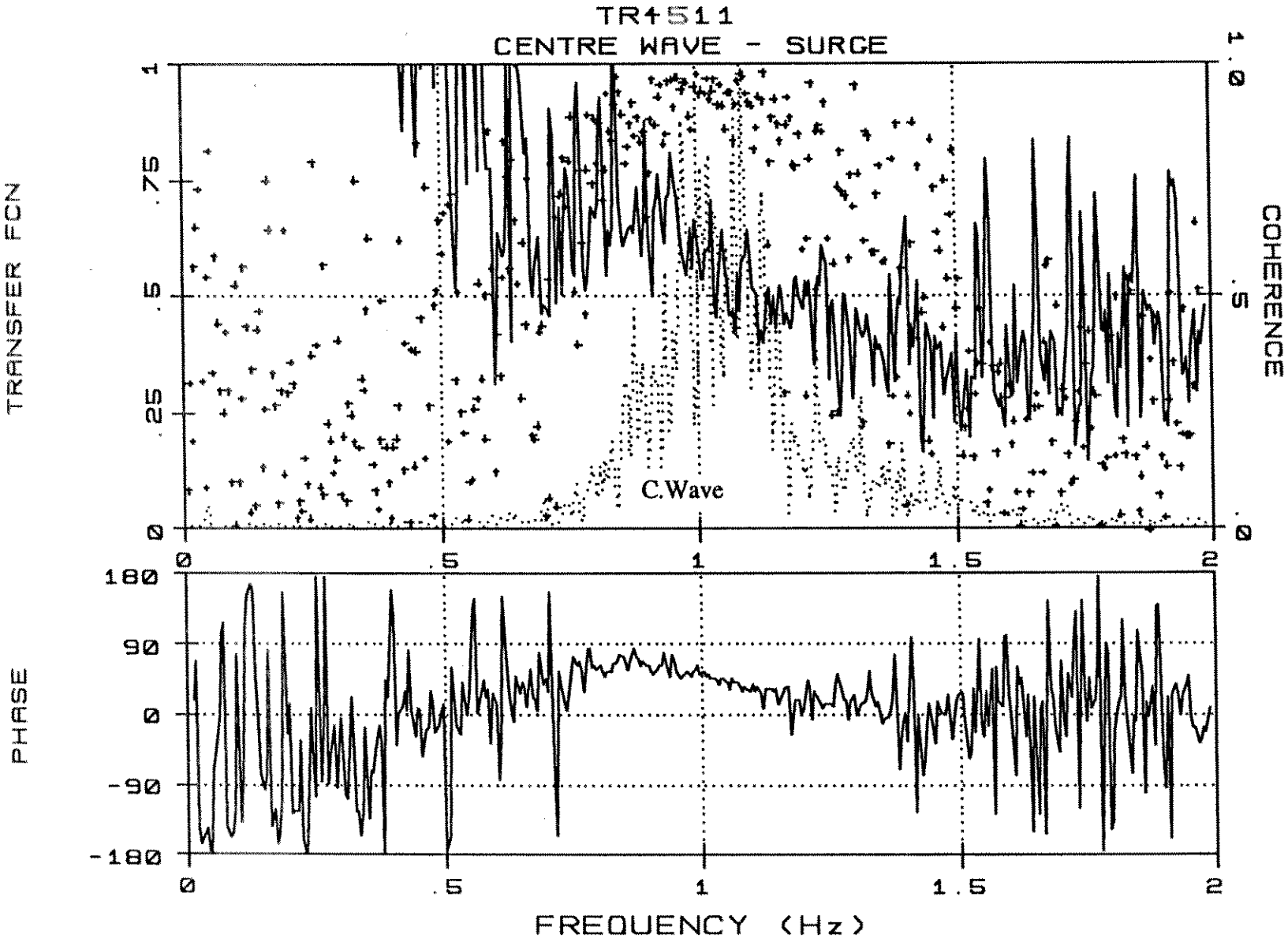
TR4511
CENTRE WAVE - SURGE
TRANSFER FCN
COHERENCE
C.Wave
PHASE
FREQUENCY (Hz)
1
.75
.5
.25
0
1.0
.5
0
180
90
0
-90
-180
0
.5
1
1.5
2

TR4511.W/S.4t

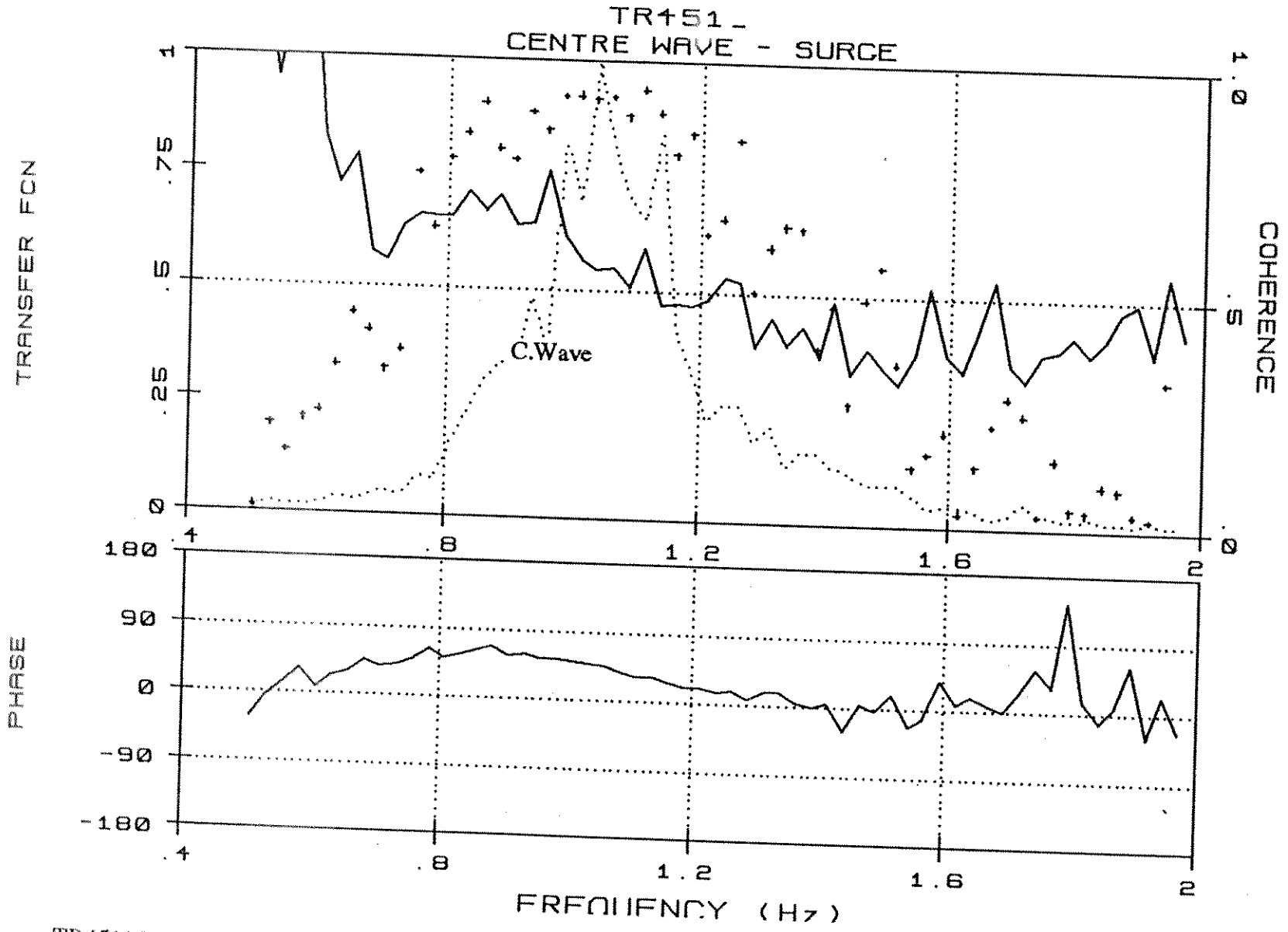
TR451_
CENTRE WAVE - SURCE
TRANSFER FCN
1
.75
.5
.25
0
C.Wave
COHERENCE
1.0
.5
0
.4
.8
1.2
1.6
2
PHASE
180
90
0
-90
-180
.4
.8
1.2
1.6
2
FREQUENCY (Hz)

TR4511.W/S.4t*

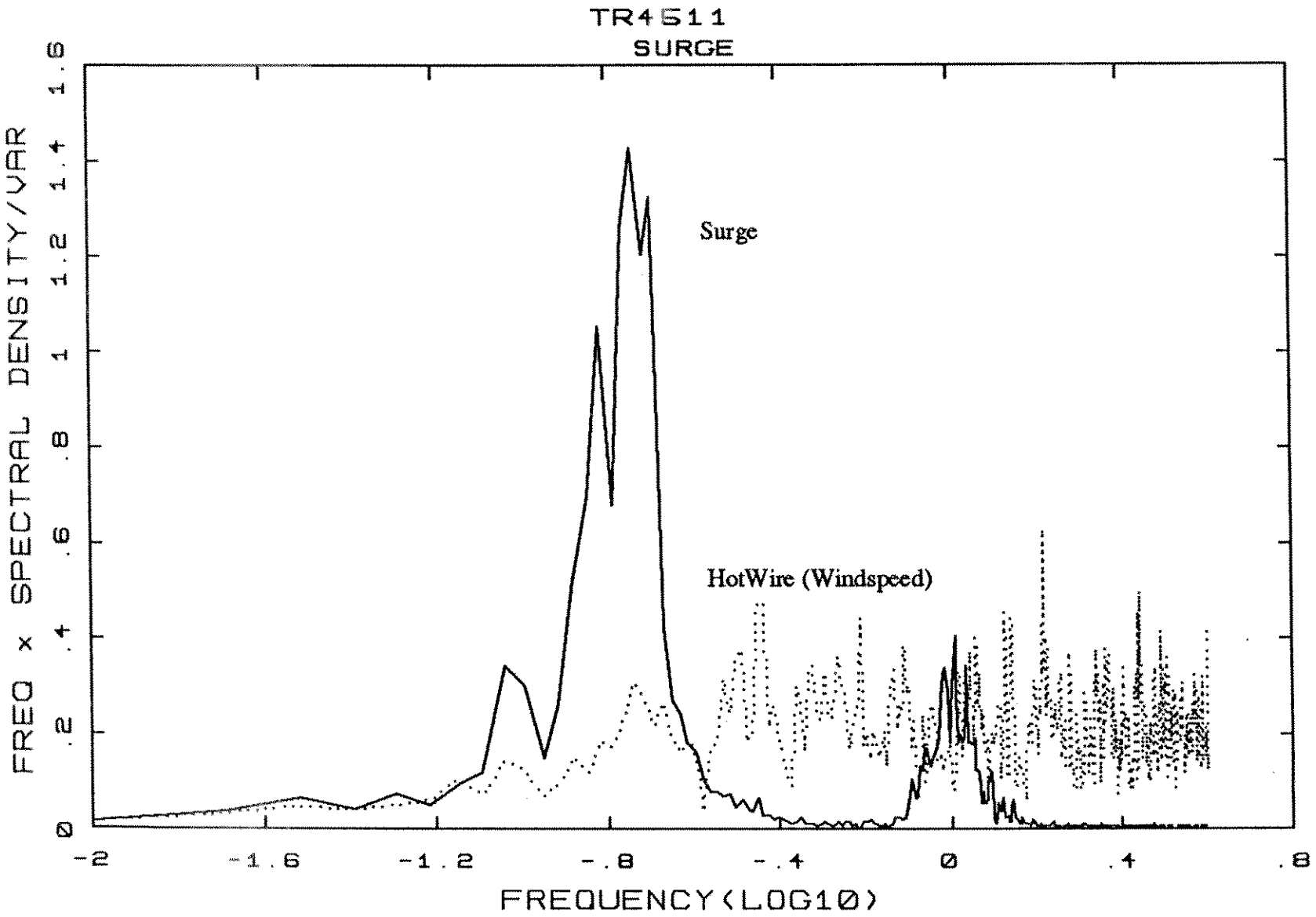
TR4511
SURGE
FREQ x SPECTRAL DENSITY/VAR
0
.2
.4
.6
.8
1
1.2
1.4
1.6
Surge
HotWire (Windspeed)
-2
-1.6
-1.2
-.8
-.4
0
.4
.8
FREQUENCY(LOG10)

TR4511.HW/S.4

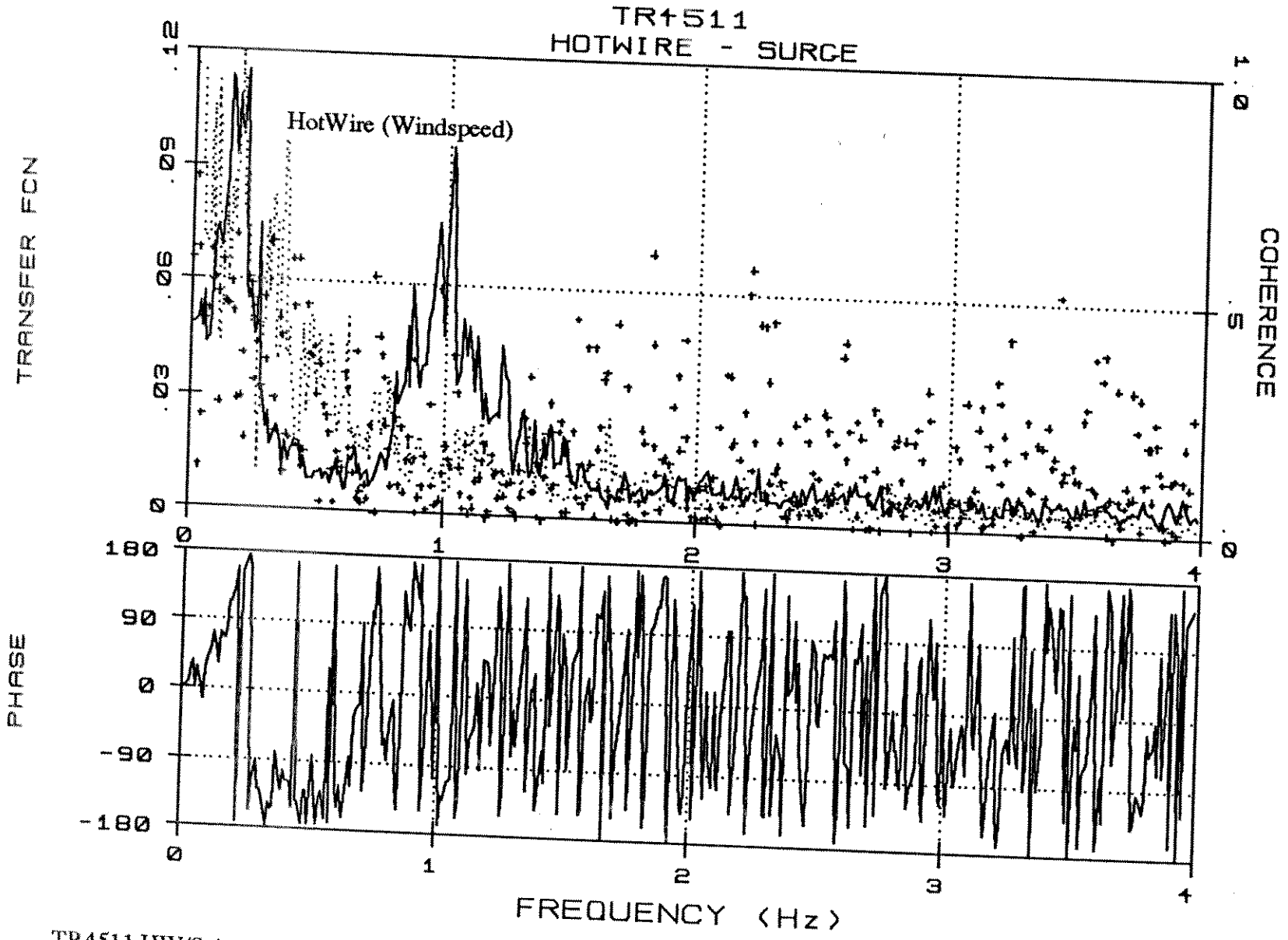

TR4511.HW/S.4t

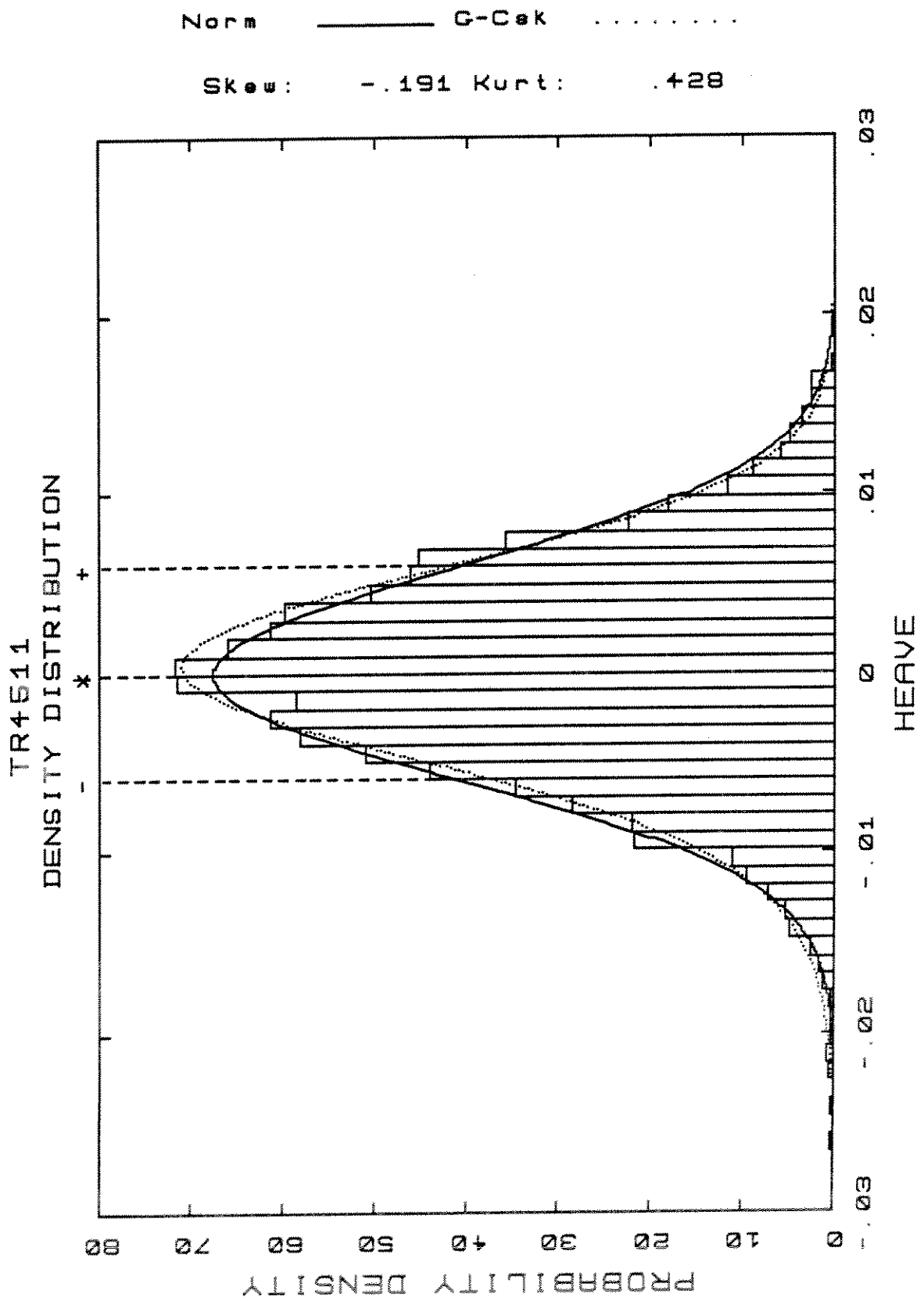
Norm
G-Cak
Skew: -.191 Kurt: .428
TR4511
DENSITY DISTRIBUTION
+
*
-
PROBABILITY DENSITY
0
10
20
30
40
50
60
70
80
-.03
-.02
-.01
0
.01
.02
.03
HEAVE

TR4511.H.1

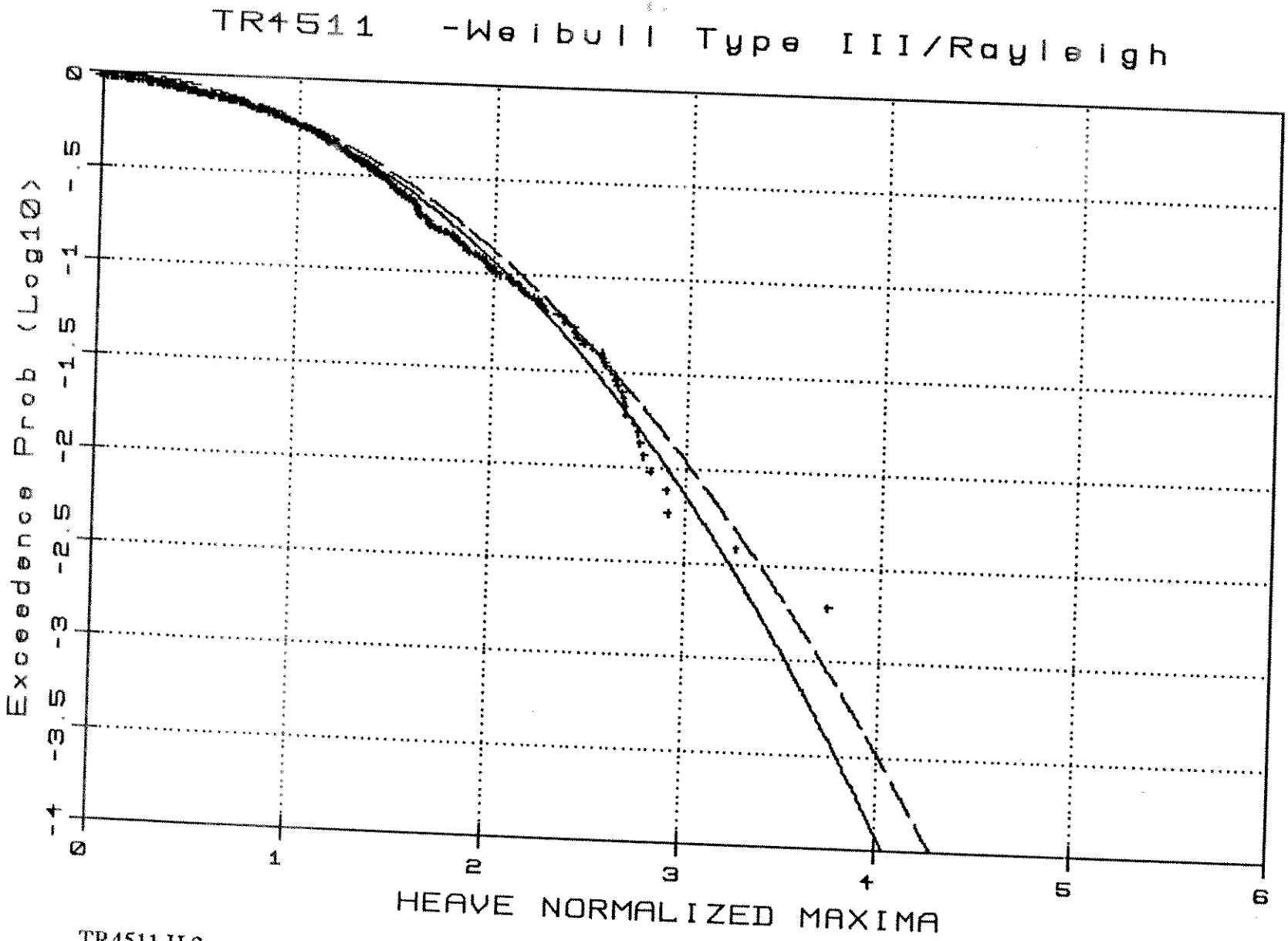
TR4511 -Weibull Type III/Rayleigh
Exceedence Prob (Log10)
0
-.5
-1
-1.5
-2
-2.5
-3
-3.5
-4
0
1
2
3
4
5
6
HEAVE NORMALIZED MAXIMA

TR4511.H.2

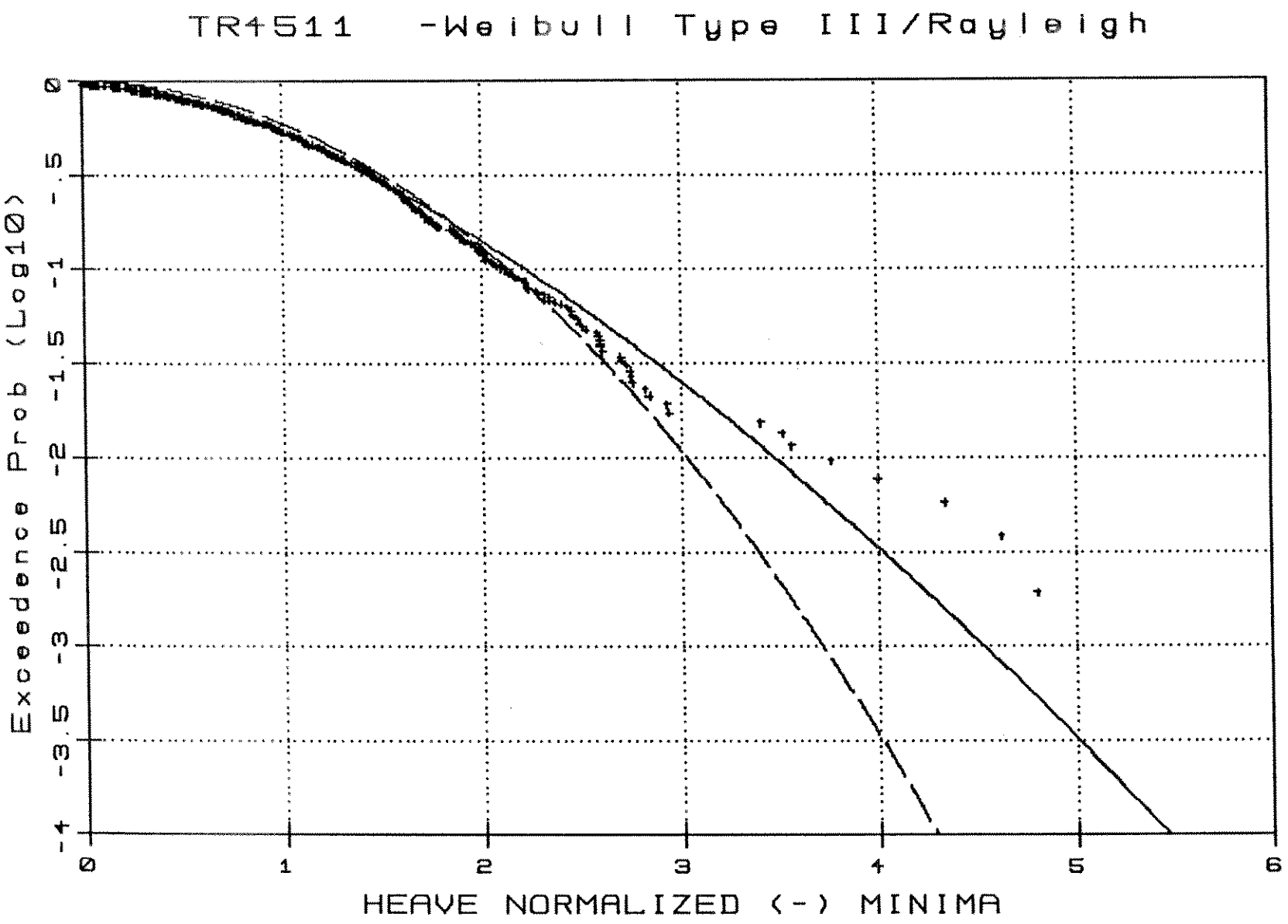
TR4511 -Weibull Type III/Rayleigh
Exceedence Prob (Log10)
0
-.5
-1
-1.5
-2
-2.5
-3
-3.5
-4
0
1
2
3
4
5
6
HEAVE NORMALIZED (-) MINIMA

TR4511.H.3

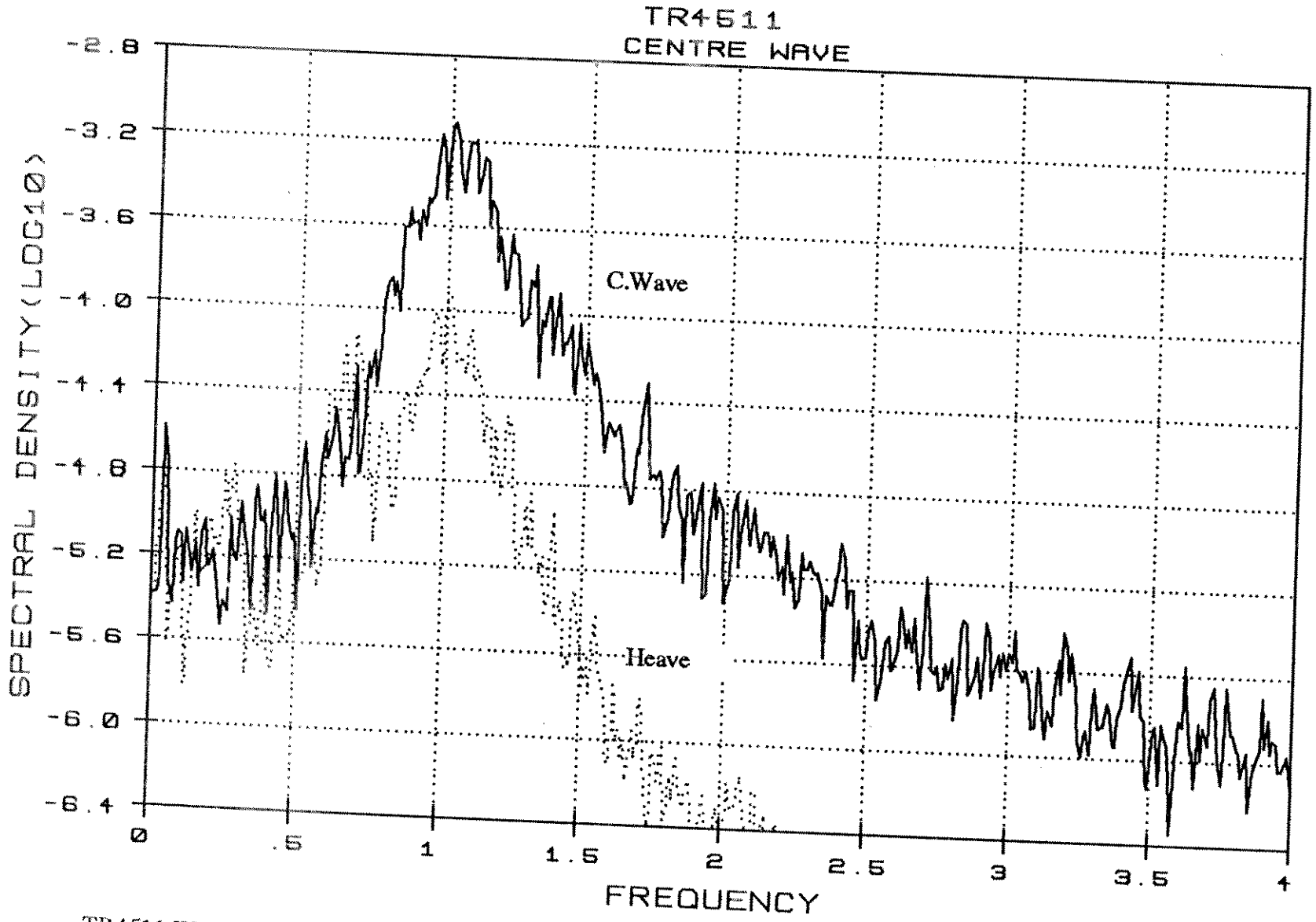
TR4511
CENTRE WAVE
SPECTRAL DENSITY(LOG10)
-2.8
-3.2
-3.6
-4.0
-4.1
-4.8
-5.2
-5.6
-6.0
-6.4
C.Wave
Heave
0
.5
1
1.5
2
2.5
3
3.5
4
FREQUENCY

TR4511.W/H.4

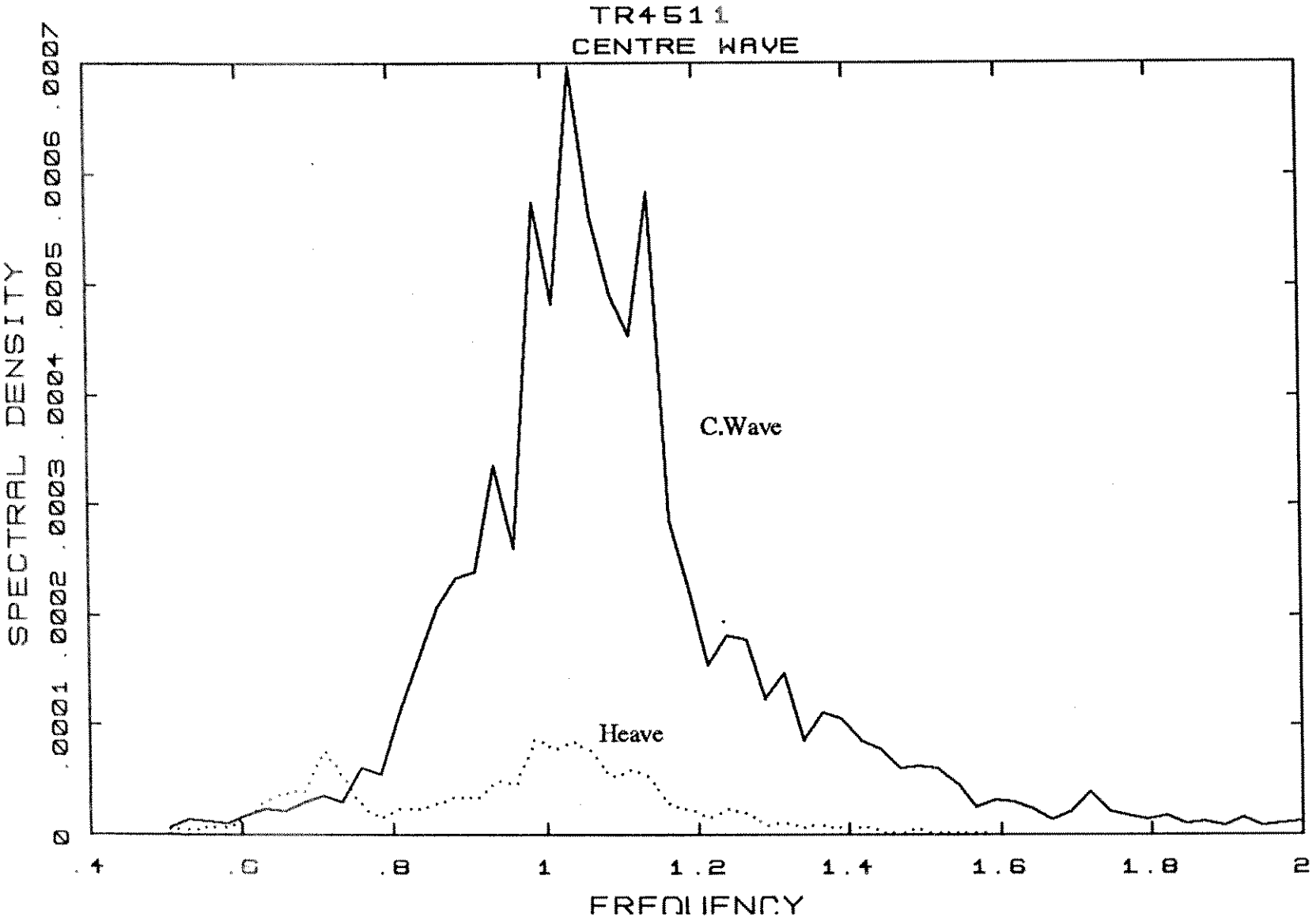
TR4511
CENTRE WAVE
SPECTRAL DENSITY
0
.0001
.0002
.0003
.0004
.0005
.0006
.0007
C.Wave
Heave
.4
.6
.8
1
1.2
1.4
1.6
1.8
2
FREQUENCY

TR4511.W/H.4*

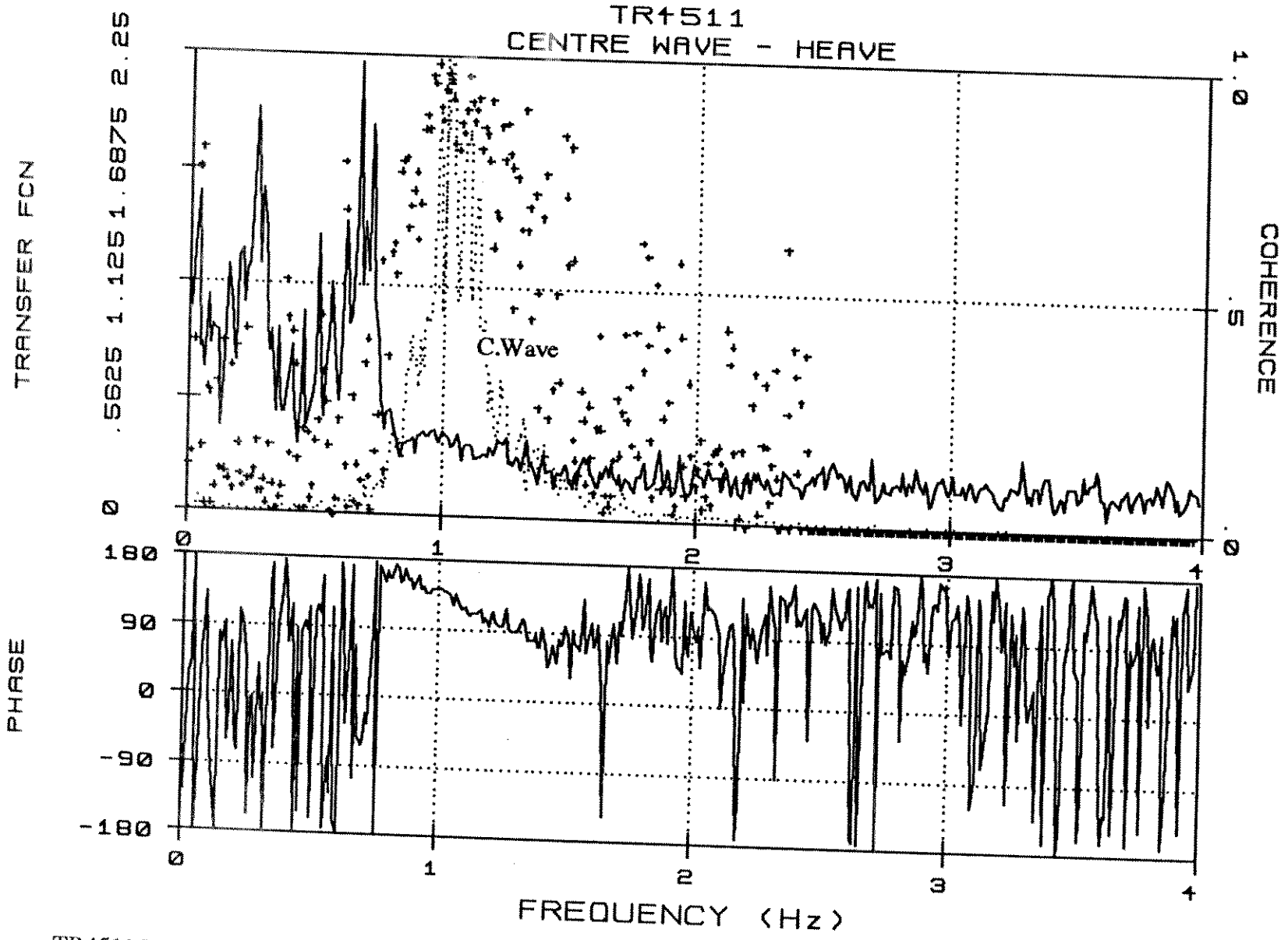
TR4511
CENTRE WAVE - HEAVE
TRANSFER FCN
.5625 1.125 1.6875 2.25
0
C.Wave
COHERENCE
1.0
.5
0
0
1
2
3
4
180
90
0
-90
-180
PHASE
FREQUENCY (Hz)

TR4511.W/H.4t

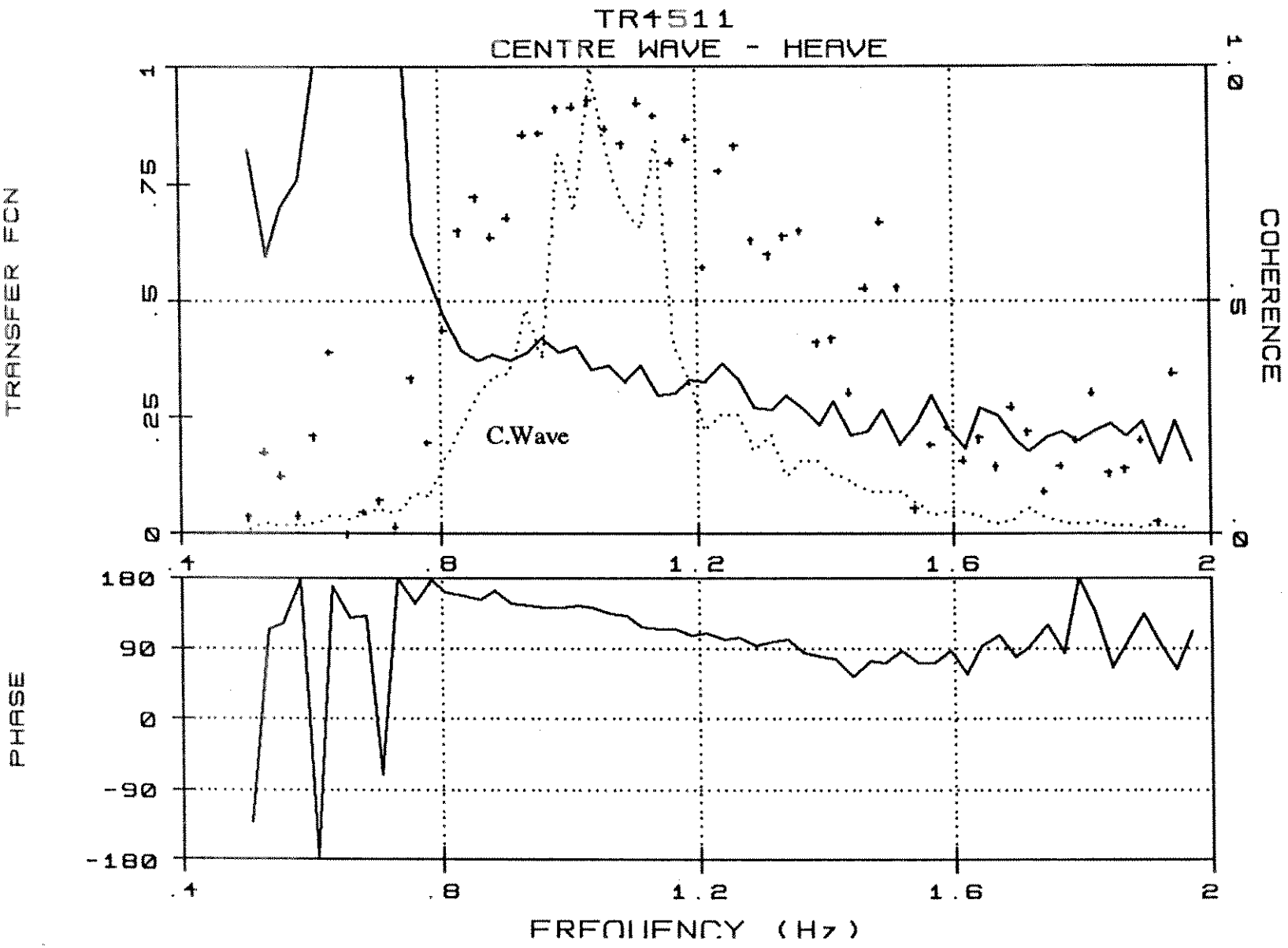
TR4511
CENTRE WAVE - HEAVE
TRANSFER FCN
COHERENCE
C.Wave
PHASE
FREQUENCY (Hz)
1
.75
.5
.25
0
1.0
.5
0
180
90
0
-90
-180
.4
.8
1.2
1.6
2

TR4511.W/H.4t*

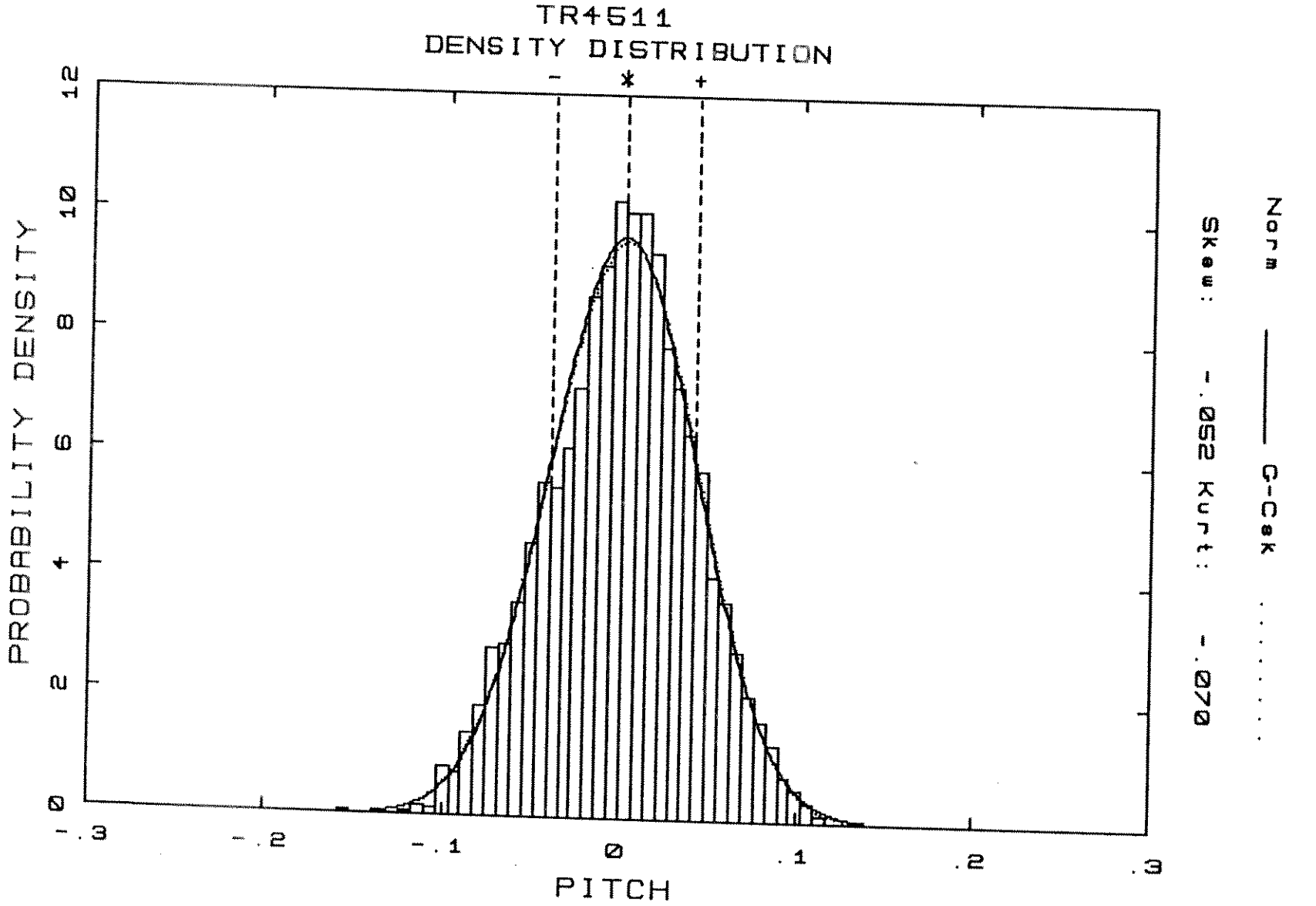
TR4511
DENSITY DISTRIBUTION
- * +
PROBABILITY DENSITY
0
2
4
6
8
10
12
-.3
-.2
-.1
0
.1
.2
.3
PITCH
Norm ——— C-Cek .....
Skew: -.052 Kurt: -.070

TR4511.Pi.1

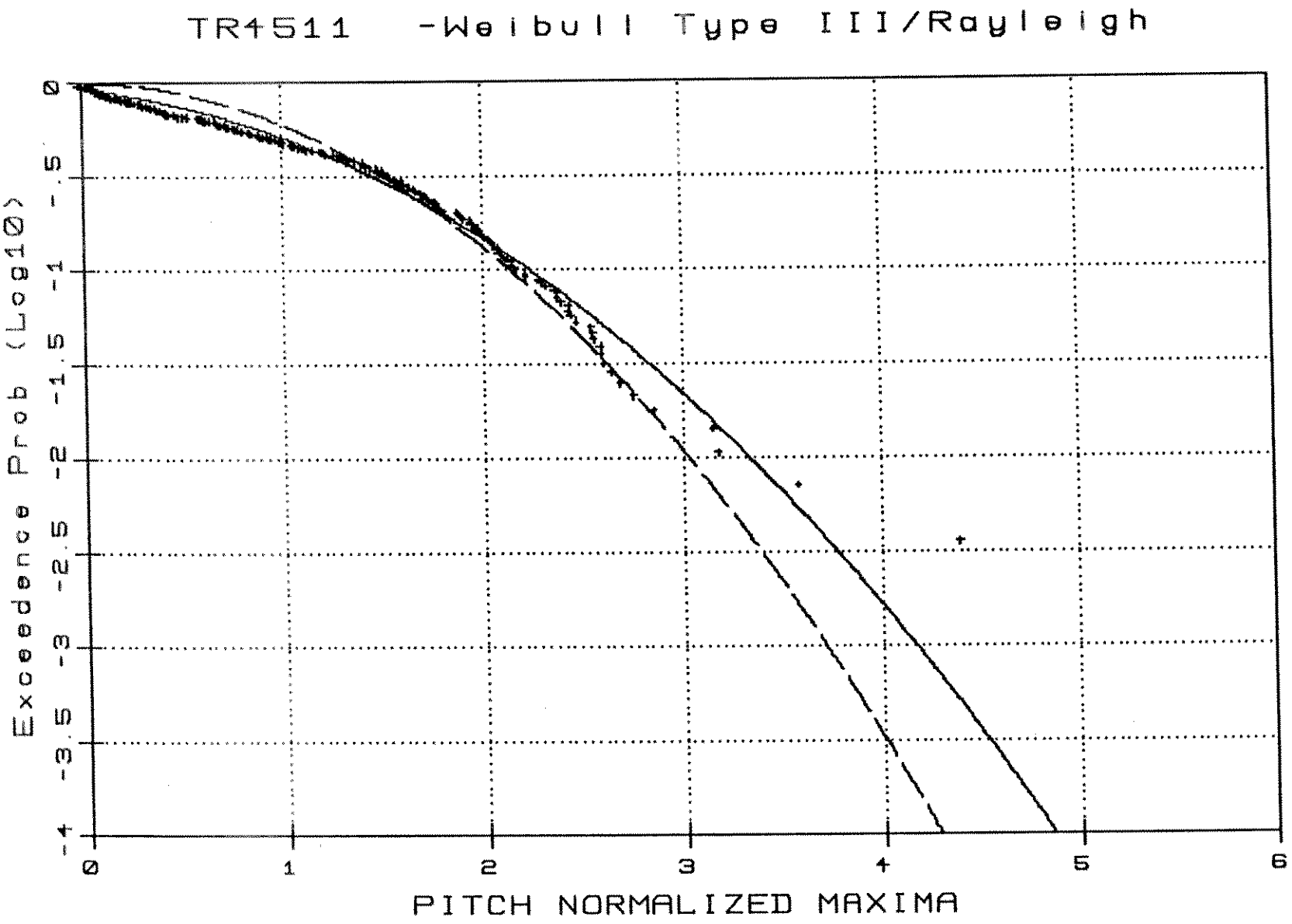
TR4511 -Weibull Type III/Rayleigh
Exceedence Prob (Log10)
0
-.5
-1
-1.5
-2
-2.5
-3
-3.5
-4
0
1
2
3
4
5
6
PITCH NORMALIZED MAXIMA

TR4511.Pi.2

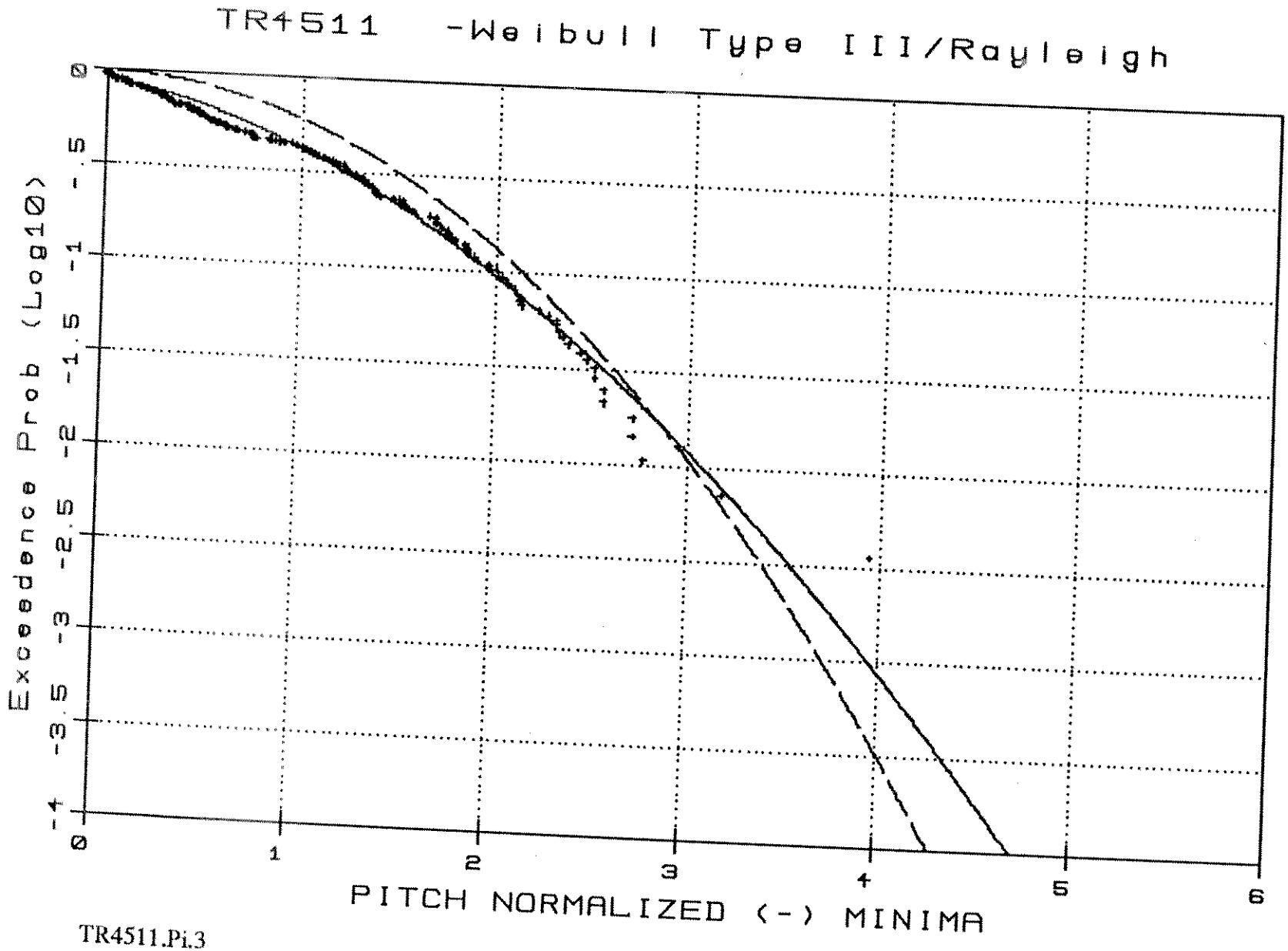
TR4511 -Weibull Type III/Rayleigh
Exceedence Prob (Log10)
0
-.5
-1
-1.5
-2
-2.5
-3
-3.5
-4
0
1
2
3
4
5
6
PITCH NORMALIZED (-) MINIMA

TR4511.Pi.3

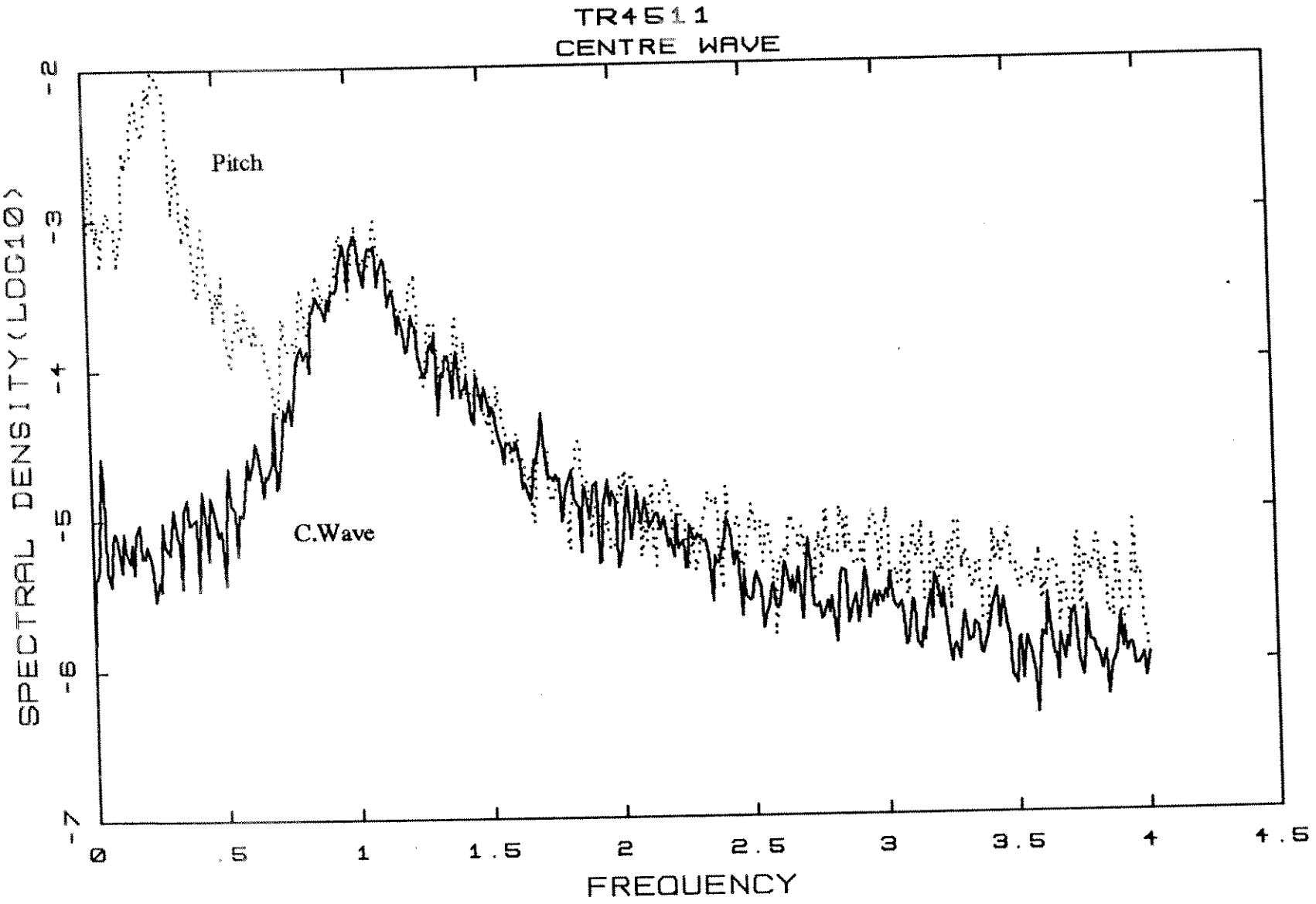
TR4511
CENTRE WAVE
Pitch
C.Wave
SPECTRAL DENSITY(LOG10)
-2
-3
-4
-5
-6
-7
0
.5
1
1.5
2
2.5
3
3.5
4
4.5
FREQUENCY

TR4511.W/Pi.4

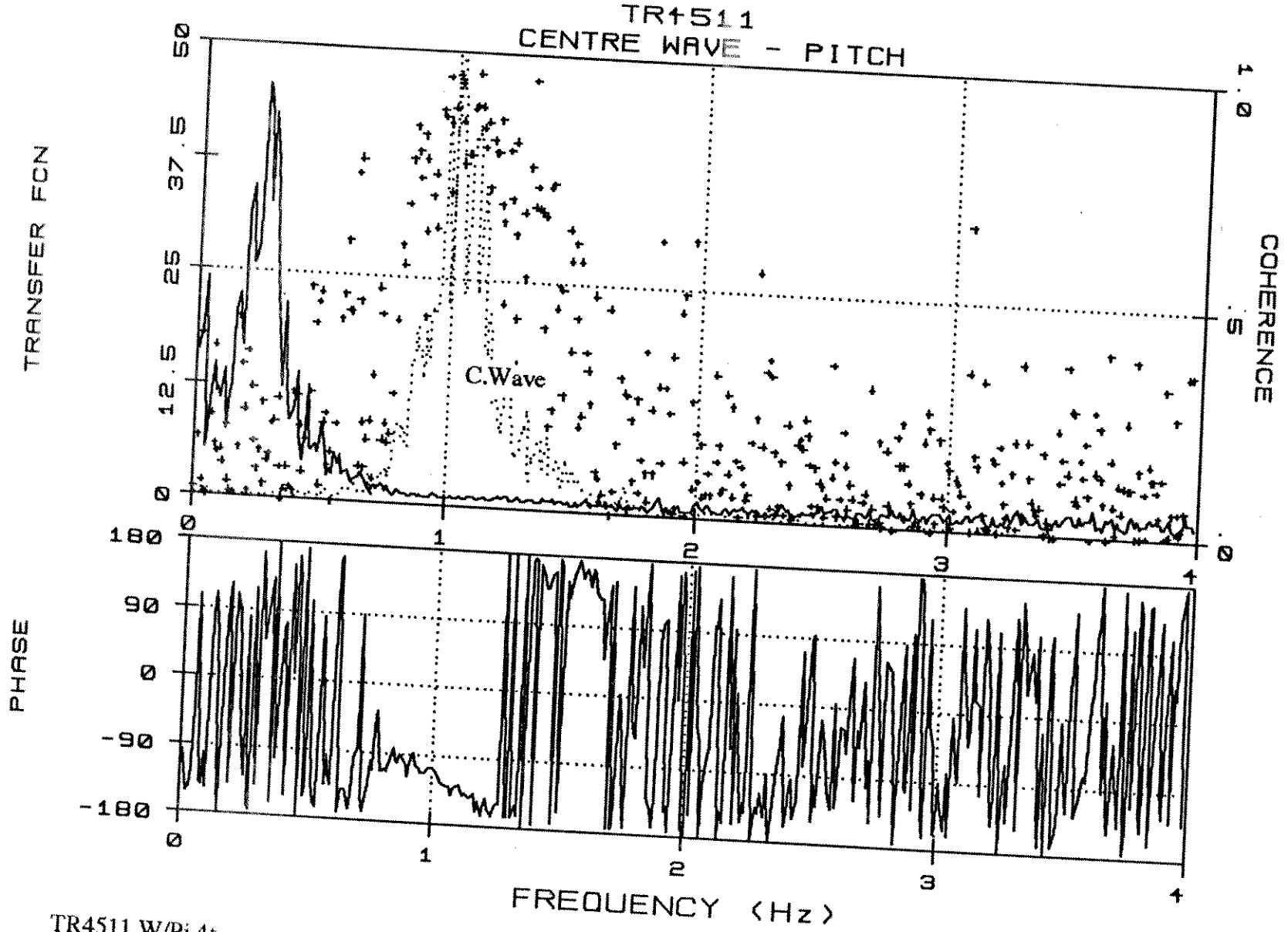

TR4511.W/Pi.4t

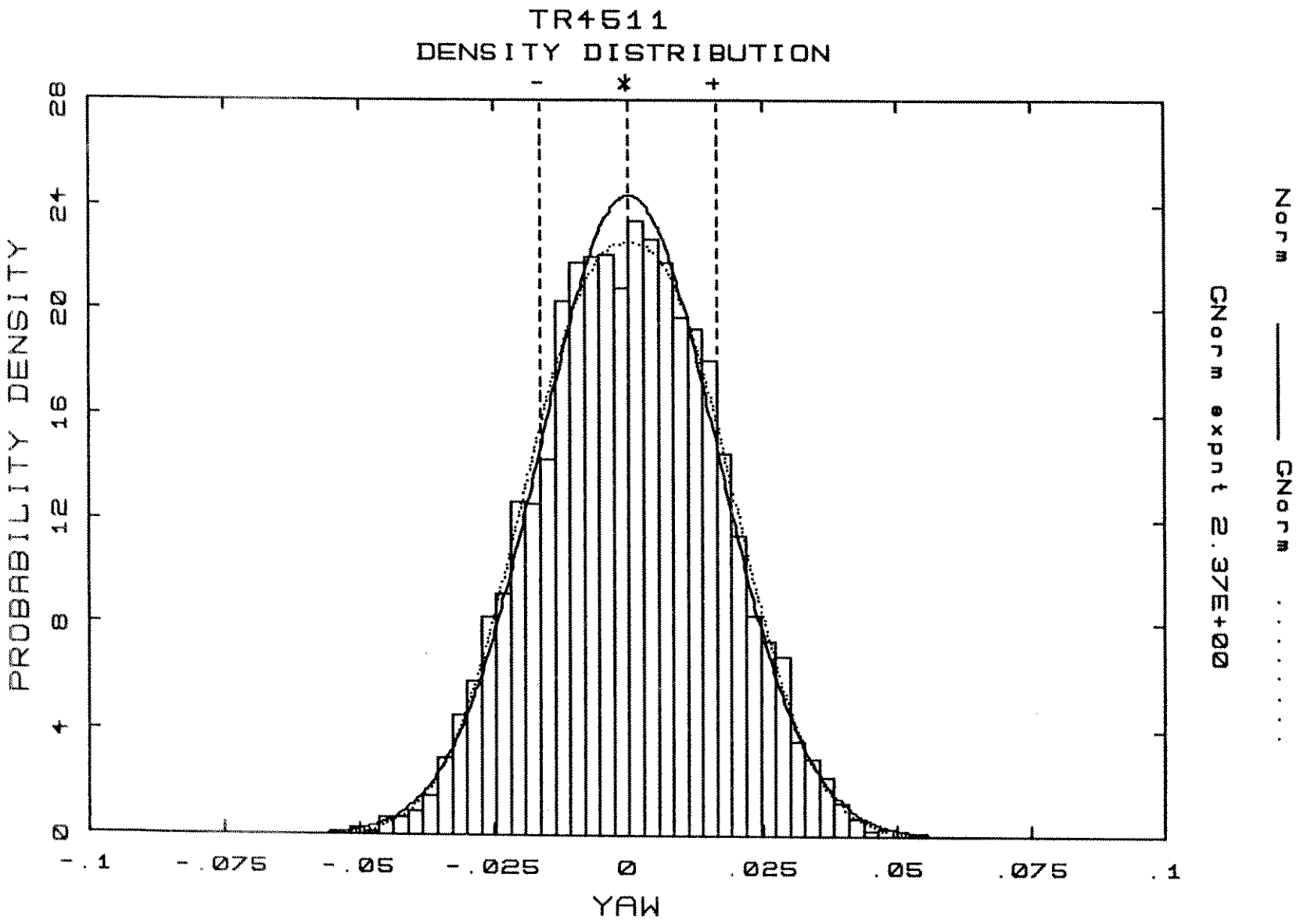
TR4511
DENSITY DISTRIBUTION
- * +
PROBABILITY DENSITY
0
4
8
12
16
20
24
28
-.1
-.075
-.05
-.025
0
.025
.05
.075
.1
YAW
Norm
GNorm
GNorm expnt 2.37E+00

TR4511.Y.1

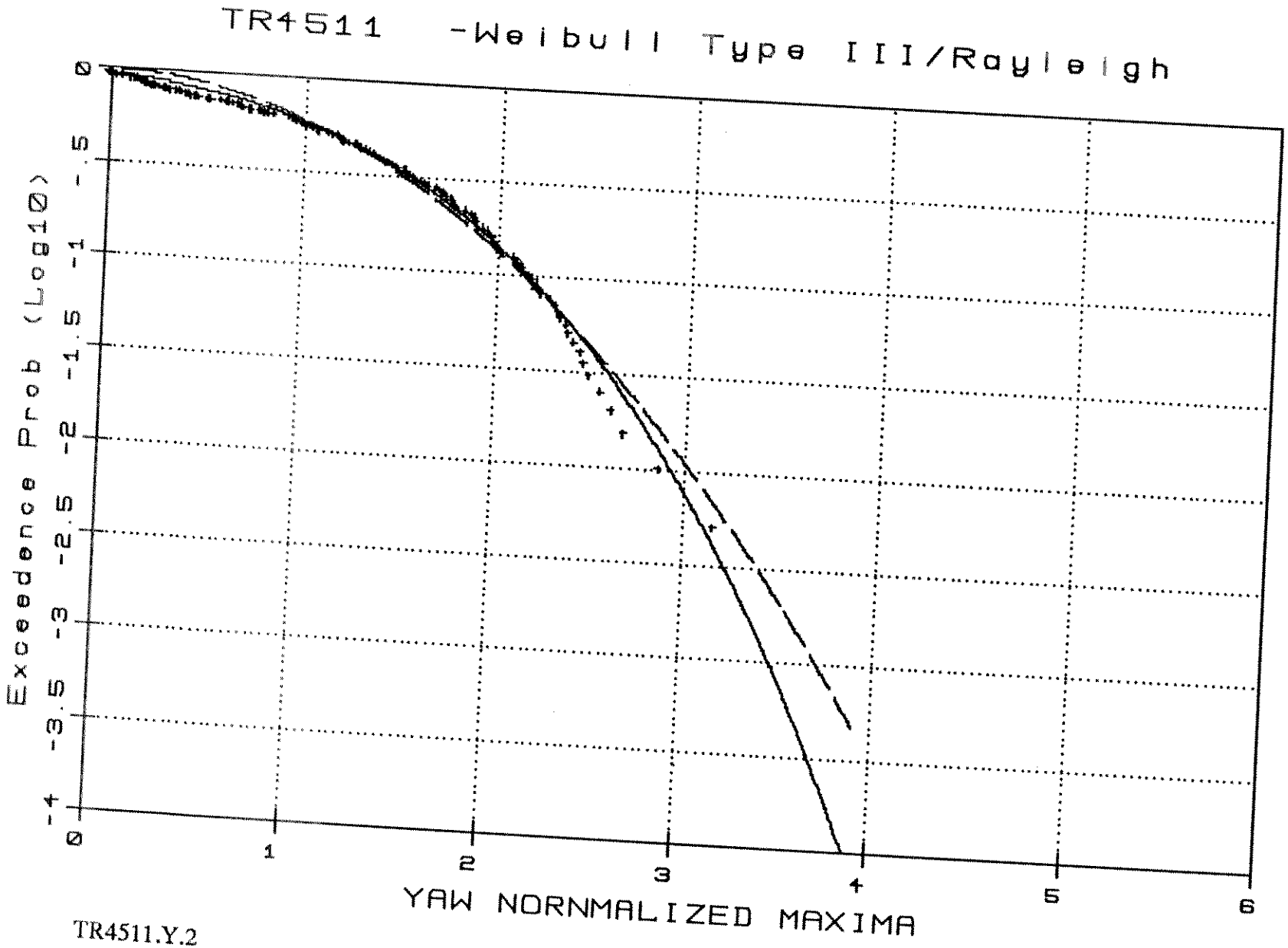
TR4511 -Weibull Type III/Rayleigh
Exceedence Prob (Log10)
0
-.5
-1
-1.5
-2
-2.5
-3
-3.5
-4
0
1
2
3
4
5
6
YAW NORNMALIZED MAXIMA

TR4511.Y.2

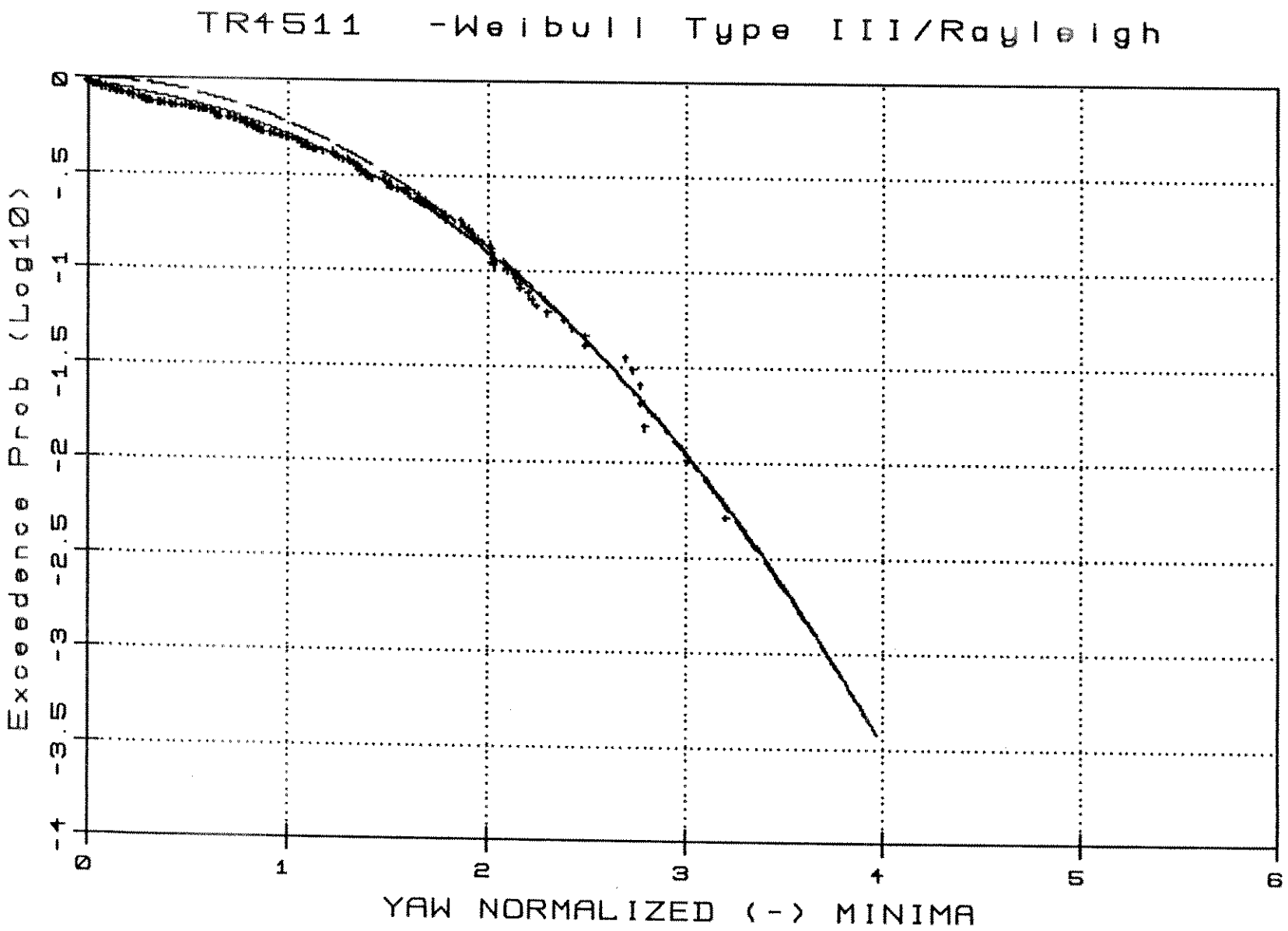
TR4511 -Weibull Type III/Rayleigh
Exceedence Prob (Log10)
0
-.5
-1
-1.5
-2
-2.5
-3
-3.5
-4
0
1
2
3
4
5
6
YAW NORMALIZED (-) MINIMA

TR4511.Y.3

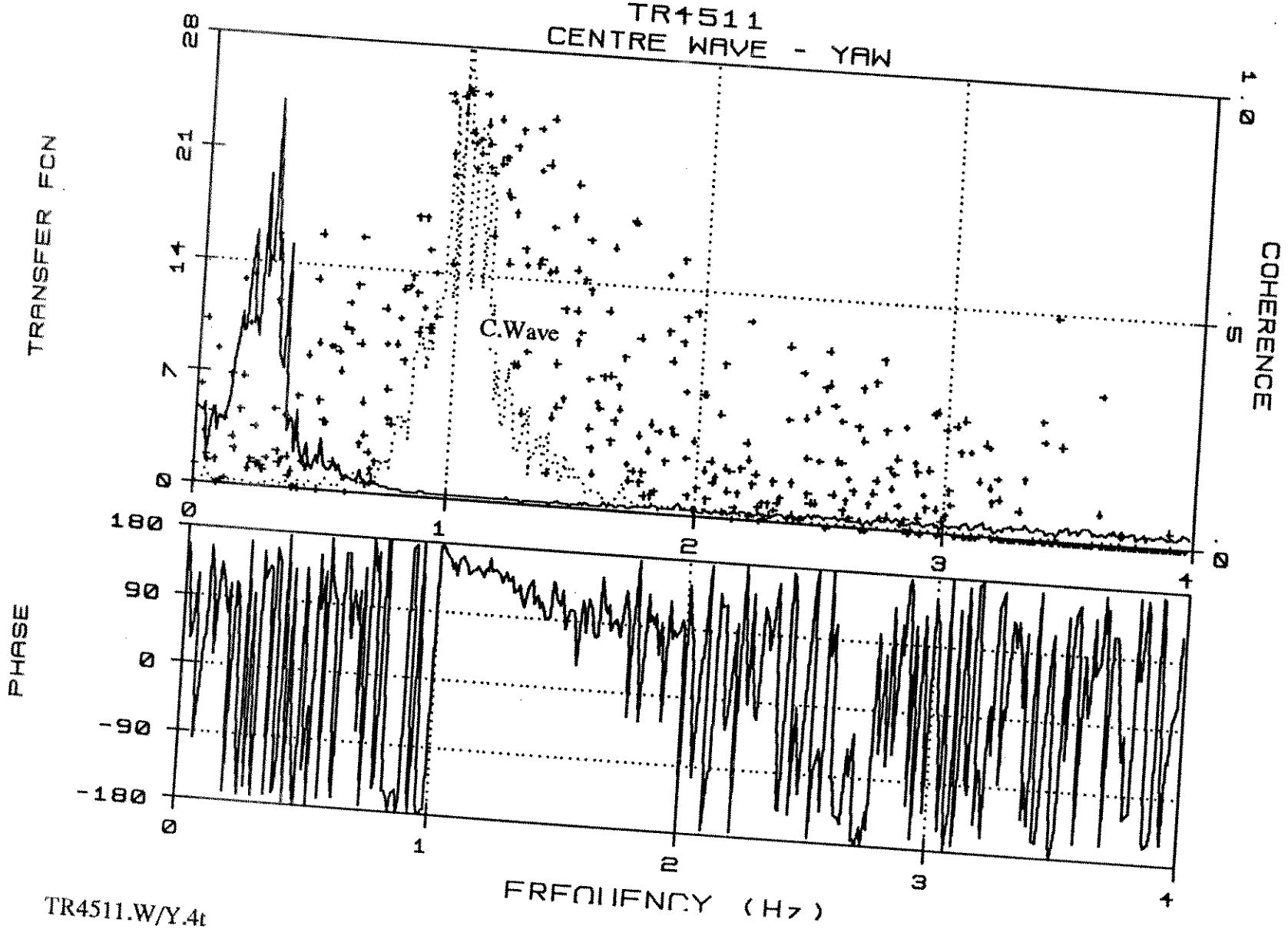
TR4511
CENTRE WAVE - YAW
TRANSFER FCN
28
21
14
7
0
C.Wave
COHERENCE
1.0
.5
0
0
1
2
3
4
PHASE
180
90
0
-90
-180
FREQUENCY (Hz)

TR4511.W/Y.4t

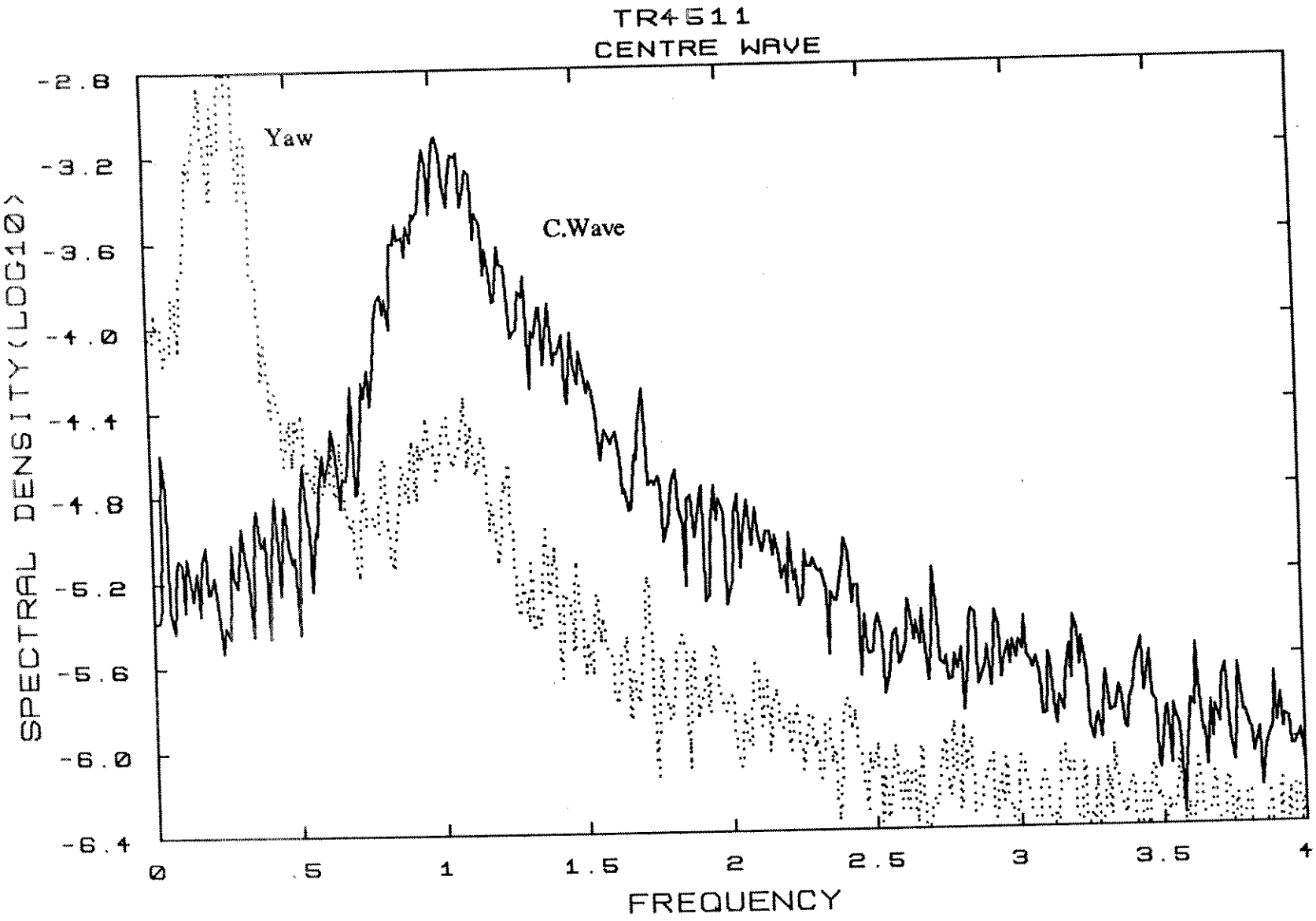
TR4511
CENTRE WAVE
Yaw
C.Wave
SPECTRAL DENSITY(LOG10)
-2.8
-3.2
-3.6
-4.0
-4.4
-4.8
-5.2
-5.6
-6.0
-6.4
0
.5
1
1.5
2
2.5
3
3.5
4
FREQUENCY

TR4511.W/Y.4

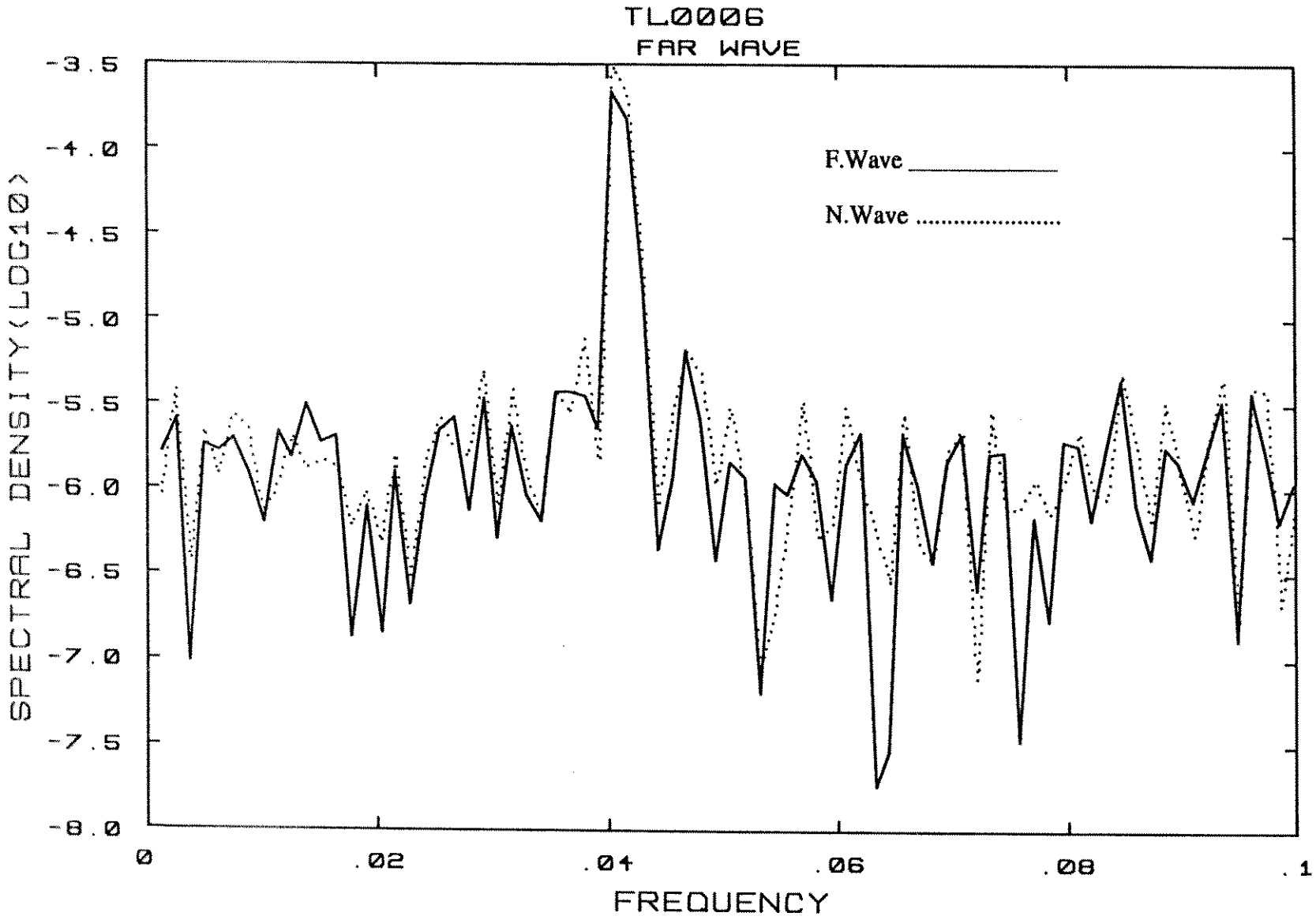

TL0006.FW/NW.4B

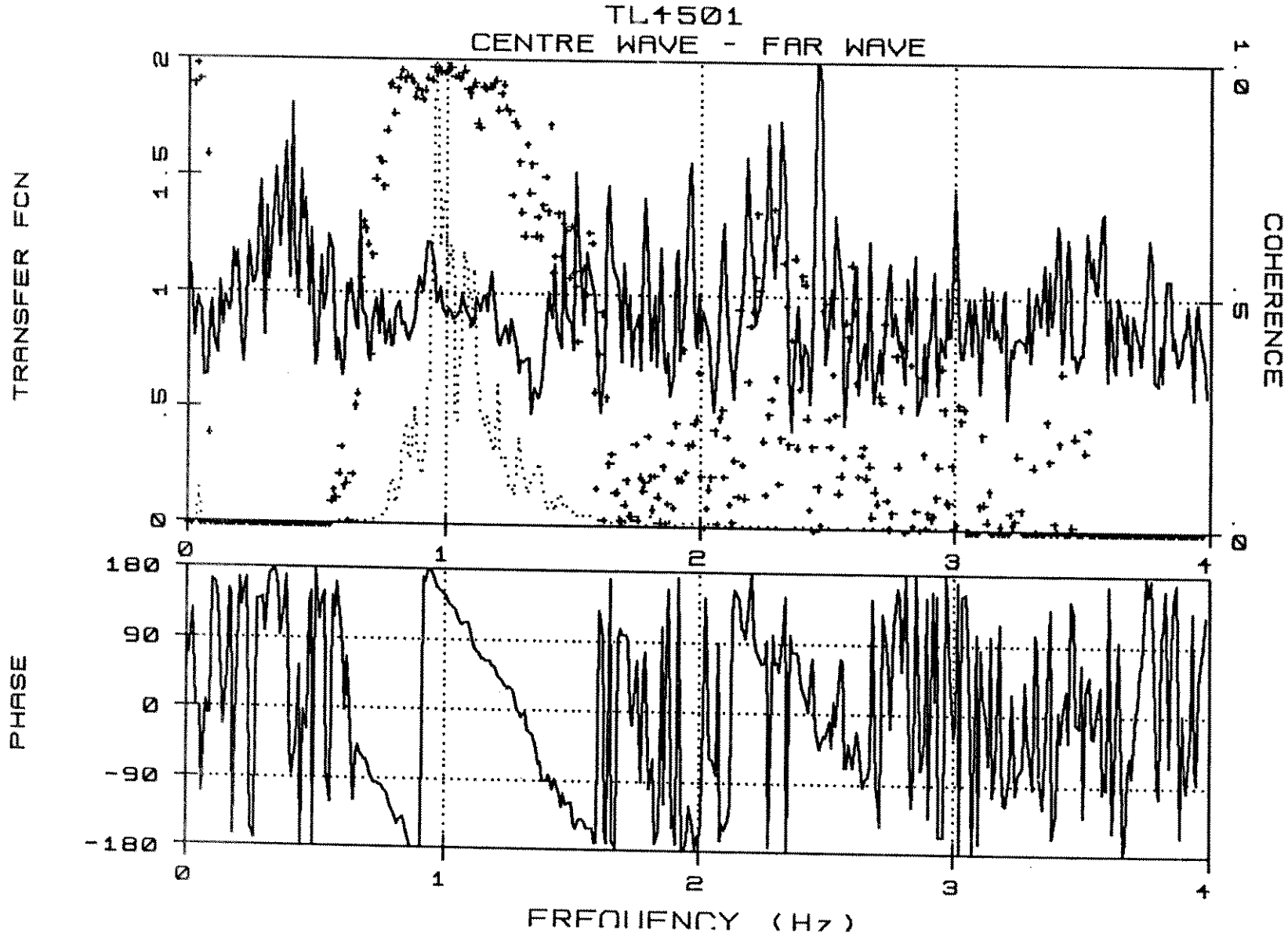

TL4501.CW.FW.4t

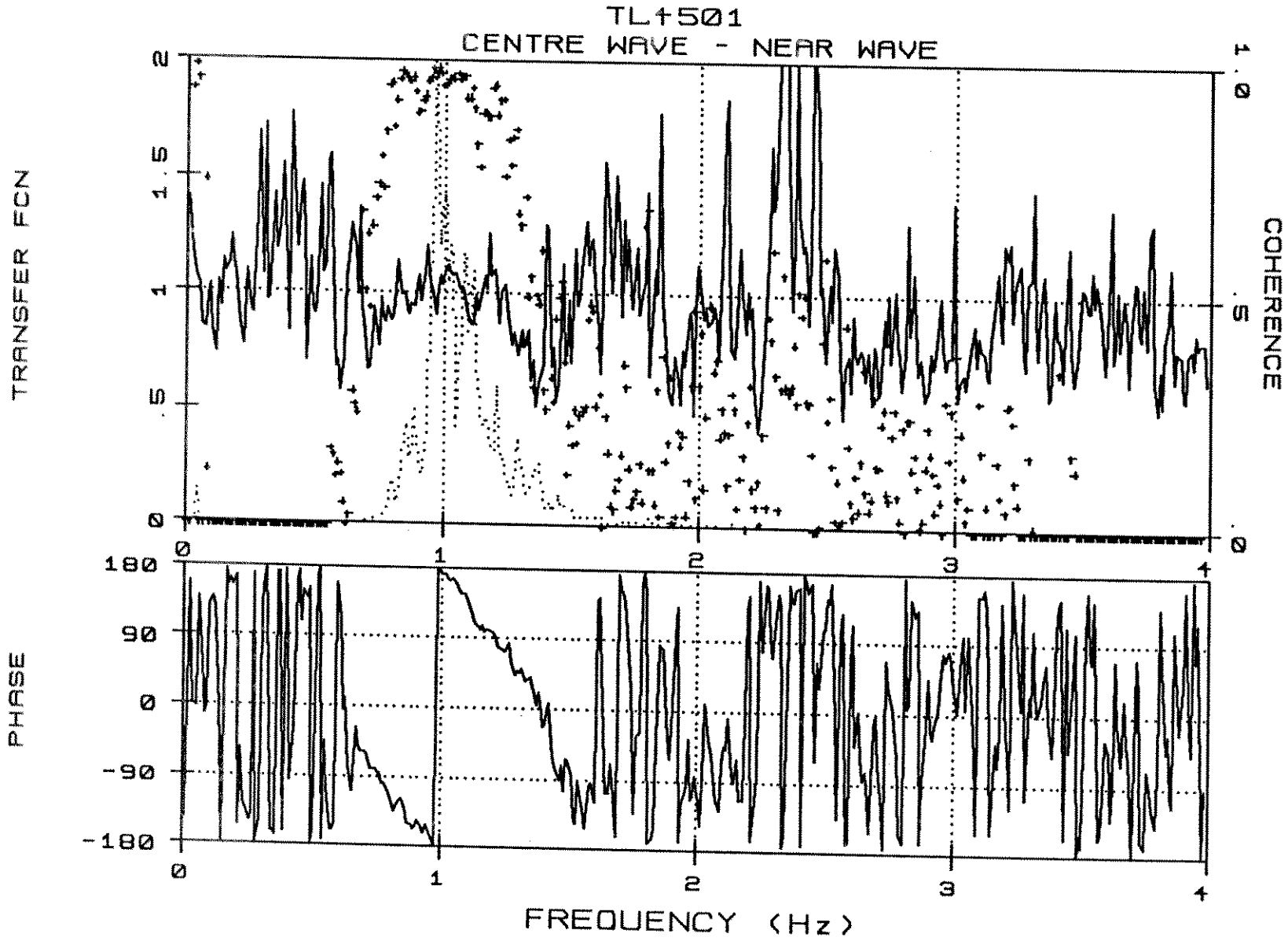

TL4501.CW/NW.4t

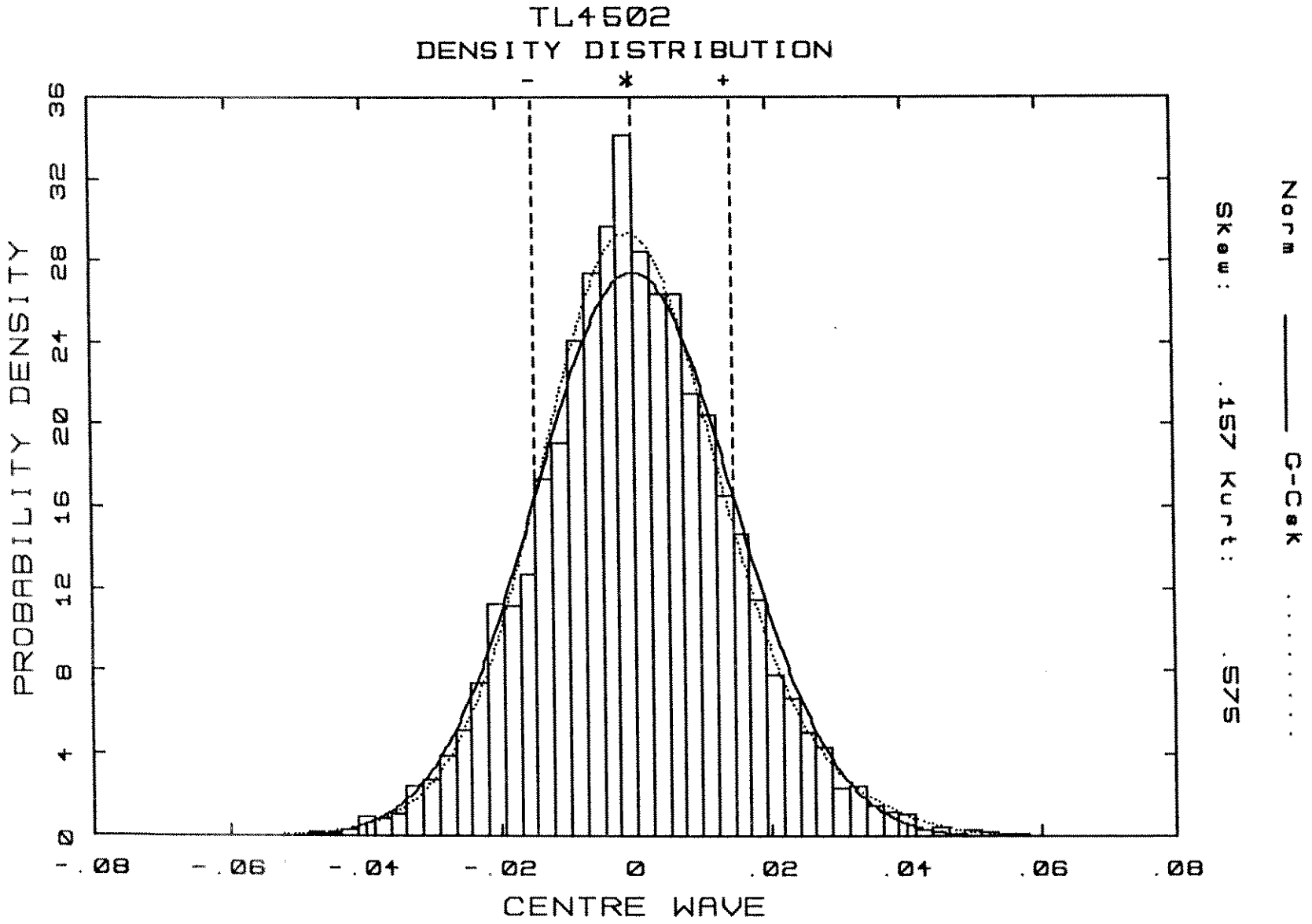
TL4502
DENSITY DISTRIBUTION
- * +
PROBABILITY DENSITY
0 4 8 12 16 20 24 28 32 36
-.08 -.06 -.04 -.02 0 .02 .04 .06 .08
CENTRE WAVE
Norm ——— G-Cak .....
Skew: .157 Kurt: .575

TL4502.W.1

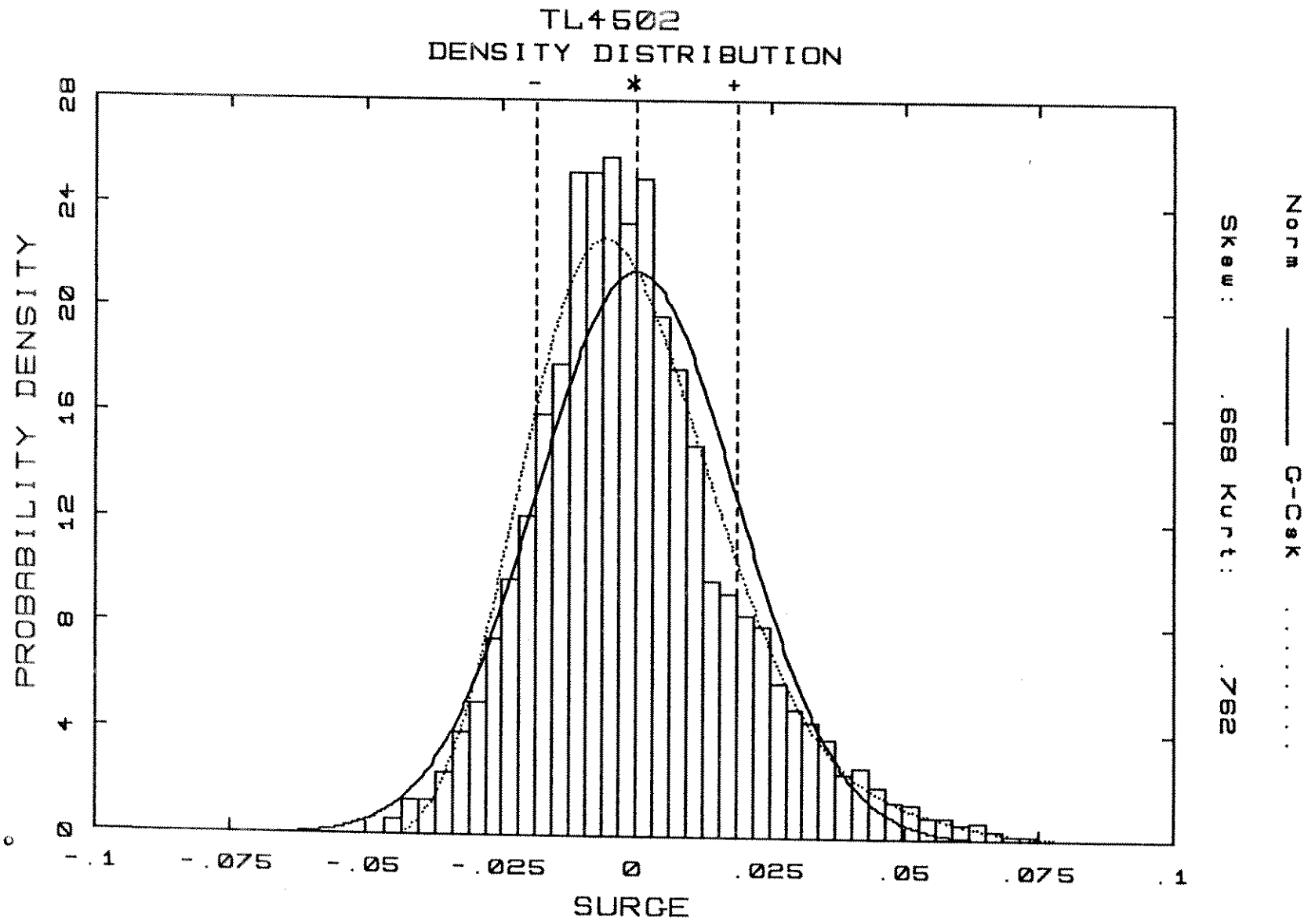
TL4502
DENSITY DISTRIBUTION
PROBABILITY DENSITY
0
4
8
12
16
20
24
28
- * +
-.1
-.075
-.05
-.025
0
.025
.05
.075
.1
SURGE
Norm
Q-Osk
Skew: .668 Kurt: .762

TL4502.S.1

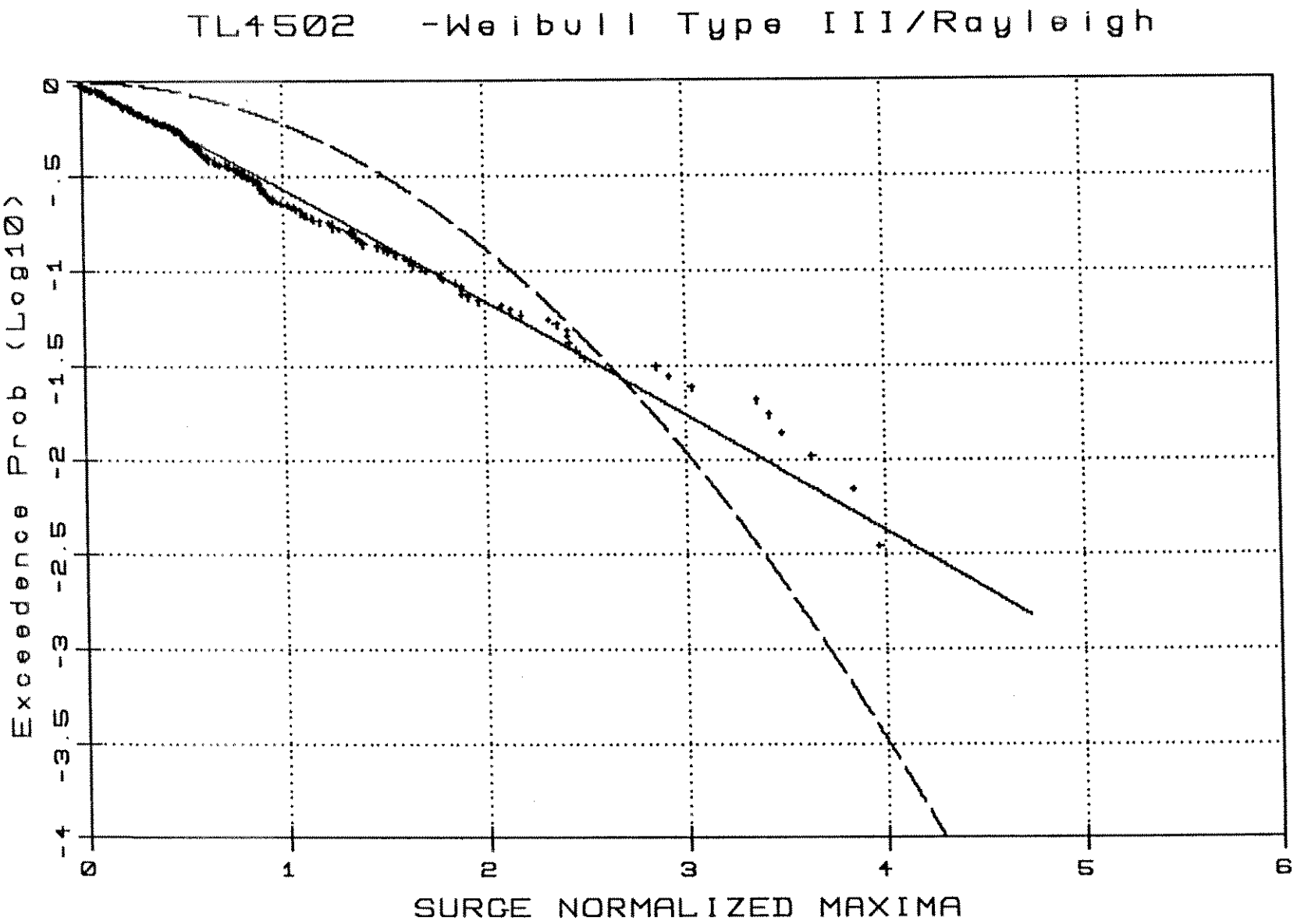
TL4502 -Weibull Type III/Rayleigh
Exceedence Prob (Log10)
0
-.5
-1
-1.5
-2
-2.5
-3
-3.5
-4
0
1
2
3
4
5
6
SURGE NORMALIZED MAXIMA

TL4502.S.2

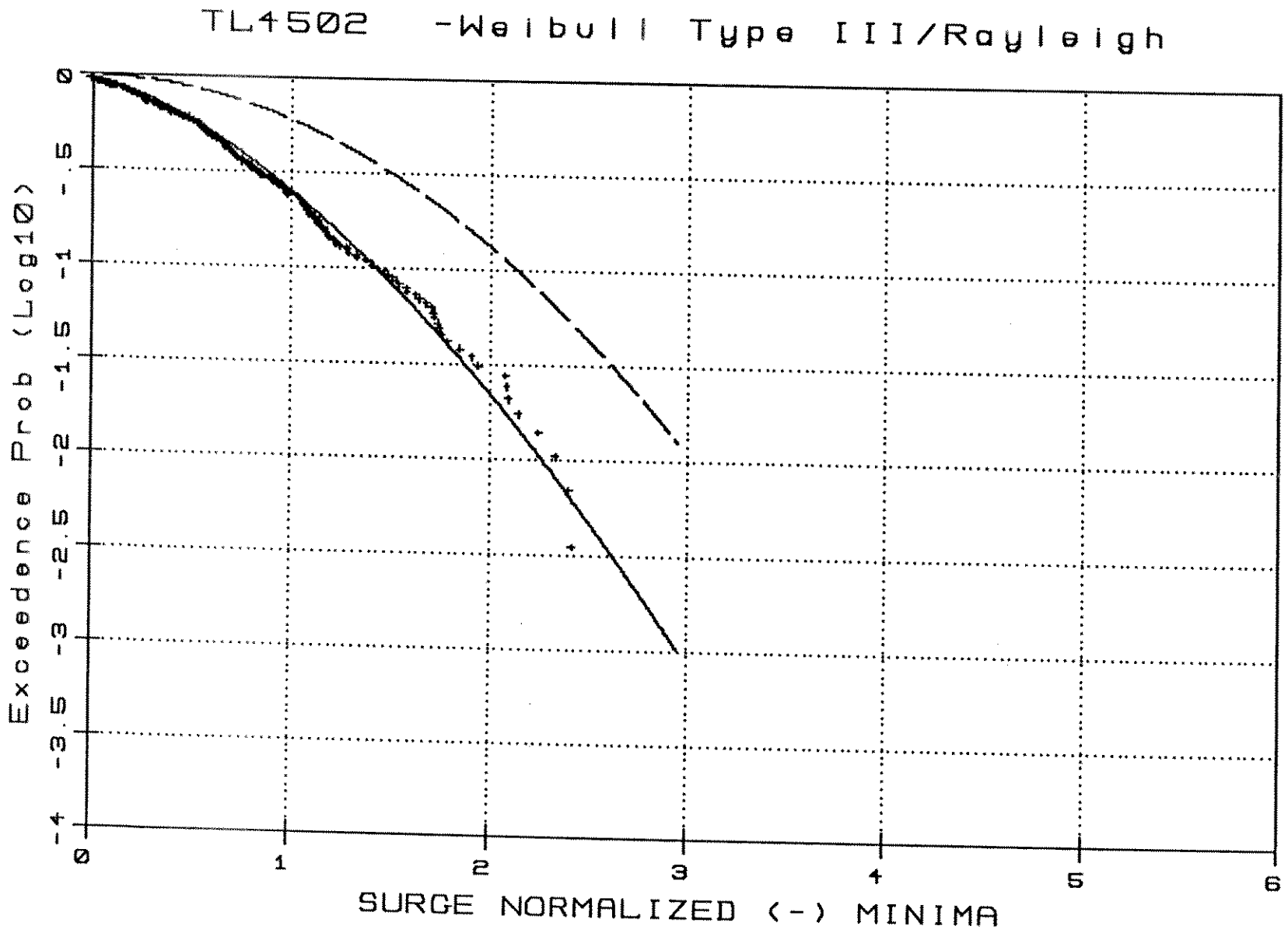
TL4502 -Weibull Type III/Rayleigh
Exceedence Prob (Log10)
0
-.5
-1
-1.5
-2
-2.5
-3
-3.5
-4
0
1
2
3
4
5
6
SURGE NORMALIZED (-) MINIMA

TL4502.S.3

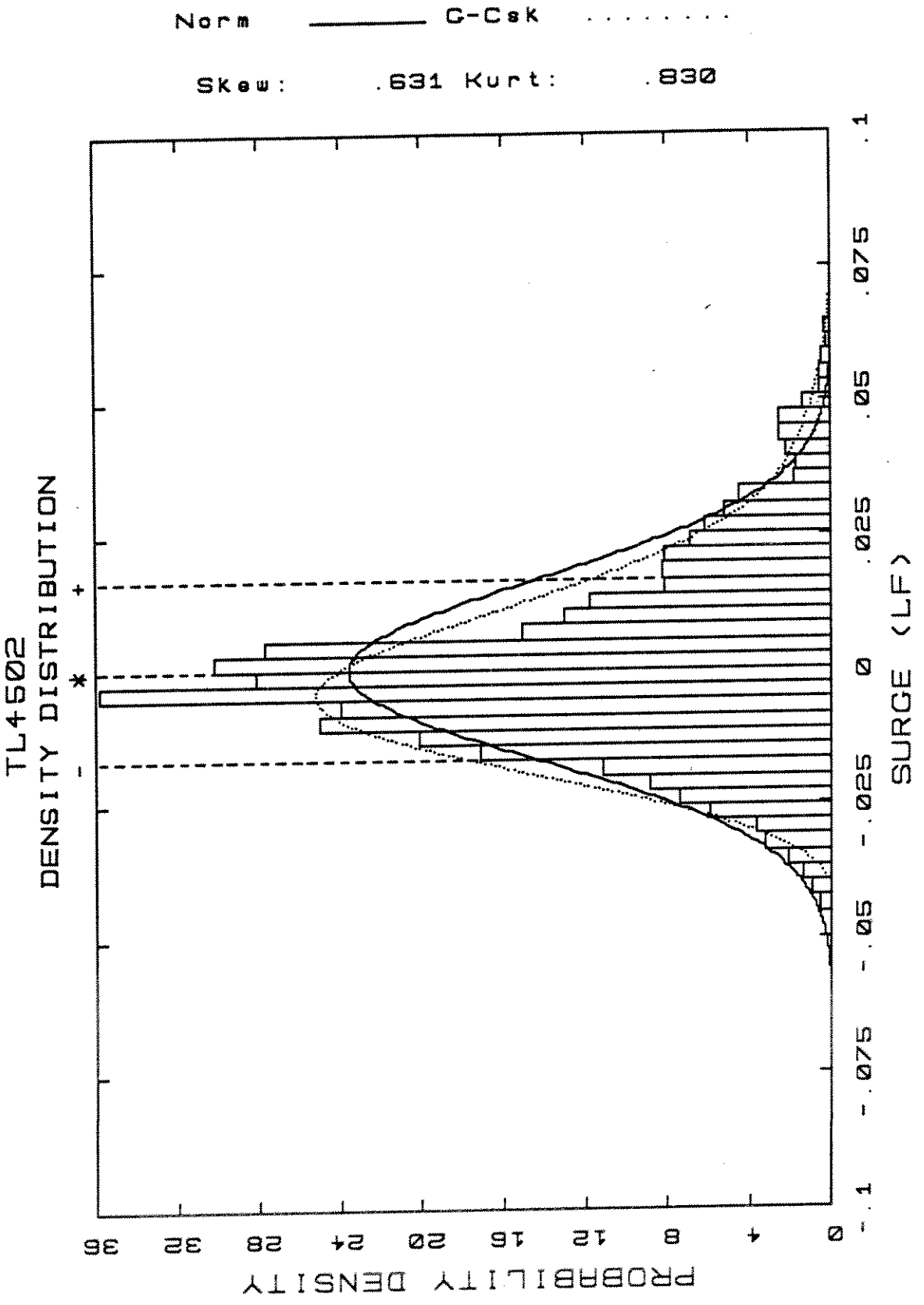
Norm
C-Csk
Skew: .631 Kurt: .830
TL4502
DENSITY DISTRIBUTION
+
*
-
PROBABILITY DENSITY
0
4
8
12
16
20
24
28
32
36
SURGE (LF)
.1
.075
.05
.025
0
-.025
-.05
-.075
-.1

TL4502.SLF.1

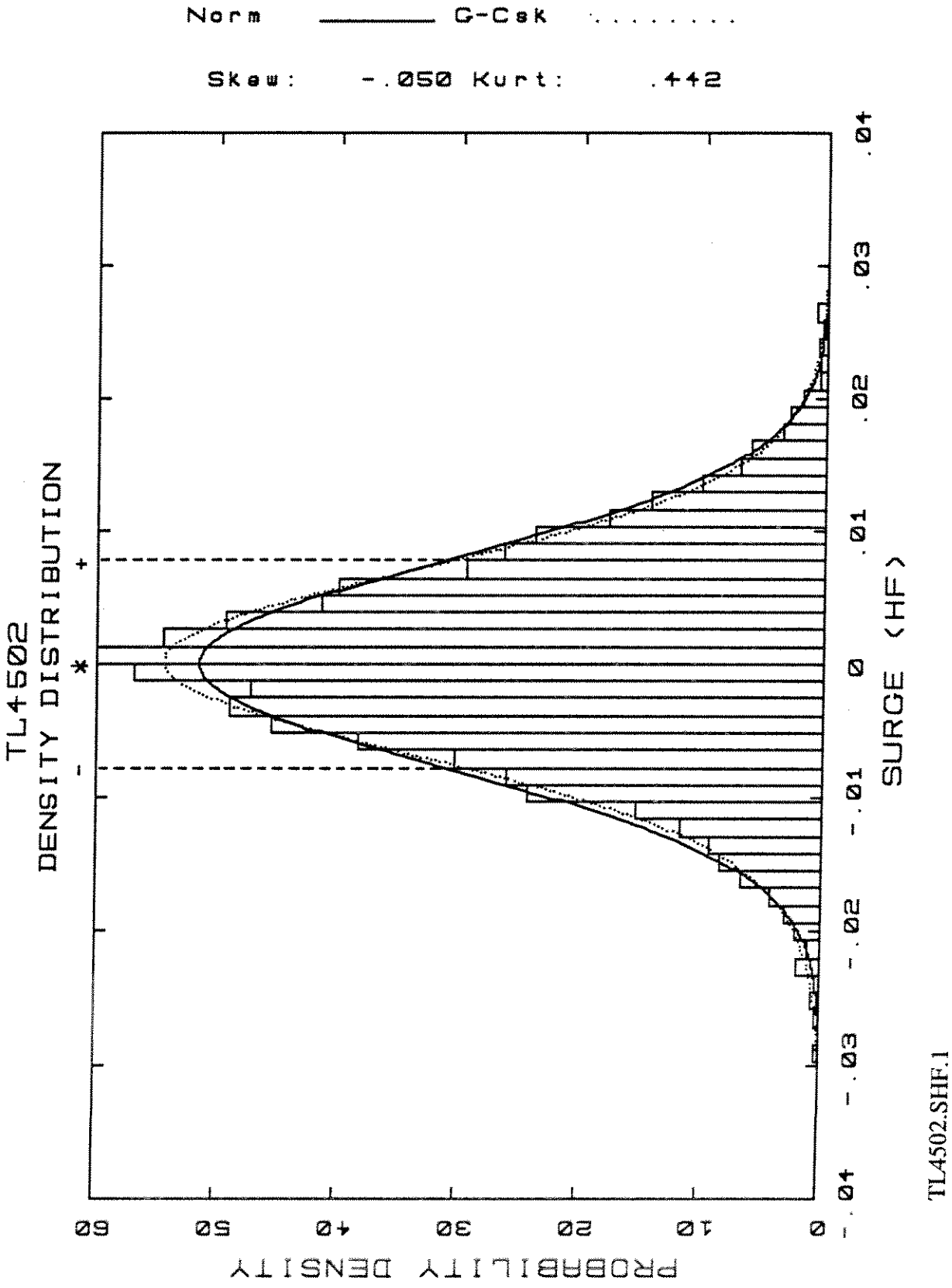
Norm
C-Csk
Skew: -.050 Kurt: .442
TL4502
DENSITY DISTRIBUTION
+
*
-
PROBABILITY DENSITY
0
10
20
30
40
50
60
-.04
-.03
-.02
-.01
0
.01
.02
.03
.04
SURGE (HF)

TL4502.SHF.1

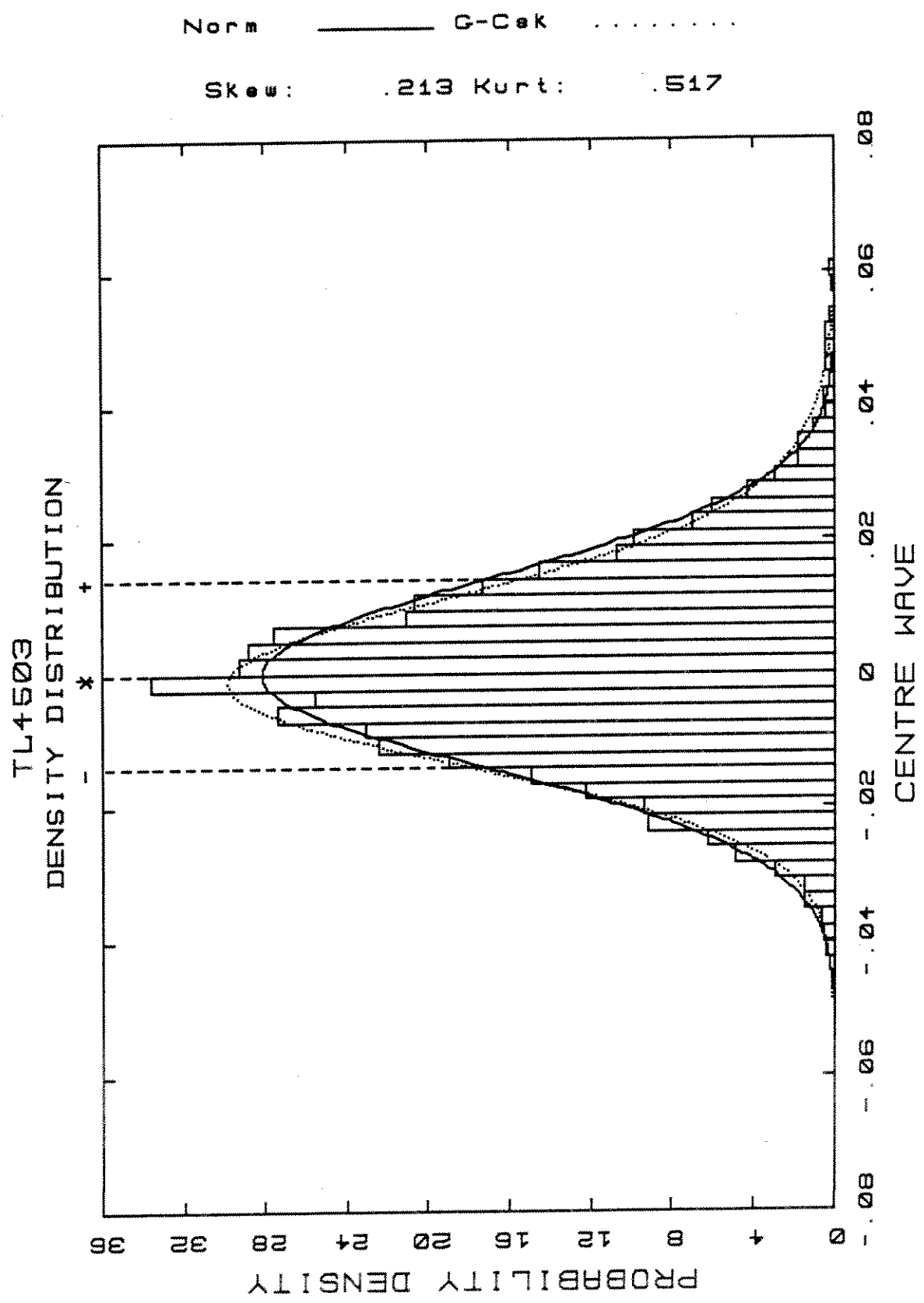
Norm
G-Cek
Skew: .213 Kurt: .517
TL4503
DENSITY DISTRIBUTION
+
*
-
PROBABILITY DENSITY
0
4
8
12
16
20
24
28
32
36
-.08
-.06
-.04
-.02
0
.02
.04
.06
.08
CENTRE WAVE

TL4503.W.1

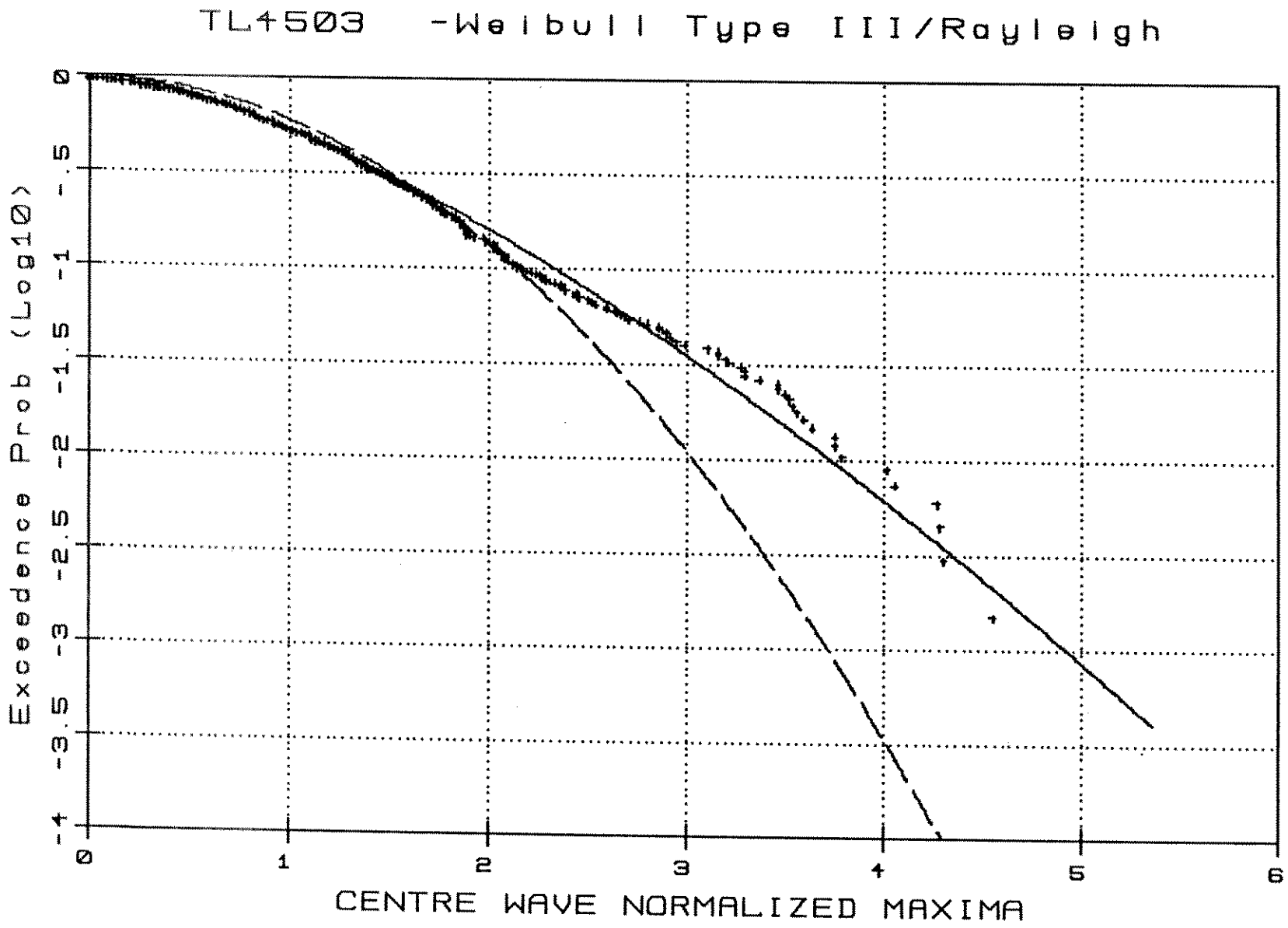
TL4503 -Weibull Type III/Rayleigh
Exceedence Prob (Log10)
0
-.5
-1
-1.5
-2
-2.5
-3
-3.5
-4
0
1
2
3
4
5
6
CENTRE WAVE NORMALIZED MAXIMA

TL4503.W.2

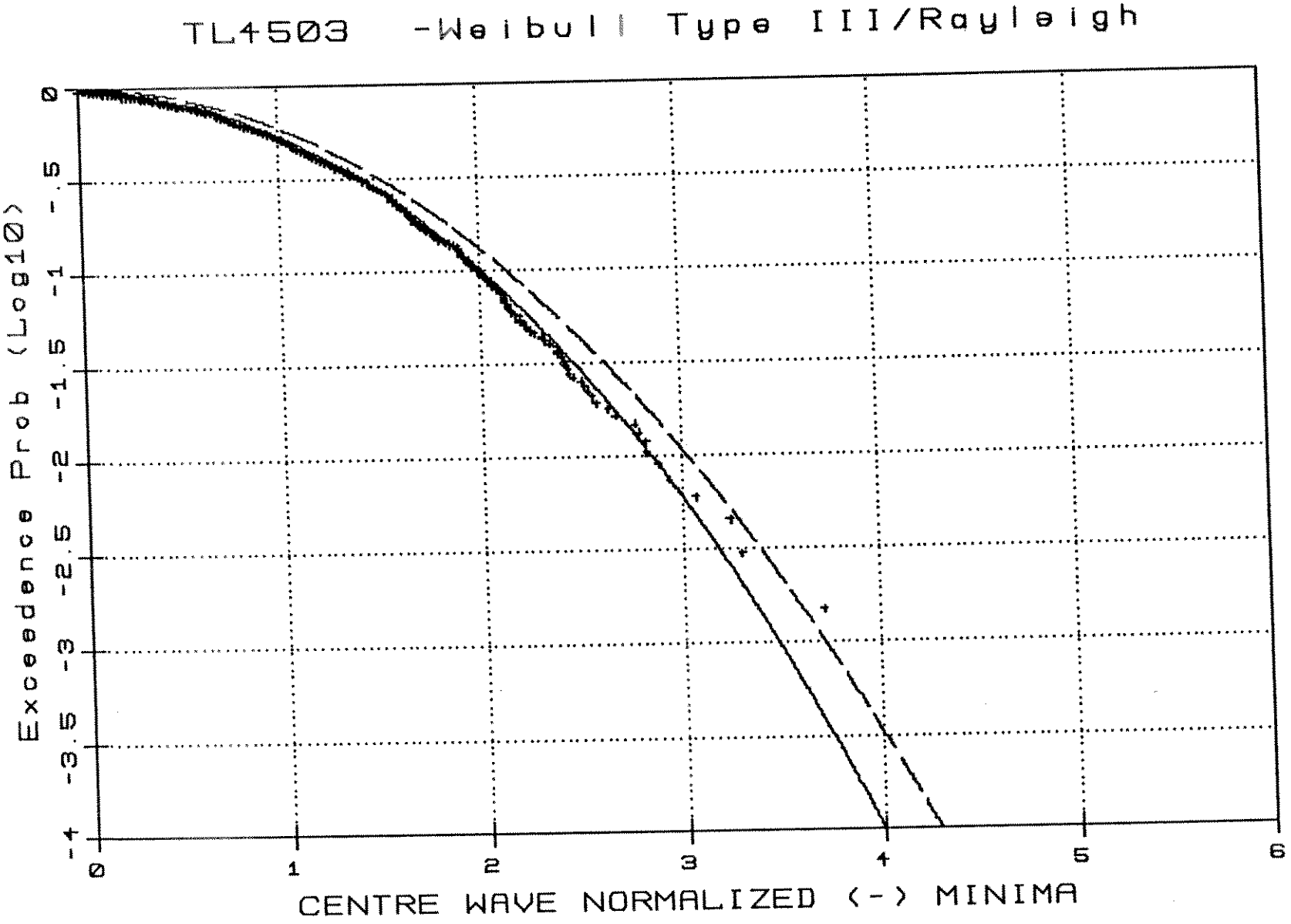
TL4503 -Weibull Type III/Rayleigh
Exceedence Prob (Log10)
0
-.5
-1
-1.5
-2
-2.5
-3
-3.5
-4
0
1
2
3
4
5
6
CENTRE WAVE NORMALIZED (-) MINIMA

TL4503.W.3

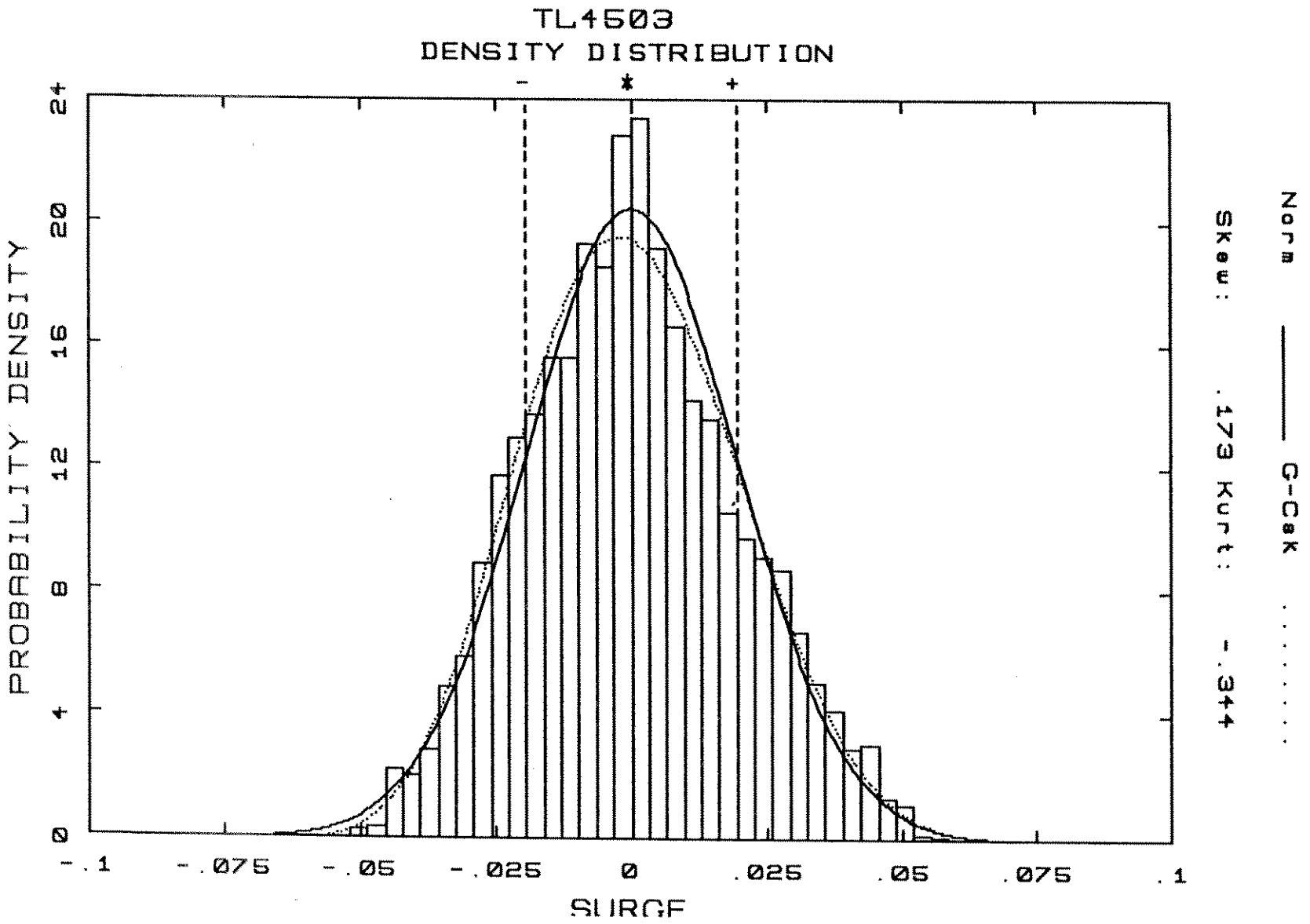
TL4503
DENSITY DISTRIBUTION
PROBABILITY DENSITY
0
4
8
12
16
20
24
- .1
- .075
- .05
- .025
0
.025
.05
.075
.1
SURGE
Norm
G-Cak
Skew: .173 Kurt: -.344

TL4503.S.1

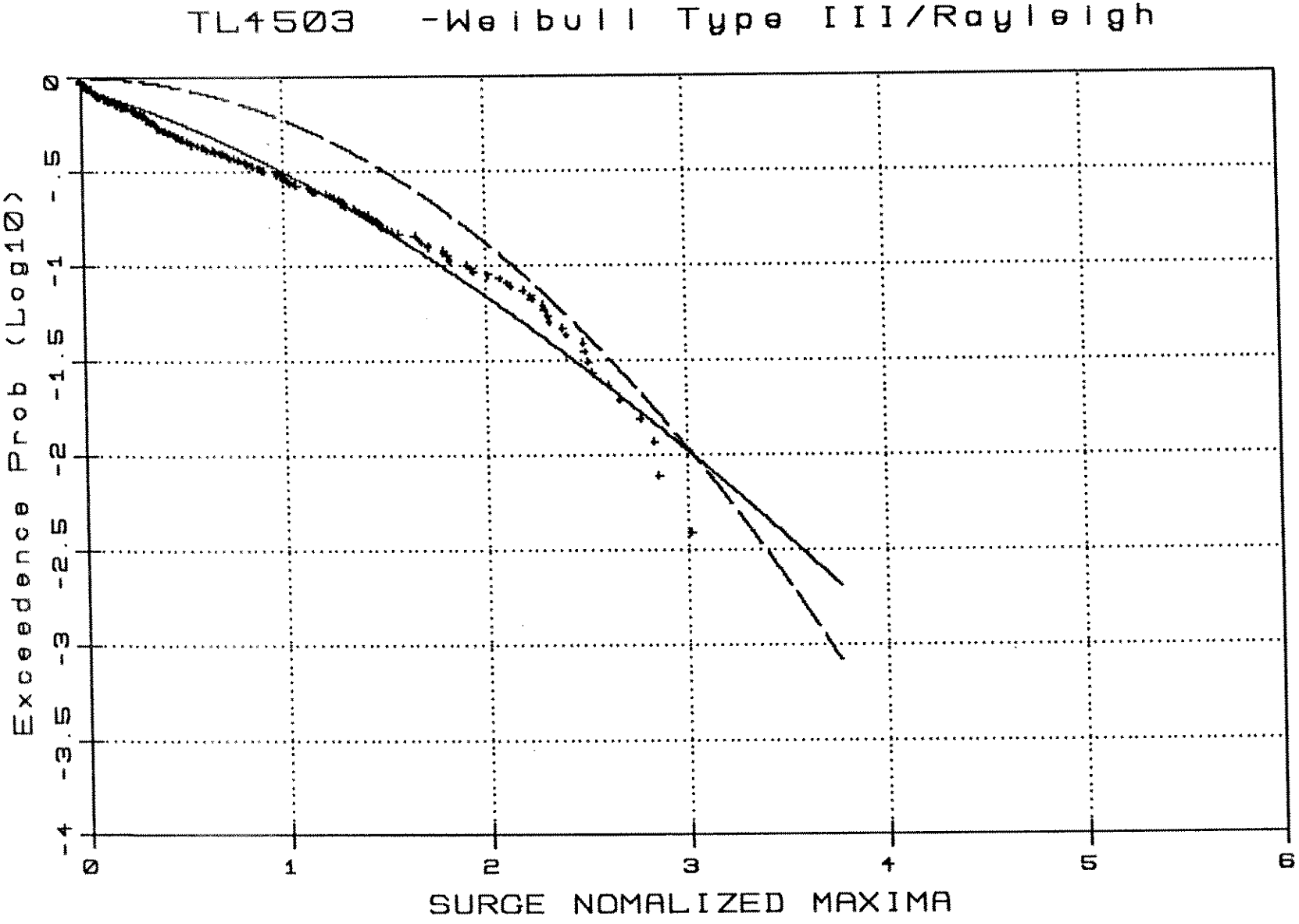
TL4503 -Weibull Type III/Rayleigh
Exceedence Prob (Log10)
0
-.5
-1
-1.5
-2
-2.5
-3
-3.5
-4
0
1
2
3
4
5
6
SURGE NOMALIZED MAXIMA

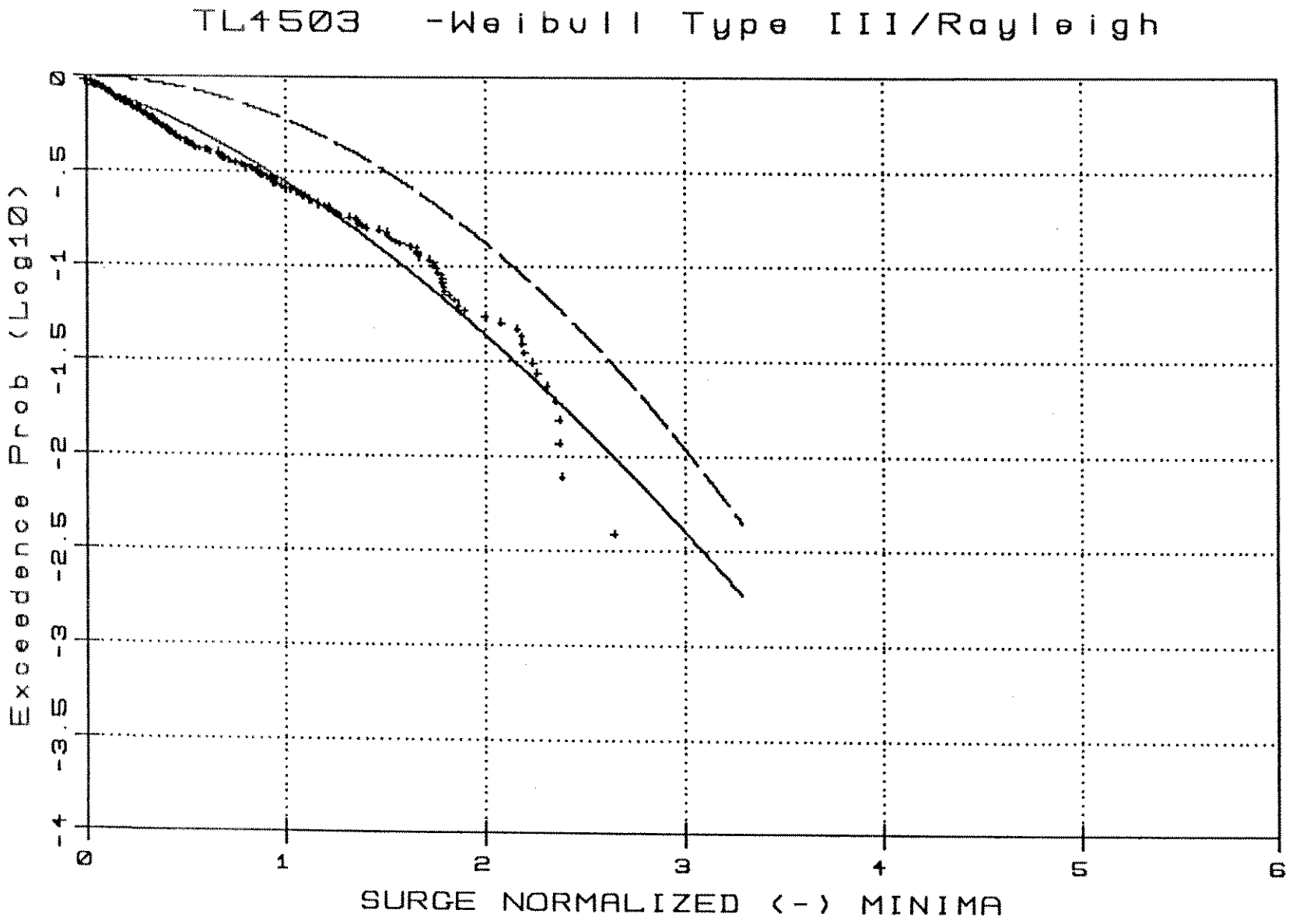
TL4503 -Weibull Type III/Rayleigh
Exceedence Prob (Log10)
0
-.5
-1
-1.5
-2
-2.5
-3
-3.5
-4
0
1
2
3
4
5
6
SURGE NORMALIZED (-) MINIMA

TL4503.S.3

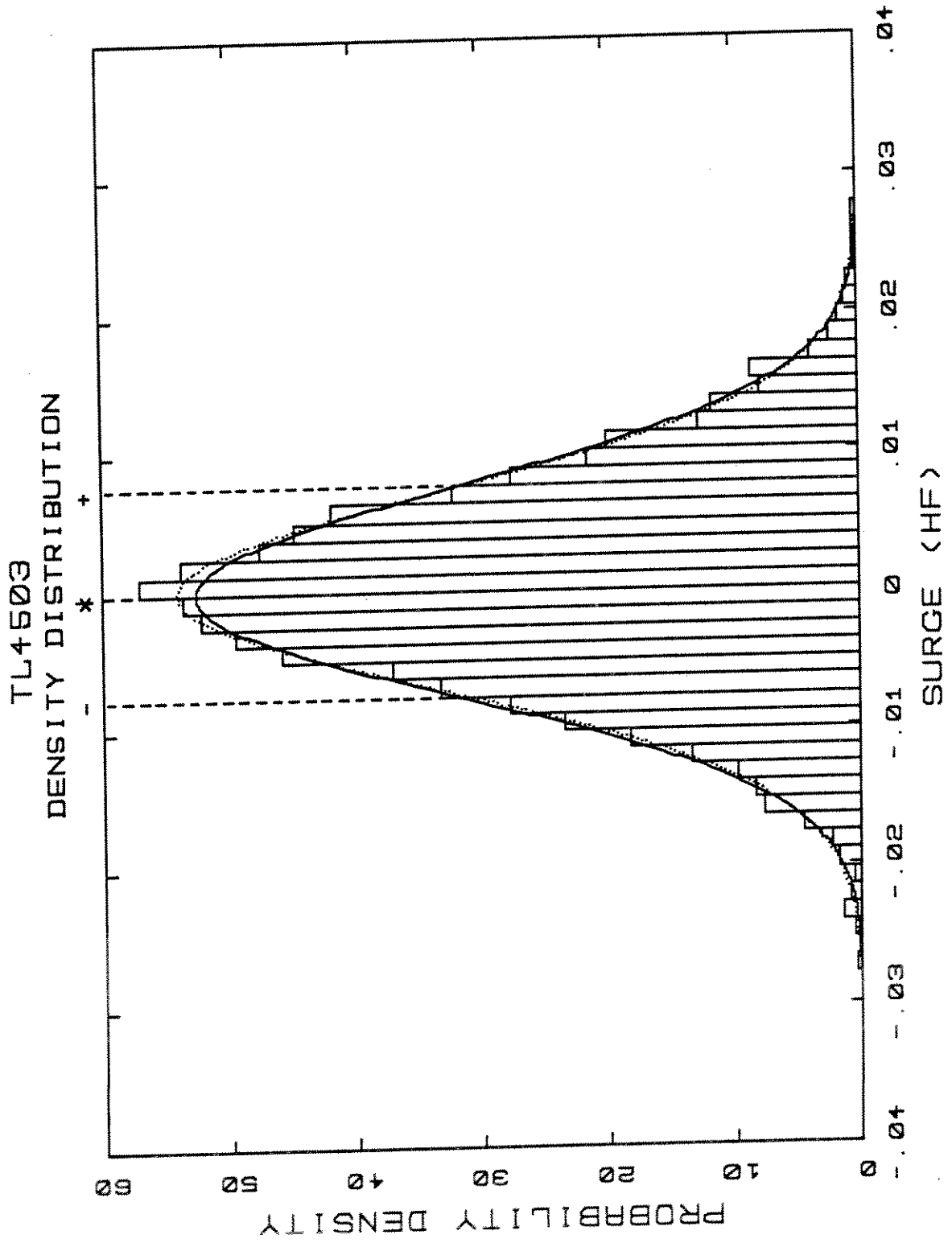
Norm
C-Cak
Skew: -.029 Kurt: .221
TL4503
DENSITY DISTRIBUTION
+
*
-
PROBABILITY DENSITY
60
50
40
30
20
10
0
-.04
-.03
-.02
-.01
0
.01
.02
.03
.04
SURGE (HF)

TL4503.SHF.1

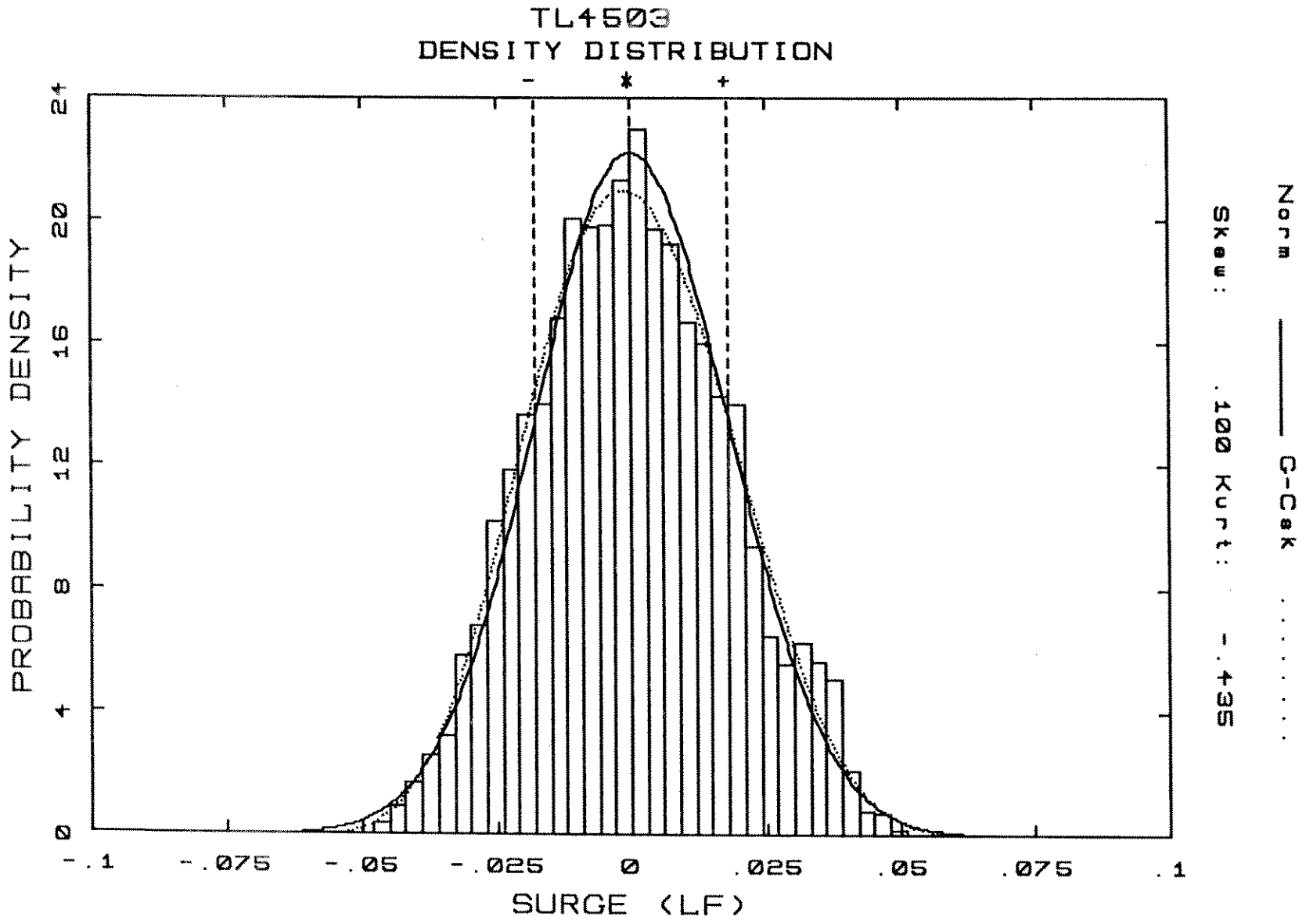
TL4503
DENSITY DISTRIBUTION
- * +
PROBABILITY DENSITY
0
4
8
12
16
20
24
-.1
-.075
-.05
-.025
0
.025
.05
.075
.1
SURGE (LF)
Norm
C-Cak
Skew: .100 Kurt: -.435

TL4503.SLF.1

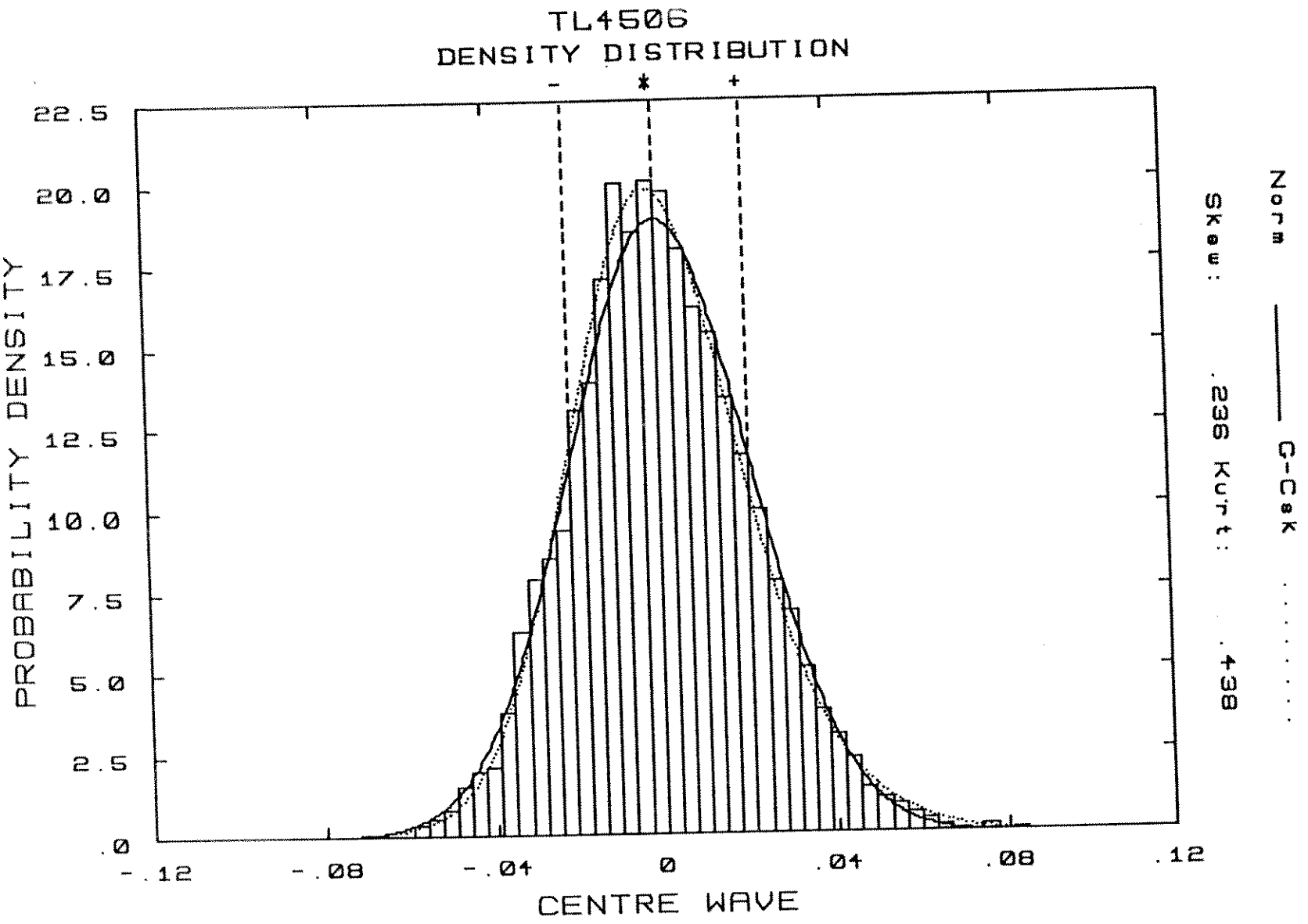
TL4506
DENSITY DISTRIBUTION
- * +
22.5
20.0
17.5
15.0
12.5
10.0
7.5
5.0
2.5
.0
PROBABILITY DENSITY
-.12
-.08
-.04
0
.04
.08
.12
CENTRE WAVE
Norm
G-Gek
Skew: .236 Kurt: .438

TL4506.W.1

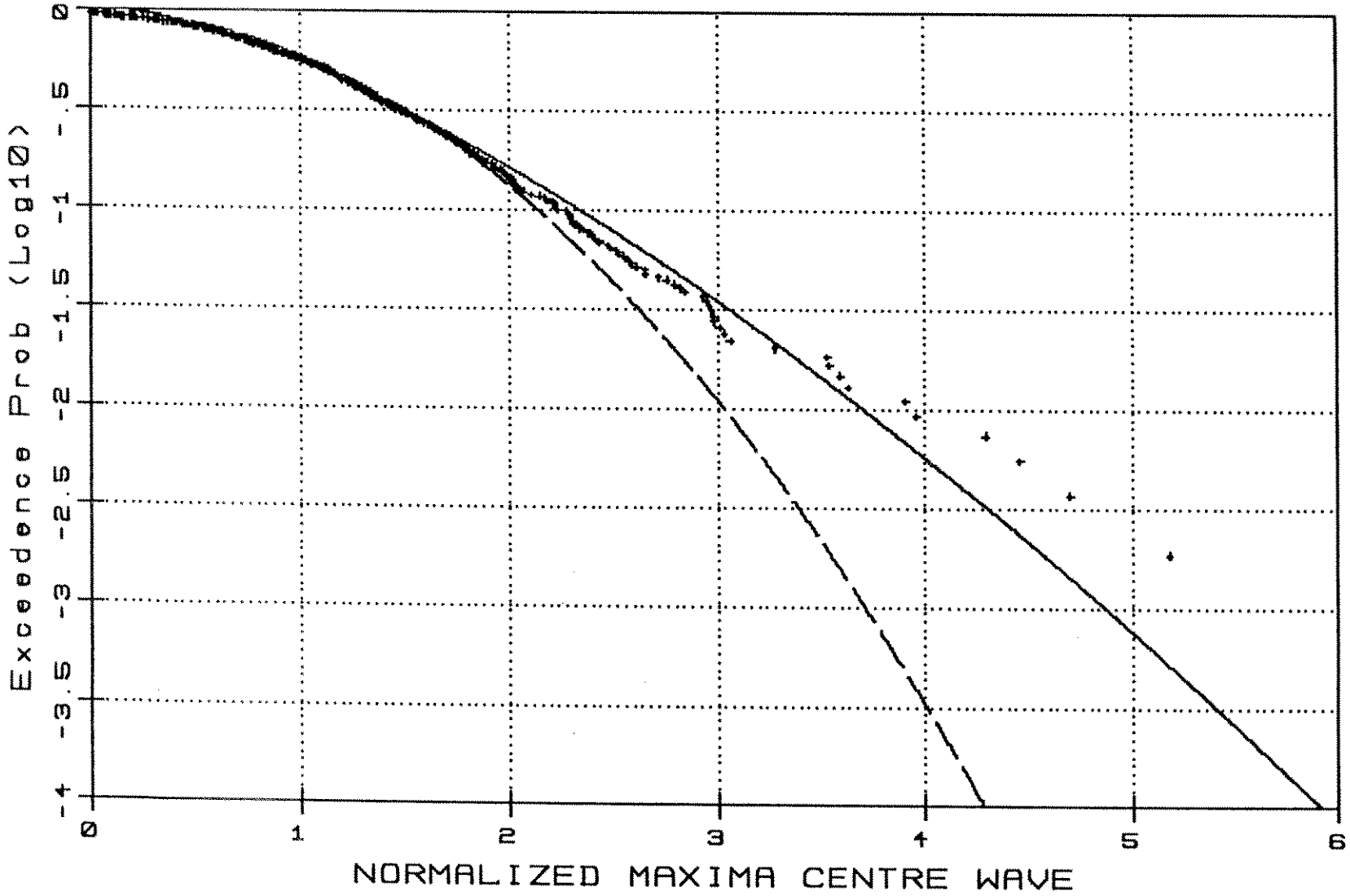
TL4506 -Weibull Type III/Rayleigh
Exceedence Prob (Log10)
0
-.5
-1
-1.5
-2
-2.5
-3
-3.5
-4
0
1
2
3
4
5
6
NORMALIZED MAXIMA CENTRE WAVE

TL4506.W.2

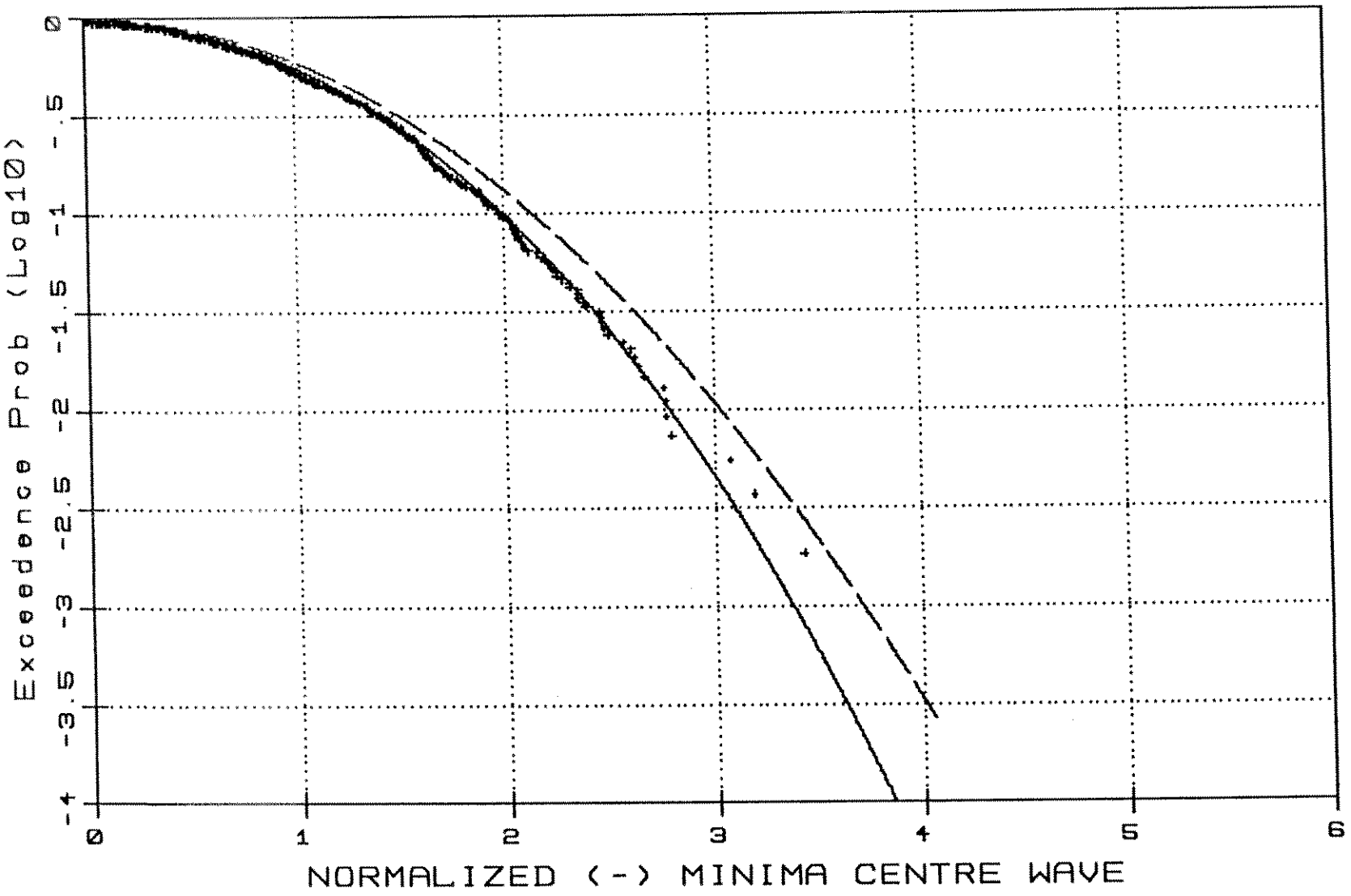
TL4506 -Weibull Type III/Rayleigh
Exceedence Prob (Log10)
0
-.5
-1
-1.5
-2
-2.5
-3
-3.5
-4
0
1
2
3
4
5
6
NORMALIZED (-) MINIMA CENTRE WAVE

TL4506.W.3

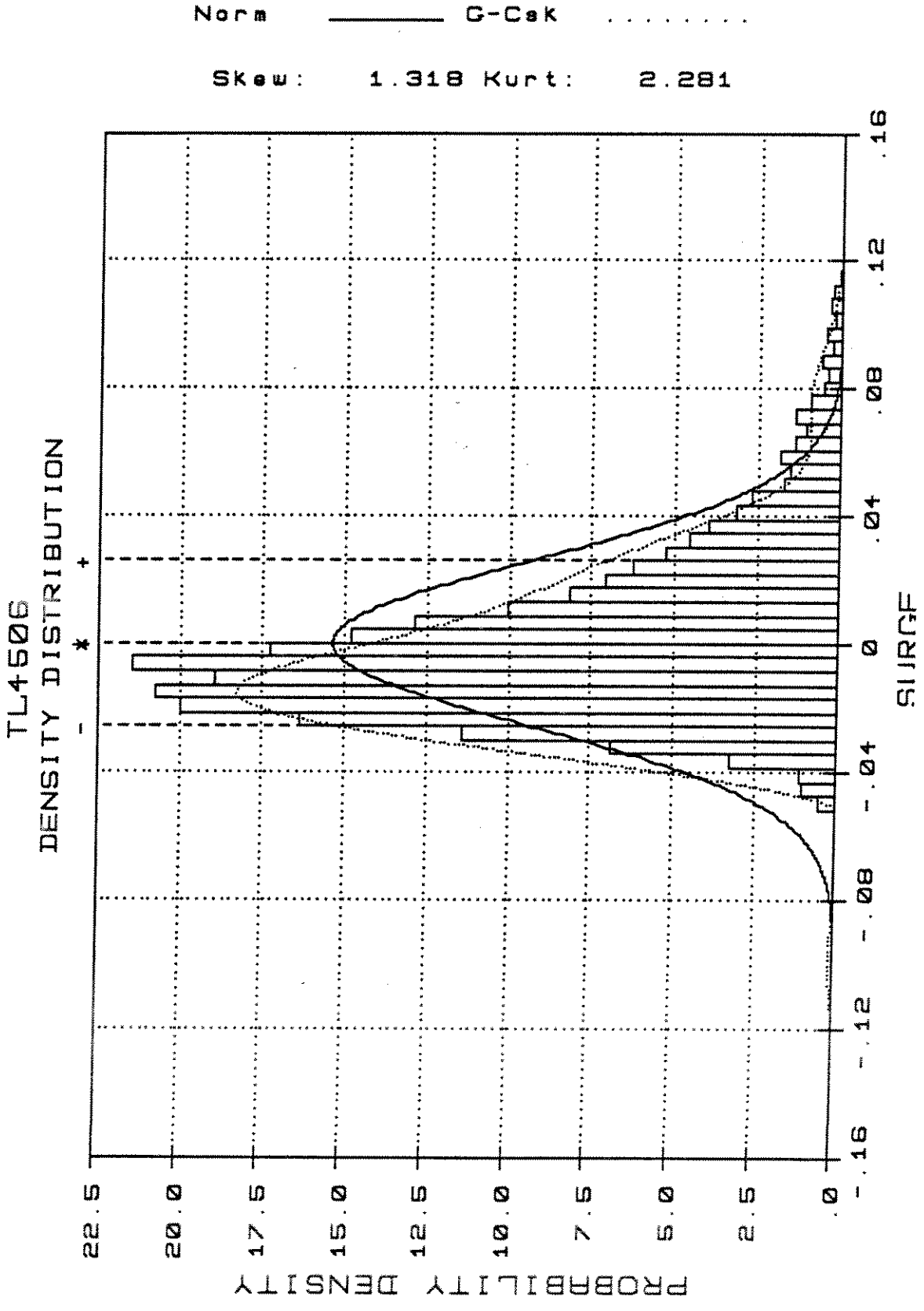
Norm
G-Cak
Skew: 1.318 Kurt: 2.281
TL4506
DENSITY DISTRIBUTION
PROBABILITY DENSITY
SURGE
22.5
20.0
17.5
15.0
12.5
10.0
7.5
5.0
2.5
0
-.16
-.12
-.08
-.04
0
.04
.08
.12
.16

TL4506.S.1

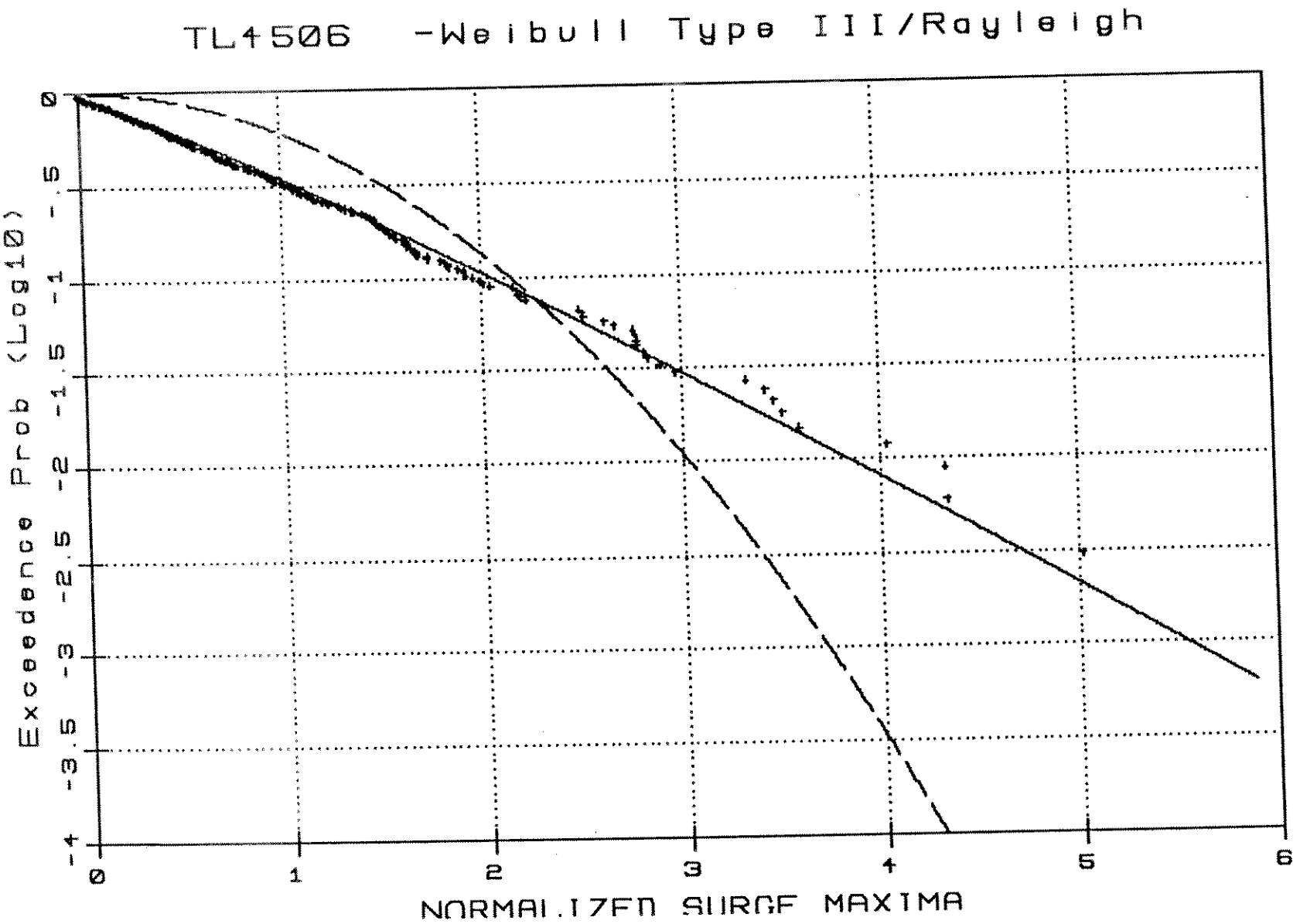
TL4506 -Weibull Type III/Rayleigh
Exceedence Prob (Log10)
0
-.5
-1
-1.5
-2
-2.5
-3
-3.5
-4
0
1
2
3
4
5
6
NORMALIZED SURGE MAXIMA

TL4506.S.2

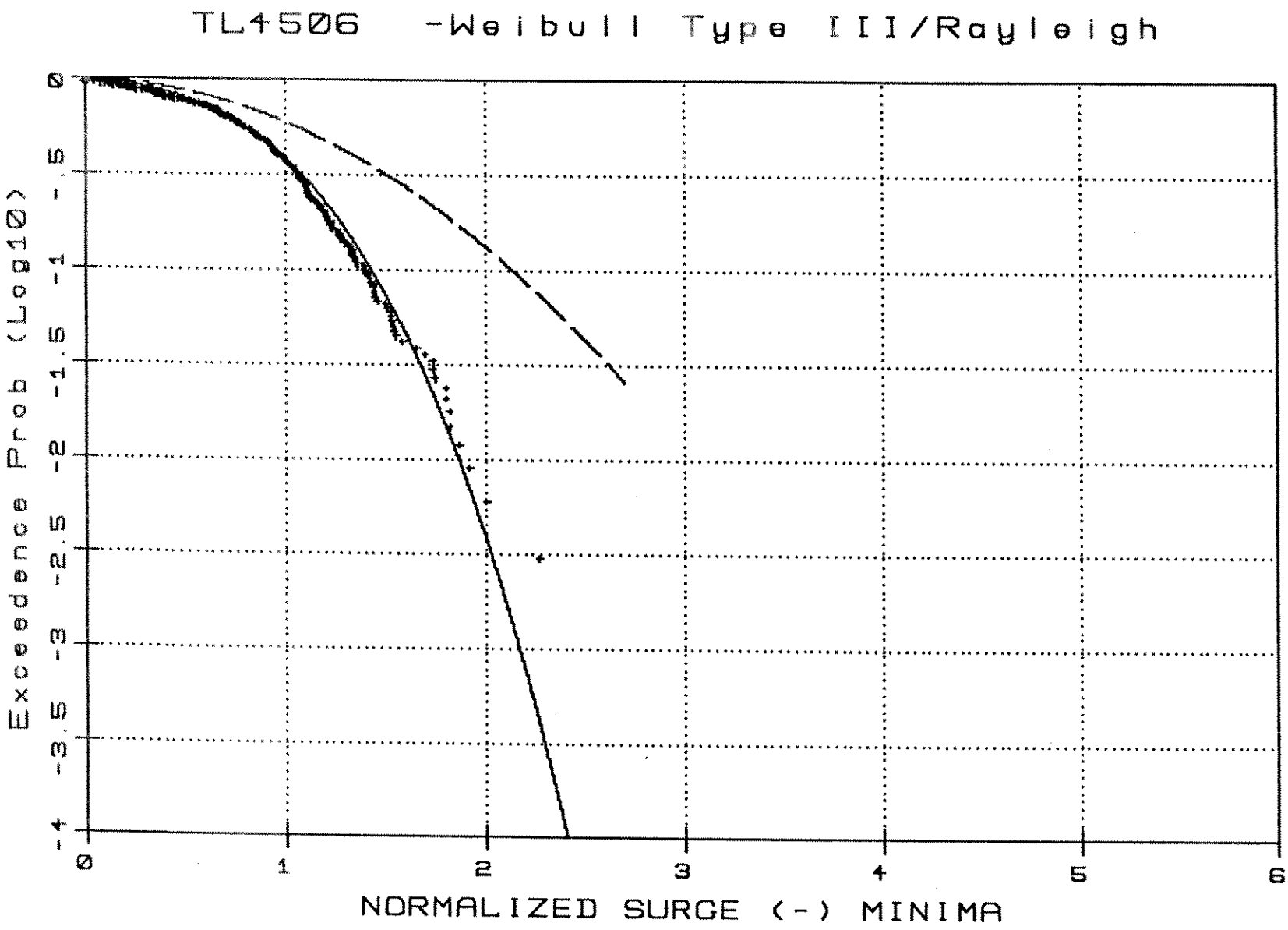
TL4506 -Weibull Type III/Rayleigh
Exceedence Prob (Log10)
0
-.5
-1
-1.5
-2
-2.5
-3
-3.5
-4
0
1
2
3
4
5
6
NORMALIZED SURGE (-) MINIMA

TL4506.S.3

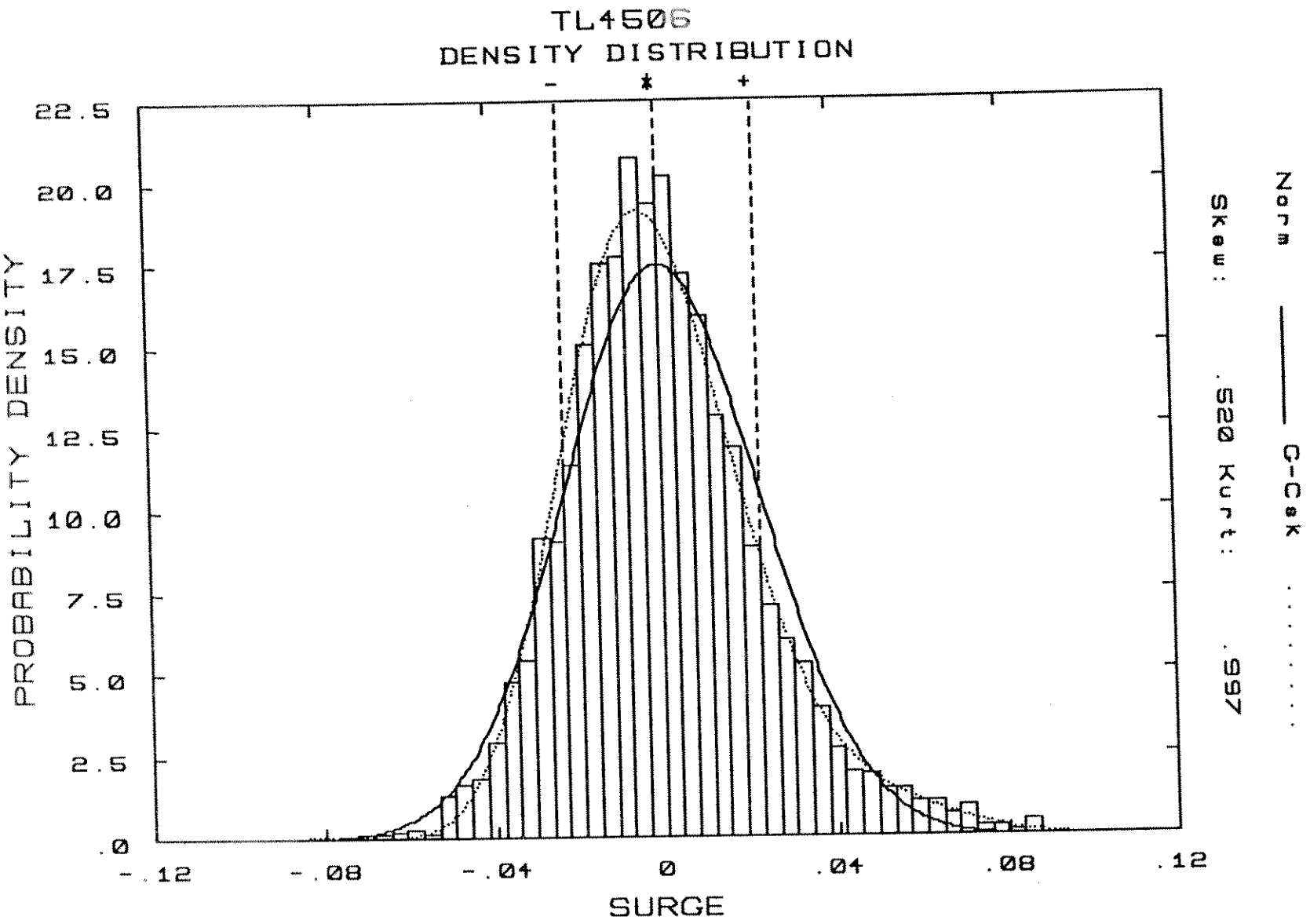
TL4506
DENSITY DISTRIBUTION
- * +
PROBABILITY DENSITY
22.5
20.0
17.5
15.0
12.5
10.0
7.5
5.0
2.5
.0
-.12
-.08
-.04
0
.04
.08
.12
SURGE
Norm
G-Cak
Skew: .520 Kurt: .997

TL4506.SHP.1

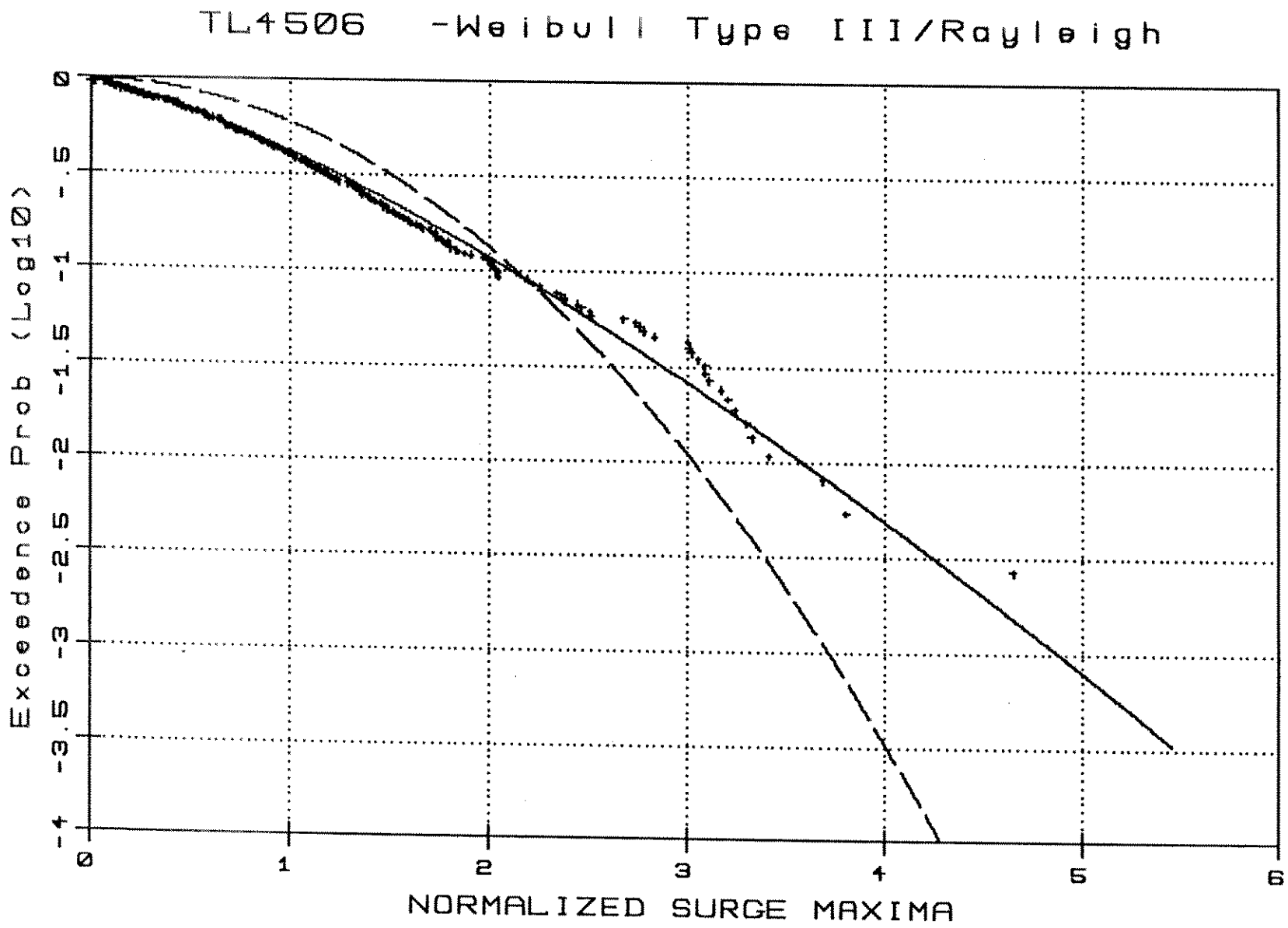
TL4506 -Weibull Type III/Rayleigh
Exceedence Prob (Log10)
0
-.5
-1
-1.5
-2
-2.5
-3
-3.5
-4
0
1
2
3
4
5
6
NORMALIZED SURGE MAXIMA

TL4506.SHP.2

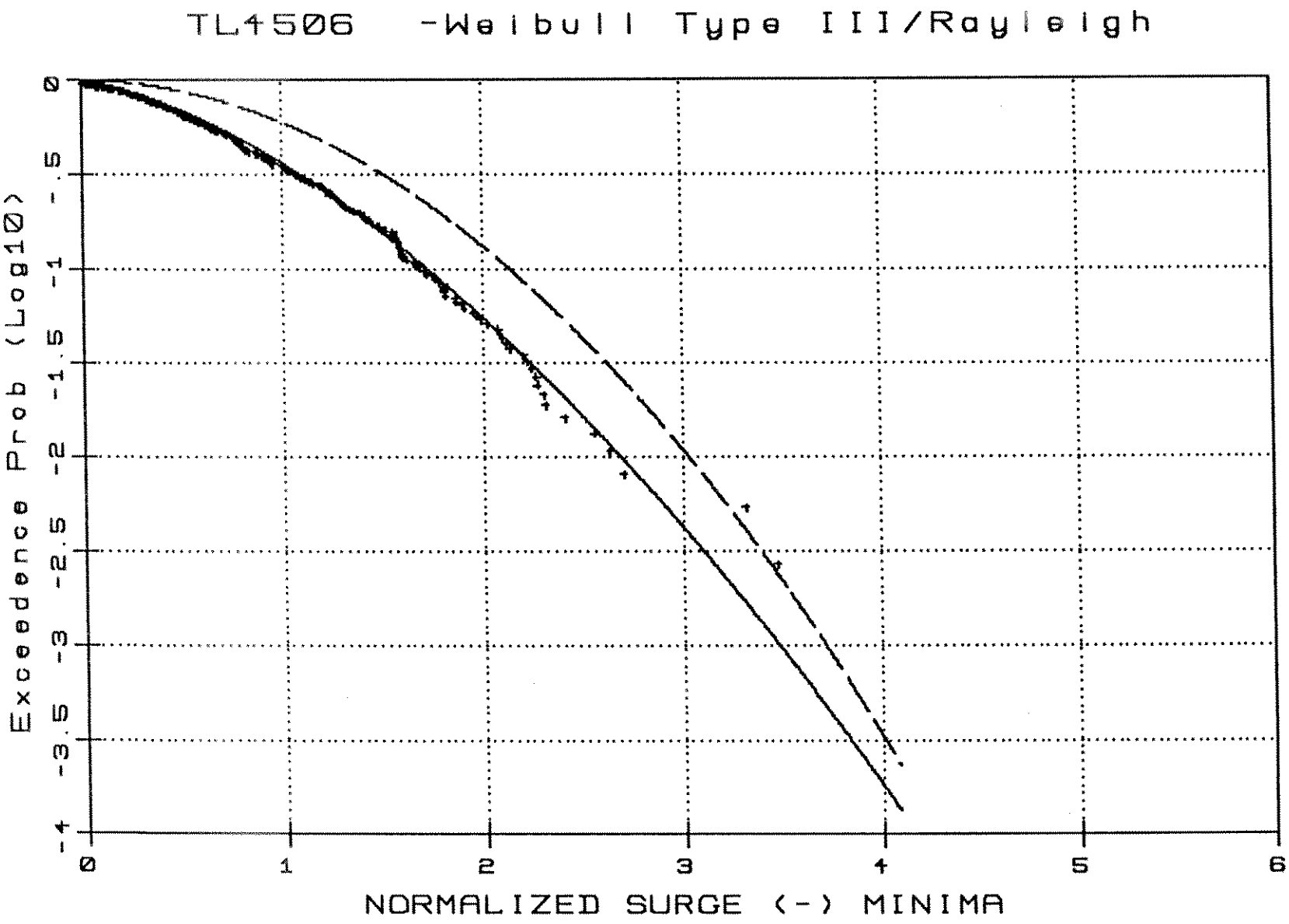
TL4506 -Weibull Type III/Rayleigh
Exceedence Prob (Log10)
0
-.5
-1
-1.5
-2
-2.5
-3
-3.5
-4
0
1
2
3
4
5
6
NORMALIZED SURGE (-) MINIMA

TL4506.SHP.3

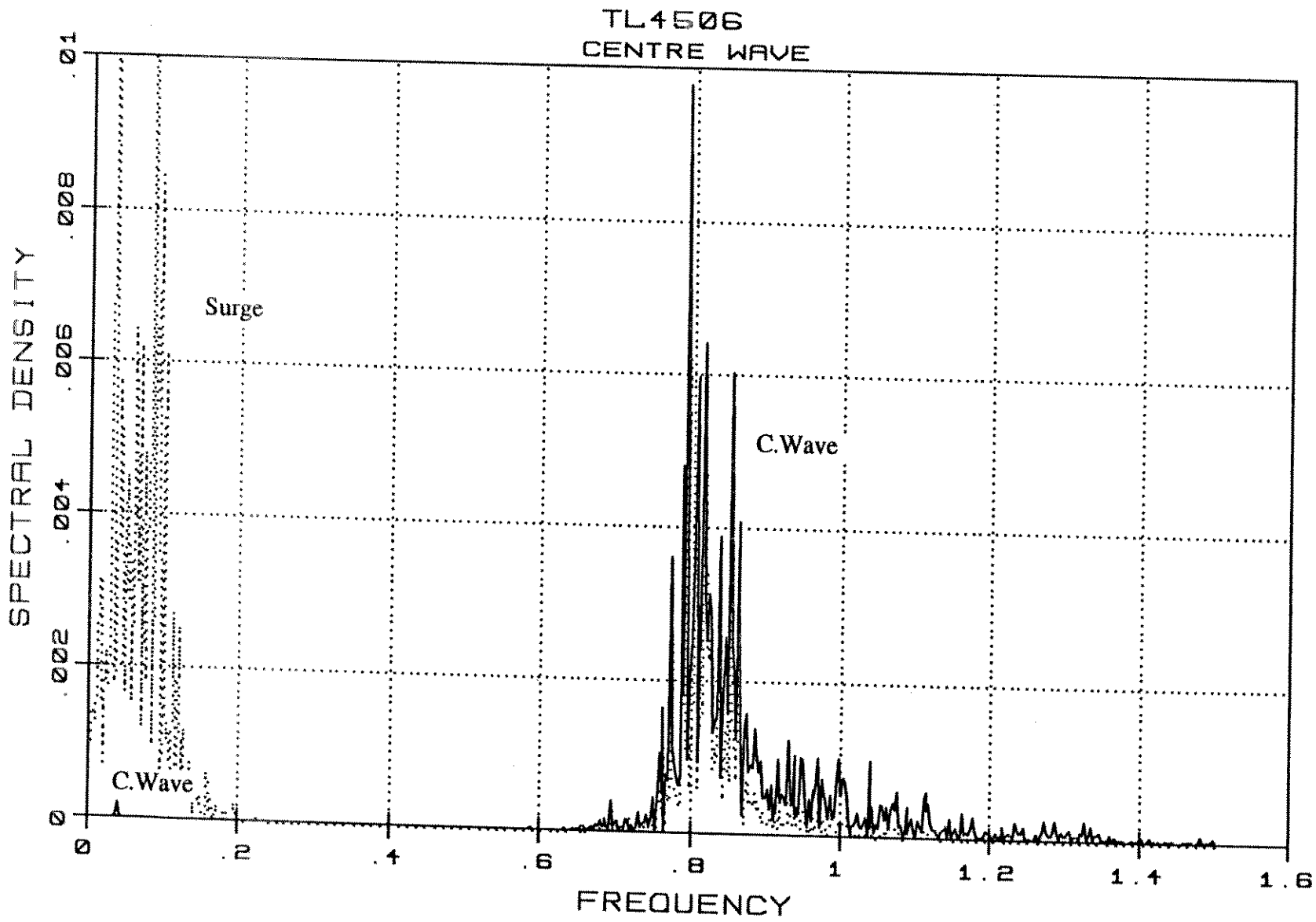
TL4506
CENTRE WAVE
SPECTRAL DENSITY
.01
.008
.006
.004
.002
0
Surge
C.Wave
C.Wave
0
.2
.4
.6
.8
1
1.2
1.4
1.6
FREQUENCY

TL4506.W/S.4

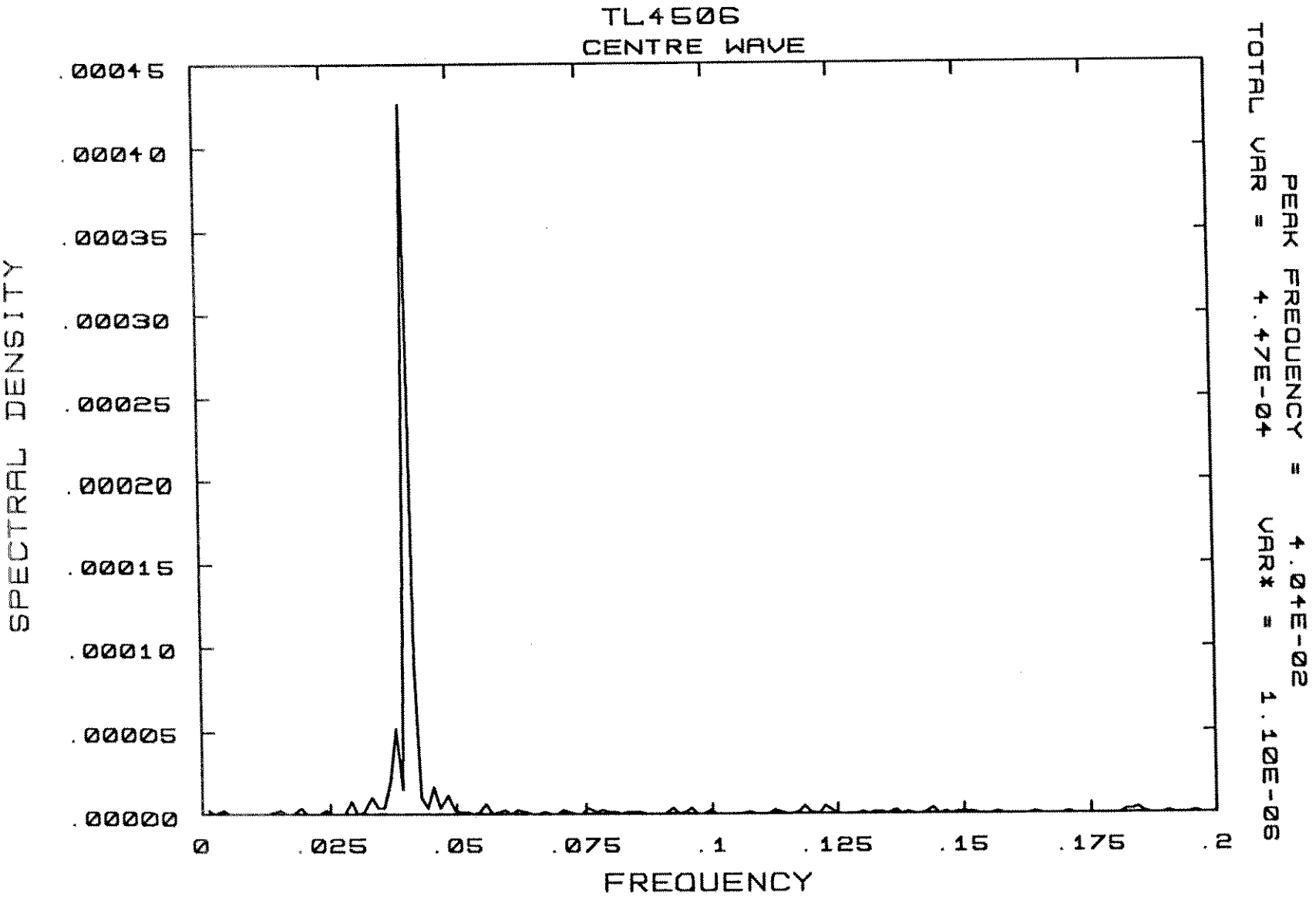
TL4506
CENTRE WAVE
SPECTRAL DENSITY
.00045
.00040
.00035
.00030
.00025
.00020
.00015
.00010
.00005
.00000
0
.025
.05
.075
.1
.125
.15
.175
.2
FREQUENCY
PEAK FREQUENCY = +.0+E-02
TOTAL VAR = +.47E-0+
VAR* = 1.10E-06

TL4606.W.4A

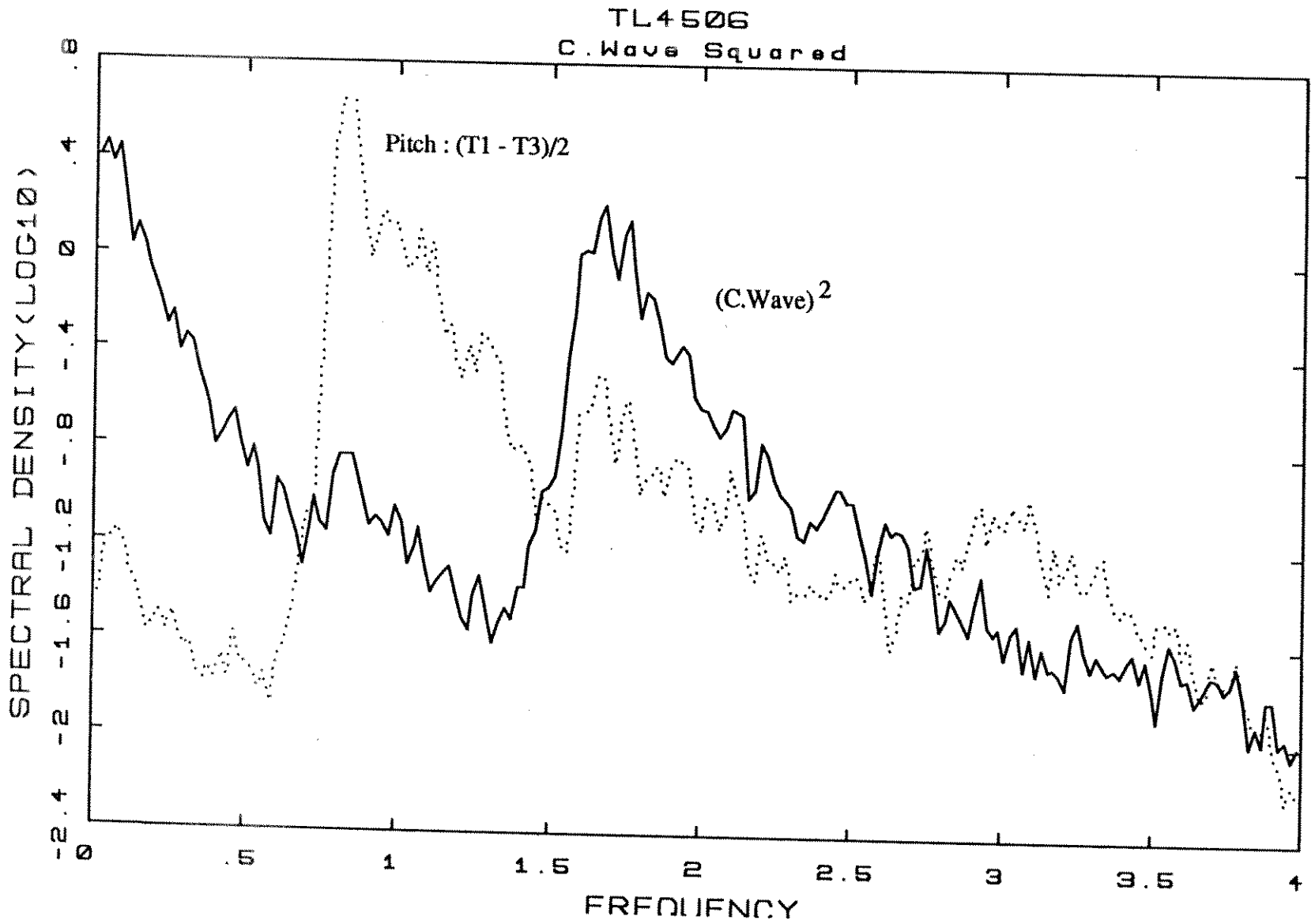

TL4506.WSQ/PiT13.4
C.Wave Squared and Pich are normalized

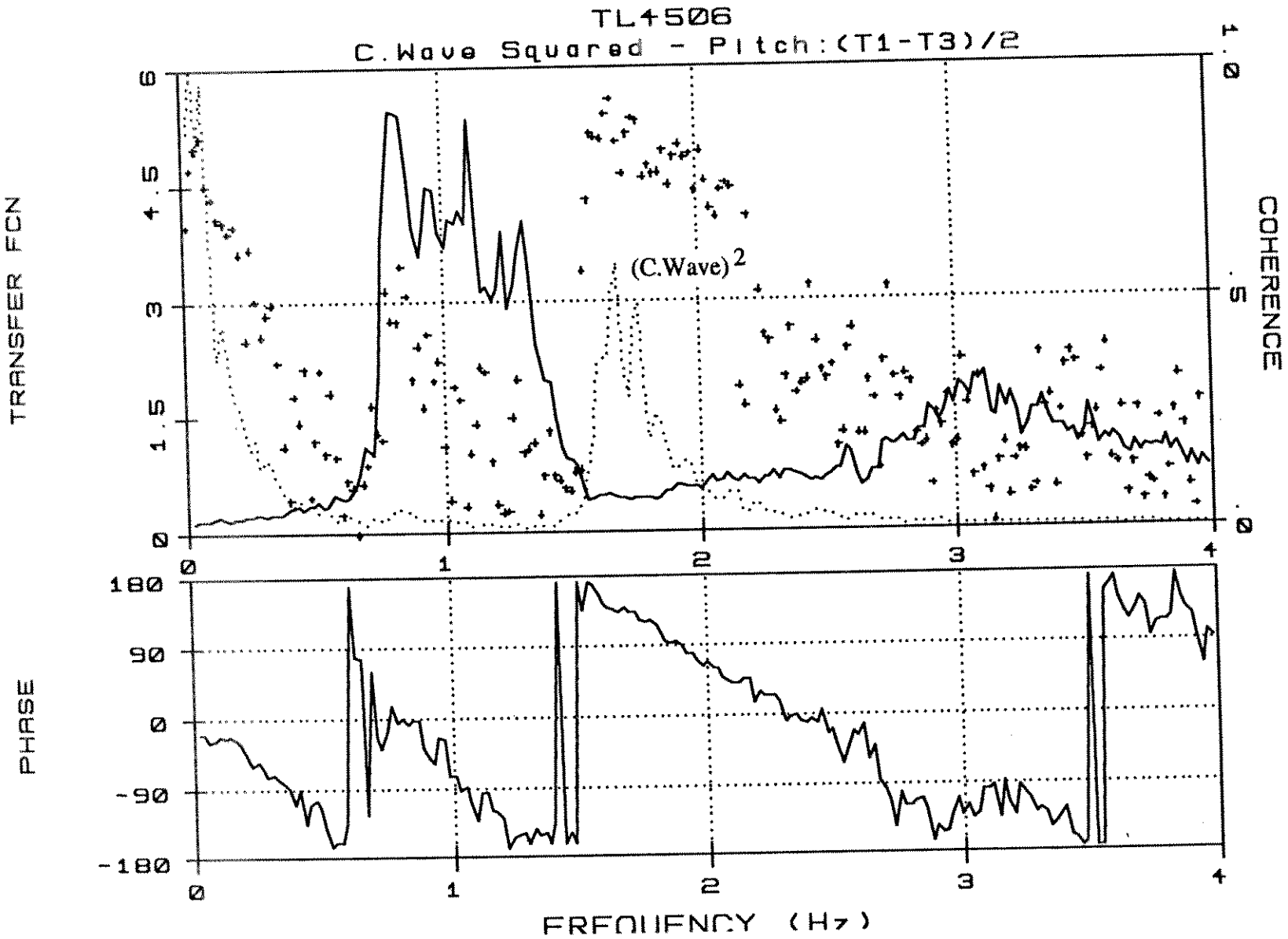

TL4506.WSQ/PiT13.4t
C.Wave Squared and Pitch are normalized

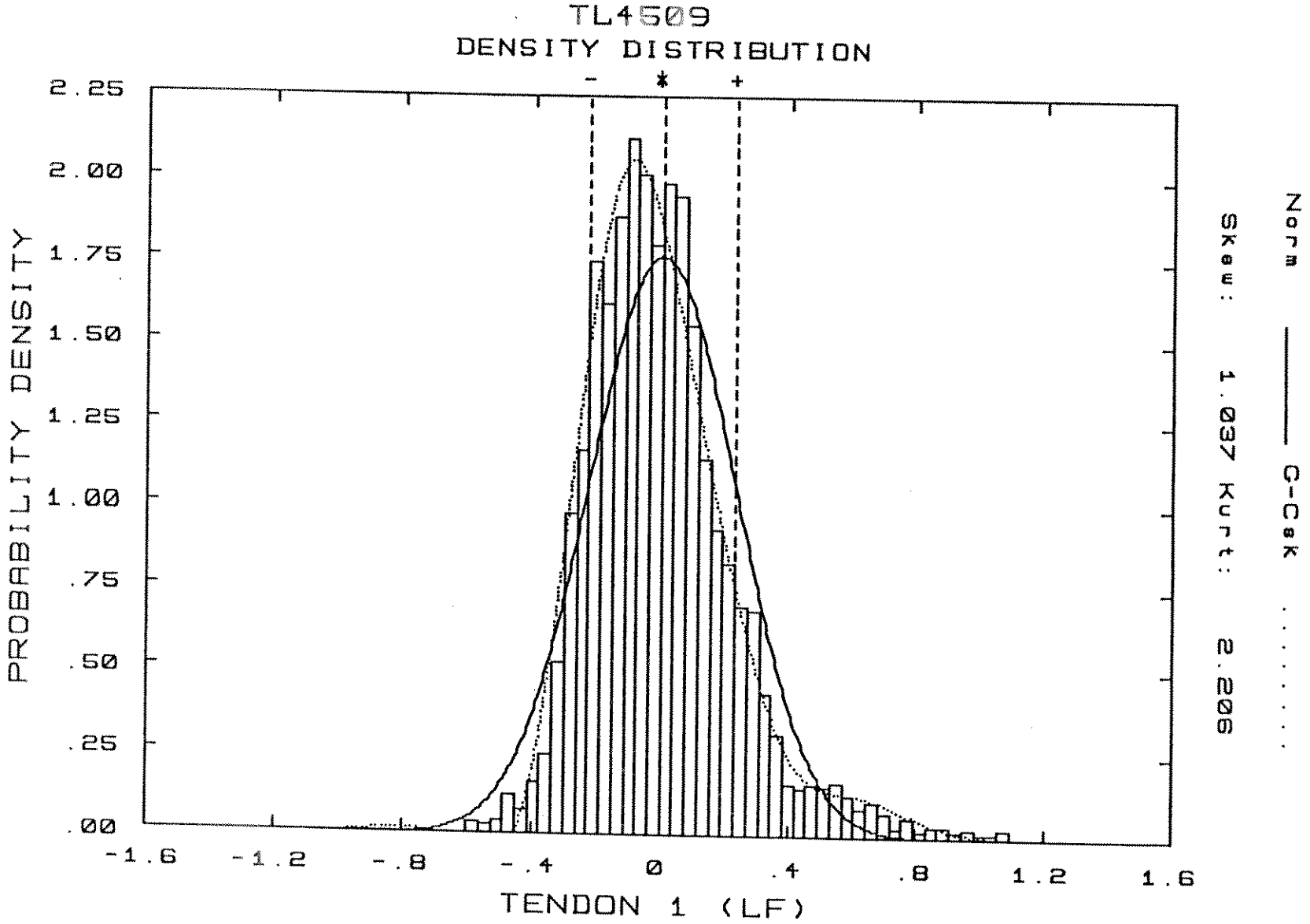

TL4509.TEN1HF.1

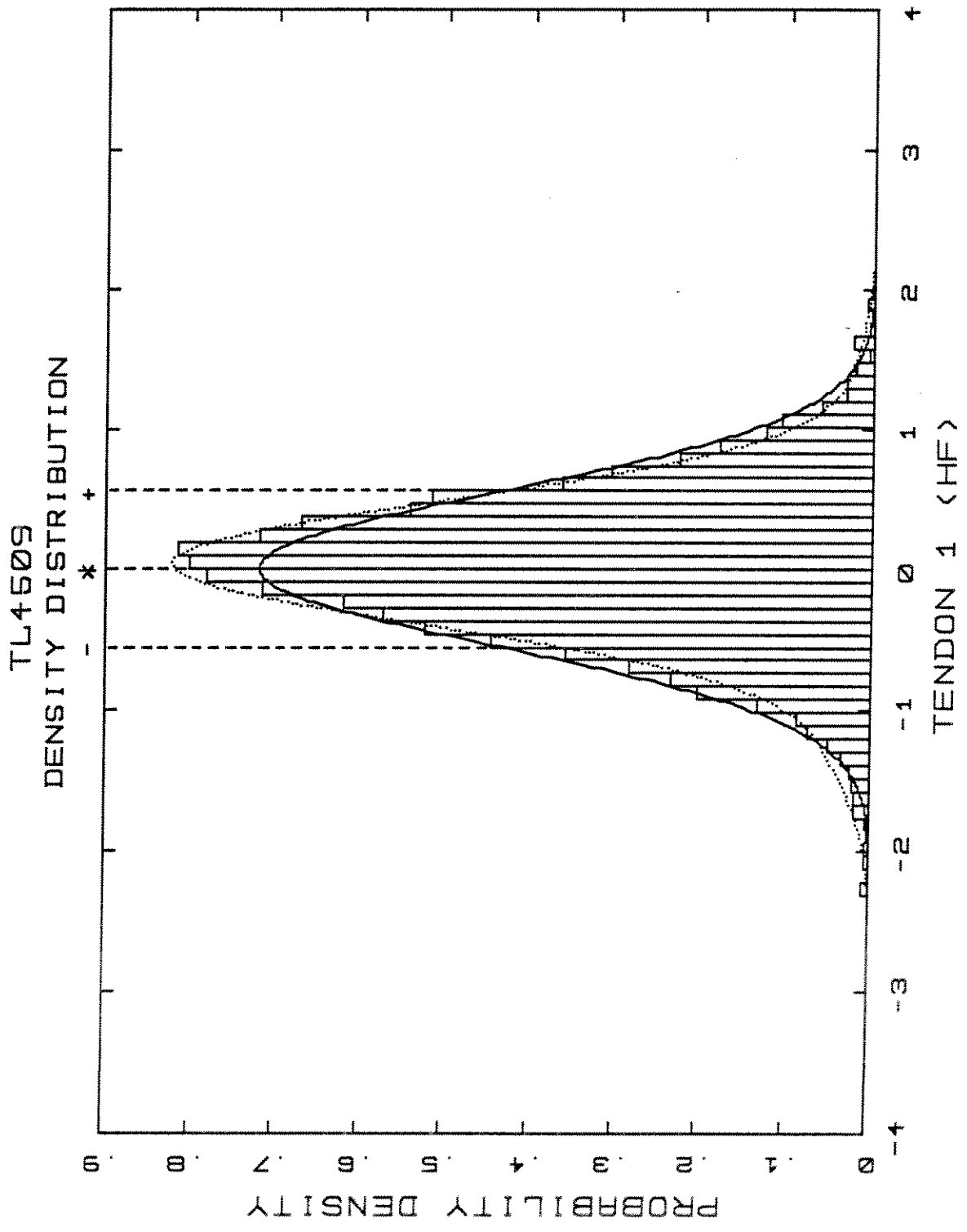
Norm
C-Cak
Skew: -.215 Kurt: 1.182
TL4509
DENSITY DISTRIBUTION
TENDON 1 (HF)
PROBABILITY DENSITY
TL4509.TENLF.1

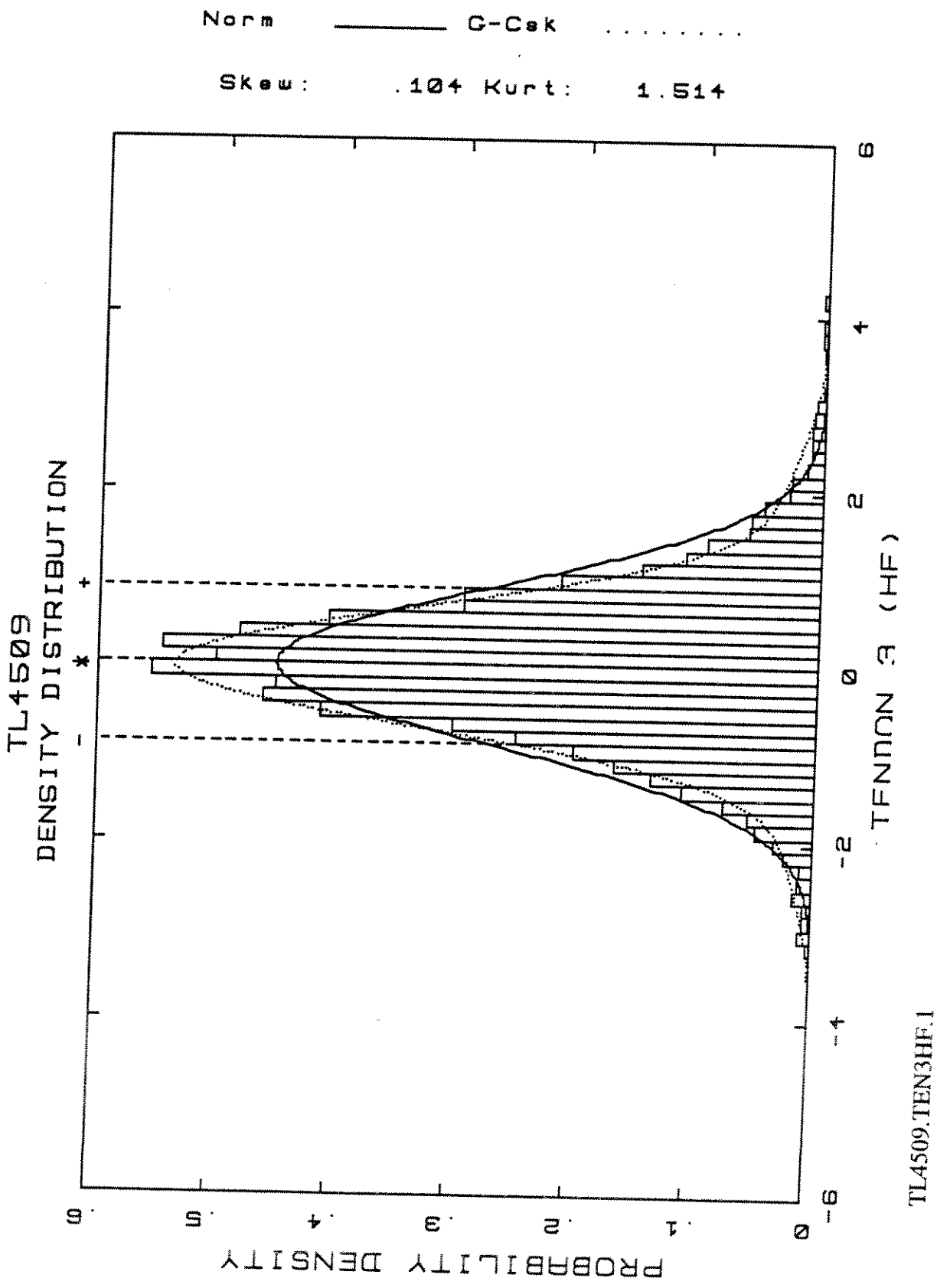

TL4509.TEN3HF.1

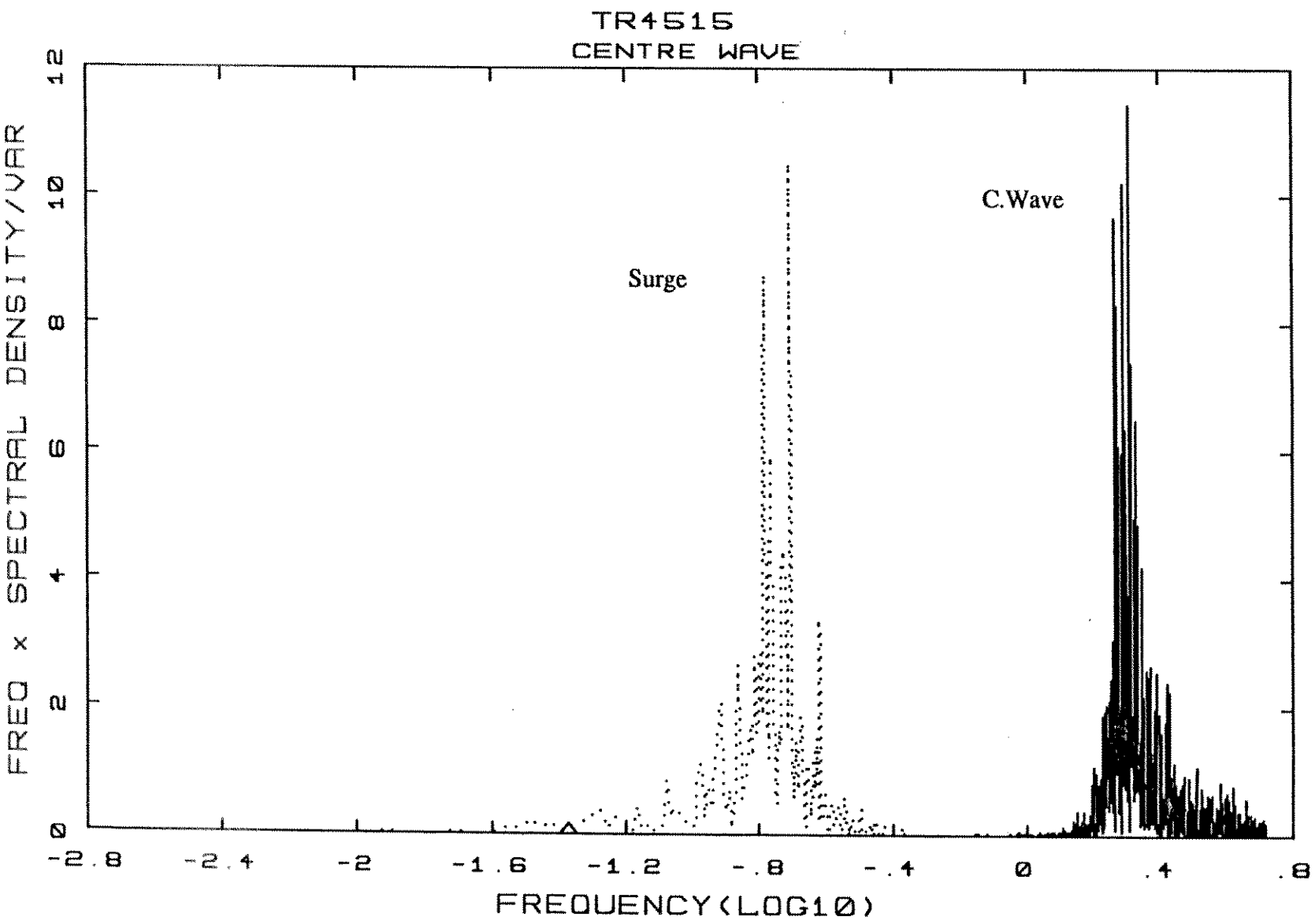

TR4515.WS
Wind 4. m/s
No Wave

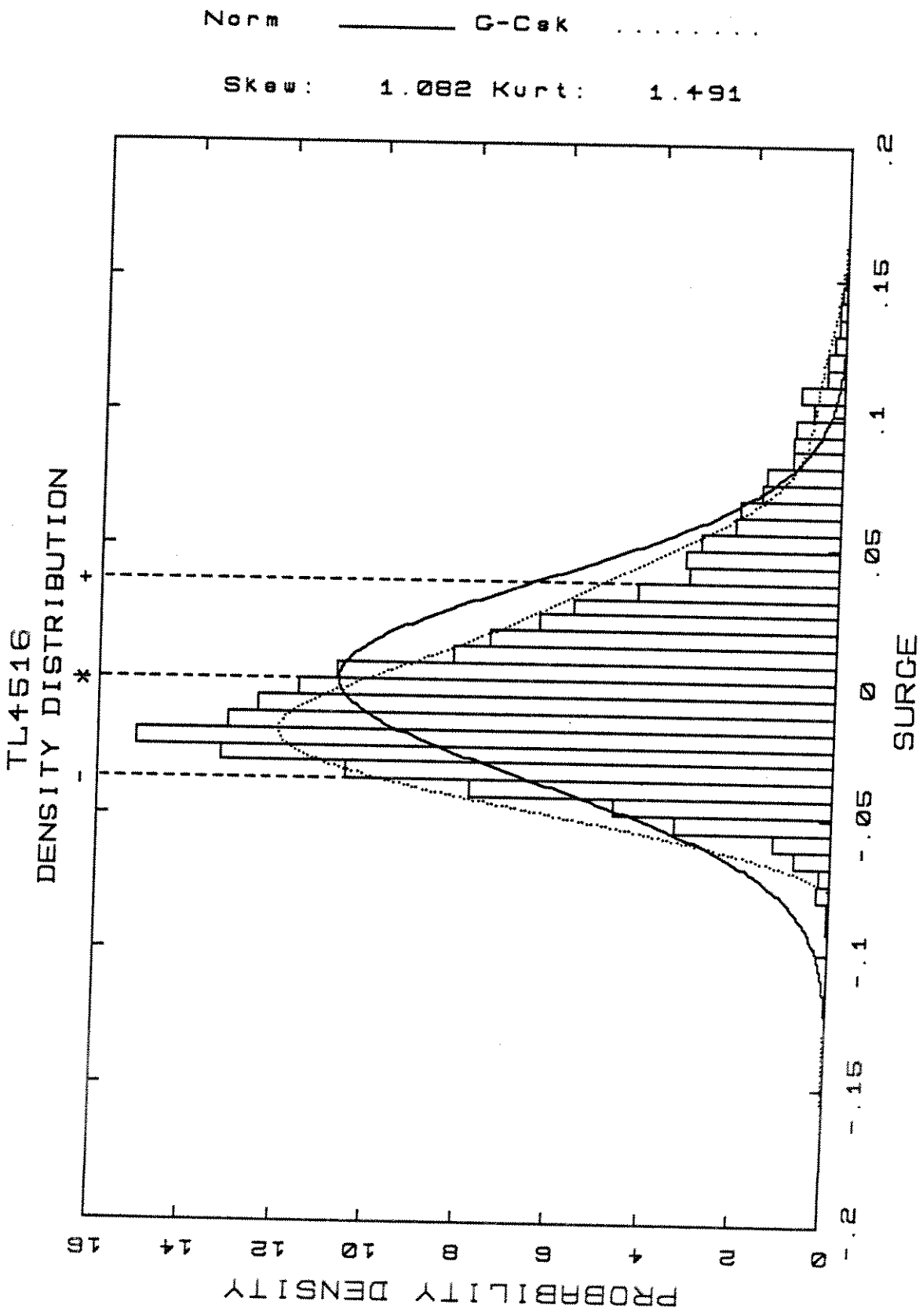
Norm
G-Cak
Skew: 1.082 Kurt: 1.491
TL4516
DENSITY DISTRIBUTION
+
*
-
PROBABILITY DENSITY
0
2
4
6
8
10
12
14
16
SURGE
.2
.15
.1
.05
0
-.05
-.1
-.15
-.2

TL4516.S.1

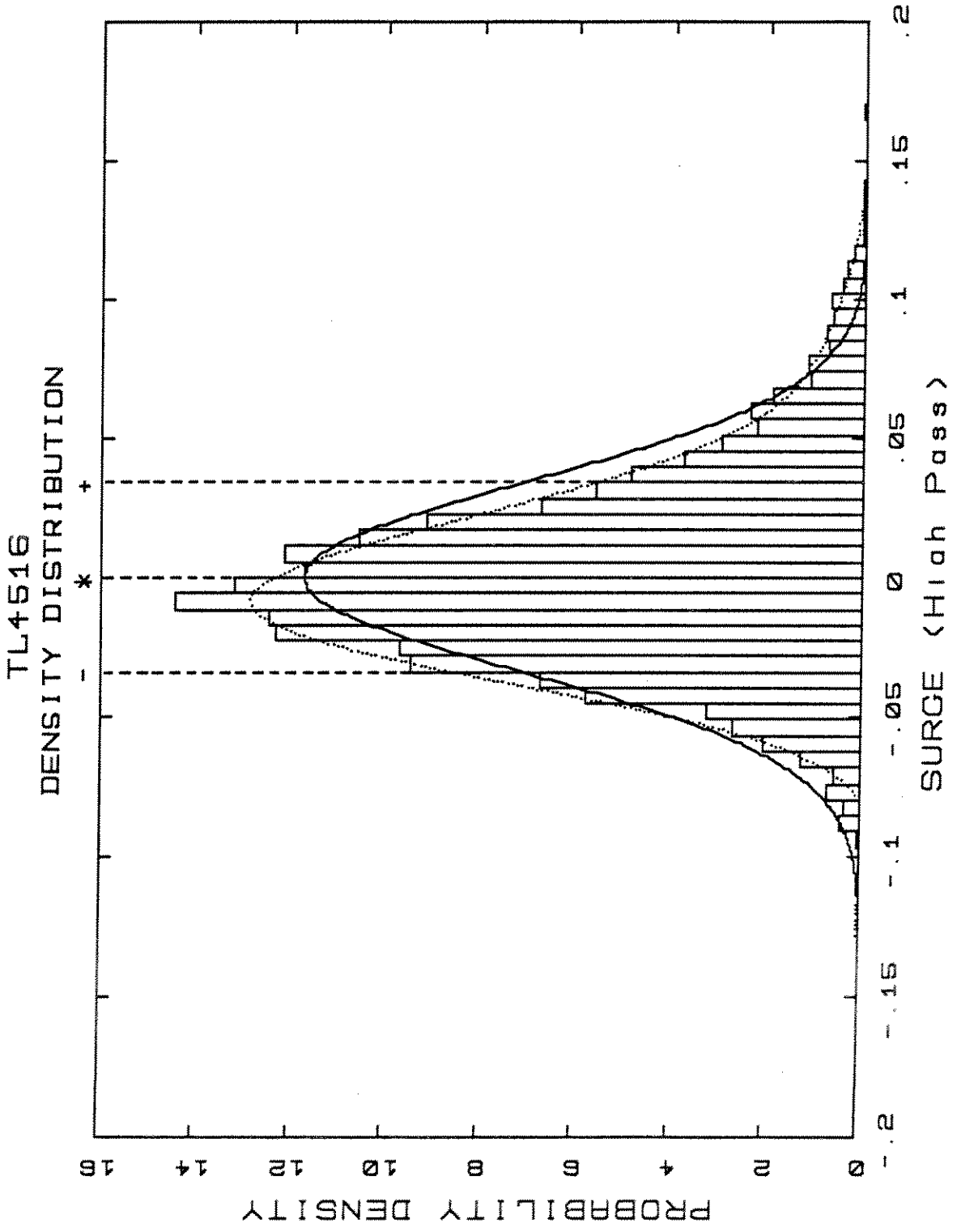
Norm
G-Cek
Skew: .641 Kurt: 1.118
TL4516
DENSITY DISTRIBUTION
PROBABILITY DENSITY
SURGE (High Pass)
0
2
4
6
8
10
12
14
16
.2
.15
.1
.05
0
-.05
-.1
-.15
-.2
+
*
-

TL4516.SHP.1

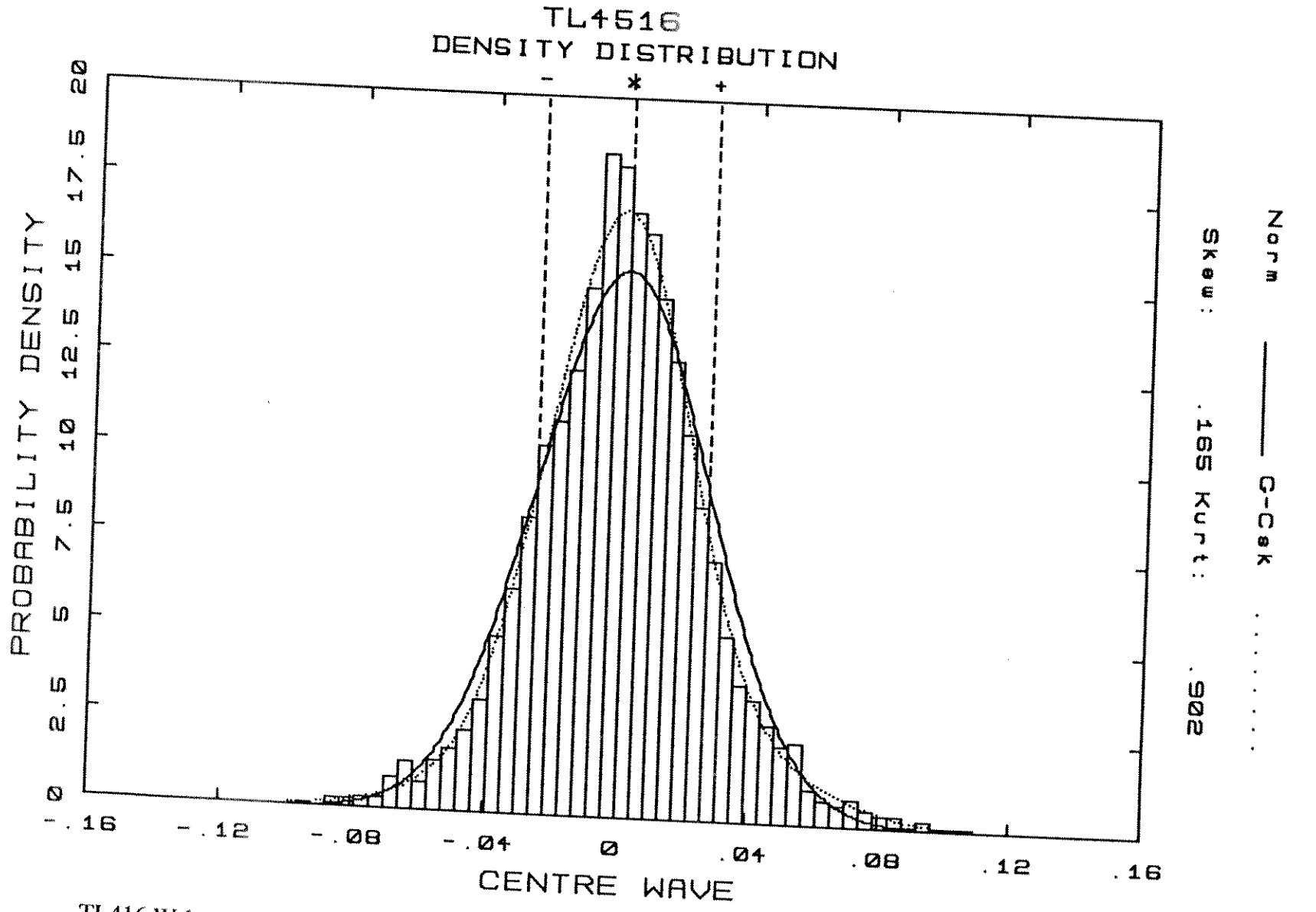
TL4516
DENSITY DISTRIBUTION
- * +
PROBABILITY DENSITY
0 2.5 5 7.5 10 12.5 15 17.5 20
-.16 -.12 -.08 -.04 0 .04 .08 .12 .16
CENTRE WAVE
Norm ——— C-Cek .....
Skew: .165 Kurt: .902

TL416.W.1

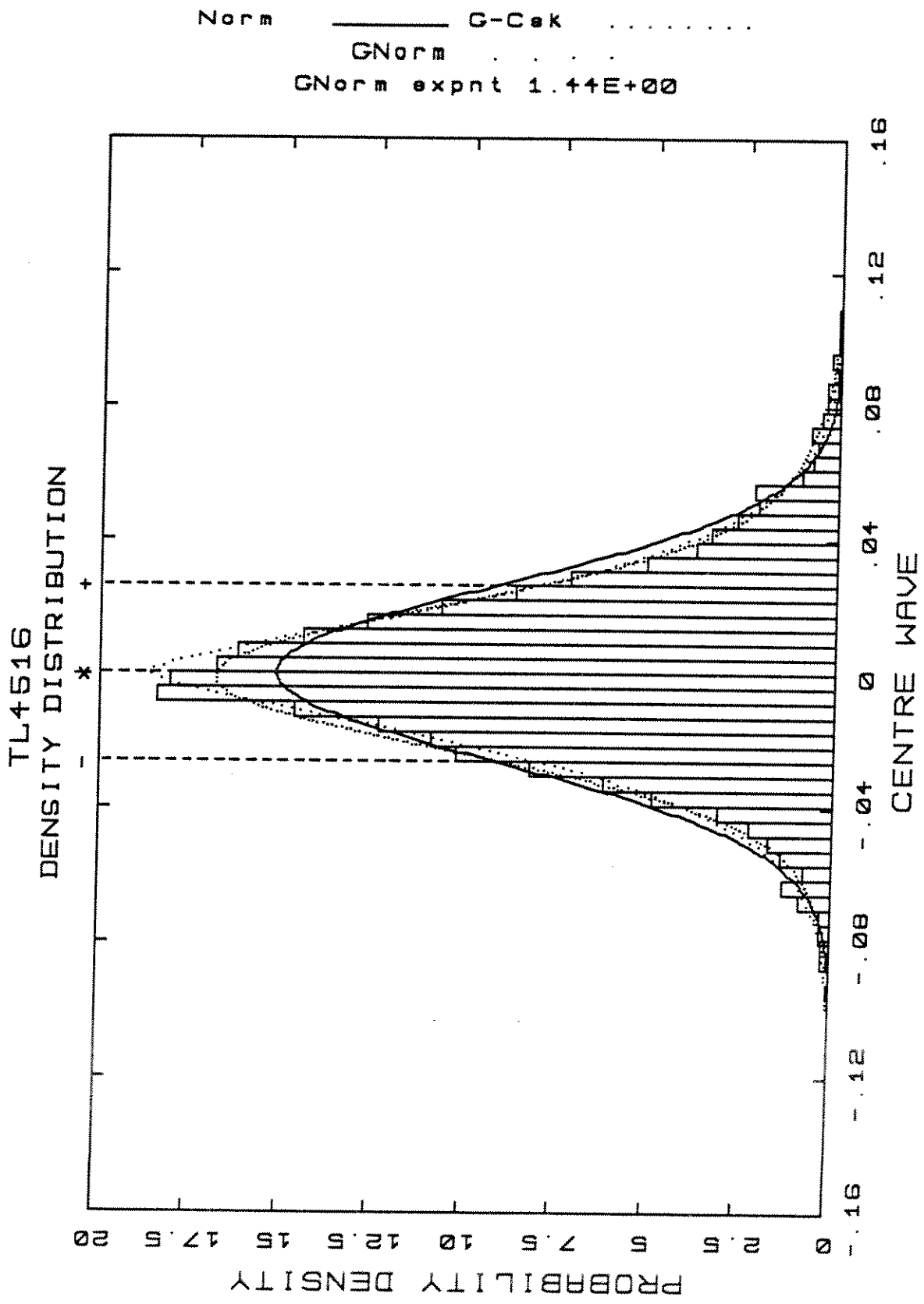
Norm
G-Cak
GNorm
GNorm expnt 1.44E+00
TL4516
DENSITY DISTRIBUTION
+
*
-
PROBABILITY DENSITY
0
2.5
5
7.5
10
12.5
15
17.5
20
.16
.12
.08
.04
0
-.04
-.08
-.12
-.16
CENTRE WAVE

TL4516.W.1A

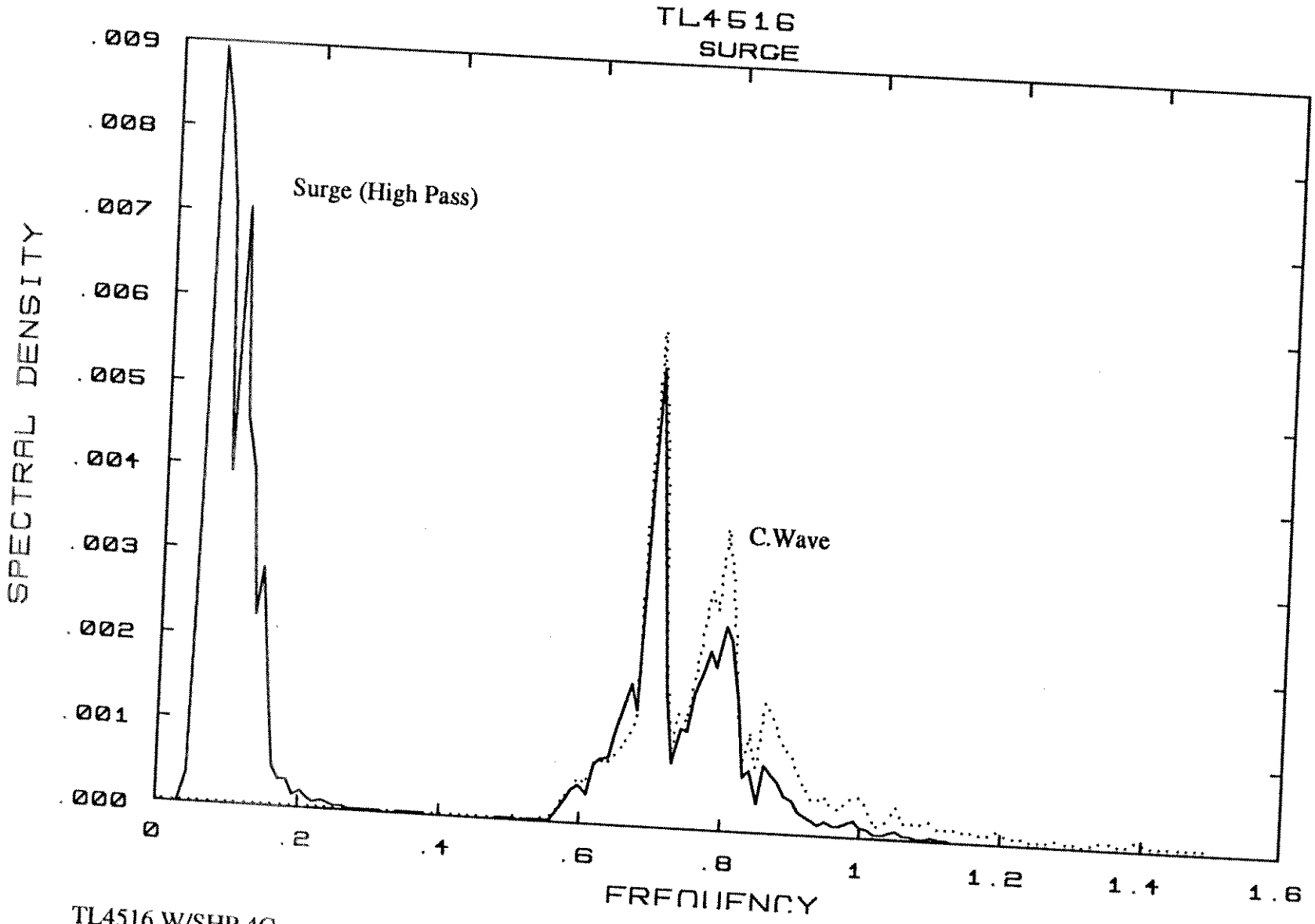

TL4516.W/SHP.4C

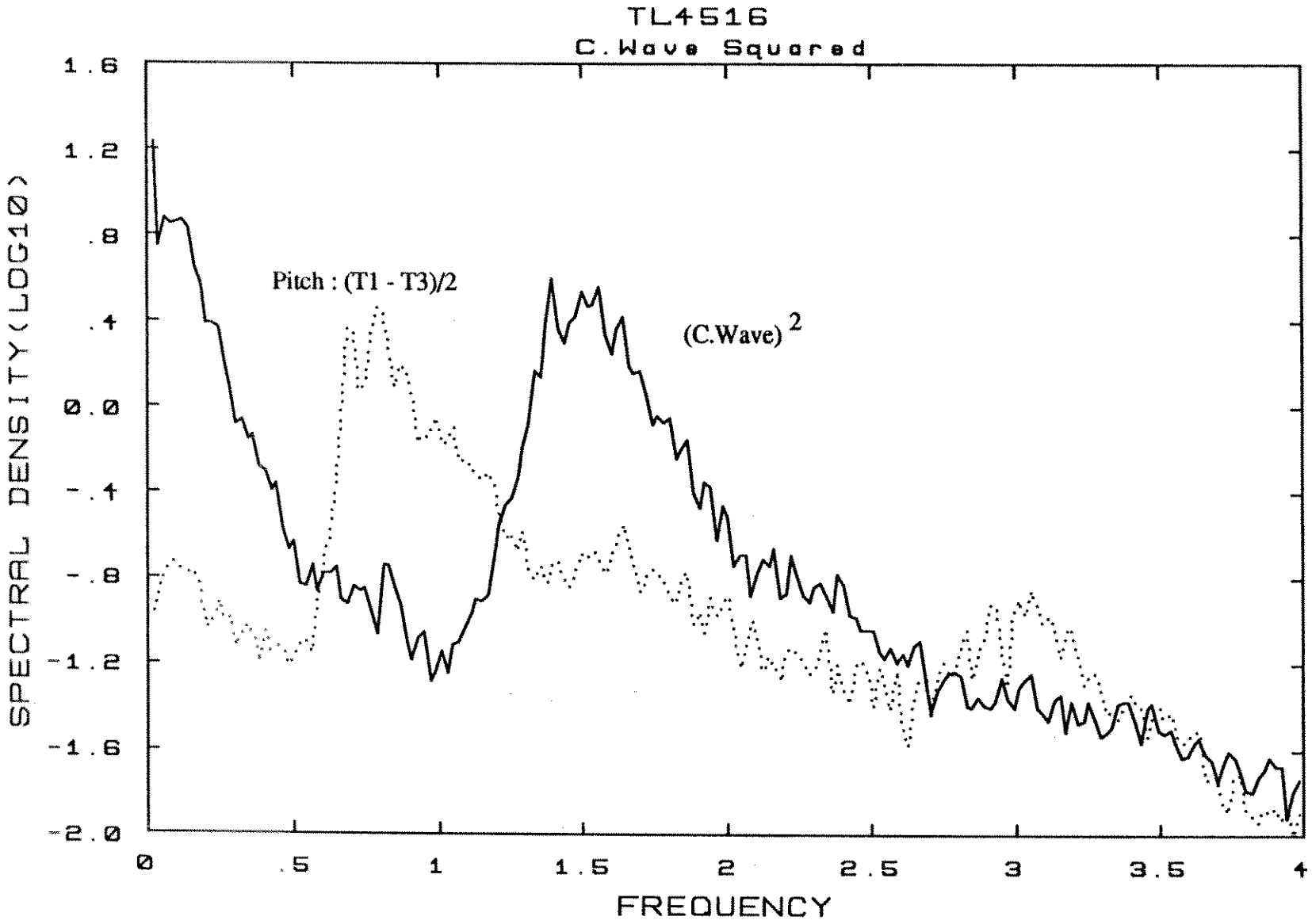

TL4516.WSQ/PiT13.4
C.Wave Squrared and Pitch are normalized

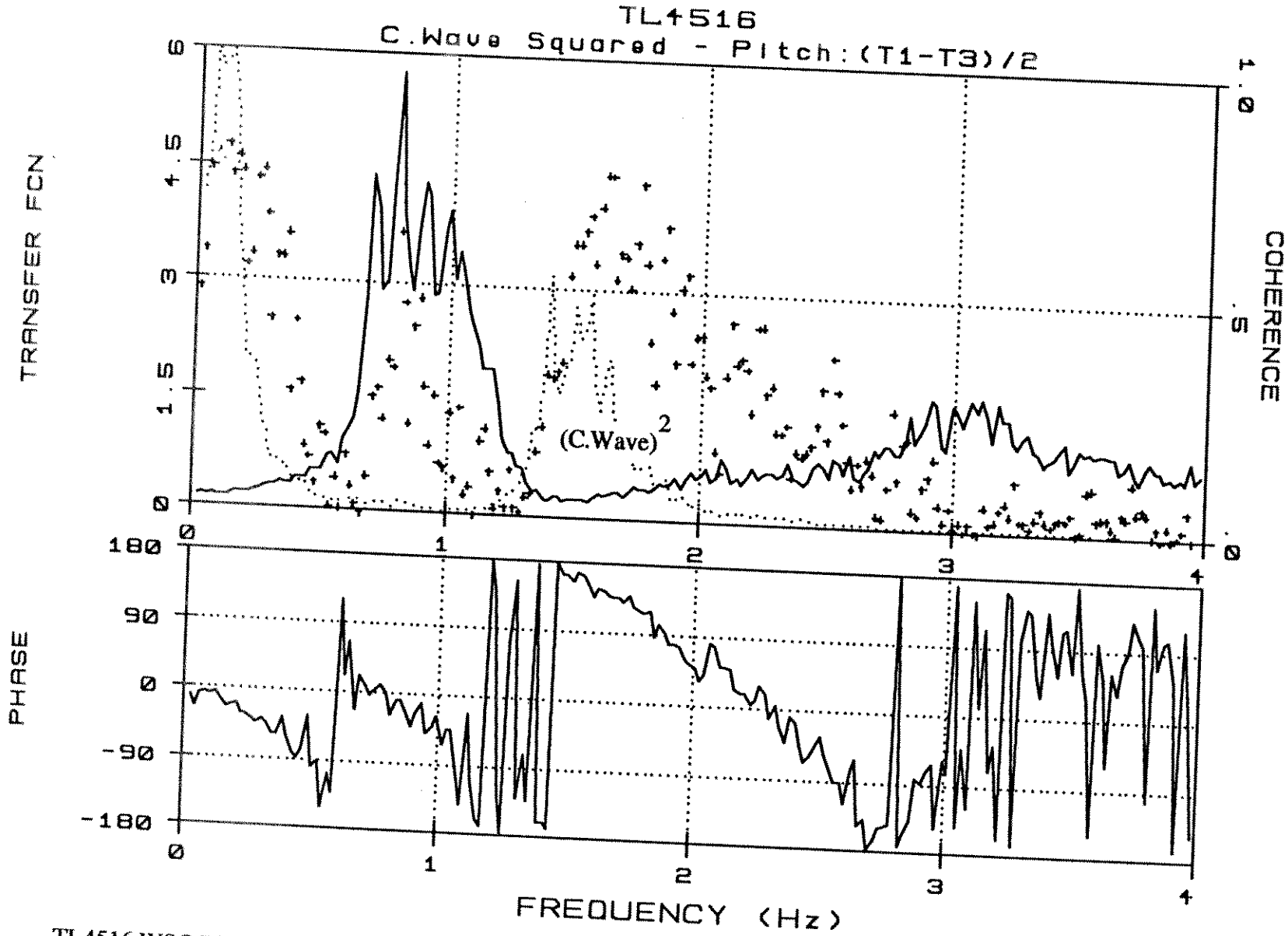

TL4516.WSQ/PiT13.4t
C.Wave Squrared and Pitch are normalized

DET NORSKE
VERITAS

A.S Veritas Research

ADDRESS: Veritasveien 1, Høvik
POSTAL ADDRESS: P.O.Box 300, N-1322 Høvik, Norway
TELEPHONE: (47 2) 47 75 00
CABLE ADDRESS: Veritas, Oslo
TELEX: 76 192 vertt n
FACSIMILE: (47 2) 47 98 71
BANKER: Den norske Creditbank, Acc.No. 7131.05.26821

TECHNICAL REPORT

		Date: May 25, 1990	
A.S Veritas Research Report No.: 90-2025	Subject Group: C1 D45 P5	Department: VR40	Project No.: 48200
Title of Report: Evaluation of Wind Load Models for Compliant Platforms		Approved by: N. Skomedal	
Client/Sponsor of project: Boundary Layer Wind Tunnel Laboratory		Client/Sponsor ref.: Dear R. Skomedal	
Work carried out by: J. Mathisen		Reporters sign.: J. Mathisen	
Work verified by: T. Vada		Verifiers sign.	

Summary

The accuracies of two mathematical models for wind loads are evaluated on the basis of model test data obtained for the deck structures of a semisubmersible and a tension leg platform. The test data comprise both wind velocities and wind loads, measured under severe environmental conditions, including realistic wind turbulence. A simple drag formula and a formula utilising aerodynamic admittance are considered. Drag coefficients and admittances are first derived from the model test data, and then used to calculate wind load time histories on the basis of the wind speed time histories. Comparison of the calculated and measured wind loads demonstrates the accuracy of the mathematical models.

4 indexing terms

wind loads
drift forces
drag
aerodynamic loads

Distribution statement:

- [X] No distribution without permission from the responsible department.
- [ ] Limited distribution within A.S Veritas Research.
- [ ] Free distribution.

Date of last revision	Rev.no.		Number of pages
-			31pages

Contents

1. Introduction

This report is part of a

Joint Industry Project to Study
Wind Loads and Wind/Wave Interactions on Offshore Structures:
Semi-Submersibles, Tension Leg Platforms and Compliant Towers,

organised by the Boundary Layer Wind Tunnel Laboratory, London, Ontario, and supported by the following organizations:

Amoco Production Company
Exxon Production Research Company
Institute for Marine Dynamics
Mobil Research and Development Corporation
Statoil
ARCO Oil and Gas Company
Institut Francais de Petrole
Minerals Management Service
Saga Petroleum a.s.
A.S. Veritas Research

The object of the present report is to quantify the accuracy of two mathematical models for wind loads, that could be used in the numerical simulation of slow drift motions of compliant offshore platforms. The two mathematical models are

(a) a simple drag force formula,

(b) a formula utilising aerodynamic admittance to include load dependence on frequency of the wind turbulence.

Estimation of drag coefficients and admittances from measured model test data for wind speeds and wind loads is described in chapter 2. The calculation of simulated wind load time histories from the estimated drag coefficients, admittances, and measured wind speed is described in chapter 3. Chapter 4 then gives details of the model test data utilised, and of the comparison between measured and calculated wind loads.

2. Estimation

It is assumed that the following signals are available from measurements of the wind loads on a bluff body:

u_i	wind speed, characteristic for loading	[m/s]
x_i	drag force, in line with wind direction	[N]
y_i	transverse force, normal to wind direction	[N]
r_i	torsional moment about a vertical axis	[Nm]

where i=1,2, . . . ,m denotes the sequence of discrete time instants at which the signals are sampled. Slow drift motions in a horizontal plane are usually taken to be of primary interest, thus leading to a focus on the three load components listed above.

2.1. Drag Coefficients

The simple drag force formula may be written as

$$x(t) = \tfrac{1}{2}\,\rho\, C_D\, B^2\, u^2(t) \tag{2.1}$$

where C_D is a drag coefficient, ρ is the air density, B is a characteristic dimension of the structure subject to the wind action, and t is time. Assuming the mean wind speed $\bar{u}$ is large compared to the speed fluctuations $\tilde{u}(t)$, this expression may be expanded, and the second order term in the fluctuating velocity may be neglected

$$\begin{aligned} x(t) &= \tfrac{1}{2}\,\rho C_D\, B^2[\bar{u}^2 + 2\,\bar{u}\,\tilde{u}(t) + \tilde{u}^2(t)] \\ &\approx \tfrac{1}{2}\,\rho C_D\, B^2[\bar{u}^2 + 2\,\bar{u}\,\tilde{u}(t)] \end{aligned} \tag{2.2}$$

Instead of using a single drag coefficient, two drag coefficients may be introduced into this expression, one for the mean drag force C_{x-m}, and one for the fluctuating drag force $C_{x-\sigma}$

$$x(t) = \tfrac{1}{2}\,\rho\, B^2[C_{x-m}\,\bar{u}^2 + 2\,C_{x-\sigma}\,\bar{u}\,\tilde{u}(t)] \tag{2.3}$$

This mean drag coefficient corresponds to normal practice, but the author of this report is not aware if this fluctuating drag coefficient is in general use. However, when this formulation is extended to transverse forces and torsional moments, it provides a possibility for non-zero fluctuating loads together with zero mean loads, a situation which certainly occurs in the model tests.

On this basis, drag load coefficients may be estimated from mean loads or standard deviations of the loads. The mean drag force is calculated as

$$\bar{x} = \frac{1}{m}\sum_{i=1}^{i=m} x_i \tag{2.4}$$

where the bar denotes a mean value, and the standard deviation of the drag force is calculated as

$$\sigma_x = \left[\frac{1}{m-1}\sum_{i=1}^{i=m}(x_i - \bar{x})^2\right]^{1/2} \tag{2.5}$$

Mean values and standard deviations for the other two load components and for the wind speed are obtained in a similar manner. The mean drag coefficient (or more accurately, the mean-based drag coefficient) is then estimated by

$$C_{x-m} = \bar{x} \,/\, (\tfrac{1}{2}\,\rho\, B^2\,\bar{u}^2) \tag{2.6}$$

and the fluctuating drag coefficient (or the coefficient for the fluctuating drag force) is

obtained as

$$C_{x-\sigma} = \sigma_x \,/\, (\rho\, B^2\, \bar{u}\, \sigma_u) \tag{2.7}$$

Extending the above formulation to transverse loads amd torsional moments, the corresponding force coefficients may be obtained as follows: for the transverse force,

$$C_{y-m} = \bar{y} \,/\, (\tfrac{1}{2}\, \rho\, B^2\, \bar{u}^2) \tag{2.8}$$

$$C_{y-\sigma} = \sigma_y \,/\, (\rho\, B^2\, \bar{u}\, \sigma_u) \tag{2.9}$$

and for the torsional moment,

$$C_{r-m} = \bar{r} \,/\, (\tfrac{1}{2}\, \rho\, B^3\, \bar{u}^2) \tag{2.10}$$

$$C_{r-\sigma} = \sigma_r \,/\, (\rho\, B^3\, \bar{u}\, \sigma_u) \tag{2.11}$$

The mean force coefficients given above corespond to the definitions given by Ramsay et al. 1989a, while the fluctuating force coefficients are different from the "rms force coefficients" therein. The difference is mainly due to use of standard deviation of the wind speed above, and is significant if different turbulence intensities $\sigma_u \,/\, \bar{u}$ are envisaged.

2.2. Aerodynamic Admittance

The equation for estimation of drag force aerodynamic admittance $\chi_x^2(f)$, given by Ramsay et al. 1989b is adopted here with one modification; viz. the fluctuating drag force coefficient defined above is used instead of the mean drag force coefficient.

$$\chi_x^2(f) = \frac{S_{xx}(f)}{(C_{x-\sigma}\, \rho\, B^2\, \bar{u})^2\, S_{uu}(f)}\,; \qquad f > 0 \tag{2.12}$$

where $S_{xx}(f)$ is the drag force spectrum, $S_{uu}(f)$ is the wind speed spectrum, and f represents frequency. The corresponding expression for the transverse force aerodynamic admittance is

$$\chi_y^2(f) = \frac{S_{yy}(f)}{(C_{y-\sigma}\, \rho\, B^2\, \bar{u})^2\, S_{uu}(f)}\,; \qquad f > 0 \tag{2.13}$$

and for the torsional moment aerodynamic admittance

$$\chi_r^2(f) = \frac{S_{rr}(f)}{(C_{r-\sigma}\, \rho\, B^3\, \bar{u})^2\, S_{uu}(f)}\,; \qquad f > 0 \tag{2.14}$$

The reason for applying a modified definition of the admittance may now be apparent, since these last two expressions would be incorrect if the mean transverse force or torsional moment were zero, and a force coefficient based on the mean force were used.

When calculating the spectra;

- a time series is split into a number of segments,
- a Parzen taper function is applied to each segment,
- a fast Fourier transform is used to obtain a periodogram for each segment,
- the final spectrum is obtained by averaging across the segments.

3. Wind Load Simulation

3.1. Loads from Drag Coefficients (Model A)

Originally, it was intended that a wind load model based on a single force coefficient would be utilised for each load component considered. However, the discussion of the results in chapter 4 shows this simplest model to be so inaccurate, that it was discarded. Instead, two coefficients are utilised to model each load component. The wind loads are then simulated using force coefficients, estimated as described in chapter 2, and the time series of the measured wind speed.

The drag force is simulated by

$$x_A(t) = \tfrac{1}{2}\,\rho\,B^2[C_{x-m}\,\bar{u}^2 + 2\,C_{x-\sigma}\,\bar{u}\,\tilde{u}(t)] \tag{3.1}$$

the transverse force is simulated by

$$y_A(t) = \tfrac{1}{2}\,\rho\,B^2[C_{y-m}\,\bar{u}^2 + 2\,C_{y-\sigma}\,\bar{u}\,\tilde{u}(t)] \tag{3.2}$$

and the torsional moment is simulated by

$$r_A(t) = \tfrac{1}{2}\,\rho\,B^2[C_{r-m}\,\bar{u}^2 + 2\,C_{r-\sigma}\,\bar{u}\,\tilde{u}(t)] \tag{3.3}$$

where the subscript A signifies loads calculated by mathematical model A.

3.2. Loads from Aerodynamic Admittances (Model B)

A drag force aerodynamic admittance function is defined in terms of force and wind speed spectra in equation (2.12). Inversion of this definition provides a straight-forward basis for calculation of drag force spectra, but does not explicitly provide an expression for drag force time histories. The requisite basis for simulation of drag forces from an aerodynamic admittance function may conveniently be developed by first considering the associated impulse response function. Such an impulse response function $h_x(\tau)$ may be obtained via an inverse Fourier transform of the square root of the corresponding aerodynamic admittance $\chi_x^2(f)$

$$h_x(\tau) = \int_{-\infty}^{\infty} \chi_x(f)\, e^{i2\pi f\tau}\, df \tag{3.4}$$

The drag force time history may be expressed by convolution of this impulse response function with the fluctuating wind speed, with the addition of a mean force term

$$x_B(t) = \tfrac{1}{2}\,\rho\,B^2\left[C_{x-m}\,\bar{u}^2 + 2\,C_{x-\sigma}\,\bar{u}\int_{-\infty}^{\infty} h_x(\tau)\,\tilde{u}(t-\tau)\,d\tau\right] \tag{3.5}$$

In practice, numerical computation of such convolutions tends to be inefficient, and it is preferable to replace the convolution by a multiplication in the frequency domain. Thus, for this mathematical model, the drag force time series is simulated by

- splitting the wind speed time series into segments of suitable length,
- using a fast Fourier transform to obtain Fourier series coefficients for each segment,
- multiplying the Fourier coefficients by the corresponding values of the square root of the aerodynamic admittance, and the fluctuating drag coefficient (while omitting the mean value terms),
- transforming each segment back to the time domain with an inverse fast Fourier transform,

- adding in the mean drag force computed from the mean force coefficient and the mean wind speed.

Corresponding procedures are used to obtain the transverse force and torsional moment time series.

4. Results

4.1. Model test Data

The present analysis is carried out using data from model tests performed by the Boundary Layer Wind Tunnel Laboratory, and described by Ramsay et al. 1988 and Ramsay et al. 1989c. Two structural models are considered here; viz. the deck structures of a tension leg platform (TLP) and a semisubmersible platform. During the model tests, each deck structure was suspended over the water surface, and subjected to the effects of a turbulent wind field, with a nominal mean speed of 3 m/s (or 40 m/s prototype scale) at deck height. Regular waves were generated by a wave flap in some of the tests, in addition to the wind-generated waves. Wind speeds and loads on the deck structure were measured. These results were transmitted to Veritas Research by means of a magnetic tape, referred to as the "wettim" tape, and received in November 1989.

The data on the tape are multiplexed, and sampled at 20 Hz. Table 4.1 gives the channel assignments and calibration factors required to obtain signals in physical units, at model scale, from the tape data. Each test on the tape has a duration of 600 seconds (or about 2 hours at prototype scale).

no.	channel	units	calib. factor
1	Moment about longit. axis	Nm	0.228
2	Moment about transv. axis	Nm	0.229
3	disregard	V	1.0
4	disregard	V	1.0
5	disregard	V	1.0
6	Lift force	N	2.196
7	Front lateral load cell	V	1.0
8	Rear lateral load cell	V	1.0
9	Transverse force	N	0.1146
10	Torsional moment	Nm	0.0116
11	Drag force	N	0.238
12	Pitot (far)	m/s	2.884
13	Pitot (near)	m/s	2.884
14	Wave probe (far)	m	0.113
15	Wave probe (near)	m	0.117
16	Hot wire	m/s	2.85

(wind speed from pitot = calib. factor $\times \sqrt{pitot\ volts}$)

Table 4.1 Calibration factors for data on "wettim" tape.

Only the drag, transverse force, torsional moment, and hot wire wind speeds are utilised here. Initial inspection of the data appeared to show a satisfactory data quality, so no additional treatment of the data was applied prior to the present analysis.

The following two parameter values are applied throughout, in the calculation of the force coefficients:

ρ=1.25 kg/m^3, air density,

B=0.381 m, characteristic length of model, (equivalent to 15 inches, as specified by Ramsay et al. 1989a).

In addition to the tests with no waves generated by the wave flap, results are also analysed from tests with the wave flap running at a frequency of 0.65 Hz, for two wave heights.

The results labelled "High waves" refer to nominal wave heights of 0.17m and 0.11m, while "Low waves" refer to 0.07m and 0.06m for the TLP and semisubmersible, respectively. These nominal wave heights are calculated as $2\sqrt{2}$ times the standard deviations from the wave probe signals (as would be appropriate for purely sinusoidal waves).

4.2. Moments and Coefficients

Mean values of the signals are given in Table 4.2, and standard deviations are given in Table 4.3. Table 4.3 includes an additional column taken from the spectral plots in Ramsay et al. 1989c, which agrees quite well with the present results, confirming that the data have been interpreted in the same manner. Only a few of the tests reported by Ramsay et al 1989c are included here, and the trends shown by the present results differ somewhat from the trends reported for the whole set of tests; viz.

- the mean wind speed is higher in the presence of additional waves,
- the wind speed standard deviation is less with low waves, and greater with high waves, as compared to the no waves cases,
- the mean drag forces are less with low waves, and greater with high waves, as compared to the no waves cases,
- the load standard deviations are larger with waves than without, but for the semisubmersible, they are largest in low waves.

	Response	No waves	High waves	Low waves
tlp	Wind speed [m/s]	2.76	2.84	2.79
	Drag force [N]	0.385	0.407	0.355
	Transverse force [N]	0.00250	0.00267	0.00227
	Torsional moment[N]	-0.00151	-0.00146	-0.00184
semisub	Wind speed [m/s]	2.76	2.77	2.81
	Drag force [N]	0.265	0.309	0.243
	Transverse force [N]	0.00240	0.00459	0.00361
	Torsional moment [Nm]	0.00084	0.00102	0.00056

Table 4.2 Mean values of measured signals

	Response	No waves	High waves	Low waves	Prelim.report no.4 No waves
tlp	Wind speed [m/s]	0.345	0.364	0.335	0.346
	Drag force [N]	0.0574	0.0648	0.0617	0.0588
	Transverse force [N]	0.0247	0.0296	0.0262	0.0248
	Torsional moment [Nm]	0.00409	0.00423	0.00411	0.0041
semisub	Wind speed [m/s]	0.352	0.356	0.349	0.353
	Drag force [N]	0.0410	0.0456	0.0486	0.0415
	Transverse force [N]	0.0137	0.0151	0.0155	0.0138
	Torsional moment [Nm]	0.00235	0.00239	0.00244	0.0024

Table 4.3 Standard deviations of measured signals

Except for the mean transverse forces and torsional moments, which are negligible, the standard errors in the estimated mean loads and load standard deviations are about 1% to 2%. Hence, the statistical uncertainty of the results in Table 4.2 and Table 4.3 should not invalidate the discussion of the load variations above.

Mean wind load coefficients, as defined by equations (2.6), (2.8) and (2.10) are calculated from the signal mean values, and given in Table 4.4. Note that the actual mean wind speed calculated from each test is used in the calculations, rather than the nominal wind speed of 3 m/s (the nominal wind speed is apparently used in the wind load coefficient calculations by Ramsay et al. 1989c).

	Response	No waves	High waves	Low waves
tlp	Drag force	0.560	0.556	0.503
	Transverse force	0.0036	0.0036	0.0032
	Torsional moment	-0.0058	-0.0052	-0.0068
semisub	Drag force	0.383	0.443	0.340
	Transverse force	0.0035	0.0066	0.0051
	Torsional moment	0.0032	0.0039	0.0021

Table 4.4 Mean wind load coefficients

Fluctuating wind load coefficients, as defined by equations (2.7), (2.9) and (2.11) are calculated from the signal standard deviations, and given in Table 4.5.

	Response	No waves	High waves	Low waves
tlp	Drag force	0.333	0.345	0.364
	Transverse force	0.143	0.158	0.155
	Torsional moment	0.062	0.059	0.064
semisub	Drag force	0.233	0.255	0.274
	Transverse force	0.078	0.085	0.087
	Torsional moment	0.035	0.035	0.036

Table 4.5 Fluctuating wind load coefficients

It is apparent from Tables 4.4 and 4.5, that the mean load coefficients for transverse forces and torsional moments are negligible in comparison with the fluctuating load coefficients. Hence, these mean load coefficients would be unsuitable for normalisation of the corresponding aerodynamic admittance functions. If the platform deck models are orientated differently with respect to the wind direction, then the symmetry of the situation may be reduced and significant mean transverse and torsional loads may arise.

The variations in the mean drag coefficients and in all the fluctuating load coefficients between the three different test conditions (high, low and no waves) are quite small, typically of the order of ±5%. The drag coefficient for the semisubmersible varies somewhat more, up to 14% from the average value of the three tests. There is a tendency for a slight increase in the fluctuating force coefficients in waves, as compared to no waves.

The present definitions of the load coefficients make the numerical values of the mean and fluctuating coefficients directly comparable. The mean drag coefficients are 50% to 60% larger than the fluctuating drag coefficients for both platform types. Hence, if the fluctuating drag forces should be modelled on the basis of the mean drag coefficents only, this would lead to a bias of this magnitude in the fluctuating loads. Conversely, if the mean drag forces should be modelled on the basis of the fluctuating drag coefficients, then the mean drag forces would be underestimated by about one third. In the present

context, where both mean and fluctuating wind forces are expected to affect the platform response significantly, these results clearly show the inadequacy of a drag force model utilising a single drag coefficient. Both mean and fluctuating drag coefficients are necessary. The same line of reasoning also applies to the transverse and torsional wind loads.

Simulated wind loads have been calculated using mathematical models A and B, and based on the load coefficients obtained from the tests with no waves. Mean values and standard deviations of these simulated wind loads have also been calculated and compared with the corresponding results from the measured loads. The numerical results of this comparison are not included here. Excellent agreement between measured and simulated results was obtained for the test with no waves, with no differences exceeding 3%. Somewhat larger differences were obtained from the tests with waves, but these differences closely reflect the differences in the load coefficients between the various tests, as discussed above. (Remember that all the simulated loads are based on coefficients and admittances obtained from the tests with no waves.)

4.3. Time Series

Sample time histories of the measured wind loads are shown in Fig. 4.1 to 4.6, with time axes covering the full extent of these tests. These plots serve to confirm that the data are reasonably stationary, and that no obvious drop-outs appear to be present. The near-zero mean values of the transverse forces and torsional moments are also obvious, while the drag forces may be seen to have mean values that are generally larger than the fluctuations. The corresponding plots from tests with waves are similar in appearance, and are not included here.

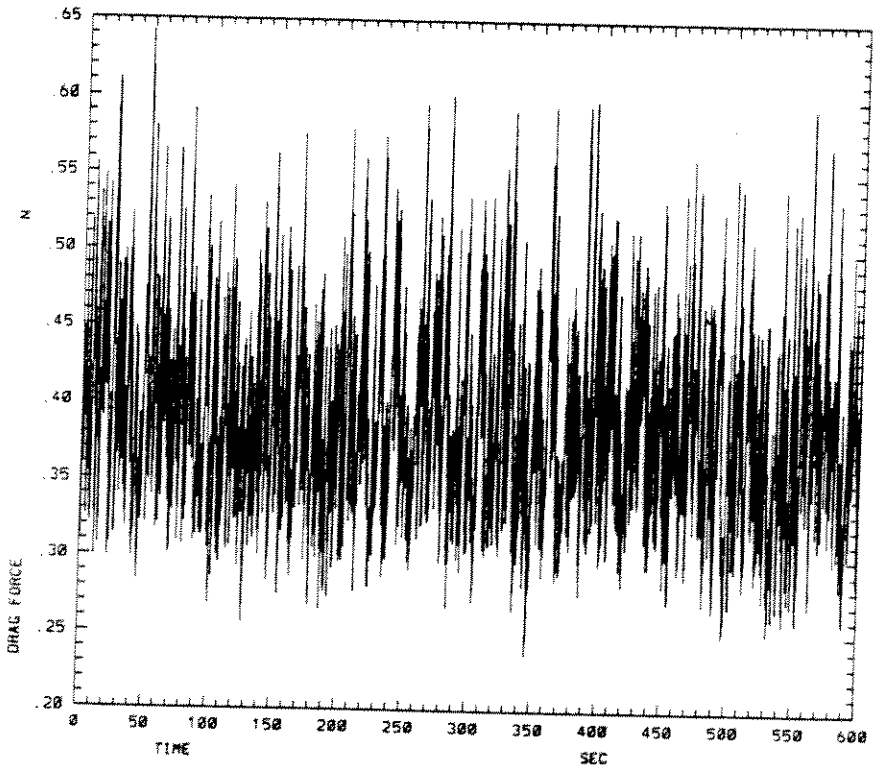

Fig. 4.1 Drag force time history for TLP - no waves.

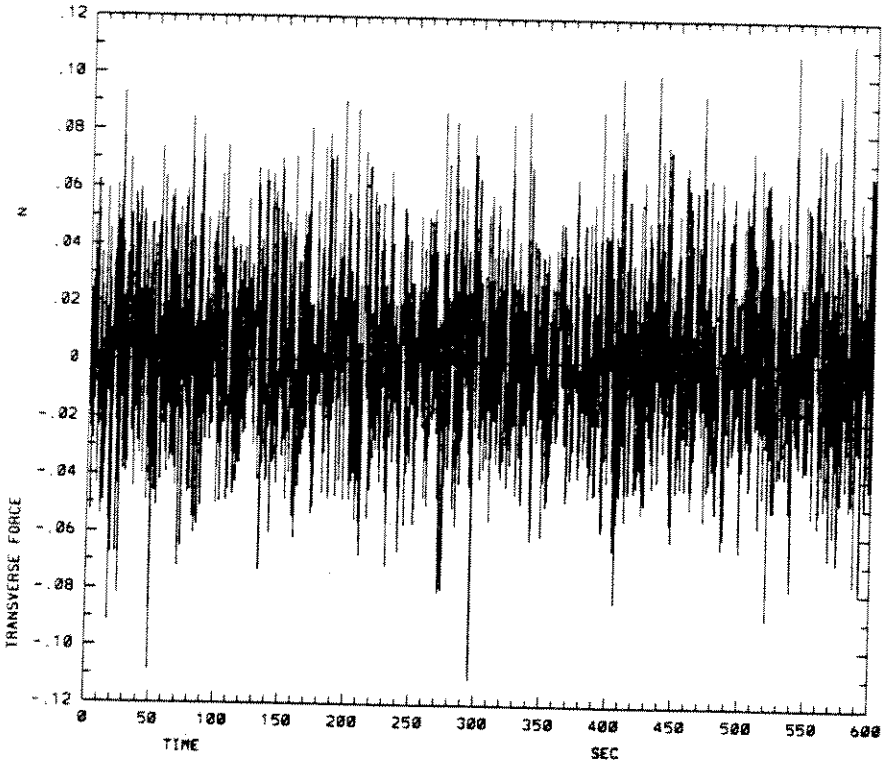

Fig. 4.2 Transverse force time history for TLP - no waves.

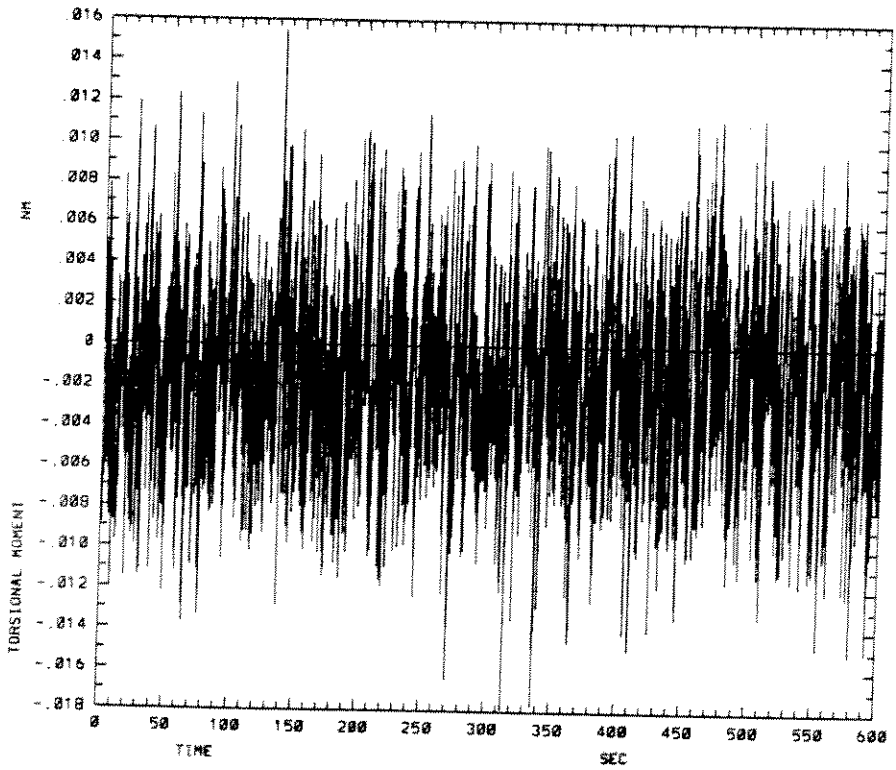

Fig. 4.3 Torsional moment time history for TLP - no waves.

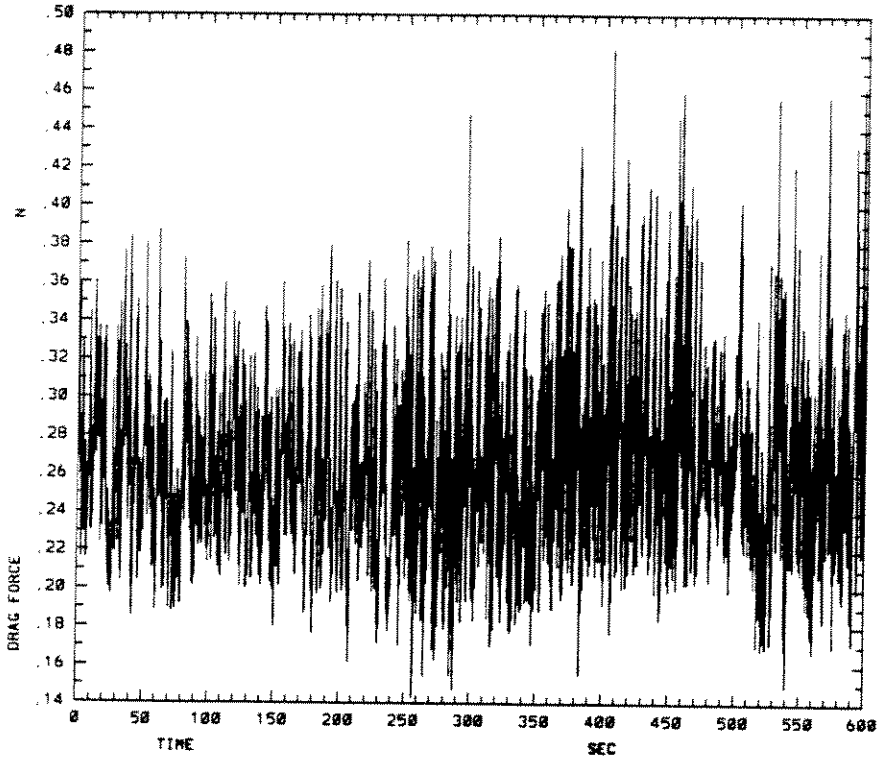

Fig. 4.4 Drag force time history for semisubmersible - no waves.

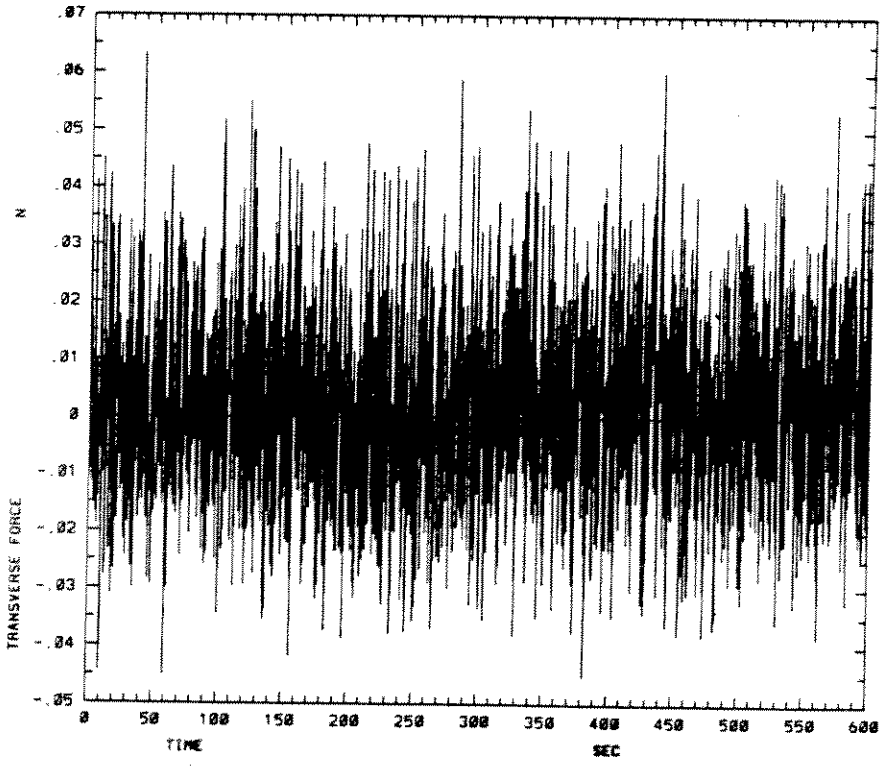

Fig. 4.5 Transverse force time history for semisubmersible - no waves.

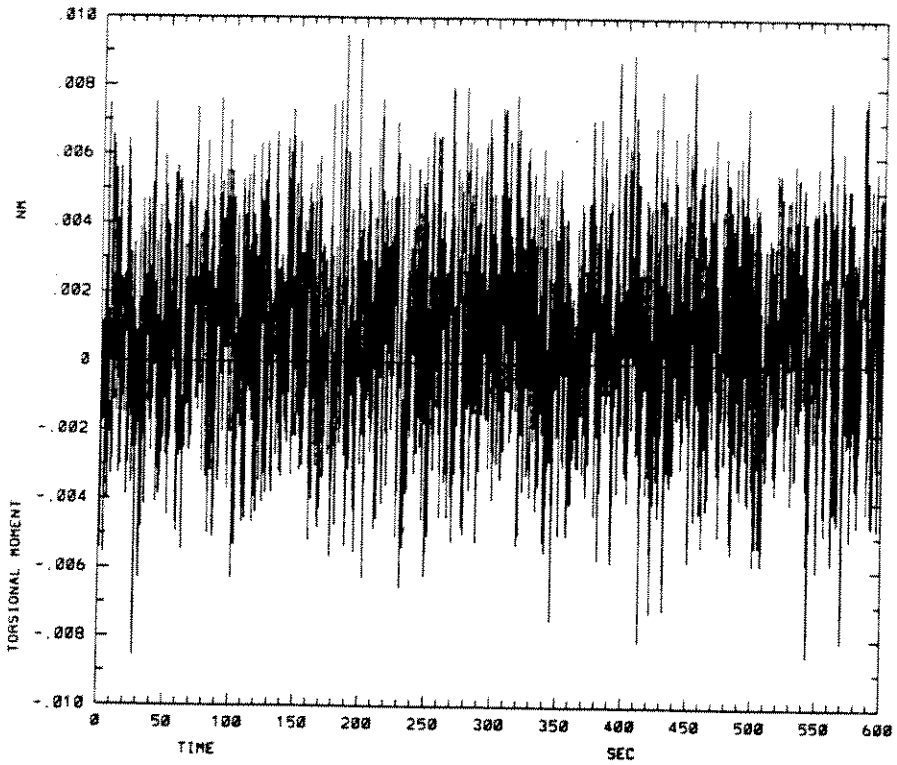

Fig. 4.6 **Torsional moment time history for semisubmersible - no waves.**

Extracts from the time histories giving comparisons of the measured loads with the two sets of simulated loads (model A and model B) are shown in Fig. 4.7 to 4.12. These extracts are located around the time instants giving the largest drag forces in the tests with no waves. The mean loads agree well in all cases, and the general magnitude of the load fluctuations also seem reasonable, while the details of the measured and simulated fluctuations differ considerably. It is notable that the two sets of simulated loads agree much better with each other than with the measured loads. This reflects the strong correlation between both the simulated loads and the wind speed, while the correlation between the wind speed and the measured loads is much weaker. The comparisons also seem to indicate that the sign of the simulated load fluctuations is random, or irregular in some way, relative to the measured fluctuations.

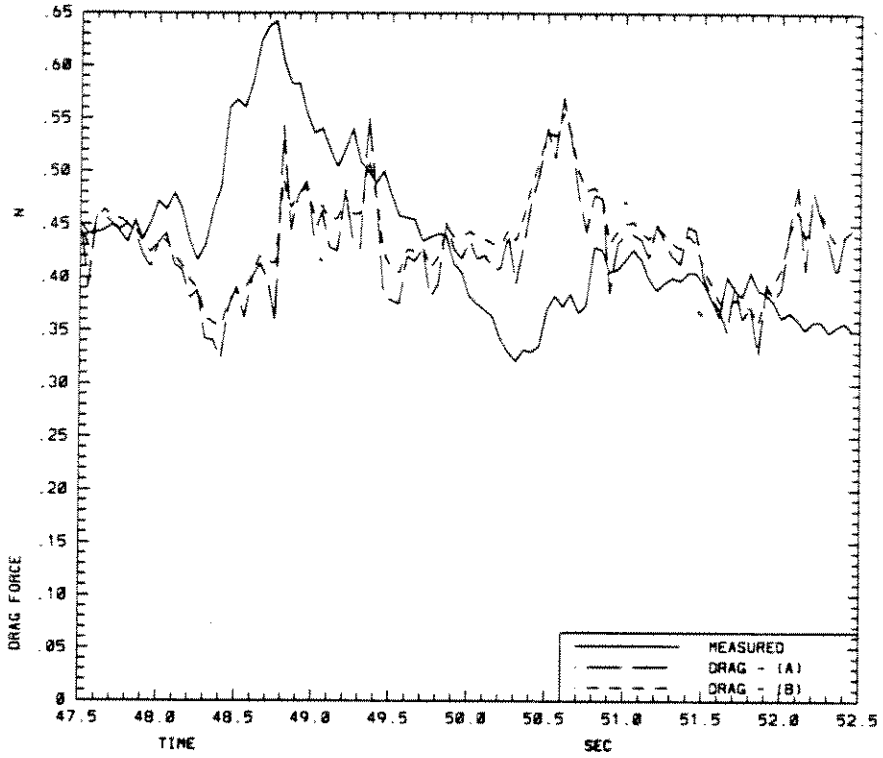

Fig. 4.7 Comparison of measured and simulated drag force time history for TLP - no waves.

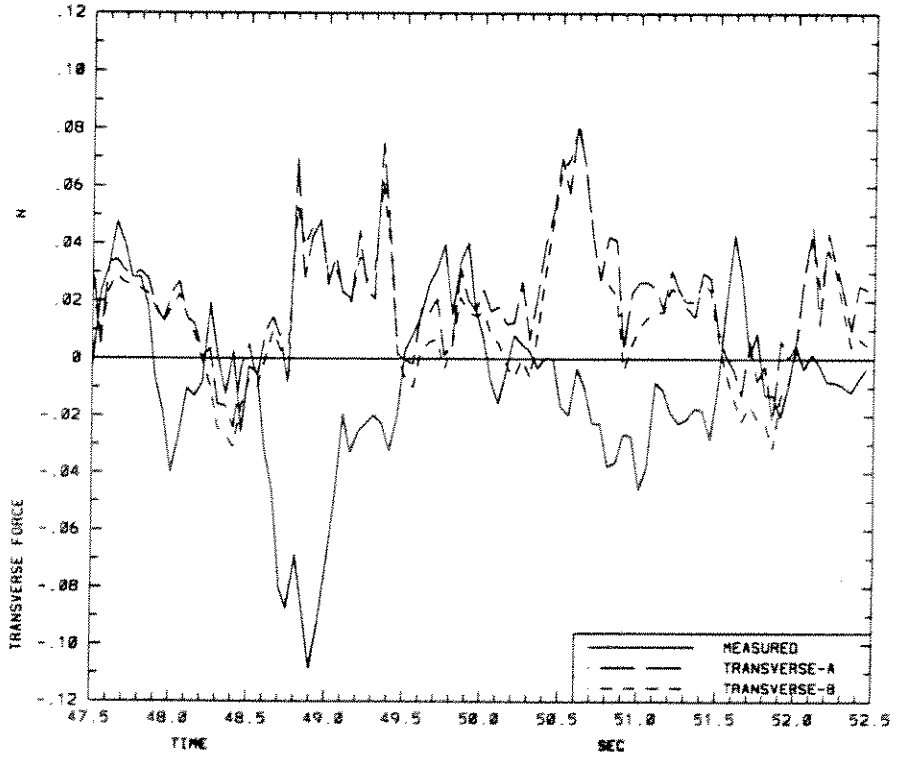

Fig. 4.8 Comparison of measured and simulated transverse force time history for TLP - no waves.

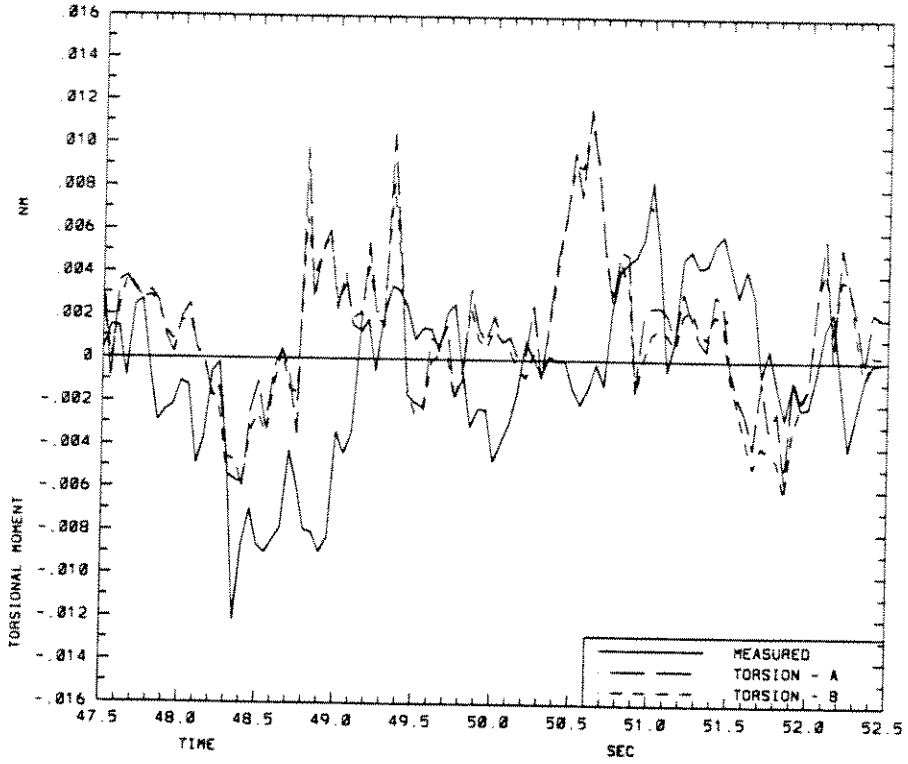

Fig. 4.9 Comparison of measured and simulated torsional moment time history for TLP - no waves.

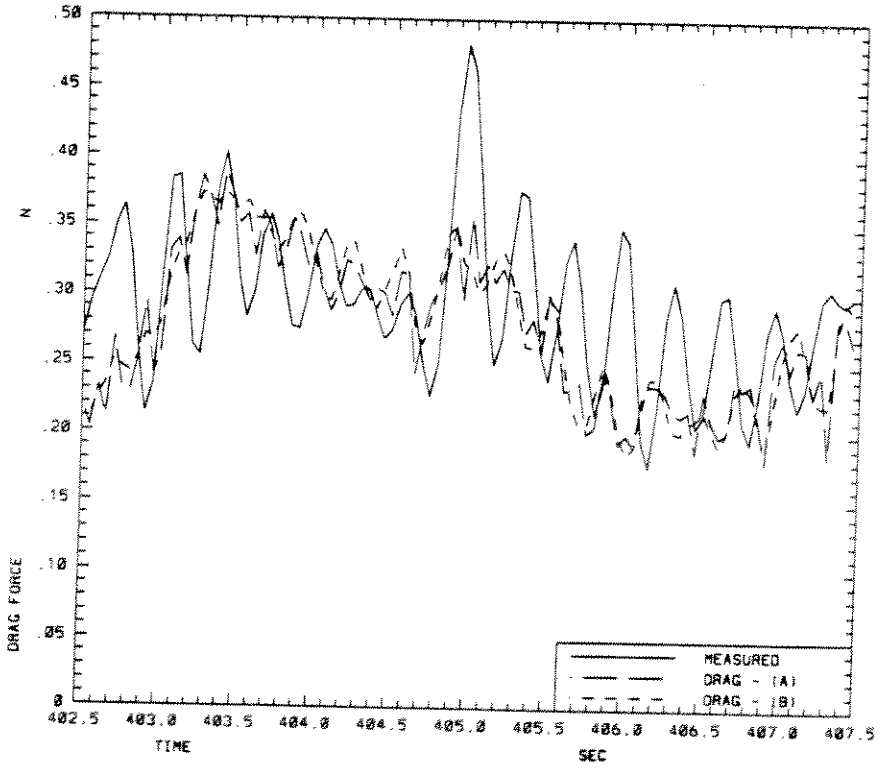

Fig. 4.10 Comparison of measured and simulated drag force time history for semisubmersible - no waves.

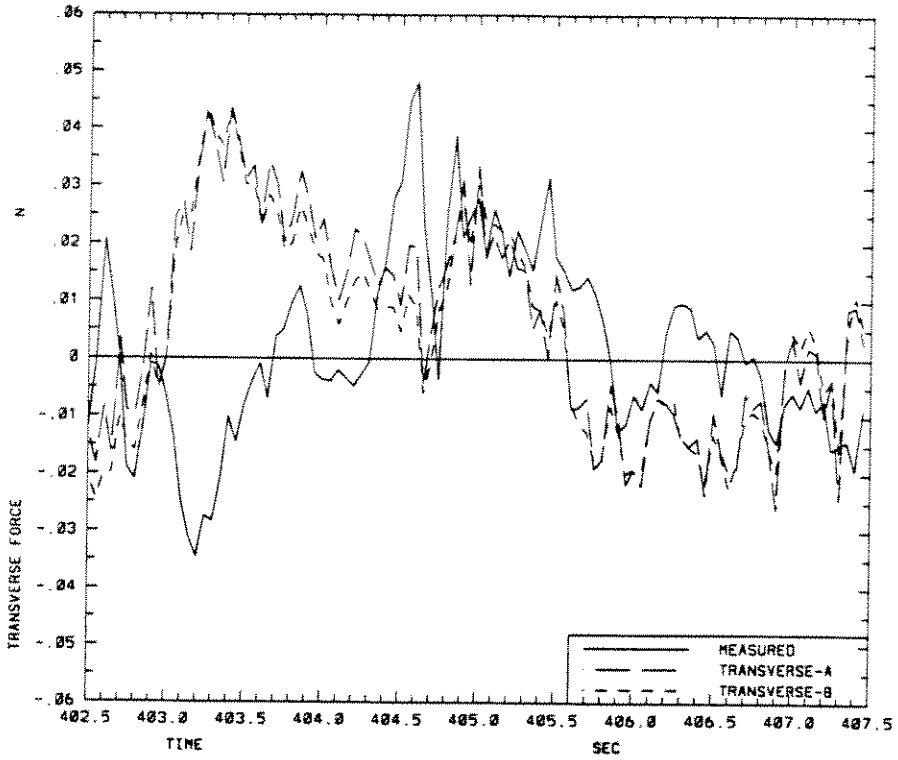

Fig. 4.11 Comparison of measured and simulated transverse force time history for semisubmersible - no waves.

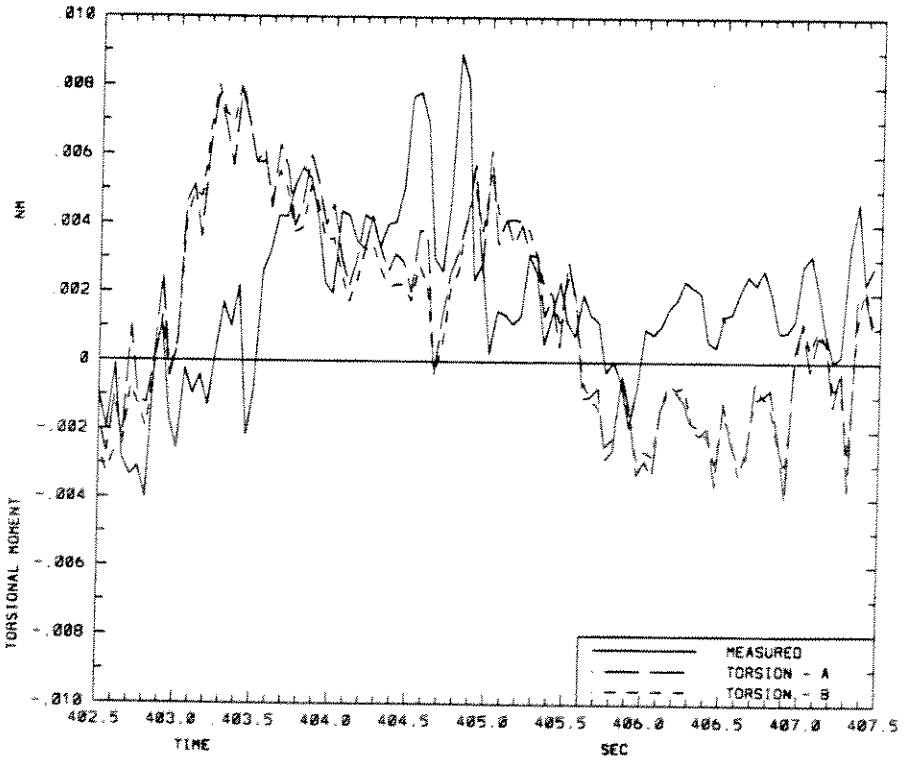

Fig. 4.12 Comparison of measured and simulated torsional moment time history for semisubmersible - no waves.

4.4. Admittances and Spectra

Aerodynamic admittance functions, are shown in Fig. 4.13 to 4.18. These functions have been calculated with a resolution of 0.1 Hz between each point on the frequency axes, allowing 55 periodograms to be averaged in the spectrum calculations, and implying a coefficient of variation of about $1/\sqrt{55} = 0.14$ for the individual spectral ordinates. Since the admittance functions are obtained from the ratio of two spectra, the uncertainty associated with individual points on the admittance functions should be expected to be somewhat higher than indicated by this coefficient of variation. The figures show comparisons of the admittance functions obtained from tests with the three types of wave conditions. The difference between the results from the various tests seems to be compatible with the level of uncertainty indicated above.

The rapid decrease in the drag force admittance function, as the frequency increases from zero, shown in Fig 4.13 and Fig. 4.16, reflects the difference found between the mean and fluctuating drag force coefficients. Fig. 4.16 shows a spurious peak in the drag force admittance for the semisubmersible, around a frequency of 3Hz. Ramsay et al. 1989c indicate that this peak may be due to a loose connection, leading to an unwanted vibration of the model.

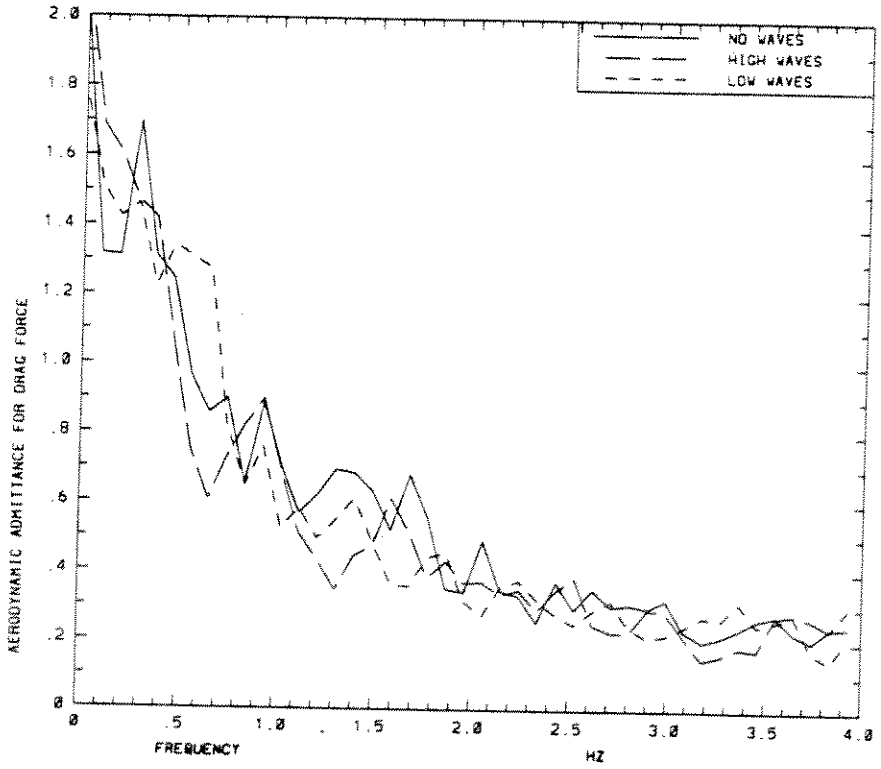

Fig. 4.13 Comparison of drag force aerodynamic admittance for TLP - 3 wave conditions.

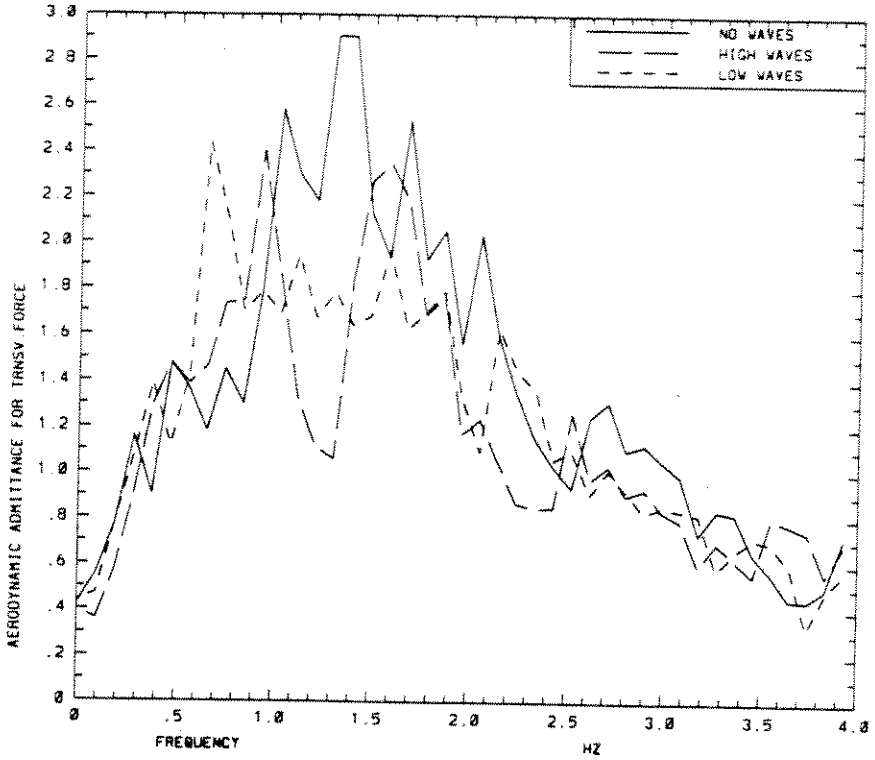

Fig. 4.14 Comparison of transverse force aerodynamic admittance for TLP - 3 wave conditions.

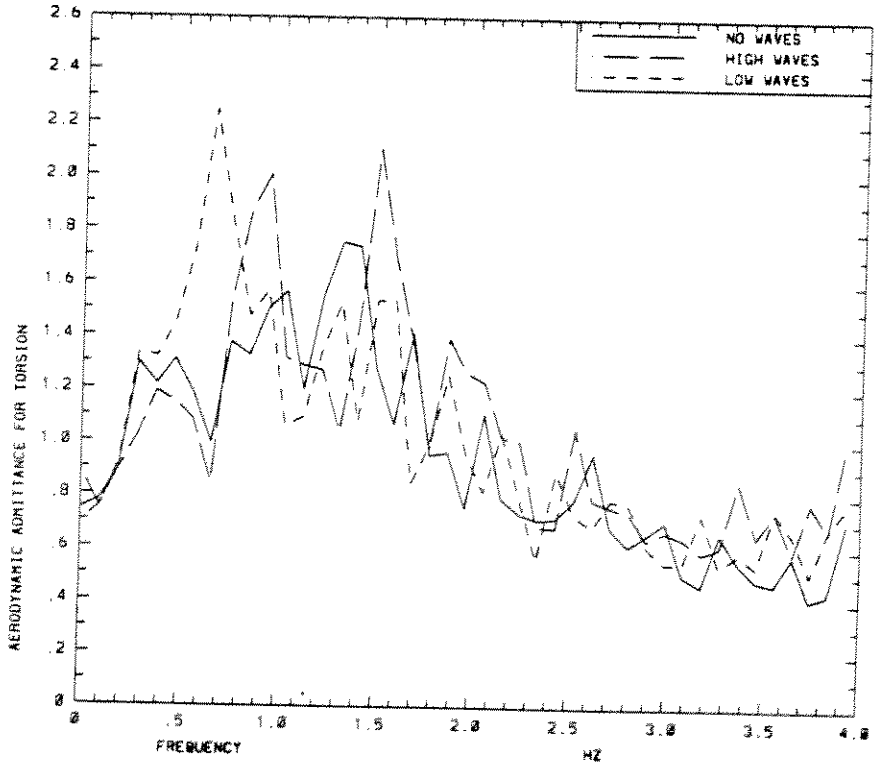

Fig. 4.15 Comparison of torsional moment aerodynamic admittance for TLP - 3 wave conditions.

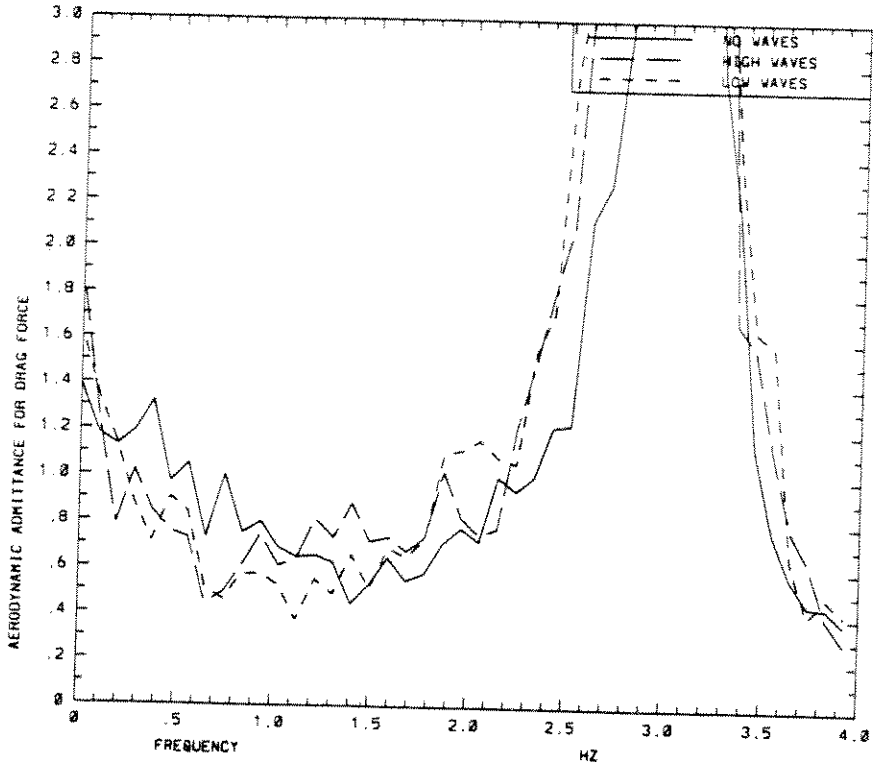

Fig. 4.16 Comparison of drag force aerodynamic admittance for semisubmersible - 3 wave conditions.

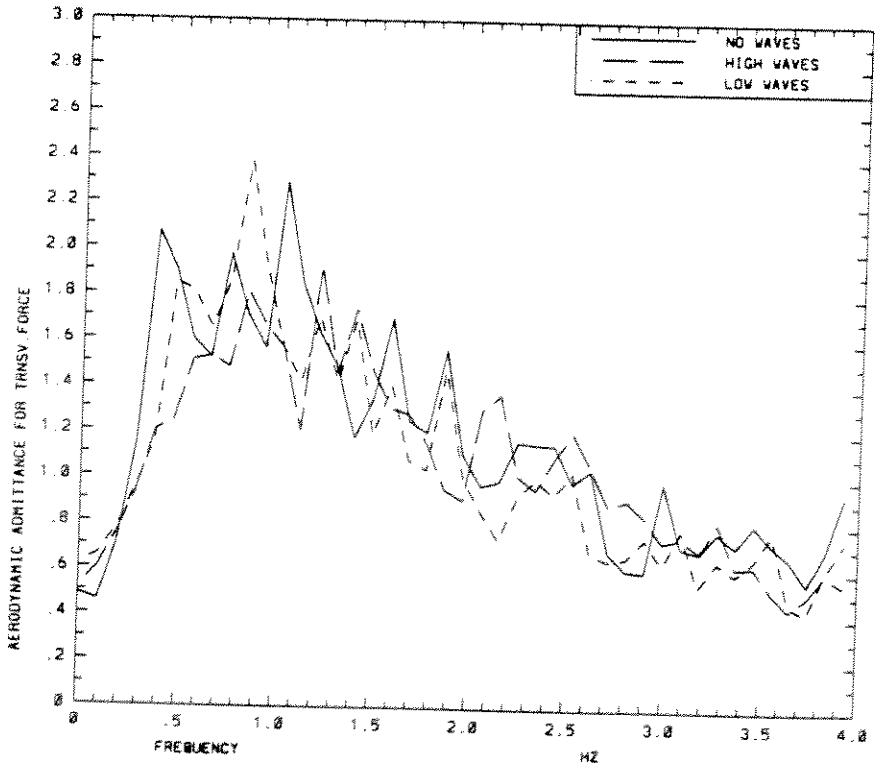

Fig. 4.17 Comparison of transverse force aerodynamic admittance for semisubmersible - 3 wave conditions.

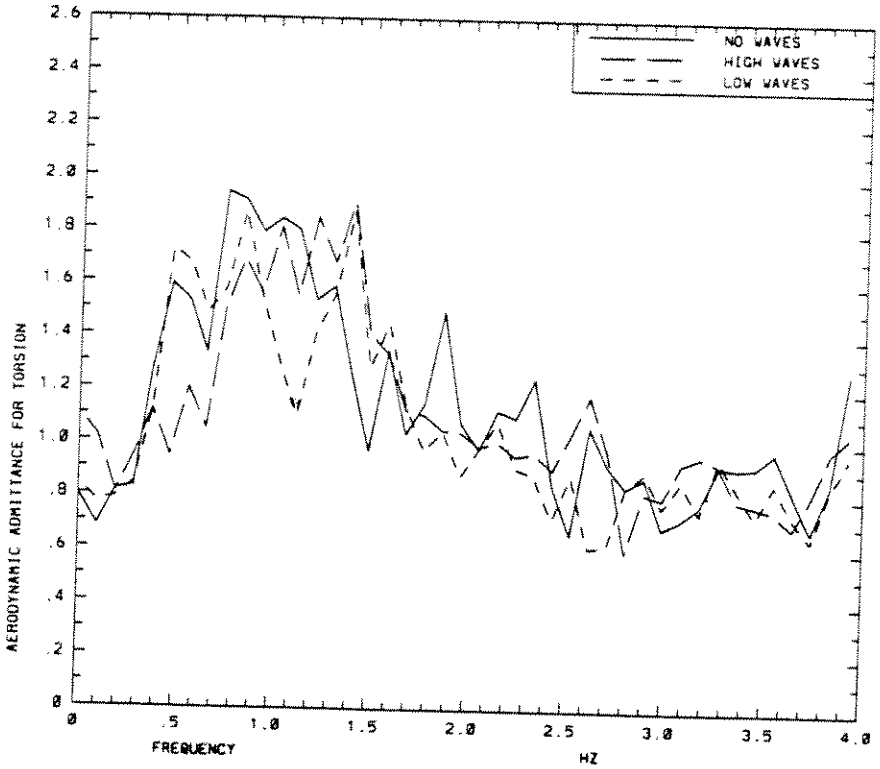

Fig. 4.18 **Comparison of torsional moment aerodynamic admittance for semisubmersible - 3 wave conditions.**

Comparisons of measured and calculated wind load spectra are shown in Fig. 4.19 to 4.24. The curves for the calculated loads are labeled to correspond to the two models, A based on load coefficients, and B based on admittance functions. These figures apply to tests where no waves were generated by the wave flap. In general, there is fair agreement between the measured and calculated wind loads. The loads calculated from the admittance functions (B) follow the measured spectra more closely. Fig. 4.19 and Fig. 4.22 show that the drag loads based on force coefficients (A) are a little on the low side for the smallest frequencies, but the loss in drag variance is recouped at higher frequencies. The opposite trend applies to both transverse forces and torsion in Fig. 4.20 - 4.21 and Fig. 4.23 - 4.24, where the load coefficient model (A) is high at the smallest frequencies and low at higher frequencies.

Corresponding figures for the tests with additional waves, but with calculated loads based on coefficients obtained from the tests without waves, showed slightly larger differences between measured and calculated loads. This reflects the differences in the load coefficients estimated from the various tests, as discussed in section 4.2.

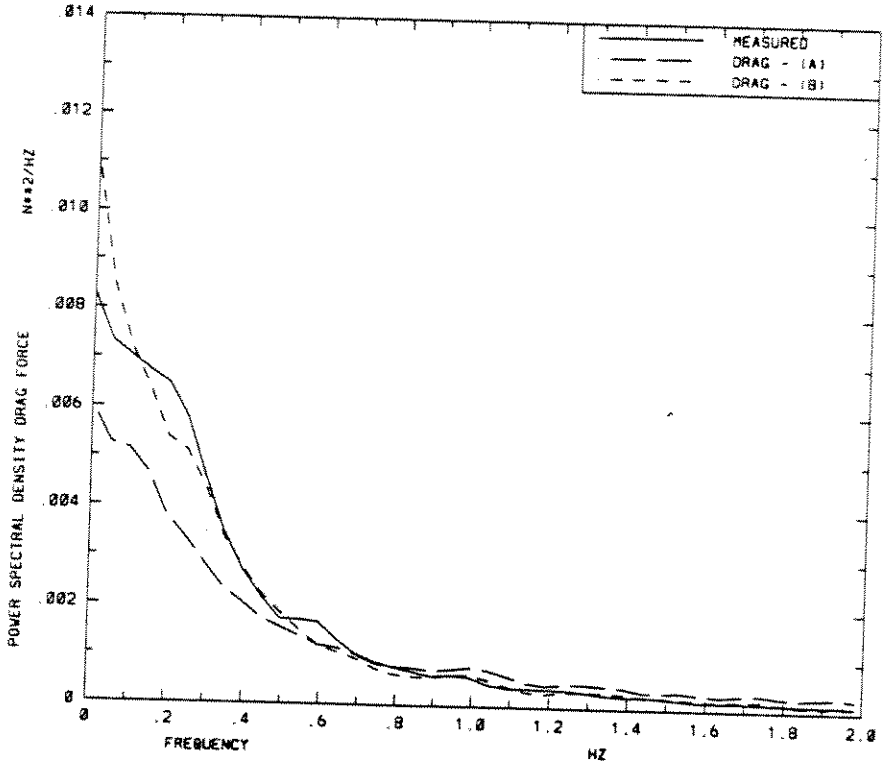

Fig. 4.19 Comparison of measured and calculated drag force spectra for TLP - no waves.

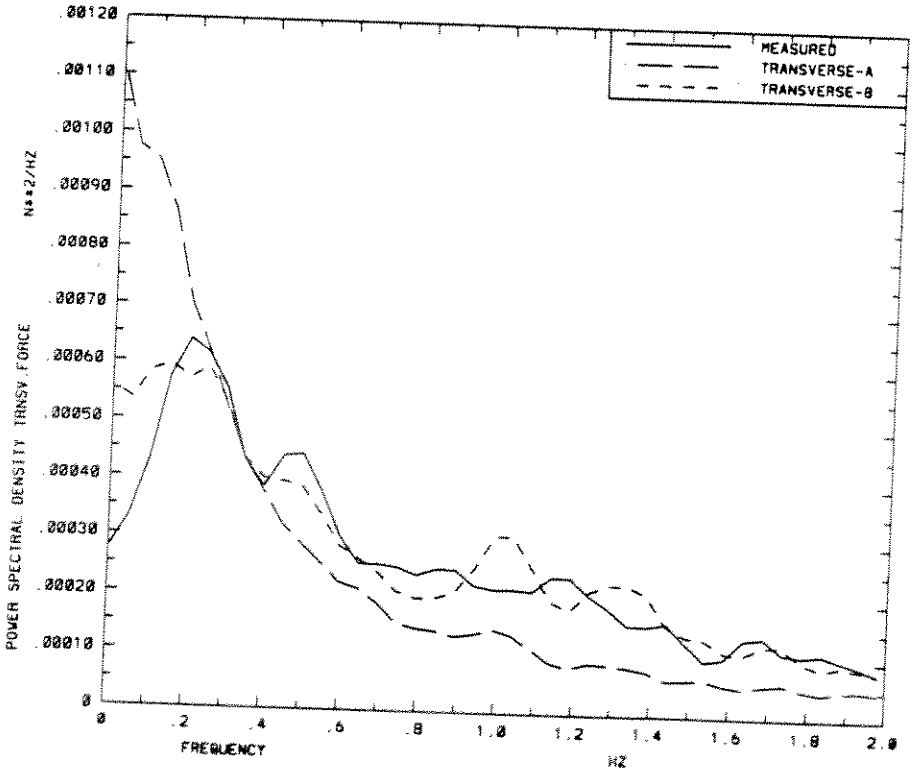

Fig. 4.20 Comparison of measured and calculated transverse force spectra for TLP - no waves.

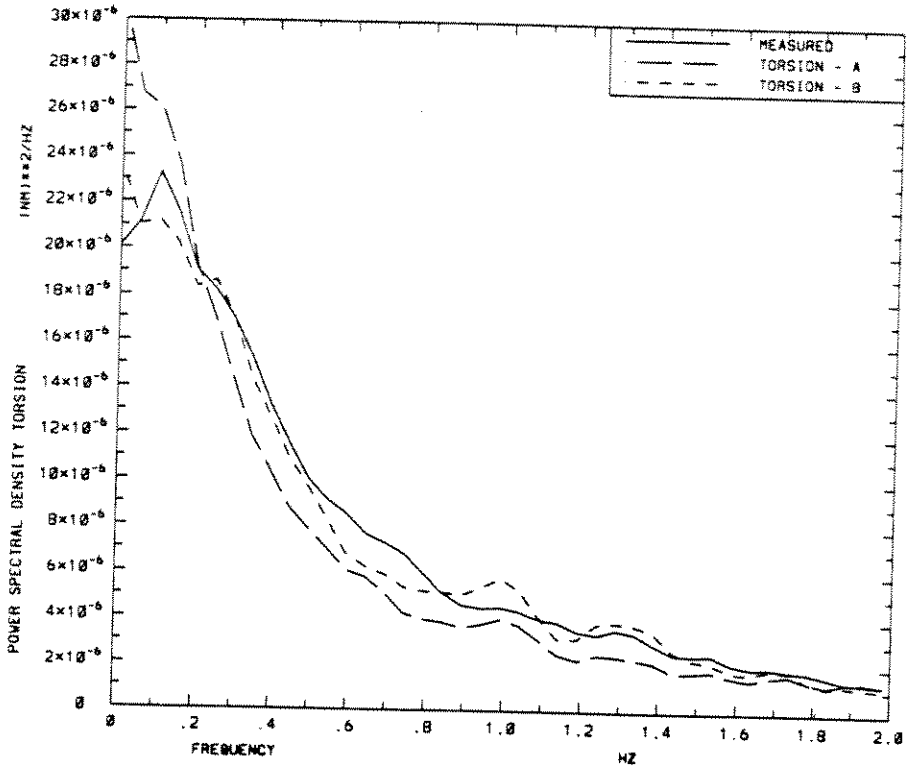

Fig. 4.21 Comparison of measured and calculated torsional moment spectra for TLP - no waves.

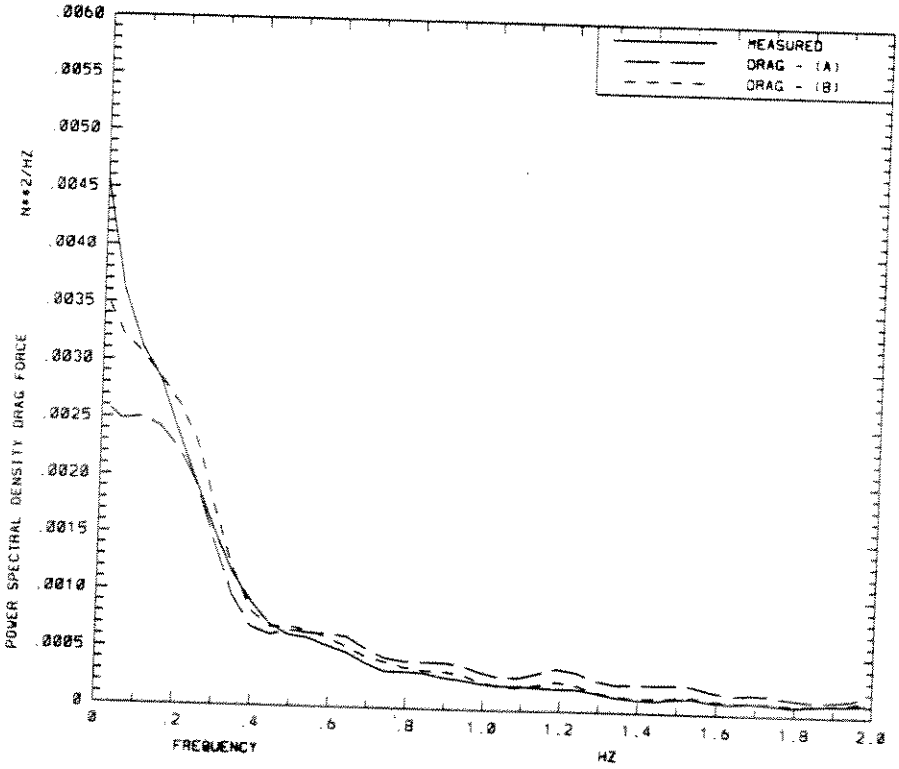

Fig. 4.22 Comparison of measured and calculated drag force spectra for semisubmersible - no waves.

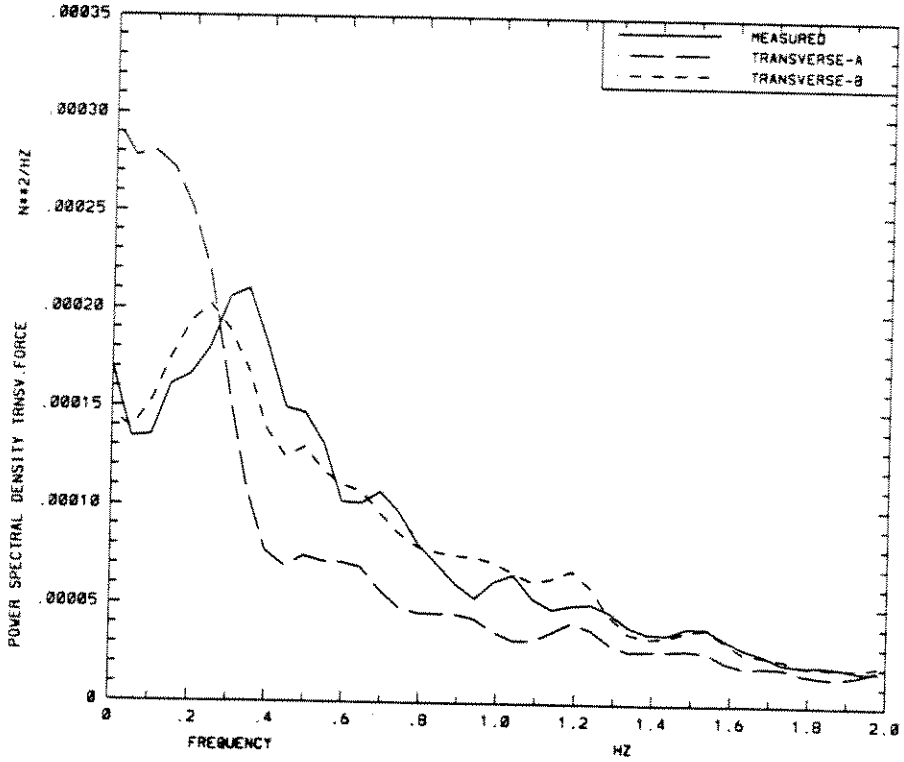

Fig. 4.23 Comparison of measured and calculated transverse force spectra for semi-submersible - no waves.

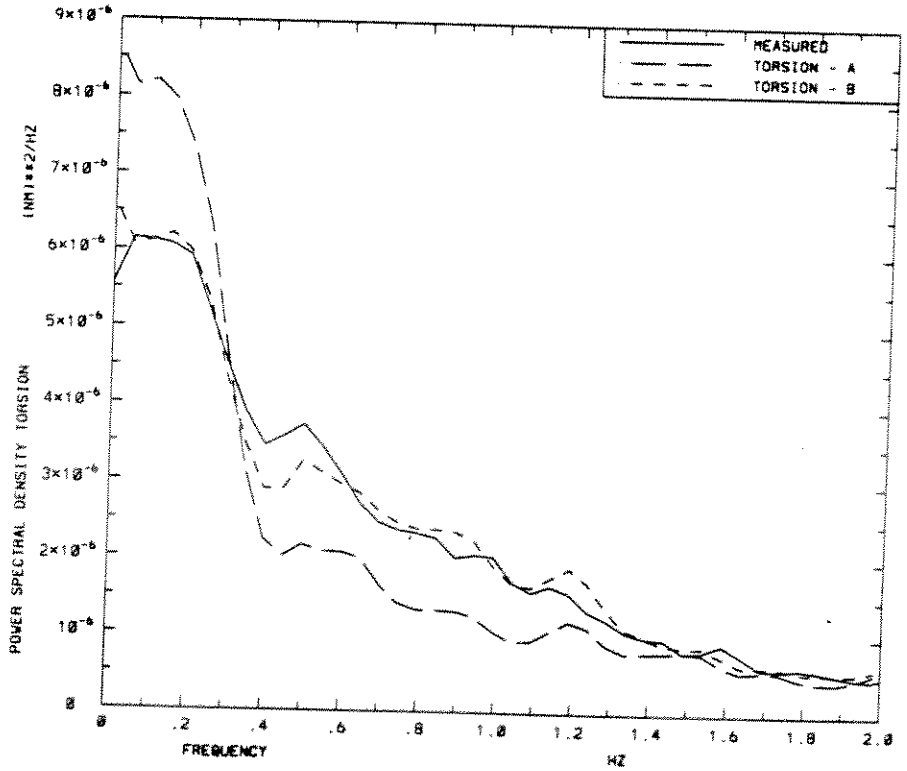

Fig. 4.24 Comparison of measured and calculated torsional moment spectra for semi-submersible - no waves.

4.5. Probability Distributions

Empirical distributions for measured and calculated wind loads are shown in Fig. 4.25 to Fig. 4.30. These results are again based on the tests with no additional waves generated by the wave flap. The distributions are plotted on normal probability paper, on which normal distributions appear as straight lines. Fairly good agreement between measured and calculated loads is shown in all cases, and the distributions do not generally deviate too much from a straight line. The drag force distributions in Fig. 4.25 and Fig. 4.28 show some curvature, indicating somewhat increased drag forces, as compared to a normal distribution. This trend is in part explained by comparison with the corresponding wind speed distributions in Fig. 4.31 and Fig. 4.32, but the curvature for the measured drag forces is slightly larger.

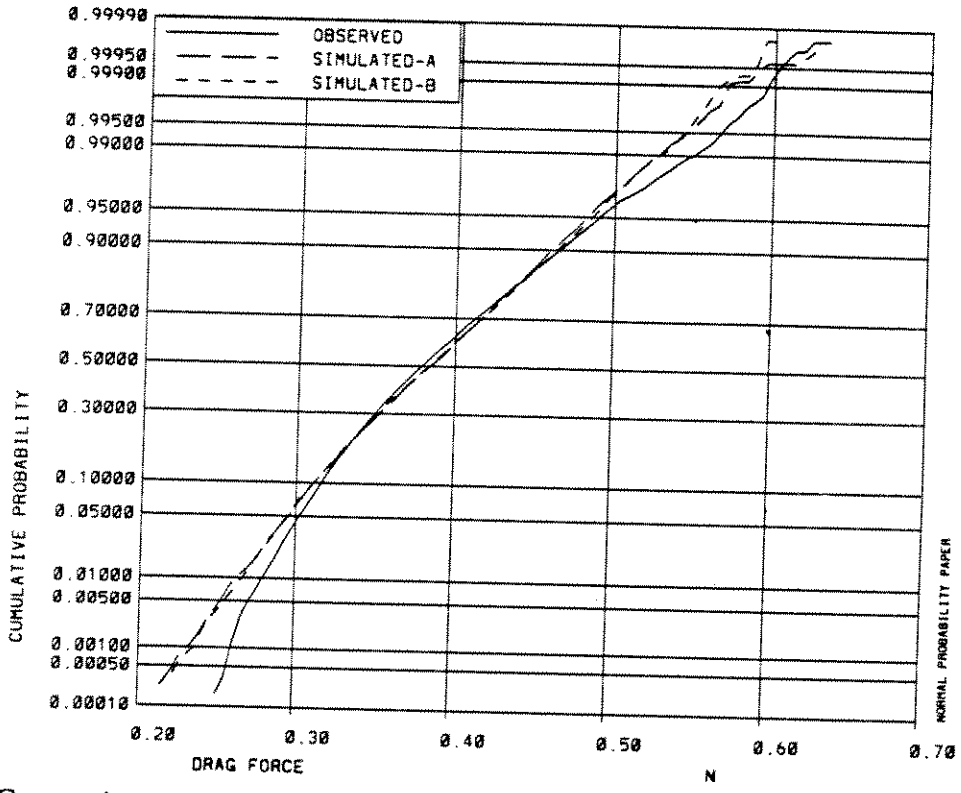

Fig. 4.25 Comparison of measured and calculated drag force distribution for TLP - no waves.

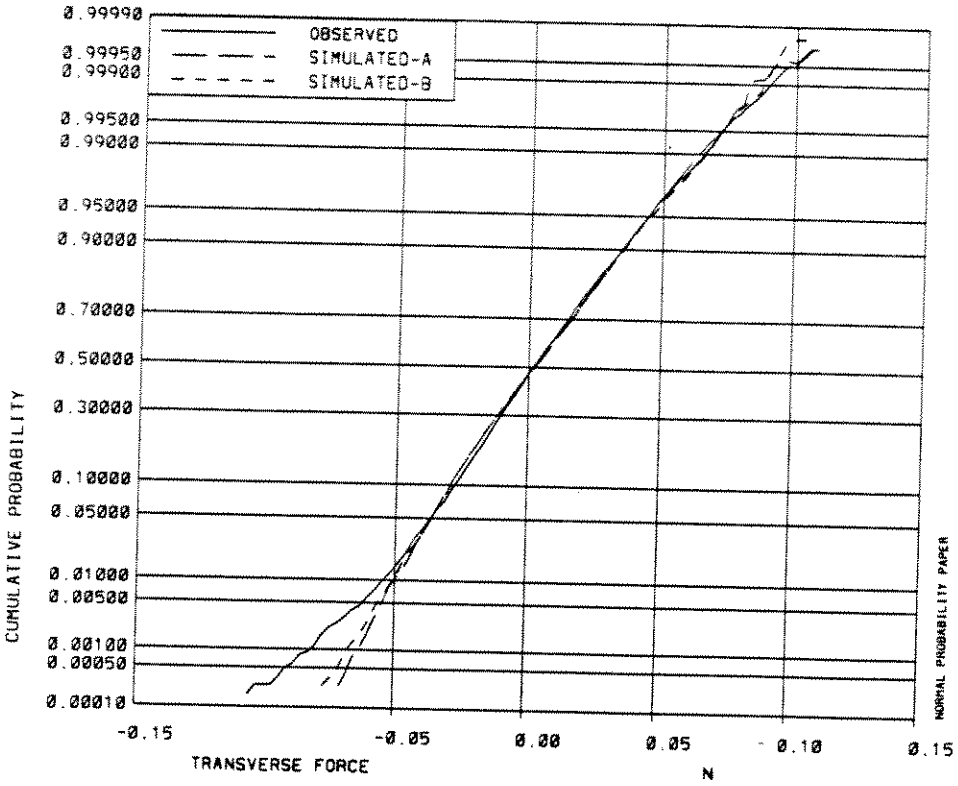

Fig. 4.26 Comparison of measured and calculated transverse force distribution for TLP - no waves.

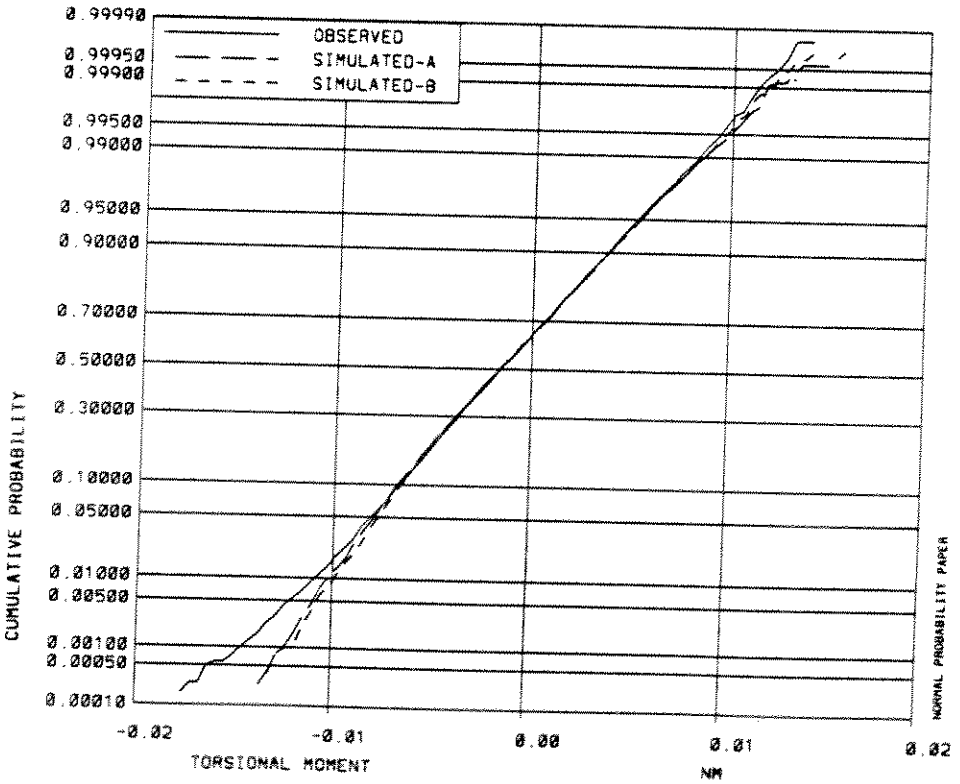

Fig. 4.27 Comparison of measured and calculated torsional moment distribution for TLP - no waves.

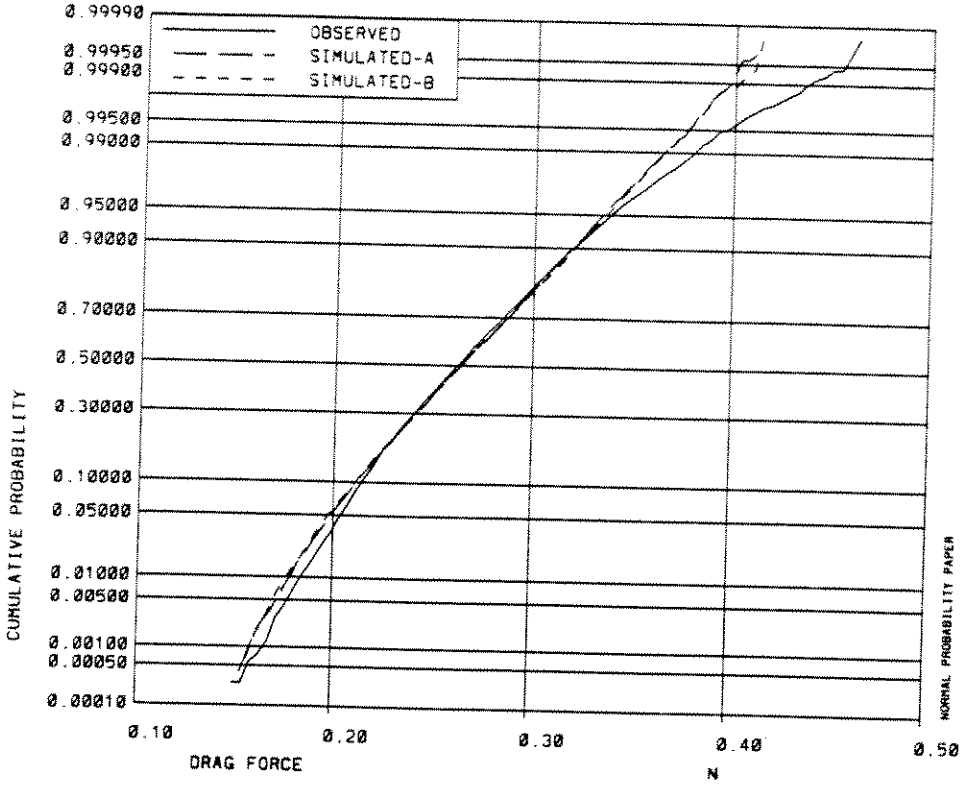

Fig. 4.28 Comparison of measured and calculated drag force distribution for semisubmersible - no waves.

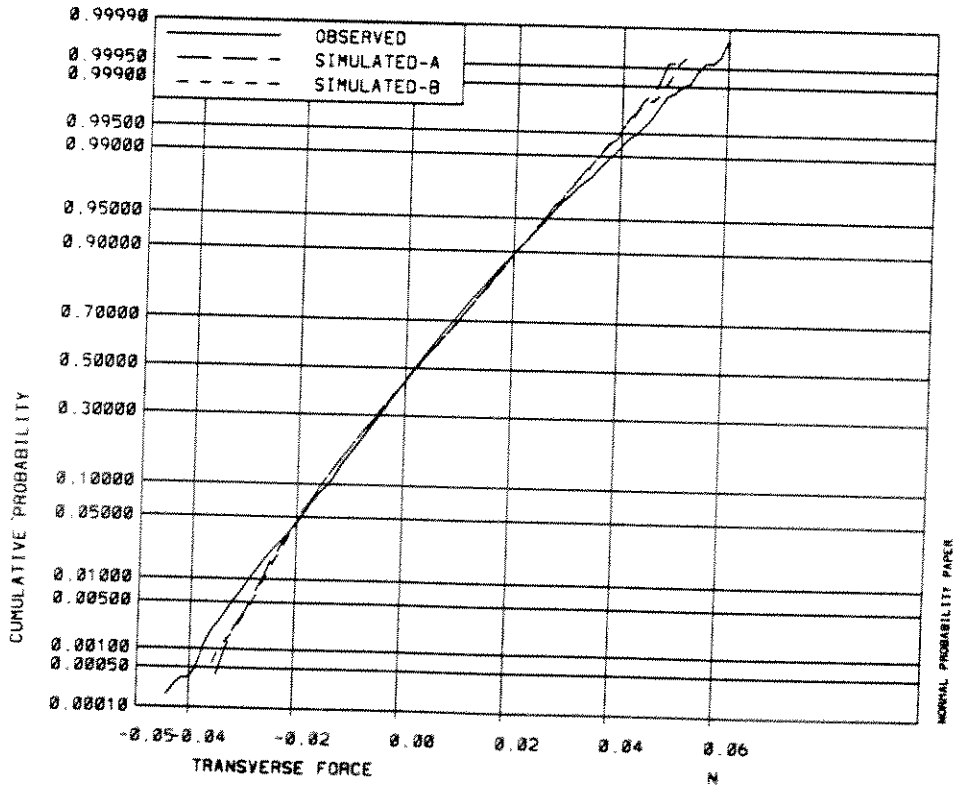

Fig. 4.29 Comparison of measured and calculated transverse force distribution for semisubmersible - no waves.

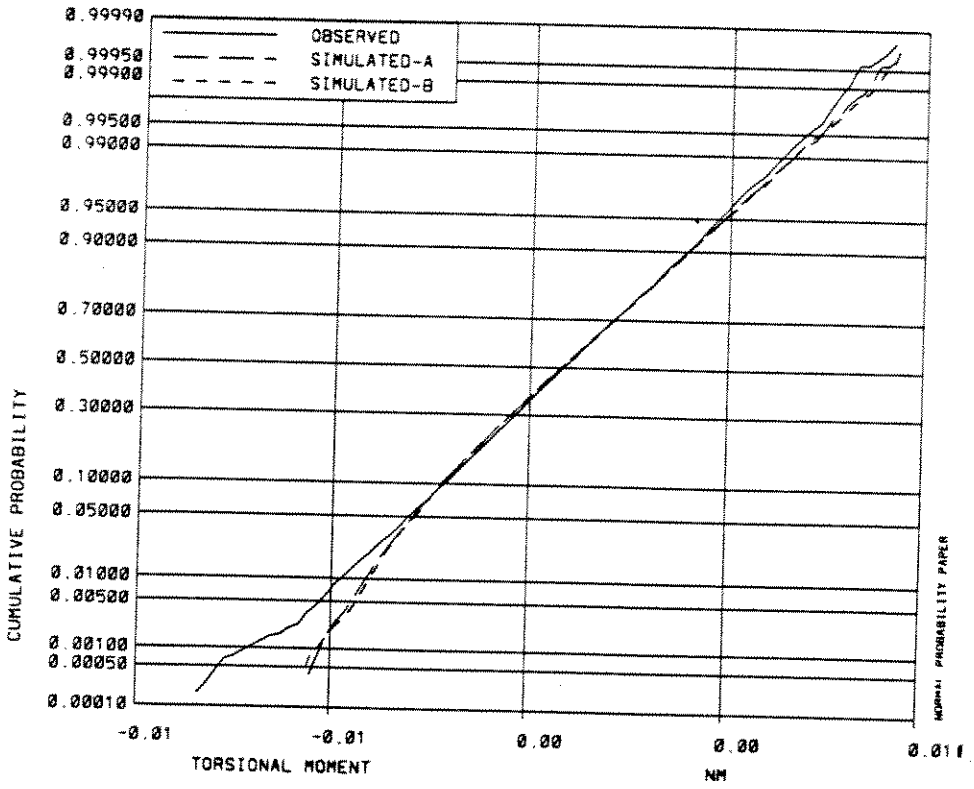

Fig. 4.30 Comparison of measured and calculated torsional moment distribution for semisubmersible - no waves.

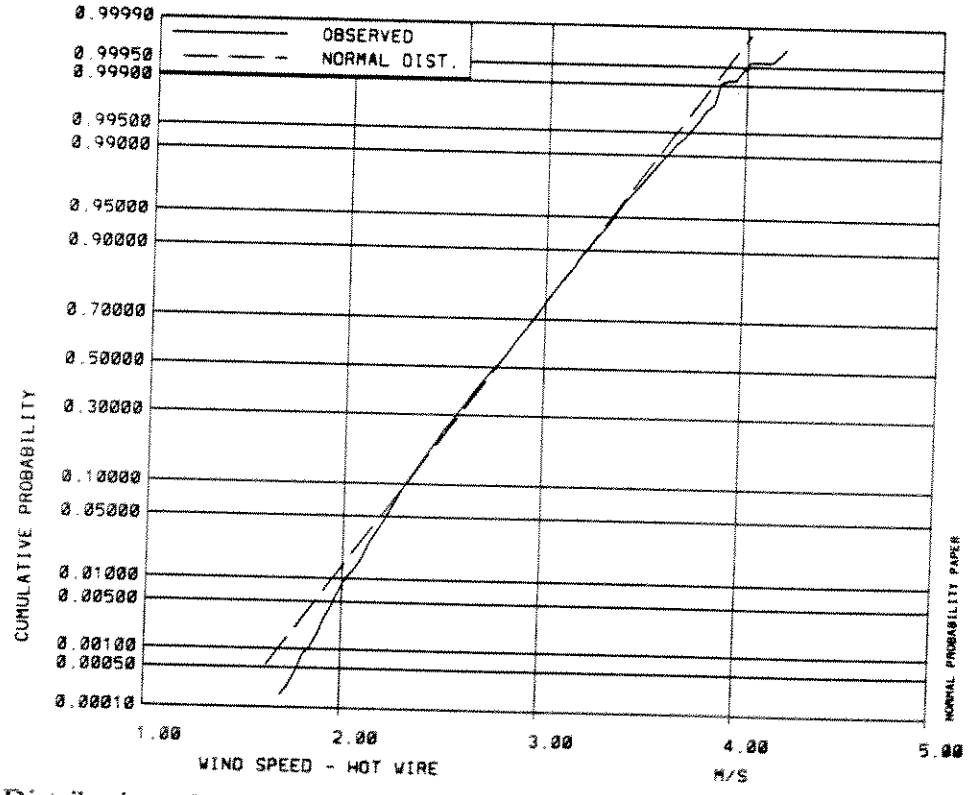

Fig. 4.31 Distribution of measured wind speed for TLP - no waves.

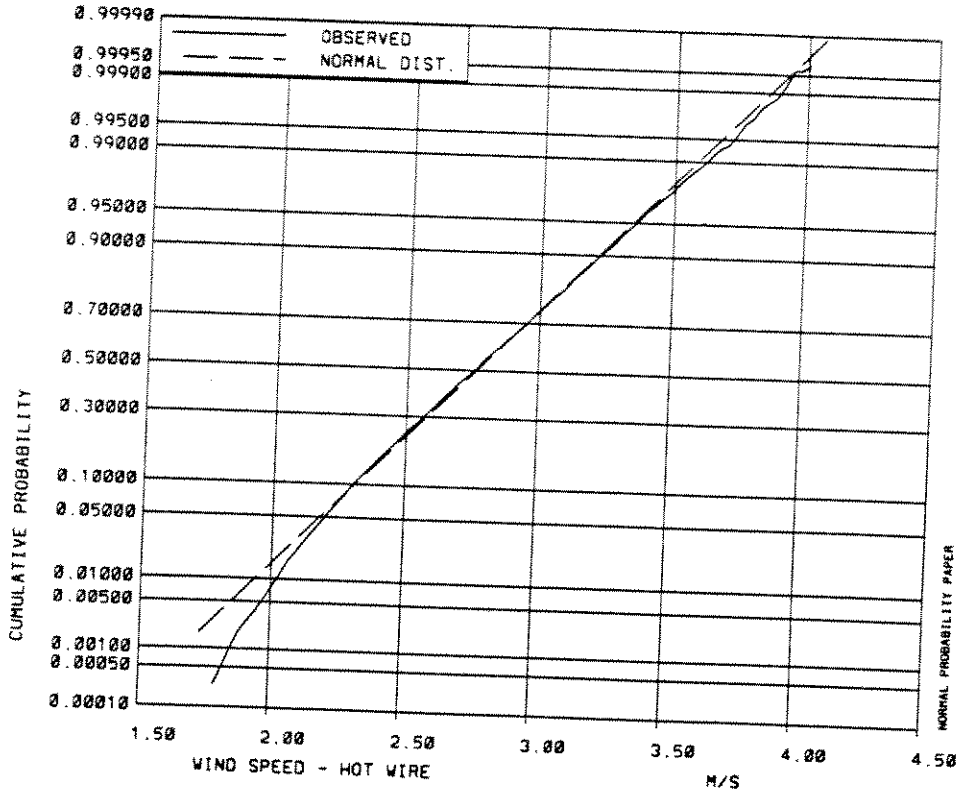

Fig. 4.32 Distribution of measured wind speed for semisubmersible - no waves.

5. Conclusions

Measured wind speeds and wind loads acting on models of the deck structure of a tension leg platform and a semisubmersible have been analysed. Wind load coefficients and aerodynamic admittance functions for drag, transverse, and torsional loads have been estimated from the model test analysis. Calculated wind loads have been simulated, using these results and the measured wind speed signal. The measured and calculated wind loads have been compared, in order to evaluate the accuracy of the mathematical models used to calculate the wind loads. It was found that:

- A drag force model using a single drag coefficient was inadequate to provide an acceptable drag force time history. If the mean drag coefficient was used, then the fluctuating drag forces were overestimated by 50% to 60%. If the fluctuating drag force coefficient was used instead, then the mean drag forces were underestimated by about one third.
- Acceptable wind loads could be obtained by using either

  (A) a model with both mean and fluctuating wind load coefficients,

  or

  (B) by a model based on aerodynamic admittance coefficients.
- Mean values and standard deviations of simulated wind loads based on either model (A) or (B), agreed with measured loads, from the same test, within ±3%. If the load coefficients or admittance were estimated from a different test, then the difference between measured and simulated results was generally increased by about ±5%. This difference increased to 14% for the drag force on the semisubmersible.
- Spectral analysis showed both models (A and B) to provide a reasonable variation in wind loading with frequency, with more accurate results provided by the admittance functions (B).
- Both calculated and measured loads appeared to follow a normal probability distribution reasonably well.
- The detailed time history of the simulated loads did not follow the measured loads at all closely. This may be due to phase shifts between wind speed frequency components and wind load components, which are not handled by either of the mathematical models.

Note that these results are all based on model tests with a single nominal mean wind speed and wind spectrum. The variations in the results primarily reflect different realisations of the same nominal conditions, and also the effect of additional waves generated by a wave flap. It seems reasonable to anticipate larger differences between measured and simulated wind loads if the wind spectrum varies significantly. If the relationship between wind speed and wind load fluctuations is predominantly linear, then the admittance model (B) should be expected to handle variations in the wind speed spectrum better than the drag coefficient model (A).

6. References

Ramsay et al. 1988

Ramsay, S.R., Vickery, B.J., and Judge, M.M. "Joint Industry Project Wind/Wave Interaction on Compliant Offshore Structures Preliminary Report No.1 Flow Structure, Sea States, Models," University of Western Ontario, Faculty of Engineering Science Research Report BLWTL-SS31-1988, November 1988

Ramsay et al. 1989a

Ramsay, S.R., Vickery, B.J., and Ng, J.Y., "Joint Industry Project Wind/Wave Interaction on Compliant Offshore Structures Preliminary Report No.2 Aerodynamic Tests - Force Coefficients," University of Western Ontario, Faculty of Engineering Science Research Report BLWTL-SS02-1989, January 1989

Ramsay et al. 1989b

Ramsay, S.R., Vickery, B.J., and Ng, J.Y. "Joint Industry Project Wind/Wave Interaction on Compliant Offshore Structures Preliminary Report No.3 Aerodynamic Tests - Spectra," University of Western Ontario, Faculty of Engineering Science Research Report BLWTL-SS03-1989, January 1989

Ramsay et al. 1989c

Ramsay, S.R., Vickery, B.J., and Ng, J.Y. "Joint Industry Project Wind/Wave Interaction on Compliant Offshore Structures - Preliminary Report No.4 Aerodynamic Tests over Water," University of Western Ontario, Faculty of Engineering Science Research Report BLWTL-SS12-1989, (Draft Version), June 1989